

Non-LOCA Methodology

Non-Proprietary Version

June 2013

**© 2013 Mitsubishi Heavy Industries, Ltd.
All Rights Reserved**

OFFICIAL USE ONLY - PROPRIETARY INFORMATION



UNITED STATES
NUCLEAR REGULATORY COMMISSION
WASHINGTON, D.C. 20555-0001

May 14, 2013

Mr. Yoshiki Ogata, General Manager
APWR Promoting Department
Mitsubishi Heavy Industries, Ltd.
16-5, Konan 2-Chome, Minato-Ku
Tokyo, 108-8215 Japan

SUBJECT: UNITED STATES - ADVANCED PRESSURIZED WATER REACTOR
FINAL TOPICAL REPORT SAFETY EVALUATION FOR TOPICAL
REPORT MUAP-7010-P, REVISION 4, "NON-LOCA METHODOLOGY"

Dear Mr. Ogata:

The U.S. Nuclear Regulatory Commission (NRC) staff has prepared a proprietary and non-proprietary final Topical Report Safety Evaluation (TRSE) for Topical Report MUAP-07010-P, Revision 4, "Non-LOCA Methodology." This action is supported by letter dated April 29, 2013 (Agencywide Documents Access and Management System accession number ML13105A219), whereby the Advisory Committee on Reactor Safeguards agrees with the NRC staff's conclusions, within the limits and conditions that are specified in the TRSE. This is also in support of the United States - Advanced Pressurized Water Reactor design certification submitted by Mitsubishi Heavy Industries, Ltd. (MHI) on December 31, 2007.

The staff requests that MHI publish the accepted proprietary and non-proprietary versions of this topical report within one month of receipt of this letter. The accepted versions of the topical report shall include an "-A" (designated accepted) following the report identification number, as well as incorporate this letter along with the enclosed final TRSE.

If the NRC's criteria or regulations change, so that its conclusion that the accepted topical report is invalidated, MHI and/or the applicant referencing the topical report will be expected to revise and resubmit its respective documentation, or submit justification for continued applicability of the topical report without revision of the respective documentation.

Document transmitted herewith
contains sensitive unclassified
information. When separated from the
enclosure, this document is
"DECONTROLLED."

OFFICIAL USE ONLY - PROPRIETARY INFORMATION

Y. Ogata

- 2 -

If you have any questions or comments concerning this matter, I can be reached at (301) 415-6391 or via e-mail address at Jeff.Ciocco@nrc.gov.

Sincerely,

A handwritten signature in cursive script that reads "Jeffrey Ciocco".

Jeffrey Ciocco, Senior Project Manager
Licensing Branch 2
Division of New Reactor Licensing
Office of New Reactors

Docket No. 52-021

Enclosure:
As stated

cc w/o encl.: See next page

DC Mitsubishi - US APWR Mailing List

(Revised 02/06/2013)

cc:

Mr. Robert E. Sweeney
IBEX ESI
4641 Montgomery Avenue
Suite 350
Bethesda, MD 20814

Mr. Gary Wright, Director
Division of Nuclear Facility Safety
Illinois Emergency Management Agency
1035 Outer Park Drive
Springfield, IL 62704

DC Mitsubishi - US APWR Mailing List

pbessette@morganlewis.com (Paul Bessette)
plarimore@talisman-intl.com (Patty Larimore)
rebecca_steinman@mnes-us.com (Rebecca Steinman)
RJB@NEI.org (Russell Bell)
ryan_sprengel@mnes-us.com (Ryan Sprengel)
sabinski@suddenlink.net (Steve A. Bennett)
sfrantz@morganlewis.com (Stephen P. Frantz)
stephan.moen@ge.com (Stephan Moen)
stramgb@westinghouse.com (George Stramback)
Tansel.Selekler@nuclear.energy.gov (Tansel Selekler)
tgilder1@luminant.com (Tim Gilder)
tmatthews@morganlewis.com (T. Matthews)
tom.miller@hq.doe.gov (Tom Miller)
Tony.Robinson@areva.com (Tony Robinson)
trsmith@winston.com (Tyson Smith)
Vanessa.quinn@dhs.gov (Vanessa Quinn)
vijukrp@westinghouse.com (Ronald P. Vijuk)
Wanda.K.Marshall@dom.com (Wanda K. Marshall)
whorin@winston.com (W. Horin)
yoshiki_ogata@mhi.co.jp (Yoshiki Ogata)

DC Mitsubishi - US APWR Mailing List

pbessette@morganlewis.com (Paul Bessette)
plarimore@talisman-intl.com (Patty Larimore)
rebecca_steinman@mnes-us.com (Rebecca Steinman)
RJB@NEI.org (Russell Bell)
ryan_sprengel@mnes-us.com (Ryan Sprengel)
sabinski@suddenlink.net (Steve A. Bennett)
sfrantz@morganlewis.com (Stephen P. Frantz)
stephan.moen@ge.com (Stephan Moen)
strambgb@westinghouse.com (George Stramback)
Tansel.Selekler@nuclear.energy.gov (Tansel Selekler)
tgilder1@luminant.com (Tim Gilder)
tmatthews@morganlewis.com (T. Matthews)
tom.miller@hq.doe.gov (Tom Miller)
Tony.Robinson@areva.com (Tony Robinson)
trsmith@winston.com (Tyson Smith)
Vanessa.quinn@dhs.gov (Vanessa Quinn)
vijukrp@westinghouse.com (Ronald P. Vijuk)
Wanda.K.Marshall@dom.com (Wanda K. Marshall)
whorin@winston.com (W. Horin)
yoshiki_ogata@mhi.co.jp (Yoshiki Ogata)

FINAL SAFETY EVALUATION BY THE OFFICE OF NEW REACTORS
 TOPICAL REPORT MUAP-07010-P, REVISION 4
 “NON-LOCA METHODOLOGY”
 MITSUBISHI HEAVY INDUSTRIES, Ltd
 DOCKET NO. 52-021

Contents

1.0	INTRODUCTION	- 4 -
2.0	SYSTEM DESCRIPTION	- 5 -
2.1	Primary System Components	- 5 -
2.1.1	Reactor Core and Reactor Vessel.....	- 5 -
2.1.2	Reactor Coolant System	- 5 -
2.2	Emergency Core Cooling System	- 6 -
2.2.1	Accumulator System	- 7 -
2.2.2	High-Head Injection System.....	- 7 -
2.3	Secondary System Components.....	- 7 -
2.3.1	Main Steam System Components.....	- 7 -
2.3.2	Main Feedwater System Components	- 8 -
2.3.3	Emergency Feedwater System Components	- 8 -
2.4	Containment Vessel.....	- 8 -
3.0	REGULATORY BASIS	- 9 -
4.0	SUMMARY OF MUAP-07010-P	- 12 -
5.0	TECHNICAL EVALUATION.....	- 15 -
5.1	Code Descriptions and Validations	- 15 -
5.1.1	MARVEL-M Code	- 15 -
5.1.2	MARVEL-M Code Validation	- 20 -
5.1.3	TWINKLE-M	- 23 -
5.1.4	VIPRE-01M	- 28 -
5.1.5	ANC.....	- 28 -
5.2	Event-Specific Methodology.....	- 28 -
5.2.1	Uncontrolled RCCA Bank Withdrawal at Power.....	- 30 -
5.2.2	Complete Loss of Forced Reactor Coolant Flow.....	- 31 -
5.2.3	Spectrum of RCCA Ejection	- 33 -
5.2.4	Steam System Piping Failure	- 42 -
5.2.5	Feedwater System Pipe Break.....	- 50 -
5.2.6	Steam Generator Tube Rupture.....	- 53 -
5.3	Independent Analyses.....	- 55 -
5.3.1	RELAP5/MOD3.3 Simulations.....	- 56 -
5.3.2	MARVEL-M Simulations.....	- 62 -
5.4	Appendix A - Review of the MARVEL-M computer code	- 63 -
A.0	Introduction.....	- 63 -
A.1	Neutron Kinetics Equation.....	- 63 -
A.1.1	Decay Heat and Fission Power	- 63 -
A.1.2	Reactivity Coefficient.....	- 64 -
A.2	Fuel Rod and Core Thermal Kinetics Equation	- 65 -
A.2.1	Fuel Thermal Model.....	- 65 -
A.2.2	Reactor Core Flow Model and Core Power Distribution.....	- 66 -
A.2.3	Hot Channel Fuel Thermal Model.....	- 67 -

A.2.4	DNBR Evaluation Model.....	- 68 -
A.3	Equations for Reactor Coolant Flow Sections.....	- 68 -
A.3.1	Reactor Core Coolant Thermal Kinetics Equation (HEAT).....	- 69 -
A.3.2	Mixing Plenum Equation (MIXG).....	- 69 -
A.3.3	Transport in Pipe (SLUG).....	- 70 -
A.3.4	SG Primary Side Equation (HEEX).....	- 72 -
A.3.5	Dead Volume (Reactor Vessel Head Volume) (MIXD).....	- 73 -
A.3.6	Reactor Vessel Upper Plenum (MIXS).....	- 73 -
A.3.7	Pressure Gradient in Reactor Coolant System.....	- 73 -
A.3.8	Thick Metal Effect.....	- 73 -
A.4	Mixing and Flow Model in Reactor Vessel.....	- 74 -
A.4.1	Mixing in the Downcomer, Reactor Vessel Lower Plenum and Upper Plenum...- 74 -	
A.4.2	Core Bypass Flow.....	- 76 -
A.5	SG Model.....	- 76 -
A.5.1	Heat Transfer Coefficient.....	- 76 -
A.5.2	SG Water Level.....	- 77 -
A.5.3	Heat Transfer Area.....	- 78 -
A.5.4	SG Secondary-Side Thermal Kinetics Equation.....	- 79 -
A.5.5	Other Special Models.....	- 79 -
A.6	Pressurizer.....	- 80 -
A.6.1	Water Phase Model.....	- 80 -
A.6.2	Steam Phase Model.....	- 81 -
A.6.3	Pressurizer Pressure Control.....	- 82 -
A.7	Transient Flow Performance.....	- 83 -
A.7.1	Reactor Coolant Pump Models and Flow Transient.....	- 83 -
A.7.2	Natural Circulation Model.....	- 85 -
A.7.3	Approximated Analytical Solution of Flow Coast-Down.....	- 85 -
A.8	Secondary Steam System Model.....	- 86 -
A.8.1	Distribution of Steam Flow.....	- 86 -
A.8.2	Steam Relief and Safety Valves.....	- 88 -
A.8.3	Steam Turbine Flow.....	- 88 -
A.9	Engineered Safeguards Features.....	- 88 -
A.10	Reactor Coolant System Small Break or Leak.....	- 89 -
A.11	Reactor Control System.....	- 89 -
A.12	Chemical Volume Control System.....	- 90 -
A.13	Reactor Protection System and ESFAS.....	- 90 -
A.14	Realistic Models - Descriptions and Model.....	- 90 -
A.15	Specific Computation Techniques.....	- 91 -
A.16	Appendix A References.....	- 93 -
6.0	CONCLUSIONS, LIMITATIONS AND CONDITIONS.....	- 95 -
7.0	REFERENCES.....	- 96 -
8.0	ACRONYMS.....	- 101 -

Tables

Table 1 Sensitivity of Key MARVEL-M Parameters to Core Inlet Mixing Assumption for the MSLB with Loss of Offsite Power..... - 44 -
Table 2 Sequence of Events for Loss of Load MDNBR Case. - 56 -
Table 3 Calculated Sequences of Events for SGTR Radiological Dose Evaluation Case..... - 58 -

Figures

Figure 1 MDNBR for the LOL Cases - 57 -
Figure 2 Peak Pressure for the LOL Overpressure Cases - 57 -
Figure 3 SGTR Event - Break Flow - 59 -
Figure 4 SGTR Event - Pressurizer Pressure - 59 -
Figure 5 SGTR Event - Safety Valve Flow in Affected SG - 60 -
Figure 6 MSLB Event - RCS Pressure..... - 61 -
Figure 7 MSLB Event - Normalized Reactor Power..... - 61 -
Figure 8 FWLB Event - Liquid Volume in the Pressurizer..... - 62 -

1.0 INTRODUCTION

By letter dated July 20, 2007, Mitsubishi Heavy Industries, LTD (MHI), the applicant, submitted to the U.S. Nuclear Regulatory Commission (NRC) for review and approval of Topical Report MUAP-07010-P, Revision 0, "Non-LOCA Methodology" [Reference 1] in support of the United States - Advanced Pressurized Water Reactor (US-APWR) Design Certification (DC) Application. This report was later superseded by letter dated October 29, 2010, which transmitted Topical Report MUAP-07010-P, Revision 1 [Reference 2], by letter dated August 31, 2011, which transmitted Topical Report MUAP-07010-P, Revision 2 [Reference 3], by letter dated April 5, 2012, which transmitted Topical Report MUAP-07010-P, Revision 3 [Reference 52] and by letter dated May 11, 2012, which transmitted Topical Report MUAP-07010-P, Revision 4 [Reference 53]. Topical Report MUAP-07010-P describes the codes and the general evaluation models used to perform Non-Loss of Coolant Accident (Non-LOCA) simulations of the US-APWR reactor design to determine the consequences of such transients and accidents on the reactor core and associated piping systems. The purpose of these evaluations is to demonstrate that, for a given transient scenario, reactor fuel failures and peak system pressures on both the primary and secondary sides of the heat transfer loops remain within acceptable ranges, and to demonstrate that onsite and offsite radiological releases remain within acceptable limits. The analyses of the US-APWR transient and accident analyses are described in the US-APWR Design Control Document (DCD) [Reference 4] Tier 2 Chapter 15, "Transient and Accident Analysis."

The applicant also provided a report for the MARVEL-M computer program. MARVEL-M is described in MHI's report GEN0-LP-480, "MARVEL-M A Digital Computer Code for Transient Analysis of a Multi-Loop PWR System." GEN0-LP-480, Revision 6, was provided in March 2009 [Reference 5]. The current version, Revision 12, was provided in October 2010 [Reference 6].

This safety evaluation (SE) documents the NRC staff's review of Topical Report MUAP-07010-P and report GEN0-LP-480. Section 2 of this SE describes the US-APWR reactor systems in the context of the Non-LOCA analysis. The regulatory basis and acceptance criteria for Standard Review Plan Chapter 15 Non-LOCA analyses are provided in Section 3. A summary of MUAP-07010-P, including the computer codes used in the Non-LOCA analysis is provided in Section 4. The NRC staff technical evaluation of Topical Report MUAP-07010-P is provided in Section 5. Discussions of requests for additional information (RAIs) issued as a part of the review are provided, along with staff evaluations of the applicant's RAI responses and the acceptability of the corresponding analytical models. Section 6 provides the staff's conclusions regarding the adequacy of the codes and methods described in Topical Report MUAP-07010-P for representing the relevant phenomena and demonstrating compliance with the regulatory acceptance criteria, as well as any conditions and limitations on the codes and methods for licensing calculations. References are listed in Section 7. The NRC staff evaluation of GEN0-LP-480 is provided in Section 5 as Appendix A.

2.0 SYSTEM DESCRIPTION

The general system configuration of the US-APWR is equivalent to that of a Westinghouse designed four-loop pressurized-water reactor (PWR), with the thermal-hydraulic volume, flow area, and diameter of reactor components and their piping sized to accommodate the larger thermal output of US-APWR. The US-APWR is rated at 4,451 megawatt thermal (MWT).

The US-APWR systems that must be modeled and analyzed include:

- Primary System (reactor core, reactor vessel (RV), reactor coolant system (RCS), emergency core cooling system (ECCS))
- Secondary System (main steam system, main feedwater system (MFWS), emergency feedwater system (EFWS))
- Containment Vessel

The reactor coolant primary and steam generator (SG) secondary systems are modeled in the Non-LOCA calculations. Primary system modeling includes the reactor internals and vessel, the SGs, the reactor coolant pumps, the pressurizer, the reactor coolant piping and pressurizer surge line, the accumulators and the high-head safety injection system. Secondary system modeling includes the SG secondary side, and the main feedwater, main steam and EFW lines, their isolation valves, and safety and relief valves.

2.1 Primary System Components

The primary system includes the reactor core, RV, RCS and the ECCS, which are included in the US-APWR MARVEL-M Non-LOCA model.

2.1.1 Reactor Core and Reactor Vessel

The US-APWR fuel assembly utilizes a 17x17 array of 264 fuel rods, 24 control rod guide thimbles and one in-core instrumentation guide tube. The fuel rod and thimble components are bundled by grid spacers. The fuel design uses 11 grid spacers that span the approximately 14-ft (4.2-m) active fuel length.

The RV internals consist of the lower and upper core support assemblies and the neutron reflector. These RV internals support the core, maintain fuel assembly and control rod alignments, limit fuel assembly movement, direct the coolant flowing through the fuel assemblies, guide the in-core instrumentation and provide RV radiation shielding.

2.1.2 Reactor Coolant System

The RCS consists of the RV, the SGs, the reactor coolant pumps (RCPs), the pressurizer, and the reactor coolant pipes and valves connecting to and interconnecting those components.

The RV, which contains the structures discussed above in Section 2.1.1, has four inlet nozzles, four outlet nozzles, and four safety injection nozzles located between the RV upper flange and the top of the core. The SG is a vertical shell U-tube evaporator with integral moisture separating equipment.

The RCPs are vertical single-stage centrifugal pumps, of design similar to Westinghouse 93A pumps used in four-loop PWRs, driven by three-phase induction motors. A flywheel on the shaft above the motor provides additional inertia to extend pump coast-down. The pump suction is located at the bottom of the pump, and the discharge on the side of the pump. The US-APWR has an automatic RCP trip, with a three-second delay, on an ECCS safety injection signal generated by low pressurizer pressure or high containment pressure, as required by Three Mile Island (TMI) Action Item II.K.3.5 "Automatic RCP Trip during a LOCA."

The pressurizer functions to control the RCS pressure and to accommodate changes in the coolant volume. The pressurizer is a vertical vessel with hemispherical top and bottom heads. Electrical immersion-type heaters are installed vertically through the bottom head of the vessel. The spray nozzle and relief line connections to the relief and safety valves are located on the top head of the vessel.

2.2 Emergency Core Cooling System

The ECCS injects borated water into the RCS following some anticipated operational occurrences and postulated accidents and performs the following functions:

- Following a LOCA, the ECCS cools the reactor core, prevents the fuel and fuel cladding from serious damage, and limits the zirconium-water reaction of the fuel cladding to a very small amount.
- Following an inadvertent opening of a steam generator relief or safety valve or a main steam line break (MSLB), the ECCS provides negative reactivity to shut down the reactor.
- In the event that the normal chemical and volume control system (CVCS) letdown and boration capability is lost, the ECCS provides emergency letdown and boration of the RCS.

The ECCS design is based on the following requirements:

- (1) In combination with control rod insertion, the ECCS is designed to shut down and cool the reactor during the following accidents:
 - Large-break LOCA and small-break LOCA of the primary piping,
 - Control rod ejection,
 - inadvertent opening of a steam generator relief or safety valve,
 - Main steam line break,
 - Steam generator tube rupture (SGTR).

- (2) The ECCS is designed with sufficient redundancy (four independent trains) to accomplish the specified safety functions assuming a single failure of an active component following an accident with one train out of service for maintenance, or a single failure of an active component or passive component for the long term core cooling following an accident with one train out of service.
- (3) The ECCS is automatically initiated by a safety injection (SI) signal.
- (4) The emergency electrical power to the essential components is provided so that the design functions can be maintained during a loss of offsite power (LOOP).

The ECCS includes the accumulator system, the high-head injection system (HHIS) system, and the emergency letdown system. The accumulator system and HHIS system are included in the US-APWR Non-LOCA evaluation model.

2.2.1 Accumulator System

The accumulator system, which is a passive safety component, consists of four accumulators, and the associated valves and piping, one for each RCS loop. The system is connected to the cold legs of the reactor coolant piping and injects borated water when the RCS pressure falls below the accumulator operating pressure. Pressurized nitrogen gas forces borated water from the tanks into the RCS. The accumulator performs the large flow injection to refill the reactor vessel, and then provides a smaller injection flow during core reflooding in association with the HHIS injection pumps. The HHIS provides long term core cooling.

2.2.2 High-Head Injection System

The HHIS, which is an active safety component, consists of four independent trains, each containing a safety injection pump (SIP) and the associated valves and piping. The safety coolant is directly injected into the downcomer using direct vessel injection (DVI). The SIPs start automatically upon receipt of the SI signal. One of four independent safety electrical buses is available to each SIP. The SIPs are aligned to take suction from the refueling water storage pit (RWSP) and to deliver borated water to the SI nozzles on the RV. Two SI trains are capable of meeting the design cooling function for a large break LOCA (LBLOCA) or small break LOCA (SBLOCA). This capability ensures adequate emergency core cooling (ECC) delivery in the case where it is assumed that there is a single failure in one train and a second train is out of service for maintenance.

The RWSP, in the containment, provides a continuous borated water source for the SIPs. This configuration eliminates the need for realignment from the refueling water storage tank to the containment sump, which is employed in existing PWR plants.

2.3 Secondary System Components

The secondary system consists of the main steam system (MSS), the MFWS, the EFWS, and the power conversion system.

2.3.1 Main Steam System Components

The MSS includes the main steam lines from the SG outlets to the turbine inlet steam chests and equipment and piping connected to the main steam lines. The main steam safety and relief

valves are installed upstream of the main steam isolation valve (MSIV). They prevent excessive steam pressure and maintain cooling of the RCS if the turbine bypass is not available. The total capacity of the main steam safety valves (MSSV) exceeds 100 percent of the rated main steam flow rate. Branch pipes for driving the turbine-driven emergency feedwater (EFW) pumps are connected upstream of the MSIVs. The secondary sides of SGs are included in the US-APWR Non-LOCA MARVEL-M model, up to the turbine. The steam line relief and isolation valves, and the steam dump control valve, are included in the MARVEL-M model.

2.3.2 Main Feedwater System Components

The MFWS supplies the SGs with heated feedwater in a closed steam cycle using regenerative feedwater heating. The system is composed of the condensate subsystem, the feedwater subsystem, and a portion of the SG feedwater piping. The feedwater control valves, the feedwater bypass control valves, the SG water filling control valves, and the feedwater isolation valves that are installed on the feedwater lines. The feedwater control and isolation valves on the secondary sides of the SGs are included in the MARVEL-M model.

2.3.3 Emergency Feedwater System Components

The EFWS consists of two motor-driven pumps, two steam turbine-driven pumps, two EFW pits, and associated piping and valves. The four EFW pumps take suction from two EFW pits. The EFWS removes reactor decay heat and RCS residual heat through the SGs following transient conditions or postulated accidents. The EFWS is modeled as a fill system in the MARVEL-M model.

2.4 Containment Vessel

The containment vessel is designed to completely enclose the reactor and RCS and to ensure that essentially no leakage of radioactive materials to the environment would result even if a major failure of the RCS were to occur. The containment vessel is a pre-stressed, post-tensioned concrete structure with an inside steel lining. The containment vessel is designed to contain the energy and radioactive materials that could result from a postulated LOCA. In the MARVEL-M model, an atmospheric condition inside the containment is assumed as the pressure boundary condition for systems that interact with the containment.

3.0 REGULATORY BASIS

Title 10 of the *Code of Federal Regulations* (10 CFR), Part 50, Section 34, paragraphs (a)(4) and (b)(4) specifies that each boiling or pressurized light-water nuclear power reactor must provide the following:

... analysis and evaluation of the design and performance of structures, systems, and components of the facility with the objective of assessing the risk to public health and safety resulting from operation of the facility and including determination of the margins of safety during normal operations and transient conditions anticipated during the life of the facility, and the adequacy of structures, systems, and components provided for the prevention of accidents and the mitigation of the consequences of accidents.

The NRC has provided guidance regarding how the above regulatory criteria can be met. Regulatory Guide (RG) 1.203 [Reference 7] describes acceptable approaches to develop the computer programs to conduct transient and accident analyses. RG 1.206 [Reference 8], Section 3.I.15 provides guidance for the evaluation of transients and accidents. Section 15 of the standard review plan (SRP) [Reference 9] discusses specific acceptance criteria for each transient.

The acceptance criteria are based on meeting the relevant requirements of the following Commission regulations:

1. 10 CFR Part 20, "Standards for Protection Against Radiation"
2. 10 CFR Part 50, "Domestic Licensing of Production and Utilization Facilities" (especially 10 CFR 50.46 and Appendix A)
3. 10 CFR Part 100, "Reactor Site Criteria"
4. 10 CFR part 52, "Early Site Permits; Standard Design Certification; and Combined Licenses for Nuclear Power Plants"

The following General Design Criteria (GDC) from Appendix A to 10 CFR 50 are relevant to Section 15 of SRP:

1. GDC 4 as it relates to the requirement that structures, systems, and components (SSC) important to safety be designed to accommodate the effects of and be compatible with the environmental conditions associated with normal operation, maintenance, testing, and postulated accident conditions, including such effects as pipe whip and jet impingement.
2. GDC 10, as it relates to the reactor coolant system (RCS) being designed with appropriate margin to ensure that specified acceptable fuel design limits (SAFDL) are not exceeded during normal operations including anticipated operational occurrences (AOO).
3. GDC 13, as it relates to instrumentation and controls provided to monitor variables over anticipated ranges for normal operation, for AOOs, and for accident conditions.

4. GDC 15, as it relates to the RCS and its associated auxiliaries being designed with appropriate margin to ensure that the pressure boundary will not be breached during normal operations, including AOOs.
5. GDC 17, as it relates to the requirement that an onsite and offsite electric power system be provided to permit the functioning of SSCs important to safety.
6. GDC 20, as it relates to the reactor protection system (RPS) being designed to initiate automatically the operation of appropriate systems, including the reactivity control systems, to ensure that the plant does not exceed SAFDLs during any condition of normal operation, including AOOs.
7. GDC 25, as it relates to the requirement that the RPS be designed to ensure that SAFDLs are not exceeded for any single malfunction of the reactivity control system, such as accidental withdrawal of control rods.
8. GDC 26, as it relates to the reliable control of reactivity changes to ensure that SAFDLs are not exceeded even during AOOs.
9. GDC 27 and 28, as they relate to the reactivity control system being designed with appropriate margin to ensure that SAFDLs are not exceeded and that the capability to cool the core is maintained.
10. GDC 29, as it relates to the design of the protection and reactivity control systems and their performance (i.e., to accomplish their intended safety functions) during AOOs.
11. GDC 34, as it relates to the capability to transfer heat and other residual heat from the reactor so that fuel and pressure boundary design limits are not exceeded.
12. GDC 35, as it relates to the RCS and associated auxiliaries being designed to provide abundant emergency core cooling.
13. GDC 55, as it relates to the isolation requirements of small-diameter lines connected to the primary system.

SRP 15.0, "Introduction – Transient and Accident Analyses." defines anticipated operational occurrences (AOOs) and postulated accidents (PAs) as the following:

AOOs, as defined in Appendix A to 10 CFR Part 50, are those conditions of normal operation that are expected to occur one or more times during the life of the nuclear power unit.

PAs are unanticipated occurrences (i.e., they are postulated but are not expected to occur during the life of the nuclear power plant).

The acceptance criteria for the safety analyses of the AOOs and PAs for compliance with the above relevant regulations and GDCs are specified in SRP Section 15.0 as described below.

The following are the acceptance criteria specified in SRP 15.0 necessary to meet the requirements GDCs for AOOs:

- i. Pressure in the reactor coolant (P_{RCS}) and main steam (P_{MS}) systems should be maintained below 110 percent of the design values in accordance with the American Society of Mechanical Engineers (ASME) Boiler and Pressure Vessel Code.
- ii. Fuel cladding integrity is maintained by ensuring that the minimum departure from nucleate boiling ratio (DNBR) remains above the 95/95 DNBR limit.
- iii. An AOO should not generate a postulated accident without other faults occurring independently or result in a consequential loss of function of the RCS or reactor containment barriers.

GDC 10 within Appendix A to 10 CFR 50 establishes that SAFDLs should not be exceeded during any condition of normal operation, including the effects of AOOs.

The following are the acceptance criteria specified in SRP 15.0 necessary to meet the requirements of the GDCs for PAs:

- i. Pressure in the reactor coolant and main steam systems should be maintained below acceptable design limits.
- ii. Fuel cladding integrity will be maintained if the minimum DNBR remains above the 95/95 DNBR limit for PWRs. If the minimum DNBR does not meet this limit, then the fuel is assumed to have failed.
- iii. The release of radioactive material shall not result in offsite doses in excess of the guidelines of 10 CFR Part 100.
- iv. The postulated accident shall not, by itself, cause a consequential loss of required functions of systems needed to cope with the fault, including those of the RCS and the reactor containment system.

For the Reactivity Initiated Accidents (RIAs), SRP 4.2 Appendix B provides the following additional fuel cladding failure acceptance criteria:

The high cladding temperature failure criteria for zero power conditions is a peak radial average fuel enthalpy greater than 170 cal/gm (306 Btu/lbm) for fuel rods with an internal rod pressure at or below system pressure and 150 cal/gm (270 Btu/lbm) for fuel rods with an internal rod pressure exceeding system pressure. For intermediate (greater than 5 percent rated thermal power) and full power conditions, fuel cladding failure is presumed if local heat flux exceeds thermal design limits (e.g. DNBR).

The pellet cladding mechanical interaction (PCMI) failure criteria is a change in radial average fuel enthalpy greater than the corrosion-dependent limit shown in Figure B-1 of SRP 4.2 Appendix B.

Appendix B of SRP 4.2 also specifies the following additional acceptance criteria regarding core coolability

1. Peak radial average fuel enthalpy must remain below 230 cal/gm (414 Btu/lbm).
2. Peak fuel temperature must remain below incipient fuel melting conditions.

3. Mechanical energy generated as a result of (1) non-molten fuel-to-coolant interaction and (2) fuel rod burst must be addressed with respect to pressure boundary, reactor internals, and fuel assembly structural integrity.
4. No loss of coolable geometry due to (1) fuel pellet and cladding fragmentation and dispersal and (2) fuel rod ballooning.

4.0 SUMMARY OF MUAP-07010-P

In Section 1.0 of the subject topical report the applicant provided a high-level overview of the codes and methods used for US-APWR Non-LOCA safety analysis, the pedigree of each code, and an outline for the rest of the report.

Section 2.0 of the topical report provided specific details regarding the methods embedded in each of the computer codes employed for US-APWR Non-LOCA evaluations. It contains descriptions of modifications that MHI made to Westinghouse Electric Corporation (WEC) codes MARVEL and TWINKLE. All changes have been made under MHI's formal Quality Assurance Program (QAP), documented in [Reference 16].

For Non-LOCA safety analysis, MHI uses MARVEL-M [Reference 6] to calculate the plant system response to transient conditions, TWINKLE-M [Reference 11] to evaluate spatial neutron kinetics for those transients when necessary, and VIPRE-01M [Reference 12] to calculate detailed core subchannel thermal-hydraulics and fuel temperature transients. Both MARVEL-M and TWINKLE-M are applicant modified versions of WEC codes MARVEL and TWINKLE. MARVEL-M is based on an early version of MARVEL which has not received NRC approval (see RAI 2.1-21 [Ref. 20], response for details). TWINKLE-M is based on the NRC approved version of TWINKLE [Reference 14]. Section 2.1.3, "Theoretical Models of MARVEL-M Improvement" of MUAP-07010 describes improvements to the MARVEL-M theoretical model. The MARVEL-M code is the same as the original MARVEL code from the perspective of the constitutive and principal models. The main differences between the original MARVEL code and MARVEL-M are the extension from two-loop simulation to four-loop simulation and the addition of a built-in RCP model. The other refinements include a pressurizer surge line node, a hot spot heat flux simulation model, and improved numerical solution and conversion techniques.

VIPRE-01M is the MHI-specific version of the VIPRE-01 [Reference 15] subchannel thermal-hydraulics code developed by Battelle Pacific Northwest Laboratory under Electric Power Research Institute (EPRI) sponsorship. VIPRE-01 has been approved for use in the United States for pressurized water reactor licensing analysis.

The staff notes that the advanced nodal code (ANC) core simulation code [Reference 17] is not specifically identified in topical report Section 2.0 as a code used for the Non-LOCA analyses. However, Sections 3, 5, and 6 of the topical report describe use of the ANC code and results in the Non-LOCA methodology as a basis for models, the validation and assessment of models, and the checking and generating of core reactivities and power distributions.

Section 3.0 of the topical report provided the code validation evaluation performed by MHI for MARVEL-M and TWINKLE-M.

To validate the adequacy of the modifications included in the MARVEL-M code, MHI performed analyses of four events (Uncontrolled rod cluster control assembly (RCCA) Bank Withdrawal at Power, Complete Loss of Forced Reactor Coolant Flow, Partial Loss of Forced Reactor Coolant Flow, and Reactor Coolant Pump Shaft Seizure) using the MARVEL-M code and the four-loop LOFTRAN [Reference 18], and compared the calculated results.

The solution methods and constitutive models of the TWINKLE-M code have not changed from the original version, but the maximum number of spatial mesh points was expanded from 2,000 points to a variable number input by the user.

The three-dimensional calculation using the TWINKLE-M code was verified by comparing the power distribution with that from the core simulator ANC code [Reference 17]. For three-dimensional transient analyses, it is desirable to use as coarse a mesh as possible while maintaining sufficient accuracy. A second objective of the validation was to compare the results of a two-by-two coarse mesh simulation for the rod ejection accident to a four-by-four fine mesh simulation for the same accident with the same cross-section data using TWINKLE-M for both. Cases with and without an ejected rod under steady-state conditions were analyzed. Sensitivity studies were also performed to compare the TWINKLE-M results for different mesh size assumptions.

Section 4.0 of the topical report provided information on event classifications and acceptance criteria for SRP Chapter 15 Non-LOCA events. The US-APWR analyses for Non-LOCA events are grouped into six categories. The topical report lists the events within each category, their classifications, the computer codes employed in the analysis and the event-specific acceptance criteria. The staff reviewed the acceptance criteria for the design basis events specified in Tables 4.2-1, "Events in Increase in Heat Removal from the Primary System," 4.3-1, "Events in Decrease in Heat Removal by the Secondary System," 4.4-1, "Events in Decrease in Reactor Coolant System Flow Rate," 4.5-1, "Events in Reactivity and Power Distribution Anomalies," 4.6-1, "Events in Increase in Reactor Coolant Inventory," and 4.7-1, "Events in Decrease in Reactor Coolant Inventory," and found them consistent with the regulatory acceptance criteria.

Section 5.0 of the topical report provided a description of the event-specific methodology. Depending on the nature and computational capabilities needed for adequate simulation of specific transients and accidents, the methodology employs a single computer code, or a combination of computer codes, such that the analyses fall into one of the following three categories:

- Analyzed using MARVEL-M only.
- Analyzed using MARVEL-M and VIPRE-01M in sequence.
- Analyzed using TWINKLE-M and VIPRE-01M in sequence.

The first category that uses MARVEL-M alone includes most of the Non-LOCA transients that challenge the design limits for the RCS and main steam system pressure limits, as well as loop-symmetric accidents at full-flow conditions that fall within the capabilities of the simplified MARVEL-M DNBR model. These accidents do not require detailed calculation of localized fuel parameters and do not require spatially dependent transient calculations for accident-specific power levels or power distributions.

The second category that uses MARVEL-M in combination with the VIPRE-01M subchannel thermal-hydraulic code is used for accidents that challenge the DNB design limits under reduced flow conditions such as the partial loss of flow, complete loss of flow, locked RCP rotor, or RCP sheared shaft conditions. The loop-dependent and core total flow, core inlet conditions, pressure, and power are calculated using the MARVEL-M program, and then the VIPRE-01M code is used to determine the hot channel or hot spot fuel response including DNBR, fuel temperatures, and cladding temperature.

The third category that uses TWINKLE-M in combination with the VIPRE-01M code is reserved for rapid reactivity transients requiring space- and time-dependent nuclear power and power distribution calculations for input to a detailed fuel response calculation. The evaluation of the Spectrum of RCCA Ejection event was provided as an example, including the 3-D TWINKLE-M capabilities as needed.

Section 6.0 of the topical report provided the sample transient analysis results for six events:

- Uncontrolled RCCA Bank Withdrawal at Power.
- Complete Loss of Forced Reactor Coolant Flow.
- Spectrum of RCCA Ejection.
- Steam System Piping Failure.
- Feedwater System Pipe Break.
- SGTR.

Section 7.0 of the topical report provided the applicant's conclusion that the existing codes and methodologies are appropriate for US-APWR analyses.

5.0 TECHNICAL EVALUATION

5.1 Code Descriptions and Validations

Section 2 of MUAP-07010-P(R4), "Non-LOCA Methodology" [Reference 53] describes MARVEL-M, TWINKLE-M and VIPRE-01M; and Section 3 provides MARVEL-M and TWINKLE-M code validation. The staff review of Section 2 (computer code description) and Section 3 (code validation) of that report is presented here.

5.1.1 MARVEL-M Code

In Section 2.1 of the Non-LOCA methodology topical report, the applicant discussed the history of MARVEL-M development, an overview of the MARVEL-M code, and the mathematical model improvements in the MARVEL-M code. In support of the Non-LOCA methodology topical report, the applicant also submitted MARVEL-M code manual report GEN0-LP-480, "MARVEL-M, A Digital Computer Code for Transient Analysis of a Multi-Loop PWR System," (References 5 and 6), which provides detailed descriptions of various models in MARVEL-M.

The MARVEL-M code simulates the reactor core, reactor vessel, reactor coolant loops, SGs, control and protection systems, and safety injection systems of two-, three-, and four-loop PWRs. Topical report Section 2.1.2, "General Description – Overview," gives an overview of various models in MARVEL-M. The details of these models are described in the MARVEL-M manual GEN0-LP-480. Therefore, the staff evaluation of MARVEL-M is based on the detailed description in the MARVEL-M manual.

The MARVEL-M code was developed by modifying the original two-loop MARVEL code [Reference 13] to expand its capability for four-loop simulation. Topical report Section 2.1.3, "Theoretical Models of MARVEL-M Improvement," describes the mathematical model improvements in the MARVEL-M code. The improvements include the expansion to the four-loop reactor coolant system model; four-loop flow mixing model in the reactor vessel; reactor coolant pump and flow transient mode; secondary steam system model; and other model refinements in the pressurizer surge line model, hot-spot fuel kinetics model, core void simulation, feedline break blowdown simulation, and conversion of RCS volume balance by pressure search.

It was noted that the applicant did not base the development of MARVEL-M on the approved version of MARVEL, but rather on an earlier version. RAI 2.1-21 therefore asked the applicant to detail the difference between MARVEL-M and the approved version of MARVEL. In its response to RAI 2.1-21 [Ref. 20], the applicant confirmed that the development of MARVEL-M was based on a version which preceded the approved version of MARVEL and that it was developed independently of Westinghouse. The applicant identified the additional features in the approved version of MARVEL from the base MARVEL version which MHI used to develop MARVEL-M. The applicant first incorporated equivalent models for these additional features into the base version of MARVEL, and verified them by comparison of MARVEL-M to the LOFTRAN [Ref. 18] simulations. The applicant then incorporated its own specific modifications and improvements into the final version of MARVEL-M. This response clearly describes the lineage of MARVEL-M and helped focus the staff's review. However, because of extensive changes from the MARVEL code, the staff conducted a detailed review of the MARVEL-M code described in GEN0-LP-480 and the methods used for verification of the modified code. The detailed staff review of MARVEL-M is described in Appendix A of this report.

This section summarizes the staff's evaluation of major model improvements and refinements described in Section 2.1.3 of the topical report.

Four-Loop Reactor Coolant System Model:

One major MARVEL-M improvement over MARVEL, described in Section 2.1.3.1 of the topical report, is the ability to simulate up to four reactor coolant loops. Although the hydraulic and thermal models of the individual reactor coolant flow sections and the model of the SGs and pressurizer are the same as the original MARVEL two-loop models, the MARVEL-M RCS flow nodalization has been expanded to up to four reactor coolant loops that can be simulated by the code, and the algorithms for core mixing in the reactor vessel and the steam lines, respectively, have changed to accommodate the expansion of the number of coolant loops.

The original MARVEL code used six different flow modules to describe the thermal behavior of the RV and coolant loops: a HEAT model for the core heated section; a MIXG module for mixing plenums including the RV outlet plenum, SG inlet and outlet headers, RV inlet plenum, and reactor core bypass; a MIXD module to evaluate the thermal-hydraulic behavior in the reactor vessel upper head dead volume; a MIXS module for the upper plenum region; a SLUG module to model the reactor coolant system pipes where the fluid flow is such that exit fluid properties are not affected by inlet fluid properties; and a HEEX module for the primary side SG tubes. MARVEL-M maintains the same flow modules. Section 1.3 of GEN0-LP-480 provides detailed descriptions of these flow modules. The staff's review of these flow modules is described in Section A.3 of Appendix A of this report. Figure 2.1-3, "Reactor Coolant System Flow Model," of the topical report shows the MARVEL-M nodal representation of the four-loop reactor coolant system. This flow model is the same as the MARVEL model except that the RCS flow loop is increased to four loops, the downcomer and lower plenum include four MIXG flow channels each, and the reactor core is expanded to four HEAT flow channels.

In RAI 2.1-3, the staff requested the applicant provide a MARVEL/MARVEL-M code comparison for a typical two-loop configuration calculation. In its response to RAI 2.1-3 [Ref. 19], the applicant provided detailed comparisons between the MARVEL and MARVEL-M simulations of the "Loss of Load" (a uniform event) and the "Feedwater Pipe Break" (a non-uniform event). The MARVEL-M calculations modeled all four loops separately, while MARVEL modeled one loop separately and the other three loops lumped together. The results for the two code simulations were essentially identical. These comparisons demonstrate that the MARVEL and MARVEL-M predictions are very similar and therefore provide reasonable assurance that the four-loop modeling is correctly implemented in MARVEL-M.

Flow Mixing in Reactor Vessel (Four-Loop Model):

The MARVEL-M algorithm for flow mixing in the RV was changed from the original MARVEL model as described in topical report Section 2.1.3.2. The changes to the flow mixing algorithm were made to accommodate the expansion of the modeling capability from two to four loops. There is no fundamental change in the mixing phenomenology, and the basic assumptions are the same as in the two-loop MARVEL version. The reactor coolant fluid circulating in the reactor coolant loops is introduced into the reactor vessel through the inlet nozzles (cold legs). Thus the mixing in the RV inlet and outlet plenum is imperfect. In order to take this into consideration in the analysis of the RV thermal kinetics behavior, an azimuthal as well as an axial analysis is necessary. The azimuthal effect is considered by using a maximum of four separate flow channels for each loop simulated.

The thermal and hydraulic behaviors are simulated by simple mixing models using representative or conservative user inputs of the mixing factors for the mixing in the reactor vessel downcomer/lower plenum and upper plenum, respectively. The input mixing factors can be derived from the 1/7 scale mixing tests as described in Topical Report MUAP-07022-P, "US-APWR Reactor Vessel Lower plenum 1/7 Scale Model Flow Test Report," [Ref. 23]. As discussed in Appendix A, Section A.4 of this report, the staff evaluated and found the flow mixing algorithm acceptable.

Secondary Steam Generator Model (Four-Loop Model):

Topical report Section 2.1.3.4 describes the improvements of the MARVEL-M SG and secondary system model for expansion to four-loop capability. Figure 2.1-6, "Steam Line Model," shows the main steam lines from each SG are connected together at a common steam header, each via an isolation valve and a check valve. If the operating conditions of the SGs are different from each other, the steam outputs from the SGs are unbalanced. The steam flow distribution is then dependent upon the steam pressure of each SG and upon the pressure losses through the steam lines. A detailed description of the secondary steam generator model is provided in Section 1.8 of GEN0-LP-480. As described in Section A.8 of Appendix A of this report, the staff's evaluation of the secondary SG model and the method of evaluating the steam flow distribution found it acceptable.

Reactor Coolant Pump and Flow Transient Model:

The original MARVEL code used a simplified empirical flow coastdown model and a transition from this flow model to natural circulation. MARVEL-M uses an explicit RCP model. Topical report Section 2.1.3.3 describes the RCP and flow transient models. The fundamental flow transient equations are based on a momentum balance around each reactor coolant loop and across the RV, flow continuity, and RCP characteristics with or without electrical power supply. The RCP head is derived from the homologous curve of the RCP, which depends on the pump speed. When the electric power supply to an RCP is lost, the pump motor torque is lost and flow coastdown results. The pump head decreases according to the decrease in pump speed and is eventually lost, which results in natural circulation. MARVEL-M includes the RCP hydraulic kinetic model, flow coastdown model, and natural circulation elevation head model. The detailed description of the transient RCS flow performance is provided in Section 1.7 of GEN0-LP-480. As described in Section A.7 of Appendix A of this report, the staff found the RCP and RCS flow transient model acceptable.

Pressurizer Surge Line Model:

As shown in Figure 2.1-3, "Reactor Coolant System Flow Model," in Section 2.1.3.1 of the topical report, MARVEL-M adds a flow section in the pressurizer surge line between the hot leg connection and the pressurizer. The addition of the surge line section in the RCS flow model is a MARVEL-M refinement to more realistically model pressurizer insurge enthalpy. If the surge line is not simulated, hot leg coolant water directly enters the pressurizer during insurge, which may result in over-predicting cooling of the pressurizer liquid phase and may cause a larger pressurizer pressure reduction for a subsequent outsurge. This refinement resulted from the observation of a transient test during a reactor plant preoperational test. The staff agrees that explicitly modeling the pressurizer surge line rather than lumping it with the pressurizer will result in more accurately representing the hydraulic behavior occurring during pressurizer insurge and out-surge. Therefore, the staff finds this MARVEL-M modeling refinement acceptable.

The MARVEL-M core and RCS thermal-hydraulic model does not simulate the pressure gradient in the system except for the pressurizer and the RCS at the hot-leg pressurizer surge line connection. The reactor coolant flow is treated as a homogeneous equilibrium mixture. The staff questioned what model MARVEL-M uses for two-phase flow and how the user deals with conditions in which homogeneous two-phase flow is not applicable. In its response to RAI 2.1-4 [Ref. 19], the applicant noted that, for the majority of Non-LOCA events, voids exist only in the pressurizer and RV upper head region, and that boiling beyond homogeneous two-phase flow does not occur for Non-LOCA conditions. Furthermore, MARVEL-M provides a message to the analyst if boiling occurs, warning the analyst to review the results to evaluate the significance of the voiding on the calculated results. This is acceptable because MARVEL-M will not be applied to events exhibiting non-homogeneous flow.

Hot-Spot Fuel Thermal Kinetics Model:

The hot-spot fuel thermal kinetics model in the original MARVEL code was similar to the fuel thermal kinetics model for the average channel. MARVEL-M includes a more detailed fuel thermal kinetics model adopted from the Westinghouse FACTRAN code [Ref. 51], which had been approved by the NRC. The FACTRAN code has the ability to model up to 10 radial sections in the fuel pellet, cladding and clad surface to compute the transient fuel temperature and heat flux. The MARVEL-M hot spot fuel model is for the computation of the heat flux transients at the surface of the cladding at the hot spot. The normalized hot-spot heat flux can be used as an option (the largest heat flux between the average channel and hot spot is used) to calculate DNBR using the simplified DNBR model in MARVEL-M. The fuel pellet thermal properties can be input by the user. This model is described in Section 1.2.3 of GEN0-LP-480. As described in Section A.2.3 of Appendix A of this report, the staff's evaluation finds this model acceptable.

Core Void Simulation:

MARVEL-M has a model to calculate the boiling of coolant or void fraction in the core when the core power increases enough to cause voiding or if the core coolant temperature exceeds the saturation temperature. However, this core thermal-hydraulic model is not sufficiently detailed to compute the void formation at accidents such as rod ejection that could cause locally high void fraction in a high power region in the core. Rapid excessive void formation in the core results in an in-surge to the pressurizer and a pressure increase. To adequately predict the pressure increase, the MARVEL-M model includes a feature scheme to accept void transients calculated by an external, detailed thermal-hydraulic code, such as VIPRE-01M [Ref. 12], which can compute void formation taking into account subcooled boiling, detached boiling, and bulk boiling. This feature is only used to assure that the RCS pressure is conservatively high for the rod ejection accident where local voids in the core could impact the peak pressure.

As stated in Section A.15 of Appendix A of this report, the safety analysis of the rod ejection event uses the VIPRE-01M code to calculate the void transient data input to MARVEL-M for the purpose of calculating the peak RCS pressure. The staff finds this core void simulation feature acceptable as VIPRE-01M has the detailed thermal-hydraulic modes to determine the core void fraction (See the RAI 4.1-3 response and staff review described in Section A.15 of this SE).

Feedline Break Blowdown Simulation:

During a feedwater line break with water release, when the SG is rapidly depressurized below the feedwater saturation pressure, feedwater contained in the feedline flashes and a mixture of steam and water can be released into the SG shell side.

MARVEL-M includes a feedline blowdown simulation model to simulate this phenomenon. Each feedwater line is assumed to contain fluid with the enthalpy of the feedwater when the feedwater line isolation valves are closed. After the individual SG pressure falls below the saturation pressure of the feedwater enthalpy, water is assumed to push into the SG by void formation. This feedwater flashing model is described in Section 1.5.5 of GEN0-LP-480. The applicant states that this feedwater flashing model is only used in the DCD Chapter 6, "Engineered Safety Features," mass and energy release analysis. As described in Section A.5.5 of Appendix A of this report, the staff did not perform an evaluation since this model is not used for Chapter 15, "Transient and Accident Analyses," analysis.

Conversion of RCS Volume Balance by Pressure Search:

[(Proprietary information withheld under 10 CFR 2.390)

] This method is also described in Section 4.0(1) of GEN0-LP-480. The staff's evaluation, described in Section A.15 of Appendix A of this report, finds this method acceptable.

Realistic Models

MARVEL-M contains "Realistic Models" as options for simulation of real plant transient behavior, as discussed in Section 2.1.4 of the topical report. The applicant stated that these models are code options and are not used for licensing evaluations of reactor plants. Therefore, the staff does not evaluate the realistic models.

Limitations for MARVEL-M Application

MUAP-07010, Section 2.1.5.1 summarizes the limitations of range of operating variables for the application of MARVEL-M in terms of the RCS temperature and pressure, pressurizer water level, SG steam pressure and water inventory, reactor coolant loop flow, and reactor core kinetics. These limitations are consistent with the approved version of MARVEL. Topical report Section 2.1.5.2 discusses the applicability of MARVEL-M to the scenarios of licensing analysis. Since MARVEL-M uses space independent point neutron kinetics, the reactivity initiated events, such as an inadvertent RCCA withdrawal from subcritical condition, should be analyzed with other codes such as TWINKLE-M which is a 1 or 3 dimensional model to capture spacial effects.

Since MARVEL-M uses a simplified DNBR calculation, those transients, such as a loss of flow for which the minimum DNBR is heavily dependent on changes in reactor coolant flow, should utilize other subchannel codes such as VIPRE-01M for the DNBR calculation. Also since MARVEL-M assumes homogeneous equilibrium two-phase flow for the RCS flow, it should not be used for LOCA analysis.

In addition, as described in Section A.6.3 of Appendix A of this report, since MARVEL-M has not been qualified for simulating the discharge of liquid through the pressurizer safety and relief valves, the usage of MARVEL-M is restricted to events which only discharge steam through the pressurizer safety and relief valves.

Topical report Section 4 describes the computer codes used for each of the Chapter 15 Non-LOCA design basis events. The original MARVEL was approved for use to analyze only four events: (1) steam line rupture, (2) feedwater line rupture, (3) startup of an inactive reactor coolant loop, and (4) excessive heat removal due to a feedwater system malfunction. MARVEL-M is used to analyze many more events than these four events. In its response to RAI 2.1-23 [Ref. 20], regarding the acceptability of MARVEL-M for the Non-LOCA events not listed above the applicant noted that while the MARVEL code was not approved for analyzing other Non-LOCA events, it still produced acceptable results for those events. The applicant noted that the disturbances caused by many Non-LOCA events were milder than those events for which MARVEL was approved. In its responses to RAI 2.1-17, and RAIs 3.1-2 through 3.1-5 [Ref. 19], the applicant also noted that LOFTRAN has been approved by the NRC for Non-LOCA event analyses and that the comparisons of the MARVEL-M results to LOFTRAN results were good as shown in Sections 3.1.1 through 3.1.4 of the topical report. MARVEL-M results have also been favorably compared to results from the original two-loop MARVEL (response to RAI 2.1-3 [Ref. 19]), and to the measured data from a four-loop plant for a partial loss of forced reactor coolant flow and a complete loss of forced reactor coolant flow (response to RAI 2.1-16 [Ref. 21]). These comparisons demonstrated that MARVEL-M was acceptable for DCD Tier 2 Chapter 15 Non-LOCA analyses. Based on its review of the RAI responses (i.e., MARVEL-M compares well with LOFTRAN and plant data), and the MARVEL-M validation as described in Section 5.1.2 of this report, the staff agrees with the applicant's conclusion that MARVEL-M is acceptable for use in Non-LOCA events.

5.1.2 MARVEL-M Code Validation

Section 3.1 of the topical report discusses the validation of the MARVEL-M code. The validation of MARVEL-M for US-APWR Non-LOCA analysis consisted of comparing calculated results to those of the four-loop LOFTRAN code (Ref. 18). The applicant stated that a code-to-code comparison is sufficient for validation because LOFTRAN had been used extensively in the licensing analysis of currently operating nuclear plants in the United States for the events that are analyzed with MARVEL-M. The applicant presented code comparisons for four events: uncontrolled RCCA bank withdrawal at power, partial loss of forced reactor coolant flow, complete loss of forced reactor coolant flow, and reactor coolant pump shaft seizure. Based on the information provided by the applicant, the staff agrees that MARVEL-M and LOFTRAN are in agreement but the Staff issued follow-on RAIs regarding the uncontrolled RCCA bank withdrawal event.

Topical report Section 3.1.1 describes the comparison between the MARVEL-M and LOFTRAN analysis results of the uncontrolled RCCA bank withdrawal at power event. The staff requested the applicant to provide documentation of MARVEL-M/LOFTRAN code comparisons that may not be in agreement, along with any explanations for the deviations. In its response to RAI

3.1-2 [Ref. 19], the applicant presented the results of an Uncontrolled RCCA Bank Withdrawal at Power event with an active pressure control system. For this case there were small differences in the responses for reactor power, core heat flux, average RCS temperature and pressurizer pressure between the MARVEL-M and LOFTRAN results. The applicant explained that the differences could be attributed to the following differences between the spray models in LOFTRAN and MARVEL-M:

MARVEL-M

- Saturated steam is assumed in the pressurizer.
- If cold water is sprayed, the saturated steam quickly condenses.

LOFTRAN

- Superheated steam is assumed in the pressurizer.
- If cold water is sprayed, the spray first removes the superheat maintaining pressurizer pressure (the steam phase does not condense but shrinks).
- After sufficient water has been sprayed the pressurizer reaches a saturated condition and condensation of the saturated steam begins.

Follow-up RAI 3.1-2-1 asked if the Uncontrolled RCCA Bank Withdrawal at Power event with an active pressure control system exhibited the largest differences between LOFTRAN and MARVEL-M. In its response [Ref. 22], the applicant noted that only cases which resulted in significant differences between the results of MARVEL-M and LOFTRAN were investigated further to determine reasons for the differences. Staff's review of the uncontrolled RCCA bank withdrawal at power, partial loss of forced reactor coolant flow, complete loss of forced reactor coolant flow, and reactor coolant pump shaft seizure transient cases found that the uncontrolled RCCA bank withdrawal case showed the largest differences in core power, average RCS temperature and pressure. The differences in these predicted plant parameters were very small and within typical code uncertainties.

The responses to RAI 3.1-2 and RAI 3.1-2-1 are acceptable because they demonstrate that the MARVEL-M simulations of US-APWR DCD Tier 2 Chapter 15 events compare well with LOFTRAN, which is NRC-approved for simulating such events. The applicant has adequately explained the source of differences in the two code simulations for the RCCA bank withdrawal event. However, the staff does not agree that good agreement between LOFTRAN and MARVEL-M is, by itself, a sufficient basis for approving MARVEL-M.

Topical report Sections 3.1.2, 3.1.3 and 3.1.4, respectively, provide comparisons between the MARVEL-M and LOFTRAN analysis results of a partial loss of forced RCS flow, complete loss of forced RCS flow, and RCP shaft seizure. The results show that the reactor powers, core heat fluxes, loop flow rates, and pressurizer pressures calculated by the two codes are in close agreement. The staff requested the applicant to provide the DNBR versus time predicted by both MARVEL-M and LOFTRAN for the three events analyzed for code validation. In its responses to RAIs 3.1-3, 3.1-4 and 3.1-5 [Ref. 19], the applicant explained that DNBR is calculated by the VIPRE-01M code [Ref. 12] for these events using power and flow calculated by either MARVEL-M or LOFTRAN. Figure 3.1-3.1, "Partial Loss of Forced Reactor Coolant Flow Comparison between MARVEL-M and LOFTRAN," Figure 3.1-4.1, "Complete Loss of Forced Reactor Coolant Flow Comparison between MARVEL-M and LOFTRAN," and Figure 3.1-5.1, "Reactor Coolant Pump Shaft Seizure Comparison between MARVEL-M and LOFTRAN" were provided to demonstrate that the VIPRE-01M calculated DNBRs were nearly identical whether MARVEL-M or LOFTRAN boundary conditions were used. This is acceptable

because the resultant DNBRs were nearly the same for each of the systems codes used to provide boundary conditions to VIPRE-01M.

The applicant used comparisons to LOFTRAN as one of the means to validate MARVEL-M. Such comparisons are only meaningful if the algorithms, numerical methods and correlations in the two codes are different, or developed independently. The staff asked if MARVEL-M shares any significant algorithms, numerical methods, or correlations with the version of LOFTRAN used for the comparison. In its response to RAI 3.1-8 [Ref. 22], the applicant stated that MARVEL-M and LOFTRAN are completely different codes with respect to the FORTRAN programming and that the two codes were developed independently by different individuals. While there are many features of MARVEL-M and LOFTRAN that were developed independently, a comparison of the documentation for MARVEL-M and for LOFTRAN shows that the underlying numerical algorithms of the two codes are very similar. Therefore comparison of MARVEL-M to LOFTRAN was not considered by the staff as a complete validation of MARVEL-M. However, the two codes show good agreement and LOFTRAN has been validated [Ref. 24] against experimental data.

The topical report does not provide an SGTR analysis for the MARVEL-M validation. RAI 3.1-6 requested the applicant to present MARVEL-M validation data for the SGTR event. [

(Proprietary information withheld under 10 CFR 2.390)

] The response to RAI 3.1-6 is acceptable because it demonstrates the ability of MARVEL-M to calculate the phenomena associated with an SGTR event. However, the staff's acceptance of MARVEL-M for analyzing the SGTR event is predominately based on the independent comparisons of MARVEL-M and the staff's RELAP5/MOD3.3 SGTR simulations described in Section 5.3.1 of this report and in the Technical Report ISL-NSAO-TR-10-01, "US-APWR NON-LOCA RELAP5/MOD3.3 Confirmatory Runs," [Ref. 25].

In summary, the staff evaluated the MARVEL-M code validation provided in Section 3.1 of the topical report. The applicant responses satisfactorily resolved all of the staff's concerns addressed in the RAIs. The combination of the applicant's MARVEL-M/LOFTRAN comparisons, comparison to plant data and the staff's independent RELAP5/MARVEL-M comparisons provide reasonable assurance that MARVEL-M is acceptable for analyzing the US-APWR Non-LOCA transients.

5.1.3 TWINKLE-M

The applicant described TWINKLE-M in Section 2.2 and the validation of TWINKLE-M in Section 3.2 of the topical report.

TWINKLE-M [Ref. 11], the applicant's version of TWINKLE [Ref. 14], is a multi-dimensional spatial neutron kinetics code which solves two-group transient diffusion equations using a finite-difference technique. The code is used to predict the kinetic behavior of a reactor for those transients that cause a major perturbation in spatial neutron flux, specifically rod ejection accidents and uncontrolled control rod assembly withdrawal from subcritical.

The fundamental basis for the TWINKLE-M reactor kinetics code was the TWINKLE code developed by the Westinghouse Electric Corporation and approved for use to calculate the neutronics aspect of reactivity transients by the Atomic Energy Commission in 1975 [Ref. 14]. TWINKLE was a multi-dimensional neutron kinetics analysis code. TWINKLE-M employed a time-dependent hot channel factor based on the three-dimensional kinetics model in the TWINKLE code for the analysis of RCCA ejection from the hot zero power condition. The solution method and constitutive models of TWINKLE-M have not changed from the base TWINKLE code, but the maximum number of spatial mesh points is expanded from 2000 points to a variable number input by the user.

Since TWINKLE-M evolves from the NRC-approved TWINKLE code, the staff requested that the applicant list and describe all the differences between TWINKLE-M and TWINKLE; and elaborate further on the development history of TWINKLE-M. In its responses to RAIs 2.2-1 and 2.2-2 [Ref. 19 and 20] respectively, the applicant presented Figure 2.2-2.1, "Historical Development of the TWINKLE Code" showing the historical relationship of TWINKLE and TWINKLE-M and stating that the solution methods and constitutive models in the two codes were identical. However, TWINKLE-M has an expanded spatial mesh to support three-dimensional core calculations and uses a discontinuity factor to improve the representation of the local power distribution in three-dimensional calculations. All other differences were confined to the treatment of input and output.

The fuel effective temperature model used to calculate Doppler feedback is of particular importance because it limits the reactor power increase caused by a reactivity insertion. In RAI REA-3, the staff requested that the applicant verify that the effective fuel temperature model used in TWINKLE-M was identical to that used in the original TWINKLE code, and to justify its applicability in light of other effective fuel temperature models developed since TWINKLE was approved (for example, the model used in the OECD PWR REA Benchmark experiment documented in NEACRP-L-335 [Ref. 26]).

In its response to RAI REA-3 [Ref. 27], the applicant provided a description of the effective fuel temperature model used in TWINKLE-M, and compared it with the model specified in NEACRP-L-335 [Ref. 26]. Using VIPRE-01M calculated radial fuel temperature distributions, the applicant demonstrated that the difference between the effective fuel temperature using the TWINKLE-M model [(Proprietary information withheld under 10 CFR 2.390)]. The applicant also provided sensitivity calculations using both effective fuel temperature models for US-APWR rod ejection transients at Beginning of Cycle (BOC) Hot Full Power (HFP) conditions and End of Cycle (EOC) Hot Zero Power (HZP) conditions. This sensitivity analysis demonstrated that there is negligible difference in the calculated maximum fuel centerline temperature, fuel average temperature, and peak reactor power for each case. Finally, the applicant provided the results

of pin-level Monte Carlo calculations that indicated the use of the TWINKLE-M model for effective fuel temperature versus using a fine-node temperature distribution from VIPRE-01M resulted [(Proprietary information withheld under 10 CFR 2.390)] conditions. Based on these calculations, and noting the empirical nature of any effective fuel temperature calculation methodology, the applicant states that the model contained within TWINKLE-M is sufficient. This is reinforced by the conservative 20 percent reduction in Doppler feedback employed within the applicant's safety analysis methodology. The staff agrees that the effective fuel temperature model in TWINKLE-M is acceptable as the applicant has demonstrated that it is similar to TWINKLE and has negligible effect on Chapter 15 analysis results.

In light of the calculations presented by the applicant, the staff finds the methods employed by the applicant to calculate the effective fuel temperature for Doppler feedback to be acceptable, especially in concert with the conservative 20 percent reduction in Doppler feedback.

Another model embedded within TWINKLE-M the staff reviewed, based upon its ranking in the phenomena identification and ranking table (PIRT) [Ref. 28], was the fuel specific heat capacity. This particular material property received an importance ranking of "High" in an NRC-sponsored PIRT [Ref. 28] due to its importance in determining the transient fuel temperature during a rod ejection event, which impacts the calculated Doppler feedback and the magnitude of the power excursion. The TWINKLE topical report [Ref. 14] describes a simple linear model for fuel specific heat capacity that was developed in the early 1970's. More accurate models have been developed in subsequent years and published in the Material Properties database [Ref. 29]. No reference to this updated model was found in the applicant's responses to RAIs requesting that the applicant detail changes made from TWINKLE to TWINKLE-M; thus the staff issued RAI REA-13 requesting that the applicant justify continued use of the original TWINKLE model.

In its response to RAI REA-13 [Ref. 30], the applicant explained that in the process of updating the fuel property models in TWINKLE-M, the MATPRO model for fuel specific heat capacity was incorporated into the code. The original TWINKLE model was retained in TWINKLE-M, but for licensing analysis the MATPRO model is used. The applicant committed to updating the TWINKLE-M input manual to reflect clearly the source of the MATPRO model in TWINKLE-M and mandate its usage for licensing analysis. The updated MATPRO model is included in Revision 3 of the TWINKLE-M manual (Ref. 11), and is used for licensing analysis. This is acceptable because the MATPRO database is considered an industry standard for fuel specific data, including fuel specific heat.

RAI 3.2-1 asked why the introduction of discontinuity factors was not considered a change to the constitutive models. The applicant presented a figure, Figure 2.2-1.1, "Flowchart of the Discontinuity Factor Process," in its response to RAI 2.2-1 [Ref. 19], showing that the addition of the discontinuity factor can be viewed as a pre-processing and post-processing activity outside the solution algorithm of the TWINKLE-M code and therefore does not represent a change to the constitutive model. The applicant's response is acceptable because it does not change the fundamental diffusion equations used by TWINKLE-M to solve for the neutron flux.

Topical Report Section 3.2 provides the TWINKLE-M code validation of the three-dimensional capability by comparing core power distribution and other parameters with the ANC code [Ref. 17]. A sensitivity study of the radial mesh size is also provided Section 3.2.2. The applicant concluded that a 2x2 mesh per assembly was sufficient for use in accident analysis.

Section 3.2.1 presented a comparison between TWINKLE-M and ANC for cases with and without an ejected rod under steady-state conditions. The three comparison cases presented

are: (1) BOC HFP with all rods out, (2) EOC HZP with all rods at the zero power insertion limit, and (3) EOC HZP with all but one rod inserted. The first two cases are characterized by radial and axial power distributions in the normal operating condition. The third case represents a highly peaked radial power distribution characteristic of an RCCA ejection accident from HZP condition. All comparisons were done at steady state conditions because, although TWINKLE-M is a transient code, ANC is a steady state code. Topical report Figures 3.2.1-2, "Radial Power Distribution Comparison with ANC and TWINKLE-M Case 1, BOC HFP All RCCAs Out," 3.2.1-3, "Radial Power Distribution Comparison with ANC and TWINKLE-M Case 2, EOC HZP RCCA at Insertion Limit," and 3.2.1-4, "Radial Power Distribution Comparison with ANC and TWINKLE-M Case 3, EOC HZP One RCCA Ejected," respectively, show the radial power distribution comparison between the TWINKLE-M and ANC for the three cases analyzed. Topical report Figure 3.2.1.5, "Average Axial Power Distribution Comparison with ANC and TWINKLE-M," shows the TWINKLE-M/ANC comparison of the average axial power distributions for the three cases. The results show good agreement between the two codes.

In reviewing the analysis of the three cases for the TWINKLE-M validation, the staff also requested the applicant to address RAI 3.2-3 through RAI 3.2-6.

RAI 3.2-3 requested an explanation of the treatment of the core-reflector boundary condition. In its response [Ref. 19], the applicant stated that the diffusion coefficient of the reflector region was modified externally with region-specific multipliers so that the TWINKLE-M power distribution agreed with the ANC calculation, both before and after the rod ejection. RAI 3.2-3-1 requested that the applicant confirm that the modification was made to both the radial reflector region and the two axial reflector regions. In its response [Ref. 22], the applicant stated that the fast group diffusion coefficient was modified for all reflector regions. RAI 3.2-3-2 requested a detailed explanation of the modification process. In its response [Ref. 22], the applicant stated [

(Proprietary information withheld under 10 CFR 2.390)

]

RAIs 3.2-4 and 3.2-5 requested an elaboration of the differences between TWINKLE-M and ANC for the HZP all rods in (ARI) and the HFP all rods out (ARO) cases, respectively. In its response [Ref. 19], the applicant stated that the differences were predominantly due to different numerical solution algorithms used in the two codes. The applicant noted that the largest difference between the results with the two codes for the HZP ARI case occurred near the inserted rods, whereas, for the HFP ARO comparison, the largest differences occurred where fresh fuel was adjacent to high burnup fuel. These locations were characterized by steep flux gradients. The nodal expansion method used in ANC calculates steep flux gradients more accurately than the finite difference method used in TWINKLE-M. RAI 3.2-4-1 requested further information regarding burnup differences being responsible for code differences. In its response [Ref. 22], the applicant provided a radial map of assembly burnups for the HFP ARO case and demonstrated that the largest differences between TWINKLE-M and ANC were at locations where adjacent assemblies had much different burnups.

RAI 3.2-6 requested a comparison of the Doppler reactivity coefficient calculated by ANC and by TWINKLE-M for the rod ejection accident. For large ejected rod worths Doppler feedback inserts negative reactivity which limits the reactor power excursion. Therefore, the staff asked how ANC, which is a modern nodal code compares with TWINKLE-M. In its response [Ref. 19], the applicant showed the two calculated values to be identical.

RAI 3.2-2 requested the applicant provide additional verification of TWINKLE-M when used to predict rod ejection behavior. In its response [Ref. 21], the applicant provided a comparison of

radial power distributions of a typical three-loop operating plant to the TWINKLE-M calculations and stated that the good agreement between the two demonstrated the accuracy of the TWINKLE-M 3-D steady state calculation. As verification of the transient capability of TWINKLE-M, the applicant presented the results of a TWINKLE 3-D calculation of the OECD rod ejection benchmark problem. The agreement between TWINKLE-M and the reference solutions was good. Therefore, the staff finds this additional verification acceptable.

Based on the above evaluation, the staff concludes that the TWINKLE-M three-dimensional capability validation is successfully demonstrated by the TWINKLE-M/ANC comparison.

Topical report Section 3.2.2 presents the sensitivity study of the mesh size in the TWINKLE-M analysis of a rod ejection accident in order to determine the optimal spatial mesh size. The sensitivity study is performed for two cases: with an 2x2 meshes and an 4x4 meshes per fuel assembly, respectively, in the radial direction. [(Proprietary information withheld under 10 CFR 2.390)] Topical report Figures 3.2.2-1 and 3.2.2-2 show the comparisons of the nuclear power and hot channel factor, respectively, of the 2x2 and 4x4 mesh results. The results show good agreement between the two mesh configurations of the maximum nuclear power and maximum hot channel factor.

RAI 3.2-7 requested additional information regarding calculated ejected rod worth, fuel temperature, hot channel factors, and axial mesh sensitivity. RAI 3.2-10 also requested the sensitivity of the computed results to axial mesh size. In its response [Ref. 21], the applicant provided the requested information and demonstrated that the 2x2 mesh simulation was in good agreement with the 4x4 simulation. The applicant's response also showed that doubling the axial mesh size resulted in axial power profiles that were generally closer to the ANC calculation but not significantly so. RAI 3.2-7-1 questioned whether the 4x4 results were converged. In its response [Ref. 22], the applicant stated that one would expect a better agreement between the ANC and TWINKLE-M power distributions as mesh size was decreased in TWINKLE. The applicant noted, however, that the key output parameters for the rod ejection accident were not highly dependent on small differences in power distributions. Hence, using a smaller mesh size would not significantly alter the final result.

The time step sizes used in TWINKLE-M are provided in the response to RAI 3.2-7-2 [Ref. 22]. RAI 3.2-7-3 requested why the diffusion coefficient was not adjusted when the axial mesh size was changed. In its response [Ref. 22], the applicant stated that its goal was to show the effect of axial nodalization without any diffusion coefficient adjustment. Had such an adjustment been made, the power traces from the two axial nodalization cases would have been much closer. The responses are acceptable because they demonstrate that the TWINKLE-M model's mesh size is adequate and the results are converged.

RAI 3.2-8 and 3.2-9, respectively, requested why the neutron lifetime and the delayed neutron fraction were listed as a calculation condition in the mesh sensitivity study. In its response [Ref. 19], the applicant explained that inputs to both sensitivity cases were adjusted so that both cases had identical values of neutron lifetime and delayed neutron fraction. When the appropriate adjustments were made, these parameters did not affect the results of the sensitivity study of mesh size for the rod ejection simulations. RAI 3.2-8-1 and RAI 3.2-9-1 asked the applicant to clarify whether the adjustments to neutron lifetime and delayed neutron fraction were done only for the mesh sensitivity study. In its response [Ref. 22], the applicant stated that the adjustments were made as part of each TWINKLE-M analysis so that the parameters' values match the safety limit values. These responses demonstrate that the

parameters were adjusted to the appropriate safety limit values for each transient; and therefore, are acceptable.

The staff recognized that, while the applicant had provided numerous comparisons between TWINKLE-M and other reactor physics computer codes in the topical report and RAI responses, no comparisons had been presented between TWINKLE-M results and experimental data. Therefore, RAI REA-1 requested that the applicant perform such a comparison, or justify why lack of such a comparison is acceptable.

In its response to RAI REA-1 [Ref. 27], the applicant provided a comparison of SPERT III E-Core Test No. 60 (hot startup conditions), as documented in IDO-17281 [Ref. 32]. SPERT III was an experimental reactor kinetics facility operated at the Idaho National Engineering Laboratory in the late 1960's to provide validation data for reactor analysis codes such as TWINKLE. The E-Core configuration consisted of a small, uranium-oxide fueled core arranged in a lattice geometry generally similar to operating pressurized water reactors, with representative coolant flow rates and pressures. [

(Proprietary information withheld under 10 CFR 2.390)

]

The applicant presented the core geometry modeled in the TWINKLE-M code to represent the SPERT III reactor, and the experimental conditions at the time of the test. [

(Proprietary information withheld under 10 CFR 2.390)

]

In a follow-up for RAI REA-1, the staff requested in RAI REA-9, that the applicant provide the source of the nuclear data (cross sections, diffusion coefficients, etc.) used to perform the simulation of SPERT-III E-Core Test No. 60.

In its response to RAI REA-9 [Ref. 33], the applicant provided electronic files containing the requested nuclear data. [

(Proprietary information withheld under 10 CFR 2.390)

]

The applicant provided the requested validation of the TWINKLE-M code using data from the SPERT III experiment, which demonstrates satisfactory agreement between calculated and measured data. The applicant also provided the requested source of the nuclear data used in the TWINKLE-M simulation of the experiment. Therefore, the staff finds the responses to RAI REA-1 and RAI REA-9 acceptable.

In summary, the staff evaluated the TWINKLE-M code description provided in Section 2.2 and the TWINKLE-M validation presented in Section 3.2 of Topical Report MUAP-07010-P (R2) [Ref. 3]. The staff identified the key issues related to this area of review and issued numerous RAIs. The applicant responses satisfactorily resolved all of the staff's concerns addressed in the RAIs. Based on comparisons between TWINKLE-M and the applicant's core design code ANC, comparisons between TWINKLE and other reactor kinetics codes, and the comparisons of TWINKLE-M calculations with the SPERT III experiment measured data, the staff concludes that the verification and validation matrix of the TWINKLE-M code is sufficient to demonstrate that TWINKLE-M is capable of adequately simulating the transient response of a reactor core to a large reactivity insertion.

5.1.4 VIPRE-01M

VIPRE-01M [Ref. 12] is the applicant's version of VIPRE-01 [Ref. 15], which is a subchannel analysis code used for thermal-hydraulic analyses in reactor cores. VIPRE-01M is primarily used to evaluate the reactor core thermal limit, the minimum departure from nucleate boiling ratio (MDNBR). In the Non-LOCA methodology, VIPRE-01M is used together with TWINKLE-M for the analysis of the uncontrolled control rod assembly withdrawal from subcritical and control rod ejection events. VIPRE-01M is also used in Non-LOCA methodology for the analysis of other events whenever the computed MDNBRs from MARVEL-M are outside the range of the MDNBR tables built into MARVEL-M. The acceptability of VIPRE-01M for use in the Non-LOCA methodology is addressed in a separate staff review of the applicant's thermal design methodology in [Ref. 12].

Condition. The Non-LOCA methodology described in MUAP-07010 Revision 4 is acceptable provided that it includes an approved method to model detailed core sub-channel thermal-hydraulic conditions. For the US-APWR DC application, that method is based on VIPRE-01M as documented in MUAP-07009 which is under NRC review.

5.1.5 ANC

PARAGON/ANC [Ref. 17] is an NRC approved core design code system.

As discussed in the topical report [Ref. 53] and in Sections 4.0, 5.1.3, and 5.2 of this SER, the ANC code and results obtained with it are used by the applicant as a basis for models, the validation and assessment of models, and the checking and generating of core reactivities and power distributions. As discussed in Section 5.2 of this SER, ANC is used to provide a standard for establishing the TWINKLE-M core initial power distributions for the Spectrum of RCCA Ejection event, and in combination with MARVEL-M in the analysis of the Inadvertent Opening of an SG Relief or Safety Valve and Steam Line Piping Failure events, for which it is used to calculate local peaking factors if the reactor is determined to return to power following scram.

The staff's evaluation finds that ANC is acceptable for use in the US-APWR Non-LOCA methodology for DCD Tier 2 Chapter 15 analyses based on the staff's review documented in the DCD Chapter 4 SE. [Ref. 4].

5.2 Event-Specific Methodology

This SER section evaluates the US-APWR event-specific Non-LOCA methodology, which is presented by the applicant in Section 5.0 of the topical report [Ref. 53].

The staff grouped the Non-LOCA events into four categories, based on the computer codes used in the event analyses. The four categories are given below, along with the events the applicant selected for presenting detailed descriptions of the application of its Non-LOCA methodology, including the use of sample calculations:

- Analyzed using MARVEL-M only
 - Uncontrolled RCCA Bank Withdrawal at Power
- Analyzed using MARVEL-M and VIPRE-01M in sequence
 - Complete Loss of Forced Reactor Coolant Flow
- Analyzed using TWINKLE-M and VIPRE-01M in sequence
 - Spectrum of RCCA Ejection
- Analyzed using special code models in MARVEL-M
 - Steam System Piping Failure
 - Feedwater System Pipe Break
 - Steam Generator Tube Rupture

It is noted that the sample transients selected by the applicant and presented in Section 6 of the topical report are for the purpose of illustrating the detailed event-specific analysis methods described in Section 5 of the topical report. These illustrations facilitate the evaluation of the Non-LOCA methodology, which is the subject of this SER. The staff evaluation of the safety analyses for all accident and transient events is documented in a separate SER that reviews Chapter 15 of the US-APWR DCD [Ref. 4].

The staff's review of topical report Section 5.0 began with consideration of the common elements of the methods employed by the applicant for the analysis of the Non-LOCA transient and accident events.

In its response to RAI Gen-2 [Ref. 36], the applicant noted that the core pressure was restricted to an upper limit on plotted input for those analyses which use the DNBR lookup tables in MARVEL-M. The upper limit was set by user input variable [

(Proprietary information withheld under 10 CFR 2.390)

]

The value given in DCD Tier 2 Table 4.1-1 is the value which conservatively bounds the uncertainties related to the bypass flow estimation. The best estimate value is determined based on a statistical combination of uncertainties related to bypass flow as described in [Ref. 37]. The applicant's response explains how the bypass input value for MARVEL-M was derived and why it differs from the DCD Tier 2 Table 4.1-1 value. Since the value being used is appropriate, the response to RAI Gen-8 is acceptable.

To calculate the maximum RCS pressure for overpressure events, the applicant adds the absolute value of [

(Proprietary information withheld under 10 CFR 2.390)

] The response is acceptable because it demonstrates that MARVEL-M adds a conservative bias to its maximum calculated pressure in the RCS.

The staff's evaluations of the application of the Non-LOCA methodology to each of the events described in Section 5 of the topical report are presented below.

5.2.1 Uncontrolled RCCA Bank Withdrawal at Power

The applicant presented the specific analysis methodology and a sample analysis for this event in Sections 5.1 and 6.1, respectively, of the topical report.

The uncontrolled RCCA bank withdrawal at power is categorized as an AOO. It results in an increase in power and reactor coolant temperature. Unmitigated, the increases in core power and coolant temperature would eventually reach a DNB, overpower, or RCS pressure limit. This AOO is mitigated, however, by the following Reactor Protection System (RPS) trips, only two of which were credited in the analysis:

- Neutron flux high trip (credited)
- Neutron flux rate high trip
- Over power delta-T high trip
- Over temperature delta-T high trip (credited)
- Pressurizer pressure high trip
- Pressurizer water level high trip

This event is analyzed using only MARVEL-M. Minimum DNBR is calculated by the MARVEL-M code using DNBR data tables input to MARVEL-M. (The staff review of the MARVEL-M DNBR model is addressed in Section A.2.4 of Appendix A of this report.) The data tables were constructed by performing several VIPRE-01M calculations with constant core flow and various core heat fluxes, core inlet temperatures, and pressures. A comparison of DNBR calculated by the tables in MARVEL-M to DNBR calculated by VIPRE-01M was presented in MUAP-07010, Appendix A of [Ref. 1]. In its response to RAI App.A-1 [Ref. 19], the applicant clarified that the DNB tables in MARVEL-M were generated assuming a constant core inlet flow rate and a constant core power distribution. Therefore the DNB tables can be used for each AOO which has a constant core flow and a power distribution bounded by the distribution used

in generation of the table. The applicant further noted that the comparison in Appendix A demonstrates that the MARVEL-M interpolation methodology adequately calculated DNBR for the uncontrolled RCCA bank withdrawal at power event. The implementation of the DNBR tables into MARVEL-M is acceptable to the staff.

The Non-LOCA methodology for this analysis requires the use of conservative trip delays and a conservative reactor scram insertion curve. The event is evaluated at both BOC and EOC conditions, and over a range of reactivity insertion rates up to the maximum insertion rate of 75 pcm/s (percent mili/s). The staff reviewed the sample calculation and found it to be reasonable because the behavior of key parameters was similar to that seen in the analysis of this event in other reactors using different computer codes.

In summary, the assumptions and application of the Non-LOCA methodology and the results of the sample calculation of the RCCA Bank Withdrawal at Power event were reviewed. The calculated results were reasonable. Therefore, the staff finds the applicant's Non-LOCA methodology acceptable for evaluating the US-APWR RCCA Bank Withdrawal at Power.

5.2.2 Complete Loss of Forced Reactor Coolant Flow

The applicant presented the specific analysis methodology and a sample analysis for this event in Sections 5.2 and 6.2, respectively, of the topical report [Ref. 53].

The complete loss of flow (CLOF) event is an AOO which results from a loss of electrical supply to the reactor coolant pumps. If the reactor is at power when the event occurs the loss of flow results in a rapid increase in core temperature and an erosion of the DNBR margin. The Non-LOCA methodology assumes the following RPS trips are available to provide protection:

- Reactor coolant pump low speed trip
- Reactor coolant flow low trip

This event is analyzed using MARVEL-M and VIPRE-01M. The reactor system response is calculated using MARVEL-M. The DNBR tables in MARVEL-M are not used for this event because they are based on constant core flow; core flow is decreasing in this event. MARVEL-M generates a file of time-dependent core flow and power for input to VIPRE-01M. The VIPRE-01M code calculates the MDNBR assuming a constant design limit enthalpy rise in the hot channel and a design limit axial power distribution. For conservatism the increase in core pressure during the event is not credited in the VIPRE-01M calculation. Conservative values of RCP inertia, trip delays, scram insertion, and reactivity coefficients are used.

In its response to RAI 5.2-1 [Ref. 19], the applicant performed a sensitivity study to show the effect of RCP inertia. The CLOF calculation was done using the design value of RCP inertia and compared to the base calculation which used a conservative value of RCP inertia. The study demonstrated that the rate of flow coast-down was faster when the conservative RCP inertia was used and the MDNBR was slightly lower. The response demonstrates that the value used for the RCP inertia was conservative; and is therefore, acceptable.

RAI 5.2-2 requested details regarding the DNB correlation used for the CLOF analysis. In its response [Ref. 19], the applicant stated that the US-APWR analysis applies the WRB-2 correlation and referred to Topical Report MUAP-07009, "Thermal Design Methodology"

[Ref. 12] for detailed information on the DNB correlation. The requested information was located in the topical report; therefore, the response to RAI 5.2-2 is acceptable.

In its response to RAI 6.2-1 [Ref. 19], the applicant explained that the revised thermal design procedure (RTDP) is used to statistically account for uncertainties in the input parameters such as reactor power, RCS pressure, flow rate, and average temperature; and conservative values are used for other parameters such as reactor trip simulation and reactivity coefficients. Since the RTDP has been approved by NRC [Ref. 55], the staff finds the uncertainty treatment to be acceptable.

The staff performed an independent mass balance on the pressurizer for the CLOF sample problem and found that mass conservation was violated. In its response to RAI CLOF-2 [Ref. 36], the applicant noted that the parameters used in the mass balance calculation were misidentified in the input manual and were not what they were believed to be in the staff's independent calculation. The description was corrected in the MARVEL-M theory manual. The applicant recreated the mass balance calculation using pertinent parameters and showed that mass conservation was not violated. The response is acceptable because the MARVEL-M theory manual was corrected to show mass conservation.

When the steam and liquid temperatures for the CLOF sample problem were reviewed it was noted that the initial steam temperature indicated subcooled steam. RAI CLOF-3 requested the applicant to explain why the steam temperature was below saturation. In its response [Ref. 36], the applicant stated that the request was about parameters that are only used for information; they are not used in internal calculations. The response is acceptable because the temperature discrepancy noted by the staff has no effect on the MARVEL-M calculations.

Since the CLOF sample problem had no fluid leaving or entering the primary system it was used to check mass and energy conservation in MARVEL-M. Using Excel spreadsheets and the information from MARVEL-M edits, the staff calculated the primary system mass and energy at 0, 6, and 10 seconds. The evaluation indicated that approximately 5 percent of the total energy had disappeared by 6 seconds and 10 percent by 10 seconds. RAI CLOF-4 requested the applicant to explain the apparent non-conservation of energy in the MARVEL-M calculation. In its response [Ref. 36], the applicant noted that the calculations had omitted a term used to account for the energy stored in the SG tube metal. The applicant explained how MARVEL-M accounts for this stored energy and modified the staff spreadsheets to include the metal stored energy. When this was done, the difference in the primary system total energy at 0 and 6 seconds was 1 percent, and the difference between the energy at 0 and 10 seconds was 0.7 percent.

These differences were within the uncertainty of the calculations. The staff reviewed the calculations as modified by the applicant, and confirmed the applicant's conclusion that MARVEL-M provides a reasonable conservation of mass and energy.

In its response to CLOF-5 [Ref. 36], the applicant noted that the SG tube metal mass calculation is controlled by the input variable [

(Proprietary information withheld under 10 CFR 2.390)

] and is acceptable.

In summary, the staff reviewed the application of the Non-LOCA methodology and the results of the sample calculation of the CLOF event which are reasonable and conservative. Therefore, the staff finds the Non-LOCA methodology acceptable for evaluating the US-APWR CLOF event.

5.2.3 Spectrum of RCCA Ejection

The applicant presented the specific analysis methodology and a sample analysis for this event in Sections 5.3 and 6.3, respectively, of the topical report [Ref. 53].

The RCCA ejection is a PA. An assumed failure of a control rod drive mechanism pressure housing results in the rapid ejection of the RCCA and its drive shaft. The RCCA ejection leads to a rapid positive reactivity insertion and an increase in local power peaking and possible localized fuel failure. The RCCA ejection event nuclear excursion is terminated by Doppler reactivity feedback from increased fuel temperature. The following RPS trips are available to trip the reactor for RCCA ejection events; trips that are not credited are identified:

- Neutron flux high trip - high setting
- Neutron flux high trip - low setting
- Neutron flux rate high trip (not credited)
- Over temperature ΔT trip (credited only for events where power does not reach setpoint for neutron flux high trip)
- Low pressurizer pressure trip (credited only for events where power does not reach setpoint for neutron flux high trip)

The analysis method described in Section 5.3 of the topical report uses primarily TWINKLE-M and VIPRE-01M to analyze the RCCA ejection event. TWINKLE-M is used to determine the transient core average and local power behavior. For HZP conditions a three-dimensional model of the core is used in TWINKLE-M. For HFP conditions a one-dimensional TWINKLE-M model is used. VIPRE-01M calculates the fuel centerline temperature, cladding temperature, fuel enthalpy, and DNBR. For the HZP analysis the VIPRE-01M calculation uses two interface files created by TWINKLE-M; one is the time-dependent core average power and the second is the hot channel power factor. For the HFP event the VIPRE-01M calculation uses only the time-dependent average core power interface file. The hot channel peaking factor is assumed constant at the design limit for the HFP VIPRE-01M calculation. The VIPRE-01M analysis uses a one-eighth core model in which each subchannel of the hot assembly is represented.

For large reactivity insertions which could potentially challenge fuel centerline melt or PCMI criteria the HFP, 1-D TWINKLE-M cases insert the design limit reactivity within 0.1 seconds.

The reactivity insertion is accomplished by modifying the TWINKLE-M eigenvalue to yield the design limit RCCA reactivity worth. As described in the staff's evaluation of RAIs 5.3-1-3 [Ref. 22] and RAI 5.3-1 [Ref. 19] below, this was found to be an acceptable way of inserting the design limit reactivity. For the HZP, 3-D analysis the ejected rod worth is increased by changing the local absorption cross section. If the design limit reactivity is not met the eigenvalue is modified to reach the design limit reactivity. Adjusting the eigenvalue, if the design limit reactivity is not met, is conservative as the localized Doppler feedbacks would be larger if the RCCA worth was increased as described in the response to RAI 5.3-3 below [Ref. 19].

For both HFP and HZP cases Doppler reactivity feedback is reduced by [

(Proprietary information withheld under 10 CFR 2.390)

] is conservative for determining the maximum fuel centerline temperature, fuel enthalpy and fuel enthalpy rise.

In RAI REA-8 and REA-12.2, the staff asked the applicant if low ejected rod worths which don't reach the high flux trip point had been evaluated. In its response to RAI REA-12 [Ref. 33], the applicant described a methodology which addressed rod ejections which don't reach the high flux setpoint and depressurize the RCS (note that the methodology in the response to REA-8 is not used). Low rod worth ejections could yield a higher number of DNB fuel failures as reactivity feedbacks are not as great and the reactor trip either does not occur or is delayed relative to high flux trip. The applicant analyzed low ejected rod worths by using the methodology described in the RAI REA-12.2 response by evaluating the accident with three, HFP, bounding steady state scenarios. The first scenario evaluated the short-term effects at peak core power and peaking factor conditions while holding thermal-hydraulic conditions constant. The second scenario evaluated a long-term, rapid RCS depressurization, while the third evaluated a long-term, slow RCS depressurization. The rapid and slow RCS depressurization cases correspond to different RCS hole size assumptions. The 3-D TWINKLE-M, VIPRE-01M and ANC codes were used in the evaluations.

The short term analysis assumes that RCS pressure remains constant; [

(Proprietary information withheld under 10 CFR 2.390)

] The total numbers of failed rods are determined and compared to the assumed value in DCD Chapter 15.4.8.

Several RAIs were issued regarding the use of a 1-D vs. 3-D TWINKLE-M model and the use of a 1/8 core VIPRE-01M model for the rod ejection analyses.

In its response to RAI 5.3-6 [Ref. 19], the applicant stated that the 1/8 core model is used simply to assure consistency of the VIPRE-01M model input with the core thermal design model. In its response to RAI 5.3-6 [Ref. 19], and RAI 5.3-6-1 [Ref. 22], the applicant explained that the 1/8-core representation used in the VIPRE-01M model allows flow redistribution from the hot assembly. This flow redistribution results in a more limiting coolant condition in the hot assembly. The staff finds the VIPRE-01M model acceptable for the intended analyses.

RAI 5.3-9 requested the applicant explain why the 3-D TWINKLE-M model wasn't used for both the HZP and the HFP rod ejection analyses. In its response [Ref. 19], the applicant stated that the 3-D model was necessary to properly capture the effect of Doppler feedback in an event where the power distribution was highly skewed. Since the rods were mostly out of the core for the HFP event the power distribution was much less skewed in the HFP event relative to the HZP event. Therefore, there was no real advantage to using the 3-D model for the HFP event analysis. The applicant chose to use the 1-D model to simplify the analysis. RAI 5.3-7 requested an explanation of how the TWINKLE-M 1-D model was obtained and how the 1-D model's axial power distribution compared to the 3-D models. In its response to this RAI [Ref. 19] and followup RAI 5.3-7-1 [Ref. 22], the applicant showed how the macroscopic cross sections, diffusion coefficients, and delayed neutron data were collapsed from 3-D to 1-D. The applicant also presented a comparison of the two models' axial power distribution for BOC, HFP, ARO conditions and concluded that the two models agreed very well. The response to RAI 5.3-7-2 [Ref. 22] noted that small differences in axial power shape would have no significant impact on the number of rods calculated to be in DNB. Based on the axial similarities of the 3-D and 1-D axial power shapes the staff agrees that a 1-D TWINKLE model is acceptable for the HFP analysis where rod insertion limits prevent a large radial power distribution distortion. A 3-D analysis at HZP is acceptable as the radial power distribution is more skewed due to the deeper rod insertion. One of the analysis assumptions made for the reactivity feedback of the RCCA ejection calculation is to apply a conservative multiplier on the fast absorption cross section to yield a conservative Doppler feedback. RAI 5.3-8 requested the applicant to elaborate on the conservative multiplier. In its response [Ref. 19], the applicant provided the equation for adjusting the fast absorption cross section and showed a conservative factor was applied to the change in the calculated effective fuel temperature yielding a conservative Doppler feedback. The staff agreed that reducing the fast absorption cross section using the applicant's method will reduce the Doppler feedback making the transient analysis results more conservative.

The important parameters for the RCCA ejection analysis are fuel temperature, PCMI, energy deposition to the fuel, and DNBR. The applicant's methodology applies conservatism for the RCCA ejection analysis depending on the figure of merit. First, a conservatively large reactivity, the design limit, is inserted within 0.1 seconds. In HZP cases the inserted reactivity is calculated directly by changing the local absorption cross section caused by the ejection of the most reactive RCCA. In its response to RAI 5.3-1 [Ref. 19], the applicant explained that because this directly calculated reactivity was less than the design reactivity, the difference between it and the design value was inserted by linearly changing the eigenvalue in the 3D TWINKLE-M calculation. This is an appropriate conservative procedure and is acceptable. Additional conservatism is applied in the treatment of the hot channel factors. In the HZP analysis the hot channel power factors from TWINKLE-M are scaled by a multiplier so that the maximum value passed to VIPRE-01M is at the design limit. VIPRE-01M then calculates a maximum fuel centerline temperature, the maximum fuel enthalpy and an adiabatic fuel enthalpy rise for comparison to the appropriate safety limit values. RAI 5.3-2 and RAI 5.3-2-3 requested the applicant explain why the important safety parameters were not obtained directly from TWINKLE-M instead of VIPRE-01M. In its responses to RAI 5.3-2 [Ref. 19] and RAI 5.3-2-3 [Ref. 22], respectively, the applicant explained that the TWINKLE-M calculation uses a [(Proprietary information withheld under 10 CFR 2.390)] It passes its mesh-wise fuel enthalpy to VIPRE-01M. VIPRE-01M then constructs the hot assembly, pin-by-pin enthalpy distribution. The staff finds this approach acceptable as it conservatively sets all 17 hot assembly pin powers to the design limit value.

In its response to RAI 5.3-3 [Ref. 19], the applicant noted that the hot channel factor from TWINKLE-M run was not at the design limit power because the margin associated with the design limit value is not accounted for in TWINKLE-M. This is conservative for the core kinetics calculation because the lower hot channel factor decreases the local Doppler feedback. By raising the pin power to the design limit in VIPRE-01M a conservative calculation of hot spot fuel temperature and enthalpy is obtained. The response to RAI 5.3-8 [Ref. 19] noted another conservative feature in the Doppler feedback calculated by TWINKLE-M: A 20 percent reduction in the calculated increase of the fast group absorption cross section caused by a fuel temperature change. The responses are acceptable because they explain the incorporation of conservatisms into the RCCA ejection accident analysis.

PCMI fuel failure is evaluated by first calculating the local adiabatic fuel enthalpy rise, ΔH , at each mesh point in TWINKLE-M. The peak TWINKLE-M mesh power is then adjusted upward to the maximum hot spot enthalpy in VIPRE-01M. This adjustment (ratio) is then applied to determine all the TWINKLE-M mesh enthalpies. Since the burnup distribution is specified in TWINKLE-M, a relationship between the burnup and ΔH can be established. The relationship between local oxide thickness to cladding wall thickness and the local burnup is available from fuel design calculations. This is used, along with the burnup/ ΔH relationship, to establish the ΔH versus oxide/wall thickness distribution for the core. Finally, this distribution is compared to the PCMI fuel failure criteria given in SRP Chapter 4.2 Revision 3 Appendix B, Figure B-1, "PWR PCMI Fuel Cladding Failure Criteria." If any rod in a TWINKLE-M mesh point exceeds the failure criteria then all rods within that mesh point are assumed to fail.

RAI 5.3-1-3 requested the applicant show the impact of changing the eigenvalue of the 3D TWINKLE-M calculation rather than changing local absorption cross sections to add reactivity to the 3D TWINKLE-M calculation as described in Section 5.3 of the Non-LOCA topical report. In its response [Ref. 22], the applicant presented the results of two HZP RCCA ejection cases. In

[

(Proprietary information withheld under 10 CFR 2.390)

] The response to RAI 5.3-2-2 confirms that VIPRE-01M uses the design limit hot channel factor which is conservative when determining fuel centerline temperature and fuel average enthalpy.

In its response to RAI 6.3-1 [Ref. 19], the applicant clarifies the role of the ANC computer code [Ref. 17] in the rod ejection accident. It states that ANC is used to calculate power peaking factor for the rod ejection accident and to calculate the core radial power distribution for the

steam line break (SLB) event. Since ANC is an NRC-approved code, its usage in calculating power peaking factor is acceptable.

RCS pressure associated with the RCCA ejection is calculated using MARVEL-M and VIPRE-01M. VIPRE-01M generates an interface file containing the time-dependent total core void fraction and core heat flux. MARVEL-M reads this file and calculates the resulting RCS pressure transient.

Prior to performing a transient rod ejection analysis, it is necessary to initialize the simulated core at steady-state conditions with respect to core power distribution. For this initialization, the applicant uses a method in which the TWINKLE-M-calculated steady-state power distribution is compared with the power distribution calculated using steady-state core simulator ANC [Ref. 17]. ANC uses a higher-order nodal method to solve the neutron diffusion equation relative to the coarse-mesh finite difference technique used by TWINKLE-M. Therefore, the ANC-generated power distribution is expected to be closer to reality than the raw TWINKLE-M calculation, especially in regions where the flux gradient is the strongest (for example, near the core periphery/heavy neutron reflector interface). In order to improve the agreement between the TWINKLE-M and ANC power distributions, the applicant manually and iteratively adjusts the fast-neutron group nuclear data in the reflector regions of the TWINKLE-M core model. The staff was concerned about the effect of performing such an adjustment at steady-state conditions and expecting it to remain valid for transient conditions, since the flux-weighted cross sections of the peripheral assemblies and the reflector region will change as the power distribution becomes perturbed by a localized reactivity insertion. To address this concern, RAI REA-4 requested that the applicant justify the TWINKLE-M initialization approach used for the analysis of transient events.

In its response to RAI REA-4 [Ref. 27], the applicant provided additional details regarding the adjustment methods used. In short, separate modifications are made to the reflector regions on the top, bottom, flat, and corner regions of the reflector in the form of multipliers to the fast neutron group diffusion coefficient. The applicant stated that once these adjustments are made for a particular core configuration at steady state conditions, they remain valid regardless of transient changes in the core power distribution.

To illustrate this point, the applicant provided reference to a comparison of TWINKLE-M and ANC calculated static power distributions at EOC HZP conditions presented in Topical Report MUAP-07010-P. For this case, the reflector adjustments were made in the TWINKLE-M model with the control rods at their insertion limits to match the ANC model power distribution within approximately [

(Proprietary information withheld under 10 CFR 2.390)

] percent. The applicant concluded that this demonstrates that the adjustments made at the initial conditions remain valid for conditions in which the core flux profile is strongly skewed.

Additionally, the applicant provided a number of mesh sensitivity studies demonstrating that if the axial and radial meshes in the TWINKLE-M model are refined, reflector data adjustments are no longer necessary to bring the TWINKLE-M and ANC power distribution into acceptable agreement. A series of TWINKLE-M HZP transient simulations was provided in which the results using the base simulation's "coarse mesh" model (2x2 radial nodes per assembly,

[

(Proprietary information withheld under 10 CFR 2.390)

] where no reflector adjustments were necessary. The results from the three cases show excellent agreement in ejected rod worth, maximum core power, and maximum hot spot relative power. The applicant concluded that this comparison demonstrates that the reflector adjustments made at steady-state conditions are not invalidated as the core transient progresses.

As a final demonstration of the insensitivity of the reflector adjustments on the core power distribution, the applicant provided a comparison between the base case HZP rod ejection transient, using licensing methodology assumptions as documented in the topical report, with a total of four sensitivity cases. In the sensitivity cases, the initial power distributions were skewed relative to the base case towards the edge of the core, the interior of the core, the top of the core, and bottom of the core. The power distributions were skewed by adjusting the appropriate reflector multiplier relative to the base case. The same ejected rod worth was used in all calculations. The applicant provided the resulting maximum core power and maximum hot spot relative power calculated by TWINKLE-M, the maximum hot spot relative power used in the subsequent VIPRE-01M analysis, and the resulting fuel enthalpy rise. The applicant concluded that, even though some of the sensitivity cases demonstrated a greater core power transient and maximum relative local power as calculated by TWINKLE-M, the cases with higher power had a lower local peaking factor, and vice versa. Additionally, the applicant stated that the conservatism in the licensing methodology (increasing the hot channel power factor to the design limit) when transferring TWINKLE-M results to the VIPRE-01M model is sufficient to bound any effects due to minor variations in the initial core power distribution.

The staff finds the applicant's adjustment of the radial reflector neutron data in order to better the agreement between the TWINKLE-M and ANC steady-state power distributions acceptable. This position is based on the analyses presented by the applicant which show very little impact of the reflector modifications on the calculation of a highly-skewed radial power distribution; sensitivity calculations which show convergence of the reflector modifications to unity as the core spatial mesh is refined; and comparisons between the licensing methodology and sensitivity cases demonstrating abundant margin in the calculated figure of merit (in this case, fuel enthalpy rise) even under conservative analysis conditions

In order to demonstrate compliance with the allowable fuel enthalpy rise related to PCMI in SRP, Section 4.2, Appendix B, the applicant's rod ejection accident (REA) analysis must be performed with the distribution of cladding corrosion within the reactor core. In Section 5.3 of the topical report, the applicant provided a high-level overview of the process used that was not sufficiently detailed for the staff to make a conclusion regarding its acceptability. RAI REA-5 requested more detail from the applicant about the method used.

In its response to RAI REA-5 [Ref. 27], the applicant describes the method by which the nodal fuel enthalpy rise is evaluated and correlated to nodal burnup. First, the nodal enthalpy rise is calculated in the TWINKLE-M code by integrating the local power and power density in each node up to a pre-determined point in the transient.

Then, the node-wise enthalpy rise is increased using the rod-wise peak-to-average ratio within the mesh obtained from the VIPRE-01M hot-spot results. The detailed nodal burnup distribution based on the equilibrium cycle is obtained from the reactor core design code ANC. Thus, for

each node in the TWINKLE-M/VIPRE-01M mesh, a corresponding local burnup from ANC is assigned.

Next, the applicant described the process in which a relationship between local burnup and oxide-to-wall thickness is obtained using the fuel design methods. Due to the axial temperature gradient present in a PWR core, the axial dependence of the corrosion thickness must be evaluated. The applicant states that several potential power histories are calculated in order to determine the limiting case. [(Proprietary information withheld under 10 CFR 2.390)]

Using the results described above, the applicant conservatively determines the relationship between nodal enthalpy rise from the REA calculations and local oxide-to-wall thickness from the fuel design calculations. The resulting relationship is plotted against the SRP 4.2 Appendix B acceptance criterion to verify compliance. For the US-APWR, the applicant states that the maximum enthalpy rise resulting from the REA simulation is less than the minimum value permitted for any oxide-to-wall thickness. Therefore, even with conservative analysis methods, the US-APWR will meet the criterion with sufficient margin.

In follow-up RAI REA-11, the staff requested more detailed information on the method used for increasing the enthalpy rise within the mesh calculated with TWINKLE-M using the rod-wise peak-to-average ratio inside the mesh from the VIPRE-01M hot spot calculation results. In its response to RAI REA-11 [Ref. 54], the applicant provided an example of the method employed using the data from base case TWINKLE-M and VIPRE-01M calculations described in Table REA-4.6 [Ref. 27]. The applicant explained that the enthalpies calculated by TWINKLE-M are compensated so that the maximum value matches the VIPRE-01M value. The hot spot enthalpy result calculated by VIPRE-01M is obtained by using the F_Q transient obtained from TWINKLE-M multiplied by the factor used to increase the peak-to-average ratio inside the mesh as the VIPRE-01M input. The applicant also provided ANC-calculated peak-to-average power data and showed how increasing the mesh-wise maximum hot channel factor obtained by TWINKLE-M in this manner conservatively bounds the mesh nodal powers.

Based on the elaborated discussion of the evaluation process described above, the staff finds the method in which the applicant demonstrates compliance with the SRP 4.2 Appendix B criterion regarding enthalpy rise as a function of oxide-to-wall thickness to be acceptable. The staff finds the method employed by the applicant to make this determination to be suitably conservative and to appropriately account for fuel burnup effects.

The staff determined that the initial axial power distributions used for analysis of the REA event had not been discussed in the topical report or prior RAI responses. The staff therefore issued RAI REA-6 requesting the applicant describe the axial power distributions used, the basis for their selection, and the sensitivity of the REA simulation results to variations in the initial axial power distribution.

In its response to RAI REA-6 [Ref. 27], the applicant stated that the best-estimate, equilibrium cycle power distribution, calculated by ANC, is used. As described above in the response to RAI REA-4, adjustments are made to the TWINKLE-M model to bring the TWINKLE-M and ANC power distributions into satisfactory agreement.

The applicant provided a list of conservatisms in the TWINKLE-M calculations that would compensate for any non-conservatism in the initial axial power distribution. These conservatisms include adjusting the reactivity insertion to the maximum design limit, using [(Proprietary information withheld under 10 CFR 2.390)] design value, and minimizing the

delayed neutron fraction and neutron lifetime. The applicant cited additional conservatisms in the core thermal analysis using the VIPRE-01M code, such as adjusting the local peaking factors to the design limit.

For the hot zero power analysis cases, the applicant referred to Appendix B of the topical report for a quantification of the conservatism inherent when using the above assumptions. The applicant also referred to the response to RAI REA-4, which demonstrates little sensitivity of the transient core power to the initial axial power distribution.

For the hot full power analysis cases, the applicant states that, depending on which limiting parameters are of interest in the thermal analysis, different axial power distributions are employed. For the fuel temperature analysis the VIPRE-01M model uses a chopped-cosine axial power distribution, while for the rods-in-DNB analysis the VIPRE-01M model uses a double-hump axial power distribution. Both axial power profiles are provided in DCD Figure 4.4-4. The applicant has shown for the thermal analysis of the reactor core that these power distributions are limiting.

Based on the conservatism of the assumptions used in the TWINKLE-M neutronics analysis (which maximizes the core power transient in both the hot zero and hot full power cases) and the conservatisms inherent in the thermal analysis methodology (which includes adjusting local peaking factors to design limits), the staff finds the treatment of the initial power distribution employed by the applicant for the REA analysis to be acceptable.

For the hot full power REA analysis, the one-dimensional methodology involves simulating the reactivity insertion resulting from control rod ejection by directly modifying the effective multiplication constant in the transient diffusion equation and not by simulating the change in nodal cross sections resulting from the control rod exiting the core. As a result, the power transient is simulated globally (i.e., core-wide) rather than locally. In RAI REA-7, the staff requested that the applicant explain how the local effects of the rod ejection are accounted for in the methodology.

In its response to RAI REA-7 [Ref. 27], the applicant stated that, while from a reactivity-insertion point of view the global axial power distribution does not change, there is some effect on the axial power shape prior to reactor trip due to feedback effects. However, the methodology does directly simulate the effect of reactor trip control rod insertion by changing the nodal cross sections. This causes the power shape to be significantly skewed toward the bottom of the core as the reactor trip reactivity is inserted.

The applicant acknowledged that simulating a reactivity insertion globally does not directly account for the effect of the rod ejection on axial flux shape but also indicated that the effect is minor for the hot full power cases. In its response to RAI-REA 6 [Ref. 27], the applicant stated that any non-conservatisms in the reactivity insertion are well-bounded by other conservatisms in the methodology.

To further support the applicant's position that other methodology conservatisms cover any effect of different axial power distributions, the applicant referenced the response to RAI 15.4.8-5 [Ref. 40]. Within this RAI response, best-estimate three-dimensional REA simulations were performed at HFP conditions and compared with the one-dimensional licensing methodology described in the topical report.

In each case, the resulting core power and fuel temperature transients were much more severe when using the one-dimensional licensing method than when using the three-dimensional, best-estimate method. The applicant indicated that the response to RAI 15.4.8-5 demonstrates the conservatism in the one-dimensional modeling approach, which more than compensate for the effects of variations in the initial core axial power distribution.

Based on the above discussion and the analysis presented by the applicant, the staff finds the method by which the applicant simulates the REA from hot full power conditions and the applicant response to RAI REA-7 to be acceptable. This finding is based primarily on the conservatism employed in the core thermal analysis (namely, increasing the local peaking factor to the design limit and maintaining it at the design limit for the duration of the transient), as well as the comparisons presented by the applicant between the licensing methodology and the best-estimate calculations.

The high worth rod ejection analysis methodology adds sufficient positive reactivity to reach the high flux reactor trip setpoint. The nominal trip setpoint is 109 percent and for conservatism the methodology adds an additional 9 percent. The analysis is performed assuming a setpoint of 118 percent. The staff agreed that this approach is conservative from a view of prompt energy deposition but questioned if it is also conservative from a view of rods-in-DNB. The staff issued RAI REA-8 requesting the applicant perform an analysis or evaluation where the positive reactivity addition causes the flux to get very close to, but not reach, the 118 percent trip setpoint. Of interest to the staff for such cases are what other reactor trips may occur, the reactor trip time, the percentage of rods in DNB.

As a result of considering issues related to the high flux reactor trip setpoint discussed above, the staff questioned if the 9 percent increase in the trip setpoint (from 109 percent nominal to 118 percent used in the analysis) is sufficient to bound all accident scenarios and issued RAI REA-12 requesting the applicant address the bases for the 9 percent uncertainty. As an example, the staff suggested a case where of the four ex-core flux detectors, one is out of service, another neighboring one is assumed to fail, and the ejected rod is on the core periphery mid-way between the two inoperative detectors.

In its response to RAI REA-12.1 [Ref. 42], the applicant stated that the 9 percent increase may not bound the uncertainty for all possible cases, especially considering the locations of ex-core detectors relative to the ejected rod. The power increase seen by the operable detectors may not reach the 118 percent analytical setpoint. The applicant stated that in that event, reactor trip will result from the over temperature delta temperature or low pressurizer pressure conditions, assuming RCS depressurization following break of the control rod drive mechanism (CRDM) housing. The applicant evaluated the uncertainty associated with the ex-core detectors and performed sensitivity analyses of rod ejection cases for the US-APWR first and equilibrium cores.

The applicant calculated the uncertainty between the actual and measured reactor powers for the rod ejection event DCD cases performed using TWINKLE-M (3D) for BOC and EOC conditions and three locations for the ejected rod. The uncertainty evaluation used detector weighting factors calculated separately using the neutron transport code DORT. The analysis indicated that the high power range neutron flux trip occurs when two out of four of the measured reactor power channels [(Proprietary information withheld under 10 CFR 2.390)]. If a single ex-core detector has failed, the trip occurs when the third-highest measured detector power reaches this value. The applicant indicated

that for both the BOC and EOC cases the times when third-highest detector reaches this value are slightly delayed relative to the reactor trip times in the DCD calculations.

To determine the impact of the larger power distribution uncertainty, the applicant performed a sensitivity analysis using a bounding 0.1-second reactor trip time. The applicant concluded that the impact on the overall results is negligible but that the evaluation also indicated that the uncertainty in the power distribution can be larger than that assumed as a part of the analytical limit. In light of this finding, Topical Report MUAP-07010 has been revised to include the explicit calculation of measured power described in this RAI response as shown in Section 5.3, "Spectrum of RCCA Ejection," and Appendix G, "Calculation of High Power Range Neutron Flux Reactor Trip for Rod Ejection Event" of Revision 2. The staff finds that the applicant evaluation adequately addresses the uncertainty in the power range high flux reactor trip setpoint.

To support the applicant's view that no DNB is expected to occur for rod ejection cases where the reactor high flux trip setpoint is approached but not reached, the applicant provided three DNB analysis scenarios as a part of the response to RAI REA-12.2. The analysis results show that during the short-term period the MDNBR remains above the analytical acceptance limit for BOC and EOC conditions for the first-cycle and equilibrium-cycle cores. For the long-term period, the applicant evaluated the effects of other reactor trips (low pressurizer pressure or over temperature ΔT) that occur as a result of declining RCS pressure following a rod ejection event. The sensitivity analyses indicated the maximum number of fuel rods below the MDNBR was bounded by the Chapter 15 analysis assumption. Based on the rod worth uncertainties, conservative assumptions regarding the hot channel factor, the VIPRE-01M inputs and the reduced Doppler reactivity feedback use the staff finds that the applicant's evaluation of low worth rod ejections acceptable.

In summary, the application of the Non-LOCA methodology and the results of the sample calculations of the Spectrum of RCCA Ejection event were reviewed. The staff review focused on the layout, structure and initialization of the TWINKLE-M and VIPRE-01M models, and conservatism inherent in the methodology, including the magnitude of the reactivity insertion, Doppler feedback, thermal factors affecting calculation of DNB and the calculation of the fuel enthalpy rise for the evaluation of PCMI.

The analysis assumptions in the applicant's RCCA ejection analysis conform to those given in RG 1.77 Appendix A [Ref. 38] and the analysis conservatively ignores the neutron flux rate high trip. The analysis results in a conservative assessment of the fuel centerline temperature, PCMI fuel failure, fuel enthalpy rise, and number of rods in DNB. Therefore, staff finds the Non-LOCA methodology acceptable for evaluating the US-APWR Spectrum of RCCA Ejection event.

5.2.4 Steam System Piping Failure

The applicant presented the specific analysis methodology and a sample analysis for this event in Sections 5.4 and 6.4, respectively, of the topical report.

A break in the US-APWR steam system piping results in an asymmetric cooldown of the RCS because the heat removal by the SG in one loop is much greater than the heat removal by the SGs in the other three loops. The cooldown of the RCS can cause an increase in power due to the negative value of the moderator temperature coefficient. For a large main steam line break (MSLB) the reactivity insertion may be sufficient to cause a return to power after scram has occurred. The post-scram return to power is terminated by the injection of boron into the RCS, by dry-out of the affected steam generator, or a combination of the two.

The applicant's methodology uses MARVEL-M to compute the core power and RCS thermal hydraulic responses.

For HFP initial conditions the DNBR tables within MARVEL-M are used to compute the pre-scrum MDNBR. This is acceptable because the core operating conditions are within the range of the independent variables of the DNBR tables. Post-scrum MDNBR is calculated using VIPRE-01M. The VIPRE-01M analysis is done as a steady state calculation at certain points at and around the time of the peak core heat flux computed by MARVEL-M. Core pressure and the core inlet enthalpy distribution for VIPRE-01M are obtained from MARVEL-M. In addition, the core power distribution is input to VIPRE-01M. The power distribution is computed by the ANC computer code assuming a stuck rod and the core inlet enthalpy distribution from MARVEL-M at the time of peak power.

The following engineered safeguard features are assumed to be available to mitigate the MSLB:

- Steam line isolation
- Emergency feedwater system (EFWS) isolation
- Main feedwater (MFW) isolation
- Safety injection (SI)

The following RPS trips are available to trip the reactor, initiate safety injection, and isolate systems:

- Low steam line pressure in any loop
- Over-power ΔT high trip
- Over-temperature ΔT high trip
- Pressurizer pressure low trip
- Neutron flux high trip (not credited)
- Containment pressure high trip (not credited)

The following conservatisms are part of the MSLB analysis methodology:

- No credit is taken for the check valves in the main steam lines. All SGs are assumed to blow down until the MSIVs close.
- All EFW is directed to the affected SG
- Failure of one SI train (limiting single failure)
- One SI train out of service for maintenance
- Both available SI trains inject into the unaffected sectors of the core.

As described in topical report Section 5.4 (1), the MSLB event requires the use of several unique models in MARVEL-M. The Moody model [Ref. 56] is used to calculate the break flow; furthermore, only vapor is allowed to flow from the break. This is a conservative assumption because it insures that all the liquid in the SG secondary remains available to boil off and extract heat from the primary side. The flow mixing models at the core inlet and outlet and the weighting of the core sector reactivities take on increased importance. ECCS actuation and the injection of boron play a key role in limiting the post-scrum return to power. MARVEL-M's ability to calculate natural circulation is important to those cases which simulate a loss of offsite power.

The sensitivity of the calculated MDNBR to core flow mixing for the HZP MSLB event was illustrated in Appendix E, “Sensitivity Study of the Inlet Mixing Coefficient for Steam System Piping Failure” of the topical report by presenting DNBR as a function of the mixing parameter. RAI 5.4-1 and RAI APP.E-1 [Ref. 19] requested the applicant to substantiate the applicability of the results shown in Appendix E to other AOOs and PAs. In its response [Ref. 19], the applicant stated that the non-uniformity of RCS loop temperatures was greatest for the MSLB event.

Therefore, the sensitivity of DNBR to core flow mixing in other events would be less than that shown in Appendix E. The applicant also asserted that the uniformity of vessel inlet flow mixing was increased with decreasing RCP flow. In particular, it stated that “...inlet mixing can best be approximated by perfect mixing for very low flows such as during natural circulation conditions.” RAI MSLB-10 asked the applicant to justify this assertion. In its response [Ref. 36], the applicant considered an MSLB with the power lost to the RCPs. In this scenario, the applicant stated, the cold water from the faulted loop would settle to the bottom of the reactor pressure vessel (RPV) lower plenum. In order to reach the core, it would have to rise through the warmer water above and that process would result in nearly perfect mixing. The staff did not agree with the applicant’s assessment. A likely scenario for the pumps-off case is for the cold water from the affected loop to settle to the bottom of the RPV and, after displacing the warm water there, be the only water entering the bottom of the core. This situation is similar to no-mixing rather than perfect mixing.

The staff conducted mixing sensitivity runs using MARVEL-M to determine how mixing assumptions affected three key parameters of the MSLB analysis: peak power, affected sector inlet flow at the time of peak power, and affected sector inlet temperature at the time of peak power. The MSLB HZP pumps-off scenario was considered for three core inlet mixing assumptions. The base case used the applicant’s mixing assumption. Sensitivity Case 1 assumed perfect mixing, and Sensitivity Case 2 assumed no mixing. The results of the three cases, shown in Table 1, indicate that the base case gives the highest power. The no mixing case gives a slightly smaller peak power, but has a lower inlet temperature and a higher inlet flow than the base case. Thus, the base case would give the lowest MDNBR of the three cases if the case key parameters were transferred to VIPRE-01M.

Table 1 Sensitivity of Key MARVEL-M Parameters to Core Inlet Mixing Assumption for the MSLB with Loss of Offsite Power

Parameter	Base Case	Perfect Mixing (Case 1)	No Mixing (Case 2)
Peak Power (%nom.)	6.9	4.7	6.3
Sector A Inlet Flow, kg/s	398	347	433
Sector A Inlet Temperature, C	178	179	177

Based on the above results, the staff finds that the core inlet mixing assumptions used by the applicant for the HZP pumps-off MSLB case are acceptable. There is reasonable assurance that the MDNBR calculated by the applicant is lower than would be calculated by using other core inlet mixing assumptions.

RAI 5.4-2 asked the applicant to provide the mixing model and substantiate why it is conservative. In its response to RAI 2.1-13 [Ref. 19], the applicant explained where the design and conservative values are given and stated to be based on 1/7 flow mixing experiments

conducted by the applicant and documented in Topical Report MUAP-07022-P, "Reactor Vessel Lower Plenum 1/7 Scale Model Flow Test Report," [Ref. 23]. The staff performed an independent calculation of the values of the mixing parameters using Figure 4-19, "Core Inlet Non-dimensional Temperature Distribution" of MUAP-07022-P, and confirmed that the values being used in MARVEL-M are conservative, and therefore acceptable.

RAI 6.4-1 asked if the SLB event is sensitive to the location of the break. In its response [Ref. 19], the applicant stated that the most limiting combination of single failure and break location is with the break located upstream of the main steam line check valve and isolation valves. The presence of the check valve is ignored.

Therefore, all four SGs blow down until MSIV closure, the case analyzed in Section 6.4 of the topical report, resulting in a greater cooldown of the RCS. The applicant's determination of the limiting break location is reasonable and ignoring the check valve is conservative; therefore, the response is acceptable.

It was noted that the input variable [

(Proprietary information withheld under 10 CFR 2.390)

]. The applicant's analysis is acceptable. However, while a higher saturation pressure is conservative with respect to reactivity effects, it is non-conservative with respect to MDNBR considerations. Independent calculations indicated that the upper head temperature could drop from 561 K to 555 K (550 °F to 539 °F) in the first 50 seconds of the transient, lowering the upper head saturation pressure from 7.3 MPa to 6.7 MPa (1053 psia to 970 psia). RAI MSLB-1-1 asked the applicant to address the effect that a lower saturation pressure would have on calculated MDNBR.

In its response to RAI MSLB-1-1 [Ref. 43], the applicant performed an MSLB simulation in which with the upper head bypass flow set to [(Proprietary information withheld under 10 CFR 2.390)] lower than the base case. The lower pressure resulted in increased HPSI flow relative to the base case; hence, boron reached the core sooner, terminating the post-scrum power increase. The net result was a smaller post-scrum peak power and a higher MDNBR relative to the base case. The applicant's response also provided justification [Ref. 44] for using the W-3 DNBR correlation for pressures below 6.9 MPa (1,000 psia). The response adequately addresses the effect of upper head bypass on the system's response to an MSLB, and is therefore acceptable.

In its response to RAI MSLB-2 [Ref. 36], the applicant explained that the pump loss coefficient, [(Proprietary information withheld under 10 CFR 2.390)] is used in the analysis of the locked rotor event and provides the pump pressure loss term during natural circulation conditions. While the loss coefficient for forward flow can be obtained from the homologous curves, it is provided as a user input so that a safety margin can be included. The response is

acceptable because it describes a reasonable way to conservatively model pressure losses across the RCP.

RAI MSLB-3 requested the applicant explain why the variables [

(Proprietary information withheld under 10 CFR 2.390)

was calculated and why it is conservative, thus providing an acceptable response to RAI MSLB-5 [Ref. 36].]

The staff performed an independent calculation of the time that low steam line pressure trip would occur in the SLB event using the lead/lag control system which calculates steam line pressure. [(Proprietary information withheld under 10 CFR 2.390)]

The staff inquired why the steam line pressure trip's lead and lag times were not the same in the MARVEL-M input file and the calculation memo which accompanied the input file. The response to RAI MSLB-4 [Ref. 36] explained that the values in the input file were conservatively biased by [

(Proprietary information withheld under 10 CFR 2.390)

value is acceptable for the MARVEL-M calculation.

As noted in the previous paragraph, when the reactor returns to power in the SLB analysis nearly all of the power is generated in the fuel assemblies in the affected sector, since that is where the stuck rod is. RAI MSLB-8 noted that the MARVEL-M SLB analysis distributed the

power equally to the 4 quadrants of the core rather than mainly to the affected quadrant, and requested a justification of that assumption. The applicant responded [Ref. 36] that the power is distributed uniformly because non-uniform radial power distributions cannot be utilized in MARVEL-M. It then indicated that so long as the reactivity feedback in MARVEL-M is demonstrated to be conservative the exact details of modeling the power distribution in core are not important. However, the applicant's response was not correct with respect to modeling non-uniform power distributions. [(Proprietary information withheld under 10 CFR 2.390)] successfully used in an independent MARVEL-MSLB calculation by the staff. The staff issued RAI MSLB-7-1 asking the applicant to run an MSLB simulation using a reactivity weighting scheme the staff considered more appropriate.

In its responses to RAI MSLB-7-1 [Ref. 43], and RAI-5 [Ref. 46], the applicant addressed the staff's concerns regarding reactivity weighting. An MSLB simulation was run with both uniform weighting and with almost all the weight given to the affected sector. Both runs were shown to yield nearly the same return to power, with the power for the uniform weighting case being slightly larger.

In its response to RAI-5 [Ref. 46], the applicant also addressed the staff's concern regarding the possibility that the input ANC boron concentration might be too high. The value used in ANC was the core average boron concentration calculated by MARVEL-M. The ANC calculation was redone using the minimum boron calculated by MARVEL-M. A comparison of the reactivity calculated by ANC to that calculated by MARVEL-M showed that the MARVEL-M value was conservatively high. The staff finds that the responses to the foregoing RAIs demonstrate the conservative nature of the MSLB methodology with respect to reactivity weighting and boron concentration in ANC, and are therefore acceptable.

In RAI MSLB-11 the staff asked why fluid temperature increases as one moves from the cold leg to the core inlet. In its response to RAI MSLB-11 [Ref. 36], the applicant noted that at any given time prior to SG dry-out the water at the RCP will be the coldest and this cold front will progress toward the lower plenum. Thus there will always be a temperature gradient between the lower plenum and the SG outlet plenum. The staff concurs with this explanation.

RAI MSLB-12 expressed the concern that the boron front could be smeared numerically with the result that boron would be calculated to arrive at the core sooner than it physically could. In its response [Ref. 36], the applicant stated that the safety injection nozzle in the MARVEL-M analysis was assumed to be in the cold leg whereas it actually is in the downcomer. The applicant claimed that this assumption was adequate to offset the small amount of boron smearing that occurs during the simulation. This response did not allay the staff's concern. The MARVEL-M model assumes that the SI is injected approximately [

(Proprietary information withheld under 10 CFR 2.390)

]. Therefore a better justification is needed of why the boron content in the core is conservative. It is noted that the power rise in the SLB analysis is terminated by boron reaching the core; hence, assurance that the core's boron content is conservatively calculated is important.

The staff issued follow-up RAI MSLB-12-1 which requested the applicant to provide more justification that boron is treated conservatively. In RAI MSLB-20 the staff requested the applicant explain how the ECC line sweep-out volume (volume of unborated water that is in the ECC lines when HPSI begins) is calculated. In its response to MSLB-20 [Ref. 43], the applicant provided the calculation of the sweep-out volume based on the US-APWR design data and a

conservative additive factor. This response showed that the sweep-out volumes used in MARVEL-M were conservative; they were therefore acceptable. In its response to RAI MSLB-12-1 [Ref. 43], the applicant provided a sensitivity calculation - the limiting MSLB case [(Proprietary information withheld under 10 CFR 2.390)]. The peak power for the sensitivity case was not significantly different from the base case peak power. The applicant noted that the time delay for the SI pumps to go from start to full speed is 18 seconds for the offsite power available cases being considered. The MSLB analysis imposes a conservative time delay of 20 seconds for the SI pumps to reach full power. The applicant's responses to MSLB-12-1 and MSLB-20 are acceptable; they provide the justification that boron injection was treated conservatively in the MSLB analyses.

The shutdown reactivity in the SLB analysis is 1.6 percent $\Delta k/k$. In its response to RAI MSLB-13 [Ref. 36], the applicant stated that the Mitsubishi reload evaluation methodology (Topical Report MUAP-07026-P, "Mitsubishi Reload Evaluation Methodology,") [Ref. 47] provides procedures for ensuring that this value is less than the shutdown margin for each cycle. If it is not, the SLB event will be re-analyzed. This procedure to ensure that the value used in the present analysis is conservative is acceptable.

The staff was concerned that the SLB methodology did not cover the full range of possible moderator density coefficients (MDCs). RAI MSLB-14 noted that the MDC used in the analysis ranged from [(Proprietary information withheld under 10 CFR 2.390)] ($\Delta k/k$)/(gm/cc) at a density of 0.95 gm/cc. The applicant was asked to explain how its analysis supported the value of the moderator density coefficient, 0.51 ($\Delta k/k$)/(gm/cc), used in other US-APWR DC Tier 2 Chapter 15 analyses. In its response to MSLB-14 [Ref. 36], the applicant indicated that it did not. In light of this, the staff concluded that the SLB analyses as it is performed only supports a hot full power MDC corresponding to the core loading used to generate the MDC curves used in the present analysis. If a core loading with a higher MDC occurs it must be re-analyzed. In its response to RAI MSLB-14-1 [Ref. 43], the applicant noted that the moderator defect curve used in the MSLB analysis is conservatively calculated by ANC and includes the assumption of a stuck rod. The applicant also noted that the applicant's reload evaluation methodology [Ref. 47] insures that cycle-specific values of key safety parameters, such as the moderator defect curve, are bounded by previous cycle values. If not, the relevant safety analyses are redone. The staff agrees that the moderator feedback is being treated conservatively in the MSLB analysis and finds that appropriate procedures are in place to insure future analyses are done conservatively. Therefore, the responses to RAI MSLB-14 and MSLB-14-1 are acceptable.

In its response to RAI MSLB-15 [Ref. 36], the applicant described the procedure used to develop the power defect reactivity curve. The applicant responded that the curve is developed at [(Proprietary information withheld under 10 CFR 2.390)]. Several power state points are analyzed and the eigenvalue for each is recorded. The defect curve is developed from the eigenvalue information. This procedure is acceptable because it is in accordance with standard engineering practice for developing power defect curves.

The staff issued RAI MSLB-16 to express the concern that the applicant's SLB methodology does not provide for the same moderator density distribution to be used in both VIPRE-01M and ANC. As it is formulated, the methodology calls for a single ANC run and a single VIPRE-01M. The ANC run is made using core inlet boundary conditions from the MARVEL-M run; it outputs a 3-D core power distribution. ANC calculates a core moderator density distribution based on closed channel hydraulics; that is, there is no cross flow between assemblies. The power distribution calculated by ANC is input to VIPRE-01M. VIPRE-01M then calculates a new moderator density distribution based on open channel hydraulics. Thus, it produces a density

distribution that, if it were given to ANC, would produce a power distribution different from what VIPRE-01M is using. A robust methodology should involve iteration between ANC and VIPRE-01M until they converge to a common core power distribution and common moderator density distribution. RAI MSLB-16 requested that the applicant provide justification for using inconsistent power and moderator density distributions in ANC and VIPRE-01M. In its response [Ref. 36], the applicant stated that *"...since ANC uses a closed channel thermal-hydraulic model which does not take into account fluid cross-flow between fuel assemblies, ANC overestimates the fluid density at the boiling region relative to VIPRE-01M, which does account for fluid cross-flow. The ANC power peaking therefore is larger relative to the open channel hydraulic model. As a result, it is more conservative to evaluate DNBRs based on the combination of ANC power distribution and VIPRE-01M fluid density distributions without an iterative process."* The applicant also presented results from an iterative calculation using ANC and VIPRE-01M and stated that the calculation showed that the converged solution gives a MDNBR which is greater than that given by the initial calculation. The results do not provide adequate information to support the applicant's position. More importantly, even if the hypothesis advanced by the response is true, it does not address the issue of whether the local power factors are converged. MDNBR is not the only SAFDL that should be evaluated; the fuel centerline melt (FCM) SAFDL must be evaluated.

That evaluation requires that the local power distribution be accurately determined. That determination can only be assured by insuring convergent power and density distributions in ANC and VIPRE-01M. RAI MSLB-16-1 and RAI-6 requested for additional information regarding the iterative study done by the applicant.

In its response to MSLB-16-1 [Ref. 43], the applicant supplied the axial power profile, F_q , location of F_q , axial void distribution, and MDNBR for each of [(Proprietary information withheld under 10 CFR 2.390)

] than the converged MDNBR value. In its response to RAI-6 [Ref. 46], the applicant provided a detailed explanation of the data transfers between VIPRE-01M and ANC. Based on these responses, the staff finds that there is reasonable assurance that the MDNBR and F_q values calculated by the applicant's methodology, with no iteration between VIPRE-01M and ANC, is conservative. Therefore the staff finds the data transfer procedure acceptable and RAIs MSLB-16, MSLB-16-1, and RAI-6 are resolved.

A complete transient evaluation methodology requires the evaluation of all relevant SAFDLs, not just MDNBR. Therefore, RAI MSLB-18 requested the applicant provide an evaluation of the fuel centerline temperature relative to its SAFDL and to address the possibility of fuel failure due to PCMI. In its response to RAI MSLB-18 [Ref. 43], the applicant provided the requested analyses. The fuel centerline temperature analysis showed that the calculated centerline temperature was far below the SAFDL value for the limiting MSLB case. The PCMI analysis showed the prompt fuel enthalpy [(Proprietary information withheld under 10 CFR 2.390)] MSLB case, even when very conservative assumptions were made for reactivity insertion rates and local peaking factors. Because of the large margin between the calculated fuel centerline temperature and prompt fuel enthalpy rise and their respective SAFDL limits, the staff finds that the applicant's MSLB methodology does not need to be supplemented to include the evaluation of these two safety parameters.

In RAI MSLB-19 [Ref. 43], the staff asked which DNBR correlation was used for the MSLB, LOOP analysis (i.e., low pressure and flows) and was the correlation within its applicable range during LOOP plant event. In its response to RAI MSLB-19, the applicant stated that the W-3

DNB correlation was used for the MSLB HZP LOOP case. Information to support the use of the W-3 correlation for the low mass flux calculated for this MSLB case was also presented. This supporting information demonstrated that the W-3 correlation exhibited no anomalous behavior when it was compared to CHF data with mass fluxes below the lower limit of $1360 \text{ kg/m}^2\text{-s}$ ($1 \times 10^6 \text{ lbm/hr-ft}^2$) of the W-3 correlation. The applicant also noted that the HZP pumps-off case is bounded by the HZP pumps-on case, having a peak power which is less than half of what is calculated for the limiting MSLB case. The low heat flux and high subcooling calculated for the HZP pumps-off case make the occurrence of DNB unlikely. The staff finds the use of the W-3 DNB correlation acceptable for the MSLB HZP pumps-off case. The applicant has adequately demonstrated that the correlation gives a reasonable estimate of the DNBR for the low flow condition observed in that case and the response to RAI MSLB-19 is acceptable.

In summary, the staff reviewed the application of the Non-LOCA methodology and the results of the sample calculations of the Steam System Piping Failure event. The staff's review focused on fluid mixing in the RV, core power distribution, reactivity weighting and feedback, boron injection and transport, and DNB modeling. For the reasons discussed in the above paragraphs, the staff finds the applicant's revised Non-LOCA methodology acceptable for evaluating the US-APWR Steam System Failure event.

5.2.5 Feedwater System Pipe Break

The applicant presented the specific analysis methodology and a sample analysis for this event in Sections 5.5 and 6.5, respectively, of the topical report.

The Feedwater Line Break (FWLB) event is a postulated accident and is defined as a major break in a feedwater pipe. Like the SLB, it induces asymmetric thermal hydraulic conditions into the RCS. The FWLB event can be a heat-up event, a cool-down event, or a combination of both. The FWLB as a cooldown event is bounded by the SLB event; therefore, the FWLB is analyzed as a heat-up event and analysis conditions are biased appropriately. The SLB event bounds the FWLB cooldown event because it retains liquid inventory in the SG secondary side longer.

The limiting FWLB heat-up event is a double-ended rupture between the SG feedwater nozzle and the last feedwater line check valve.

The following RPS trips are available to automatically trip the reactor and help mitigate the FWLB event:

- SG water level low trip in any loop
- Pressurizer pressure high trip (not credited)
- Pressurizer level high trip (not credited)

The following engineered safeguard features are assumed to be available to mitigate an FWLB:

- EFWS actuation, automatic
- EFWS isolation
- SI

The FWLB is modeled in MARVEL-M using the assumption that the main feedwater flow stops at the initiation of the transient. This results initially in a slow heat-up of the RCS. When the low

SG level setpoint is reached, the reactor trip signal is generated. Simultaneously, a double-ended guillotine break of the feedwater line and LOOP are assumed to occur. Break flow is assumed to be only saturated water and is computed using the Moody model [Ref 56]. These two assumptions maximize the removal of liquid from the SG and cause a conservatively-rapid loss of SG heat removal capability for the affected SG. EFW is assumed not to be available because it is automatically isolated due to a low SG pressure signal. The check valve in the affected SG steam line isolates the affected SG from the rest of the steam system.

The FWLB analysis is used to evaluate the peak RCS pressure; therefore, RCS initial conditions (core power, initial RCS pressure and temperature) and core parameters (reactivity feedback coefficients, decay heat) are selected to maximize RCS pressure. The staff reviewed the input for the FWLB sample problem and confirmed that the initial conditions listed were biased to maximize RCS pressure.

RAI 6.5-1 questioned the procedure of performing the FWLB analysis using the assumption that the main feedwater flow stops at the initiation of the event (which leads to an occurrence of an SG low level trip). It asked if the pressurizer water volume was sensitive to perturbations in this assumption. In its response [Ref. 19], the applicant stated that the procedure used is conservative in that it reduces the SG inventory available to cool down the primary system when the break opens and results in a slow heat up of the primary prior to opening of the break. This latter feature causes an in-surge into the pressurizer. Therefore, the procedure is conservative relative to maximizing the pressurizer liquid volume during the event.

RAI FWLB-1 asked if a break spectrum study had been completed. In its response to RAI FWLB-1 [Ref. 36], the applicant stated that a break spectrum had not been conducted because smaller breaks are bounded by the case presented, which is a double-ended rupture of the feedwater line. Smaller breaks would result in a slower reduction in the affected steam generator's heat removal capability and therefore less of a heat up of the primary system. The applicant's disposition of smaller breaks is reasonable.

The applicant's FWLB analysis assumes LOOP occurs coincident with the break occurrence. RAI FWLB-2 requested more information regarding the sensitivity of the analysis to LOOP timing. In its response [Ref. 36], the applicant stated that the requested information had already been submitted in its response to Question 15.0.0-3 of RAI 297-2287 [Ref. 48], and showed that assuming a minimum time delay resulted in the most severe results. The relevant RAI response was evaluated during the Chapter 15 DCD FWLB analysis and found acceptable.

In RAI 5.5-1, the applicant was asked if the FWLB transient analysis was sensitive to the timing of the transition to natural circulation and if the core flow mixing factors were the same for the forced flow and natural circulation regimes. In its response [Ref. 19], the applicant stated that there is no explicit model to transition from forced flow to natural circulation. As the RCPs coast down, the gravity head terms in the MARVEL-M flow equations increase in importance relative to the RCP head terms. Thus, the transition to natural circulation is built into the MARVEL-M numerical solution. With respect to mixing factors, the same mixing factors (FMXI and FMXO) are used for all flow conditions. The applicant asserted that the mixing in the upper and lower plena would be near perfect during natural circulation conditions. In its response to RAI 5.5-2 [Ref. 21], the applicant provided a sensitivity study to examine the effect of the mixing factor values on the FWLB results. Two sensitivity calculations were conducted. One had the inlet mixing factor value decreased by 10 percent; the second had the inlet mixing factor value increased by 10 percent. The applicant compared the results from the sensitivity calculations to

the base case simulation. The comparison showed that the ± 10 percent variation in the inlet mixing factor value had a negligible effect upon the RCS pressure response and the pressurizer water level response. The response is acceptable because it demonstrates the insensitivity of the key safety parameters to modest changes in the value of the inlet mixing factor used in the FWLB analysis.

The methodology for FWLB assumes that EFW is supplied to only two of the four SGs¹. Therefore, after the RCPs coast down, two of the loops (1 and 2) will stagnate and the other two (3 and 4) will remove core heat via natural circulation. Under these circumstances there will be little mixing between the fluids in the flowing and stagnant loops. The core inlet temperature will be nearly the same as the cold leg temperature of the flowing loops. An examination of the MARVEL-M simulation shows that the loop flows in all loops are nearly the same throughout the FWLB simulation. The difference between the hot and cold leg temperatures in the affected loop is zero for times greater than 1500 s, while the difference between the hot and cold leg temperatures in Loop 4 is [(Proprietary information withheld under 10 CFR 2.390)] percent of nominal. There is no apparent driving force for the flow in Loop 1.

The applicant selected the failure of an EFWS as the limiting single failure for the FWLB analysis. RAI FWLB-4 asked why the possibility of one EFWS being out of service for maintenance was not considered in the analysis. In its response [Ref. 43], the applicant explained that the US-APWR Technical Specifications (TS) require the EFW systems to be cross-tied if any one system is out for maintenance. Consequently, assuming a system out of service means that EFW is available to all SGs. Assuming all systems are in service means that the systems are not cross-tied. In this case, one EFW is lost due to the break and another is lost to an assumed single failure. EFW is therefore available to only two of the SGs. This is a more limiting condition than EFW available to all the SGs. Therefore the failure of an EFWS as the limiting single failure assumption for FWLB analysis is acceptable.

The MARVEL-M FWLB simulation shows that all four reactor loops have nearly the same flow after the RCPs have coasted down. This appears to be non-physical behavior since only two of the loops have primary-to-secondary heat transfer. One expects natural circulation to be established in these two loops only – flows in the other two loops should stagnate. RAI FWLB-5 requested an explanation of the MARVEL-M calculated loop flows. In its response [Ref. 43], the applicant stated that some flow would be expected in each of the four reactor loops because of the density difference between the fluid in the RPV downcomer and the core. It further stated that the loop flows would be greater in the loops with SG heat transfer if the length of the SG tubes were considered. [

(Proprietary information withheld under 10 CFR 2.390)

]. This is acceptable because the FWLB analysis is conservative with respect to pressurizer overfill.

¹ Automatic EFW isolation in the affected SG (Loop 1) and EFW lost to one intact SG (Loop 2) due to single failure.

In summary, the staff reviewed the application of the Non-LOCA methodology and the results of the sample calculations of the Feedwater System Pipe Break event. The staff's review focused on trip setpoints, systems assumed available and unavailable, break modeling and fluid mixing. The staff finds the Non-LOCA methodology acceptable for evaluating the US-APWR Feedwater System Pipe Failure event.

5.2.6 Steam Generator Tube Rupture

The applicant presented the specific analysis methodology and a sample analysis for this event in Sections 5.6, "Steam Generator Tube Rupture," and 6.6, "Steam Generator Tube Rupture," respectively, of the topical report.

The SG tube rupture (SGTR) event is postulated as the complete severance of one SG tube. The rupture causes reactor coolant to flow into the SG secondary side. The largest break flow occurs when the rupture occurs at the tube sheet on the cold leg side of the SG tube. Since the primary system water may be radioactive, the event may cause a radiation release to the steam system and potentially to the atmosphere. Radiation detectors in the steam lines alert the operator to the occurrence of a SGTR. The operator may manually scram the reactor, but a substantial period of time, usually at least 30 minutes, is assumed to pass before this action is credited.

The following signals are available to automatically trip the reactor:

- Over temperature delta-T high trip (not credited)
- Pressurizer pressure low trip
- SG water level high-high trip

The following engineered safeguard features are assumed to be available to mitigate a SGTR:

- EFWS actuation
- EFWS isolation
- SI

The SGTR event ultimately is mitigated by operator action. The operator identifies and isolates the affected SG by closing its main steam and main feedwater isolation valves. Next the operator terminates the leak flow by equalizing the RCS and affected SG secondary pressures and terminating ECCS flow. The pressure equalization is accomplished by reducing the RCS temperature (and hence the RCS pressure) through cycling the intact SG relief valves and by reducing the RCS pressure through cycling the pressurizer relief valves.

Two cases are analyzed, one to evaluate the maximum steam release to the atmosphere and a second to evaluate SG overfill. In the steam release case the EFWS train to the affected SG is assumed to fail (limiting single failure) because that increases the steam release through the affected SG safety and relief valves. Additionally, a secondary relief valve is assumed to stick open after it automatically opens. The steam release through this stuck open valve is assumed to be terminated by automatic closure of the associated block valve.

For the SG overflow case the main feedwater is isolated by the high-high steam generator water level trip signal and EFW is assumed to remain available to the affected SG for a conservative length of time.

The MARVEL-M computer code is used to simulate the plant transient response to a SGTR from inception to the time of RCS/SG secondary pressure equalization. The staff evaluation therefore is focused on the ability of MARVEL-M to adequately perform that analysis. Two specific MARVEL model features, important to the SGTR simulation, are the SG tube break flow model and the model for simulating flashing in the upper head of the reactor pressure vessel.

In Appendix F of the Topical report, the applicant claims that the break flow rate to the secondary side is conservatively calculated by first calculating the break flow based upon the initial pressures in the primary and secondary systems. The transient break flow is then computed by multiplying the initial break flow by the square root of the ratio of the transient primary-to-secondary pressure difference to the nominal primary-to-secondary pressure difference. The initial break flow is calculated using the Zaloudek correlation [Ref. 49] with C=1.0 instead of 0.95. The Zaloudek correlation is

$$G = C \sqrt{2g\rho(p_{up} - p_{sat})},$$

where G is the critical mass flux, C is a discharge coefficient, 0.95, g is the gravitational constant, ρ is the saturated liquid density, P_{up} is the upstream pressure, and P_{sat} is the saturation pressure. Several RAIs were submitted to determine exactly how the initial critical flow is calculated for the SGTR event.

In its response to RAI App.F-1 [Ref. 19], the applicant presented the equation used to compute the initial break flow. A modified version of the Zaloudek correlation was used, not the original Zaloudek correlation. Zaloudek's correlation uses the upstream stagnation pressure as a key parameter. The applicant's modification replaces the upstream stagnation pressure by the pressure at the break. The applicant provided no justification for its modification of Zaloudek's correlation. Therefore, RAI App.F-1-1 [Ref. 22] asked the applicant to provide validation for the "modified Zaloudek" correlation. In its response to RAI App.F-1-1 [Ref. 22], the applicant noted that it had compared MARVEL-M to an actual SGTR event as a MARVEL-M validation, described in response to RAI 3.1-6. In order to get MARVEL-M to accurately simulate the measured [(Proprietary information withheld under 10 CFR 2.390)] for the MARVEL-M validation. Since it is using a value of 1.0 in its US-APWR SGTR analysis, the applicant stated that the break flow for that analysis is conservative. The staff did not agree as a smaller value of the discharge coefficient may have been needed in the plant SGTR simulation because of break geometry (i.e., not a double-ended break). A discharge coefficient of 1.0 would be appropriate for the double-ended break SGTR licensing analysis and hence the applicant had not demonstrated its break flow calculation is conservative.

In its response to RAI SGTR-6 [Ref. 43], the applicant attempted to justify using the pressure at the break instead of the upstream pressure in the Zaloudek correlation. The applicant cited experimental data showing that critical flow decreases with an increase in the length-to-diameter ratio (L/D) of the discharge tube. The staff agreed with this observation but did not agree with the applicant's contention that this observation justifies the use of the break pressure instead of the upstream pressure for the Zaloudek correlation.

The staff conducted independent calculations of the SGTR event using RELAP5/MOD3.3. It also reviewed SGTR simulations for operating plants. The staff's investigation showed total calculated initial break flows lie between 18 and 29 kg/s (40 and 66 lbm/s) for the SGTR event. The 29 kg/s value corresponds to the rupture of a tube with a flow area 1.36 times larger than a US-APWR SG tube. Dividing the 29 kg/s value by 1.36 yields 21.3 kg/s (47.0 lbm/s). The staff therefore concludes that the applicant's value of 25 kg/s (55 lbm/s) for the initial break flow in the SGTR event for the US-APWR is reasonable and acceptable.

In Appendix F, "Detailed Break Flow Model for Steam Generator Tube Rupture" of the Topical report, a comparison of the integrated break flow from the above equation is compared to what is called a realistic break flow calculation. The realistic calculation accounts for the pressure loss along SG tube from the hot side to the break. It is shown that the break flow as calculated in MARVEL-M is always greater than the realistic break flow.

If the pressure in the primary system drops sufficiently and the inventory loss is sufficient to empty the pressurizer, the RV upper head may flash. RAI 5.6-1 asked if upper head flashing could affect RV upper or lower plenum mixing. In its response [Ref. 19], the applicant stated that no upper head flashing occurred in the SGTR simulation.

The applicant further explained that if flashing were to occur in the upper head it would have no impact on MARVEL-M upper plenum mixing calculations because the flow from the upper plenum would flow equally to each of the four upper plenum nodes. Lower plenum mixing would also be unaffected since upper plenum flashing would only increase loop flows and the lower plenum mixing model is independent of loop flows. The staff agrees with the applicant's assessment of the effect of RV upper head flashing on the fluid mixing calculated for the upper and lower plena.

The SGTR methodology assumes manual reactor trip at 900 seconds. RAI 6.6-1 asked for the basis for choosing 900 seconds and if the transient results would be different if the time of trip were changed. In its response [Ref. 19], the applicant responded that in the event of an SGTR the PCMS [plant control and monitoring system]-based N-16 radiation alarm will sound within two minutes and prompt the operator to trip the reactor. Therefore, the 900 second time being assumed in the analysis is a significantly conservative assumption. The applicant stated that the response time assumed will be verified to be conservative during operator training. The staff concludes that an assumption of 900 seconds for the operator to initiate reactor trip is conservative.

In summary, the staff reviewed the application of the Non-LOCA methodology and the results of the sample calculations of the SGTR event. The staff's review focused on the tube rupture break flow model, RV upper head flashing and fluid mixing and the timing of the assumed operator action to manually trip the reactor. The staff finds the applicant's Non-LOCA methodology acceptable for evaluating the US-APWR SGTR event.

5.3 Independent Analyses

The staff conducted Non-LOCA simulations for the US-APWR using both the RELAP5/MOD3.3 and MARVEL-M codes. These simulations provided independent verification that analysis conservatisms being claimed by the applicant were indeed conservative. To support these independent analyses, the applicant provided the MARVEL-M input files, instructions for obtaining plotted output from MARVEL-M, and a detailed summary of the SLB, loss of load (LOL) and SGTR input files in its responses to RAI-1, RAI-2, RAI-3, and RAI-4 [Ref. 50].

5.3.1 RELAP5/MOD3.3 Simulations

The following Chapter-15 Non-LOCA events were simulated using RELAP5/MOD3.3 (R5M33) and are documented in Technical Report ISL-NSAO-TR-10-01, "US-APWR Non-LOCA RELAP5/MOD3.3 Confirmatory Runs," [Ref. 25]:

- LOL, US-APWR DCD Tier 2 Section 15.2.1, minimum departure from nucleate boiling ratio (MDNBR) and primary system overpressure cases
- SGTR, US-APWR DCD Tier 2 Section 15.6.3, maximum radiological release case
- MSLB, US-APWR DCD Tier 2 Section 15.1.5, HZP with offsite power available.

The LOL cases and the SGTR case used a RELAP5/MOD3.3 base model that independently represents the four US-APWR reactor coolant loops. The RV is modeled with a single downcomer flow channel, and the lower plenum, upper plenum, and upper head. The core model consists of two regions: one representing a hot assembly, and the other representing the remaining assemblies. For the MSLB simulations the RELAP5/MOD3.3 base model was modified so that each coolant loop had its own corresponding RV quadrant. Mixing between the quadrants at the upper plenum and lower plenum was simulated using time-dependent junctions and the RELAP5/MOD3.3 control system model. The degree of mixing between the affected loop and the other loops was specified via user input mixing factors and could be varied from no mixing to perfect mixing. For comparisons to MARVEL-M, the mixing factors in the RELAP5/MOD3.3 model were specified to be the same as in the MARVEL-M model.

A more complete description of the RELAP5/MOD3.3 US-APWR models can be found in [Ref. 25].

LOL Confirmatory Analysis

For the LOL event, the RELAP5/MOD3.3 LOL confirmatory runs showed good agreement with the MARVEL-M results presented in the US-APWR DCD. The MDNBR calculated by MARVEL-M was lower than that calculated by RELAP5/MOD3.3, as shown in Figure 1 below. The peak RCS pressure calculated by MARVEL-M was higher than that calculated by RELAP5/MOD3.3, as shown in Figure 2 below. The timing of events and the transient responses of key variables with RELAP5 were very similar to those calculated with MARVEL-M, as shown in Table 2 below. The RELAP5/MOD3.3 LOL confirmatory runs show that MARVEL-M results in the US-APWR DCD Tier 2 are conservative.

Table 2 Sequence of Events for Loss of Load MDNBR Case.

Event	DCD	R5M33
	Time (s)	
Turbine trip, loss of main feedwater flow.	0.0	0.0
High pressurizer pressure signal.	6.7	6.3
Reactor trip initiated.	8.5	8.0
Pressurizer safety relief valves open.	8.6	8.6
MDNBR occurs.	9.5	0.0*
Main steam safety valves open.	9.7	10.0

Event	DCD	R5M33
	Time (s)	
Peak RCP outlet pressure occurs.	10.3	10.3
Peak main steam system pressure occurs.	14.3	15.0

* MDNBR of 2.013 occurs at time 0.0 s. Secondary MDNBR of 2.082 occurs at 9.7 s.

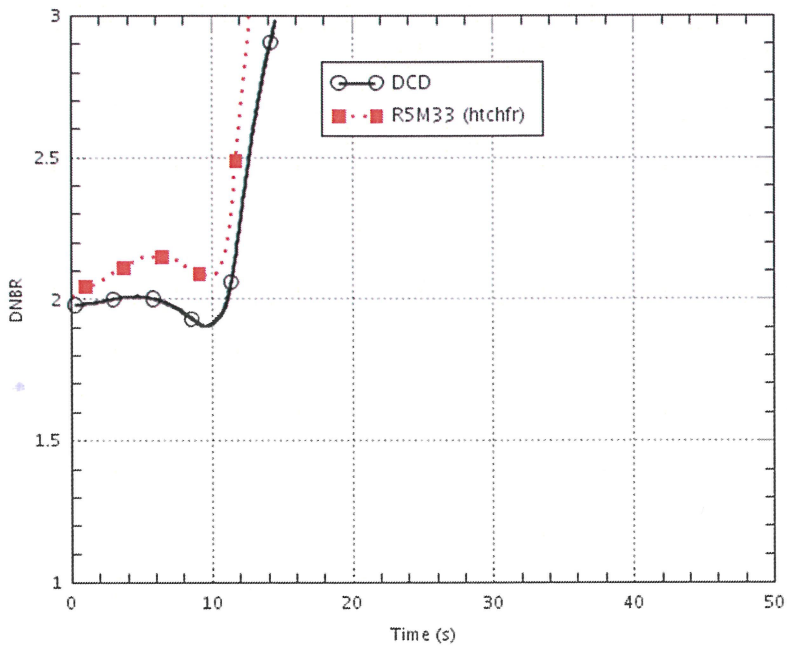


Figure 1 MDNBR for the LOL Cases

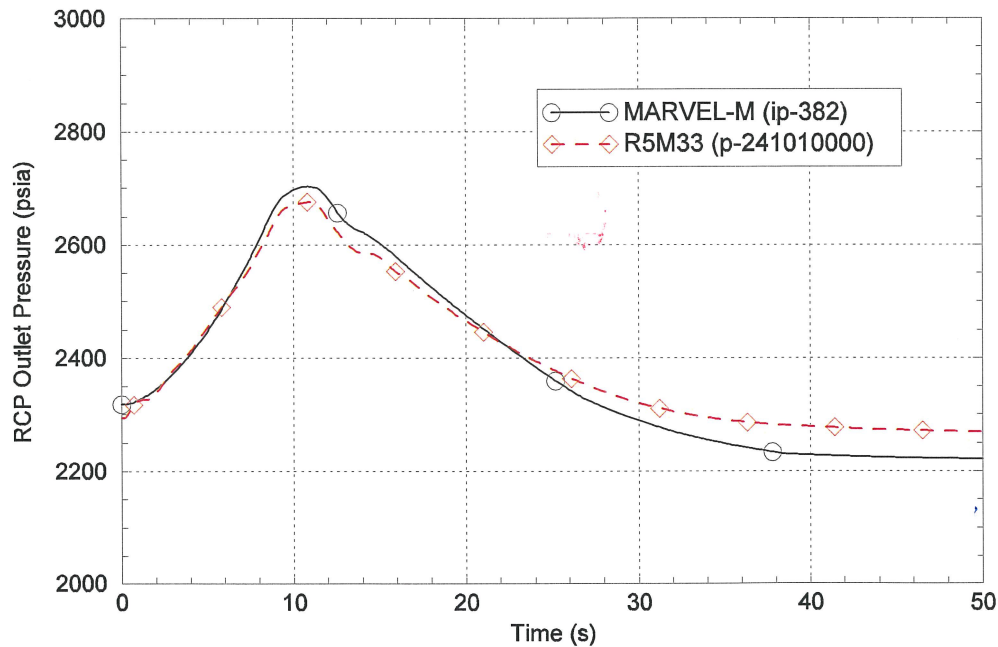


Figure 2 Peak Pressure for the LOL Overpressure Cases

SGTR Confirmatory Analysis

For the SGTR event comparison to MARVEL-M, the RELAP5/MOD3.3 SGTR simulation's break flow was adjusted to be in reasonable agreement with that calculated by MARVEL-M. Assumed operator actions and equipment failures were identical in the two simulations.

Thus, the goal of the confirmatory calculation was to see if MARVEL-M and RELAP5/MOD3.3 would give similar results when given the same initial and boundary conditions. Table 3 and Figure 3 through Figure 5 below show that the two codes provide similar results.

Regarding the results of the RELAP5/MOD3.3 SGTR confirmatory calculations, it is stated in the Staff's confirmatory analysis, ISL-NSAO-TR-10-01 [Ref. 25], that "*Considering the complexity of the SGTR radiological dose evaluation case event scenario and the significant differences between the plant modeling approaches and computer codes employed, the R5M33 and DCD calculations agree remarkably well.*" Based on this assessment it is reasonable to conclude MARVEL-M is capable of simulating the SGTR event.

Table 3 Calculated Sequences of Events for SGTR Radiological Dose Evaluation Case

Event	MARVEL-M	R5M33
	Time (s)	
Double-ended rupture of single tube in SG B.	0	0
Manual reactor trip. Scram rod insertion begins. Loss of offsite power assumed.	900	900
Reactor coolant pump power tripped.	900	900
Main feedwater isolation.	900	900
Turbine trip.	900	900
Affected SG B isolated (MSIV closed).	1,200	1,200
Initiation of RCS cooling by the operator. Operator opens MSDVs on intact SG A and intact SG C.	1,500	1,500
MSRV on affected SG B assumed to stick open.	1,500	1,500
Safety injection actuation signal. CVCS and letdown flows terminated. ECCS (HPI) flow initiated.	1,634	1,648
EFW flows initiated to intact SG A and intact SG C.	1,774	1,788
Operator assumed to isolate the flow through the stuck-open MSRV on affected SG B by closing the block valve.	1,826	1,820
Operator assumed to open the pressurizer SDV to depressurize the RCS.	2,717	2,717
RCS subcooling exceeds 50°F, operator closes MSDVs on intact SG A and intact SG C.	2,819	2,816
Operator assumed to close the pressurizer SDV.	2,848	2,848
Operator assumed to terminate ECCS flow.	2,880	2,880
RCS subcooling falls below 50°F, operator reopens MSDVs on intact SG A and intact SG C and they remain open thereafter.	3,117	3,000
Flow through the ruptured tube in SG B terminated	4,183	6,811
Calculation ended.	6,000	8,000

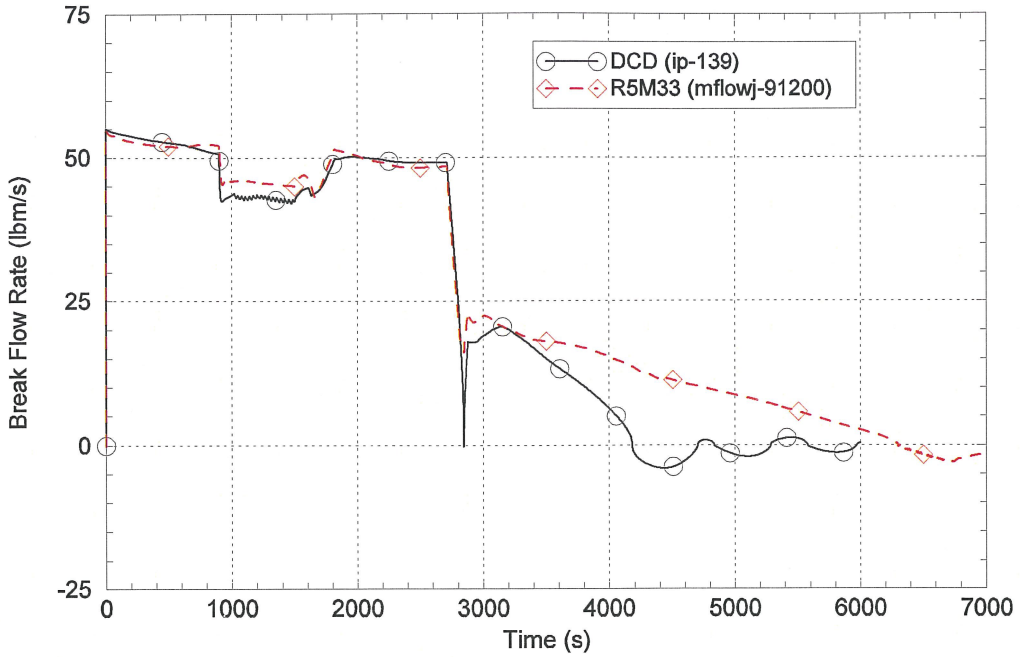


Figure 3 SGTR Event - Break Flow

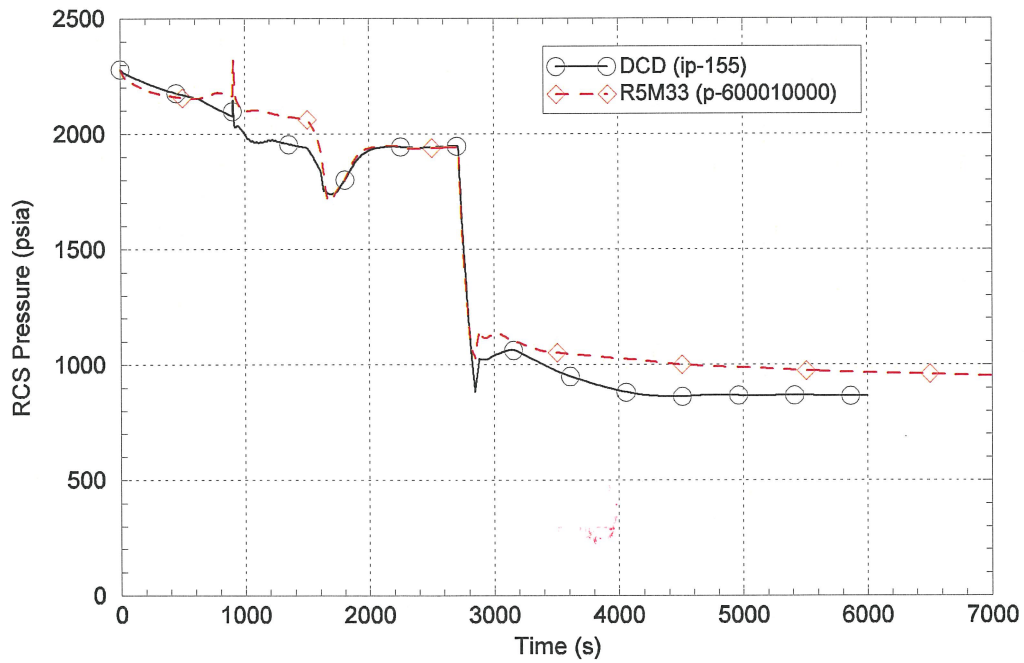


Figure 4 SGTR Event - Pressurizer Pressure

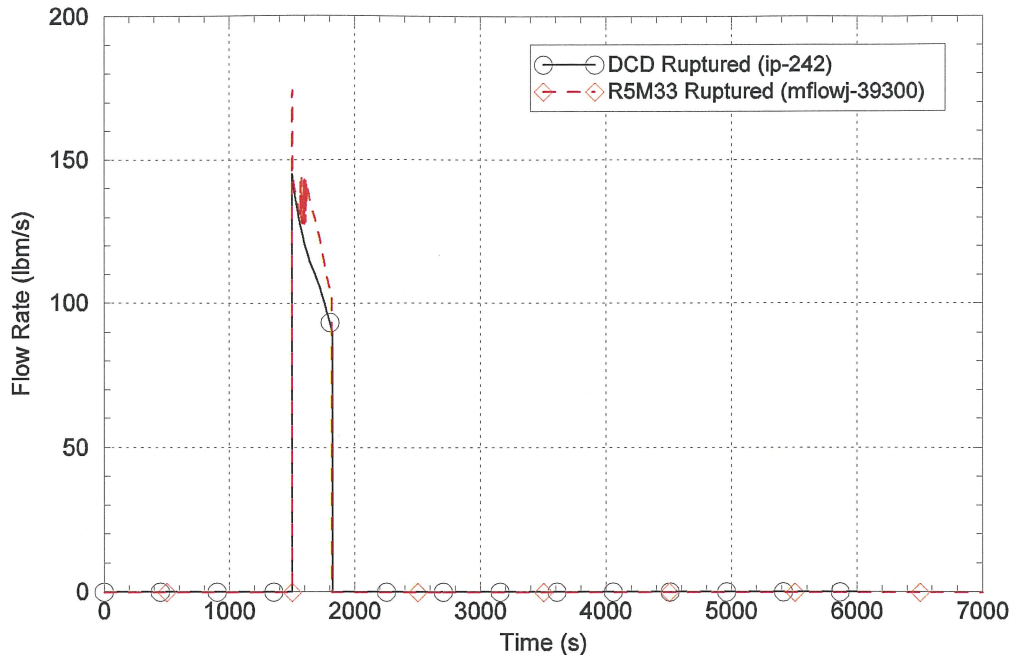


Figure 5 SGTR Event - Safety Valve Flow in Affected SG

MSLB Confirmatory Analysis

The RELAP5/MOD3.3 simulation of the HZP MSLB with RCPs running agreed closely with the MARVEL-M result. The main difference was that RELAP5/MOD3.3 calculated a slightly slower RCS pressure decline, as shown in Figure 6 below. This, in turn, caused SI injection to occur slightly later in the RELAP5/MOD3.3 calculation. In this MSLB event, the rise in core power is terminated by boron reaching the core; therefore, a delay in SI injection leads to a higher return to power. Whereas the US-APWR DCD Tier 2 calculation shows [(Proprietary information withheld under 10 CFR 2.390)], as shown in Figure 7 below. Technical Report ISL-NSAO-TR-10-01 [Ref. 25] does not identify a reason for the slight difference in the RCS pressure response with the two codes. A likely cause is that different models are used to compute the pressure in the pressurizer during a flow out-surge. This analysis demonstrates that the RELAP5/MOD3.3 MSLB confirmatory calculation is in good agreement with the corresponding MARVEL-M calculation in the DCD.

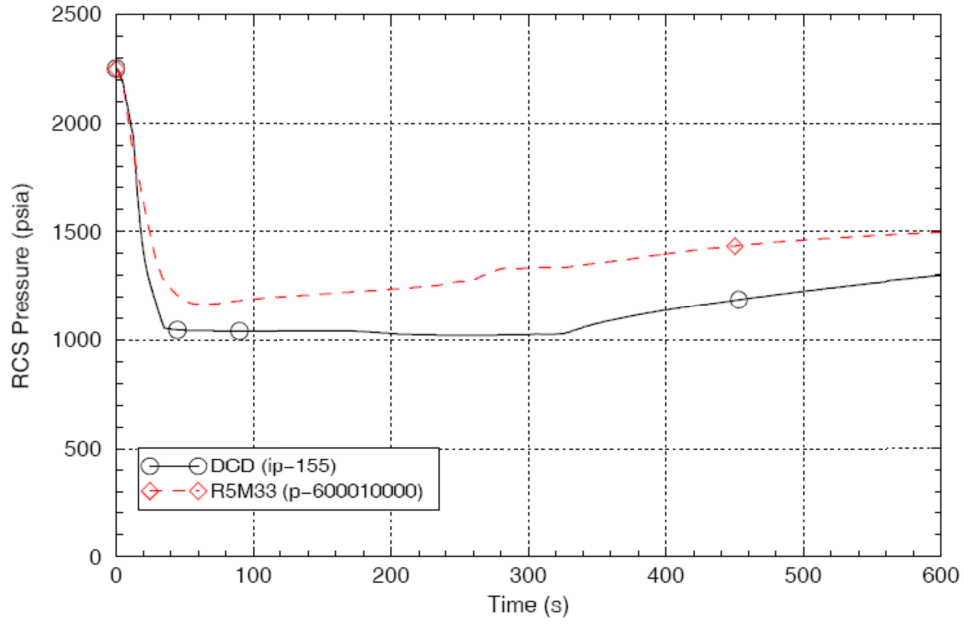


Figure 6 MSLB Event - RCS Pressure

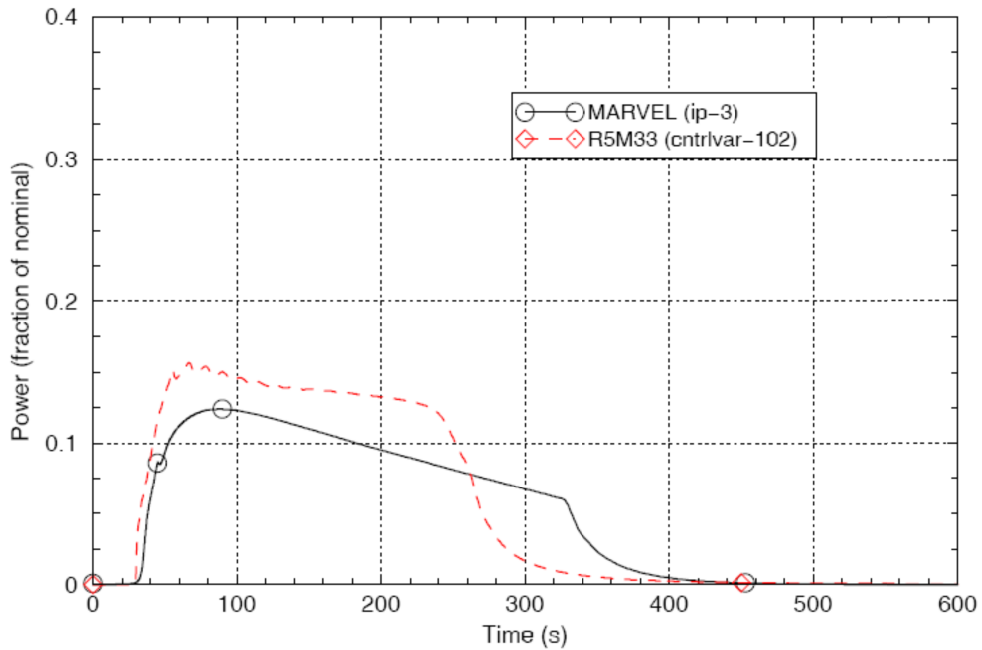


Figure 7 MSLB Event - Normalized Reactor Power

5.3.2 MARVEL-M Simulations

The staff also performed many independent MARVEL-M simulations using the code executable and DCD Chapter 15 analysis input files supplied by the applicant. These in-house calculations allowed the staff to examine the DCD analyses in much more detail than simply reviewing the information provided in the US-APWR DCD and the Non-LOCA methodology Topical report. It also assisted in the understanding of the input and modeling capabilities of MARVEL-M. These independent MARVEL-M calculations were an important part of the staff's review.

Complete Loss of Flow

Many MARVEL-M simulations of the CLOF event were conducted to perform a detailed examination of the code's conservation of mass and energy. Based on the results of the CLOF simulations, it was concluded that mass and energy were conserved in MARVEL-M.

FWLB

The US-APWR DCD FWLB simulation [

(Proprietary information withheld under 10 CFR 2.390)

] of conservatism in the calculated
pressurizer liquid volume.

(Figure 8 - Proprietary information withheld under 10 CFR 2.390)

Figure 8 FWLB Event - Liquid Volume in the Pressurizer

5.4 Appendix A - Review of the MARVEL-M computer code

A.0 Introduction

[(Proprietary information withheld under 10 CFR 2.390)

]

A.1 Neutron Kinetics Equation

A.1.1 Decay Heat and Fission Power

[(Proprietary information withheld under 10 CFR 2.390)

]

[(Proprietary information withheld under 10 CFR 2.390)

]

A.1.2 Reactivity Coefficient

[(Proprietary information withheld under 10 CFR 2.390)

]

[(Proprietary information withheld under 10 CFR 2.390)

]

A.2 Fuel Rod and Core Thermal Kinetics Equation

A.2.1 Fuel Thermal Model

[(Proprietary information withheld under 10 CFR 2.390)

[(Proprietary information withheld under 10 CFR 2.390)

]

A.2.2 Reactor Core Flow Model and Core Power Distribution

[(Proprietary information withheld under 10 CFR 2.390)

]

[(Proprietary information withheld under 10 CFR 2.390)

]

A.2.3 Hot Channel Fuel Thermal Model

[(Proprietary information withheld under 10 CFR 2.390)

]

[(Proprietary information withheld under 10 CFR 2.390)

]

A.2.4 DNBR Evaluation Model

[(Proprietary information withheld under 10 CFR 2.390)

]

A.3 Equations for Reactor Coolant Flow Sections

[(Proprietary information withheld under 10 CFR 2.390)

]

[(Proprietary information withheld under 10 CFR 2.390)

]

A.3.1 Reactor Core Coolant Thermal Kinetics Equation (HEAT)

[(Proprietary information withheld under 10 CFR 2.390)

]

A.3.2 Mixing Plenum Equation (MIXG)

[(Proprietary information withheld under 10 CFR 2.390)

]

[(Proprietary information withheld under 10 CFR 2.390)

]

A.3.3 Transport in Pipe (SLUG)

[(Proprietary information withheld under 10 CFR 2.390)

]

[(Proprietary information withheld under 10 CFR 2.390)

[(Proprietary information withheld under 10 CFR 2.390)

]

A.3.4 SG Primary Side Equation (HEEX)

[(Proprietary information withheld under 10 CFR 2.390)

]

A.3.5 Dead Volume (Reactor Vessel Head Volume) (MIXD)

[(Proprietary information withheld under 10 CFR 2.390)

]

A.3.6 Reactor Vessel Upper Plenum (MIXS)

[(Proprietary information withheld under 10 CFR 2.390)

]

A.3.7 Pressure Gradient in Reactor Coolant System

[(Proprietary information withheld under 10 CFR 2.390)

]

A.3.8 Thick Metal Effect

[(Proprietary information withheld under 10 CFR 2.390)

]

A.4 Mixing and Flow Model in Reactor Vessel

[(Proprietary information withheld under 10 CFR 2.390)

]

A.4.1 Mixing in the Downcomer, Reactor Vessel Lower Plenum and Upper Plenum

[(Proprietary information withheld under 10 CFR 2.390)

[(Proprietary information withheld under 10 CFR 2.390)

]

[(Proprietary information withheld under 10 CFR 2.390)

]

A.4.2 Core Bypass Flow

[(Proprietary information withheld under 10 CFR 2.390)

]

A.5 SG Model

[(Proprietary information withheld under 10 CFR 2.390)

]

A.5.1 Heat Transfer Coefficient

[(Proprietary information withheld under 10 CFR 2.390)

]

[(Proprietary information withheld under 10 CFR 2.390)

A.5.2 SG Water Level]

[(Proprietary information withheld under 10 CFR 2.390)

[(Proprietary information withheld under 10 CFR 2.390)

]

A.5.3 Heat Transfer Area

[(Proprietary information withheld under 10 CFR 2.390)

]

A.5.4 SG Secondary-Side Thermal Kinetics Equation

[(Proprietary information withheld under 10 CFR 2.390)

]

A.5.5 Other Special Models

[(Proprietary information withheld under 10 CFR 2.390)

]

[(Proprietary information withheld under 10 CFR 2.390)

]

A.6 Pressurizer

[(Proprietary information withheld under 10 CFR 2.390)

]

A.6.1 Water Phase Model

[(Proprietary information withheld under 10 CFR 2.390)

]

[(Proprietary information withheld under 10 CFR 2.390)

]

A.6.2 Steam Phase Model

[(Proprietary information withheld under 10 CFR 2.390)

[(Proprietary information withheld under 10 CFR 2.390)

]

A.6.3 Pressurizer Pressure Control

[(Proprietary information withheld under 10 CFR 2.390)

[(Proprietary information withheld under 10 CFR 2.390)

]

A.7 Transient Flow Performance

[(Proprietary information withheld under 10 CFR 2.390)

]

A.7.1 Reactor Coolant Pump Models and Flow Transient

[(Proprietary information withheld under 10 CFR 2.390)

]

[(Proprietary information withheld under 10 CFR 2.390)

]

[(Proprietary information withheld under 10 CFR 2.390)
]

A.7.2 Natural Circulation Model

[(Proprietary information withheld under 10 CFR 2.390)

]

A.7.3 Approximated Analytical Solution of Flow Coast-Down

[(Proprietary information withheld under 10 CFR 2.390)

]

A.8 Secondary Steam System Model

[(Proprietary information withheld under 10 CFR 2.390)
]

A.8.1 Distribution of Steam Flow

[(Proprietary information withheld under 10 CFR 2.390)

]

[(Proprietary information withheld under 10 CFR 2.390)

]

[(Proprietary information withheld under 10 CFR 2.390)

]

A.8.2 Steam Relief and Safety Valves

[(Proprietary information withheld under 10 CFR 2.390)

]

A.8.3 Steam Turbine Flow

[(Proprietary information withheld under 10 CFR 2.390)

]

A.9 Engineered Safeguards Features

[(Proprietary information withheld under 10 CFR 2.390)

]

A.10 Reactor Coolant System Small Break or Leak

[(Proprietary information withheld under 10 CFR 2.390)

]

A.11 Reactor Control System

[(Proprietary information withheld under 10 CFR 2.390)

]

A.12 Chemical Volume Control System

[(Proprietary information withheld under 10 CFR 2.390)

]

A.13 Reactor Protection System and ESFAS

[(Proprietary information withheld under 10 CFR 2.390)

]

A.14 Realistic Models - Descriptions and Model

[(Proprietary information withheld under 10 CFR 2.390)

]

A.15 Specific Computation Techniques

[(Proprietary information withheld under 10 CFR 2.390)

]

[(Proprietary information withheld under 10 CFR 2.390)

]

A.16 Appendix A References

- A1. "MARVEL-M A Digital Computer Code for Transient Analysis of a Multi-Loop PWR System," GEN0-LP-480 (R12), October 5, 2010, ADAMS Accession Number ML102850707
- A2. MARVEL-M A Digital Computer Code for Transient Analysis of a Multi-Loop PWR System," GEN0-LP-480 (R6), March 23, 2009, ADAMS Accession Number ML091050123
- A3. T. Hakata, "MARVEL – A Digital Computer Code for Transient Analysis of a Multi-loop PWR System," WCAP-7635, Westinghouse Electric Corporation, March 1971.
- A4. UAP-HF-09358, Docket No. 52-021, "MHI's 5th Response to NRC's Requests for Additional Information on US-APWR Topical Report MUAP-07010-P, Non-LOCA Methodology," July 2010. ADAMS Accession Number ML091980286.
- A5. UAP-HF-10001, Docket No. 52-021, "MHI's 6th, 7th and 8th Responses to NRC's Requests for Additional Information on MARVEL-M Theory Manual GEN0-LP-480 and US-APWR Topical Report MUAP-07010-P, Non-LOCA Methodology," January 2010. ADAMS Accession Number ML100140146.
- A6. UAP-HF-09040, Docket No. 52-021, "MHI's 4th Response to NRC's Request for Additional Information on US-APWR Topical Report MUAP-07010-P, Non-LOCA Methodology," February 2009. ADAMS Accession Number ML090490842.
- A7. UAP-HF-10101, Docket No. 52-021, "MHI's 9th and 10th Responses to NRC Requests for Additional Information on MARVEL-M Theory Manual GEN0-LP-480 and US-APWR Topical Report: Non-LOCA Methodology," MUAP-07010-P (R0)," April 2010. ADAMS Accession Number ML101480303.
- A8. UAP-HF-08245, Docket No. 52-021, "MHI's 3rd Response to NRC's Request for Additional Information on US-APWR Topical Report MUAP-07010-P, Non-LOCA Methodology," November 12, 2008. ADAMS Accession Number ML083190141-2.
- A9. UAP-HF-08141, Docket No. 52-021, "MHI's Response to NRC's Request for Additional Information on US-APWR Topical Report MUAP-07010-P, Non- LOCA Methodology," August 22, 2008. ADAMS Accession Number ML082400136.
- A10. UAP-HF-08115, Docket No. 52-021, Transmittal of MUAP-07022-P, "Reactor Vessel Lower Plenum 1/7 Scale Model Flow Test Report," June 30, 2008. ADAMS Accession Number ML081850466.
- A11. UAP-HF-08170, Docket No. 52-021, "MHI's 2nd Response to NRC's Request for Additional Information on US-APWR Topical Report MUAP-07010-P, Non-LOCA Methodology," September 2008. ADAMS Accession Number ML082600089.
- A12. UAP-HF-10226, Docket No. 52-021, "MHI's 12th Response to NRC's Requests for Additional Information on US-APWR Topical Report: Non-LOCA Methodology," MUAP-07010-P (R0), August 2010. ADAMS Accession Number ML102240215.

- A13. F. H. Clark, et al., "Review of LOFTRAN, Thermal-Hydraulic Code for Nuclear Power Plants," ORNL TER, September 24, 1982. ADAMS Accession No. 8210010258.
- A14. "RELAP5/MOD3.3 Code Manual Volume III: Developmental Assessment Problems," NUREG/CR-5535/Rev 1, December 2001.
- A15. "US-APWR Topical Report Non-LOCA Methodology," MUAP-07010-P (R2), August 31, 2011, UAP-HF-11277. ADAMS Accession Number ML11255A272.
- A16. "Summary of the July 13 - 14, 2010, Public Meeting With Mitsubishi Heavy Industries, Ltd. to Discuss the Open Items Remaining from the Review of the Non-Loss-Of-Coolant Accident Topical Report MUAP-07010, and the MARVEL-M Computer Code," August 12, 2010. ADAMS Accession Number ML102000239.
- A17. H.G. Hargrove, "FACTRAN-A Fortran IV Code for Thermal Transients in a UO₂ Fuel Rod," WCAP-7908-A, December 1989, ADAMS Accession Number ML080630436.

6.0 CONCLUSIONS, LIMITATIONS AND CONDITIONS

The staff concludes that the Non-LOCA methodology as described in MUAP-07010-P (R2), "Non-LOCA Methodology," is acceptable for analysis of the Non-LOCA design basis events described in Chapter 15 of the US-APWR Tier 2 DCD with the following restriction:

- Since MARVEL-M has not been qualified for simulating the discharge of liquid through the pressurizer safety and relief valves, the usage of MARVEL-M is restricted to events which only discharge steam through the pressurizer safety and relief valves.

The following condition applies to the staff approval of the MUAP-07010:

- The Non-LOCA methodology described in MUAP-07010 Revision 4 is acceptable provided that it includes an approved method to model detailed core sub-channel thermal-hydraulic conditions. For the US-APWR DC application, that method is based on VIPRE-01M as documented in MUAP-07009, "Thermal Design Methodology," which is under NRC review.

7.0 REFERENCES

1. "US-APWR Topical Report Non-LOCA Methodology," MUAP-07010-P (R0), July 2007, UAP-HF-07089. ADAMS Accession Number ML072150271.
2. "US-APWR Topical Report Non-LOCA Methodology," MUAP-07010-P (R1), October 29, 2010, UAP-HF-10294. ADAMS Accession Number ML103120250.
3. "US-APWR Topical Report Non-LOCA Methodology," MUAP-07010-P (R2), August 31, 2011, UAP-HF-11277. ADAMS Accession Number ML11255A272.
4. "US-APWR Design Control Document," Revision 3, March 2011, ADAMS Accession Number ML110980238.
5. "MARVEL-M A Digital Computer Code for Transient Analysis of a Multi-Loop PWR System," GEN0-LP-480 (R6), March 23, 2009, ADAMS Accession Number ML091050123.
6. "MARVEL-M A Digital Computer Code for Transient Analysis of a Multi-Loop PWR System," GEN0-LP-480 (R12), October 5, 2010, ADAMS Accession Number ML102850707.
7. Regulatory Guide (RG) 1.203 "Transient and Accident Analysis Methods," dated December 2005. ADAMS Accession Number ML053500170.
8. RG 1.206 "Combined License Applications for Nuclear Power Plants," dated June 2007, ADAMS Accession Number ML070630003.
9. NUREG-0800, "Standard Review Plan for the Review of Safety Analysis Reports for Nuclear Power Plants."
10. RG 1.70, "Standard Format and Content of Safety Analysis Reports for Nuclear Power Plants (LWR Edition)," November 1978. ADAMS Accession Number ML011340122.
11. "TWINKLE-M Input Manual," GEN0-LP-517 (R3), Mitsubishi Heavy Industries, Ltd., Revision 3, June 28, 2011, ADAMS Accession Number ML11195A049.
12. Y. Makino, et al., "Thermal Design Methodology," MUAP-07009-P, Mitsubishi Heavy Industries, Ltd., May 2007, ADAMS Accession Number ML071520271.
13. T. Hakata, "MARVEL – A Digital Computer Code for Transient Analysis of a Multi-loop PWR System," WCAP-7635, Westinghouse Electric Corporation, March 1971, ADAMS Accession Number ML080650322.
14. D. H. Risher and R. F. Barry, "TWINKLE – A Multi-Dimensional Neutron Kinetics Computer Code," WCAP-7979-P-A, Westinghouse Electric Corporation, January 1975, ADAMS Accession Number ML080650324.
15. C.W. Stewart and J. M. Cuta, et al., "VIPRE 01: A Thermal-Hydraulic Code for Reactor Cores," EPRI 1-3 (2001) NP-2511-CCM.

16. "Quality Assurance Program (QAP) for Design Certification of the US APWR," PQD-HD-18046-Rev.1, Mitsubishi Heavy Industries, Ltd., 2006.
17. MUAP-07019-P, Rev. 0, "Qualification of Nuclear Design Methodology using PARAGON/ANC." December 2007, ADAMS Accession Number ML080250232.
18. WCAP-7907-P-A, "LOFTRAN Code Description," Westinghouse Electric Corporation, April 1984, ADAMS Accession Number ML080650325.
19. UAP-HF-08141, Docket No. 52-021, "MHI's Response to NRC's Request for Additional Information on US-APWR Topical Report MUAP-07010-P, Non- LOCA Methodology," August 22, 2008. ADAMS Accession Number ML082400136.
20. UAP-HF-08245, Docket No. 52-021, "MHI's 3rd Response to NRC's Request for Additional Information on US-APWR Topical Report MUAP-07010-P, Non-LOCA Methodology," November 12, 2008. ADAMS Accession Number ML083190141-2.
21. UAP-HF-08170, Docket No. 52-021, "MHI's 2nd Response to NRC's Request for Additional Information on US-APWR Topical Report MUAP-07010-P, Non-LOCA Methodology," September 2008. ADAMS Accession Number ML082600089.
22. UAP-HF-09040, Docket No. 52-021, "MHI's 4th Response to NRC's Request for Additional Information on US-APWR Topical Report MUAP-07010-P, Non-LOCA Methodology," February 2009. ADAMS Accession Number ML090490843.
23. UAP-HF-08115, Docket No. 52-021, Transmittal of MUAP-07022-P, "Reactor Vessel Lower Plenum 1/7 Scale Model Flow Test Report," June 30, 2008. ADAMS Accession Number ML081850466.
24. F. H. Clark, et al., "Review of LOFTRAN, Thermal-Hydraulic Code for Nuclear Power Plants," ORNL TER, September 24, 1982. ADAMS Accession No. 8210010258.
25. R. Beaton and D. Fletcher, "US-APWR NON-LOCA RELAP5/MOD3.3 Confirmatory Runs," Information Systems Laboratories, Inc., ISL-NSAO-TR-10-01, January 2010.
26. H. Finnemann and A. G. Galati, "NEACRP 3-D LWR Core Transient Benchmark," NEACRP-L-335 (Revision 1), Final Specifications, October 1991 (January 1992).
27. UAP-HF-11005, Docket No. 52-021, "MHI's 13th Response to NRC's Request for Additional Information on US-APWR Topical Report MUAP-07010-P, Non-LOCA Methodology," January 14, 2011. ADAMS Accession Number ML110200306, ML110200311.
28. B. Boyack, et al., "Phenomena Identification and Ranking Tables (PIRTs) for Rod Ejection Accidents in Pressurized Water Reactors Containing High Burnup Fuel," Los Alamos National Laboratory, NUREG/CR-6742, LA-UR-99-6810, August 2001.
29. W. G. Luscher and K. J. Geelhood, "Material Property Correlations: Comparisons between FRAPCON-3.4, FRAPTRAN 1.4, and MATPRO," Pacific Northwest National Laboratory, MUREG/CR-7024, PNNL-19417, March 2011.

30. UAP-HF-11200, Docket No. 52-021, "MHI's 16th Response to NRC's Request for Additional Information on US-APWR Topical Report MUAP-07010-P, Non-LOCA Methodology," June 30, 2011. ADAMS Accession Number ML11195A047-8.
31. – Deleted –
32. "Reactivity Accident Test Results and Analyses for the SPERT III E-Core-A Small, Oxide-Fueled, Pressurized Water Reactor," IDO-17281, U. S. Atomic Energy Commission, March 1969.
33. UAP-HF-11129, Docket No. 52-021, "MHI's 15th Response to NRC's Request for Additional Information on US-APWR Topical Report MUAP-07010-P, Non-LOCA Methodology," April 28, 2011. ADAMS Accession Number ML11129A050-1. Revised 15th Response, August 12, 2011, ML11229A191-2.
34. K. Odumura, K. Kaneko and K. Tsuchihashi, "SRAC95: General Purpose Neutronics Code System," JAERI-Data/Code 96-015, March 1996.
35. NEA-0842, "SRAC-95, Cell Calculation with Burnup, Fuel Management for Thermal Reactors."
36. UAP-HF-10001, Docket No. 52-021, "MHI's 6th, 7th and 8th Responses to NRC's Requests for Additional Information on MARVEL-M Theory Manual GEN0-LP-480 and US-APWR Topical Report MUAP-07010-P, Non-LOCA Methodology," January 2010. ADAMS Accession Number ML100140146-7.
37. UAP-HF-09500, Docket No. 52-021, "Response to RAI 4.2 on Thermal Design Methodology, MUAP-07009-P," October 30, 2009. ADAMS Accession Number ML093130118-9.
38. Regulatory Guide 1.77, "Assumptions Used for Evaluating a Control Rod Ejection Accident for Pressurized Water Reactors," May 1974. ADAMS Accession Number ML00370279.
39. MUAP-09021-P(R2), "Response Time of Safety I&C System," April 2011. ADAMS Accession Number ML11129A146.
40. UAP-HF-09346, July 3, 2009, "MHI's Response to US-APWR DCD RAI No. 313-2361 Revision 2." ADAMS Accession Number ML091890118
41. UAP-HF-11118, Docket No. 52-021, "MHI's 14th Response to NRC's Request for Additional Information on US-APWR Topical Report MUAP-07010-P, Non-LOCA Methodology," April 22, 2011. ADAMS Accession Number ML11115A167.
42. UAP-HF-11264, Docket No. 52-021, "MHI's Revised 15th Response to NRC's Request for Additional Information on US-APWR Topical Report MUAP-07010-P, Non-LOCA Methodology," August 12, 2011, ADAMS Accession Number ML11229A191

43. UAP-HF-10101, Docket No. 52-021, "MHI's 9th and 10th Responses to NRC Requests for Additional Information on MARVEL-M Theory Manual GEN0-LP-480 and US-APWR Topical Report: Non-LOCA Methodology," MUAP-07010-P (R0)," April 2010. ADAMS Accession Number ML101480303.
44. Letter from A.C. Thadani (NRC) to W.J. Johnson (Westinghouse), "Acceptance for Referencing of Licensing Topical Report WCAP-9226-P/9227-NP, Reactor Core Response to Excessive Secondary Steam Releases," January 31, 1989.
45. UAP-HF-09341-P, Docket No. 52-021, "MHI's Response to US-APWR DCD RAI 302-2327 Revision 2," July 2009. ADAMS Accession Number ML091890527.
46. UAP-HF-10226, Docket No. 52-021, "MHI's 12th Response to NRC's Requests for Additional Information on US-APWR Topical Report: Non-LOCA Methodology," MUAP-07010-P (R0), August 2010. ADAMS Accession Number ML102240215.
47. UAP-HF-07187, Docket No. 52-021, Transmittal of MUAP-07026-P (R0), "Mitsubishi Reload Evaluation Methodology", December 31 2007. ADAMS Accession Number ML080290227.
48. UAP-HF-09340-P, Docket No. 52-021, "MHI's Response to US-APWR DCD RAI 297-2287 Revision 2," July 2009. ADAMS Accession Number ML091890966.
49. F. R. Zaloudek, "Steam-Water Critical Flow for High Pressure Systems," HW-80535, Hanford Laboratories, January 1964.
50. UAP-HF-09099, Docket No. 52-021, "MHI's Non-LOCA Response to NRC's Requests for Additional Information on Topical Reports MUAP-07010, MUAP-07011, and MUAP-07013, March 2009." ADAMS Accession Number ML091050114.
51. H.G. Hargrove, "FACTRAN-A Fortran IV Code for Thermal Transients in a UO₂ Fuel Rod," WCAP-7908-A, December 1989, ADAMS Accession Number ML080630436.
52. "US-APWR Topical Report Non-LOCA Methodology," MUAP-07010-P (R3), April 2012, ADAMS Accession Number ML12103A272.
53. "US-APWR Topical Report Non-LOCA Methodology," MUAP-07010-P (R4), May 2012, ADAMS Accession Number ML121460108.
54. UAP-HF-12120, Docket No. 52-021, "2nd Revision to MHI's 15th Response to NRC's Request for Additional Information on US-APWR Topical Report: Non-LOCA Methodology, MUAP-07010-P (R1)," May 11, 2012. ADAMS Accession Number ML121360496
55. Friedland, A. J. and Ray, S., Revised Thermal Design Procedure, WCAP-11397-P-A (Proprietary) and WCAP-11397-A (Non-Proprietary), April 1989.
56. F. J. Moody, "Maximum Flow Rate of a Single Component, Two-Phase Mixture", Journal of Heat Transfer, Trans American Society of Mechanical Engineers, 87 No. 1, February 1965.

57. Letter from Joseph Donoghue to Hossein Hamzehee, "SOFTWARE QUALITY ASSURANCE AUDIT REPORT FOR MITSUBISHI HEAVY INDUSTRIES, LTD. M-RELAP-5 AND VIPRE-01M COMPUTER CODES" August 31, 2011 (ADAMS Accession No. ML112430288)
58. Letter from Joseph Donoghue (U.S. NRC) to Hossein Hamzehee (U.S. NRC), "The U.S. Nuclear Regulatory Commission Report for the audit performed on May 16 and 17, 2012 regarding the Onsite Audit Report for VIPRE-01M Topical Code Review" dated June 11, 2012 (ADAMS Accession No. ML12164A837).

8.0 ACRONYMS

1D (or 1-D)	One-dimensional
3D (or 3-D)	Three-dimensional
AC	Alternating current
AFW	Auxiliary feedwater
ANS	American Nuclear Society
AOO	Anticipated operational occurrence
APWR	Advanced Pressurized Water Reactor
ASME	American Society of Mechanical Engineers
ARI	All rods in
ARO	All rods out
BOC	Beginning of cycle
CFR	Code of Federal Regulations
CHF	Critical heat flux
CLOF	Complete loss of flow
CRDM	Control Rod Drive Mechanism
CVCS	Chemical and Volume Control System
DCD	Design Control Document
DNB	Departure from nucleate boiling
DNBR	Departure from nucleate boiling ratio
DVI	Direct vessel injection
ECC	Emergency core cooling (or coolant)
ECCS	Emergency Core Cooling System
EFWS	Emergency Feedwater System
EOC	End of cycle
EPRI	Electric Power Research Institute
ESF	Engineered safety feature
ESFAS	Engineered Safety Feature Actuation System
FCM	Fuel centerline melt
FWLB	Feedwater line break
GDC	General design criteria
HFP	Hot full power
HHIS	High-Head Injection System
HPI	High pressure injection
HPSI	High pressure safety injection
HZP	Hot zero power
IPP	Indian Point Plant
LBLOCA	Large break loss-of-coolant accident
LCO	Limiting condition for operation
LHS	Left hand side
LOCA	Loss-of-coolant accident
LOL	Loss of load
LWR	Light water reactor
MDC	Moderator density coefficient
MDNBR	Minimum departure from nucleate boiling ratio
MFW	Main feedwater
MHI	Mitsubishi Heavy Industries, Ltd.
MSDV	Main Steam Depressurization Valve

MSIV	Main Steam Isolation Valve
MSLB	Main steam line break
MSRV	Main Steam Relief Valve
NR	Neutron Reflector
NRC	United States Nuclear Regulatory Commission
NSSS	Nuclear Steam Supply System
OECD	Organization for Economic Co-operation and Development
PA	Postulated accident
PAM	Post accident monitoring
PCMI	Pellet cladding mechanical interaction
PCT	Peak cladding temperature
PIRT	Phenomena identification and ranking table
PWR	Pressurized water reactor
QAP	Quality Assurance Program
RAI	Request for additional information
RCCA	Rod Cluster Control Assembly
RCP	Reactor coolant pump
RCS	Reactor coolant system
REA	Rod ejection accident
RG	Regulatory Guide
RHS	Right hand side
RIA	Reactivity initiated accident
RPS	Reactor Protection System
RPV	Reactor pressure vessel
RTD	Resistance temperature detector
RV	Reactor vessel
RWSP	Refueling Water Storage Pit
SAFDL	Specified acceptable fuel design limit
SBLOCA	Small break loss-of-coolant accident
SE	Safety evaluation
SER	Safety evaluation report
SG	Steam generator
SGTR	Steam generator tube rupture
SI	Safety injection
SIS	Safety Injection System
SLB	Steam line break
SRP	Standard Review Plan
TER	Technical evaluation report
TMI	Three Mile Island
TS	Technical specification
US-APWR	United States Advanced Pressurized Water Reactor
USNRC	United States Nuclear Regulatory Commission
WEC	Westinghouse Electric Corporation

Revision History

Revision	Page(s)	Description
0	All	Original issue
1	--	Revised for consistency with current code manual revisions, to correct typographical errors, and to incorporate changes from previous RAI responses.
2	--	Revised to update the HFP rod ejection methodology described in Section 5.3, Appendix-G and associated results in Section 6.3. (Topical Report RAI No. REA-12) Revised the HZP rod ejection results in Section 6.3 to be consistent with the DCD. Table 4.5-1 is also updated. Updated the dose evaluation acceptance criteria in Tables 4.2-1, 4.4-1, 4.5-1, and 4.7-1 for consistency with the DCD. Revised list of references in Section 8 to reflect latest versions. Corrected a typographical error in Appendix B.
3	5-13 5-14 8-1	Clarified description of fuel properties assumptions for the rod ejection methodology. Revised list of references in Section 8 to reflect latest version.
4	8-1	Revised list of references in Section 8.

© 2013
MITSUBISHI HEAVY INDUSTRIES, LTD.
All Rights Reserved

This document has been prepared by Mitsubishi Heavy Industries, Ltd. ("MHI") in connection with its request to the U.S. Nuclear Regulatory Commission ("NRC") for a pre-application review of the US-APWR nuclear power plant design. No right to disclose, use or copy any of the information in this document, other than that by the NRC and its contractors in support of MHI's pre-application review of the US-APWR, is authorized without the express written permission of MHI.

This document contains technology information and intellectual property relating to the US-APWR and it is delivered to the NRC on the express condition that it not be disclosed, copied or reproduced in whole or in part, or used for the benefit of anyone other than MHI without the express written permission of MHI, except as set forth in the previous paragraph.

This document is protected by the laws of Japan, U.S. copyright law, international treaties and conventions, and the applicable laws of any country where it is being used.

Mitsubishi Heavy Industries, Ltd.
16-5, Konan 2-chome, Minato-ku
Tokyo 108-8215 Japan

ABSTRACT

This report presents the non-LOCA methodology that will be used in the Standard Review Plan (SRP) Chapter 15 safety analysis for MHI-designed pressurized water reactors such as the US-APWR. The contents of this document include description of the computer code, code validation, acceptance criteria and event specific methodology with sample transient analysis. The methodology for the analysis of radiological consequence is not described in this topical report.

The purpose of submitting this topical report during the US-APWR pre-application phase is to provide information to the NRC to facilitate efficient and timely review of the accident analysis to be provided in the Design Certification Document (DCD) as part of the Design Certification License Application.

The report provides an overview of the applicable methodology and the description of the specific models incorporated in the following MHI codes used to analyze non-LOCA accidents, as well as a discussion of the bases for applying these codes/methods to the US-APWR. Validation of the principal models of these codes by comparison with computer codes that have been approved by the NRC is presented.

- MARVEL-M Plant system transient analysis code
- TWINKLE-M Multi-dimensional neutron kinetics code
- VIPRE-01M Subchannel thermal hydraulics analysis and fuel transient code

The event classification and associated acceptance criteria that will be used by MHI for each non-LOCA event included in the DCD are presented, ordered by the broader event categories defined by the SRP Chapter 15 and Regulatory Guide 1.206.

The following six events were selected to represent the spectrum of key analytical methods (combinations of codes), key SRP accident categories (15.1, 15.2, 15.3, 15.4, 15.6, and 15.7), and specialized models used by MHI in the non-LOCA accident analysis for the US-APWR.

- Uncontrolled RCCA Bank Withdrawal at Power
- Complete Loss of Forced Reactor Coolant Flow
- Spectrum of RCCA Ejection
- Steam System Piping Failure
- Feedwater System Pipe Break
- Steam Generator Tube Rupture

A detailed description of event sequences, method of analysis, analysis assumptions and sample transient results are provided in the topical report for each of these events. Appendices provide additional analyses to support selected methodology assumptions.

On the basis of the information in this topical report, it is concluded that the applied codes and methodologies are appropriate for US-APWR safety analyses. Also, it is concluded that the information provided in this topical report supports its purpose to provide key technical information related to the computer codes and methodology as well as the sample plant responses of the US-APWR related with the representing non-LOCA safety analysis to the

NRC during the pre-application phase to facilitate an efficient and timely review of the Design Certification Application.

ACKNOWLEDGEMENTS

Mr. Tadakuni Hakata and Mr. Hiroshi Fujishiro's contributions to the development and documentation of the MARVEL-M code are gratefully acknowledged.

Table of Contents

List of Tables	vi
List of Figures	vii
List of Acronyms	xi
1.0 INTRODUCTION	1-1
2.0 COMPUTER CODE DESCRIPTION	2-1
2.1 MARVEL-M Code	2-2
2.1.1 Introduction	2-2
2.1.2 General Description - Overview	2-4
2.1.2.1 Reactor Core Model	2-4
2.1.2.2 Reactor Coolant System Model	2-6
2.1.2.3 Reactor Coolant Flow Transient Model	2-8
2.1.2.4 Steam Generator and Secondary System Model	2-9
2.1.2.5 Safety Systems and Miscellaneous Models	2-9
2.1.2.6 Perturbations	2-11
2.1.3 Theoretical Models of MARVEL-M Improvement	2-12
2.1.3.1 Four Loop Reactor Coolant System Model	2-12
2.1.3.2 Flow Mixing in Reactor Vessel (4-Loop Model)	2-14
2.1.3.3 Reactor Coolant Pump and Flow Transient Model	2-18
2.1.3.4 Secondary Steam System Model (4-Loop Model)	2-24
2.1.3.5 Other Model Refinement	2-26
2.1.4 Realistic Models	2-27
2.1.4.1 Steam Generator Tube Rupture	2-27
2.1.5 Precautions and Limitations for the Use of the MARVEL-M Code	2-29
2.1.5.1 Range of Operating Variables	2-29
2.1.5.2 Applicability of the Code to the Scenarios of Licensing Analysis	2-29
2.2 TWINKLE-M Code	2-32
2.3 VIPRE-01M Code	2-33
3.0 CODE VALIDATION	3-1
3.1 MARVEL-M Code	3-1
3.1.1 Uncontrolled RCCA Bank Withdrawal at Power	3-1
3.1.2 Partial Loss of Forced Reactor Coolant Flow	3-5
3.1.3 Complete Loss of Forced Reactor Coolant Flow	3-8
3.1.4 Reactor Coolant Pump Shaft Seizure	3-11
3.2 TWINKLE-M Code	3-14
3.2.1 Comparison with Core Design Code	3-14
3.2.2 Sensitivity Study of Mesh Size	3-21

4.0	ACCEPTANCE CRITERIA FOR SRP CHAPTER 15 NON-LOCA EVENTS	4-1
4.1	Acceptance Criteria	4-2
4.1.1	AOO Acceptance Criteria	4-2
4.1.2	PA Acceptance Criteria	4-3
4.2	Increase in Heat Removal from the Primary System	4-4
4.3	Decrease in Heat Removal by the Secondary System	4-5
4.4	Decrease in Reactor Coolant System Flow Rate	4-6
4.5	Reactivity and Power Distribution Anomalies	4-7
4.6	Increase in Reactor Coolant Inventory	4-9
4.7	Decrease in Reactor Coolant Inventory	4-10
5.0	EVENT-SPECIFIC METHODOLOGY	5-1
5.1	Uncontrolled RCCA Bank Withdrawal at Power	5-3
5.2	Complete Loss of Forced Reactor Coolant Flow	5-5
5.3	Spectrum of RCCA Ejection	5-9
5.4	Steam System Piping Failure	5-20
5.5	Feedwater System Pipe Break	5-27
5.6	Steam Generator Tube Rupture	5-30
6.0	SAMPLE TRANSIENT ANALYSIS	6-1
6.1	Uncontrolled RCCA Bank Withdrawal at Power	6-2
6.2	Complete Loss of Forced Reactor Coolant Flow	6-11
6.3	Spectrum of RCCA Ejection	6-16
6.4	Steam System Piping Failure	6-24
6.5	Feedwater System Pipe Break	6-33
6.6	Steam Generator Tube Rupture	6-42
7.0	CONCLUSIONS	7-1
8.0	REFERENCES	8-1
	Appendix A Evaluation of MARVEL-M DNBR Calculation Method	A-1
	Appendix B Sensitivity Study of the RCCA Ejection in the 3-D Methodology	B-1
	Appendix C Doppler Weighting Factor of the RCCA Ejection in the 1-D Methodology	C-1
	Appendix D Validation of VIPRE-01M Modeling for Steam System Piping Failure	D-1
	Appendix E Sensitivity Study of the Inlet Mixing Coefficient for Steam System Piping Failure	E-1
	Appendix F Detailed Break Flow Model for Steam Generator Tube Rupture	F-1
	Appendix G Calculation of High Power Range Neutron Flux Reactor Trip for Rod Ejection Event	G-1
	Appendix H Summary of MHI's Responses to NRC's Requests for Additional Information	H-1

List of Tables

Table 2.1-1	Reactor Coolant System Flow Sections (4-Loop Model)	2-6
Table 3.2.1-1	Results of RCCA Ejection Comparison with ANC and TWINKLE-M	3-15
Table 3.2.2-1	Calculation Condition and Results of the RCCA Ejection	3-21
Table 4-1	Event Classification Categories	4-1
Table 4.2-1	Events in Increase in Heat Removal from the Primary System	4-4
Table 4.3-1	Events in Decrease in Heat Removal by the Secondary System	4-5
Table 4.4-1	Events in Decrease in Reactor Coolant System Flow Rate	4-6
Table 4.5-1	Events in Reactivity and Power Distribution Anomalies	4-7
Table 4.6-1	Events in Increase in Reactor Coolant Inventory	4-9
Table 4.7-1	Events in Decrease in Reactor Coolant Inventory	4-10
Table 6.1-1	Sequence of Events for the Uncontrolled RCCA Bank Withdrawal at Power (75 pcm/sec)	6-3
Table 6.1-2	Sequence of Events for the Uncontrolled RCCA Bank Withdrawal at Power (2.5 pcm/sec)	6-3
Table 6.2-1	Sequence of Events for the Loss of Forced Reactor Coolant Flow	6-12
Table 6.3-1	Sequence of Events for the RCCA Ejection	6-17
Table 6.4-1	Sequence of Events for the Steam System Piping Failure	6-26
Table 6.5-1	Sequence of Events for the Feedwater System Pipe Failure	6-34
Table 6.6-1	Sequence of Events for the SGTR (Radiological Consequence Analysis)	6-43
Table B-1	Calculation Condition and Results of Sensitivity Studies about an Ejected Reactivity and a Hot Channel Factor in the RCCA Ejection	B-2
Table C-1	Calculation Condition of the RCCA Ejection in the Hot Full Power	C-1
Table D-1	DNBR Calculation Model and Assumptions for the Steam System Piping Failure	D-1
Table H-1	First Set of MUAP-07010 Historical RAI Responses	H-1
Table H-2	Second Set of MUAP-07010 Historical RAI Responses	H-7

List of Figures

Figure 2.1-1	PWR Plant Systems Modeled in the MARVEL-M Code	2-4
Figure 2.1-2	Reactor Coolant Flow and Mixing in Reactor Vessel	2-7
Figure 2.1-3	Reactor Coolant System Flow Model	2-12
Figure 2.1-4	Reactor Vessel Inner Structure	2-13
Figure 2.1-5	Reactor Vessel Flow Model	2-15
Figure 2.1-6	Steam Line Model	2-24
Figure 3.1.1-1	Reactor Power, Uncontrolled RCCA Bank Withdrawal at Power Comparison with MARVEL-M and LOFTRAN	3-3
Figure 3.1.1-2	Core Heat Flux, Uncontrolled RCCA Bank Withdrawal at Power Comparison with MARVEL-M and LOFTRAN	3-3
Figure 3.1.1-3	RCS Average Temperature, Uncontrolled RCCA Bank Withdrawal at Power Comparison with MARVEL-M and LOFTRAN	3-4
Figure 3.1.1-4	Pressurizer Pressure, Uncontrolled RCCA Bank Withdrawal at Power Comparison with MARVEL-M and LOFTRAN	3-4
Figure 3.1.2-1	Reactor Power, Partial Loss of Forced Reactor Coolant Flow Comparison with MARVEL-M and LOFTRAN	3-6
Figure 3.1.2-2	Core Heat Flux, Partial Loss of Forced Reactor Coolant Flow Comparison with MARVEL-M and LOFTRAN	3-6
Figure 3.1.2-3	Loop Volumetric Flow, Partial Loss of Forced Reactor Coolant Flow Comparison with MARVEL-M and LOFTRAN	3-7
Figure 3.1.2-4	Pressurizer Pressure, Partial Loss of Forced Reactor Coolant Flow Comparison with MARVEL-M and LOFTRAN	3-7
Figure 3.1.3-1	Reactor Power, Complete Loss of Forced Reactor Coolant Flow Comparison with MARVEL-M and LOFTRAN	3-9
Figure 3.1.3-2	Core Heat Flux, Complete Loss of Forced Reactor Coolant Flow Comparison with MARVEL-M and LOFTRAN	3-9
Figure 3.1.3-3	Loop Volumetric Flow, Complete Loss of Forced Reactor Coolant Flow Comparison with MARVEL-M and LOFTRAN	3-10
Figure 3.1.3-4	Pressurizer Pressure, Complete Loss of Forced Reactor Coolant Flow Comparison with MARVEL-M and LOFTRAN	3-10
Figure 3.1.4-1	Reactor Power, Reactor Coolant Pump Shaft Seizure Comparison with MARVEL-M and LOFTRAN	3-12
Figure 3.1.4-2	Core Heat Flux, Reactor Coolant Pump Shaft Seizure Comparison with MARVEL-M and LOFTRAN	3-12
Figure 3.1.4-3	Loop Volumetric Flow, Reactor Coolant Pump Shaft Seizure Comparison with MARVEL-M and LOFTRAN	3-13
Figure 3.1.4-4	Pressurizer Pressure, Reactor Coolant Pump Shaft Seizure Comparison with MARVEL-M and LOFTRAN	3-13
Figure 3.2.1-1	Control and Shutdown Rod Location (17x17-257FA Core, 4-Loop Plant)	3-16
Figure 3.2.1-2	Radial Power Distribution Comparison with ANC and TWINKLE-M Case 1, BOC HFP All RCCAs Out	3-17
Figure 3.2.1-3	Radial Power Distribution Comparison with ANC and TWINKLE-M Case 2, EOC HZP RCCA at Insertion Limit	3-18
Figure 3.2.1-4	Radial Power Distribution Comparison with ANC and TWINKLE-M Case 3, EOC HZP One RCCA Ejected	3-19

Figure 3.2.1-5	Average Axial Power Distribution Comparison with ANC and TWINKLE-M	3-20
Figure 3.2.2-1	Nuclear Power, RCCA Ejection at EOC HZP Comparison with 2 x 2 mesh and 4 x 4 mesh in TWINKLE-M	3-22
Figure 3.2.2-2	Hot Channel Factor, RCCA Ejection at EOC HZP Comparison with 2 x 2 mesh and 4 x 4 mesh in TWINKLE-M	3-22
Figure 5.2-1	VIPRE-01M 1/8 Core Analysis Modeling (17x17-257FA Core, 4-Loop Plant)	5-7
Figure 5.2-2	Calculation Flow Diagram of the MARVEL-M/VIPRE-01M Methodology	5-8
Figure 5.3-1	Calculation Flow Diagram of the Three-Dimensional Methodology	5-15
Figure 5.3-2	Calculation Flow Diagram of the One-Dimensional Methodology	5-16
Figure 5.3-3	Calculation Flow Diagram of the Number of Rods in DNB Methodology	5-17
Figure 5.3-4	Relationship between CRDM Housing Break Size and Minimum DNBR in Long-Term Period Including Reactor Trip Protection Functions	5-18
Figure 5.3-5	Calculation Flow Diagram of the RCS Pressure Methodology	5-19
Figure 5.4-1	Steam System Configuration of US-APWR	5-20
Figure 5.4-2	Calculation Flow Diagram of the Steam System Piping Failure Methodology for the Hot Zero Power Condition	5-25
Figure 5.4-3	VIPRE-01M 1/8 Core Analysis Modeling with 5-grouped Power Distributions (17x17-257FA Core, 4-Loop Plant)	5-26
Figure 5.5-1	Emergency Feedwater System of US-APWR	5-28
Figure 6.1-1	Minimum DNBR versus Reactivity Insertion Rate (HFP, BOC)	6-4
Figure 6.1-2	Reactor Power versus Time Uncontrolled RCCA Bank Withdrawal at Power (HFP, BOC, 75 pcm/sec)	6-5
Figure 6.1-3	Hot Spot Heat Flux versus Time Uncontrolled RCCA Bank Withdrawal at Power (HFP, BOC, 75 pcm/sec)	6-5
Figure 6.1-4	RCS Average Temperature versus Time Uncontrolled RCCA Bank Withdrawal at Power (HFP, BOC, 75 pcm/sec)	6-6
Figure 6.1-5	RCS Pressure versus Time Uncontrolled RCCA Bank Withdrawal at Power (HFP, BOC, 75 pcm/sec)	6-6
Figure 6.1-6	Pressurizer Water Volume versus Time Uncontrolled RCCA Bank Withdrawal at Power (HFP, BOC, 75 pcm/sec)	6-7
Figure 6.1-7	DNBR versus Time Uncontrolled RCCA Bank Withdrawal at Power (HFP, BOC, 75 pcm/sec)	6-7
Figure 6.1-8	Reactor Power versus Time Uncontrolled RCCA Bank Withdrawal at Power (HFP, BOC, 2.5 pcm/sec)	6-8
Figure 6.1-9	Hot Spot Heat Flux versus Time Uncontrolled RCCA Bank Withdrawal at Power (HFP, BOC, 2.5 pcm/sec)	6-8
Figure 6.1-10	RCS Average Temperature versus Time Uncontrolled RCCA Bank Withdrawal at Power (HFP, BOC, 2.5 pcm/sec)	6-9
Figure 6.1-11	RCS Pressure versus Time Uncontrolled RCCA Bank Withdrawal at Power (HFP, BOC, 2.5 pcm/sec)	6-9
Figure 6.1-12	Pressurizer Water Volume versus Time Uncontrolled RCCA Bank Withdrawal at Power (HFP, BOC, 2.5 pcm/sec)	6-10
Figure 6.1-13	DNBR versus Time Uncontrolled RCCA Bank Withdrawal at Power (HFP, BOC, 2.5 pcm/sec)	6-10
Figure 6.2-1	Reactor Power versus Time Complete Loss of Forced Reactor Coolant Flow	6-13
Figure 6.2-2	Hot Channel Heat Flux versus Time Complete Loss of Forced Reactor Coolant Flow	6-13

Figure 6.2-3	RCS Total Flow versus Time Complete Loss of Forced Reactor Coolant Flow	6-14
Figure 6.2-4	RCS Average Temperature versus Time Complete Loss of Forced Reactor Coolant Flow	6-14
Figure 6.2-5	RCS Pressure versus Time Complete Loss of Forced Reactor Coolant Flow	6-15
Figure 6.2-6	DNBR versus Time Complete Loss of Forced Reactor Coolant Flow	6-15
Figure 6.3-1	Nuclear Power versus Time RCCA Ejection (BOC HFP)	6-19
Figure 6.3-2	Fuel and Cladding Temperature versus Time RCCA Ejection (BOC HFP)	6-19
Figure 6.3-3	Nuclear Power versus Time RCCA Ejection (EOC HZP)	6-20
Figure 6.3-4	Fuel Enthalpy versus Time RCCA Ejection (EOC HZP)	6-20
Figure 6.3-5	Fuel Enthalpy Rise versus Oxide/Wall Thickness RCCA Ejection (EOC HZP)	6-21
Figure 6.3-6	Nuclear Power versus Time for Short Term Period RCCA Ejection (BOC HFP, No Flux Trip)	6-22
Figure 6.3-7	DNBR versus Time for Short Term Period RCCA Ejection (BOC HFP, No Flux Trip)	6-22
Figure 6.3-8	Core Census for Rods in DNB for Long Term Period RCCA Ejection (EOC HFP, No Flux Trip)	6-23
Figure 6.4-1	Core Reactivity versus Time Steam System Piping Failure – Double-Ended Break from Hot Shutdown	6-27
Figure 6.4-2	Reactor Power versus Time Steam System Piping Failure – Double-Ended Break from Hot Shutdown	6-27
Figure 6.4-3	Core Heat Flux versus Time Steam System Piping Failure – Double-Ended Break from Hot Shutdown	6-28
Figure 6.4-4	RCS Pressure versus Time Steam System Piping Failure – Double-Ended Break from Hot Shutdown	6-28
Figure 6.4-5	Pressurizer Water Volume versus Time Steam System Piping Failure – Double-Ended Break from Hot Shutdown	6-29
Figure 6.4-6	Reactor Vessel Inlet Temperature versus Time Steam System Piping Failure – Double-Ended Break from Hot Shutdown	6-29
Figure 6.4-7	Steam Generator Water Mass versus Time Steam System Piping Failure – Double-Ended Break from Hot Shutdown	6-30
Figure 6.4-8	Steam Generator Pressure versus Time Steam System Piping Failure – Double-Ended Break from Hot Shutdown	6-30
Figure 6.4-9	Steam Flow Rate versus Time Steam System Piping Failure – Double-Ended Break from Hot Shutdown	6-31
Figure 6.4-10	Feedwater Flow Rate versus Time Steam System Piping Failure – Double-Ended Break from Hot Shutdown	6-31
Figure 6.4-11	Core Boron Concentration versus Time Steam System Piping Failure – Double-Ended Break from Hot Shutdown	6-32
Figure 6.5-1	Reactor Power versus Time Feedwater System Pipe Break	6-36
Figure 6.5-2	RCS Pressure versus Time Feedwater System Pipe Break	6-36

Figure 6.5-3	RCS Average Temperature versus Time Feedwater System Pipe Break	6-37
Figure 6.5-4	RCS Total Flow versus Time Feedwater System Pipe Break	6-37
Figure 6.5-5	Pressurizer Water Volume versus Time Feedwater System Pipe Break	6-38
Figure 6.5-6	Steam Generator Pressure versus Time Feedwater System Pipe Break	6-38
Figure 6.5-7	Feedwater Line Break Flow Rate versus Time Feedwater System Pipe Break	6-39
Figure 6.5-8	Steam Generator Water Mass versus Time Feedwater System Pipe Break	6-39
Figure 6.5-9	Temperature versus Time for the Faulted Loop Feedwater System Pipe Break	6-40
Figure 6.5-10	Temperature versus Time for the Intact Loop without EFW Feedwater System Pipe Break	6-40
Figure 6.5-11	Temperature versus Time for the Intact Loop with EFW Feedwater System Pipe Break	6-41
Figure 6.6-1	Reactor Power versus Time SGTR Radiological Consequence Analysis	6-44
Figure 6.6-2	RCS Pressure versus Time SGTR Radiological Consequence Analysis	6-44
Figure 6.6-3	Pressurizer Water Volume versus Time SGTR Radiological Consequence Analysis	6-45
Figure 6.6-4	Ruptured Loop RCS Temperature versus Time SGTR Radiological Consequence Analysis	6-45
Figure 6.6-5	Intact Loop RCS Temperature versus Time SGTR Radiological Consequence Analysis	6-46
Figure 6.6-6	Steam Generator Pressure versus Time SGTR Radiological Consequence Analysis	6-46
Figure 6.6-7	Steam Generator Water Volume versus Time SGTR Radiological Consequence Analysis	6-47
Figure 6.6-8	Feedwater Flow Rate versus Time SGTR Radiological Consequence Analysis	6-47
Figure 6.6-9	Reactor Coolant Leakage versus Time SGTR Radiological Consequence Analysis	6-48
Figure A-1	DNBR Transient, Uncontrolled RCCA Bank Withdrawal at Case 1- Full Power for a High Reactivity Insertion Rate	A-2
Figure A-2	DNBR Transient, Uncontrolled RCCA Bank Withdrawal at Case 2- Full Power for a Low Reactivity Insertion Rate	A-2
Figure B-1	Definition of the Prompt Maximum Fuel Enthalpy Time	B-2
Figure C-1	Radial Doppler Weighting Factor for 1-D Kinetics Analysis	C-2
Figure C-2	Average Axial Power Distribution Comparison with 3-D and 1-D (BOC, EOC)	C-2
Figure C-3	Nuclear Power versus Time (BOC) Comparison between 3-D and 1-D with Doppler Weighting Factor	C-3
Figure C-4	Nuclear Power versus Time (EOC) Comparison between 3-D and 1-D with Doppler Weighting Factor	C-3
Figure D-1	VIPRE-01M Full Core Analysis Modeling (17x17-257FA Core, 4-Loop Plant)	D-2

Figure D-2	5-grouped Model for Radial Power Distribution	D-3
Figure D-3	Comparison of DNBR and Local Fluid Parameters at Hot Channel between the 1/8 Core Model and the Full Core Model	D-4
Figure E-1	DNBR versus Reactor Inlet Mixing for the Steam System Piping Failure	E-1
Figure F-1	Realistic Model of the Broken SG Tube	F-2
Figure F-2	Comparison of the Calculation Result for Each Break Flow Model	F-3
Figure G-1	Location of Ex-Core Detectors and Control Rod Bank-D	G-4
Figure G-2	Actual and Measured Reactor Power - Rod Ejection (BOC)	G-5

List of Acronyms

1-D	one-dimensional
3-D	three-dimensional
AOOs	Anticipated Operational Occurrences
APWR	Advanced Pressurized Water Reactor
ASME	American Society of Mechanical Engineers
BOC	Beginning of Cycle
CFR	Code of Federal Regulations
CVCS	Chemical and Volume Control System
DNB	Departure from Nucleate Boiling
DNBR	Departure from Nucleate Boiling Ratio
ECCS	Emergency Core Cooling System
EFWS	Emergency Feed Water System
EOC	End of Cycle
EPRI	Electric Power Research Institute
GDC	General Design Criteria
HFP	Hot Full Power
HZP	Hot Zero Power
MHI	Mitsubishi Heavy Industries, Ltd
MSIV	Main Steam Isolation Valve
Non-LOCA	Non Loss of Coolant Accident
NRC	US Nuclear Regulatory Commission
NSSS	Nuclear Steam Supply System
PAs	Postulated Accidents
PCMI	Pellet Cladding Mechanical Interaction
PCT	Peak Clad Temperature
PWR	Pressurized Water Reactor
RCCA	Rod Cluster Control Assembly
RCP	Reactor Coolant Pump
RCS	Reactor Coolant System
RIA	Reactivity Initiated Accident
RIE	Reactivity Initiated Event
RPS	Reactor Protection System
RTDP	Revised Thermal Design Procedure
RWSP	Refueling Water Storage Pit
SAFDL	Specified Acceptable Fuel Design Limits
SG	Steam Generator
SGTR	Steam Generator Tube Rupture
SIS	Safety Injection System
SRP	Standard Review Plan

1.0 INTRODUCTION

The purpose of this topical report is to present the non-LOCA computer codes and methodologies that are adopted by Mitsubishi Heavy Industries, Ltd. (MHI) for the analysis of all non-LOCA events in the Standard Review Plan (SRP) Chapter 15, except LOCA and dose evaluation, for MHI-designed pressurized water reactors such as the US-APWR. The MHI non-LOCA methodology using the following codes is very similar to the conventional non-LOCA methodology used for currently operating US PWRs:

- MARVEL-M Plant system transient analysis code
- TWINKLE-M Multi-dimensional neutron kinetics code
- VIPRE-01M Subchannel thermal hydraulics analysis and fuel transient code

The MARVEL-M [Reference 1], TWINKLE-M [References 2 and 3], and VIPRE-01M [References 4 and 6] codes are MHI improved versions. The MARVEL code [WCAP-7635 and WCAP-8844] and the TWINKLE code [WCAP-7979-P-A] were originally developed by Westinghouse Electric Corporation in the 1970s and used for licensing analysis for their US PWRs. The VIPRE-01 [Reference 4] code was originally developed by Battelle Pacific Northwest Laboratories, under the sponsorship of the Electric Power Research Institute and is also used for licensing analysis in the US.

Under a licensing agreement between Westinghouse and MHI, the MARVEL and TWINKLE codes were made available to MHI, and have been applied to licensing analysis for Japanese PWRs. For the non-LOCA safety analysis in the US, MHI uses the 4-loop MARVEL-M code. The primary changes to TWINKLE-M are the increase in the maximum number of mesh points and adding the ability for the user to change certain fuel thermal properties. However, the underlying solution method remains unchanged.

The VIPRE-01M code is a MHI modified version of the original VIPRE-01 code that includes some additional options concerning DNB correlations and fuel thermal properties. The topical report "Thermal Design Methodology" [Reference 6] submitted by MHI describes the modifications and validations related to the VIPRE-01M code.

MHI performs the non-LOCA safety analysis for the SRP Chapter 15 events using these computer codes and methodologies. This report describes:

- Section 2 – Computer Codes and MHI Modifications
- Section 3 – Validation of Models Utilizing Modified Codes
- Section 4 – Acceptance Criteria for SRP Chapter 15 Non-LOCA Events
- Section 5 – Non-LOCA Methodology for Typical Non-LOCA Events
- Section 6 – Sample Non-LOCA Event Analyses

2.0 COMPUTER CODE DESCRIPTION

As described in Section 1.0 the following computer codes are used by MHI for the non-LOCA safety analysis:

- MARVEL-M Plant system transient analysis code
- TWINKLE-M Multi-dimensional neutron kinetics code
- VIPRE-01M Subchannel thermal hydraulics analysis and fuel transient code

Sections 2.1, 2.2, and 2.3 provide an overview of the plant system and mathematical models and detailed descriptions of the modifications associated with the MHI versions of each code. MHI modified these codes under Mitsubishi's Quality Assurance Program (QAP) [Reference 7].

2.1 MARVEL-M Code

2.1.1 Introduction

The MARVEL-M code is the same as the original MARVEL code from the viewpoint of constitutive and principal models. The main differences between the original MARVEL code and MARVEL-M are the extension from 2-loop simulation to 4-loop simulation and the addition of a built-in RCP model. The other refinements such as a pressurizer surge line node, a hot spot heat flux simulation model, and improved numerical solution and conversion techniques are described.

History of MARVEL-M Development

The use of digital computer techniques for safety design and safety evaluation of nuclear power plants started in the 1960s. The single loop LOFTRAN code was developed by Westinghouse Electric Corporation in the 1960s for control and protection analysis for pressurized water reactors. Limitations associated with the original single loop LOFTRAN code led to the development of BLKOUT [Reference 8], a code designed for long-term, multi-loop transient analysis for PWRs. The BLKOUT code was an improvement over single loop LOFTRAN because the BLKOUT code incorporated simulation of two loops. Additionally, the BLKOUT code utilized perfect mixing in the reactor vessel inlet, which was a reasonable assumption for analyzing long-term transients. The code was used for accident analysis, such as loss of all AC power to the station auxiliaries, loss of normal feedwater, and also for system design studies, such as the auxiliary feedwater system sizing studies.

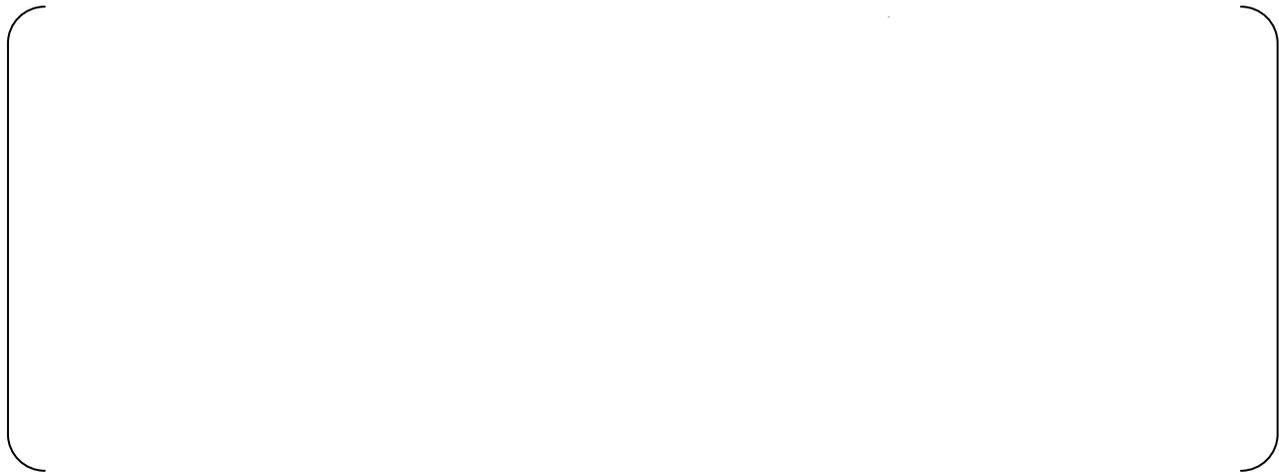
In the early 1970s the BLKOUT code was modified to handle shorter time steps necessary for the computation of fast transients. This modified version of BLKOUT eventually evolved into the 2-loop MARVEL code. The MARVEL models accounted for the effect of multiple loops more precisely than the BLKOUT code, such as the multiple azimuthal flow channels in the reactor vessel and mixing model (no mixing -partial -complete) in the reactor vessel, but otherwise adopted methods similar to LOFTRAN.

Three or four loop plants were modeled in MARVEL as a 2-loop simulation by assuming that the other loops are operated in the same way as either of the two modeled loops. The code was used for safety analysis for multi-loop reactor plant transient response where the reactor coolant loops behave in a non-uniform manner, such as start-up of an inactive reactor coolant loop and steam line break.

The original MARVEL code was licensed to Mitsubishi Heavy Industries Ltd (MHI) with other computer codes including nuclear and thermal-hydraulic codes under the licensing agreement between Westinghouse and MHI in 1971. Some model improvements were subsequently made by MHI, such as a hot-spot heat flux model similar to the Westinghouse FACTRAN code [Reference 10]. Since then the MARVEL code has been used extensively for licensing safety

analysis for various types of transients and design basis accidents, including Startup of an Inactive Reactor Coolant Loop, Loss of Reactor Coolant Flow, Inadvertent Rod Withdrawal, the Steam Line Break Accident, Feedwater Line Break Accident, and Steam Generator Tube Rupture Accident. The program has also been utilized as a tool for control studies and operating plant analysis for PWRs by MHI in Japan. In addition, certain realistic models were added as options to facilitate benchmarking and comparison with data obtained from operating plants.

In the 1990s, the original MARVEL code was expanded to a 4-loop version and added a reactor coolant pump model. This version of the code is denoted MARVEL-M. This evolution of the MARVEL-M code is graphically depicted below.



The MARVEL-M code is applicable to licensing safety analysis and control system studies and other applications for current PWR plants and for the APWR both for Japan and the US.

MARVEL-M Code Applicability to US-APWR Safety Analysis

The digital computer programs used for design and safety analysis in the Westinghouse pressurized water reactors were developed based on state-of-the-art technical and engineering knowledge at the time, and were influenced by the evolution of nuclear reactors developed by Westinghouse. As described above, the essential models of the MARVEL-M code are the same as the original MARVEL code developed by Westinghouse and approved by the NRC. The MARVEL-M code uses analytical models that are similar to those utilized in other codes, such as the LOFTRAN code, which have been used to license and continue to be used for safety analyses of their US PWRs. Due to the similarities between the US-APWR design and the current generation of US PWRs licensed by Westinghouse and the similarities between the codes used to analyze the transient response of the plant to an accident, it is concluded that the MARVEL-M code is applicable for performing the non-LOCA accident analysis for the US-APWR.

This topical report presents the overview of the MARVEL-M code in Section 2.1.2. Section 2.1.3 provides details on the improvement and refinement of certain original MARVEL models. Section 2.1.4 presents the realistic models incorporated as options in the MARVEL-M code for post-event analysis of a steam generator tube rupture event in Japan. Note that these realistic models are not used for original plant licensing. Section 2.1.5 discusses the precautions and limitations regarding the use of the MARVEL-M code.

2.1.2 General Description - Overview

MARVEL-M simulates reactor coolant loops and their associated systems; as well as the reactor core, pressurizer, control and protection system, safeguards system and others. The MARVEL-M code is applicable to 2-, 3-, and 4-loop PWR plants. A schematic diagram of the reactor systems simulated in 4-loop MARVEL-M is shown in Figure 2.1-1.

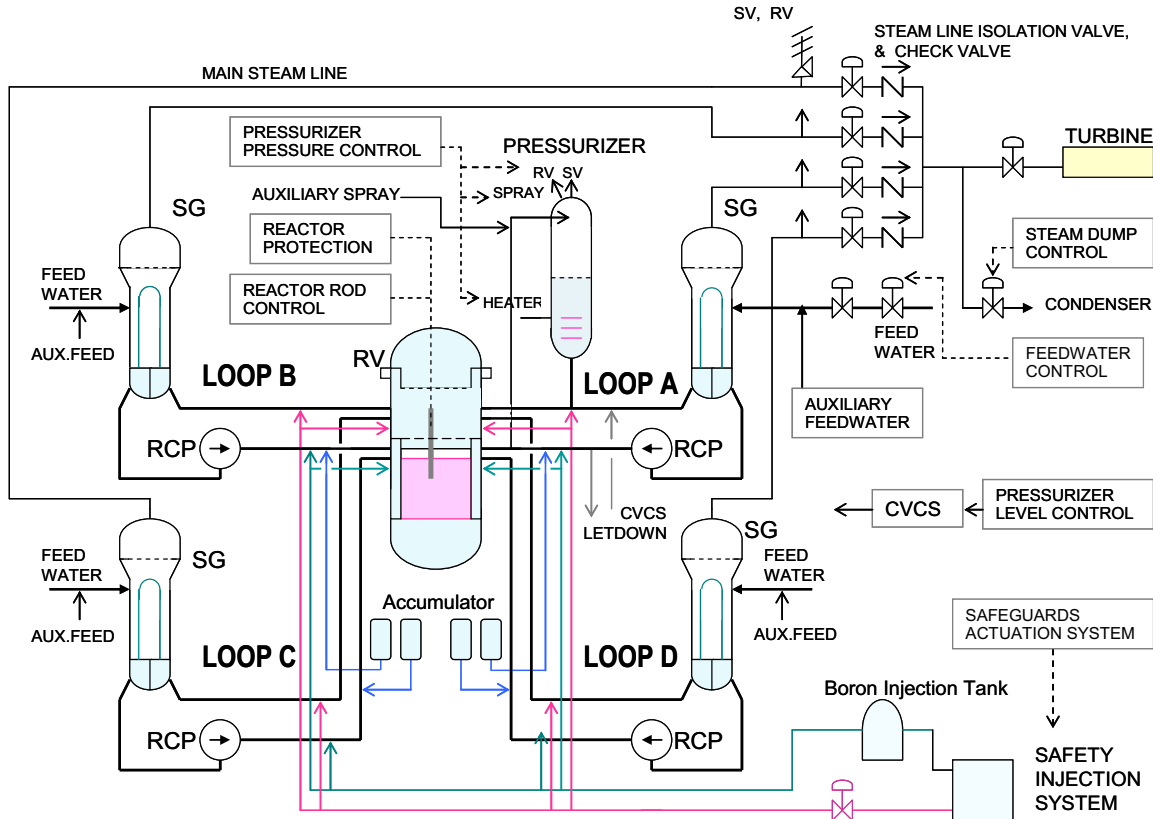


Figure 2.1-1 PWR Plant Systems Modeled in the MARVEL-M Code

2.1.2.1 Reactor Core Model

(1) Neutron Kinetics

The instantaneous power is calculated from the sum of the contribution of the instantaneous fission rate and contributions from decay heat. The rate of change of fission power is calculated by a space-independent one-energy one point neutron kinetics model with six delayed neutron groups. Reactivity is calculated as the sum of contributions due to moderator density variations (or temperature variation), boron concentration, the fuel Doppler effect, and rod motion.

The reactivity variation due to fuel Doppler effect can be calculated by the change in the fuel effective temperature and the Doppler coefficient of reactivity, or Doppler power coefficient and fuel power expressed by the normalized average fuel temperature rise. The reactivity changes due to changes in the core coolant and fuel properties in the axial meshes are

calculated from their coefficients of reactivity and the changes in core properties weighted by flux squared based on the perturbation theory approximation.

The reactor core model consists of up to four azimuthal flow sections corresponding to the coolant loops. If the core coolant properties are non-uniform, the azimuthal average of the core properties can be calculated using a user input reactivity weighting factor.

(2) Fuel Thermal Kinetics Models

The fuel rod kinetics are modeled by two equal volume concentric pellet nodes and one cladding node. The heat transfer coefficient from the clad surface to coolant is calculated using one of two different modes of heat transfer (1) subcooled convection or (2) local nucleate boiling. The total heat input to the coolant is the sum of the heat transferred from the cladding to the coolant and the heat generated in the coolant.

(3) DNBR Evaluation Model

MARVEL-M has ability to calculate the value of DNBR during a transient using a simple calculation model. The model employs user-input values of the DNBR at nominal core conditions and at selected DNBR limits represented by operating parameters of core inlet temperature, pressure and power levels. The code may accept input defining DNBR dependency on reactor coolant flow. The simplified DNBR model closely agrees with design calculations when the core operating conditions do not exceed the design flux distribution or core protection limits. When conditions exceed the limitations for the simplified model, DNBR analysis is performed by a more detailed external calculation code.

2.1.2.2 Reactor Coolant System Model

(1) Nodal Representation of the Reactor Coolant System

The thermal and hydraulic characteristics of the reactor coolant system are described by time and space dependent differential equations. They are reduced to nodal differential forms, the solutions of which are easily managed by means of finite differences. The system is divided into the following nodes or flow sections.

Table 2.1-1 Reactor Coolant System Flow Sections (4-Loop Model)

In each section, the mass and energy balance equations are solved by integration over time steps by the finite difference method, ignoring the momentum balance for forced reactor coolant flow.

Although not typically used for licensing analysis for non-LOCA accidents, MARVEL-M models two phase flow as a homogeneous equilibrium mixture (except for the pressurizer). This model is acceptable if the predicted volumetric void fraction is within the fluid flow regime where a homogeneous mixture is expected. If the predicted volumetric void fraction becomes significant, even within the homogeneous regime, the user must check whether the boiling affects the validity of the analysis for the intended purpose.

Each individual reactor coolant loop has a reactor coolant pump and a steam generator. The reactor coolant flows are variable and flow reversal is permitted unless the overall reactor vessel inlet flow becomes negative.

In the steam generators, the heat transfer rate from each flow section to the secondary side is calculated based on the log-mean temperature difference so that the power transferred is computed accurately for a limited number of tube flow sections and over a wide range of primary flow conditions including natural circulation conditions. The heat transfer coefficient and heat transfer area are treated as variables and defined as functions of the representative operating parameters.

The reactor coolant circulating through the coolant loops enter the reactor vessel through the inlet nozzles. The coolant flows downward through the downcomer into the reactor vessel lower plenum, then turns and flows upward to the reactor core. After passing through the core the coolant enters the reactor vessel upper plenum and leaves the vessel through the outlet nozzles.

A small fraction of the flow entering the reactor vessel bypasses the reactor core. The flow is not considered effective for removing core power and is modeled by two paths. A small fraction of the bypass flow directly enters the reactor vessel upper head region through the cooling spray nozzles from the top of the downcomer. The coolant in the upper head is stagnant. The rest of the bypass flow goes up a flow channel from the lower plenum to the upper plenum without core heating.

(2) Mixing Model in Reactor Vessel

The coolant from the coolant loops is mixed in the reactor vessel lower plenum before entering the core. The coolant leaving the core is also mixed in the reactor vessel upper plenum. The mixing of the loop coolant is, however, known to be imperfect from the results of mixing tests conducted in the 1970s. If the coolant loop operation is not uniform, the core may be subject to operation with azimuthally tilted temperatures and nuclear fluxes. Figure 2.1-2 shows the reactor coolant flow paths and mixing in the reactor vessel.

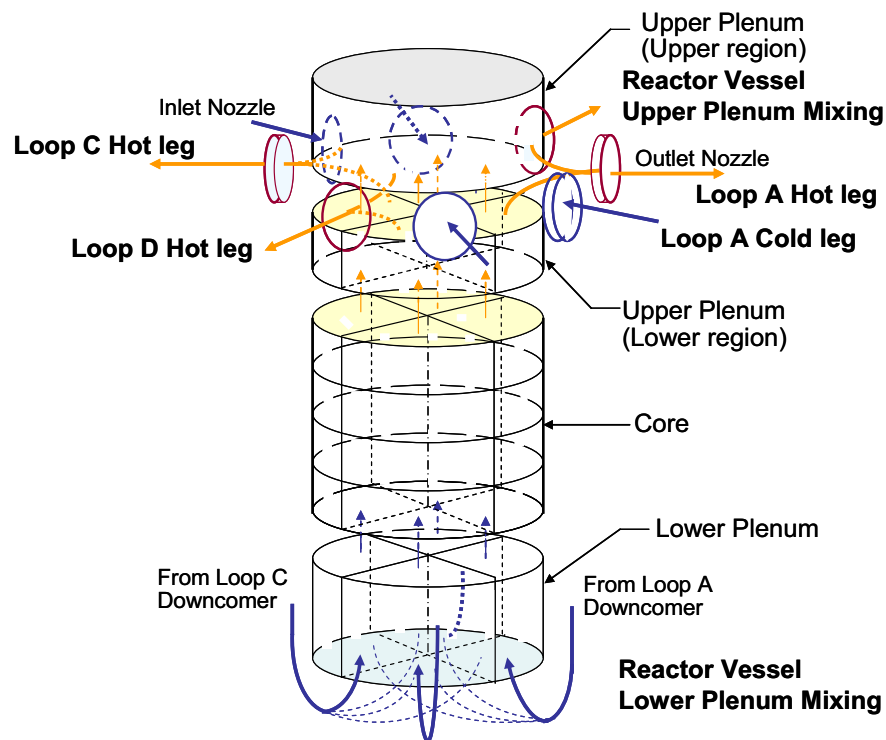


Figure 2.1-2 Reactor Coolant Flow and Mixing in Reactor Vessel

In order to simulate reactor conditions caused by imperfect mixing in the reactor vessel plenums, a maximum of four parallel flow channels can be provided in the reactor vessel as shown in Figure 2.1-2. The number of parallel flow channels is set at the actual number of

reactor coolant loops in the application. Cross flow between the flow channels is first assumed in the reactor vessel inlet downcomer sections, if the loop operation is unbalanced, so that flow rates leaving the downcomer are uniform. Mixing of reactor coolant flows between the flow channels are assumed to occur in the reactor vessel lower plenum and the upper plenum in order to account for imperfect mixing of the coolant in the reactor vessel according to user input mixing factors.

The code input mixing factor, $FMXI$, is calculated by :

$$FMXI = (1 - f_{mi}) \cdot \frac{Nloop}{(Nloop - 1)} \quad (1)$$

where

$Nloop$ = Total number of reactor coolant loops

f_{mi} = The fraction of the coolant flow emerging from an inlet nozzle which flows up the azimuthal part (per loop) of the core nearest the inlet nozzle.

$FMXI = 0$ means no mixing, while $FMXI = 1$ means perfect mixing. The mixing in reactor vessel upper plenum is specified by a factor $FMXO$ of the user input. The factor $FMXO$ is defined such that $FMXO=0$ means no mixing and $FMXO=1$ means perfect mixing. It is calculated by the following equation:

$$FMXO = (1 - f_{mo}) \cdot \frac{Nloop}{(Nloop - 1)} \quad (2)$$

where

f_{mo} = The fraction of vessel outlet flow leaving through an outlet nozzle which comes from the azimuthal part of the core nearest the outlet nozzle.

(3) Pressurizer Model

The change in the reactor coolant mass contained in the reactor coolant system (excluding the pressurizer) causes an outsurge or an insurge to the pressurizer through a pressurizer surge line which connects the pressurizer and the reactor coolant system hot leg. The pressurizer pressure is determined based upon an isentropic process during the steam expansion and contraction. An option is available that allows the isentropic process to change to a saturation process with an input time delay. After the pressurizer has emptied, the reactor coolant system pressure is determined by the compressibility of the coolant, in most cases a two phase mixture, in some part of the reactor coolant system.

2.1.2.3 Reactor Coolant Flow Transient Model

The manner in which primary system flows respond to a disturbance is important because such coolant flow removes the core heat and transfers it to the secondary fluid in the steam generators. An important phenomenon is the rapid flow decrease upon loss of reactor coolant pumping power – known as “flow coastdown”. A flow decrease occurs also when the frequency of the electric power supply decreases causing the reactor coolant pump speed to follow the frequency decay. Mechanical failures such as pump rotor seizure cause rapid flow reduction, which are analyzed as the locked rotor accident. After a complete pump loss the post-accident plant operation must rely on the plant’s capability for heat removal by natural circulation.

MARVEL-M is provided with a reactor coolant pump hydraulic and kinetics model so that flow transients can be computed by the pump model in conjunction with the existing reactor

coolant system hydraulic models. After the reactor coolant pumps are stopped, the reactor coolant flow becomes natural circulation. The natural circulation model is incorporated in the code.

2.1.2.4 Steam Generator and Secondary System Model

(1) Heat Transfer Coefficient from the Primary to the Secondary

The overall heat transfer coefficient in the steam generators consists of the four major thermal resistances: the primary convection film, the tube metal, the fouling, and the secondary side boiling heat transfer. Those resistances, except for the fouling resistance, are modeled to vary depending on changes in the appropriate parameters.

(2) Steam Generator Water Level and Heat Transfer Area

At no load conditions, the water level in the steam generators is calculated from the liquid volume contained in the steam generator shell and the geometry of the shell side volume. At power the water level is a complex function of liquid volume and other variables in the steam generator since the existence of void in the heating region in the shell side raises the water level considerably. The water level at power is modeled as a function of the water mass and the boiling rate in the secondary shell based on steam generator design calculations.

The effective heat transfer area is reduced when part of the steam generator tubes is uncovered. The effective heat transfer area is computed from the ratio of the water level to the height of the steam generator U-tube bundle. The heat transfer from the uncovered part of the steam generator tubes to the vapor in the shell side is assumed to be negligible and is not modeled.

(3) Steam Generator Secondary-Side Thermal Kinetics Equation

The steam generator secondary side contains a two-phase fluid. Assuming that most of the secondary fluid is at saturated conditions, and ignoring subcooling in the liquid in the preheat region and the downcomer, a thermal kinetics equation is derived from mass, volume and energy balance equations as a lumped saturated equilibrium mixture of vapor and liquid.

(4) Main Steam Lines and Steam Flow Distribution

MARVEL-M has the capability of simulating up to four steam generators and steam lines. The main steam lines from each steam generator are connected together at a common steam header, each via an isolation valve and a check valve.

If the operating conditions of the steam generators are different from each other, the steam outputs are unbalanced and the steam flow distribution is calculated from the steam pressure of each steam generator and the pressure losses through the steam lines to meet the total steam flow. A steam relief valve and up to three safety valves on each steam line are modeled; these valves are opened when the steam pressures increase above their respective set pressures.

2.1.2.5 Safety Systems and Miscellaneous Models

(1) Reactor Protection System - Reactor Trip

The reactor protection system is provided to protect the reactor core and plant design limits. The MARVEL-M code simulates the following reactor trips, which automatically insert the control rods to shut down the reactor when the trip signals reach or exceed their respective

setpoint. (Setpoints are usually set at the protection limit, which includes measurement error and channel error.)

- High Neutron Flux Trip
- High Flux Rate Trip
- Overtemperature ΔT Trip
- Overpower ΔT Trip
- Low Pressurizer Pressure Trip
- High Pressurizer Pressure Trip
- High Pressurizer Level Trip
- Low Steam Generator Water Level Trip
- High Steam Generator Water Level Trip
- Low Reactor Coolant Loop Flow Trip
- Turbine Trip

Overtemperature ΔT Trip and Overpower ΔT Trip protect the core operating limits, that define a region of permissible operation in terms of power, pressure, axial power distribution, and coolant temperatures.

The trip serves to protect the core against DNB and core exit boiling, accounting for all the adverse instrumentation setpoint errors and the time delays in signal measurement and processing. When the reactor coolant loop ΔT exceeds the calculated ΔT setpoint, the reactor is tripped.

Overpower ΔT Trip protects the reactor against excessive core thermal power. The protection line for the condition is a function of coolant temperatures and axial power distribution. When the reactor coolant loop ΔT exceed the calculated ΔT , the reactor is tripped.

(2) Safety Injection System (SIS)

The Safety Injection System is provided to deliver borated emergency core cooling water to the reactor coolant system to assure core cooling and reactivity control for accidents such as the main steam line break. The safety injection function is modeled in MARVEL-M, but the recirculation function used in the LOCA analysis is not modeled.

The Safety Injection System is equipped with two (or more) safety injection pumps, which take suction from the refueling water storage tank or pit and deliver borated water to the reactor through injection lines. A boron injection tank may be modeled in the cold leg injection line to promptly deliver highly concentrated boric acid. The injection system also includes accumulators, pressurized with nitrogen and connected to each cold leg, which also deliver borated water to the reactor. The gas-pressurized accumulators function as a passive injection system, discharging automatically when the reactor coolant system pressure decreases below the accumulator pressure.

(3) Safety Injection System Actuation System

The following Safety Injection System Actuators are modeled in the code

- Low Pressurizer Pressure
- Low Pressurizer Pressure in Coincidence with Low Pressurizer Level
- High Steam Flow in Coincidence with Low-Low T_{avg}
- Steam Line Differential Pressure
- Steam Line Low Pressure
- Manual Safety Injection

(4) Steam Line Isolation and Feedwater Isolation

The main steam line isolation valves are closed by a steam line isolation signal, which is generated from coincidence of high steam flow, safety injection, low T_{avg} , and/or high containment pressure signals. Manual actuation of steam line isolation is available.

A safety injection signal closes all control valves and trips the main feedwater pumps to isolate feedwater lines and close discharge valves. A low T_{avg} signal coincident with a turbine trip also actuates feedwater isolation to avoid excessive cooldown of the primary side due to continued addition of cold feedwater to the steam generators.

(5) Other Models

Thick metal effects, the Rod Control System, the Steam Dump Control System, and the Chemical and Volume Control System are also modeled.

2.1.2.6 Perturbations

Perturbations in many parameters and systems can be simulated in the code.

Examples include but are not limited to the following:

- Reactivity (e.g., rod drop)
- Core Power
- Reactor Coolant Loop Flows (e.g., partial or complete loss of flow, locked RCP rotor & sheared shaft)
- Steam Flow (e.g., turbine trip, loss of load, increase in steam flow)
- Feedwater Flow and Feedwater Enthalpy (e.g., loss of normal feedwater, increase in feedwater flow, change in feedwater temperature)
- Steam and Feedwater Isolation Valves
- Pressurizer Spray, Relief Valves and Auxiliary Spray
- Reactor Trip
- Steam Line Break
- Feedwater Line Break
- Reactor Coolant System Small Break (Including SG Tube Rupture)
- Safety Injection System Operation
- Chemical and Volume Control System Operation
- Turbine Runback and Trip
- Malfunction of Reactor Control Systems

2.1.3 Theoretical Models of MARVEL-M Improvement

This section describes the mathematical model improvements in the MARVEL-M code, including the models associated with the reactor coolant system loops and reactor coolant pump hydraulic kinetics model. This section also describes model refinements such as hot-spot fuel thermal kinetics and pressurizer surge line models.

2.1.3.1 Four Loop Reactor Coolant System Model

MARVEL-M code has the ability to simulate up to four reactor coolant loops. The hydraulic and thermal models of the individual reactor coolant flow sections and the models of the steam generators and pressurizer are the same as the original MARVEL code. The algorithm for core mixing in the reactor vessel in MARVEL-M is changed, although the basic model for each reactor coolant loop has remained the same as the original MARVEL code. The algorithm for the steam lines has changed to incorporate the expansion in the number of coolant loops that can be simulated by the code.

(1) Equation for Reactor Coolant Flow Sections

The reactor coolant system thermal kinetics equations are derived using a nodal approximation similar to the original MARVEL code. The nodes and flow sections are illustrated in Figure 2.1-3.



Figure 2.1-3 Reactor Coolant System Flow Model

One of six different flow models is used for each flow section. The six models include transport delay (denoted by *SLUG*), mixing (*MIXG*), a steam generator heat transfer section (*HEEX*), a core heated section (*HEAT*), a reactor vessel outlet plenum (*MIXS*), and an inactive coolant volume (*MIXD*). These models are functionally the same as the original MARVEL code.

(2) Dead Volume (Reactor Vessel Head Volume) (*MIXD*)

There is a plenum in the reactor upper head of the reactor vessel as shown in Figure 2.1-4. The volume is modeled as a control volume called the Dead Volume (*VDEAD*) as shown at the top of Figure 2.1-5.

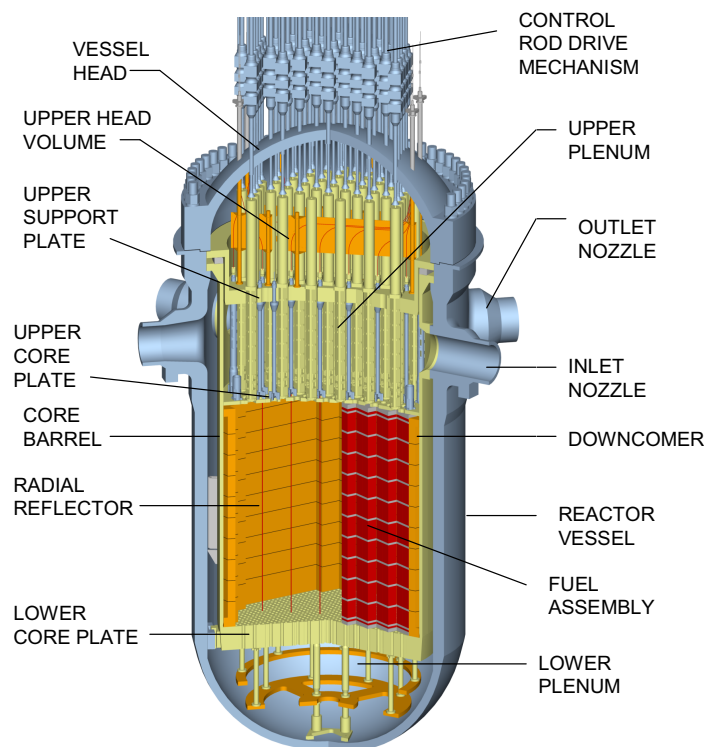


Figure 2.1-4 Reactor Vessel Inner Structure

A small fraction (*FDEAD*) of the coolant entering the reactor vessel is diverted and flows directly into the vessel head plenum (Upper Head Dead Volume) through small cooling spray nozzles. A small fraction of upper plenum flow (*FUPH*) goes up into the area through control rod guide tubes in the central area. A small rate of fluid flow exits from the dead volume to the upper plenum through control rod guide tubes in the peripheral region and is mixed with upper plenum coolant. The flow paths are modeled as shown in Figure 2.1-5.

The flow pattern is caused by the pressure difference profile across the upper support plate during forced reactor coolant flow conditions. With reactor coolant pumps stopped, the flow pattern is governed by the natural circulation head among fluids associated with elevation

differences. The coolant in the reactor vessel head plenum is stagnant and is virtually inactive during short-term transients, but the flow model determines steady-state temperatures in the upper head volume. The upper head temperature is between the hot leg and cold leg temperatures and is computed using the formula below.

$$\text{Initial Enthalpy} = (FDEAD * h_{cold} + FUPH * h_{hot}) / (FDEAD + FUPH) \quad (3)$$

h_{cold} and h_{hot} are coolant enthalpy at cold leg and hot leg, respectively.

The user-defined fraction $FUPH$ is smaller than $FDEAD$ and the initial upper head temperature is generally close to the cold-leg temperature. The value of $FUPH$ can be varied by the user to reflect different upper head temperature assumptions.

During plant cooldown or depressurizing transients the reactor coolant in the dead volume may flash and form a steam phase at the top, separated from the liquid. It may act as an alternate pressurizer to define the reactor coolant system pressure after the pressurizer is emptied. The downward flow leaving the dead volume is assumed to be single-phase liquid, even after the flashing occurs in the dead volume, until the void fraction becomes very large.

When the total mass in the reactor coolant system starts increasing, the pressurizer may begin to refill with water and, at the same time, the upper head vapor phase starts decreasing. During refilling of the boiled-off part of the dead volume, flow may occur from the reactor vessel upper plenum (below the core support plate) into the dead volume. The net incoming flow then refills the boiled-off part. This process may occur very slowly since the refilling requires condensation of the vapor existing in the dead volume. The processes in the pressurizer and the upper head depend on the reactor coolant condition. The described behavior of the dead volume is modeled in the code.

(3) Pressure Gradient in Reactor Coolant System

The core and reactor coolant system thermal-hydraulic model does not simulate the pressure gradient in the system except for the pressurizer and the reactor coolant system (at the hot-leg pressurizer surge line connection), although fluid properties in the flow sections are treated by two dimensions of specific enthalpy and pressure from subcooled to two phase flow (homogeneous).

Although, the reactor coolant system fluid in a PWR is normally pressurized and subcooled by the pressurizer, boiling of the coolant fluid may occur locally during specific transients due to excessive power increase or rapid depressurization.

The pressure gradient of the reactor coolant system is of importance for computation of pressure in the core for DNBR evaluation and the RCS maximum pressure, which usually occurs at the reactor coolant pump discharge with the pump running. The pressure differences between the pressurizer and those points are compensated for by adding pressure differences computed taking account of the pressure losses and the elevation effect.

2.1.3.2 Flow Mixing in Reactor Vessel (4-Loop Model)

The reactor coolant fluid that circulates in the reactor coolant loops is introduced into the reactor vessel through the inlet nozzles. Thus the mixing in the reactor vessel inlet and outlet plenum is imperfect. Therefore, in order to take this into consideration in the analysis of the reactor vessel thermal kinetics behavior, an azimuthal as well as an axial analysis is necessary. In this program, the azimuthal effect is considered by using a maximum of four

separate flow channels for each loop simulated. Although this model is not detailed enough to describe the exact thermal and hydraulic behaviors, by use of certain code inputs, representative or conservative prediction of reactor nuclear and thermal transients can be made. The flow model is shown in Figure 2.1-5.



Figure 2.1-5 Reactor Vessel Flow Model

(1) Mixing in the Downcomer and Reactor Vessel Lower Plenum

The flow sections $V(14,1)$ to $V(14,4)$ in Figure 2.1-5 correspond to the flow volumes of the annular volume between the vessel wall and the core barrel, including inlet nozzles, as seen in Figure 2.1-4. (These flow sections will be called the downcomers from here on.) Reactor coolant flow enters the downcomers through the reactor vessel inlet nozzles. When the direct vessel safety injection to reactor vessel option is used, the safety injection flow is introduced to the corresponding downcomer volumes. The flow lines are not shown in Figure 2.1-5.

i) Cross flows in downcomers

When loop flows are unbalanced, cross flows are assumed between downcomer flow sections $V(14,1)$ to $V(14,4)$. Cross flows are determined to satisfy the following conditions:

1. Cross flows may only exist between each downcomer section and the adjacent

downcomer sections.

2. Cross flow occurs so that coolant flow rates at the downcomer exit are uniform.
3. The cross flows are proportional to the differences between downcomer inlet flows.

ii) Mixing in lower plenum

Mixing in the reactor vessel lower plenum is assumed to occur, if specified in the code input, at the point where the coolant enters the lower plenum $V(15,1)$ to $V(15,4)$. The mixing factor $FMXI$ is defined by user input as follows:

$$\begin{aligned} & FMXI = 0 ; \text{ no mixing} \\ 0 < FMXI < 1 & ; \text{ partial mixing} \\ & FMXI = 1 ; \text{ perfect mixing} \end{aligned} \tag{7}$$

(2) Mixing in the Reactor Vessel Upper Plenum

Mixing in the reactor vessel upper plenum is assumed to exist in the flow volume $V(22,1)$ (refer to Figure 2.1-5). Partial mixing, if assumed, is simulated by taking the reactor vessel outlet flow partly from $V(22,1)$ and partly from the flow volume $V(21,i)$. (These are the volumes above the top of the active core and below the outlet nozzle center.)

The user-defined mixing factor $FMXO$ for the upper plenum is:

$$\begin{array}{ll} FMXO = 0 & ; \text{ no mixing} \\ 0 < FMXO < 1 & ; \text{ partial mixing} \\ FMXO = 1 & ; \text{ perfect mixing} \end{array} \quad (14)$$

2.1.3.3 Reactor Coolant Pump and Flow Transient Model

(1) Reactor Coolant Flow Transient Equations [Reference 11]

The fundamental flow transient equations are based on a momentum balance around each reactor coolant loop and across the reactor vessel, flow continuity, and the reactor coolant pump (RCP) characteristics with or without electrical power supply. The conservation equation for driving head, elevation head, and head losses is written for a multi-loop nuclear reactor system as follows:

$$H_{RV} + [H_{PUMP}]_i + [H_{LP}]_i + [H_{SG}]_i - \Delta P_{RV} - [\Delta P_{LP}]_i - \Delta P_{KE-RV} - [\Delta P_{KE-LP}]_i = 0, \quad i=1 \text{ to } Nloop \quad (22)$$

where

H_{RV} , H_{LP} , H_{SG} = head generated by the difference in elevation and density of fluid in the reactor vessel, cross-over leg, and steam generators, respectively

H_{PUMP} = reactor coolant pump head

ΔP_{RV} , ΔP_{LP} = pressure loss in reactor vessel and reactor coolant loop, including pipes, reactor coolant pump and steam generator
Note: if H_{PUMP} is input, ΔP_{LP} does not include pressure loss by RCP.

ΔP_{KE-RV} , ΔP_{KE-LP} = pressure head developed by fluid kinetic energy in reactor vessel and reactor coolant loop (including contributions from reactor coolant system pipes, pumps, and steam generator)

The RCP head, H_{PUMP} , is derived from the homologous curves of the RCP.

When the electrical power supply to a RCP motor is lost, the pump head, H_{PUMP} , is eventually lost. If the RCPs in the other loops continue to operate, the flow in the loop with the stopped RCP is reversed due to the reversed head between the reactor vessel inlet and outlet nozzle of the loop caused by the H_{PUMP} associated with the operating RCPs. For this condition, the stopped RCP acts as a flow resistance and the RCP performance for the reversed flow has to be prepared.

If all RCPs stop, the forced coolant flow eventually changes to natural circulation flow, if the elevation heads, H_{RV} , H_{LP} , H_{SG} , are developed. It should be noted that the head generated in the steam generator U-tubes is conservatively recommended not to be included because the head in each U-tube could be unstable.

The pressure heads developed by the fluid kinetic energy are expressed as:

$$\Delta P_{KE-RV} = \frac{1}{g} \sum \left(\frac{L}{A} \right)_{RV} \cdot \frac{dW_{RV}}{dt} \quad (23)$$

$$[\Delta P_{KE-LP}]_i = \left[\frac{1}{g} \sum \left(\frac{L}{A} \right)_{LP} \cdot \frac{dW_{LP}}{dt} \right]_i, \quad i=1 \text{ to } Nloop \quad (24)$$

where

g =acceleration due to gravity

$\left(\frac{L}{A} \right)_{RV}$, $\left(\frac{L}{A} \right)_{LP}$ = length of flow path over cross-section area of flow path for reactor vessel and loop.

W_{RV} , W_{LP} = mass flow rate in reactor vessel and in RCS loop

The pressure drop in the reactor or other sections of the coolant loops vary as a function of flow squared and the density. If the nominal full-flow conditions are known, the pressure drops are written as:

$$\begin{aligned} \Delta P_{RV} = \Delta P_{CORE}^0 \left(\frac{W_{CORE}}{W_{CORE}^0} \right)^2 \left(\frac{\rho_{CORE}^0}{\rho_{CORE}} \right) + \Delta P_{RVI}^0 \left(\frac{W_{RVI}}{W_{RVI}^0} \right)^2 \left(\frac{\rho_{RVI}^0}{\rho_{RVI}} \right) \\ + \Delta P_{RVO}^0 \left(\frac{W_{RVO}}{W_{RVO}^0} \right)^2 \left(\frac{\rho_{RVO}^0}{\rho_{RVO}} \right) \end{aligned} \quad (25)$$

$$[\Delta P_{LP}]_i = [\Delta P_{HL} + \Delta P_{SG} + \Delta P_{CL} + \Delta P_{PUMP}]_i = \left[\sum_j \Delta P_j^0 \left(\frac{W_j}{W_j^0} \right)^2 \left(\frac{\rho_j^0}{\rho_j} \right) \right]_i, \quad J=HL, SG, CL, PUMP \text{ and } i=1 \text{ to } Nloop \quad (26)$$

where

superscript: ⁰ denotes nominal value

subscripts: *CORE, RVI, RVO, HL, SG, CL, PUMP* = core, reactor vessel inlet plenum (downcomer), reactor vessel upper plenum, hot leg, steam generator, cold leg (including cross-over leg) and reactor coolant pump.

In Equation (26), $\left(\frac{W_j}{W_j^0} \right)^2$ is defined as having the same sign in the parenthesis in order to take account for the direction of the flow.

It should be noted that the pressure losses in Equations (25) and (26) are computed by mass flow squared compensated by the density, which is acceptable for turbulent flow, but is underestimated for laminar flow. Pressure loss corrections using Reynolds number are available in the code as an option (see Section 2.1.4 Realistic Models).

From basic conservation laws, the sum of the loop flows must equal the reactor vessel flow.

$$W_{RV} = \sum W_{LP} \quad (27)$$

For the steady-state condition, the reactor coolant flows are determined by Equations (22) to (27), assuming $\Delta P_{KE} = 0$.

(2) Reactor Coolant Pump Model

The sum of various torques in the RCP must equal the pump motor torque:

$$T_{KE} + T_H + T_W = T_M \quad (28)$$

where

T_{KE} = pump kinetic torque

T_H = pump hydraulic torque

T_W = pump windage and friction torque

T_M = pump motor torque

The pump motor torque, T_M , is given by the speed-torque curve of the pump motor. The torque generated by an induction motor is a function of the difference between motor speed and the synchronous speed.

Flow Coastdown

When the electrical power to a pump motor is interrupted, the motor torque, T_M in Equation (28), becomes zero and a flow coastdown results, which is characterized by a decreasing reactor coolant flow in each affected loop.

$$T_{KE} + T_H + T_W = 0 \quad (29)$$

In the fundamental Equation (22), the reactor coolant pump head, H_{PUMP} , decreases according to the decrease of the pump speed. During the flow coastdown the pump head is generated by the inertia of the pump and the coupling between the pump and the system fluid is considered.

The kinetic energy of rotating parts of the reactor coolant pump is:

$$KE = \frac{1}{2g} I_P \varpi^2 \quad (30)$$

where

I_P = moment of inertia of rotating parts of reactor coolant pump

ϖ = angular speed of rotating parts of reactor coolant pump

The kinetic energy is dissipated into several losses and the power developed by the inertia is given by differentiating Equation (30). Dividing by the speed gives the total torque developed by the depletion of the kinetic energy.

$$T_{KE} = \frac{1}{g} I_P \cdot \frac{d\varpi}{dt} \quad (31)$$

The hydraulic torque is defined as

$$T_H = \frac{W \Delta P_P}{\varpi \eta \rho} \quad (32)$$

where

W = fluid flow rate

ΔP_P = reactor coolant pump pressure head

η = hydraulic efficiency of reactor coolant pump

ρ = fluid density

The pump windage and friction torque is defined as

$$T_W = K_W \omega^n \quad (32a)$$

where

K_W = friction and windage coefficient

n = constant

The pump head H_{PUMP} is determined from head versus flow characteristics of the pump which depends on the pump speed. The effect of a change in pump speed on the head-flow curve is defined according to the following affinity law:

$$H_{PUMP} = f_{HF}(\omega, W) \quad (33)$$

The above equations can be solved exactly if the pump characteristics, reactor system pressure losses, friction, windage and retardation torques are known.

Pump Motor Power Frequency Decay

If the frequency of the pump power decays, the motor torque, T_M in Equation (28), decreases depending on the pump motor speed-torque characteristics, causing decrease of the pump speed and the pump hydraulic torque. Because the RCPs use synchronous AC motors, the reactor coolant flow decreases by about the same rate as the pump speed and frequency decay. The frequency decay rate is determined from the electrical network strength against failures in some of the power generating stations in the network.

Reactor Coolant Pump Locked Rotor

If a RCP rotating part is locked and the rotation of the impeller instantly stops, the reactor coolant pump hydraulic torque is lost and the loop coolant flow rapidly decreases. Eventually the loop flow is reversed due to the head of the intact reactor coolant pump in the other loops. The flow change is calculated using the reactor coolant pump hydraulic characteristics with the rotor locked. In such a case, the reactor coolant flow in the core also decreases rapidly causing a rapid reduction in core heat removal.

All the models described by the above equations have been incorporated in the MARVEL-M code and coupled with the reactor coolant system models. The code can compute flow transients from the various causes, allowing different flows in up to four loops. If all the reactor coolant pumps stop, the flow transient proceeds to natural circulation condition continually.

The flow transients are integrated with the other nuclear and thermal-hydraulic performance. The flow models are applicable to the reactor transient analysis for partial loss of flow, complete loss of flow (including due to pump motor power frequency decay) and locked rotor.

(3) Natural Circulation Elevation Head Model

When the electrical power to a pump motor is interrupted, the reactor coolant pump torque becomes zero and the reactor flow coasts down and the pump eventually stops rotating.

If the elevation heads, H_{RV} , H_{LP} , H_{SG} , are developed, natural circulation flow is established. The natural flow conditions are calculated by the overall balance equation, Equation (22), using the relevant equations for the associated variable terms.

The driving forces in the case of natural circulation are calculated from the difference in the fluid densities around the circuit as follows:

$$H_{RV} = \int_{RVI}^{RVO} \rho \cdot dz = (Z_{CORE} + Z_{PL})\rho_{RVI} - Z_{CORE}\rho_{CORE} - Z_{PL}\rho_{RVO} \quad (34)$$

$$[H_{LP}]_i = \int_{RVO}^{RVI} \rho \cdot dz = [Z_{CL} (\rho_{CL}^{SG} - \rho_{CL}^{RCP})]_i, \quad i=1 \text{ to } Nloop \quad (35)$$

$$[H_{SG}]_i = \int_{RVO}^{RVI} \rho \cdot dz = [Z_{SG} (\rho_{SGO} - \rho_{SGI}) + Z_{TUBE} (\rho_{SGC} - \rho_{SGH})]_i, \quad i=1 \text{ to } Nloop \quad (35a)$$

where

Z_{CORE} = core height (active fuel region)

Z_{PL} = height of reactor vessel outlet nozzle centerline above top of core (active fuel region)

Z_{SG} = height of steam generator tube sheet above the hot leg centerline

Z_{TUBE} = height of average steam generator U-tube

Z_{CL} = height of reactor coolant cross-over piping (cold leg reactor vessel inlet nozzle centerline above bottom of cross-over centerline)

ρ_{RVI} , ρ_{RVO} = fluid density in reactor vessel inlet plenum (downcomer) and upper plenum, respectively

ρ_{CORE} = average fluid density in core

ρ_{SGI} = average of fluid density in hot-leg piping, rising part to SG, and fluid density in SG hot leg side plenum

ρ_{SGO} = average of fluid density in SG cold leg side plenum and cold-leg piping from SG to the level of reactor vessel inlet nozzle centerline

ρ_{SGC} = average fluid density in steam generator cold leg side tubes

ρ_{SGH} = average fluid density in steam generator hot leg side tubes

ρ_{CL}^{SG} , ρ_{CL}^{RCP} = fluid density in the cross-over leg. Superscripts of SG , RCP denote steam generator side and reactor coolant pump side, respectively

(4) Solution of Flow Transient Equations

Equation (22) with the relevant equations for the various associated variable is reduced to the following set of simultaneous equations for changes in the loop flow,

$$\frac{1}{g} \left(\frac{L}{A} \right)_{LP} \cdot \left[\frac{\Delta W_{LP}}{\Delta t} \right]_i + \frac{1}{g} \left(\frac{L}{A} \right)_{RV} \cdot \frac{\Delta W_{RV}}{\Delta t} = [H_{PUMP}]_i + H_{RV} + [H_{LP}]_i + [H_{SG}]_i - \Delta P_{RV} - [\Delta P_{LP}]_i, \quad i=1 \text{ to } Nloop \quad (36)$$

When the reactor coolant pump in a reactor coolant loop is running, the head of the reactor coolant pump $[H_{PUMP}]_i$ is calculated from Equations (29) to (33). If some pumps are not running, the idle reactor coolant loop flow for the loop associated with the idle pump is reversed, and the pump head is replaced with a pressure loss. When all the reactor coolant pumps are not operating, all the pump heads, $[H_{PUMP}]_i$ are replaced with pressure losses and the reactor coolant flow transitions to natural circulation. The natural circulation flow in the multiple loops depends primarily on the power generation in the reactor core and the heat

removal in the loops at the steam generators. The flow transition from the forced circulation to the natural circulation is calculated using Equation (36).

In solving Equation (36) the unknown parameter of interest is the loop flow, W_{LP} . This equation is a second order equation for W_{LP} . Then MARVEL-M solves for W_{LP} using the quadratic formula. All anticipated and postulated reactor coolant system flow transients are computed by Equation (36) with the boundary conditions specified in the input data.

2.1.3.4 Secondary Steam System Model (4-Loop Model)

(1) Distribution of Steam Flows

The main steam lines from each steam generator are connected together at a common steam header, each via an isolation valve and a check valve, as illustrated in Figure 2.1-6.

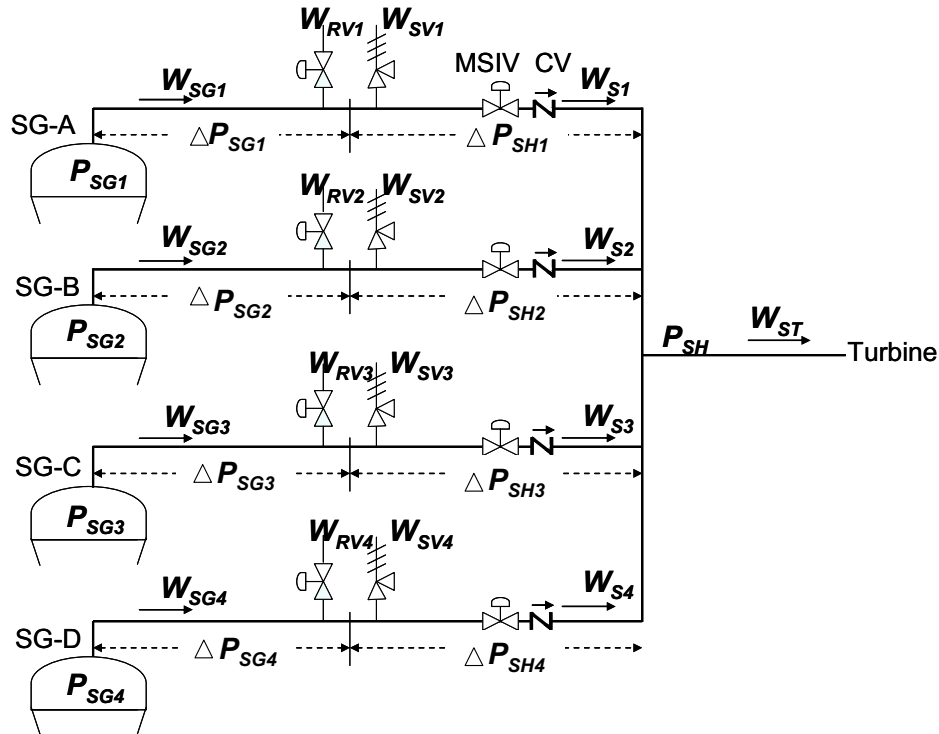


Figure 2.1-6 Steam Line Model

If the operating conditions of the steam generators are different from each other, the steam outputs from the steam generators are unbalanced. The steam flow distribution is then dependent upon the steam pressure of each steam generator and upon the pressure losses through the steam lines. The steam flow distribution can be obtained by solving the following basic equations:

$$\left[P_{SG} + \frac{\Delta P_{SG}^0}{\rho} \cdot (\bar{W}_{SG})^2 + \frac{\Delta P_{SH}^0}{\rho} \cdot (\bar{W}_S)^2 \right] = [P_{SH}]_i, \quad i=1 \text{ to } Nloop \quad (37)$$

$$\bar{W}_S = \bar{W}_{SG} - \bar{W}_{RV} - \bar{W}_{SV} \quad (37a)$$

$$\bar{W}_{ST} = \sum_{i=1, N} [\bar{W}_S]_i \quad (38)$$

$$[P_{SH}]_i = P_{SH} \quad (39)$$

where $\bar{W}_{SG}, \bar{W}_{RV}, \bar{W}_{SV}$ are steam generator, relief valve and safety valve mass flow rates normalized by the rated loop steam flow rate.

To solve the four non-linear equations of (37) for a multi-loop plant, the following predictions of the steam generator pressures at the next time step are introduced for stable computation, since changes in steam flow change steam generator pressures and vice versa.

For a 3- and 4-loop plant, simultaneous second-order equations are solved by iterative computation to converge the entire solution.

When $[P_{SH}]_i$ becomes higher than the set pressure of the relief valves or safety valves, the valves open and steam is relieved. For the relief valves, the entire relief valve flow is added to the total turbine steam flow in Equation (38). Since the actual plant design has lock-up features in the relief valve trip open functions, MARVEL-M incorporates a steam generator relief valve lock-up to prevent oscillations from occurring in this on/off situation. For the safety valves, the valves open and steam is relieved as necessary to maintain the pressure at the setpoint. If the necessary steam relief is greater than the maximum relief rate, the maximum is relieved and $[P_{SH}]_i$ is allowed to increase.

If some of the steam line isolation valves are closed, the steam flow from those steam lines becomes zero and the steam flow to the turbine, W_{ST} , is provided from the steam generators with their respective steam isolation valve open. If the main steam check valves are modeled, reverse steam flow is not allowed and the steam lines are all treated independently after turbine trip.

Note:

In solving equations (37) to (39), pressure losses $[\Delta P_{SH}]_i$ (between the secondary safety/relief valves and common steam header) are assumed to be zero for simplification. This assumption is reasonable since the MARVEL-M model assumes the valves are close to the common steam header and the pressure loss for the entire steam line in this configuration is dominated by the pressure losses at the steam generator exit nozzle (with integral flow restrictor).

(2) Steam Safety and Relief Valves

Multiple safety valves with slightly different set pressures are provided in each steam line. The simulation of those safety valves includes a maximum of three valves with different set pressures and the valve pressure accumulation when opened.

Relief valves can be controlled by automatic proportional controllers to maintain steam pressure at the set-point. Manual control is also simulated. Steam released from safety and relief valves is released to the atmosphere. The MARVEL-M code has the capability to integrate atmospheric relief flow for use in the radiological assessment of certain accidents.

2.1.3.5 Other Model Refinement

MARVEL-M contains some other additional refinements beyond what has been described in the previous sections. Items (1) through (4) are MHI refinements made in the 1970s, while item (5) is a refinement of the numerical solution methodology adopted in the MARVEL-M code.

(1) Pressurizer Surge Line Model

A flow section has been added in the pressurizer surge line to the original MARVEL code between the reactor coolant system hot leg connection and the pressurizer. This is to more realistically model pressurizer insurge water enthalpy. If the pressurizer surge line is not simulated, hot leg coolant water directly enters the pressurizer during pressurizer insurge. This may result in overpredicting cooling of the pressurizer liquid phase and may cause a larger pressurizer pressure reduction for a subsequent outsurge. This refinement resulted from the observation of a transient test during a reactor plant pre-operational test.

(2) Hot-Spot Fuel Thermal Kinetics Model

A hot-spot fuel thermal kinetics model is provided in the original MARVEL code. The model was similar to the fuel thermal kinetics model for the average channel.

A more detailed hot-spot fuel thermal kinetics model is included in the MARVEL-M code. The basic model is the same as the FACTRAN code by Westinghouse, which was approved by the NRC [Reference 10]. The FACTRAN code has the ability to model of up to 10 radial sections in the fuel pellet, cladding and clad surface heat transfer coefficient to compute the transient fuel temperature and heat flux. FACTRAN also has the capability to handle post-DNB transition film boiling heat transfer, Zircaloy-water reaction, and partial melting of the pellet material. The use of the model added to MARVEL-M is limited to the computation of the heat flux transients at the surface of the cladding at a hot-spot. The normalized hot-spot heat flux can be used as an option (the largest heat flux between the average channel and the hot spot is used) to calculate DNBR using the simplified DNBR model in MARVEL-M. The fuel pellet thermal properties can be input by the user.

(3) Core Void Simulation

Boiling can occur in the reactor core when the core power increases excessively or if the core coolant temperature exceeds the saturation temperature. The void causes insurge to the pressurizer, resulting in an increase in pressurizer pressure. The MARVEL-M code has an internal model to calculate the void fraction in the core. The MARVEL-M code has added a scheme to accept void transients calculated by an external detailed thermal-hydraulic code, which can compute void formation taking into account subcooled boiling, detached boiling, as well as bulk boiling. The VIPRE-01M code can be used for that purpose. This feature is

only used to assure that the RCS pressure is conservatively high for the rod ejection accident where local void formation in the core could impact the peak pressure.

(4) Feedline Break Blowdown Simulation

Licensing feedline break analysis uses the water release rate computed by the Moody correlation. During the water release, when the steam generator is depressurized below the feedwater saturation pressure, feedwater contained in the feedline flashes and a mixture of steam and water can be released into the steam generator shell side. This phenomenon is simulated by a flow section connected to the steam generator secondary side.

(5) Conversion of Reactor Coolant System Volume Balance by Pressure Search

2.1.4 Realistic Models

The original MARVEL code was developed for transient and accident analysis (excluding LOCA events) and control system design studies for pressurized water reactor plants. The models are sufficiently accurate for the purposes of design and licensing safety analysis. The code has also been used for various other applications, such as analysis for operating instruction development, support for plant transient tests (start-up tests), and post-event analysis of operating plant events (e.g. the steam generator tube rupture event at Mihama Unit 2 in 1993). Through those analyses the MARVEL code has been refined and various models have been added in order to simulate real plant transient behavior. Selected model refinements for these realistic analyses are described in this section, although they are typically not used for licensing safety evaluation of reactor plants. Use of these models is optional and is controlled by user input in the MARVEL-M code.

2.1.4.1 Steam Generator Tube Rupture

A steam generator tube rupture event (a single double ended tube rupture) occurred at the Mihama Unit No.2 (a 2 loop PWR plant designed by Westinghouse and constructed by Mitsubishi for Kansai Electric). During the actual event many systems were actuated and operated (e.g., Low Pressurizer Pressure reactor trip, Low-Low Pressurizer Pressure Safety Injection, manual actions for reactor coolant system (RCS) cooldown using a secondary relief

valve, depressurization of the RCS by auxiliary pressurizer spray, termination of the SG leak in the failed SG by termination of SI, etc.). Many reactor system transient behaviors were also observed, including emptying the pressurizer, recovery of pressurizer water level, natural circulation in the primary loops, the failed SG secondary side transients such as steam pressure increase to actuate steam relief valves repeatedly, and SG water level increase. The reactor plant was safely shut down without significant radioactivity release.

(1) Event analysis by MARVEL-M code

The event was analyzed using the MARVEL-M code to ascertain the adequacy of the reactor system operation and to aid in the response to detailed regulatory questions and examination.

The MARVEL-M code and the models for SGTR event were evaluated and verified to be able to analyze such an accident with sufficient accuracy.

(2) Realistic SGTR Models

To obtain better agreement between the MARVEL-M analysis and the trend records of the event several realistic models were developed and added to the MARVEL-M code during the post-accident analysis of the event.

The essentially important models are:

- Pressure transient after pressurizer emptied and water level recovery
- Failed SG secondary response (SG steam pressure, water level, etc.)
- Tube leak model

(a) Reactor Vessel Upper Head Model

After the pressurizer is emptied RCS pressure is maintained by the stagnant fluid in the upper head volume, where vapor phase is formed and acts as an alternate pressurizer. High Pressure Safety Injection also acts to maintain the system pressure. Essential models of the upper head are already incorporated in the code as described in this document. To obtain closer agreement between the reactor coolant system pressure and the pressurizer level transient, the following realistic models were investigated and added to the MARVEL-M code. Some Japanese PWRs used to be designed to trip the electric cross-tie breakers between the non-safeguards busses and the safeguard busses on a Safety Injection signal. That causes loss of power supply to the reactor coolant pumps, resulting in natural circulation flow.

- i) During natural circulation, flow through the cooling spray nozzle in the upper head may exist due to elevation heads caused by temperature differences between the downcomer and reactor vessel upper plenum.
- ii) Condensing heat transfer may occur between the vapor phase and the upper head metal and liquid in the upper head volume.

(b) Realistic Steam Generator Tube Leak Flow Model

The following conservative realistic model to compute SGTR leak flow has been added to the MARVEL-M code. The initial primary-to-secondary leak flow at steam generator tube rupture is computed as the critical flow, and the leak flow transitions to orifice-type flow (not critical) later when the pressure difference between the primary and secondary sides is reduced. In the calculation the pressure losses along the tube from the tube inlet or outlet to the break point are included. A conservative, but realistic SGTR analysis can be performed with a user-defined discharge coefficient of 1.0 for critical flow.

(c) Reverse Heat Transfer Coefficient

When the steam generator shell-side temperature is higher than the primary side temperature, heat is transferred from the shell side to the primary side. A constant value for the reverse heat transfer coefficient can be input. An internal calculation can also be selected using either the McAdam's or Kreith correlation.

(d) The steam in the failed SG and steam line can be compressed because of the increase in SG level due to leakage from the primary side. Steam in the steam line may be condensed by condensate heat transfer to the pipe wall.

(e) Coolant leaking from the primary side may not be completely mixed with the secondary water. A two-node model for the water portion of the steam generator secondary is added to account for cooling of a portion of the steam generator water when the RCS temperature is below the steam generator temperature.

2.1.5 Precautions and Limitations for the Use of the MARVEL-M Code

2.1.5.1 Range of Operating Variables

The program is designed to be run within the following ranges of operating variables.

- Reactor Coolant System Temperature and Pressure
 - Temperature : 50°F to approximately 1100°F
 - Pressure : 50 psia to critical pressure (about 3200 psia)
- Pressurizer Water Level
 - From empty to full including water discharge (After the pressurizer is emptied, the program may analyze the system behavior until the coolant in the reactor vessel inactive volume (dead volume) is boiled off.)
- Steam Generator
 - Steam Pressure : 14 psia to 1500 psia
 - Water Inventory : Empty to moderately high level
- Reactor Coolant Loop Flow
 - Forward, reverse and natural circulation flows are computed. Two phase flows are also permitted as a homogeneous equilibrium mixture of vapor and liquid
- Reactor Core Kinetics
 - Reactor power : neutron source level to overpower level
 - Reactivity : sub-critical to super-prompt critical.

The program is intended to cover a very wide range of operating parameters. However, when the plant operating variables deviate excessively from the normal operating conditions, care must be used in interpreting the results in context with the accuracy and limitations of the code models over the regions where the variables are extreme.

2.1.5.2 Applicability of the Code to the Scenarios of Licensing Analysis

The MARVEL-M code is used for multiple transients and accidents. The code is provided with the models for most of the scenarios in the design basis transients and accidents for pressurized water reactor plants except for Loss of Coolant Accident. However, other appropriate codes should be used for specific transients and accidents in part or as a whole, since the following models are not sufficiently detailed for certain specific transients.

- Space independent one point neutron kinetics equations are used.

- A simplified DNBR calculation is modeled, but detailed DNBR calculation should be performed by an external code.
- Two phase flows in the reactor coolant system are modeled assuming homogeneous equilibrium mixture of vapor and fluid, except for the pressurizer and the upper head volume where vapor and liquid are separated and not at equilibrium.

The following events should not be evaluated with MARVEL-M. The use of another appropriate code is recommended.

(1) Transients

- (a) Transients that are classified as reactivity initiated events (RIE), e.g. Inadvertent Rod Withdrawal from Sub-critical Condition, should be analyzed by a code developed for the specific purposes. (The TWINKLE-M code is used for the US-APWR.)
- (b) Transients for which the minimum DNBR is heavily dependent on changes in reactor coolant flow. For example, the Loss of Flow should use a thermal-hydraulic code which can compute the local fuel kinetics and DNBR correctly using the output of plant operating variables by MARVEL code. (The VIPRE-01M code is used for the US-APWR.)

(2) Accidents

- (a) Reactivity Initiated Accidents, e.g. RCCA Ejection, should be analyzed using a spatial neutron kinetics code. (TWINKLE-M code is used for the US-APWR.)
- (b) DNBR calculations for the large steam line break from a shutdown or hot standby condition should be calculated by an appropriate external thermal-hydraulic code with capability of computing DNBR, in conjunction with a spatial neutron kinetics code if a large transient distortion of the flux distribution is to be taken into account.
- (c) LOCA should be analyzed by LOCA codes.

(3) Conservatism in Models

Safety analysis for Chapter 15 for a safety analysis report of a reactor plant should be performed with adequate conservatism to assure the safety of the reactor plant for Anticipated Operational Occurrences (AOOs) and Postulated Accidents (PAs). The conservatism or safety margins should be assured by the computer models, assumptions and safety criteria, and input data used for the analysis, depending on the scenarios of the transients and accidents.

The MARVEL-M code may be regarded as a code between best estimate (BE) and evaluation model (EM). Key conservatisms in the models are:

- (a) The pressurizer pressure calculation is based on the isentropic process of the vapor phase for short-term that gives conservatively higher pressure increase for insurge transients.
- (b) The steam generator secondary side thermal model is based on equilibrium of the vapor and liquid at saturation, neglecting the subcooling in the downcomer and the preheat region. This model is generally conservative: i.e. subcooled water, if modeled, could absorb some energy following a loss of load, loss of normal feedwater flow and feedline break and also for a SG tube rupture accident.
- (c) MARVEL-M computes the pressurizer pressure and the reactor coolant system pressure at the connection of the pressurizer surge line. The pressure differences between the surge line connection, core, and the maximum pressure point (usually at the discharge of the reactor coolant pump) are corrected at each time step by adding a conservative bias. For the purpose of calculating fluid properties, the RCS pressure is

assumed to be constant around the RCS loop, because the RCS coolant is subcooled in a PWR.

- (d) The model of the reactor coolant mixing in the reactor vessel allows conservative mixing by selecting the mixing factors bounding the best estimation based on the experimental data.

The MARVEL-M code may be regarded as a realistic conservative evaluation code as a whole. The transient and accident analyses performed using the MARVEL-M code are expected to give sufficiently conservative results by using conservative assumptions and conservative values of plant data depending on the scenarios of the transient and accident.

2.2 TWINKLE-M Code

The TWINKLE-M code is the multi-dimensional spatial neutron kinetics code which solves two-group transient diffusion equations using a finite-difference technique. The code uses six delayed neutron groups and contains the detailed fuel-clad-coolant heat transfer model for calculating mesh-wise Doppler and moderator feedback effects. The code is used to predict the kinetic behavior of a reactor for the transients that cause a major perturbation in the spatial neutron flux after steady-state initialization.

Aside from basic cross-section data and thermal-hydraulic parameters, the code accepts the following types of basic input parameters: inlet temperature, pressure, flow, boron concentration, control rod motion, and others. Various outputs are produced (for example, channel-wise power, axial offset, enthalpy, volumetric surge, point-wise power, and fuel temperatures).

The original TWINKLE code was approved by the NRC (WCAP-7979-P-A) [Reference 3] as a multi-dimensional neutron kinetics analysis code. The code was licensed to MHI under the licensing agreement between Westinghouse and MHI. Since then the code has been applied to licensing analysis for Japanese PWRs. At the beginning, a conservative methodology based on one-dimensional kinetics with the assumption of a constant hot channel factor during transient was applied to the RCCA ejection for fuel enthalpy evaluation.

In 1993 the fuel failure threshold for the RIE (Reactivity Initiated Event) for Japanese PWRs was required to be lowered and expressed as a function of local fuel burnup. This change was in response to the results of the RIE fuel failure testing at NSRR (Nuclear Safety Research Reactor) experiments. In order to comply with the new threshold, MHI introduced a more realistic methodology for the RCCA ejection from hot zero power condition. This methodology employed a time-dependent hot channel factor based on the three-dimensional kinetics model in the TWINKLE code. The maximum number of spatial mesh points had to be increased to allow a full three-dimensional core representation. In addition, a discontinuity factor consistent with a core simulator ANC code [Reference 12] was incorporated to present the local power distribution more accurately. This new version of TWINKLE is now referred to as TWINKLE-M.

MHI has used the TWINKLE-M three-dimensional kinetics code to validate the use of a one-dimensional model for plant licensing in Japan. This is supported by the following:

- The TWINKLE code was originally approved by the NRC as a multi-dimensional kinetics code.
- The TWINKLE three-dimensional static calculation is in good agreement with the ANC.
- The TWINKLE three-dimensional kinetics is used as a reference solution for a recent nodal kinetics code SPNOVA developed by Westinghouse. The SPNOVA code was approved by the NRC [Reference 13].

MHI has had significant experience in using the 1-D and 3-D capabilities of the TWINKLE-M code over many years.

Section 3 presents validation of the three-dimensional calculation. This information supports the use of TWINKLE-M 1-D and 3-D capabilities for licensing new reactors in the US.

2.3 VIPRE-01M Code

VIPRE-01M is the MHI version of VIPRE-01, which is a subchannel analysis code that is developed to perform thermal-hydraulic analyses in reactor cores. Using the original VIPRE-01 code as the basis, MHI incorporated certain added functions for more flexible design applications. VIPRE-01M is used to evaluate reactor core thermal limits related to the minimum DNBR, reactor core coolant conditions, and fuel temperature and heat flux in normal and off-normal conditions.

The original version of VIPRE-01 was developed by Battelle Pacific Northwest Laboratories, under the sponsorship of Electric Power Research Institute (EPRI). Its basic components are from the well-known COBRA code series. VIPRE-01 divides the reactor core into a number of flow channels. The size of each flow channel could be as small as the flow area surrounded by four fuel rods (fuel rods and/or control rod guide thimble) situated on a square lattice, or be formed by a number of fuel rod bundles. Conservation equations of mass, momentum (in axial and lateral directions), and energy are solved to determine axial mass flux distributions, lateral flow rate per unit length, and enthalpy distributions. Fluid properties are functions of the local enthalpy and a uniform but time-varying system pressure. Transient thermal behavior of the fuel rod is also analyzed in association with the determined thermal-hydraulic analysis results.

Specific constitutive models which prescribe optional flow resistance, turbulent mixing, and subcooled as well as saturated boiling, are selected in VIPRE-01M analyses to provide adequate results for the purpose of the applications.

VIPRE-01M has incorporated mainly the following features into the original VIPRE-01.

- DNB correlations for design applications
- Fuel thermal properties for design applications
- Options for hot spot PCT analysis

The original solution methods and constitutive models are not changed at all. Therefore, the VIPRE-01M code is virtually identical to the original VIPRE-01. The conclusion of validation for the original VIPRE-01 code by EPRI still remains valid.

The details concerning calculation models, additional DNB correlation, fuel properties of the VIPRE-01M code and validation to transient analysis are described in Reference 6.

3.0 CODE VALIDATION

3.1 MARVEL-M Code

The MARVEL-M code is the same as the original MARVEL code from the viewpoint of constitutive and principal models. The main differences between the original MARVEL code and MARVEL-M are the extension from 2-loop simulation to 4-loop simulation and the addition of a built-in RCP model. The other refinements such as a pressurizer surge line node, a hot spot heat flux simulation model, and improved numerical solution and conversion techniques are described in Section 2.1.3.5.

This section provides a comparison of the calculated results between the MARVEL-M code and the 4-loop LOFTRAN* code in order to validate the adequacy of the modifications included in the MARVEL-M code. A code-to-code comparison is sufficient for this purpose because the LOFTRAN code has been used extensively in the licensing analysis of currently operating nuclear plants in the US for the accidents that are affected by the new MARVEL-M models.

*MHI has the source code, as well as sample input and output, for the 4-loop LOFTRAN code under a licensing agreement with Westinghouse.

The uncontrolled RCCA bank withdrawal at power has been chosen because both the LOFTRAN and MARVEL-M codes use simplified internal DNBR calculations to demonstrate the adequacy of the reactor protection system for uniform transients. The loss of flow accidents (partial loss of flow, complete loss of flow, and locked rotor) have been chosen because both LOFTRAN and MARVEL-M use an internal reactor coolant pump model for calculating the loop and total core flow transient. Comparison of other key parameters for these accidents such as nuclear power, core thermal power, RCS average temperature, and pressurizer pressure further confirm that the reactivity, pressure, and power models in the MARVEL-M code remain valid.

3.1.1 Uncontrolled RCCA Bank Withdrawal at Power

(1) Event Description

The Uncontrolled RCCA Bank Withdrawal at Power event initiates from nominal power operation. The event produces a positive reactivity insertion, and nuclear power increases until a reactor protection system setpoint is reached.

The Uncontrolled RCCA Bank Withdrawal at Power has been chosen because both the LOFTRAN and MARVEL-M codes calculate power and RCS parameters to demonstrate the adequacy of the reactor protection system for uniform transients. In this way, the transient validates the overall adequacy of the point kinetics model, fuel heat transfer model, and RCS thermal hydraulic model. Parameters of interest include reactor power, core average heat flux, RCS average temperature, and pressurizer pressure.

The maximum control rod insertion reactivity case (75 pcm/sec) is selected because it results in the maximum perturbation to the parameters of interest.

(2) Analysis Assumption

Analysis assumptions and calculation conditions in the typical 4-loop plant with a 17x17, 257 fuel assembly (17x17-257FA) core are as follows.

(a) Initial condition	Nominal power, Nominal T_{avg} , Nominal RCS pressure
(b) Reactor trip	118% nominal power
(c) Insertion reactivity rate	75 pcm/sec
(d) Feedback reactivity	Minimum feed back
(e) Trip reactivity	-4% $\Delta K/K$
(f) Pressure control system	Off

(3) Results and Conclusions

Comparison results of MARVEL-M and LOFTRAN are shown in Figures 3.1.1-1 through 3.1.1-4. The results demonstrate that the two codes have equivalent capabilities and are in close agreement.

It is concluded that the MARVEL-M code is suitable for use in analyzing uniform non-LOCA transients assuming constant RCS flow that challenge the reactor protection system.

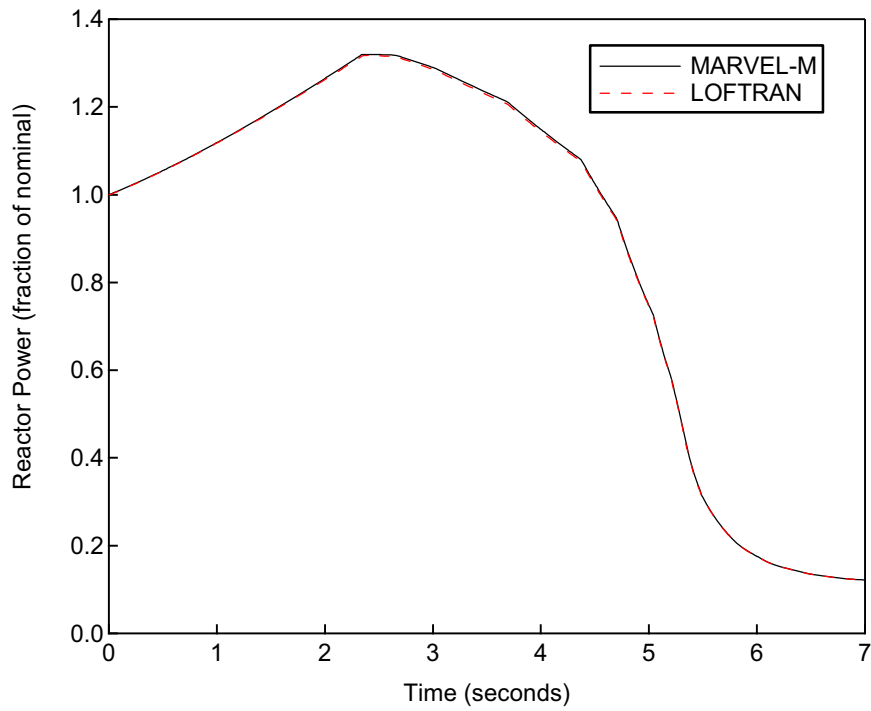


Figure 3.1.1-1 Reactor Power, Uncontrolled RCCA Bank Withdrawal at Power Comparison with MARVEL-M and LOFTRAN

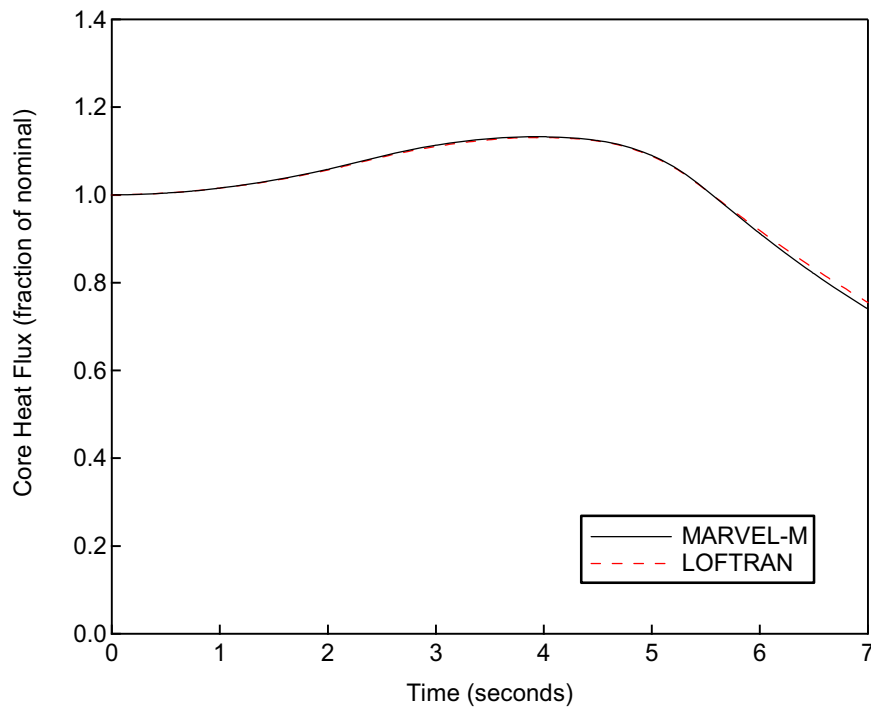


Figure 3.1.1-2 Core Heat Flux, Uncontrolled RCCA Bank Withdrawal at Power Comparison with MARVEL-M and LOFTRAN

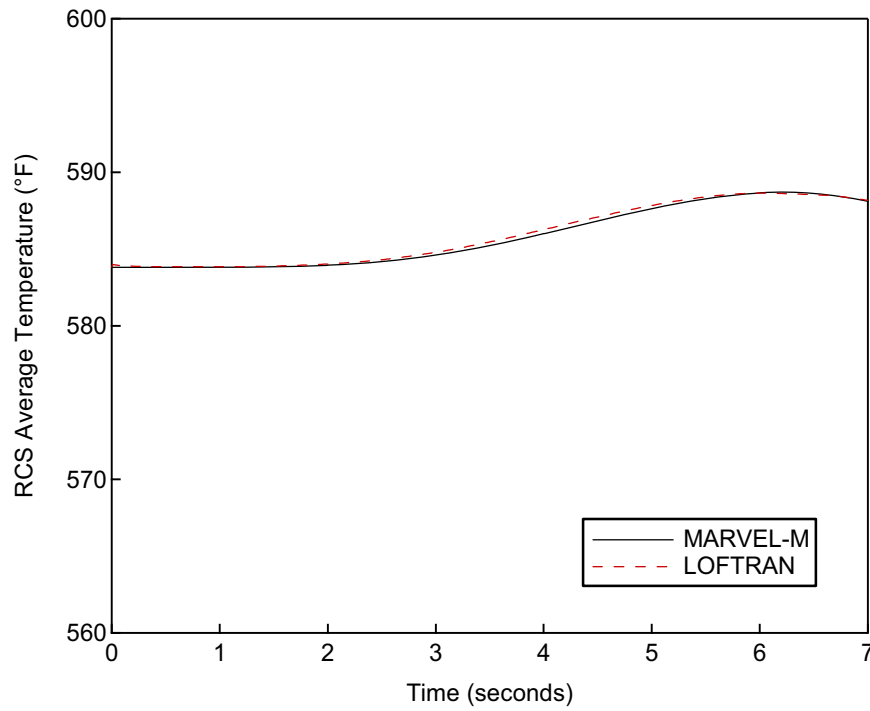


Figure 3.1.1-3 RCS Average Temperature, Uncontrolled RCCA Bank Withdrawal at Power Comparison with MARVEL-M and LOFTRAN

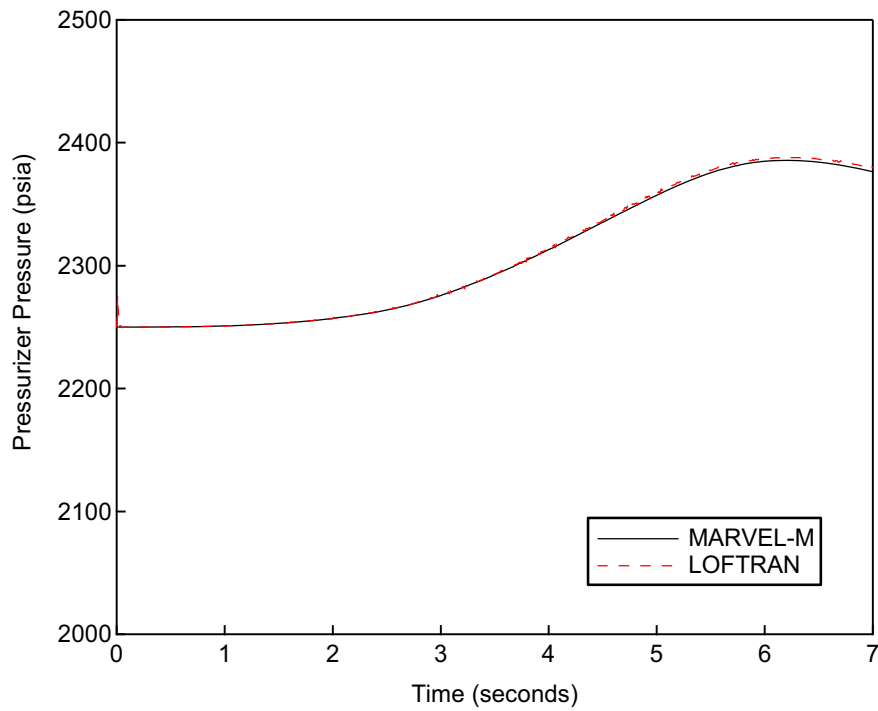


Figure 3.1.1-4 Pressurizer Pressure, Uncontrolled RCCA Bank Withdrawal at Power Comparison with MARVEL-M and LOFTRAN

3.1.2 Partial Loss of Forced Reactor Coolant Flow

(1) Event Description

The Partial Loss of Forced Reactor Coolant Flow event initiates from nominal power operation. The event includes cases where either one or two RCPs coast down, resulting a DNBR decrease due to core flow reduction until a reactor protection setpoint is reached.

The Partial Loss of Reactor Coolant Flow has been chosen because both the LOFTRAN and MARVEL-M codes use an internal reactor coolant pump model to calculate the loop and total core flow transients. In this way, the transient validates the adequacy of the MARVEL-M expansion from 2-loop to 4-loop simulation and the built-in RCP model. Two RCPs coasting down are analyzed in this case. Parameters of interest include reactor power, core average heat flux, loop flow rate, and pressurizer pressure.

(2) Analysis Assumption

Analysis assumptions and calculation conditions in the typical 4-loop plant with a 17x17-257FA core are as follows.

- | | |
|---------------------------|---|
| (a) Initial condition | Nominal power, Nominal T_{avg} , Nominal RCS pressure |
| (b) Reactor trip | Low Reactor Coolant Loop Flow |
| (c) RCP coast down number | Two RCPs |
| (d) Feedback reactivity | Minimum Density feedback and maximum Doppler feedback |
| (e) Trip reactivity | -4% $\Delta K/K$ |

(3) Results and Conclusions

Comparison results of MARVEL-M and LOFTRAN are shown in Figures 3.1.2-1 through 3.1.2-4. The results demonstrate that the two codes have equivalent capabilities and are in close agreement.

It is concluded that the MARVEL-M code is suitable for use in analyzing a flow coastdown in one or more loops for the purpose of calculating time-dependent parameters input to the VIPRE-01M code (RCS flow rate and reactor power) for heat flux at the hot channel and DNBR calculations.

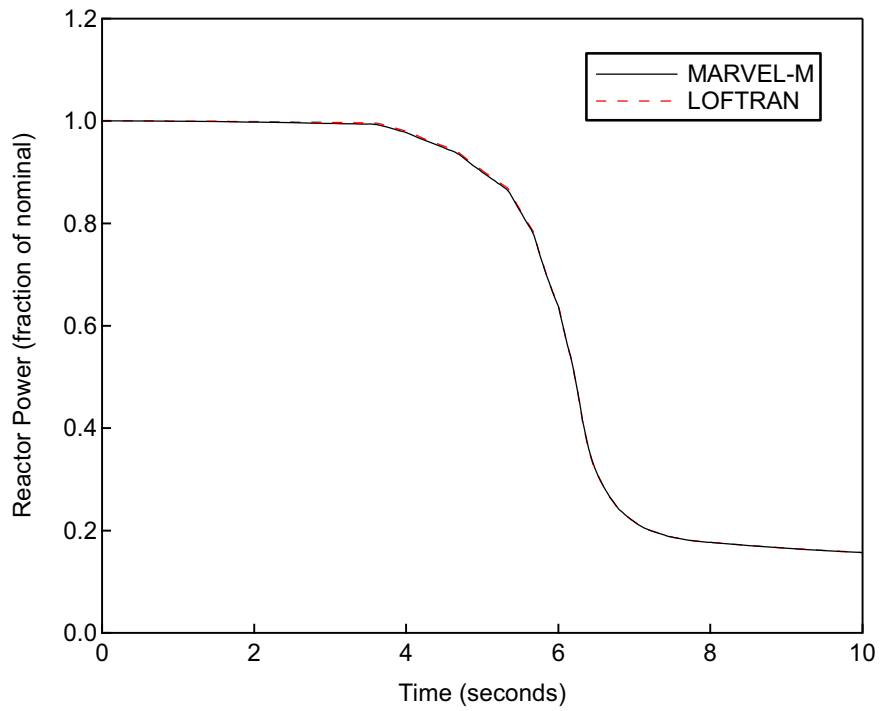


Figure 3.1.2-1 Reactor Power, Partial Loss of Forced Reactor Coolant Flow Comparison with MARVEL-M and LOFTRAN

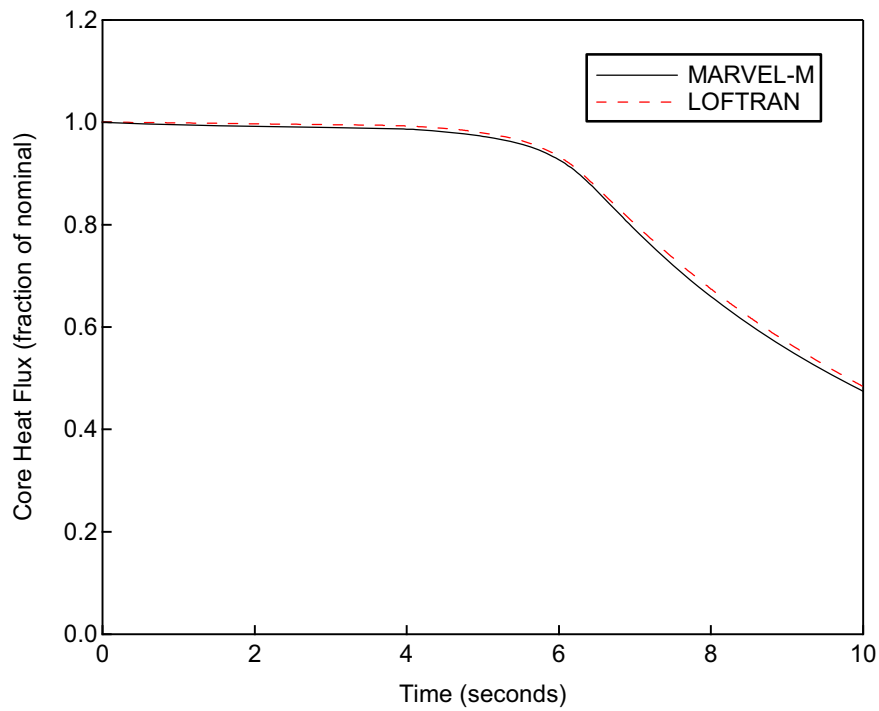


Figure 3.1.2-2 Core Heat Flux, Partial Loss of Forced Reactor Coolant Flow Comparison with MARVEL-M and LOFTRAN

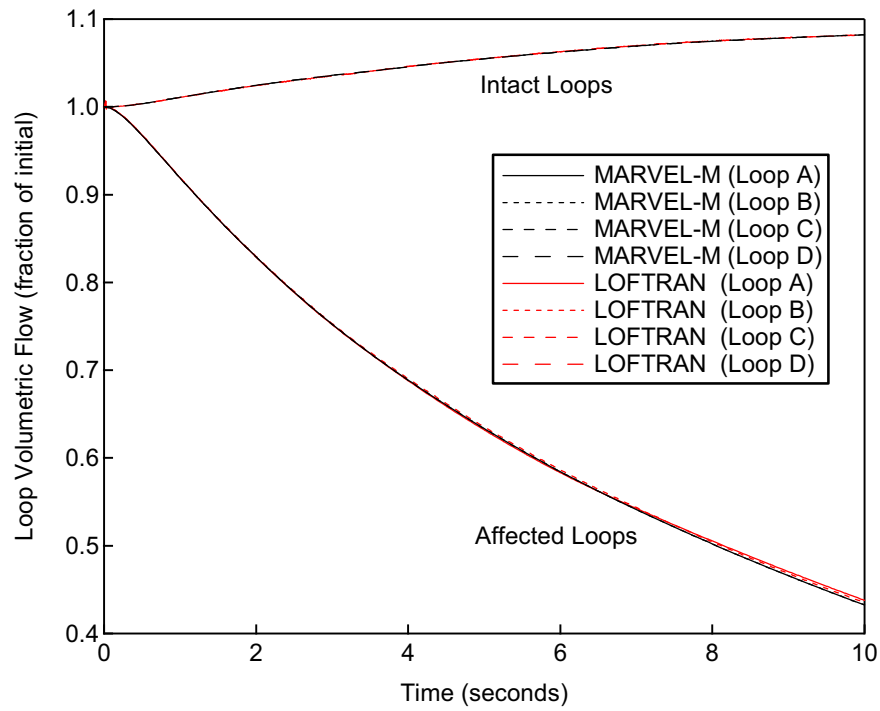


Figure 3.1.2-3 Loop Volumetric Flow, Partial Loss of Forced Reactor Coolant Flow Comparison with MARVEL-M and LOFTRAN

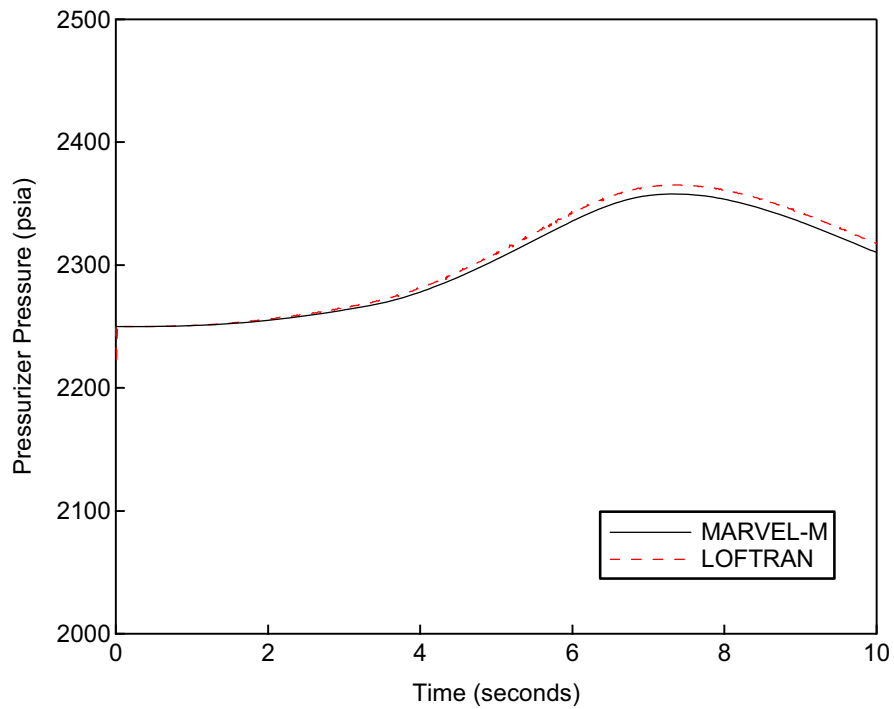


Figure 3.1.2-4 Pressurizer Pressure, Partial Loss of Forced Reactor Coolant Flow Comparison with MARVEL-M and LOFTRAN

3.1.3 Complete Loss of Forced Reactor Coolant Flow

(1) Event Description

The Complete Loss of Forced Reactor Coolant Flow event initiates from nominal power operation. All RCPs coast down and DNBR decreases due to core flow reduction until a reactor protection setpoint is reached.

The Complete Loss of Flow event has been chosen because both the LOFTRAN and MARVEL-M codes use an internal reactor coolant pump model to calculate the loop and total core flow. In this way, the transient validates the adequacy of the built-in RCP model for the purpose of calculating parameters used in calculating DNBR. The parameters of interest include reactor power, core heat flux, loop flow rate, and pressurizer pressure.

(2) Analysis Assumption

Analysis assumptions and calculation conditions in the typical 4-loop plant with a 17x17-257FA core are as follows.

- | | |
|-------------------------|---|
| (a) Initial condition | Nominal power, Nominal T_{avg} , Nominal RCS pressure |
| (b) Reactor trip | Low RCP speed |
| (c) RCP coast down | All RCPs |
| (d) Feedback reactivity | Minimum Density feedback and maximum Doppler feedback |
| (e) Trip reactivity | -4% $\Delta K/K$ |

(3) Results

Comparison results of MARVEL-M and LOFTRAN are shown in Figures 3.1.3-1 through 3.1.3-4. The results demonstrate that the two codes have equivalent capabilities and are in close agreement.

It is concluded that the MARVEL-M code is suitable for use in analyzing a uniform flow coastdown in all loops for the purpose of calculating time-dependent parameters input to the VIPRE-01M code (RCS flow rate and reactor power) for heat flux at the hot channel and DNBR calculations.

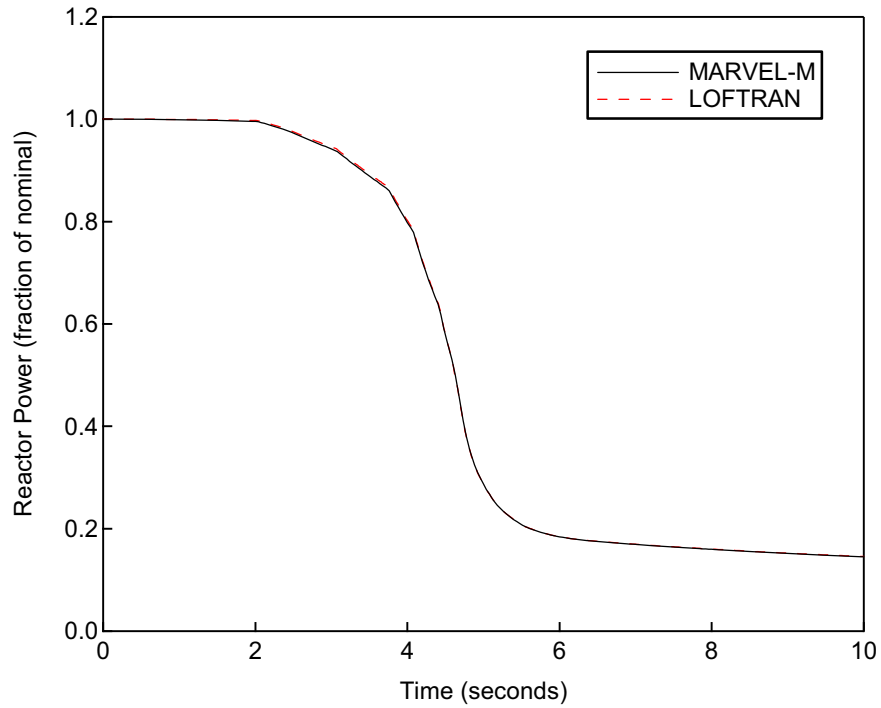


Figure 3.1.3-1 Reactor Power, Complete Loss of Forced Reactor Coolant Flow Comparison with MARVEL-M and LOFTRAN

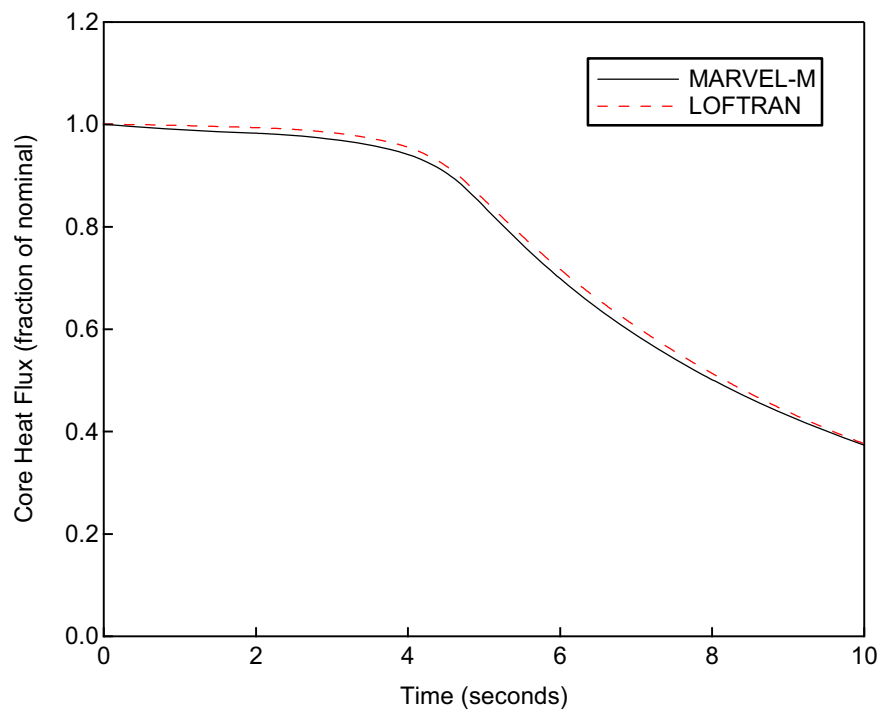


Figure 3.1.3-2 Core Heat Flux, Complete Loss of Forced Reactor Coolant Flow Comparison with MARVEL-M and LOFTRAN

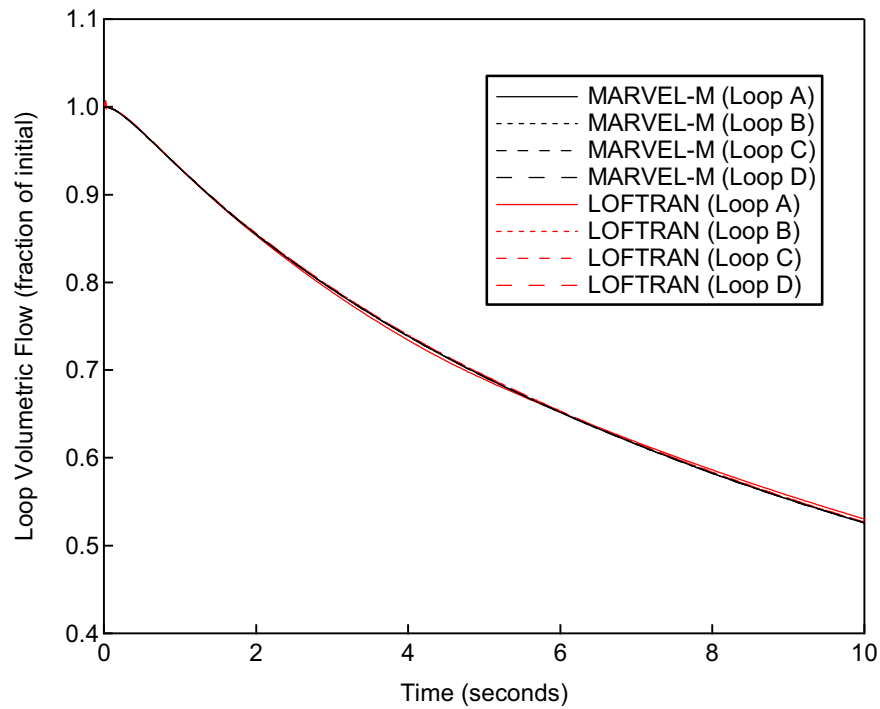


Figure 3.1.3-3 Loop Volumetric Flow, Complete Loss of Forced Reactor Coolant Flow Comparison with MARVEL-M and LOFTRAN

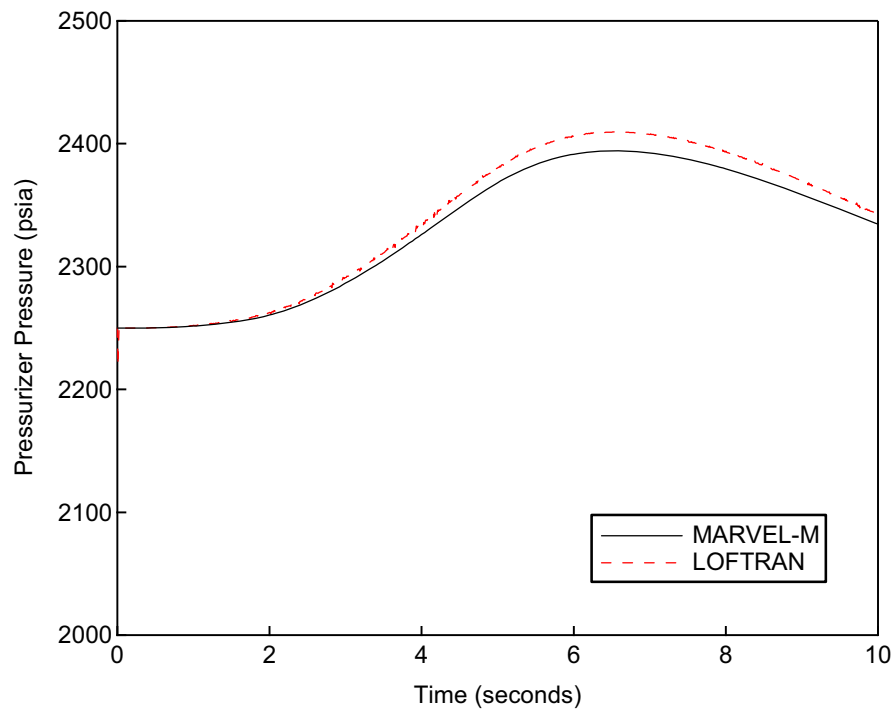


Figure 3.1.3-4 Pressurizer Pressure, Complete Loss of Forced Reactor Coolant Flow Comparison with MARVEL-M and LOFTRAN

3.1.4 Reactor Coolant Pump Shaft Seizure

(1) Event Description

The Reactor Coolant Pump Shaft Seizure event initiates from nominal power operation. In this event, one RCP shaft seizes (Locked Rotor) and DNBR decreases due to rapid flow reduction in the core until a reactor protection system setpoint is reached.

The Reactor Coolant Pump Shaft Seizure accident has been chosen because both the LOFTRAN and MARVEL-M codes use an internal reactor coolant pump model to calculate the loop and total core flow. In this way, the transient validates the extension from 2-loop to 4-loop simulation and the built-in RCP model. Parameters of interest include reactor power, core average heat flux, loop flow rate, and pressurizer pressure.

(2) Analysis Assumption

Analysis assumptions and calculation conditions in the typical 4-loop plant with a 17x17-257FA core are as follows.

- | | |
|-------------------------|---|
| (a) Initial condition | Nominal power, Nominal T_{avg} , Nominal RCS pressure |
| (b) Reactor trip | Low Reactor Coolant Loop Flow |
| (c) RCP Shaft Seizure | One RCP locked at 0 seconds |
| (d) Feedback reactivity | Minimum Density feedback and maximum Doppler feedback |
| (e) Trip reactivity | -4% $\Delta K/K$ |

(3) Results and Conclusions

Comparison results of MARVEL-M and LOFTRAN are shown in Figures 3.1.4-1 through 3.1.4-4. The results for loop flow rate and reactor power are in close agreement.

Pressurizer pressure of the MARVEL-M code is slightly lower than that of the LOFTRAN code due to the difference in average core heat flux. Although those minor differences exist, both codes have equivalent capability for this accident.

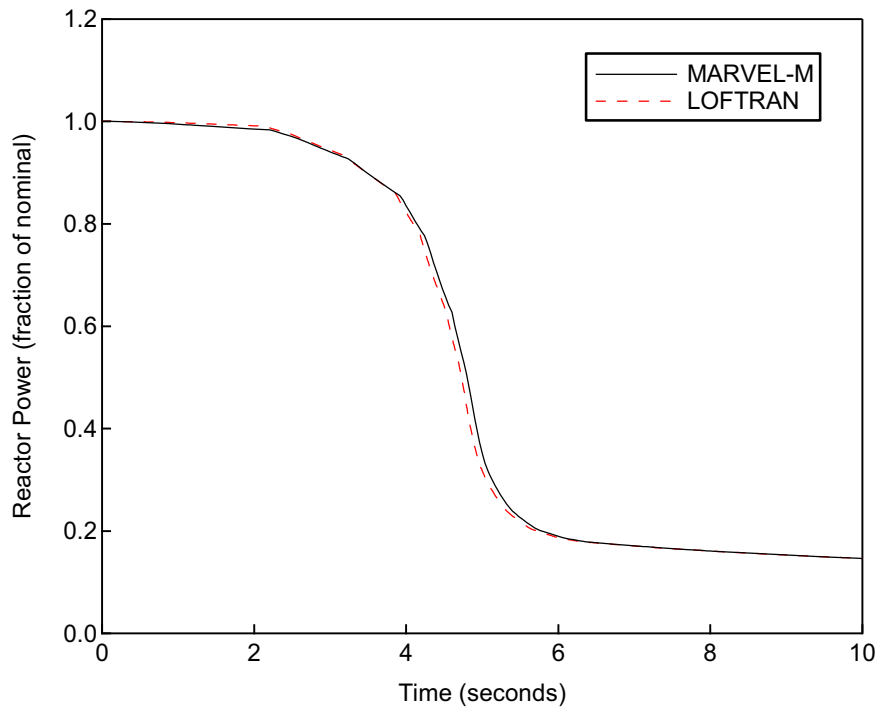


Figure 3.1.4-1 Reactor Power, Reactor Coolant Pump Shaft Seizure Comparison with MARVEL-M and LOFTRAN

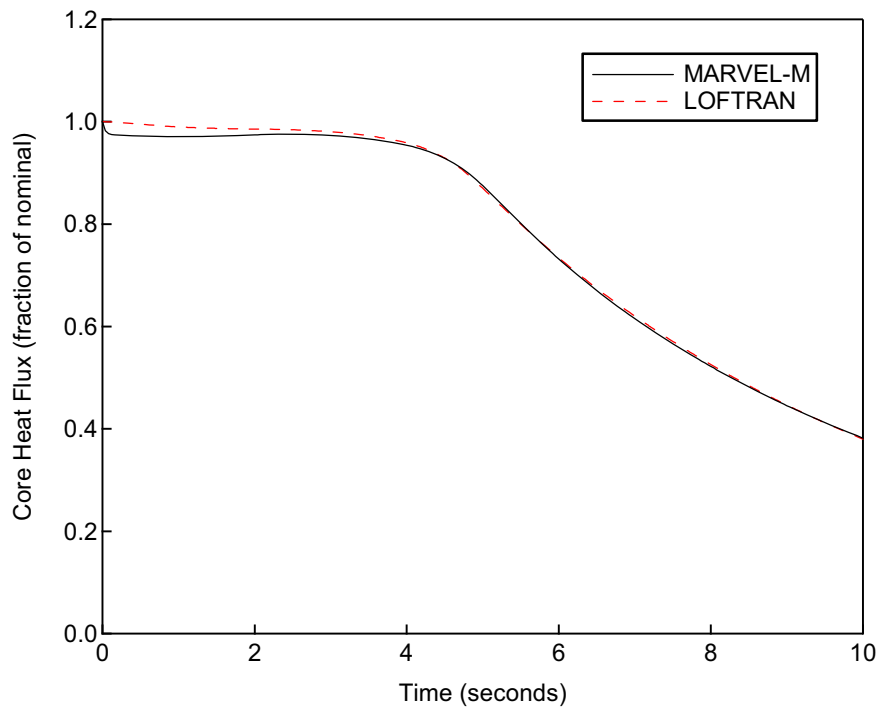


Figure 3.1.4-2 Core Heat Flux, Reactor Coolant Pump Shaft Seizure Comparison with MARVEL-M and LOFTRAN

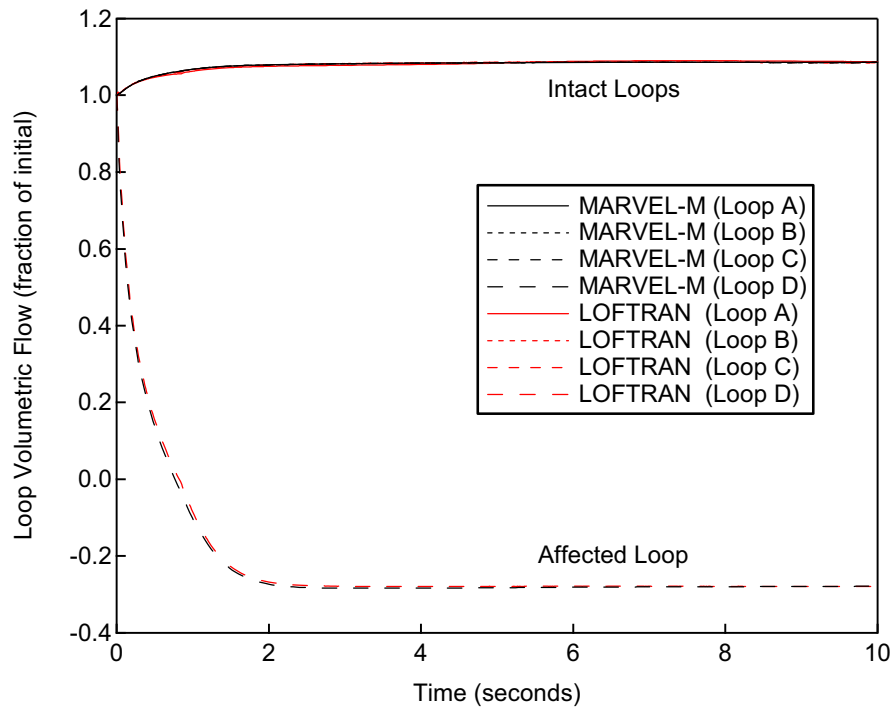


Figure 3.1.4-3 Loop Volumetric Flow, Reactor Coolant Pump Shaft Seizure Comparison with MARVEL-M and LOFTRAN

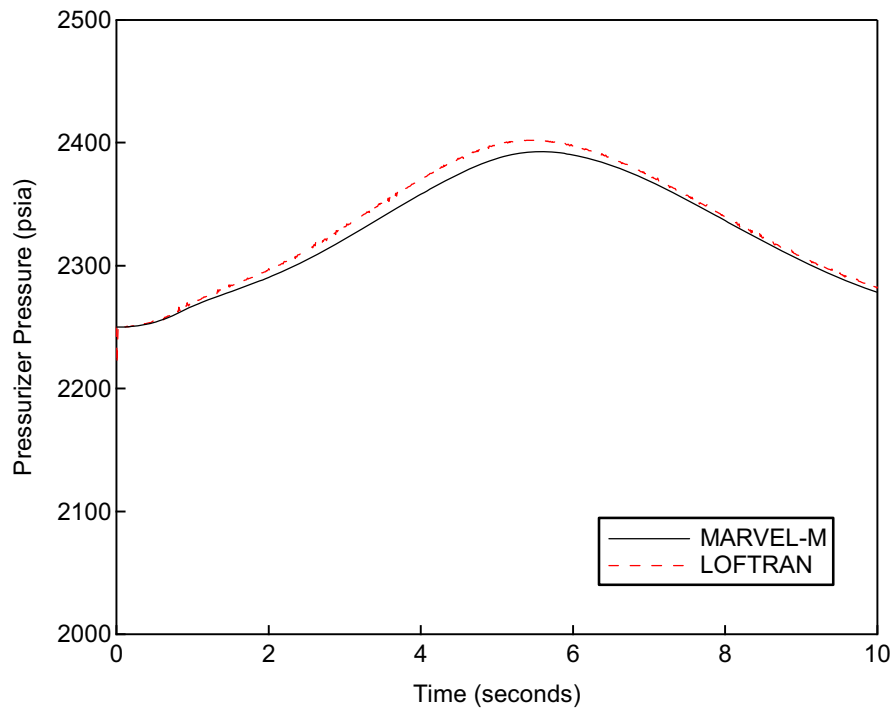


Figure 3.1.4-4 Pressurizer Pressure, Reactor Coolant Pump Shaft Seizure Comparison with MARVEL-M and LOFTRAN

3.2 TWINKLE-M Code

The solution methods and constitutive models of the TWINKLE-M code have not changed from the original version, but the maximum number of spatial mesh points is expanded from 2,000 points to a variable number input by the user.

First, the three-dimensional calculation by the TWINKLE-M code is verified by comparing the power distribution with that from the core simulator ANC code. A two-by-two (2 x 2) mesh per assembly in the radial direction are used by both codes allowing confirmation that the expanded number of mesh points in TWINKLE-M has been properly implemented.

For three-dimensional transient analyses, it is desirable to use as coarse a mesh as possible while maintaining sufficient accuracy. A second objective of the validation is to compare the results of a two-by-two (2 x 2) coarse mesh simulation of the rod ejection accident to a four-by-four (4 x 4) fine mesh simulation of the same accident with the same cross-section data using TWINKLE-M for both.

Section 3.2.1 describes a TWINKLE-M to ANC comparison for cases with and without an ejected rod under steady-state conditions. Section 3.2.2 compares the sensitivity of the TWINKLE-M results to different mesh size assumptions.

3.2.1 Comparison with Core Design Code

In this section the validity of the three-dimensional capabilities of the TWINKLE-M code are confirmed by comparing core power distribution and other parameters with the ANC. Three cases are defined to cover the range of conditions for which TWINKLE-M will be used in the non-LOCA accident analysis. The first case is hot full power with fuel temperatures at their full power values and all rods are fully withdrawn. The second case is hot zero power with uniform temperature distribution and RCCAs at the zero power insertion limit. Both cases are characterized by radial and axial power distributions in the normal operating condition. The third case is representative of a highly peaked radial power distribution characteristic of one RCCA ejection accident from the hot zero power condition.

It is important to note key differences between TWINKLE-M and ANC that are relevant to the comparison of the two codes. The TWINKLE-M code solution methodology is based on a finite difference technique, whereas ANC uses a nodal methodology. This is important because the two methods treat the core-reflector boundary condition differently. The TWINKLE-M code uses a multiplier to the diffusion coefficient for reflector regions in order to more accurately predict core power for peripheral core regions. In addition, ANC is a steady-state 3-D core simulator code whereas TWINKLE-M is a 3-D core transient analysis code. As a result, all of the comparison cases are done at steady-state conditions.

(1) Analysis Assumptions

The end-of-cycle hot zero power condition is selected for this validation because the hot channel factor after RCCA ejection becomes largest for every core condition. A control and shutdown rod location in the typical 4-loop plant with a 17x17, 257 fuel assembly (17x17-257FA) core is shown in Figure 3.2.1-1. And analysis assumptions and calculation conditions are as follows:

(a) Core condition	Case 1: 24 month equilibrium core, beginning-of-cycle (BOC) Case 2,3: 24 month equilibrium core, end-of-cycle (EOC)
(b) Initial condition	Case 1: Hot full power Case 2,3: Hot zero power
(c) RCCA position	Case 1: All RCCAs out Case 2: Bank-D is fully inserted. Bank-C and B are partially inserted. Case 3: One RCCA from Bank-D is ejected from core. The rest are same as Case 2
(d) Mesh division	2 x 2 meshes per assembly in the radial direction () in the axial direction for the active core region

(2) Results and Conclusions

Radial power distribution comparison between ANC and TWINKLE-M for the hot full power case and the hot zero power RCCA insertion limit case are shown in Figure 3.2.1-2 and 3.2.1-3, respectively. A similar comparison for the one RCCA ejected case is shown in Figure 3.2.1-4. Axial power distribution comparison for all the cases is shown in Figure 3.2.1-5.

In the full power case, the radial and axial power distributions for both codes are in good agreement with small differences in some assemblies. In the zero power cases, the maximum error in the assembly average power distribution appears at RCCA locations, which is expected due to the limitations associated with the differences between the two codes modeling methodologies. Additionally, the average axial power distributions for both codes are in good agreement.

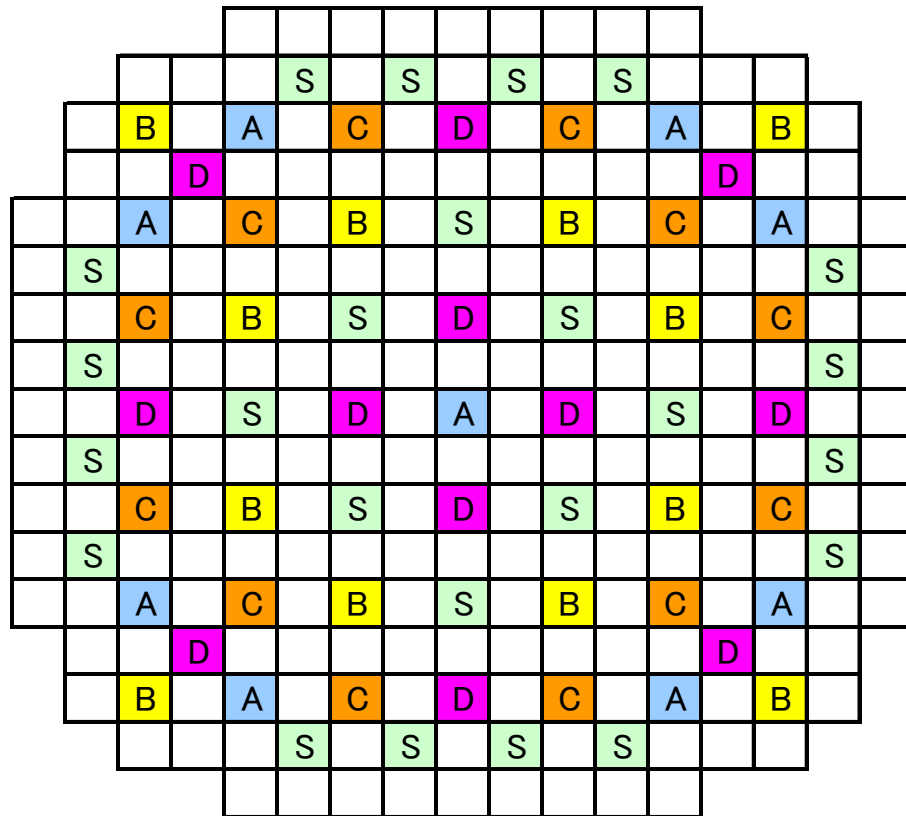
The results of ejected worth, hot channel factor and axial offset shown in Table 3.2.1-1 also demonstrate agreement between the codes.

These results indicate the validity of the three-dimensional TWINKLE-M calculation of core power utilizing the expanded number of mesh points.

Table 3.2.1-1 Results of RCCA Ejection Comparison with ANC and TWINKLE-M

	Ejected worth (pcm)	Hot channel factor	Axial offset (%)
ANC	603	27.3*	90.4
TWINKLE-M	600	27.7	90.0

* Node average value (Maximum is 29.5 rod wise)



Control group bank A	9
Control group bank B	12
Control group bank C	12
Control group bank D	12
Shutdown group bank S	24

**Figure 3.2.1-1 Control and Shutdown Rod Location
(17x17-257FA Core, 4-Loop Plant)**

TWINKLE-M

				0.43	0.50	0.49	0.51	0.50	0.51	0.49	0.50	0.43				
		0.40	0.64	1.31	1.10	0.93	1.04	1.06	1.04	0.93	1.10	1.31	0.64	0.40		
	0.40	1.09	1.01	1.26	1.03	1.08	1.10	1.06	1.10	1.08	1.03	1.26	1.01	1.09	0.40	
		0.64	1.01	0.95	1.02	1.14	1.28	1.15	1.09	1.15	1.28	1.14	1.02	0.95	1.01	0.64
0.43	1.31	1.26	1.02	1.26	1.14	1.06	1.13	1.18	1.13	1.06	1.14	1.26	1.02	1.26	1.31	0.43
0.50	1.10	1.03	1.14	1.14	1.04	1.21	1.35	1.15	1.35	1.21	1.04	1.15	1.14	1.03	1.10	0.50
0.49	0.93	1.08	1.28	1.06	1.21	1.36	1.10	1.17	1.10	1.36	1.21	1.06	1.28	1.08	0.93	0.49
0.51	1.04	1.10	1.15	1.13	1.35	1.10	1.18	1.09	1.18	1.10	1.35	1.13	1.15	1.10	1.04	0.51
0.50	1.06	1.06	1.09	1.18	1.15	1.17	1.09	0.92	1.09	1.17	1.15	1.18	1.09	1.06	1.06	0.50
0.51	1.04	1.10	1.15	1.13	1.35	1.10	1.18	1.09	1.19	1.10	1.35	1.13	1.15	1.10	1.04	0.51
0.49	0.93	1.08	1.28	1.06	1.21	1.36	1.10	1.17	1.10	1.36	1.21	1.06	1.28	1.08	0.93	0.49
0.50	1.10	1.03	1.14	1.15	1.04	1.21	1.35	1.15	1.36	1.21	1.04	1.15	1.14	1.03	1.10	0.50
0.43	1.31	1.26	1.02	1.26	1.15	1.06	1.13	1.18	1.13	1.06	1.15	1.26	1.02	1.26	1.31	0.43
		0.64	1.01	0.95	1.02	1.14	1.28	1.15	1.09	1.15	1.28	1.14	1.02	0.95	1.01	0.64
		0.40	1.09	1.01	1.26	1.03	1.08	1.10	1.06	1.10	1.08	1.03	1.26	1.01	1.09	0.40
			0.40	0.64	1.31	1.10	0.93	1.04	1.06	1.04	0.93	1.10	1.31	0.64	0.40	
				0.43	0.50	0.49	0.51	0.50	0.51	0.49	0.50	0.43				

ANC

				0.43	0.51	0.49	0.52	0.51	0.52	0.49	0.51	0.43				
		0.40	0.65	1.23	1.08	0.94	1.03	1.06	1.03	0.94	1.08	1.23	0.65	0.40		
	0.40	1.03	1.01	1.24	1.04	1.08	1.12	1.08	1.12	1.08	1.04	1.24	1.01	1.03	0.40	
		0.65	1.01	0.97	1.03	1.15	1.27	1.11	1.16	1.27	1.15	1.04	0.97	1.01	0.65	
0.43	1.23	1.24	1.04	1.24	1.16	1.08	1.15	1.19	1.15	1.08	1.16	1.24	1.03	1.24	1.23	0.43
0.51	1.08	1.04	1.15	1.16	1.07	1.22	1.33	1.16	1.33	1.22	1.07	1.16	1.15	1.04	1.08	0.51
0.49	0.94	1.08	1.27	1.08	1.22	1.34	1.11	1.17	1.11	1.34	1.22	1.08	1.27	1.08	0.94	0.49
0.52	1.03	1.12	1.16	1.15	1.33	1.11	1.15	1.07	1.15	1.11	1.33	1.15	1.17	1.12	1.03	0.52
0.51	1.06	1.08	1.11	1.19	1.16	1.17	1.07	0.90	1.07	1.17	1.16	1.19	1.11	1.08	1.06	0.51
0.52	1.03	1.12	1.17	1.15	1.33	1.11	1.15	1.07	1.15	1.11	1.33	1.15	1.16	1.12	1.03	0.52
0.49	0.94	1.08	1.27	1.08	1.22	1.34	1.11	1.17	1.11	1.34	1.22	1.08	1.27	1.08	0.94	0.49
0.51	1.08	1.04	1.15	1.16	1.07	1.22	1.33	1.16	1.33	1.22	1.07	1.16	1.15	1.04	1.08	0.51
0.43	1.23	1.24	1.03	1.24	1.16	1.08	1.15	1.19	1.15	1.08	1.16	1.24	1.04	1.24	1.23	0.43
		0.65	1.01	0.97	1.04	1.15	1.27	1.16	1.11	1.27	1.15	1.03	0.97	1.01	0.65	
		0.40	1.03	1.01	1.24	1.04	1.08	1.12	1.08	1.12	1.08	1.04	1.24	1.01	1.03	0.40
			0.40	0.65	1.23	1.08	0.94	1.03	1.06	1.03	0.94	1.08	1.23	0.65	0.40	
				0.43	0.51	0.49	0.52	0.51	0.52	0.49	0.51	0.43				

TWINKLE-M / ANC

				1.00	0.99	0.99	0.99	0.98	0.99	0.99	0.99	1.00				
		0.99	0.98	1.06	1.02	1.00	1.01	1.01	1.01	1.00	1.02	1.06	0.98	0.99		
	0.99	1.06	0.99	1.02	0.98	1.00	0.98	0.98	0.98	1.00	0.98	1.02	0.99	1.06	0.99	
		0.98	0.99	0.98	0.99	0.99	1.01	0.99	0.98	0.99	1.01	0.99	0.98	0.99	0.99	0.98
1.00	1.06	1.02	0.99	1.01	0.99	0.98	0.98	0.99	0.98	0.98	0.99	1.01	0.99	1.02	1.06	1.00
0.99	1.02	0.98	0.99	0.99	0.98	0.99	1.01	0.99	1.01	0.99	0.98	0.99	0.99	0.98	1.02	0.99
0.99	1.00	1.00	1.01	0.98	0.99	1.01	0.99	1.00	0.99	1.01	0.99	0.98	1.01	1.00	1.00	0.99
0.99	1.01	0.98	0.99	0.98	1.01	0.99	1.03	1.01	1.03	0.99	1.01	0.98	0.99	0.98	1.01	0.99
0.98	1.01	0.98	0.98	0.99	0.99	1.00	1.02	1.02	1.02	1.00	0.99	0.99	0.98	0.98	1.01	0.98
0.99	1.01	0.98	0.99	0.98	1.01	0.99	1.03	1.02	1.03	0.99	1.01	0.98	0.99	0.98	1.01	0.99
0.99	1.00	1.00	1.01	0.98	0.99	1.01	0.99	1.00	0.99	1.01	0.99	0.98	1.01	1.00	1.00	0.99
0.99	1.02	0.98	0.99	0.99	0.98	0.99	1.01	0.99	1.02	0.99	0.98	0.99	0.99	0.98	1.02	0.99
1.00	1.06	1.02	0.99	1.01	0.99	0.98	0.98	0.99	0.98	0.98	0.99	1.01	0.99	1.02	1.06	1.00
		0.98	0.99	0.98	0.99	0.99	1.01	0.99	0.98	0.99	1.01	0.99	0.99	0.98	0.99	0.98
		0.99	1.06	0.99	1.02	0.98	1.00	0.98	0.98	0.98	1.00	0.98	1.02	0.99	1.06	0.99
			0.99	0.98	1.06	1.02	1.00	1.01	1.01	1.01	1.00	1.02	1.06	0.98	0.99	
				1.00	0.99	0.99	0.99	0.98	0.99	0.99	0.99	1.00				

Legend		
~	±3%	~
~	±5%	~
~	±8%	~

Figure 3.2.1-2 Radial Power Distribution Comparison with ANC and TWINKLE-M Case 1, BOC HFP All RCCAs Out

TWINKLE-M

				0.52	0.68	0.73	0.77	0.74	0.77	0.73	0.68	0.52				
		0.35	0.64	1.21	1.30	1.29	1.41	1.37	1.41	1.29	1.30	1.21	0.64	0.35		
	0.35	0.65	0.97	1.22	0.92	0.61	1.27	0.69	1.27	0.61	0.92	1.22	0.97	0.65	0.35	
	0.64	0.97	0.44	0.74	1.16	1.18	1.38	1.15	1.38	1.18	1.16	0.74	0.44	0.97	0.64	
0.52	1.21	1.22	0.74	0.59	1.09	0.75	1.14	1.50	1.14	0.75	1.09	0.59	0.74	1.22	1.21	0.52
0.68	1.30	0.92	1.16	1.09	1.02	1.44	1.46	1.13	1.46	1.44	1.02	1.09	1.16	0.92	1.30	0.68
0.73	1.29	0.61	1.18	0.75	1.44	1.53	1.03	0.73	1.03	1.53	1.44	0.75	1.18	0.61	1.29	0.73
0.77	1.41	1.27	1.38	1.14	1.46	1.03	1.04	0.96	1.04	1.03	1.46	1.14	1.38	1.27	1.41	0.77
0.74	1.37	0.69	1.15	1.50	1.13	0.73	0.96	0.85	0.96	0.73	1.13	1.50	1.15	0.69	1.37	0.74
0.77	1.41	1.27	1.38	1.14	1.46	1.03	1.04	0.96	1.04	1.03	1.46	1.14	1.38	1.27	1.41	0.77
0.73	1.29	0.61	1.18	0.75	1.44	1.53	1.03	0.73	1.03	1.53	1.44	0.75	1.18	0.61	1.29	0.73
0.68	1.30	0.92	1.16	1.09	1.02	1.44	1.46	1.13	1.46	1.44	1.02	1.09	1.16	0.92	1.30	0.68
0.52	1.21	1.22	0.74	0.59	1.09	0.75	1.14	1.50	1.14	0.75	1.09	0.59	0.74	1.22	1.21	0.52
	0.64	0.97	0.44	0.74	1.16	1.18	1.38	1.15	1.38	1.17	1.16	0.74	0.44	0.97	0.64	
	0.35	0.65	0.97	1.22	0.92	0.61	1.27	0.69	1.27	0.61	0.92	1.22	0.97	0.65	0.35	
	0.35	0.64		1.21	1.30	1.29	1.41	1.37	1.41	1.29	1.30	1.21	0.64	0.35		
				0.52	0.68	0.73	0.77	0.74	0.77	0.73	0.68	0.52				

ANC

				0.52	0.68	0.74	0.77	0.75	0.77	0.74	0.68	0.52				
		0.35	0.63	1.16	1.27	1.27	1.38	1.35	1.38	1.27	1.27	1.16	0.63	0.35		
	0.35	0.65	0.97	1.21	0.94	0.65	1.27	0.73	1.27	0.65	0.94	1.21	0.97	0.65	0.35	
	0.63	0.97	0.46	0.76	1.15	1.18	1.36	1.16	1.36	1.18	1.15	0.76	0.46	0.97	0.63	
0.52	1.16	1.21	0.76	0.62	1.10	0.80	1.16	1.50	1.15	0.80	1.10	0.62	0.76	1.21	1.16	0.52
0.68	1.27	0.94	1.15	1.10	1.03	1.44	1.44	1.13	1.44	1.44	1.03	1.10	1.15	0.94	1.27	0.68
0.74	1.27	0.65	1.18	0.80	1.44	1.52	1.04	0.76	1.04	1.52	1.44	0.80	1.18	0.65	1.27	0.74
0.77	1.38	1.27	1.36	1.15	1.44	1.04	1.03	0.95	1.03	1.04	1.44	1.16	1.36	1.27	1.38	0.77
0.75	1.35	0.73	1.16	1.50	1.13	0.76	0.95	0.84	0.95	0.76	1.13	1.50	1.16	0.73	1.35	0.75
0.77	1.38	1.27	1.36	1.16	1.44	1.04	1.03	0.95	1.03	1.04	1.44	1.16	1.36	1.27	1.38	0.77
0.74	1.27	0.65	1.18	0.80	1.44	1.52	1.04	0.76	1.04	1.52	1.44	0.80	1.18	0.65	1.27	0.74
0.68	1.27	0.94	1.15	1.10	1.03	1.44	1.44	1.13	1.44	1.44	1.03	1.10	1.15	0.94	1.27	0.68
0.52	1.16	1.21	0.76	0.62	1.10	0.80	1.16	1.50	1.15	0.80	1.10	0.62	0.76	1.21	1.16	0.52
	0.63	0.97	0.46	0.76	1.15	1.18	1.36	1.16	1.36	1.18	1.15	0.76	0.46	0.97	0.63	
	0.35	0.65	0.97	1.21	0.94	0.65	1.27	0.73	1.27	0.65	0.94	1.21	0.97	0.65	0.35	
	0.35	0.63		1.17	1.27	1.27	1.38	1.35	1.38	1.27	1.27	1.16	0.63	0.35		
				0.52	0.68	0.74	0.77	0.75	0.77	0.74	0.68	0.52				

TWINKLE-M / ANC

				1.01	1.00	0.99	1.00	0.98	0.99	0.99	1.00	1.02				
		1.01	1.01	1.04	1.03	1.02	1.02	1.01	1.02	1.02	1.03	1.04	1.01	1.01		
	1.01	1.00	1.00	1.01	0.98	0.94	1.00	0.94	1.00	0.94	0.98	1.01	1.00	1.00	1.01	
1.02	1.04	1.01	0.98	0.95	0.99	0.94	0.99	1.00	0.99	0.94	0.99	0.95	0.98	1.01	1.04	1.01
1.00	1.03	0.98	1.01	0.99	0.99	1.01	1.01	1.00	1.01	1.00	0.99	0.99	1.01	0.98	1.03	1.00
0.99	1.02	0.94	1.00	0.94	1.01	1.01	1.00	0.97	0.99	1.01	1.00	0.94	1.00	0.94	1.02	0.99
0.99	1.02	1.00	1.01	0.99	1.01	1.00	1.01	1.01	1.02	1.00	1.01	0.99	1.01	1.00	1.02	0.99
0.98	1.01	0.94	0.99	1.00	1.00	0.97	1.01	1.01	1.01	0.97	1.00	1.00	0.99	0.94	1.01	0.98
1.00	1.02	1.00	1.01	0.99	1.01	1.00	1.02	1.01	1.02	0.99	1.01	0.99	1.01	1.00	1.02	0.99
0.99	1.02	0.94	1.00	0.94	1.00	1.01	0.99	0.97	1.00	1.01	1.00	0.94	1.00	0.94	1.02	0.99
0.99	1.02	0.98	1.01	0.99	0.99	1.00	1.01	1.00	1.01	1.00	0.99	0.99	1.01	0.98	1.02	1.00
1.01	1.04	1.01	0.98	0.95	0.99	0.94	0.99	1.00	0.99	0.94	0.99	0.95	0.98	1.01	1.04	1.02
	1.01	1.00	0.94	0.98	1.01	1.00	1.01	0.99	1.01	1.00	1.01	0.98	0.94	1.00	1.01	
	1.01	1.00	1.00	1.01	0.98	0.94	1.00	0.94	1.00	0.94	0.98	1.01	1.00	1.00	1.01	
	1.01	1.01		1.04	1.02	1.02	1.02	1.01	1.02	1.02	1.02	1.04	1.00	1.01		
				1.02	1.00	0.99	0.99	0.98	0.99	0.99	0.99	1.01				

Legend		
	~	±3%
	~	±5%
	~	±8%

Figure 3.2.1-3 Radial Power Distribution Comparison with ANC and TWINKLE-M Case 2, EOC HZP RCCA at Insertion Limit

TWINKLE-M

				0.11	0.14	0.15	0.16	0.16	0.16	0.16	0.14	0.11				
		0.08	0.15	0.27	0.29	0.28	0.31	0.30	0.31	0.28	0.29	0.27	0.15	0.08		
	0.10	0.16	0.23	0.29	0.22	0.14	0.30	0.16	0.30	0.14	0.22	0.29	0.23	0.16	0.10	
		0.19	0.28	0.12	0.20	0.31	0.32	0.37	0.31	0.37	0.32	0.31	0.20	0.12	0.28	0.19
0.17	0.38	0.38	0.24	0.19	0.35	0.24	0.36	0.47	0.36	0.24	0.35	0.19	0.24	0.38	0.38	0.17
0.23	0.45	0.32	0.42	0.41	0.39	0.55	0.54	0.41	0.54	0.55	0.39	0.41	0.42	0.32	0.45	0.23
0.28	0.50	0.24	0.49	0.32	0.64	0.68	0.46	0.33	0.46	0.68	0.64	0.32	0.49	0.24	0.50	0.28
0.33	0.61	0.58	0.67	0.59	0.78	0.56	0.60	0.57	0.60	0.56	0.78	0.59	0.67	0.58	0.62	0.33
0.36	0.67	0.36	0.66	0.93	0.76	0.54	0.74	0.67	0.74	0.54	0.76	0.93	0.66	0.36	0.68	0.36
0.42	0.79	0.76	0.91	0.84	1.26	1.01	1.08	0.99	1.08	1.01	1.26	0.84	0.91	0.76	0.79	0.42
0.46	0.82	0.42	0.92	0.68	1.54	1.87	1.40	1.04	1.40	1.87	1.54	0.68	0.92	0.42	0.83	0.46
0.48	0.97	0.76	1.07	1.21	1.34	2.17	2.56	2.15	2.56	2.17	1.34	1.21	1.07	0.76	0.97	0.48
0.41	1.01	1.13	0.80	0.83	1.86	1.46	2.67	3.73	2.67	1.46	1.86	0.83	0.80	1.13	1.01	0.41
	0.62	1.07	0.62	1.36	2.43	3.02	4.38	4.11	4.39	3.02	2.43	1.36	0.62	1.07	0.62	
		0.41	0.87	1.68	2.49	2.19	1.85	5.16	5.17	1.85	2.19	2.49	1.68	0.87	0.41	
			0.57	1.22	2.65	3.34	4.07	5.53	6.13	5.54	4.08	3.34	2.66	1.22	0.57	
				1.22	1.79	2.31	2.85	2.96	2.85	2.31	1.80	1.22				

Ejected Rod

ANC

				0.11	0.15	0.16	0.16	0.16	0.16	0.16	0.15	0.11				
		0.09	0.15	0.26	0.28	0.28	0.30	0.30	0.30	0.28	0.28	0.26	0.15	0.09		
	0.10	0.17	0.24	0.29	0.22	0.15	0.30	0.17	0.30	0.15	0.22	0.29	0.24	0.17	0.10	
		0.19	0.28	0.13	0.20	0.31	0.32	0.37	0.32	0.37	0.32	0.31	0.20	0.13	0.28	0.19
0.17	0.37	0.38	0.25	0.20	0.35	0.25	0.36	0.47	0.36	0.25	0.35	0.20	0.25	0.38	0.37	0.17
0.24	0.44	0.33	0.42	0.41	0.39	0.54	0.53	0.41	0.53	0.54	0.39	0.41	0.42	0.33	0.44	0.24
0.28	0.49	0.26	0.50	0.35	0.64	0.67	0.46	0.34	0.46	0.67	0.64	0.35	0.50	0.26	0.49	0.28
0.33	0.61	0.58	0.67	0.60	0.77	0.56	0.59	0.56	0.59	0.56	0.77	0.60	0.67	0.59	0.61	0.34
0.37	0.68	0.38	0.67	0.93	0.76	0.55	0.73	0.66	0.73	0.55	0.76	0.93	0.67	0.38	0.68	0.37
0.43	0.78	0.77	0.91	0.86	1.25	1.01	1.06	0.98	1.06	1.02	1.25	0.86	0.91	0.77	0.78	0.43
0.47	0.82	0.45	0.93	0.73	1.54	1.86	1.40	1.07	1.40	1.86	1.54	0.73	0.93	0.45	0.82	0.47
0.49	0.96	0.78	1.07	1.23	1.36	2.16	2.52	2.13	2.52	2.17	1.36	1.23	1.07	0.78	0.96	0.49
0.41	0.99	1.13	0.83	0.87	1.87	1.55	2.69	3.70	2.69	1.55	1.87	0.87	0.83	1.13	0.99	0.41
	0.62	1.08	0.66	1.38	2.40	3.00	4.30	4.11	4.31	3.01	2.40	1.38	0.66	1.08	0.62	
		0.41	0.87	1.67	2.45	2.22	1.94	5.11	5.19	5.13	1.95	2.22	2.45	1.67	0.87	0.41
			0.56	1.20	2.54	3.24	4.00	5.41	6.03	5.42	4.00	3.25	2.55	1.20	0.56	
				1.20	1.80	2.33	2.86	3.00	2.86	2.33	1.80	1.20				

TWINKLE-M / ANC

				1.01	0.99	0.98	0.99	0.98	0.99	0.99	0.99	1.00				
		0.99	0.99	1.02	1.01	1.00	1.01	1.00	1.01	1.00	1.01	1.02	0.99	0.99		
	0.99	0.99	0.99	1.00	0.97	0.94	0.99	0.94	1.00	0.94	0.97	1.00	0.99	0.99	0.99	
		0.99	0.99	0.93	0.97	1.00	0.99	1.01	0.99	1.01	0.99	1.00	0.97	0.93	0.99	0.99
1.01	1.03	1.00	0.97	0.95	0.99	0.94	0.99	1.00	0.99	0.94	0.99	0.95	0.97	1.00	1.03	1.01
0.99	1.01	0.97	1.00	0.99	0.99	1.01	1.01	1.00	1.02	1.01	0.99	0.99	1.00	0.97	1.01	0.98
0.98	1.00	0.93	0.99	0.94	1.01	1.01	1.00	0.97	1.00	1.01	1.00	0.93	0.99	0.93	1.00	0.98
0.99	1.01	0.99	1.01	0.99	1.01	0.99	1.02	1.02	1.02	0.99	1.01	0.98	1.01	0.99	1.01	0.98
0.97	1.00	0.93	0.98	0.99	1.00	0.97	1.01	1.01	1.02	0.97	1.00	0.99	0.98	0.93	1.00	0.97
0.98	1.01	0.99	1.01	0.98	1.01	0.99	1.01	1.01	1.01	0.99	1.01	0.98	1.01	0.99	1.01	0.98
0.98	1.00	0.93	0.99	0.93	1.00	1.01	1.00	0.97	0.99	1.01	1.00	0.93	0.99	0.93	1.00	0.98
0.98	1.01	0.97	1.00	0.99	0.99	1.00	1.02	1.01	1.02	1.00	0.99	0.98	1.00	0.97	1.01	0.98
1.00	1.02	1.00	0.96	0.95	0.99	0.94	0.99	1.01	0.99	0.94	0.99	0.95	0.97	1.00	1.02	1.00
	0.99	0.99	0.94	0.98	1.01	1.00	1.02	1.00	1.02	1.00	1.01	0.98	0.94	0.99	0.99	
		1.00	0.99	1.01	1.02	0.99	0.95	1.01	1.00	1.01	0.95	0.99	1.02	1.01	0.99	1.00
			1.02	1.02	1.04	1.03	1.02	1.02	1.02	1.02	1.02	1.03	1.04	1.02	1.02	
				1.02	1.00	0.99	1.00	0.99	1.00	0.99	1.00	0.99	1.00	1.02		

Legend		
~	±3%	~
~	±5%	~
~	±8%	~

Figure 3.2.1-4 Radial Power Distribution Comparison with ANC and TWINKLE-M Case 3, EOC HZP One RCCA Ejected

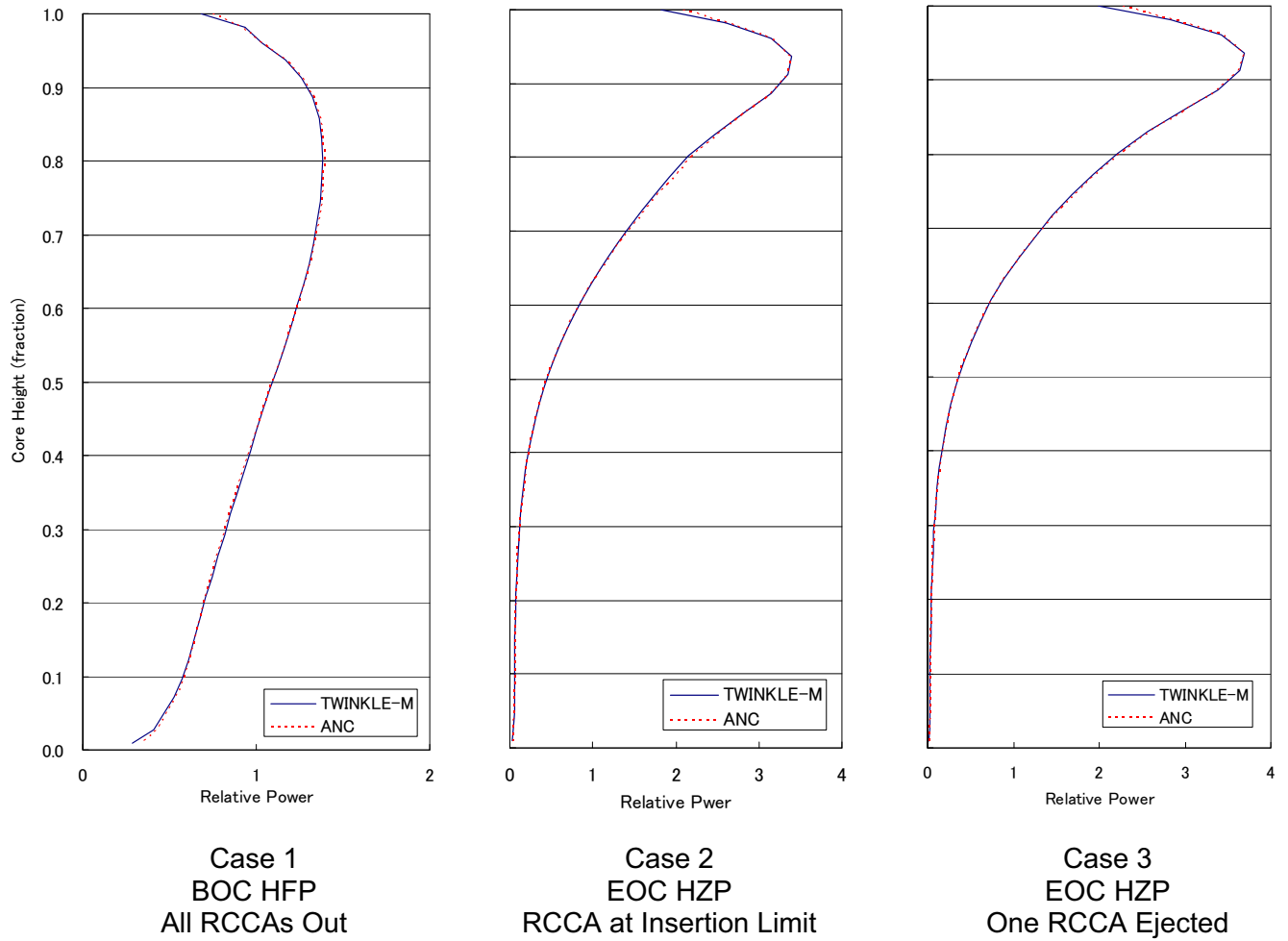


Figure 3.2.1-5 Average Axial Power Distribution Comparison with ANC and TWINKLE-M

3.2.2 Sensitivity Study of Mesh Size

In the ejected rod accident simulation, reactivity insertion and reactivity feedback including Doppler feedback are most important parameters. In the three-dimensional calculation, these effects are dependent on calculational mesh size. The coarseness of the spatial mesh generally influences the accuracy of three-dimensional finite-difference techniques for solving the diffusion equations. A sensitivity study of spatial mesh division utilizing the same cross-section data is performed in order to determine the optimal spatial mesh size.

In this study, sensitivity analysis of the mesh division is performed in the radial direction. Using a fine mesh analysis in the finite-difference technique provides the most accurate results.

(1) Analysis Assumptions

Analysis assumptions and calculation conditions in the typical 4-loop plant with a 17x17-257FA core are as follows. The end-of-cycle hot zero power condition is selected for comparison because it represents the most severe case in the RCCA ejection accident.

- (a) Core condition 24 month equilibrium core end-of-cycle
- (b) Initial condition Hot zero power
- (c) RCCA position Insertion limit at initial
- (d) Mesh division Case 1: 2 x 2 meshes per assembly in the radial direction
Case 2: 4 x 4 meshes per assembly in the radial direction
() in the axial direction in the active core region (both cases)
- (e) Ejected rod One RCCA ejected from fully inserted Bank-D within 0.1 seconds

(2) Results and Conclusions

Results of the RCCA ejection analysis including the main calculation conditions using a 2 x 2 mesh and a 4 x 4 mesh are shown in Table 3.2.2-1. The transient response of the core average power and the hot channel factor is shown in Figures 3.2.2-1 and 3.2.2-2, respectively.

The results indicate that the 2 x 2 mesh calculation is sufficient for use in the accident analysis.

Table 3.2.2-1 Calculation Condition and Results of the RCCA Ejection

	Case 1 2 x 2 mesh	Case 2 4 x 4 mesh
Initial power (fraction of nominal)	10 ⁻⁹	
Average coolant temperature (F)	557	Same as 2 x 2
RCS pressure (psia)	2250	
Ejected worth (pcm)	600	595
Delayed neutron fraction (%)	0.44	Same as 2 x 2
Neutron lifetime (microseconds)	8.0	Same as 2 x 2
Maximum core power (fraction of nominal)	3.12	2.98
Maximum hot channel factor	27.5	27.3

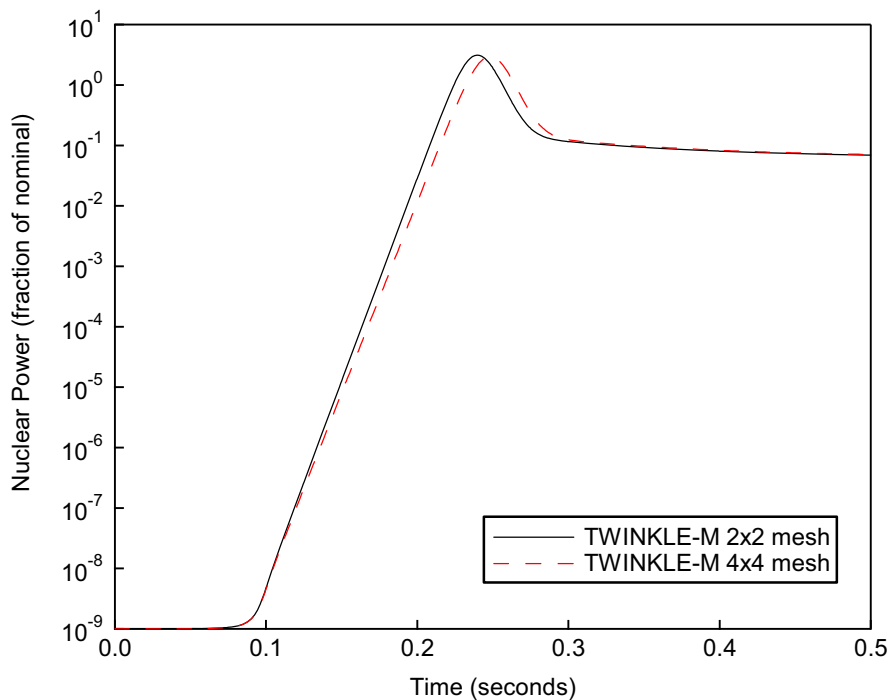


Figure 3.2.2-1 Nuclear Power, RCCA Ejection at EOC HZP Comparison with 2 x 2 mesh and 4 x 4 mesh in TWINKLE-M

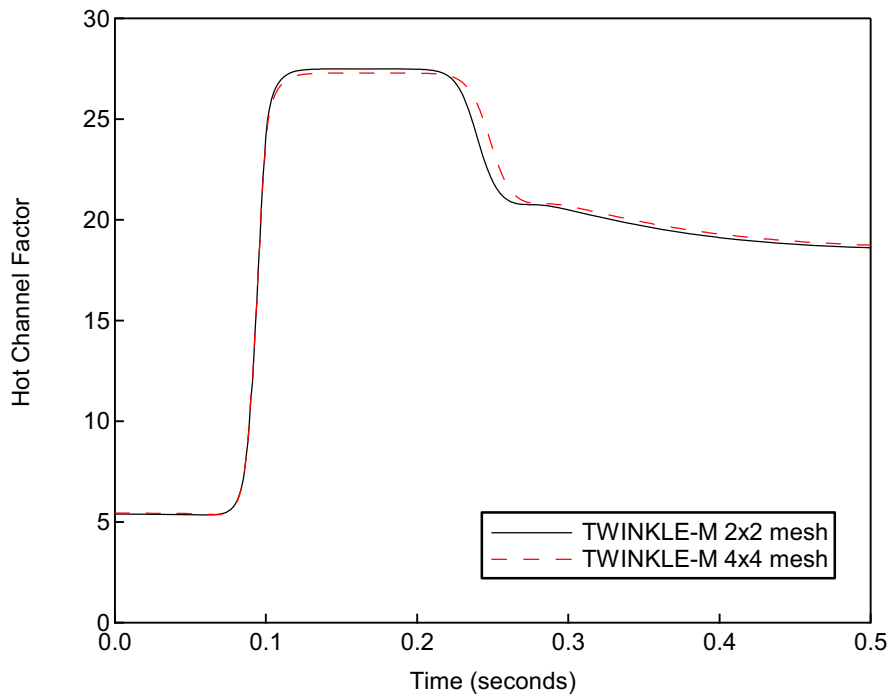


Figure 3.2.2-2 Hot Channel Factor, RCCA Ejection at EOC HZP Comparison with 2 x 2 mesh and 4 x 4 mesh in TWINKLE-M

4.0 ACCEPTANCE CRITERIA FOR SRP CHAPTER 15 NON-LOCA EVENTS

The methodology described in this Topical Report is applicable to the US-APWR plant design and modes of plant operation addressed in the non-LOCA accident analysis. In particular, the methodology described is related to the thermal-hydraulic aspects of the SRP Chapter 15 non-LOCA events for US-APWR that challenge the cladding and reactor coolant system fission product barriers; the non-LOCA methodology does not include the dose consequence analysis of radiological releases, accidents that only apply to Boiling Water Reactors, or events that are beyond the design basis.

The accident analysis in the Design Certification and Combined License Applications will be organized consistent with the categories shown below in Table 4-1, as defined in the Standard Review Plan (SRP) NUREG-0800 and the most recent version of Regulatory Guide 1.206. Regulatory Guide 1.206 will serve the same purpose (format and content guide) for new plants licensed under Part 52 as Regulatory Guide 1.70 serves for the current operating US plant Updated Final Safety Analysis Reports.

Table 4-1 Event Classification Categories

Category Number	Event Categorization By Effect on the Plant
15.1	Increase in Heat Removal by the Secondary System
15.2	Decrease in Heat Removal by the Secondary System
15.3	Decrease in Reactor Coolant System Flow Rate
15.4	Reactivity and Power Distribution Anomalies
15.5	Increase in Reactor Coolant Inventory
15.6	Decrease in Reactor Coolant Inventory

Due to the similarity between the MHI US-APWR and the current generation of PWRs in the United States, MHI has determined that no new categories of events (determined by effect on the plant) are required to bound the possible initiating events.

Each of the event categories in Table 4-1 have different potential initiating events that can be further categorized according to their expected frequency of occurrence. Historically, the frequency of each event was categorized as a fault of moderate frequency (ANSI 18.2 Category II), limiting fault (Category III), or design basis fault (Category IV), and frequency-class-based acceptance criteria associated with each category applied to specific accidents. For new plants, the current SRPs no longer use the historical frequency categories by name or number, but instead, re-categorize each event as either an Anticipated Operational Occurrence (AOO) or Postulated Accident (PA). The following definitions of AOO and PA are derived from the SRPs:

- Anticipated operational occurrences (AOOs), as defined in Appendix A to 10 CFR Part 50, are those conditions of normal operation that are expected to occur one or more times during the life of the plant. The SRP reiterates the 10 CFR 50 Appendix A definition of the term AOOs and adds that AOOs are also known as Condition II and Condition III events (referring to events that are categorized in Regulatory Guide 1.70 and Regulatory Guide 1.206 as incidents of moderate frequency

and infrequent events). Incidents of moderate frequency and infrequent events have also been previously known as ANSI 18.2 Condition II and Condition III events, respectively.

- Postulated accidents (PAs) are unanticipated occurrences (i.e., they are postulated but are not expected to occur during the life of the plant.) They are analyzed to confirm the adequacy of plant safety systems. These accidents have also been previously known as ANSI 18.2 Condition IV events or “Design Basis Accidents”.

Section 4.1 documents the acceptance criteria MHI plans to use for AOOs and PAs based on the SRPs, modified as needed, to identify the key criteria and additional more restrictive criteria imposed by MHI for each of the non-LOCA accidents to be provided in the Design Certification Application Design Control Document (DCD). The six event categories in Table 4-1 are then expanded in Sections 4.2 through 4.7 to define all of the related initiating events, each of which will be quantitatively analyzed in the US-APWR Design Certification Document (DCD).

4.1 Acceptance Criteria

Licensing analyses are performed to demonstrate that an operating plant can meet the applicable acceptance criteria for a limiting set of AOOs and PAs. This section provides the acceptance criteria used for the accident analyses of the US-APWR.

The General Design Criteria (GDC) are written such that the risk of an event, defined as the product of an event’s frequency of occurrence and its consequences, is approximately equal across the spectrum of AOOs and PAs. The first two sub-sections of Section 4.1 provide the general SRP acceptance criteria for the AOO and PA categorization of accidents. Additional event-specific criteria, including event-specific SRP criteria such as PCMI cladding failure limit or internal MHI acceptance criteria, are described in the appropriate event classification discussion.

4.1.1 AOO Acceptance Criteria

The following are the generic criteria necessary to meet the requirements of GDC for AOOs:

- i. Pressure in the reactor coolant (P_{RCS}) and main steam (P_{MS}) systems should be maintained below 110 percent of the design values in accordance with the American Society of Mechanical Engineers (ASME) Boiler and Pressure Vessel Code.
- ii. Fuel cladding integrity is maintained by ensuring that the minimum departure from nucleate boiling ratio (DNBR) remains above the 95/95 DNBR limit.
- iii. An AOO should not generate a postulated accident without other faults occurring independently or result in a consequential loss of function of the reactor coolant system (RCS) or reactor containment barriers.

General Design Criterion (GDC) 10 within Appendix A to 10 CFR 50, establishes that specified acceptable fuel design limits (SAFDLs) should not be exceeded during any condition of normal operation, including the effects of AOOs. Further guidance for interpreting this regulation is provided in SRP 4.2.

4.1.2 PA Acceptance Criteria

A list of the basic criteria necessary to meet the requirements of GDC for postulated accidents appears below.

- i. Pressure in the reactor coolant and main steam systems should be maintained below acceptable design limits.
- ii. Fuel cladding integrity is maintained by ensuring that the minimum DNBR remains above the 95/95 DNBR limit. If the minimum DNBR does not meet this limit, then the fuel is assumed to have failed.
- iii. The release of radioactive material shall not result in offsite doses in excess of the guidelines of 10 CFR Part 100. Any event-specific accident limits for allowable radiological releases are described in the appropriate section (i.e., for specific reactivity initiated accidents) below.
- iv. The postulated accident shall not, by itself, cause a consequential loss of required functions of systems needed to cope with the fault, including those of the RCS and the reactor containment system.

For the Reactivity Initiated Accidents (RIA), SRP 4.2 Appendix B provides the following additional acceptance criteria regarding core coolability (which are considered an extension of criteria iv above):

- Peak radial average fuel enthalpy must remain below 230 cal/g.
- Peak fuel temperature must remain below incipient fuel melting conditions.
- Mechanical energy generated as a result of (1) non-molten fuel-to-coolant interaction and (2) fuel rod burst must be addressed with respect to pressure boundary, reactor internals, and fuel assembly structural integrity.
- No loss of coolable geometry due to (1) fuel pellet and cladding fragmentation and dispersal and (2) fuel rod ballooning.

4.2 Increase in Heat Removal from the Primary System

This category covers events that lead to heat removal exceeding the heat generation in the core potentially leading to a decrease in moderator temperature resulting in an increased power level and reduced shutdown margin. The following table summarizes the five initiating events considered for the US-APWR, their associated event classification, the computer codes used to analyze the event for compliance with applicable codes and regulations, and a listing of the event-specific acceptance criteria.

Table 4.2-1 Events in Increase in Heat Removal from the Primary System

Event	Class	Code	Acceptance Criteria
1. Decrease in feedwater temperature	AOO	MARVEL-M	<ul style="list-style-type: none"> • max P_{RCS} & $P_{MS} < 110\%$ design • min DNBR > 95/95 DNBR limit^{*1}
2. Increase in feedwater flow	AOO	MARVEL-M	<ul style="list-style-type: none"> • max P_{RCS} & $P_{MS} < 110\%$ design • min DNBR > 95/95 DNBR limit^{*1} • no SG overfill^{*1}
3. Increase in steam flow	AOO	MARVEL-M	<ul style="list-style-type: none"> • max P_{RCS} & $P_{MS} < 110\%$ design • min DNBR > 95/95 DNBR limit^{*1}
4. Inadvertent opening of a steam generator relief or safety valve	AOO	MARVEL-M, VIPRE-01M ^{*2}	<ul style="list-style-type: none"> • max P_{RCS} & $P_{MS} < 110\%$ design • min DNBR > 95/95 DNBR limit^{*1}
5. Steam system piping failure a. Minor break	AOO	MARVEL-M, VIPRE-01M ^{*2}	<ul style="list-style-type: none"> • max P_{RCS} & $P_{MS} < 110\%$ design • min DNBR > 95/95 DNBR limit^{*1}
b. Major break (double-ended)	PA	MARVEL-M, VIPRE-01M ^{*2}	<ul style="list-style-type: none"> • max P_{RCS} & $P_{MS} < \text{acceptable design limits}$ • min DNBR > 95/95 DNBR limit^{*1, *3} • site boundary dose limited to 10% and 100% of 10 CFR 100 values

^{*1} Indicates the key parameter / acceptance limit of concern.

^{*2} Steady-state analysis

^{*3} MHI internal design criterion does not allow DNB to occur.

4.3 Decrease in Heat Removal by the Secondary System

This category covers events that lead to unplanned decreases in heat removal by the secondary system. The following table summarizes the six initiating events considered for the US-APWR, their associated event classification, the computer codes used to analyze the event for compliance with applicable codes and regulations, and a listing of the event-specific acceptance criteria.

Table 4.3-1 Events in Decrease in Heat Removal by the Secondary System

Event	Class	Code	Acceptance Criteria
1. Loss of external electrical load and/or turbine trip	AOO	MARVEL-M	<ul style="list-style-type: none"> • max P_{RCS} & $P_{MS} < 110\%$ design^{*1} • min DNBR > 95/95 DNBR limit
2. Inadvertent closure of main steam isolation valves	AOO	MARVEL-M	<ul style="list-style-type: none"> • max P_{RCS} & $P_{MS} < 110\%$ design^{*1} • min DNBR > 95/95 DNBR limit
3. Loss of condenser vacuum and other events resulting in turbine trip	AOO	MARVEL-M	<ul style="list-style-type: none"> • max P_{RCS} & $P_{MS} < 110\%$ design^{*1} • min DNBR > 95/95 DNBR limit
4. Loss of non-emergency ac power to the station auxiliaries	AOO	MARVEL-M	<ul style="list-style-type: none"> • max P_{RCS} & $P_{MS} < 110\%$ design • min DNBR > 95/95 DNBR limit • establish natural circulation flow^{*1, *3}
5. Loss of normal feedwater flow	AOO	MARVEL-M	<ul style="list-style-type: none"> • max P_{RCS} & $P_{MS} < 110\%$ design^{*1} • min DNBR > 95/95 DNBR limit
6. Feedwater system pipe break a. Minor break	AOO	MARVEL-M	<ul style="list-style-type: none"> • max P_{RCS} & $P_{MS} < 110\%$ design^{*1} • min DNBR > 95/95 DNBR limit • pressurizer does not fill^{*3} • evaluate hot leg boiling^{*3}
b. Major break (double-ended)	PA	MARVEL-M	<ul style="list-style-type: none"> • max P_{RCS} & $P_{MS} < 120\%$ design^{*1} • min DNBR > 95/95 DNBR limit^{*2} • pressurizer does not fill^{*3} • evaluate hot leg boiling^{*3}

^{*1} Indicates the key parameter / acceptance limit of concern.

^{*2} If the DNBR falls below this value, fuel failure (rod perforation) must be assumed for all rods that do not meet these criteria unless it can be shown, based on an acceptable fuel damage model that includes the potential adverse effects of hydraulic instabilities, that fewer failures occur. If rod internal pressure exceeds system pressure, then fuel rods may balloon shortly after entering DNB. The effect of ballooning fuel rods must be evaluated with respect to flow blockage and DNB propagation. Any fuel damage calculated to occur must be sufficiently limited to the extent that the core will remain in place and intact with no loss of core cooling capability.

^{*3} MHI internal acceptance criterion

4.4 Decrease in Reactor Coolant System Flow Rate

This category covers events that lead to a decrease in reactor coolant flow that could result in fuel damage if certain specified acceptable fuel design limits (SAFDLs) are exceeded. The following table summarizes the four initiating events considered for the US-APWR, their associated event classification, the computer codes used to analyze the event for compliance with applicable codes and regulations, and a listing of the event-specific acceptance criteria.

Table 4.4-1 Events in Decrease in Reactor Coolant System Flow Rate

Event	Class	Code	Acceptance Criteria
1. Partial loss of forced reactor coolant flow	AOO	MARVEL-M, VIPRE-01M	<ul style="list-style-type: none"> • max P_{RCS} & P_{MS} < 110% design • min DNBR > 95/95 DNBR limit^{*1}
2. Complete loss of forced reactor coolant flow	AOO	MARVEL-M, VIPRE-01M	<ul style="list-style-type: none"> • max P_{RCS} & P_{MS} < 110% design • min DNBR > 95/95 DNBR limit^{*1}
3. Reactor coolant pump shaft seizure (locked rotor)	PA	MARVEL-M, VIPRE-01M	<ul style="list-style-type: none"> • max P_{RCS} & P_{MS} < acceptable design limits • min DNBR > 95/95 DNBR limit^{*1, *2} • site boundary dose limited to 10% of 10 CFR 100 values • long-term core coolability maintained
4. Reactor coolant pump shaft break	PA	MARVEL-M, VIPRE-01M	<ul style="list-style-type: none"> • max P_{RCS} & P_{MS} < acceptable design limits • min DNBR > 95/95 DNBR limit^{*1, *2} • long-term core coolability maintained

^{*1} Indicates the key parameter / acceptance limit of concern.

^{*2} If the DNBR falls below this value, fuel failure (rod perforation) must be assumed for all rods that do not meet these criteria unless it can be shown, based on an acceptable fuel damage model that includes the potential adverse effects of hydraulic instabilities, that fewer failures occur. If rod internal pressure exceeds system pressure, then fuel rods may balloon shortly after entering DNB. The effect of ballooning fuel rods must be evaluated with respect to flow blockage and DNB propagation. Any fuel damage calculated to occur must be sufficiently limited to the extent that the core will remain in place and intact with no loss of core cooling capability.

4.5 Reactivity and Power Distribution Anomalies

This category covers events associated with unintended fuel rod movement or core flow parameter (temperature, boron concentration, etc.) changes that alter reactivity or power distribution. The following table summarizes the six initiating events considered for the US-APWR, their associated event classification, the computer codes used to analyze the event for compliance with applicable codes and regulations, and a listing of the event-specific acceptance criteria. It should be noted that the event classification of the withdrawal of a single RCCA has been defined as PA. Limited fuel damage has traditionally been allowed for this event when it was classified as a Condition III event per ANSI 18.2. This classification is consistent with its low expected frequency and the multiple failures required to initiate a single rod withdrawal.

Table 4.5-1 Events in Reactivity and Power Distribution Anomalies

Event	Class	Code	Acceptance Criteria
1. Uncontrolled RCCA bank withdrawal from a subcritical or low power startup condition	AOO	TWINKLE-M, VIPRE-01M	<ul style="list-style-type: none"> • max P_{RCS} & $P_{MS} < 110\%$ design • min DNBR > 95/95 DNBR limit^{*1}
2. Uncontrolled RCCA bank withdrawal at power	AOO	MARVEL-M	<ul style="list-style-type: none"> • max P_{RCS} & $P_{MS} < 110\%$ design^{*1} • min DNBR > 95/95 DNBR limit^{*1}
3. RCCA misalignment a. Dropped RCCA b. Static misalignment	AOO AOO	MARVEL-M, VIPRE-01M ^{*2}	<ul style="list-style-type: none"> • max P_{RCS} & $P_{MS} < 110\%$ design • min DNBR > 95/95 DNBR limit^{*1,2}
c. Withdrawal of a single RCCA	PA	MARVEL-M, VIPRE-01M ^{*2}	<ul style="list-style-type: none"> • max P_{RCS} & $P_{MS} < 110\%$ design • min DNBR > 95/95 DNBR limit^{*1, *7}
4. Startup of an inactive reactor coolant pump at an incorrect temperature	AOO	N/A	N/A ^{*3}
5. CVCS malfunction that results in a decrease in boron concentration in the reactor coolant	AOO	N/A ^{*4}	<ul style="list-style-type: none"> • max P_{RCS} & $P_{MS} < 110\%$ design • min DNBR > 95/95 DNBR limit^{*1} • See Note^{*5}
6. Spectrum of RCCA ejection accidents	PA	TWINKLE-M, VIPRE-01M, MARVEL-M	<ul style="list-style-type: none"> • max reactor pressure < ASME "Service Limit C" criteria • min DNBR > 95/95 DNBR limit^{*1, *7, *8} • PCMI fuel failure^{*1, *6} • site boundary dose limited to 25% of 10 CFR 100 values • core coolability maintained^{*6}

*1 Indicates the key parameter / acceptance limit of concern.

*2 Steady-state analysis

*3 N-1 loop operation not allowed per plant Tech Specs

*4 This event is evaluated without the use of a computer code.

-
- *5 The following minimum time intervals are available for operator actions between the time an alarm announces an unplanned moderator dilution and the time shutdown margin is lost:
- A. During refueling: 30 minutes.
 - B. During startup, cold shutdown, hot shutdown, hot standby, and power operation: 15 minutes.
- *6 The RCCA ejection (RIA) follows SRP 4.2 Appendix B
- *7 If the DNBR falls below this value, fuel failure (rod perforation) must be assumed for all rods that do not meet these criteria unless it can be shown, based on an acceptable fuel damage model that includes the potential adverse effects of hydraulic instabilities, that fewer failures occur. If rod internal pressure exceeds system pressure, then fuel rods may balloon shortly after entering DNB. The effect of ballooning fuel rods must be evaluated with respect to flow blockage and DNB propagation. Any fuel damage calculated to occur must be sufficiently limited to the extent that the core will remain in place and intact with no loss of core cooling capability.

4.6 Increase in Reactor Coolant Inventory

This category covers events that lead to fuel damage or over-pressurization of the RCS due to an unexpected increase in RCS inventory. The following table summarizes the two initiating events considered for the US-APWR, their associated event classification, and identifies the computer codes used to analyze the event for compliance with applicable codes and regulations.

Table 4.6-1 Events in Increase in Reactor Coolant Inventory

Event	Class	Code	Acceptance Criteria
1. Inadvertent operation of the emergency core cooling system during power operation	AOO	N/A	N/A ^{*2}
2. CVCS malfunction that increases reactor coolant inventory	AOO	MARVEL-M	<ul style="list-style-type: none"> • max P_{RCS} & $P_{MS} < 110\%$ design • min DNBR $> 95/95$ DNBR limit^{*1}

^{*1} Indicates the key parameter / acceptance limit of concern.

^{*2} Safety injection pump shut off head is below normal operation pressure.

4.7 Decrease in Reactor Coolant Inventory

This category covers events that lead to accidental depressurization of the RCS. The following table summarizes the two initiating events considered for the US-APWR, their associated event classification, and identifies the computer codes used to analyze the event for compliance with applicable codes and regulations.

Table 4.7-1 Events in Decrease in Reactor Coolant Inventory

Event	Class	Code	Acceptance Criteria
1. Inadvertent opening of a pressurizer safety valve ^{*3}	AOO	MARVEL-M	<ul style="list-style-type: none"> •max P_{RCS} & $P_{MS} < 110\%$ design •min DNBR > 95/95 DNBR limit^{*1}
2. Steam generator tube rupture	PA	MARVEL-M	<ul style="list-style-type: none"> •max P_{RCS} & $P_{MS} < 110\%$ design^{*4} •min DNBR > 95/95 DNBR limit^{*2} •SG does not fill^{*1, *2} •site boundary dose limited to 10% and 100% of 10 CFR 100 values

*1 Indicates the key parameter / acceptance limit of concern.

*2 MHI internal acceptance criteria.

*3 The non-LOCA scope of this accident includes the short-term analysis to evaluate fuel and NSSS response. The LOCA aspects of this accident are outside the scope of this non-LOCA analysis topical report.

*4 MHI internal criterion to assure that rupture of primary or steam system piping does not occur.

5.0 EVENT-SPECIFIC METHODOLOGY

The objective of this topical report is to provide methods of analysis, details, and examples of the application of the MHI non-LOCA accident analysis to the US-APWR such that questions or issues can be identified as early as possible in the licensing process. As discussed in Section 2, the MARVEL-M, VIPRE-01M, and TWINKLE-M computer codes are the principal computer codes that will be used by MHI for the US-APWR non-LOCA analyses. Depending on the specific nature and computational capabilities needed for specific accidents, these programs are either used alone or in combination with another. Events utilizing computer codes for the non-LOCA accident analysis fall into one of the following three categories based on the combination of codes used:

- Analyzed using MARVEL-M only
- Analyzed using MARVEL-M and VIPRE-01M in sequence
- Analyzed using TWINKLE-M and VIPRE-01M in sequence

The first category that uses MARVEL-M alone includes most of the non-LOCA transients that challenge the design limits for the RCS and main steam system pressure limits, as well as loop-symmetric accidents at full-flow conditions that fall within the capabilities of the simplified MARVEL-M DNBR model. These accidents do not require detailed calculation of localized fuel parameters and do not require spatially dependent transient calculations for accident-specific power levels or power distributions. The RCCA Bank Withdrawal at Power event is such a transient.

The second category that uses MARVEL-M in combination with the VIPRE-01M fuel rod code is used for accidents that challenge the DNB design limits under reduced flow conditions such as the partial loss of flow, complete loss of flow, locked RCP rotor, or RCP sheared shaft conditions. The loop-dependent and core total flow, core inlet conditions, pressure and power are calculated using the MARVEL-M program, and then the VIPRE-01M code is used to determine the hot channel or hot spot fuel response including DNBR, fuel temperatures, and cladding temperature. The Complete Loss of Forced Reactor Coolant Flow is an example of such an event. The flow transient is calculated in the MARVEL-M code using the internal reactor coolant pump model in conjunction with the core and reactor coolant loop characteristics.

The third category that uses TWINKLE-M in combination with the VIPRE-01M fuel rod code is reserved for rapid reactivity transients requiring space- and time-dependent nuclear power and power distribution calculations for input to a detailed fuel response calculation. The Spectrum of RCCA Ejection event is an example of an event requiring these capabilities, including 3-D TWINKLE-M capabilities if needed.

There are several other events that make use of special models or code capabilities of the MARVEL-M code.

- The Steam System Piping Failure is a transient that is characterized by a non-uniform cooldown in combination with the assumption that the most reactive control rod be fully withdrawn. The steam line break flow calculation is unique to this event, and reactor vessel inlet mixing and reactivity weighting models in MARVEL-M are used to conservatively predict core reactivity and nuclear power using point kinetics. In addition, certain ECCS functions such as steamline isolation, EFWS actuation, feedwater isolation, and RCS boration using the safety injection system are modeled in

this event. The VIPRE-01M code is used to confirm that the DNB design limit is met for selected steady-state points characterized by temperature, pressure, power, power distribution, inlet temperature distribution, and flow conditions unique to the steamline break event.

- The Feedwater System Pipe Break is another non-uniform accident that involves modeling break flow from one of the secondary loops. The feedwater system pipe break models loss of inventory from the saturated liquid water mass in the steam generator and unlike the steamline break cooldown, results in RCS heatup and pressurization. This event also uses the 4-loop capability of the MARVEL-M code to model the failure of EFWS to feed one of the intact steam generators.
- The Steam Generator Tube Rupture event uses the MARVEL-M capability to calculate primary-to-secondary flow based on primary and secondary pressures calculated by the code. Operator actions to establish steam generator cooling using the non-faulted steam generators, manual opening of the steam generator relief valves, and manual opening of a pressurizer depressurization valve are also modeled by MARVEL-M for this accident.

In summary, the following six events have been selected to demonstrate the wide spectrum of key analytical methods (combinations of codes) and specialized models used by MHI in the non-LOCA accident analysis for the US-APWR. These events also represent the SRP accident categories for cooldown events (15.1), heatup events (15.2), flow reduction events (15.3), reactivity events (15.4), and reactor coolant inventory reduction events (15.6).

Analyzed using MARVEL-M only

- Uncontrolled RCCA Bank Withdrawal at Power

Analyzed using MARVEL-M / VIPRE-01M sequence

- Complete Loss of Forced Reactor Coolant Flow

Analyzed using TWINKLE-M / VIPRE-01M sequence

- Spectrum of RCCA Ejection

Requiring special treatment

- Steam System Piping Failure (VIPRE-01M core modeling)
- Feedwater System Pipe Break (4-loop MARVEL-M capability)
- Steam Generator Tube Rupture (primary-to-secondary flow model)

A detailed description of the methodology for each of these events is provided in separate subsections of Section 5, and sample transient results for each of the events are provided in Section 6.

5.1 Uncontrolled RCCA Bank Withdrawal at Power

Event Description

The uncontrolled RCCA bank withdrawal at power results in an increase in both the nuclear power and core heat flux. Because the heat removal from the steam generator lags the core power generation until the steam generator relief or safety valves open, there is an increase in the reactor coolant temperature. Unmitigated, the power increase and concurrent coolant temperature rise could eventually exceed a DNB, overpower, or RCS pressure limit. In order to avoid damage of the fuel cladding, the protection system trips listed below are designed to terminate any such transient before a design limit is exceeded.

This transient is categorized in AOO and the acceptance criteria are shown in Section 4.5.

Reactor Protection

The following automatic reactor trip signals are assumed to be available to provide protection from this transient:

- Neutron flux high trip (high setting)
- Neutron flux rate high trip
- Over power ΔT high trip
- Over temperature ΔT high trip
- Pressurizer pressure high trip
- Pressurizer water level high trip

The reactor protection system overpower and overtemperature ΔT trips are designed to provide margin to the core protection design limits.

Method of Analysis

(1) Analysis Code

The MARVEL-M code is used to determine the plant transient following an uncontrolled RCCA bank withdrawal at power. A reactivity insertion into the core is simulated by external reactivity. Minimum DNBR is calculated by the MARVEL-M code using DNBR data tables with average and hot spot heat flux, RCS pressure, and core inlet temperature. The DNBR data tables are made up of several pre-calculated conditions using the VIPRE-01M code with an assumed constant core flow rate. A suitable rod bundle DNB correlation and the Revised Thermal Design Procedure (RTDP) [Reference 14] are used for a DNBR evaluation.

Comparison of the MARVEL-M DNBR calculation using the DNBR data tables with the VIPRE-01M DNBR calculation for this transient is shown in Appendix A.

(2) Analysis Assumptions

Analysis assumptions and calculation conditions for this event are as follows.

- | | |
|-----------------------------------|--|
| (a) Initial condition | Nominal power, T_{avg} , RCS pressure for DNB evaluation |
| (b) Power distribution | Design power distribution |
| (c) Moderator Density Coefficient | Least positive (BOC), Most positive (EOC) |
| (d) Doppler Power Coefficient | Least negative (BOC), Most negative (EOC) |
| (e) Trip Parameters | Conservative reactivity insertion curve and trip delays |

-
- (f) Reactor protection Neutron flux high trip and Over temperature ΔT high trip are assumed.

(3) Calculation Case

Analyses for DNBR evaluation are performed for a range of reactivity insertion rates ranging from a small reactivity insertion rate through the maximum reactivity insertion rate of 75 pcm/sec using combinations of the following feedback conditions.

- Beginning of cycle (BOC), meaning a minimum feedback condition
- End of cycle (EOC), meaning a maximum feedback condition

Analyses for peak RCS pressure are also performed for this accident. The analysis assumptions such as initial conditions and core parameters are selected to maximize peak RCS pressure.

5.2 Complete Loss of Forced Reactor Coolant Flow

Event Description

A complete loss of forced reactor coolant flow accident results from a simultaneous loss of electrical supplies to the reactor coolant pumps. If the reactor is at power at the time of the transient, the immediate effect of a loss of coolant flow is a rapid increase in the coolant temperature, and the minimum DNBR decreases. The reactor protection trips listed below are available to provide protection for this event. In the analysis, this transient is terminated by the Reactor coolant pump speed low trip to prevent a DNB occurrence.

This transient is categorized in AOO and the acceptance criteria are shown in Section 4.4.

Reactor Protection

The following signals are assumed to be available to automatically trip the reactor and therefore provide protection from this transient.

- Reactor coolant pump speed low trip
- Reactor coolant flow low trip

Method of Analysis

(1) Analysis Code

The MARVEL-M code's built-in reactor coolant pump model is used to determine the plant transient following a complete loss of forced reactor coolant flow. The MARVEL-M code generates an interface file that includes the time-dependent histories of the nuclear power and core inlet flow rate.

The VIPRE-01M code calculates the minimum DNBR during the transient using this interface as a boundary condition assuming a constant design power distribution. A constant RCS pressure and inlet temperature is used in the DNBR calculation for conservatism. A subchannel analysis using VIPRE-01M for the typical 4-loop plant with 17x17-257FA core is performed using a one-eighth core model with a hot assembly located at the center of the core. This model assumes that the radial power distribution and inlet flow distribution are symmetric with respect to the core center [Reference 6]. A suitable rod bundle DNB correlation and Revised Thermal Design Procedure (RTDP) are used.

VIPRE-01M one-eighth core model is shown in Figure 5.2-1 and a calculation flow diagram of the MARVEL-M / VIPRE-01M methodology is shown in Figure 5.2-2.

(2) Analysis Assumptions

Analysis assumptions and calculation conditions for the MARVEL-M analysis are as follows.

- | | |
|-----------------------------------|--|
| (a) Initial condition | Nominal power, T_{avg} , RCS pressure for DNB evaluation |
| (b) Moderator Density Coefficient | Least positive |
| (c) Doppler Power Coefficient | Most negative |
| (d) Trip Parameter | Conservative reactivity insertion curve and trip delays |
| (e) Others | Conservative inertia momentum of the RCP flywheel |

Analysis assumptions and calculation conditions for the VIPRE-01M analysis are as follows:

- | | |
|------------------------|---|
| (f) Power distribution | Design limit of the nuclear enthalpy rise hot channel |
|------------------------|---|

	factor and design axial power shape
(g) RCS Pressure	Constant
(h) Core Inlet Temperature	Constant

(3) Calculation Case

Analyses for DNBR evaluation are performed at the beginning-of-cycle (BOC) for the hot full power condition.

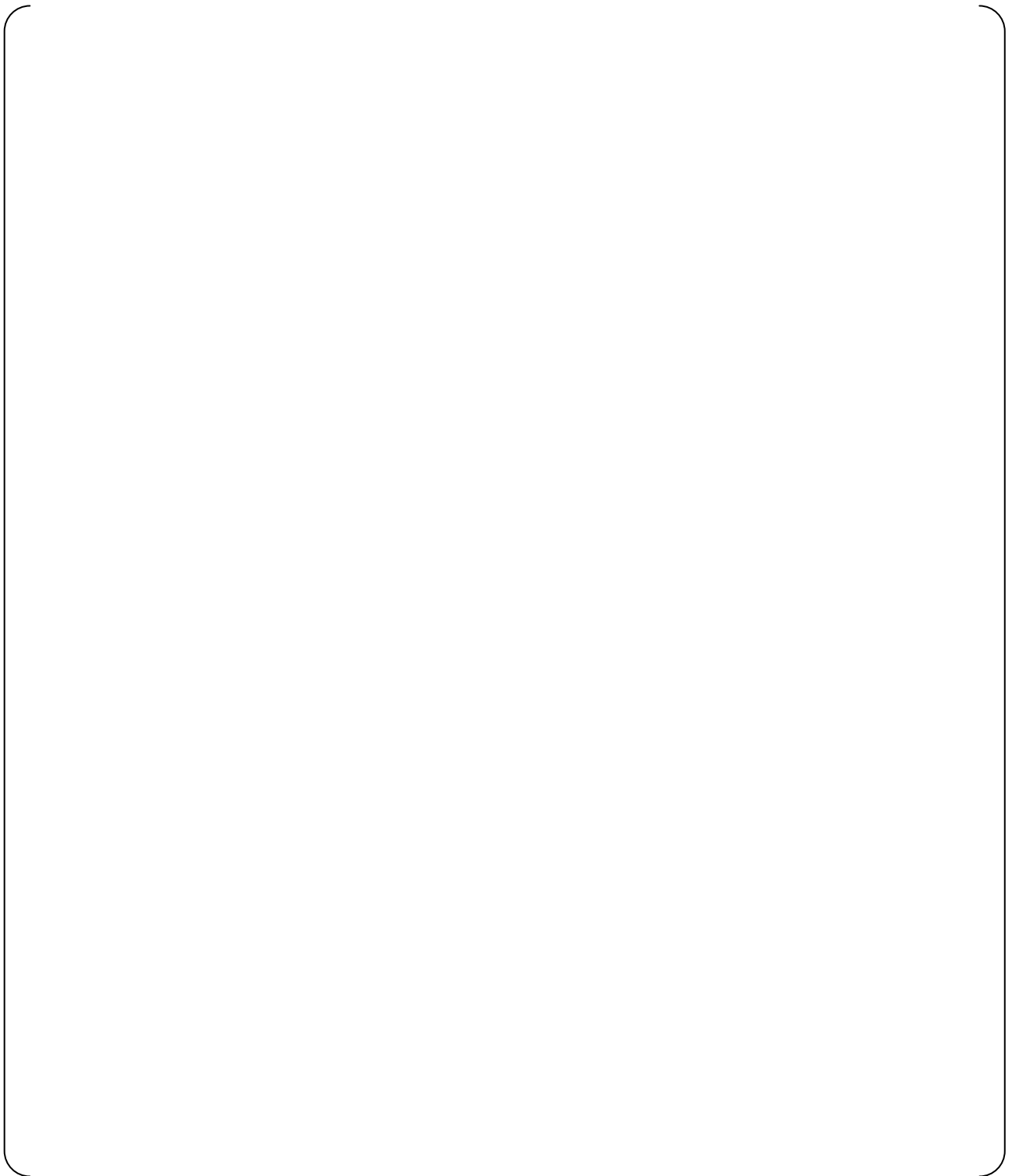


Figure 5.2-1 VIPRE-01M 1/8 Core Analysis Modeling (17x17-257FA Core, 4-Loop Plant)

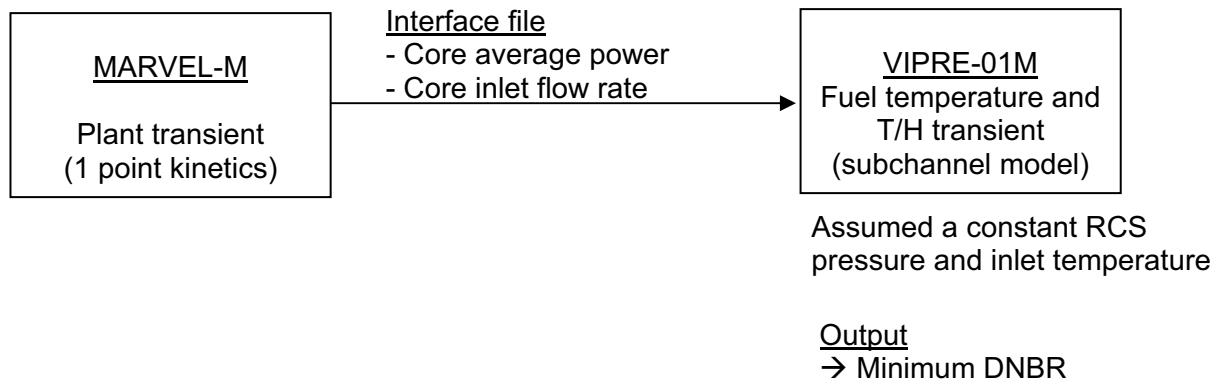


Figure 5.2-2 Calculation Flow Diagram of the MARVEL-M / VIPRE-01M Methodology

5.3 Spectrum of RCCA Ejection

Event Description

This accident is defined as the mechanical failure of a control rod drive mechanism pressure housing, resulting in the ejection of an RCCA and drive shaft. The consequence of this RCCA ejection is a rapid positive reactivity insertion with an increase of core power peaking in the short-term period, possibly leading to localized fuel rod failure, and depressurization of the RCS in the long-term period due to the CRDM housing break. The nuclear excursion is terminated by Doppler reactivity feedback from increased fuel temperature, and the core is shut down by the reactor trip.

This accident is categorized as a PA, and the acceptance criteria are shown in Section 4.5.

Reactor Protection

The following signals are assumed to be available to automatically trip the reactor and therefore provide protection from this transient.

- High power range neutron flux trip (high setting)
- High power range neutron flux trip (low setting)
- High power range neutron flux rate trip
- Over temperature ΔT trip
- Low pressurizer pressure trip

In the safety analysis, the high power range neutron flux rate trip is ignored and the reactor is tripped on high power range neutron flux. However, in some cases, the reactivity of the ejected rod is low enough that the reactor power increase does not reach the setpoint of the high power range neutron flux trip. In these cases, the core is protected by the over temperature ΔT trip or low pressurizer pressure trip during RCS depressurization.

Method of Analysis

(1) Analysis Code

The TWINKLE-M code is used to determine the core transient including core average and local power behavior following a RCCA ejection. An increase of local power and the Doppler feedback due to an increase of fuel effective temperature are calculated in each spatial mesh.

The three-dimensional method is applied to the hot zero power condition in order to conform to the PCMI (Pellet Cladding Mechanical Interaction) fuel failure criteria, which was lowered and expressed as a function of fuel oxide / wall thickness in SRP Chapter 4.2 Rev.3 Appendix B. Core mesh division is 2 x 2 meshes per assembly in the radial direction and (38 meshes) in the axial direction for the active core region for the typical 4-loop plant with 17x17-257FA core. The three-dimensional method is also used for the hot full power analysis of DNB to ensure that the core is protected even under rod ejection conditions which result in power increases less than the high power range neutron flux trip setpoint. For the bounding HFP analysis of peak fuel and cladding temperature and fuel enthalpy, a one-dimensional method is applied using () in the axial direction for the active core region.

The VIPRE-01M code calculates the fuel temperature and fuel enthalpy at the hot spot during the transient using two interface files created by the TWINKLE-M code. One of the interface files is a time-dependant history of the core average power and the other is a time-dependant

history of the hot channel factor. The hot channel factor time history is used for the three-dimensional calculation only. The VIPRE-01M analysis uses a one-eighth core model shown in Figure 5.2-1.

The MARVEL-M code is used to calculate the RCS pressure transient using the VIPRE-01M results which are core total void and heat flux histories.

(2) Hot Zero Power Application

A calculation flow diagram of the three-dimensional methodology applied to the hot zero power condition including the hot spot temperature analysis and the PCMI fuel failure evaluation is shown in Figure 5.3-1.

Hot spot fuel temperature analysis

PCMI fuel failure evaluation

- (a) A local adiabatic fuel enthalpy rise (ΔH) is calculated in the TWINKLE-M code by integration of local power and power density (cal/g-s) in each mesh. This ΔH is considered a peak / average ratio in the mesh using the VIPRE-01M hot spot results. In this way, a relation of between the fuel enthalpy rise (ΔH) and the local burnup is obtained.
- (b) A relation of between the local oxide / wall thickness and the local fuel burnup is evaluated in fuel design.
- (c) Then, a relation of between the fuel enthalpy rise (ΔH) and the local oxide / wall thickness can be obtained. The fuel integrity is confirmed by comparing the calculated fuel enthalpy rise and oxide / wall thickness data with the new PCMI fuel failure criteria.

The three-dimensional calculation is generally the most realistic method to predict localized fuel behavior. The MHI three-dimensional methodology used in the hot zero power RCCA ejection safety analysis is established based on the following separate calculation conservatisms:

A sensitivity study of the conservatism of the reactivity and the hot channel factor treatment is

shown in Appendix B.

(3) Hot Full Power Application

A calculation flow diagram of the one-dimensional methodology for the hot spot temperature analysis is shown in Figure 5.3-2. The number of rods in DNB methodology is shown in Figure 5.3-3 and the RCS pressure methodology is shown in Figure 5.3-5. The relationship between the CRDM housing break size and minimum DNBR in the long-term period, including the protection function provided by both low pressurizer pressure and over temperature ΔT reactor trips, is shown in Figure 5.3-4.

Hot spot fuel temperature analysis

- (a) The TWINKLE-M code analyzes the RCCA ejection using a one-dimensional model for the hot full power initial condition. The reactivity insertion to the core is simulated by an external reactivity insertion by changing the eigenvalue of the neutron kinetics. Other conservative assumptions are described in (4).
- (b) The TWINKLE-M code outputs the interface file for the VIPRE-01M code including histories of core average power. The hot channel factor used as the VIPRE-01M input data is assumed a constant during the transient after a RCCA ejection.
- (c) The VIPRE-01M code reads the interface file and calculates a fuel temperature transient at the hot spot with conservative parameters and assumptions described in (5). Then a maximum fuel center temperature, a peak fuel enthalpy and a peak clad temperature are obtained.

RCS pressure analysis

- (a) The TWINKLE-M code analyzes the core average power histories using the same manner as the hot spot analysis.
- (b) The VIPRE-01M code analyzes the fuel temperature and the thermal hydraulics using the same manner as the hot spot analysis.
- (c) The VIPRE-01M code generates the interface file including a time-dependant core total void fraction and core heat flux.
- (d) The MARVEL-M code analyzes a plant transient for maximum RCS pressure using the interface file generated by VIPRE-01M.

Short-term DNB analysis

Long-term DNB analysis (Rapid Depressurization Case)

Long-term DNB analysis (Slow Depressurization Case)

(4) Analysis Assumptions for the Core Kinetics

Analysis assumptions and calculation conditions are as follows. These conditions follow Regulatory Guide 1.77 Appendix A.

(a) Initial Condition

- 24 month equilibrium core at the beginning-of-cycle (BOC) and end-of-cycle (EOC)
- Hot full power with initial uncertainty for fuel temperature evaluation
 - Hot zero power for fuel enthalpy evaluation

24 month first core and equilibrium core at BOC and EOC

- Hot full power for DNB evaluation

(b) Reactivity Insertion

For the bounding peak fuel and cladding temperature, fuel enthalpy and RCS pressure analyses, a conservative large reactivity is chosen as the design limit.

For the rods in DNB analyses, a reactivity insertion is modeled based on the value calculated by ANC plus an additional () margin. This reactivity of the ejected rod worth is much lower than the design limit values and therefore the short-term reactor power increase due to the ejected rod may not reach the setpoint of the high power range neutron flux trip and the event will continue until the reactor trips on low pressurizer pressure or over temperature ΔT during the RCS depressurization.

In the case of three-dimensional methodology, the reactivity insertion is modeled by three-dimensional change in the cross section due to the ejected rod.. The difference in reactivity compared with the target reactivity is externally added to the core by changing the eigenvalue of the neutron kinetics. In the case of one-dimensional methodology, the target reactivity is externally added to the core within 0.1 seconds.

(c) Feedback

The Doppler feedback is applied as a conservative multiplier to the change in the fast absorption cross-section for the given change in the calculated fuel effective temperature.

The moderator reactivity feedback is calculated by multiplying the moderator slowing down cross section by a conservative multiplier.

(d) Doppler Weighting Factor for 1-D Method

In the MHI one-dimensional methodology, a small Doppler weighting factor is used to compensate for collapsing the 3-D problem into a 1-D axial model. The suitability and conservatism of this approach is confirmed by a comparison between the three-dimensional and one-dimensional kinetic results presented in Appendix C.

(e) Trip Parameters

The reactor trip is simulated by dropping partially and fully withdrawn rod banks into the core. The calculation of the high power range neutron flux reactor trip (high setpoint) for the rod ejection analysis is described in Appendix G. Maximum time delay from reactor trip signal to rod motion and a conservative RCCA insertion curve are simulated. The trip reactivity used is the design limit, which is $-4\% \Delta K/K$ for the hot full power case and $-2\% \Delta K/K$ for the hot zero power case, respectively.

(f) Other Parameters

Minimum delayed neutron fraction and minimum neutron lifetime are used.

(5) Analysis Assumptions for the Fuel Temperature Transient

Analysis assumptions and calculation conditions are as follows.

(a) Initial Condition

Same as (4)(a)

(b) Hot Channel Factor

[

In the case of one-dimensional methodology, the hot channel factor is assumed to instantaneously increase to the design limit and is conservatively assumed to remain constant, ignoring feedback effects during the transient.

(c) Fuel Properties

Initial condition of fuel temperature at hot spot is consistent with the results of the fuel design code FINE [Reference 15]. Pellet and cladding gap conductance in the transient are assumed to be conservative values according to the evaluation purpose.

- Remains constant at the initial value for the fuel temperature and enthalpy analysis
- Instantaneously decreases to zero for the adiabatic fuel enthalpy analysis
- Rapidly increases to the maximum value for the clad temperature analysis
- Realistic increases based on the transient change in gap width for the RCS pressure analysis
- Assumptions for rods in DNB analyses are described in (6) and (7) below.

(6) Analysis Assumptions for the Short-Term DNB Transient

Analysis assumptions and calculation conditions are as follows.

(a) Initial Condition

Same as (4)(a)

(b) Nuclear Enthalpy Rise Hot Channel Factor ($F_{\Delta H}^N$)

(c) Fuel Properties

(7) Analysis Assumptions for the Long-term DNB Steady State Analysis (Rapid Depressurization Case)

Analysis assumptions and calculation conditions are as follows.

(8) Calculation Cases

Analyses of the spectrum of RCCA ejection are performed for the following cases.

- Hot full power initial condition at beginning-of-cycle
- Hot full power initial condition at end-of-cycle
- Hot zero power initial condition at beginning-of-cycle
- Hot zero power initial condition at end-of-cycle

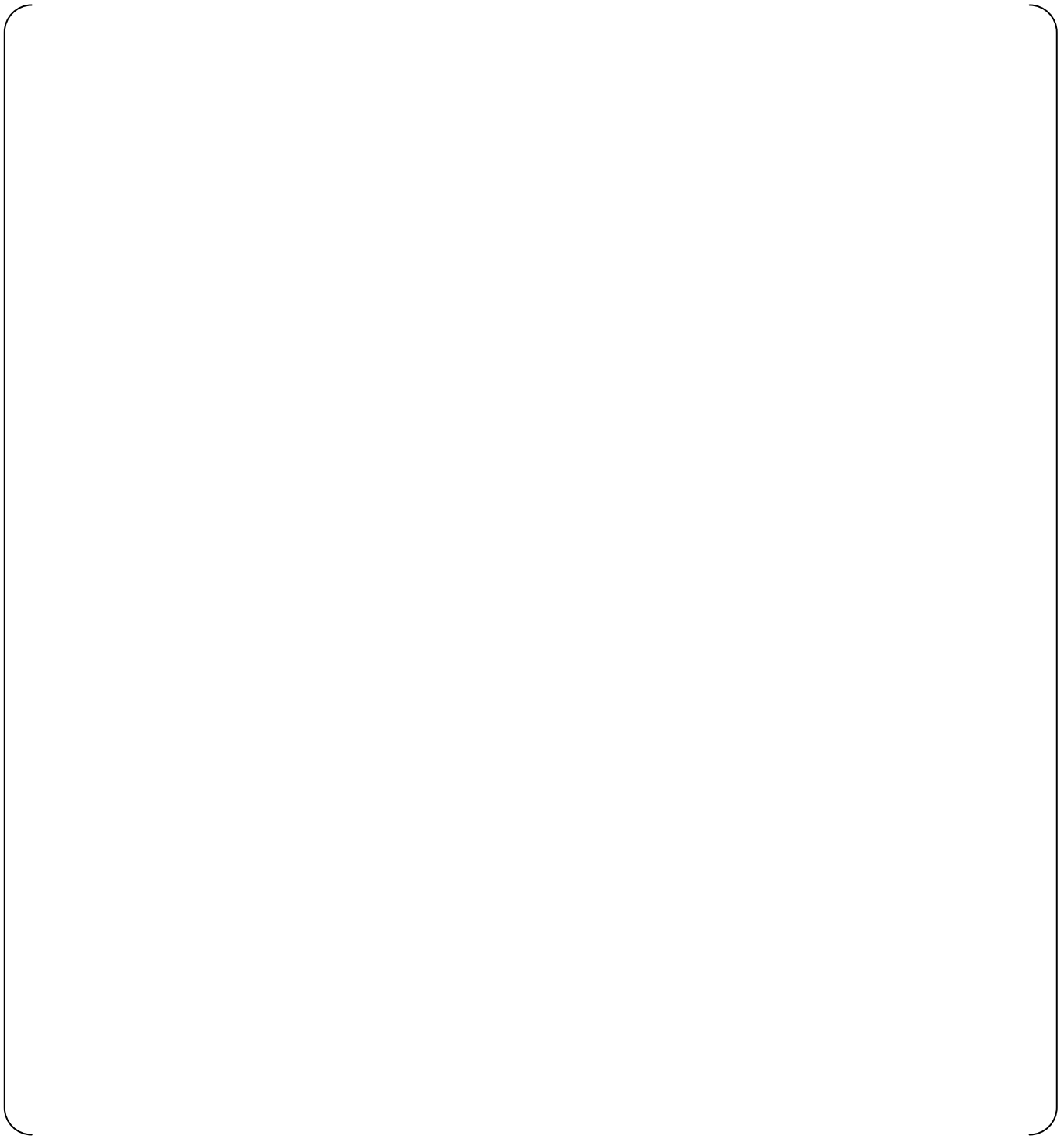


Figure 5.3-1 Calculation Flow Diagram of the Three-Dimensional Methodology

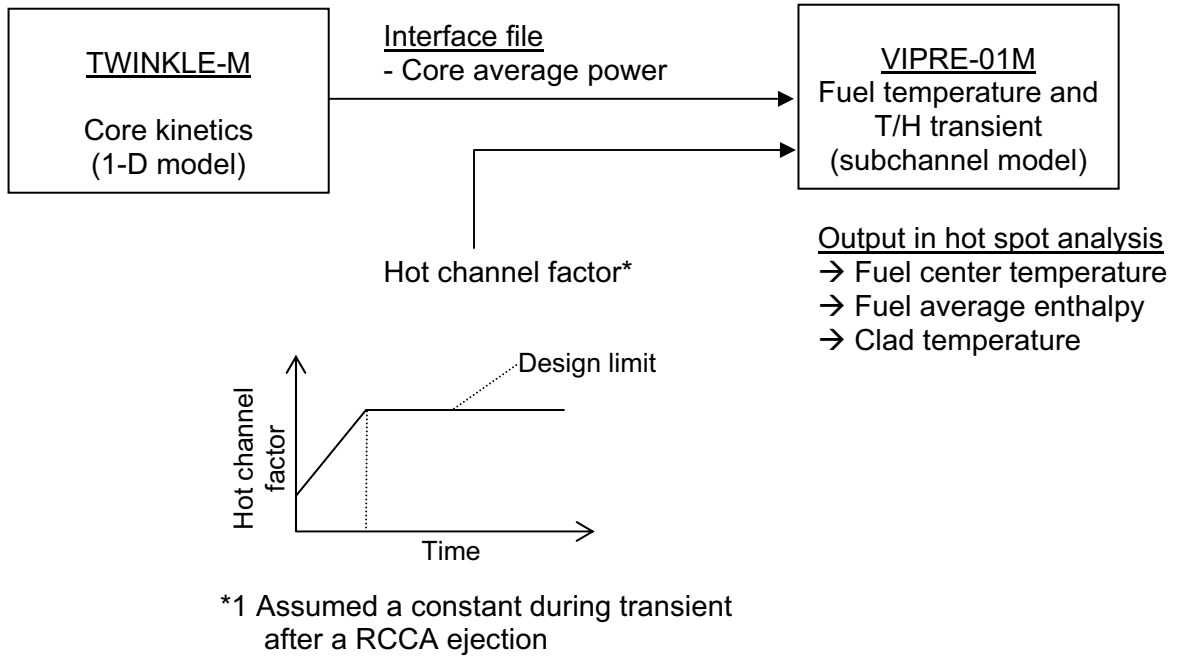


Figure 5.3-2 Calculation Flow Diagram of the One-Dimensional Methodology

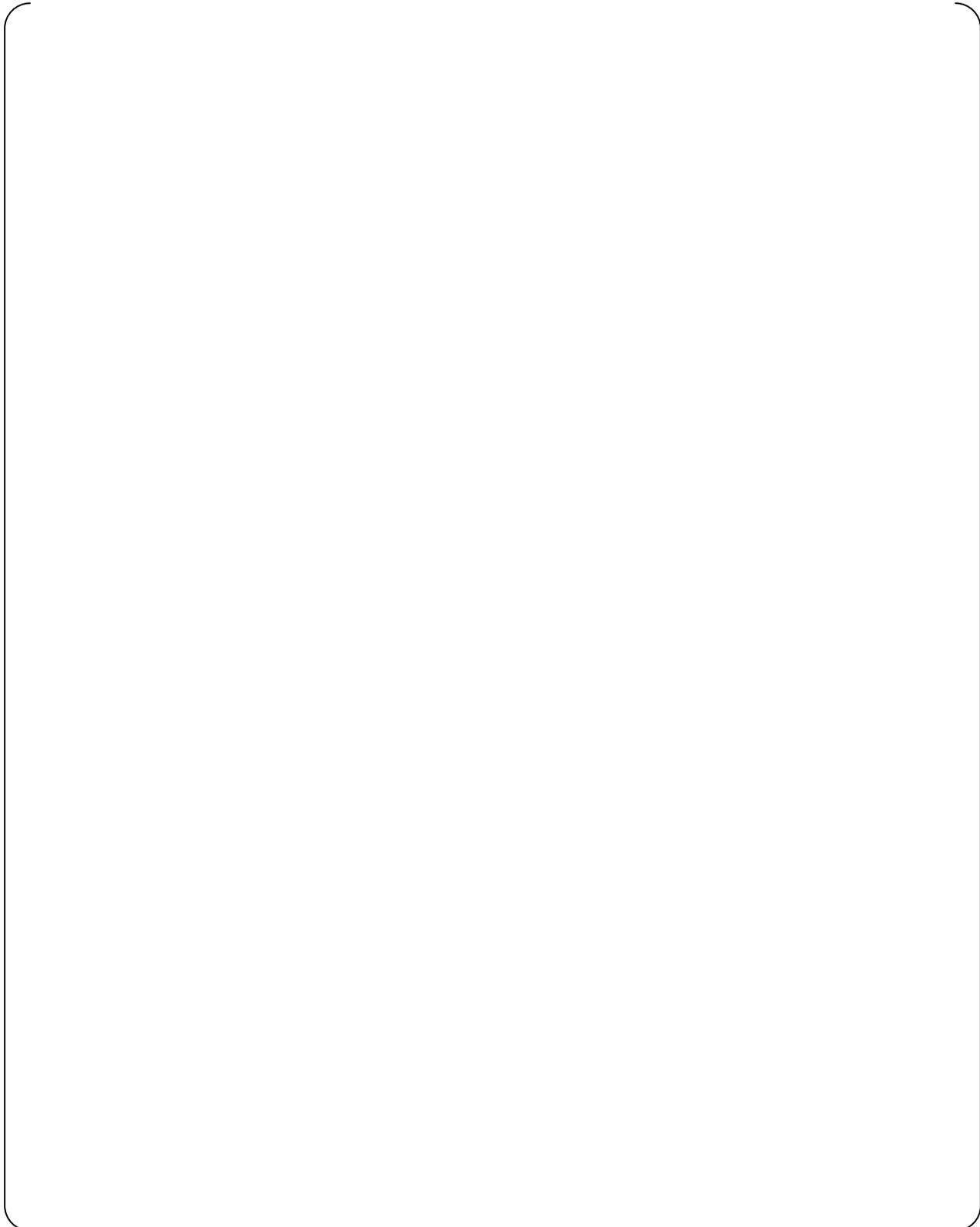


Figure 5.3-3 Calculation Flow Diagram of the Number of Rods in DNB Methodology



Figure 5.3-4 Relationship between CRDM Housing Break Size and Minimum DNBR in Long-Term Period Including the Reactor Trip Protection Functions

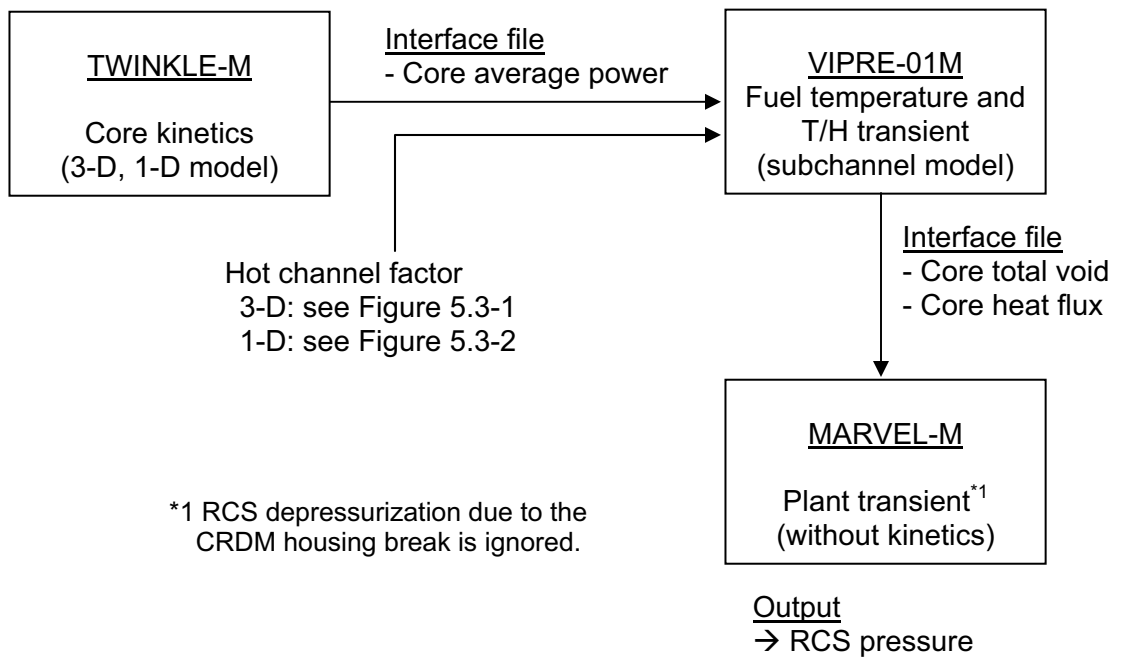


Figure 5.3-5 Calculation Flow Diagram of the RCS Pressure Methodology

5.4 Steam System Piping Failure

The Steam System Piping Failure is a transient that is characterized by asymmetric power generation in the core due to a non-uniform cooldown, which is caused by single steam system piping failure in combination with the assumption that the most reactive control rod be fully withdrawn. The steam line break flow calculation is unique to this event. The specific models for the core inlet mixing and consequent reactivity weighting are used in MARVEL-M analysis to conservatively predict core reactivity and nuclear power using point kinetics. In addition, the reactor coolant flow condition can be natural circulation. Certain Emergency Core Cooling System (ECCS) functions such as steam line isolation, EFWS actuation, feedwater isolation, and RCS boration using the safety injection system are included in the analysis. The VIPRE-01M code is used to calculate minimum DNBR and confirm that the DNB design basis is met in conjunction with other parameters calculated by the MARVEL-M code.

The steam system piping and valve arrangement for US-APWR is shown in Figure 5.4-1.

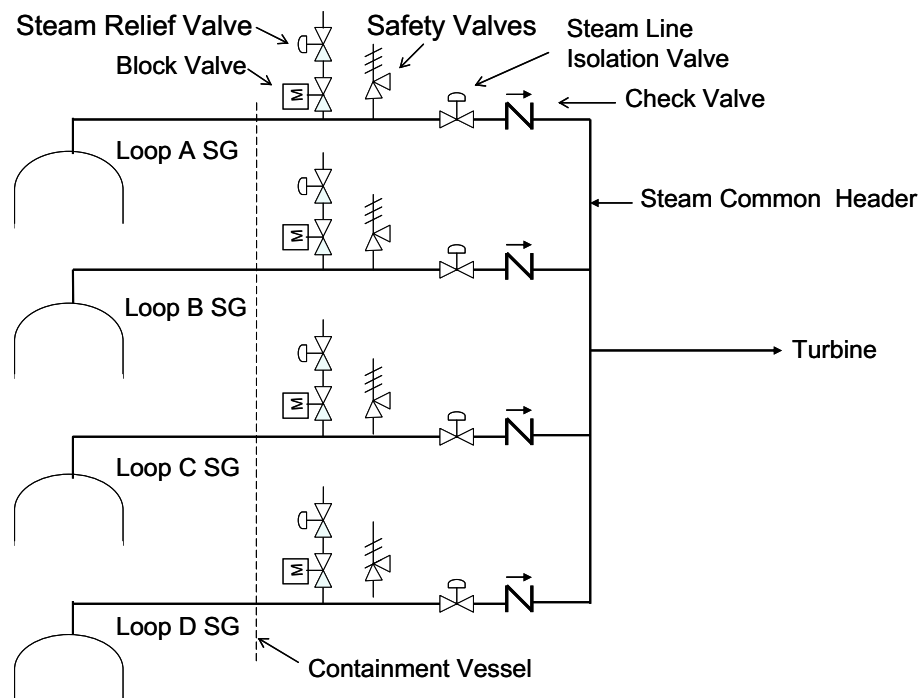


Figure 5.4-1 Steam System Configuration of US-APWR

A steam line break at a steam generator exit nozzle located at inside of the containment and a pipe break at the steam common header are postulated for Chapter 15 accident analysis.

Event Description

- 1) Steam piping failure inside containment
A double-ended steam pipe break at a SG exit nozzle is assumed. The break causes

uncontrolled steam release from the faulted SG into the containment until the SG is dried out. Assuming the check valve in the faulted SG steam line does not function as designed, the model accounts for steam release from the other SGs until the steam line isolation valve associated with the faulted SG is completely closed.

2) Steam piping failure outside containment

A double ended pipe break at the steam common header is assumed. The steam pipe break causes steam release from all the SGs until the steam line isolation valves are closed. One of the steam line isolation valves is assumed to fail to close and the steam release continues from that SG until the SG is dried out.

Although the above two steam system piping failure scenarios are different, the effects on the reactor coolant system are very similar.

The major steam pipe rupture results in an initial increase in steam flow, which decreases during the accident as the steam pressure falls. Although an integral flow restrictor is installed in the SG exit nozzle to mitigate the steam flow, a double-ended steam line break causes a large steam flow from the faulted SG to induce a rapid cooldown of the SG secondary side. The energy removal from the reactor coolant system causes a reduction in coolant temperature and pressure. The colder fluid in the loop with the faulted SG is mixed with the flow from the other intact loops. The core inlet temperature distribution and the cooldown of the core water are non-uniform due to the imperfect mixing of the loop flows in the reactor vessel inlet.

In the presence of a negative moderator temperature coefficient, the cooldown results in an insertion of positive reactivity. The effect is the largest at the end of core cycle. If the event occurs at nominal operating conditions, a core power increase results. If the event occurs at hot zero power condition and the most reactive RCCA is assumed stuck in its fully withdrawn position after reactor trip, there is an increased possibility that the core becomes critical and returns to power. A return to power following a steam line rupture is a potential problem mainly because of the existing high radial power peaking factors, assuming the most reactive RCCA to be stuck in its fully withdrawn position.

When the steam pressure in the failed steam generator falls below the Main Steam Line Pressure Low setpoint (in any loop), the ECCS is actuated. The ECCS signal also actuates functions such as EFWS, steam line isolation, and feedwater isolation to isolate the failed SG.

The core is ultimately shut down by a combination of the high concentration boric acid water delivered by the ECCS and the termination of the cooldown when the steam generator inventory is depleted.

The large double-ended steam pipe rupture is categorized as a PA and the acceptance criteria are described in Section 4.2. The MHI analysis conservatively uses a criterion of no DNB for the limiting steam line break, to preclude DNB propagation in the low pressure environment of the fuel.

The steam system piping failure inside the containment causes a containment pressure and temperature increase due to the steam release. The mass and energy release is calculated by the MARVEL-M code as a function of time for analysis of the containment integrity.

Reactor Protection

The following signals are assumed to be available to automatically trip the reactor and therefore provide protection from this transient.

- ECCS Actuation (low steam line pressure signal in any loop or low pressurizer pressure or high-1 containment pressure)
- Over power ΔT high trip
- Over temperature ΔT high trip
- Pressurizer pressure low trip
- Neutron flux high trip

Engineered Safeguards Features

The following features are assumed to be available to mitigate the accident.

- Steam line isolation
- EFWS isolation
- Safety injection
- Main feedwater isolation

Method of Analysis

(1) Analysis code

The MARVEL-M, ANC and VIPRE-01M codes are used for this steam system piping failure analysis. A calculation flow diagram is shown in Figure 5.4-2.

(a) System analysis by the MARVEL-M code

The MARVEL-M code is used to analyze the plant transient following steam piping ruptures. The break flow rate from the SGs is calculated using the Moody correlation. The released steam is conservatively assumed saturated and dry without moisture carry-over, since steam release without carry-over causes the maximum energy release and cooldown.

The overall primary-to-secondary heat transfer coefficient in the steam generators is modeled in the code by the four major thermal resistance components: the primary convection film resistance, the tube metal resistance, the fouling resistance, and the secondary side boiling heat transfer resistance, taking account of the dependency on the relevant operating conditions, such as temperature, pressure and flow. The model is applicable over the wide range of the operating conditions characteristic of the SG during a steam pipe break event.

The RCS model in the code can analyze the non-uniform reactor system transient response to the event. The steam system model in the code can simulate steam flow redistribution from SGs (described in Section 2.1.3.4). The flow mixing in the reactor vessel is modeled in the code. The mixing factors for the reactor vessel inlet and outlet plenums are defined conservatively by the input referring to the mixing test results by the 1/7 scale reactor vessel model (Section 2.1.3.2).

A weighting factor for reactivity feedback can be also input to take account of the azimuthal tilt of the core coolant properties.

The safeguards system and the ECCS sub-system necessary for such non-LOCA analysis are modeled in the code.

(b) DNBR calculation

In the hot zero power condition, the VIPRE-01M code calculates the minimum DNBR. These DNBR calculations are steady-state calculations at pre-selected conditions, using the MARVEL-M calculated values of core average heat flux, RCS pressure, core inlet coolant temperatures, core inlet flow rate and boron concentration, for a certain number of state points around the time the highest core average heat flux is reached. Additionally, the core inlet coolant enthalpy distribution coupled with core power distribution, which is calculated by the ANC code considering a steady-state condition assuming a stuck rod, is also input to the VIPRE-01M code. The history files used in the more standard MARVEL-M / VIPRE-01M sequences are not used for the steam piping failure. A suitable bundle DNB correlation is used at the low RCS pressure conditions characteristic of this accident.

A VIPRE-01M subchannel analysis is performed using a one-eighth core model with a hot assembly assumed at the center of the core as shown in Figure 5.2-1 as well as the other DNB concerned transients. However the fuel rods and flow channels are divided into 5 groups shown in Figure 5.4-3 to express the power distribution and inlet enthalpy distribution. Each group is associated with the hot channel, the neighbor channels to hot channel, the remains in the hot assembly, the neighbor assemblies to hot assembly and the remains in the core, respectively. Radial power distributions calculated by the ANC code and inlet enthalpy distribution are averaged for each group. Axial power distributions are represented by a 3 shapes, which are associated with the hot assembly (group 1 through 3), neighbors to the hot assembly (group 4) and the remains (group 5). This symmetric model is validated by the comparison with the asymmetric full core model as described in Appendix D. This comparison demonstrates that the symmetric model can provide minimum DNBR with sufficient accuracy during the steam piping failure transient.

For the hot full power condition, the MARVEL-M code calculates the minimum DNBR using its internal DNBR data tables, with core average heat flux, RCS pressure, and core inlet temperature in the same manner as is used for the RCCA Bank Withdrawal at Power described in Section 5.1. The internal DNBR table used is evaluated by using RTDP and applicable rod bundle DNB correlation. This methodology is acceptable, since the core operating condition is within the range of the pre-evaluated DNBR table in MARVEL-M, because the minimum DNBR occurs within a short time after the reactor trip is initiated. The one rod stuck assumption is considered in defining the shutdown reactivity, but is not meaningful for the period up to reaching the minimum DNBR in the at-power transients of this kind.

(c) Mass and Energy Release Analysis

The MARVEL-M code is used to generate the mass and energy release data as a function of time for the case of Steam Piping Failure inside containment, taking into consideration the following models:

- i) The RCS thick metal effect in the MARVEL-M code is used.
- ii) When the SG steam pressure decreases below the saturation pressure of the hot feedwater remaining in the feedwater system piping of the faulted SG, it could flash into the shell side of the SG through the feedwater nozzle. This results in an increased mass and energy release to the containment. The effect is calculated by modeling a single mass volume attached to the SG secondary side in the MARVEL-M code for this purpose.

The containment response due to the release of the mass and energy is not addressed in this topical report.

(2) Analysis Assumptions

Analysis assumptions and calculation conditions used in MARVEL-M for the analysis of the core response to the double-ended break from the hot zero power condition are as follows:

- (a) Break Size: Double-ended rupture
- (b) Moderator Density Coefficient: Maximum positive considering a stuck rod effect
- (c) Doppler Power Coefficient: Minimum considering a stuck rod effect
- (d) Shutdown Margin: Minimum considering the most reactive rod stuck out of the core
- (e) Core inlet mixing modeled to reflect non-uniform effects based on the 1/7 scale reactor vessel model. Sensitivity study of inlet mixing coefficient is shown in Appendix E. The minimum DNBR is not extremely sensitive to small changes of the mixing coefficient near the expected value.
- (f) Single Failure: Safety Injection train
- (g) Reactivity weighting factor for fluid properties is considered
- (h) Steam Quality: Dry steam (100%)

Analysis assumptions and calculation conditions used in VIPRE-01M for the analysis of the core response to the double-ended break from the hot zero power condition are as follows:

- (i) Power Distribution: Calculated by detailed core analysis considering a stuck rod in the cold core sector

Comparison of the results from the detailed core analysis with the MARVEL-M predictions verifies the overall conservatism of the methodology. That is, the specific power, temperature, and flow conditions used to perform the DNB analysis are conservative.

Analysis assumptions and calculation conditions used in MARVEL-M for the analysis of the core response to a spectrum of break sizes from the hot full power condition are as follows:

- (a) Moderator Density Coefficient: At EOC not considering a stuck rod
- (b) Doppler Power Coefficient: Least negative
- (c) Minimum Trip Reactivity: Same as RCCA bank withdrawal at power
- (d) Power Distribution: DNBR data input to MARVEL-M
- (e) Core Inlet Mixing: Same as HZP scenario
- (f) Single Failure: RPS train (response unaffected)
- (g) Steam Quality: Dry steam (100%)

Analysis assumptions and calculation conditions used in MARVEL-M for the analysis of the mass and energy release evaluation are the same as the assumptions above except thick metal effects and feedwater line water flashing due to SG depressurization are modeled.

- (a) Moderator Density Coefficient: At EOC not considering a stuck rod
- (b) Doppler Power Coefficient: Least negative
- (c) Minimum Trip Reactivity: Same as RCCA bank withdrawal at power
- (d) Power Distribution: Not applicable
- (e) Core Inlet Mixing: Same as HZP scenario
- (f) Single Failure: Safety Injection train
- (g) Reactivity Weighting Factor: Same as HZP
- (h) Steam Quality: Dry steam (100%)

(3) Calculation Case

Safety analysis is performed for the following cases in the spectrum of steam system piping failures.

Hot full power initial condition at end of cycle

Hot zero power initial condition at end of cycle (with and without offsite power)

DNBR, M&E

Post-scram: double ended rupture, EOC hot zero power

Pre-scram: Spectrum of break sizes and power levels, EOC

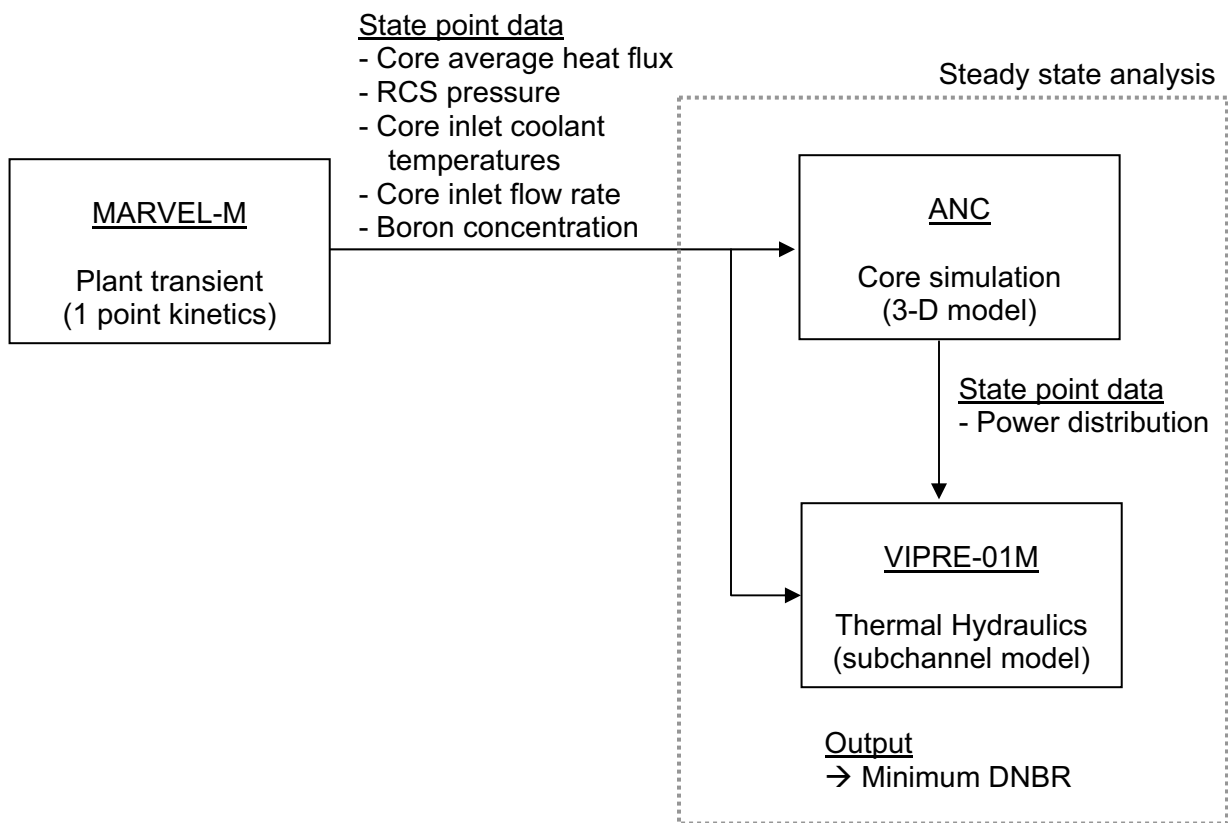


Figure 5.4-2 Calculation Flow Diagram of the Steam System Piping Failure Methodology for the Hot Zero Power Condition

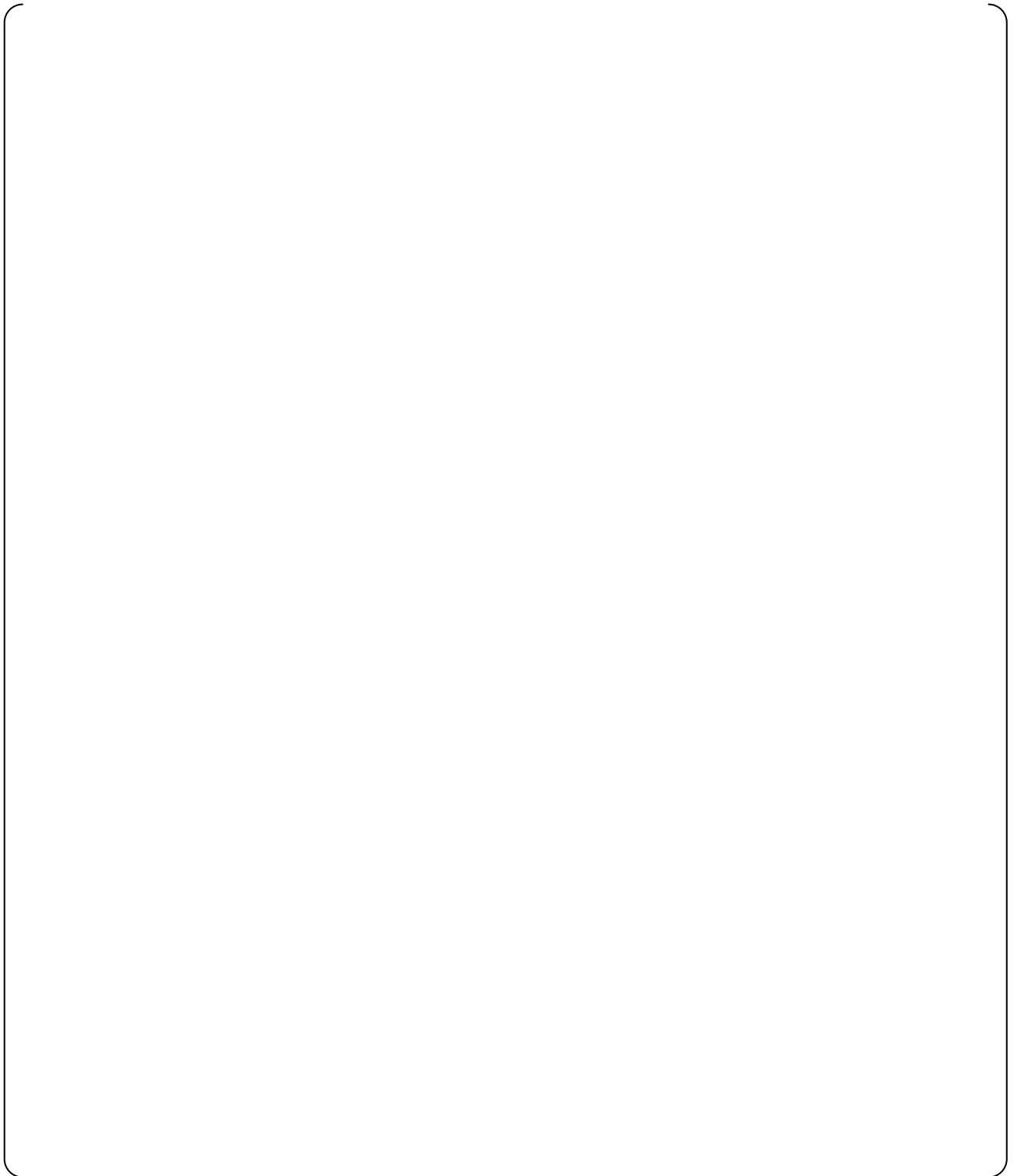


Figure 5.4-3 VIPRE-01M 1/8 Core Analysis Modeling with 5-grouped Power Distributions (17x17-257FA Core, 4-Loop Plant)

5.5 Feedwater System Pipe Break

The Feedwater System Pipe Break is another non-uniform accident that involves modeling break flow from one of the secondary loops. The feedwater system pipe break causes loss of inventory from the saturated liquid water mass in the steam generator and unlike the steamline break cooldown, results in RCS heatup and pressurization. This event also uses the 4-loop capability of the MARVEL-M code to model the failure of EFWS to feed one of the intact steam generators.

Event Description

A major feedwater line rupture is a break in a feedwater line large enough to prevent the addition of sufficient feedwater to the steam generators in order to maintain shell-side fluid inventory in the steam generators. If the break is postulated in a feedwater line between the check valve and the steam generator, fluid from the steam generator may also be discharged through the break.

The feedwater line rupture reduces the ability to remove heat generated by the core from the reactor coolant system for the following reasons:

- Feedwater flow to the steam generators is reduced. Because feedwater is subcooled, its loss may cause reactor coolant temperatures to increase prior to reactor trip.
- Fluid in the steam generator may be discharged through the break and would not be available for decay heat removal after trip.
- The break may be large enough to prevent the addition of main feedwater after trip.

For breaks that are small enough to not be considered a major feedwater line rupture, the plant continues to operate without the need for reactor protection system or engineered safeguards feature actuation. For breaks resulting in continued feedwater addition but at a rate insufficient to maintain steam generator level, the loss of normal feedwater response will bound these breaks. In the limiting case, the double-ended rupture inside the main feedwater check valve will bound the remaining larger breaks.

The double-ended feedwater system pipe break accident is categorized as a PA and the acceptance criteria are described in Section 4.3.

If the postulated double-ended feedwater system pipe break occurs, the RCS heats up and the pressurizer water level and pressure increase. Unless the heatup of the RCS is mitigated, there will be possibility of water relief through the pressurizer safety valve.

The protective actions to mitigate the accident are isolation of the failed SG by closing the feedwater isolation valve and terminating the emergency feedwater supply to the faulted SG, and cooling of the RCS by supplying emergency feedwater to the intact SGs. The emergency feedwater system (EFWS) has two motor-driven and two turbine-driven emergency feedwater pumps. The associated valve arrangement is shown in Figure 5.5-1.

Each emergency feedwater pump supplies emergency feedwater independently to each SG taking water from the emergency feedwater pits. The EFWS is sized to have the capability of supplying sufficient emergency feedwater to preclude the pressurizer filling with water during a

postulated feedwater system pipe break, assuming a single failure in one of the sub-systems of the EFWS. The protective actions are automated for the US-APWR.

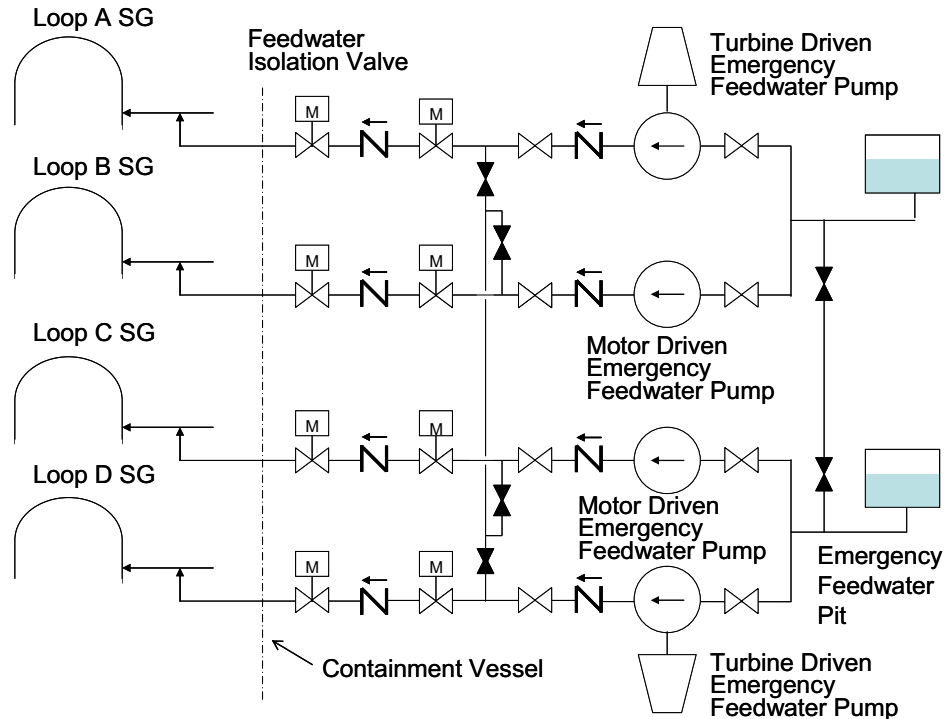


Figure 5.5-1 Emergency Feedwater System of US-APWR

Reactor Protection

The following signals are assumed to be available to automatically trip the reactor and therefore provide protection from this transient.

- Steam generator water level low trip in any loop
- Pressurizer pressure high trip
- Pressurizer water level high trip

Engineered Safeguards Features

The following features are assumed to be available to mitigate the accident.

- EFWS
- EFWS isolation
- Safety Injection

Method of Analysis

(1) Analysis code

The MARVEL-M code is used to determine the plant transient following a feedwater line rupture. The code describes the reactor thermal kinetics, reactor coolant system (including natural

circulation), pressurizer, steam generators, and feedwater system responses. MARVEL-M also computes related variables, including the pressurizer pressure, pressurizer water level, and reactor coolant average temperature.

The feedwater system pipe break causes non-balanced operation, e.g. a faulted SG loop, intact loops with emergency feedwater supply and an intact loop without emergency feedwater supply. The capability to model up to 4 separate loops in the MARVEL-M code is used for the analysis.

The break flow at the feedwater system pipe break is conservatively calculated by the Moody correlation, taking account of the flow restriction at the feedwater inlet nozzle.

In reality, the feedline water discharge could entrain steam when the water level in the faulted SG decreases significantly. In this case, the energy removed from the RCS from the steam release could mitigate the heatup of the RCS. This effect is conservatively neglected in the analysis to present the worst-case RCS heatup results for the feedwater system pipe break event.

(2) Analysis Assumptions

Analysis assumptions and calculation conditions are as follows.

- | | |
|-----------------------------------|---|
| (a) Break Size and Location: | Double-ended rupture downstream of the feedwater line check valve |
| (b) Initial SG Mass: | Loss of normal feedwater is assumed at 0 second until the reactor trip |
| (c) Reactor trip: | SG water level low trip |
| (d) Break Flow and Timing: | Feedwater pipe break is assumed to occur just after trip |
| (e) Break Quality: | 0% (saturated liquid) |
| (f) Limiting Single Failure: | EFWS train failure is assumed (One SG is ruptured and associated EFWS is not effective. Another SG is intact and without EFWS, due to the single failure. The remaining SGs are intact and are supplied with EFWS.) |
| (g) EFWS Isolation to Faulted SG: | Automatic isolation of EFWS to faulted SG by secondary low pressure signal |

Analyses for peak RCS pressure are performed for this accident. The analysis assumptions such as initial conditions and core parameters are selected for this analysis to maximize peak RCS pressure.

Due to the steam line check valve feature, the faulted SG pressure will decrease rapidly after the reactor trip is initiated. The pressure in the intact SGs pressure will go up to relief or safety valve setpoints.

(3) Calculation Case

One case is analyzed, the double-ended rupture of the main feedwater pipe at the beginning of cycle (BOC) from hot full power conditions with maximum decay heat assuming loss of offsite power at time of turbine trip.

5.6 Steam Generator Tube Rupture

The Steam Generator Tube Rupture event uses the MARVEL-M capability to calculate primary-to-secondary flow based on the primary and secondary pressures calculated by the code. The SGTR event involves the loss of the reactor coolant due to the leakage to the ruptured SG secondary side, which causes a decrease in the pressurizer water level, eventually emptying the pressurizer. The decrease in the pressurizer pressure may actuate the ECCS. Operator actions to establish steam generator cooling using the intact steam generators, manual opening of the steam generator relief valves, and manual opening of the pressurizer depressurization valve are also modeled by MARVEL-M for this accident.

Event Description

The accident examined is the complete severance of a single steam generator tube. The accident is assumed to take place at power. The SG tube rupture causes the reactor coolant to leak to the SG secondary side through the double-ended breaks from the inlet side and the outlet side. The largest break flow occurs when the rupture location is near the tube sheet in the colder side. The steam output of the ruptured SG may be contaminated with the radioactivity of the leaked primary coolant water. The SG tube break can be detected by N-16 radiation detectors installed on the main steam line that alarms the occurrence of the SG tube rupture. The SG leak causes a reduction in the pressurizer pressure that may trip the reactor by either a Pressurizer Pressure Low signal or a Steam Generator Water Level High-High signal from the ruptured SG. The leak rate is comparatively small for a large 4-loop PWR plant such as the US-APWR. The operator may manually trip the reactor, if the automatic actuation of a reactor trip is delayed. If the pressurizer pressure decreases below the Pressurizer Pressure Low-Low setpoint, the ECCS is actuated. The ECCS signal trips the RCS pumps which then coast down to natural circulation flow. The actuation of the high pressure safety injection sub-system of the ECCS tends to prolong the SG tube leakage, causing a continued increase in the water level and the increase in the steam pressure that may lift the steam relief valve of the ruptured SG.

The operators have to take the following recovery actions:

a) Isolate the ruptured SG

Operators identify the ruptured SG and isolate the ruptured SG by closing the steam line isolation valve, main feedwater isolation valve and other valves.

b) Terminate the leak flow

Operators reduce the RCS temperature of the intact loop using the steam relief valves of the intact SGs or turbine bypass system, depressurize the RCS using a pressurizer depressurization valve until primary-to-secondary pressure balance is attained, and terminate the ECCS flow. These actions in turn terminate the leak flow.

For the radiological analysis, the reactor coolant system water is assumed to contain some radioactive fission products corresponding to continuous operation with a limited number of defective fuel rods at the maximum allowance of the Technical Specifications. The accident leads to an increase in contamination of the secondary system due to leakage of radioactive coolant from the reactor coolant system. In the event of a coincident loss of offsite power, or a failure of the condenser steam dump system, discharge of radioactivity to the atmosphere takes place via the steam generator relief valves or the safety valves. This provides a pathway for the release of radioactivity to the environment.

The acceptance criteria set by MHI for this accident are to preclude additional fuel failures and to not allow the ruptured SG to fill with water. Filling the SG could result in radioactive water relief through the secondary relief valve, further increasing the radioactivity released to the environment. Additionally, the site boundary dose must meet the 10 CFR 100 requirements.

Reactor Protection

The following signals are assumed to be available to automatically trip the reactor and therefore provide protection from this transient.

- Pressurizer pressure low trip
- Over temperature ΔT high trip
- Steam generator water level high-high trip
- ECCS Actuation

Engineered Safeguards Features

The following features are assumed to be available to mitigate the accident.

- EFWS
- EFWS isolation
- Safety Injection

Method of Analysis

(1) Analysis code

The MARVEL-M code is used to calculate the reactor plant transient following a steam generator tube rupture until the primary-to-secondary break flow is terminated. The specific models for the analysis are discussed below:

(a) The SG tube break flow calculation

The initial break flow is conservatively determined assuming critical flow calculated using the primary pressure at the location of the break, accounting for the pressure drop between the tube inlet or outlet and the break location. The initial break flow is calculated for a break just above the tube sheet on the cold leg side to maximize the flow rate and input into MARVEL-M. From that point on, the break flow is calculated by MARVEL-M as a function of the square root of the primary-to-secondary differential pressure, scaled to match the initial flow. The break location in MARVEL-M is just above the tube sheet on the hot leg side to maximize the energy of the break flow. A comparison has been made between the conservative model described above and a more detailed model that checks for critical flow conditions and uses either critical or non-critical flow depending on primary pressure and secondary pressure at the break location. This comparison is provided in Appendix F.

(b) Reactor coolant system response after the pressurizer is emptied

When the RCS pressure decreases significantly, the reactor coolant in the reactor vessel upper head dead volume may flash and form a steam phase at the top, separated from the liquid. It may act as an alternate pressurizer to define the reactor coolant system pressure after the pressurizer is emptied. If ECCS is actuated, the system also functions to maintain the RCS pressure and the ECCS flow and RCS leak flow are balanced. The transient model of the upper head dead volume is discussed in Section 2.1.3.1.

(2) Analysis Assumptions

Analysis assumptions and calculation conditions are as follows.

- (a) Double-ended rupture
Conservative leak flow model used
- (b) Limiting single failure is assumed
EFWS train failure is typically assumed in the fluid discharge for the dose evaluation.
- (c) Conservative assumptions
A secondary relief valve is assumed to stick open after the valve is automatically opened for conservative analysis of radioactivity released for this accident. The steam release through the valve is terminated by the automatic closure of the block valve.
Conservatism in the analysis includes also primary-to-secondary leak rate model, time margins for operator actions, conservative addition of main feedwater and EFWS feedwater to the ruptured SG, and loss of off-site power at the time of reactor trip.
- (d) Operator action and the time margin
Operator actions assumed to be taken to mitigate the accident and to recover the reactor safety conditions until the SG leak is terminated are as follows:
 - (i) Detection of the accident
SGTR causes various relevant indications, including the reduction in pressurizer water level, reduction in pressurizer pressure and the increase in water level in the ruptured SG. The event can be also detected from the SG blowdown radiation monitors, the steam condenser ejector radiation monitors, as well as the main steam line N-16 high-sensitivity radiation monitors installed on each steam line (the high radiation level alarms occur within 2 minutes from the SGTR initiation).
 - (ii) Identification of the ruptured SG and reactor trip
Operators can identify the ruptured SG from the N-16 radiation monitors and from the increase in the affected SG water level.
A time margin of 10 minutes is assumed for operators to identify the ruptured SG after the audible alarms indicate the event has occurred. Operators are assumed to trip the reactor manually 15 minutes after SGTR initiation.
 - (iii) Isolation of the ruptured SG
The ruptured SG is isolated by closing the main steam line isolation valve and other isolation valves. The actions to isolate the affected SG are assumed to be completed within 5 minutes after the reactor trip.
 - (iv) Reduce the RCS temperature
Operators are assumed to start to reduce the RCS temperature by opening the secondary relief valves of the intact SGs 5 minutes after the isolation of the ruptured SG.
 - (v) Depressurize the RCS and terminate the ECCS
After the RCS hot leg temperatures of the intact loops are reduced sufficiently to assure the subcooling even when the RCS pressure is reduced to the ruptured SG steam pressure, operators reduce the RCS pressure by opening a pressurizer depressurization valve until the primary-to-secondary pressure balance is attained. The ECCS is then terminated manually according to the SI termination criteria specified in the Emergency Operating Instructions.

(3) Calculation Case

Two cases are analyzed, one to determine the maximum integrated atmospheric steam relief and the second to confirm that none of the steam generators overflow.

6.0 SAMPLE TRANSIENT ANALYSIS

As explained in Section 5, six specific events were selected for inclusion in this Topical Report so as to demonstrate the application of each of the key computer codes (or groups of codes), as well as to include certain accidents where special methods or code capabilities are used. The methodology associated with the analysis of each of these six events is described in detail in Section 5. Section 6 provides sample transient analysis results for each of these six events. The results consist of a brief summary description of the event, a sequence of events table with explanation, and figures showing the time-dependent response of key parameters. The DCD analysis for these six events will consist of a combination of event description, descriptions of applicable computer code and models, accident classification, acceptance criteria, event-specific assumptions (initial conditions, time of cycle, core parameters, etc.), results, and conclusions included in Sections 2, 4, 5, and 6 of this report. For certain events, the results presented in Section 6 are of a representative or limiting case for the purpose of illustrating the format, content, and level of detail that are presented in the DCD.

Section 6.1 provides sample results for the Uncontrolled Rod Cluster Control Assembly (RCCA) Bank Withdrawal at Power. This analysis is performed using only the MARVEL-M code and demonstrates that the DNBR acceptance criterion is met. Section 6.2 provides sample results for the Complete Loss of Forced Reactor Coolant Flow. This analysis uses the MARVEL-M code (and associated internal reactor coolant pump model) to calculate the NSSS response, and uses the VIPRE-01M code for the fuel rod and DNBR calculations. Section 6.3 provides sample results for the Spectrum of RCCA Ejection Accidents. This rapid core reactivity transient uses the multidimensional TWINKLE-M transient code to calculate the core power distribution and the VIPRE-01M code for the fuel rod response used to evaluate fuel damage due to Pellet Clad Mechanical Interaction (PCMI) or other failure mechanisms. Results from the 3-D HZP case and the 1-D HFP case are presented. Section 6.4 provides sample results for the limiting Steam System Piping Failure (Main Steamline Break). The MARVEL-M code utilizes steamline break flow models and accident-specific inlet mixing and reactivity weighting factors to calculate a conservative NSSS response, and the VIPRE-01 code is used to evaluate the DNBR for an accident-specific power distribution assuming the most reactive rod stuck out of the core. Section 6.5 provides sample results for the limiting Feedwater System Pipe Failure (Main Feedline Break). The MARVEL-M code (and its associated secondary break model and steam generator heat transfer model) is used to calculate the NSSS response. Section 6.6 provides sample results for the Steam Generator Tube Rupture event. The MARVEL-M code is used to model the primary-to-secondary flow and manual actions to terminate the accident, as well as calculate parameters used in the radiological response analysis (not included in this Topical Report).

6.1 Uncontrolled RCCA Bank Withdrawal at Power

Event Description

This event is an uncontrolled control rod bank withdrawal at power initiated by either a failure of the rod control system or an operator error. The positive reactivity insertion results in a power transient, which increases the core heat flux creating a potential challenge to the DNB limits.

Events Analyzed

A range of cases utilizing different reactivity insertion rates at both BOC and EOC will be evaluated and presented in the DCD. The sample results presented in this section include a plot of minimum DNBR as a function of reactivity insertion rate initiated from Hot Full Power (HFP) assuming minimum reactivity feedback (BOC). In addition, plots of key parameters versus time are provided for the most limiting HFP DNBR cases at BOC conditions, which per Figure 6.1-1 occur at withdrawal rates of 2.5 pcm/sec and 75 pcm/sec.

Minimum DNBR is calculated by using the Revised Thermal Design Procedure (RTDP) and the WRB-2 DNB correlation [Reference 16].

The analysis uses conservative assumptions for moderator density coefficient, Doppler power coefficient, and trip simulation (trip setpoint, trip reactivity curve, rod drop time, RPS signal processing delays) as described in Section 5.1.

Analysis Results

The overall response of the primary and secondary systems and DNBR are evaluated by the MARVEL-M code. DNBRs are calculated internal to MARVEL-M using DNBR input data separately calculated by VIPRE-01M and an algorithm that adjusts DNBR for changes in RCS parameters. Although the MARVEL-M DNBR model has the capability to model flow variations, constant RCS flow is assumed for this event. The focus of this reactivity insertion event is the challenge to the DNB design limit resulting from the power increase.

Figure 6.1-1 shows the minimum DNBR versus reactivity insertion rate (pcm/sec) for bank withdrawals initiating from HFP conditions assuming minimum feedback core physics parameters and the availability of pressure control systems (pressurizer spray). Reactor trips credited for the accident from HFP conditions include the over temperature ΔT high and power range neutron flux high trips. For slower reactivity addition rates from HFP conditions, protection is provided by the over temperature ΔT high trip. For higher insertion rates, the power range neutron flux high trip provides protection. The minimum DNBR for the HFP cases represented by Figure 6.1-1 occurs at 2.5 pcm/sec reactivity insertion rate protected by the over temperature ΔT high trip. Transient parameter plots are provided as the sample results for the uncontrolled bank withdrawal at power parameters for 75 pcm/sec reactivity insertion rate scenario in Figures 6.1-2 through 6.1-7. The same parameters are provided for the 2.5 pcm/sec insertion rate scenario in Figures 6.1-8 through 6.1-13. The sequence of events for these specific cases (HFP, minimum feedback, pressure control available) are provided in Table 6.1-1 (75 pcm/sec) and Table 6.1-2 (2.5 pcm/sec).

For the limiting 2.5 pcm/sec reactivity insertion rate, the initiation of the bank withdrawal occurs at time = 0 seconds. Power and ΔT increase until the over temperature ΔT high trip is initiated

at time = 51.9 seconds, and the minimum DNBR occurs immediately following the trip. The minimum DNBR is greater than the 95/95 DNBR Design Limit for transients using the RTDP, the peak RCS pressure remains below 2750 psia (110% of RCS design pressure), and the steam pressure remains below 1320 psia (110% of the main steam system design pressure).

**Table 6.1-1 Sequence of Events
for the Uncontrolled RCCA Bank Withdrawal at Power (75 pcm/sec)**

Event	Time (sec)
RCCA Bank Withdrawal Begins	0.0
Neutron Flux High Analysis Limit Reached	1.4
Reactor Trip Initiated (Rod Motion Begins)	2.3
Minimum DNBR Occurs	3.4
Peak Hot Spot Heat Flux Occurs	3.5

**Table 6.1-2 Sequence of Events
for the Uncontrolled RCCA Bank Withdrawal at Power (2.5 pcm/sec)**

Event	Time (sec)
RCCA Bank Withdrawal Begins	0.0
Over Temperature ΔT High Analysis Limit Reached	45.1
Reactor Trip Initiated (Rod Motion Begins)	51.9
Peak Hot Spot Heat Flux Occurs	52.2
Minimum DNBR Occurs	52.2

Conclusions

The analysis of this event demonstrates that the resulting power increase does not result in a DNB-related fuel failure. The separate RCS pressure transient is not included in this topical report, but will be described in the DCD. The DNB acceptance criteria for this AOO event as described in Section 4.5 are met.

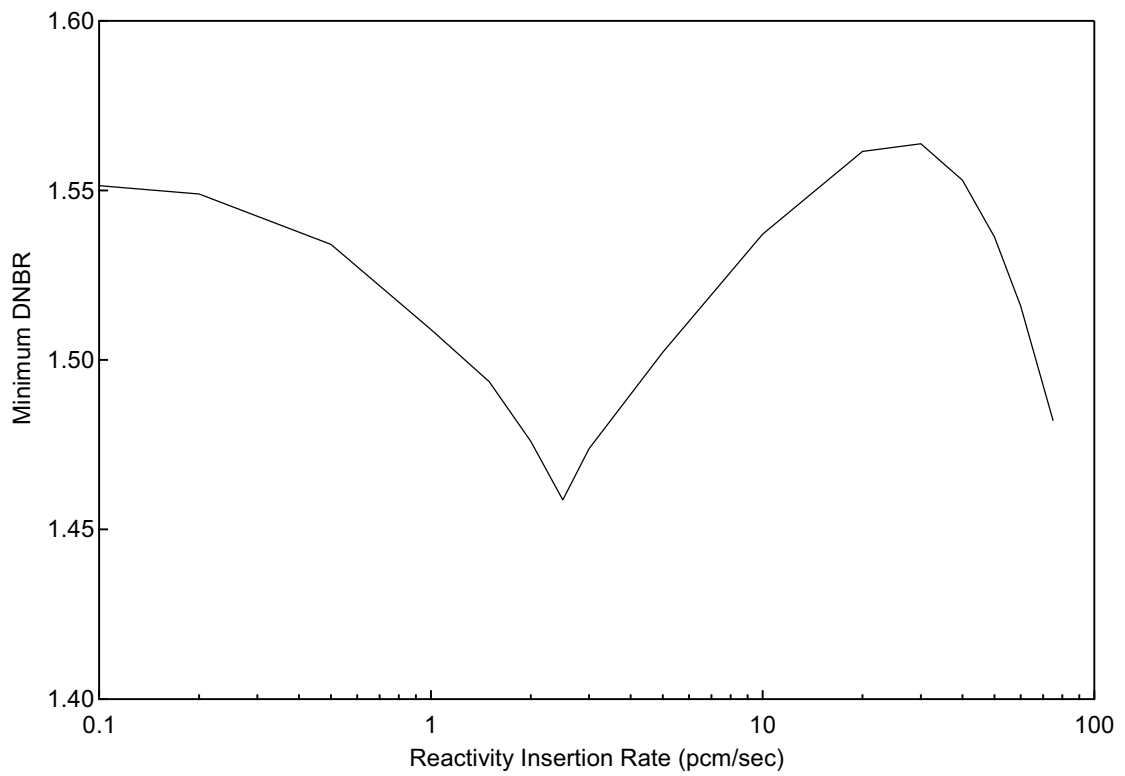


Figure 6.1-1 Minimum DNBR versus Reactivity Insertion Rate (HFP, BOC)

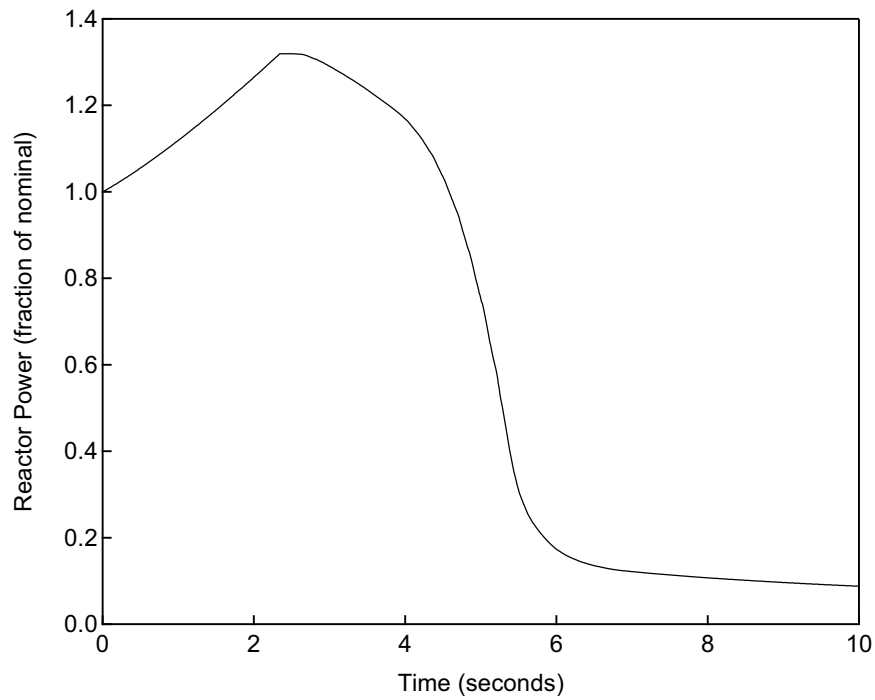


Figure 6.1-2 Reactor Power versus Time
Uncontrolled RCCA Bank Withdrawal at Power (HFP, BOC, 75 pcm/sec)

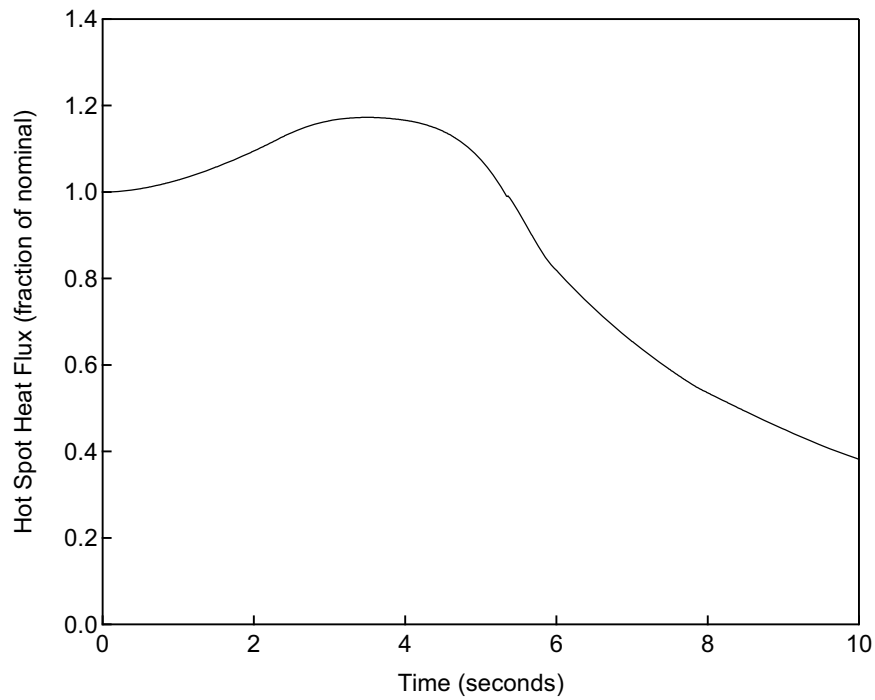
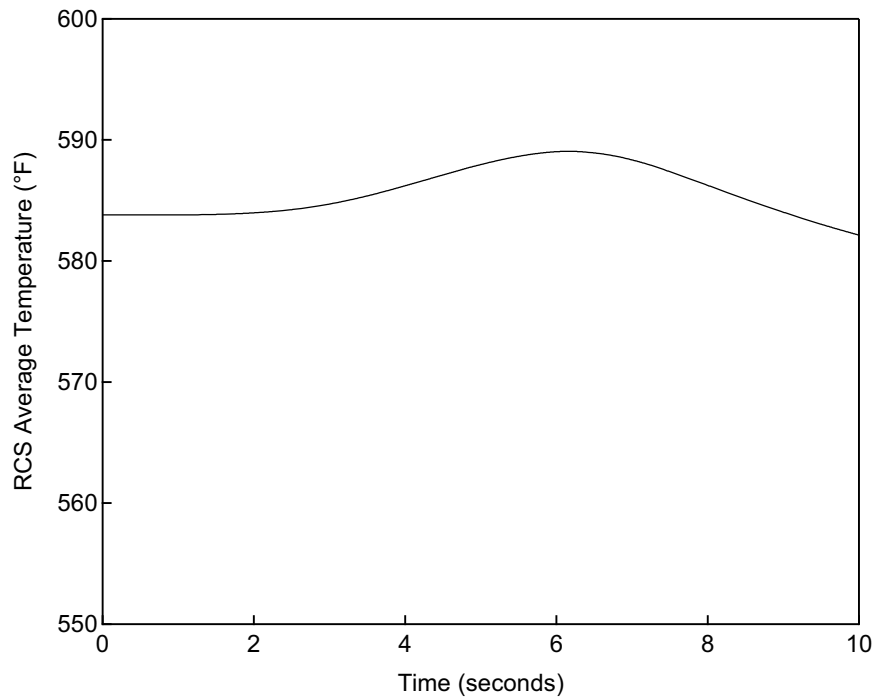
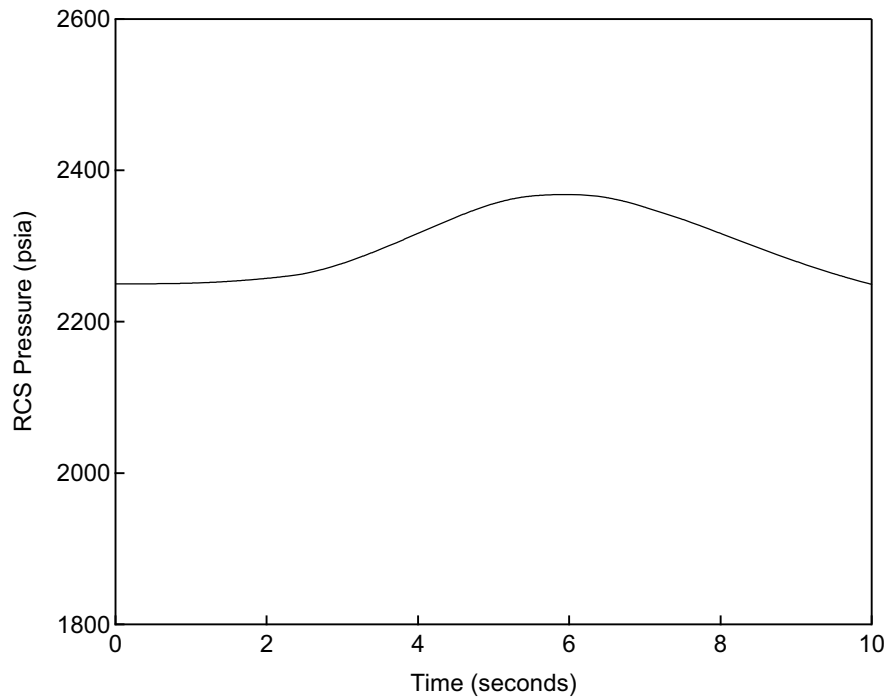


Figure 6.1-3 Hot Spot Heat Flux versus Time
Uncontrolled RCCA Bank Withdrawal at Power (HFP, BOC, 75 pcm/sec)



**Figure 6.1-4 RCS Average Temperature versus Time
Uncontrolled RCCA Bank Withdrawal at Power (HFP, BOC, 75 pcm/sec)**



**Figure 6.1-5 RCS Pressure versus Time
Uncontrolled RCCA Bank Withdrawal at Power (HFP, BOC, 75 pcm/sec)**

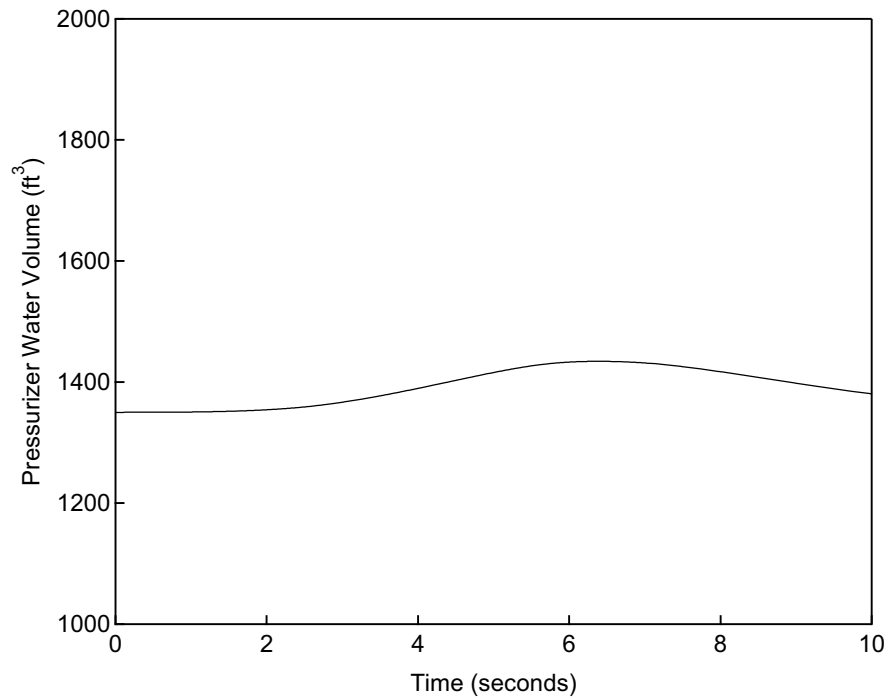


**Figure 6.1-6 Pressurizer Water Volume versus Time
Uncontrolled RCCA Bank Withdrawal at Power (HFP, BOC, 75 pcm/sec)**

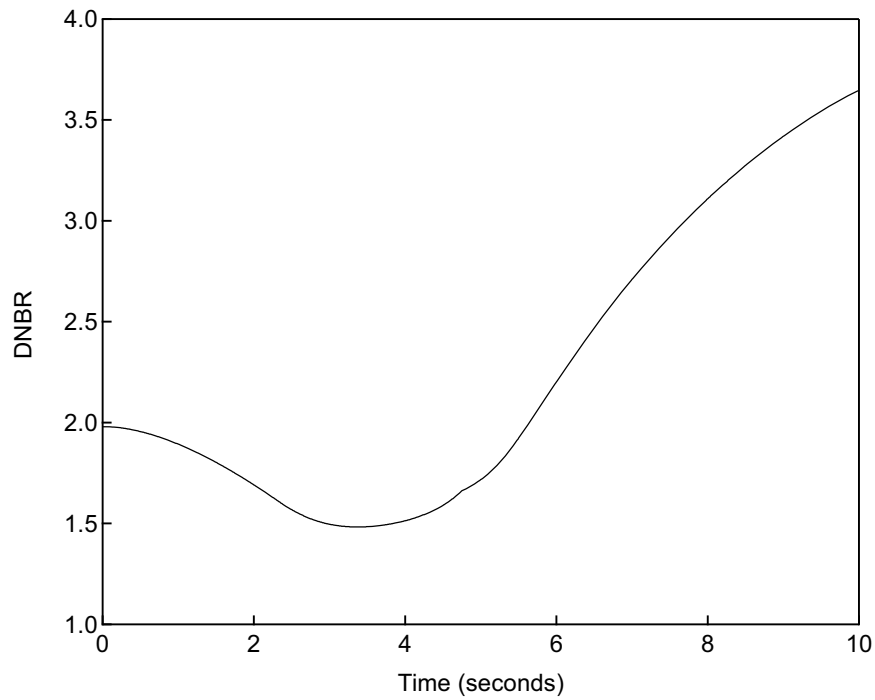


**Figure 6.1-7 DNBR versus Time
Uncontrolled RCCA Bank Withdrawal at Power (HFP, BOC, 75 pcm/sec)**

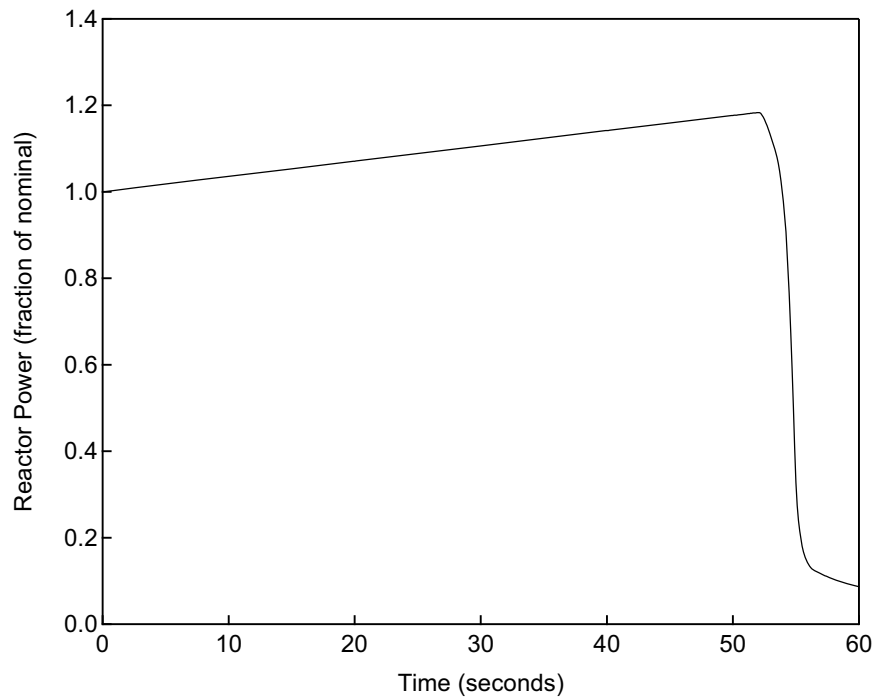


Figure 6.1-8 Reactor Power versus Time
Uncontrolled RCCA Bank Withdrawal at Power (HFP, BOC, 2.5 pcm/sec)

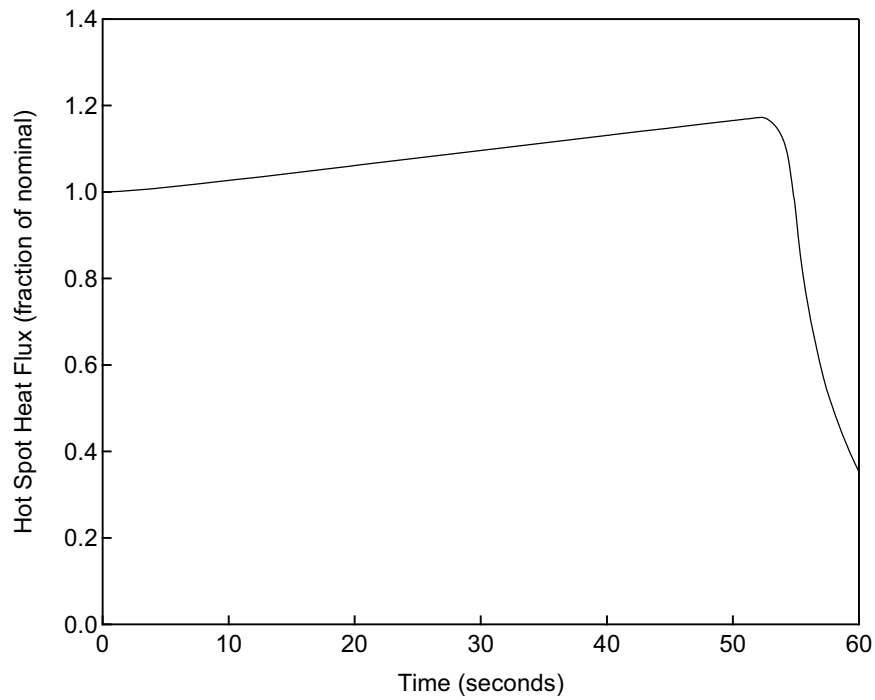
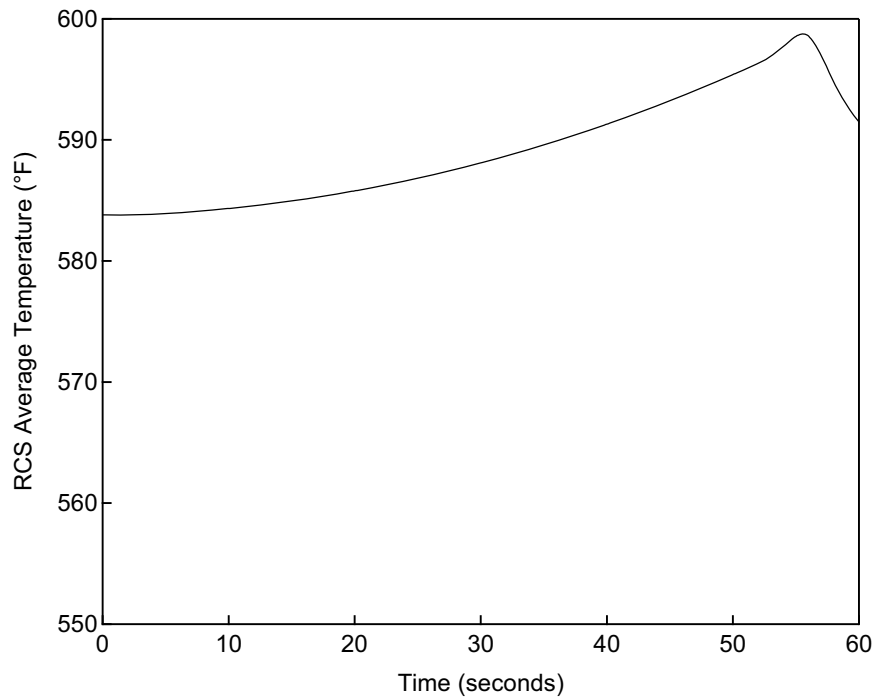
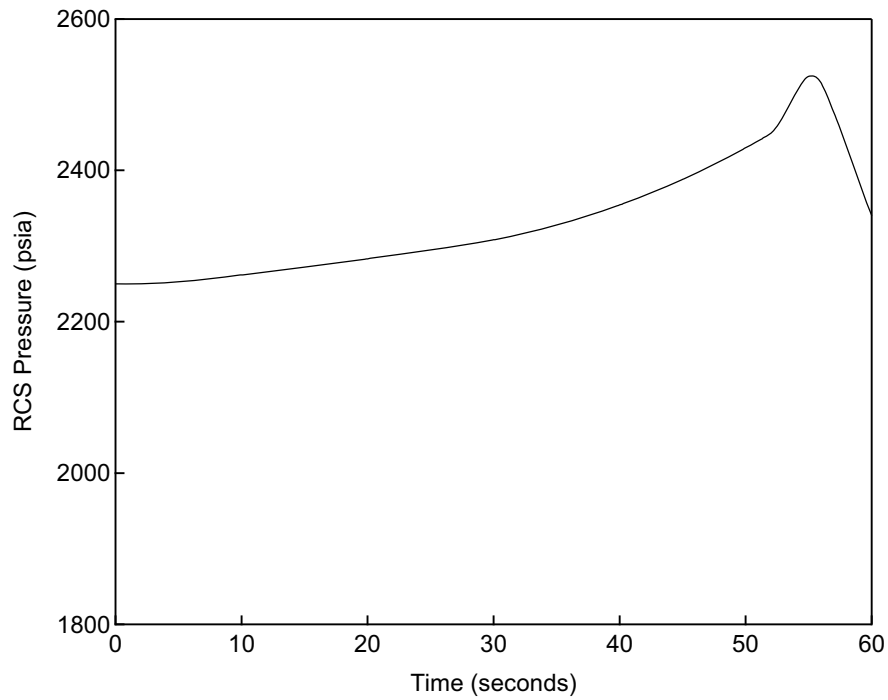


Figure 6.1-9 Hot Spot Heat Flux versus Time
Uncontrolled RCCA Bank Withdrawal at Power (HFP, BOC, 2.5 pcm/sec)



**Figure 6.1-10 RCS Average Temperature versus Time
Uncontrolled RCCA Bank Withdrawal at Power (HFP, BOC, 2.5 pcm/sec)**



**Figure 6.1-11 RCS Pressure versus Time
Uncontrolled RCCA Bank Withdrawal at Power (HFP, BOC, 2.5 pcm/sec)**

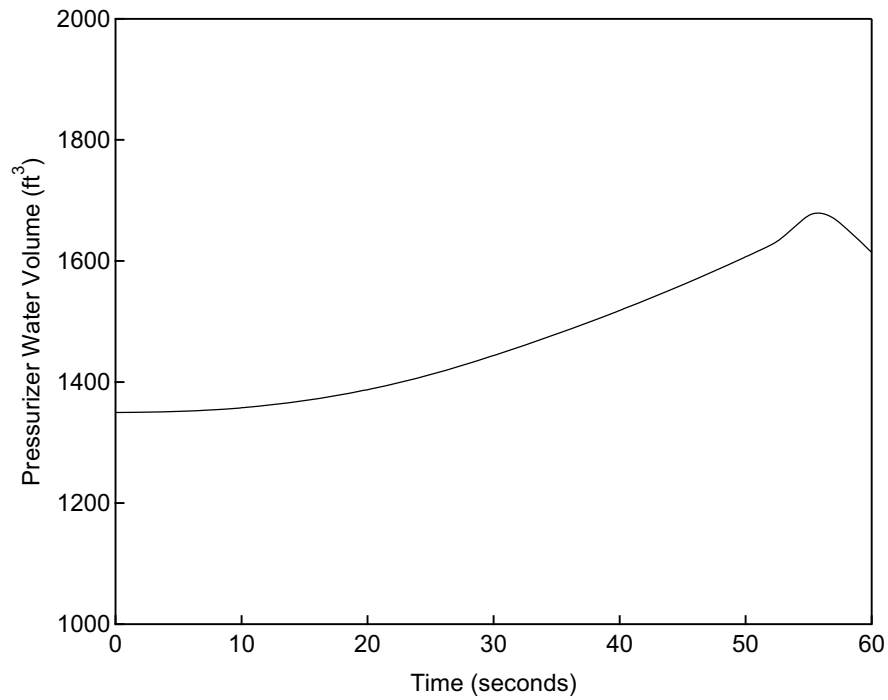


**Figure 6.1-12 Pressurizer Water Volume versus Time
Uncontrolled RCCA Bank Withdrawal at Power (HFP, BOC, 2.5 pcm/sec)**

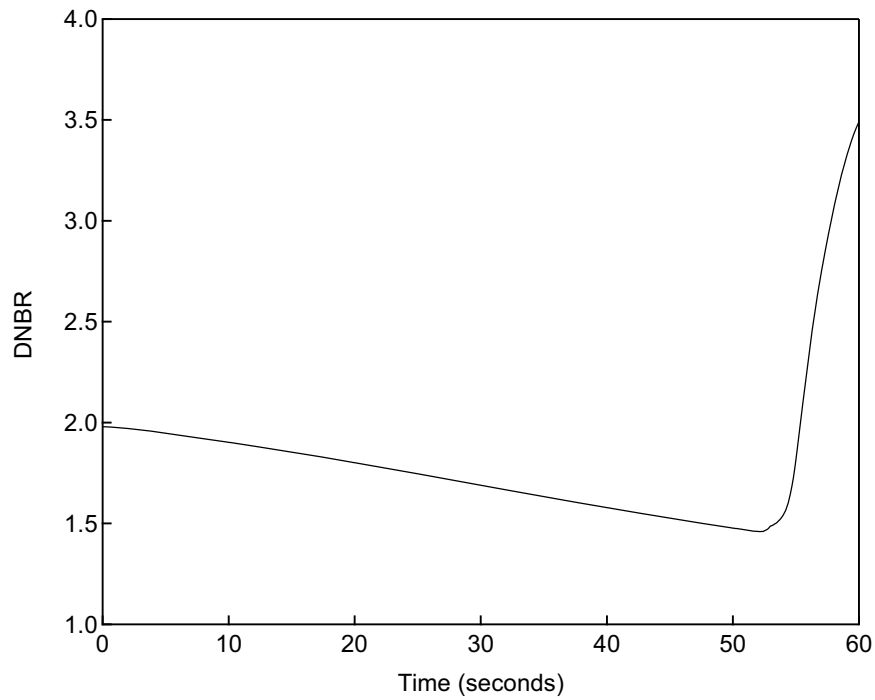


**Figure 6.1-13 DNBR versus Time
Uncontrolled RCCA Bank Withdrawal at Power (HFP, BOC, 2.5 pcm/sec)**

6.2 Complete Loss of Forced Reactor Coolant Flow

Event Description

Loss of forced reactor coolant flow events can result from a mechanical or electrical failure in one or more reactor coolant pumps (RCPs) or from a fault in the power supply to the pump motor. The complete loss of forced reactor coolant flow is initiated by malfunctions that cause the loss of electrical power to all four reactor coolant pumps during power operation, resulting in a reduction in the core cooling capabilities. Although the reduction in core cooling capability could also cause an increase in the reactor fuel temperature and in the reactor coolant temperature, the DNB limit is the primary design limit of concern due to the combination of core temperature increase and core flow decrease.

Events Analyzed

This section provides a sample transient analysis for the complete loss of forced reactor coolant flow event resulting from a loss of electrical power to all four reactor coolant pumps.

The overall response of the primary and secondary systems is evaluated using MARVEL-M. For the loss of flow transients, the MARVEL-M calculates the time-dependent core flow using the reactor coolant pump model described in Section 2.1.3. Time-dependent normalized values of core flow and core power calculated by MARVEL-M are transferred to the VIPRE-01M code for DNBR calculations using the Revised Thermal Design Procedure (RTDP) and the WRB-2 DNB correlation. Inlet temperature and RCS pressure are held constant at conservative values for the DNBR calculations.

The MARVEL-M analysis uses conservative assumptions for the RCP flywheel inertia, moderator density coefficient (least positive), Doppler power coefficient (most negative), and trip simulation (trip setpoint, trip reactivity curve, rod drop time, RPS signal processing delays), as described in Section 5.2. The initial conditions for power, RCS temperature, and RCS pressure are assumed at their nominal values, consistent with the RTDP methodology.

The RPS trips available to mitigate the complete loss of flow from full power include the low reactor coolant flow and low reactor coolant pump speed.

This event was chosen as one of the six sample analyses because it utilizes MARVEL-M to calculate the NSSS response using its internal reactor coolant pump model and performs the DNBR analysis external to MARVEL-M using the VIPRE-01M code.

Analysis Results

The complete loss of forced reactor coolant flow transient is initiated by a trip of all four RCPs. As the pumps coast down, a reactor trip signal is generated by the RCP speed low trip. Prior to the reactor trip, the power increases and the flow decreases, resulting in a decrease in DNBR. The minimum DNBR occurs shortly after the reactor trip following the sharp decrease in power. The minimum DNBR is greater than the 95/95 DNBR Design Limit for transients using the RTDP, the peak RCS pressure remains below 2750 psia (110% of RCS design pressure), and the steam pressure remains below 1320 psia (110% of the main steam system design pressure).

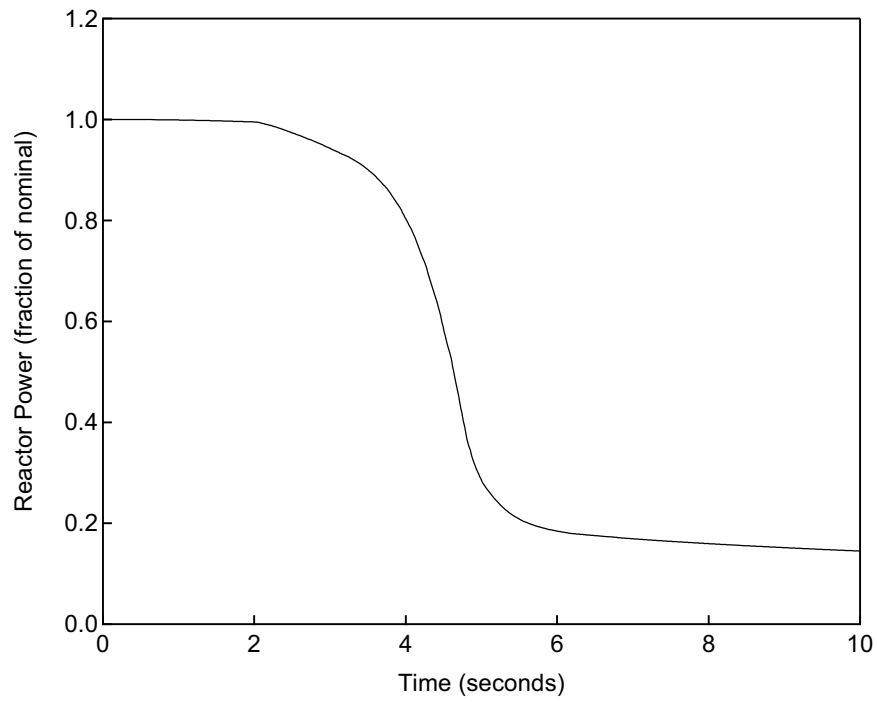
Table 6.2-1 provides the sequence of events for the complete loss of forced coolant flow event. The transient responses for key parameters are presented in Figures 6.2-1 through 6.2-6.

Table 6.2-1 Sequence of Events for the Loss of Forced Reactor Coolant Flow

Event	Time (sec)
RCPs Trip (Flow Coastdown Begins)	0.0
RCP Speed Low Analysis Limit Reached	0.8
Reactor Trip Initiated (Rod Motion Begins)	1.7
Minimum DNBR Occurs	4.0

Conclusions

The analysis of this event demonstrates that the transient does not result in a DNB-related fuel failure. Additionally, the peak pressures in the reactor coolant and main steam systems remain below 110% of the design pressure. Therefore, the AOO acceptance criteria for this event as discussed in Section 4.4 are met.



**Figure 6.2-1 Reactor Power versus Time
Complete Loss of Forced Reactor Coolant Flow**

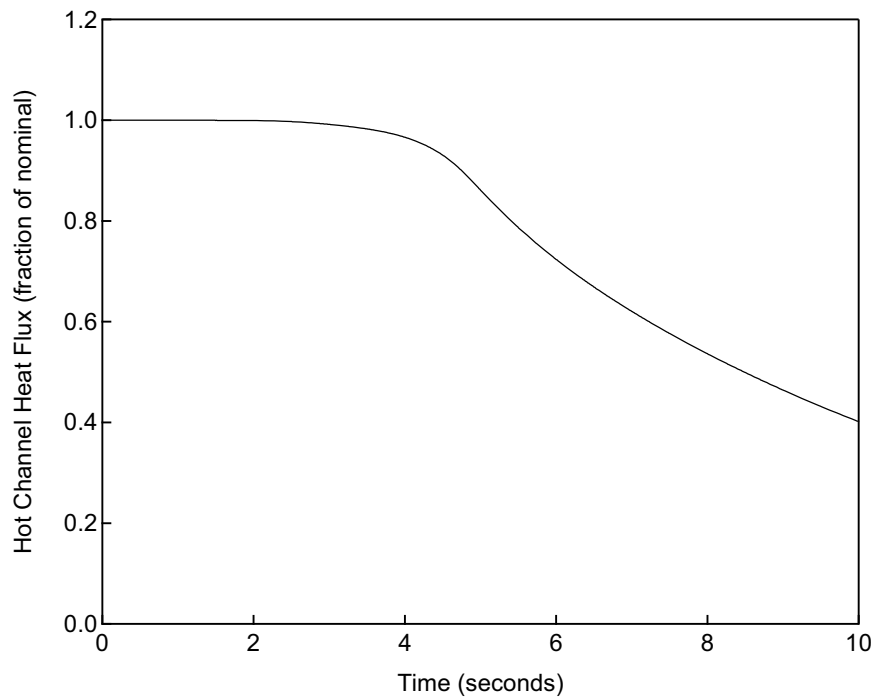


**Figure 6.2-2 Hot Channel Heat Flux versus Time
Complete Loss of Forced Reactor Coolant Flow**

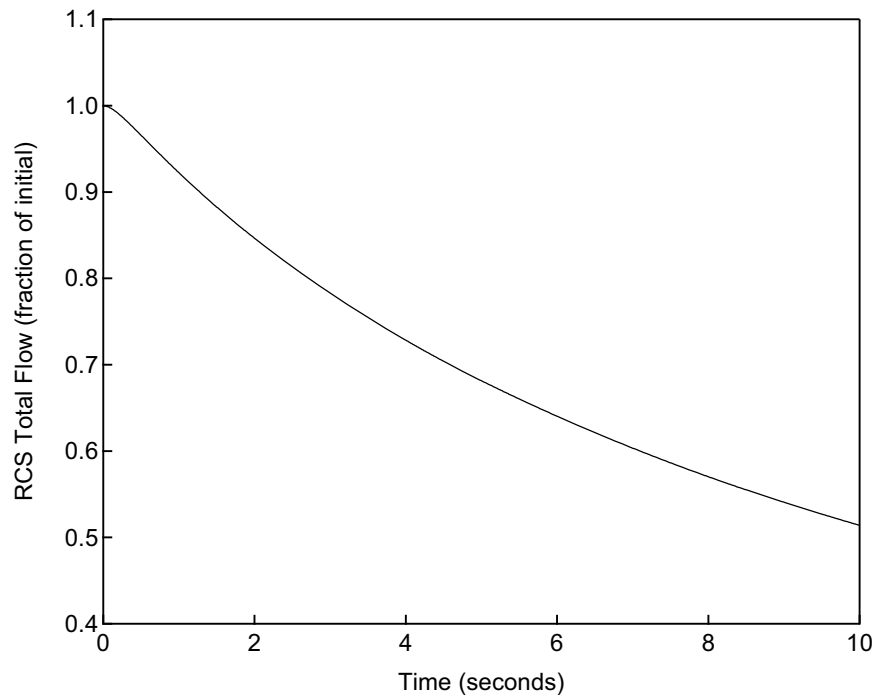


Figure 6.2-3 RCS Total Flow versus Time Complete Loss of Forced Reactor Coolant Flow

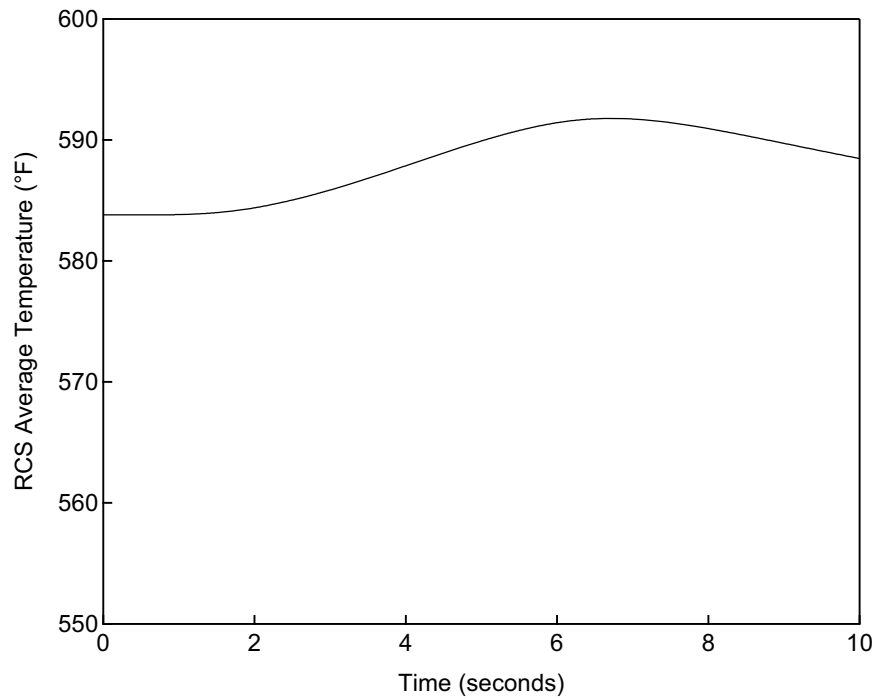
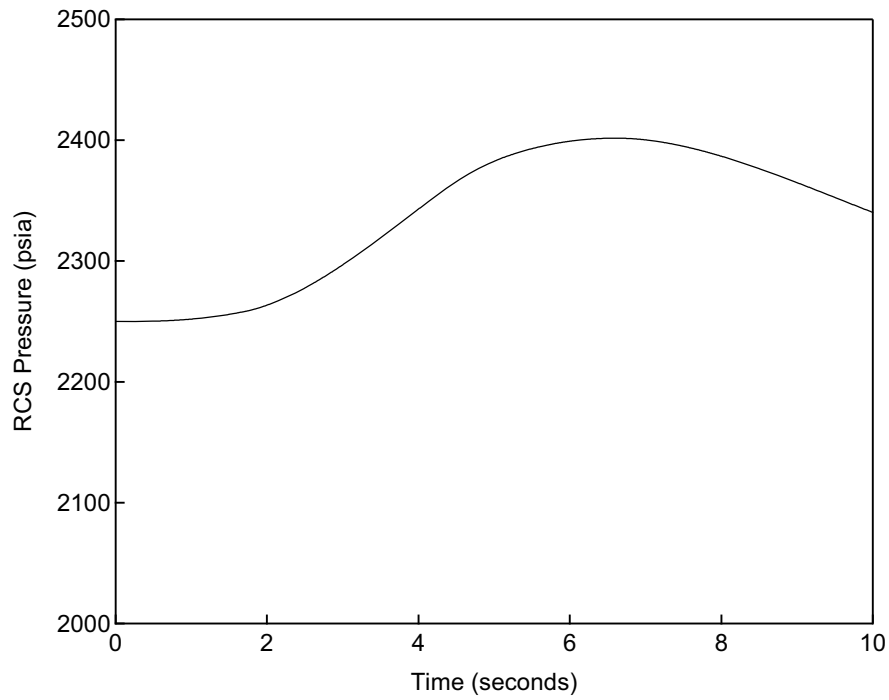
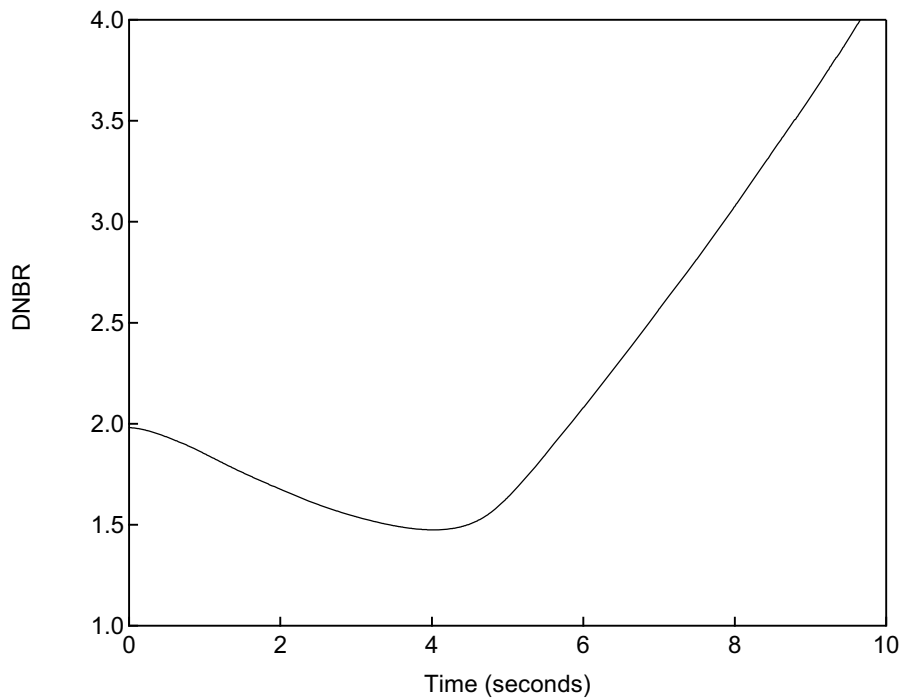


Figure 6.2-4 RCS Average Temperature versus Time Complete Loss of Forced Reactor Coolant Flow



**Figure 6.2-5 RCS Pressure versus Time
Complete Loss of Forced Reactor Coolant Flow**



**Figure 6.2-6 DNBR versus Time
Complete Loss of Forced Reactor Coolant Flow**

6.3 Spectrum of RCCA Ejection

Event Description

This event is defined as a mechanical failure of a control rod drive mechanism pressure housing, resulting in the ejection of an RCCA and drive shaft. This rapid positive reactivity insertion results in a rapid increase in core power and local peaking, challenging the fuel design limits. If the ejected rod reactivity is low, the core power increase might not be large enough to trip the reactor on high power range neutron flux, resulting in a delay until the reactor eventually trips due to the depressurization of the RCS by the CRDM housing break.

Events Analyzed

The limiting RCCA ejection cases, for both the beginning and end of cycle at both zero and full power, for both conservative and more realistic ejected rod worths, are evaluated in the DCD using the methodology described in Section 5.3 with respect to the acceptance criteria described in Section 4.5.

For the hot full power (HFP) fuel temperature and enthalpy cases, the TWINKLE-M spatial neutron kinetics code is used to determine the core average and local power generation with time. Then the VIPRE-01M code is utilized to determine the fuel response at the limiting location using local peaking factors based on design calculations (with safety margin) using the ANC code. For the hot zero power (HZP) cases, the transient is modeled using TWINKLE-M 3-D kinetics and a case-specific local peaking factor (with safety margin) is calculated for use in the VIPRE-01M fuel response analysis.

Sample results are provided for three cases, one HFP case (BOC) using design peaking factors, one HZP case (EOC) using transient-specific 3-D TWINKLE-M peaking factors, and one HFP case (EOC) that does not reach the high power range neutron flux trip setpoint.

Analysis Results

For the first HFP (BOC) case, Control Bank-D is assumed to be inserted to its insertion limit when the rod ejection occurs. A bounding maximum ejected rod worth of 110 pcm and a design hot channel factor of 5.0 are assumed to provide margin for future cores. The reactivity insertion causes a rapid increase in power and the power increase is terminated by Doppler feedback. The reactor trip is initiated by neutron flux high (high setting) and the reactor

returns subcritical following the trip. The hot spot peak fuel centerline temperature is 4232°F, which remains below the fuel melting temperature limit.

For the HZP (EOC) case, Control Bank-D is assumed to be fully inserted and the others inserted to their insertion limit when the rod ejection occurs. A bounding maximum ejected rod worth of 800 pcm and a hot channel factor of 35.0 are assumed to provide margin for future cores. The reactivity insertion causes a rapid increase in power and the power excursion is terminated by Doppler feedback. The reactor trip is initiated by neutron flux high (low setting) and the reactor returns subcritical following the trip. The hot spot peak fuel enthalpy is 72.7 cal/g. The number of PCMI failed fuel is zero.

For the second HFP case, Control Bank-D is assumed to be inserted to its insertion limit when the rod ejection occurs. A reactivity insertion with additional margin is modeled. The reactivity insertion causes a rapid increase in power and the power excursion is terminated by Doppler feedback. No reactor trip is assumed in the short-term. The reactor power stabilizes due to feedback effects and no DNB occurs in the short-term. This period is followed by depressurization of the RCS due to the CRDM housing break. The reactor trip is initiated by the low pressurizer pressure signal during rapid depressurization conditions and the over temperature ΔT signal during slower depressurization conditions. The reactor power decrease and DNB concern is mitigated after the trip. The longer-term effects of the RCS depressurization are bounded by LOCA analyses. The limiting case for the rapid depressurization results in DNB failure in () of rods. The limiting case for the slow depressurization results in DNB failure in () of rods.

The nuclear power, fuel temperature (centerline and average), and clad temperature transients for the HFP case are presented in Figures 6.3-1 and 6.3-2, and the nuclear power and fuel enthalpy transients for the HZP case are presented in Figures 6.3-3 and 6.3-4, respectively. The relationship between oxide / wall thickness and fuel enthalpy rise is presented in Figure 6.3-5 for the HZP case. The calculated pairs of points are plotted on the same graph as the acceptance criterion. The calculated sequence of events corresponding to these limiting events is provided in Table 6.3-1.

Table 6.3-1 Sequence of Events for the RCCA Ejection

Event	BOC HFP Time (sec)	EOC HZP Time (sec)
Rod Ejection Occurs	0.0	0.0
Neutron Flux High Analysis Limit Reached	0.10 (high setting) ^{*1}	0.15 (low setting)
Peak Nuclear Power Occurs	0.11	0.16
Reactor Trip Initiated (Rod Motion Begins)	0.70	0.75
Maximum Fuel Temperature Occurs	2.5	-
Maximum Fuel Enthalpy Occurs	-	1.2

*1 The reactor trip occurs when the measured neutron flux considering a single failure of one ex-core detector channel reaches the high power range neutron flux high setpoint plus uncertainty.

For the HFP case that does not result in the high power range neutron flux trip, the nuclear power and DNB transients for the short-term period are presented in Figures 6.3-6 and 6.3-7 for one of the rod ejection locations. The $F_{\Delta H}^N$ census used to calculate rods in DNB for the long-term period slow depressurization case is shown in Figure 6.3-8.

Conclusions

The analysis of this event demonstrates that the interim core coolability criteria described in SRP 4.2 Appendix B have been met, and therefore, no consequential damage occurs to the RCS or containment as a result of fuel damage. The separate RCS pressure transient using the MARVEL-M code with void data from VIPRE-01M is not included in this topical report. The fuel limit acceptance criteria for this event as described in Section 4.5 are met.

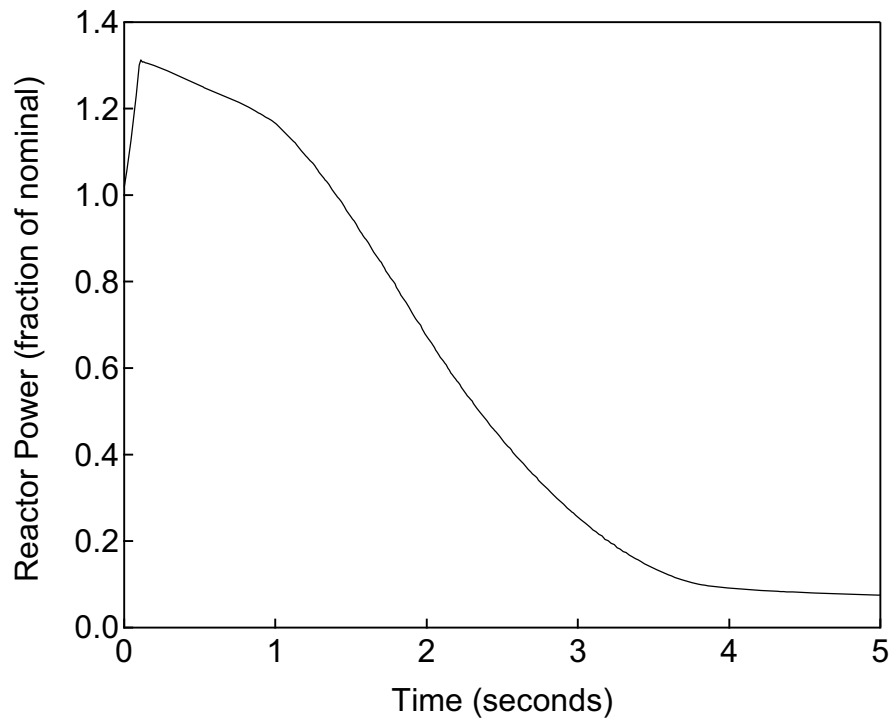


**Figure 6.3-1 Nuclear Power versus Time
RCCA Ejection (BOC HFP)**

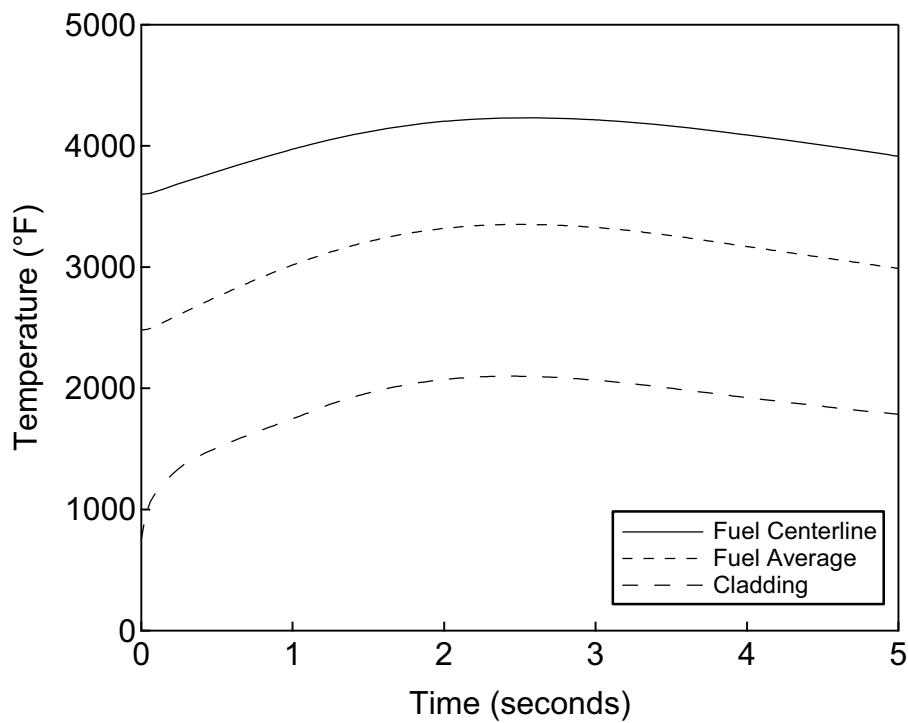


**Figure 6.3-2 Fuel and Cladding Temperature versus Time
RCCA Ejection (BOC HFP)**

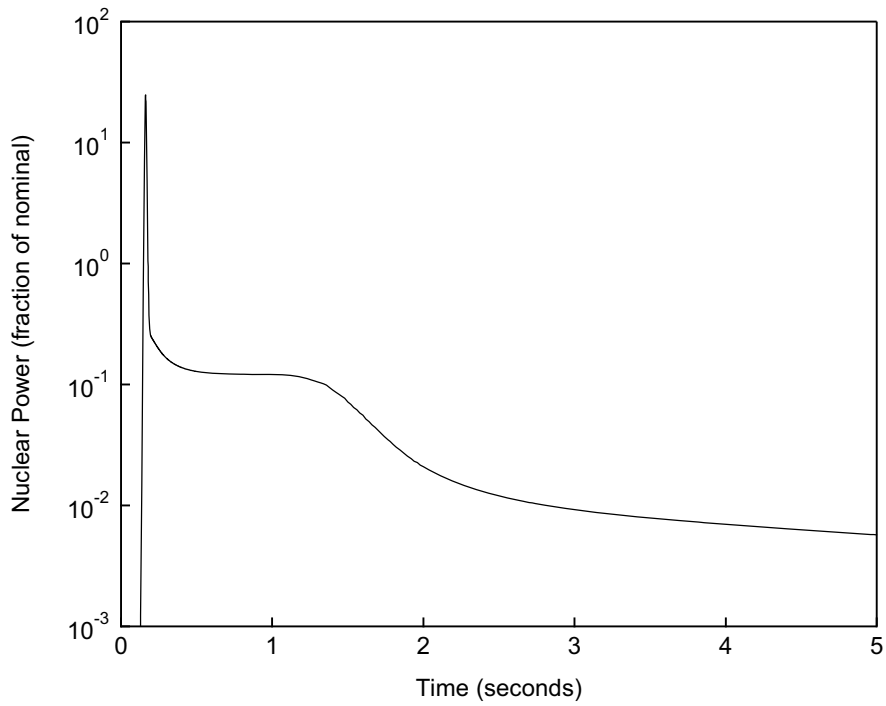


**Figure 6.3-3 Nuclear Power versus Time
RCCA Ejection (EOC HZP)**

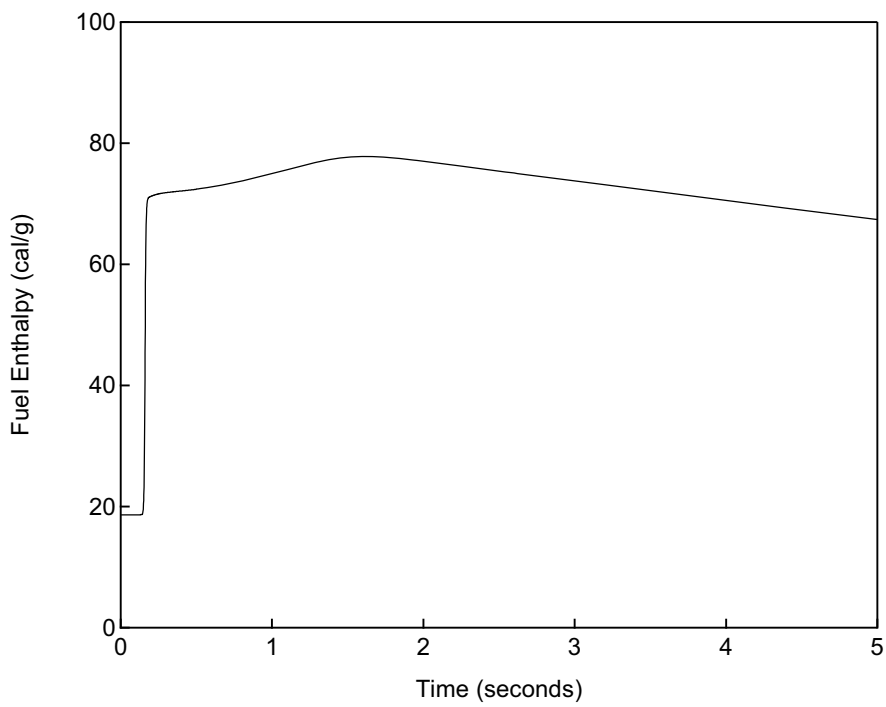


**Figure 6.3-4 Fuel Enthalpy versus Time
RCCA Ejection (EOC HZP)**



**Figure 6.3-5 Fuel Enthalpy Rise versus Oxide / Wall Thickness
RCCA Ejection (EOC HZP)**

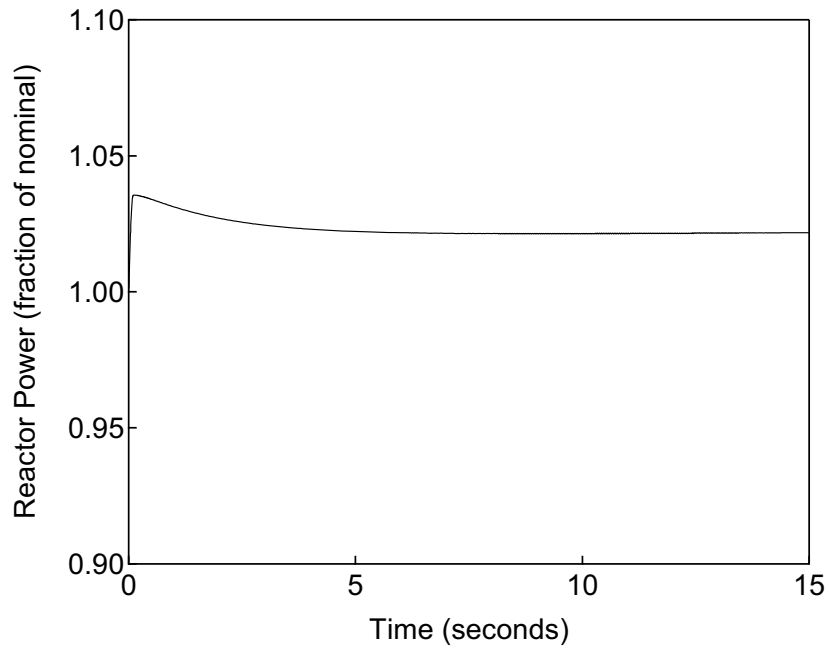


Figure 6.3-6 Nuclear Power versus Time for Short Term Period RCCA Ejection (BOC HFP, No Flux Trip)

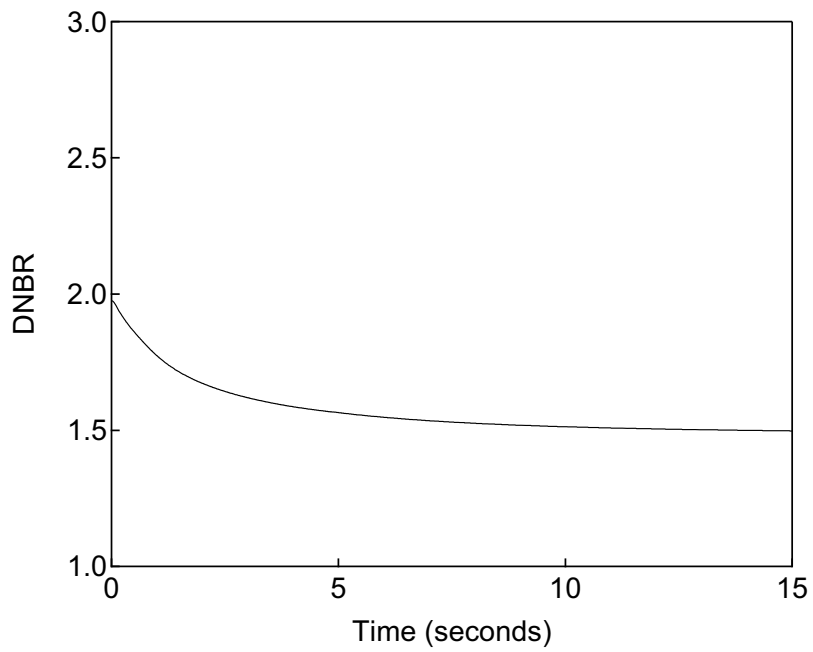


Figure 6.3-7 DNBR versus Time for Short Term Period RCCA Ejection (BOC HFP, No Flux Trip)



**Figure 6.3-8 Core Census for Rods in DNB for Long Term Period (0% to 5% Range)
RCCA Ejection (EOC HFP, No Flux Trip)**

6.4 Steam System Piping Failure

Event Description

The rupture of a main steam line results in removal of energy from the reactor coolant system through the steam generator leading to a reduction in coolant temperature and pressure. In the presence of a negative moderator temperature coefficient, the event results in a positive reactivity insertion and an increase in power level (at-power) or a return to criticality and power (hot shutdown).

Events Analyzed

The Steam System Piping Failure (Main Steamline Break) accident can be characterized as a spectrum of break sizes and locations that can occur from various operating modes (e.g., hot shutdown, at power) at various times in core life (BOL, EOL), with and without offsite power (forced reactor coolant pump flow). As discussed in Section 5.4, the event is analyzed assuming the most reactive control rod stuck out of the core, which results in both a reactivity penalty as well as a power distribution penalty. The sample results provided in this section are for an instantaneous double-ended guillotine break in a steam pipe, between the steam generator and turbine. Failure of a main steam system pipe (described in this section) is a postulated accident event as defined in Section 4.2. Effects of other minor secondary steam system pipe breaks (classified as an AOO in Section 4.2) are bounded by the analysis of the large double-ended break.

The overall response of the primary and secondary systems is evaluated using the MARVEL-M code. As discussed in Section 2, the MARVEL-M code calculates break flow and its resulting effect on reactivity, power, and RCS parameters. The VIPRE-01M code is then used to determine if DNB occurs for selected steady-state core conditions computed by the MARVEL-M code during the transient.

The analysis is performed at the end of the core cycle. The moderator density coefficient has its highest value (moderator temperature coefficient has its highest negative value) at the end of the cycle, causing the cooldown to have the maximum impact on the core transient. As described in Section 5.4, the stuck rod assumption (and its associated reactivity and power distribution effects) has no meaning prior to the minimum DNBR portion of the at-power breaks. Therefore, the at-power analysis to verify that the RPS protects the core limits is done in the same manner as the Bank Withdrawal at Power analysis using only the MARVEL-M code (and its internal DNBR calculation) as described in Sections 5.1 and 6.1. Sample results for these at-power cases are not provided in this section. The large, double-ended break from hot shutdown inside the MSIV with full reactor coolant flow is a representative case, and is the only case presented in this sample transient analysis section.

Analysis Results

Figures 6.4-1 through 6.4-11 are plots of system parameters versus time from the core response analysis for the double-ended steam line failure from hot shutdown with offsite power available. The break is assumed to occur inside the main steam isolation valve on one of the steam lines, resulting in the complete blowdown of one steam generator. If the core is at critical hot zero power conditions when the break occurs, the main steam line pressure low

ECCS actuation signal will trip the reactor, leading to a transient much like the case presented here.

Immediately following the break, a main steam line pressure low (any one steam generator) signal will occur on the affected loop, resulting in steamline isolation and reactor trip signals. The steamline pressures on the other loops will not be affected because check valves in each steam line inside the reactor building upstream of the main steam header prevent steam flow to the break. However, the effect of check valves is conservatively ignored in the analysis prior to steamline isolation. If the break were to occur outside the reactor building (downstream of the main steamline isolation valves), flow to the break would be terminated in all steam lines by the closure of the main steam isolation valves (MSIVs) actuated by the steamline isolation signal. The main steam line pressure low signal also causes an ECCS actuation signal, which in turn, starts the emergency feedwater pumps, isolates main feedwater, and starts the safety injection pumps.

As shown in Figure 6.4-1, the reactor becomes critical with the control rods inserted (assuming the single most reactive rod in the fully withdrawn position), and the reactor returns to power. The cooldown continues at a decreasing rate due to decreasing steam pressure, until the affected steam generator inventory is depleted and emergency feedwater to it is isolated. As can be seen from Figures 6.4-6 and 6.4-8, the intact loop with the pressurizer surge line connection responds differently from the other two intact loops due to the addition of warmer pressurizer outsurge to the hot leg. The steam generator pressure in the pressurizer loop remains higher than the other intact loops after steam line isolation due to this effect and the assumption of no reverse heat transfer from the steam generators to the RCS. When the RCS pressure decreases below the shutoff pressure of the safety injection pumps, borated water begins to flow to the RCS, as indicated by the boron concentration transient shown in Figure 6.4-11. A single failure of one safety injection train is assumed in the analysis. The limiting point in the transient occurs when the nuclear power and core heat flux peak, resulting from the combination of decreasing steam flow and increasing core boron concentration.

Only one steam generator blows down completely following a steam pipe failure transient. Emergency feedwater to the affected steam generator is isolated automatically on an uncompensated steam generator pressure signal as shown in Figure 6.4-10. As shown in Figure 6.4-7, the blowdown is terminated when the affected steam generator mass is depleted, terminating the rapid cooldown. After the faulted steam generator mass is depleted, the pressurizer level recovers and the differences in loop inlet temperature decrease due to mixing in the reactor vessel as shown in Figures 6.4-5 and 6.4-6. The other three steam generators remain available for removal of decay heat from the primary coolant after the initial transient is over.

A steady-state analysis is performed at the peak power point in the transient to calculate the minimum DNBR. The ANC code is used to calculate the limiting power distribution assuming the most reactive rod fully withdrawn; the limiting location is in the core quadrant associated with the broken loop. The ANC analysis also confirms the conservatism of the reactivity and nuclear power transients as calculated by the MARVEL-M code. The ANC power distribution and core inlet temperature distribution is used to perform a hot channel DNBR analysis using VIPRE-01M. Because the RCS pressures are below the applicable pressure range for the WRB-2 DNBR correlation, the W-3 correlation [Reference 17] and its associated 95/95 limit are used.

Table 6.4-1 Sequence of Events for the Steam System Piping Failure

Event	Time (sec)
Steam Pipe Rupture (Steamline Break) Occurs	0.0
Main Steam Line Pressure Low Analysis Limit Reached	1.5
MSIVs Closed	10.0
Safety Injection Pumps Start	21.5
Boron Reaches Core	44.7
Automatic Isolation of EFWS to Faulted SG	60.0
Peak Core Heat Flux Occurs	88.2
Faulted SG Water Mass Depleted	333

Conclusions

Although the Steam System Piping Failure is a Postulated Accident (fuel failures are permitted according to the acceptance criteria discussed in Section 4.1.2), the minimum DNBR does not exceed the 95/95 DNBR limit, and therefore no fuel failures are predicted as a result of the accident.

Therefore, the acceptance criteria for core damage as defined in Section 4.2 for this event are met.

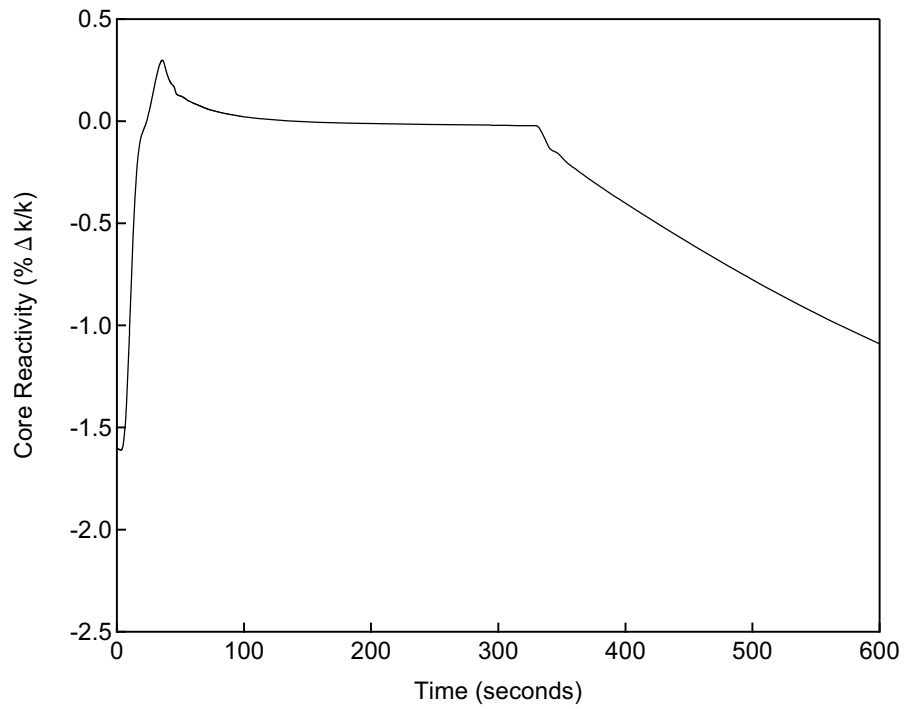


**Figure 6.4-1 Core Reactivity versus Time
Steam System Piping Failure – Double-Ended Break from Hot Shutdown**

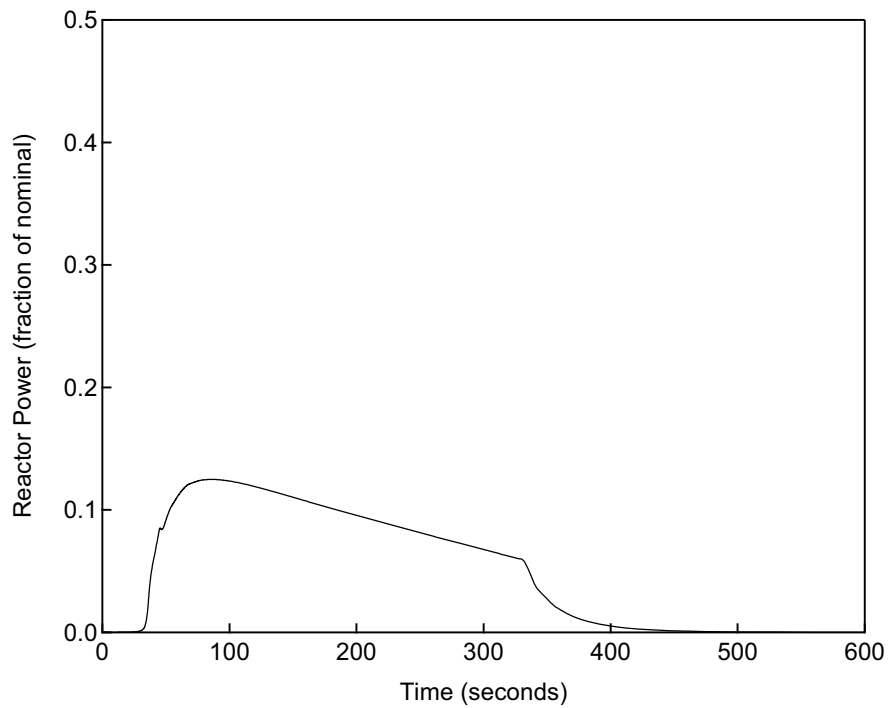


**Figure 6.4-2 Reactor Power versus Time
Steam System Piping Failure – Double-Ended Break from Hot Shutdown**

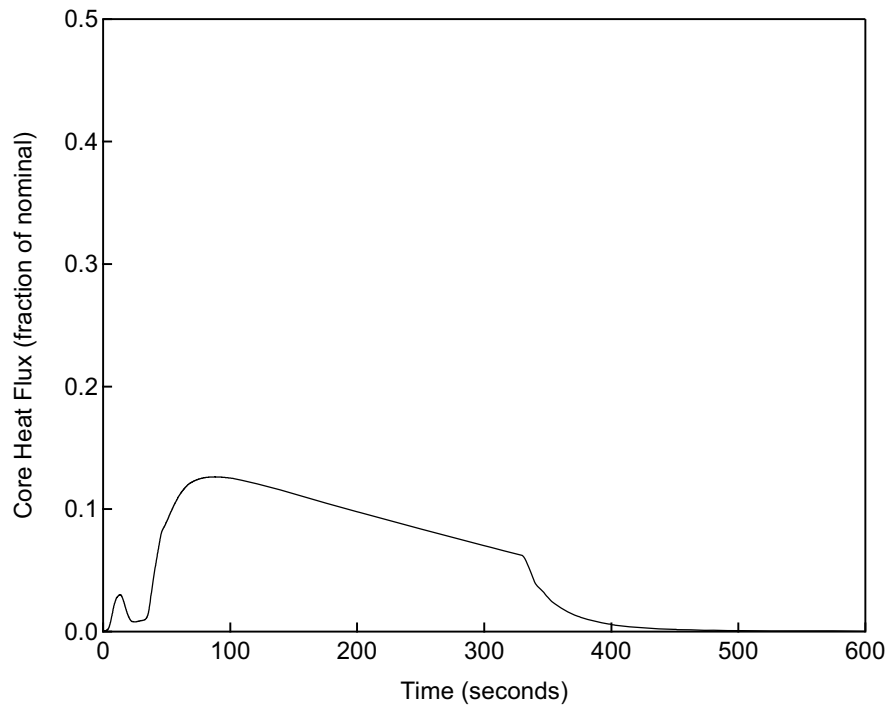


**Figure 6.4-3 Core Heat Flux versus Time
Steam System Piping Failure – Double-Ended Break from Hot Shutdown**

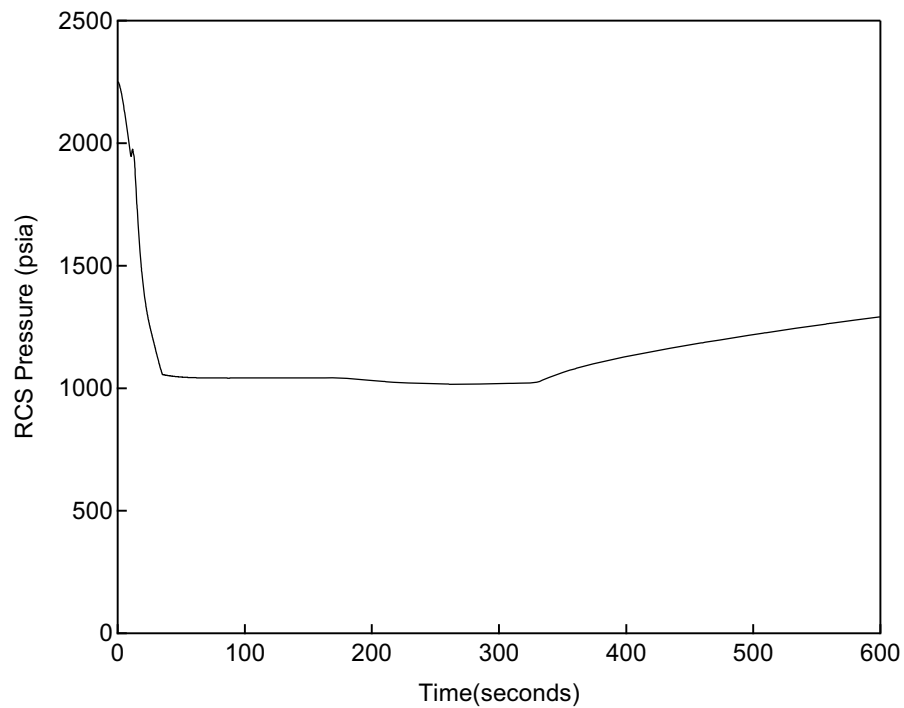


**Figure 6.4-4 RCS Pressure versus Time
Steam System Piping Failure – Double-Ended Break from Hot Shutdown**

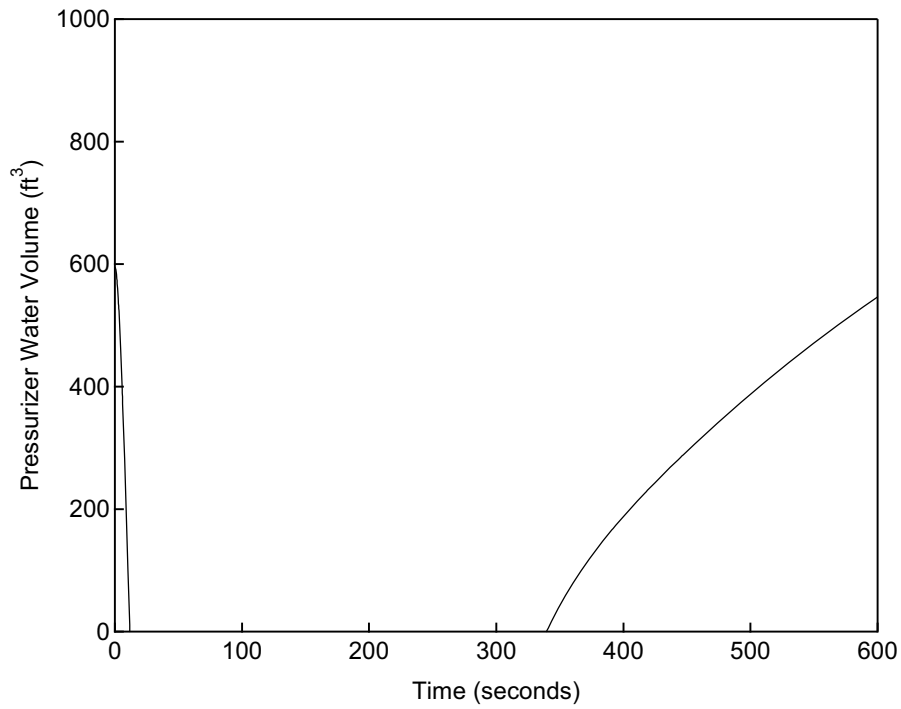


**Figure 6.4-5 Pressurizer Water Volume versus Time
Steam System Piping Failure – Double-Ended Break from Hot Shutdown**

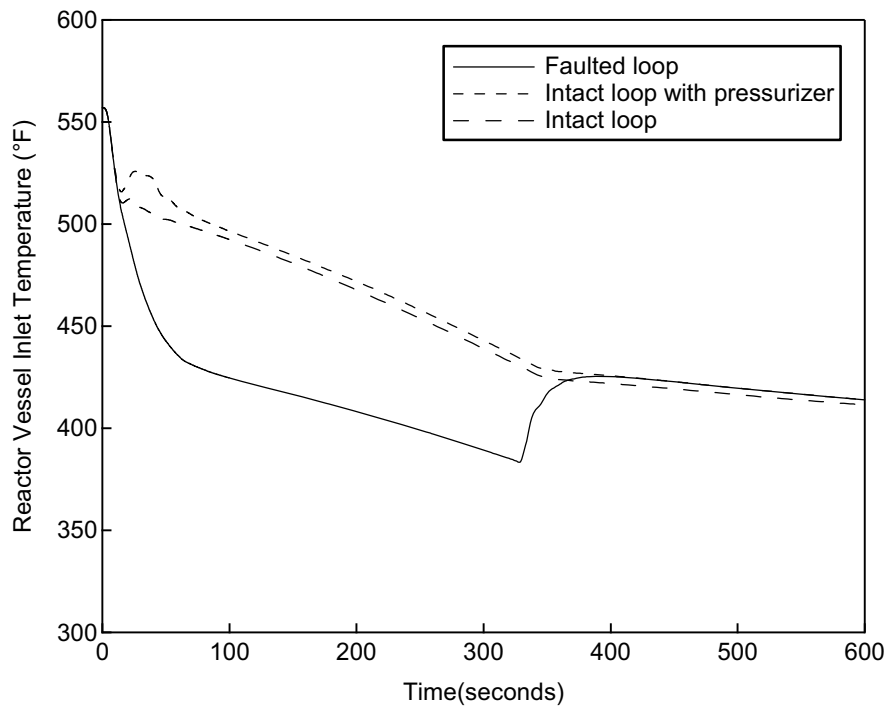


**Figure 6.4-6 Reactor Vessel Inlet Temperature versus Time
Steam System Piping Failure – Double-Ended Break from Hot Shutdown**

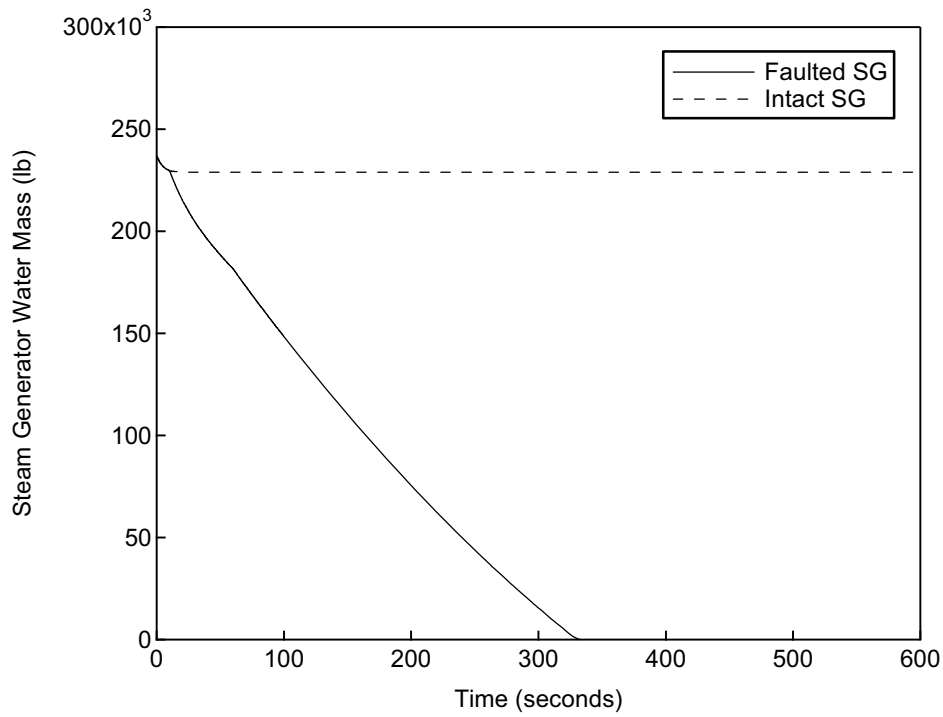


**Figure 6.4-7 Steam Generator Water Mass versus Time
Steam System Piping Failure – Double-Ended Break from Hot Shutdown**

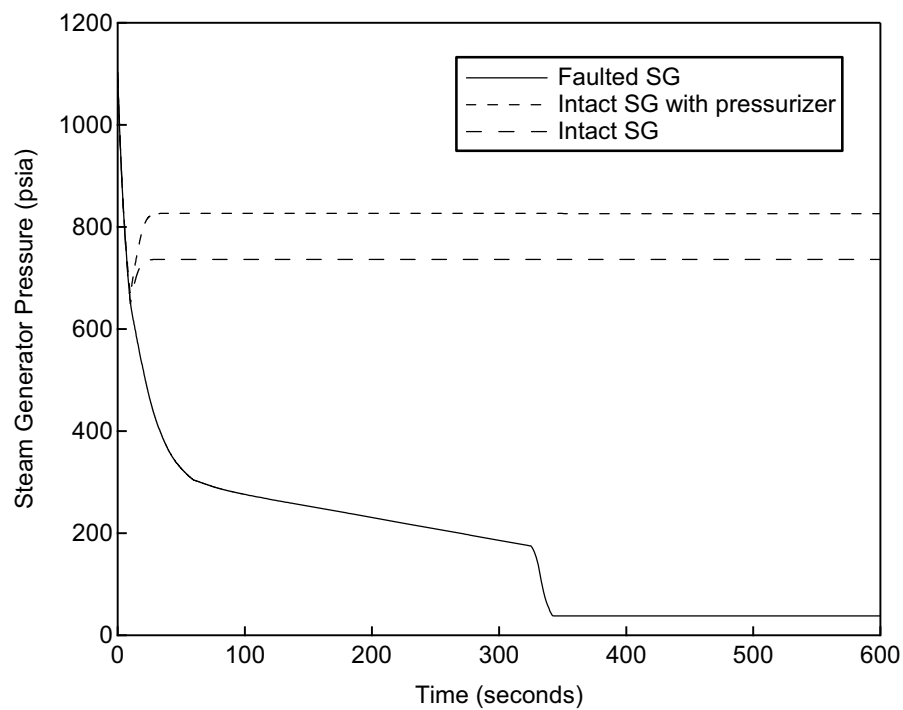


**Figure 6.4-8 Steam Generator Pressure versus Time
Steam System Piping Failure – Double-Ended Break from Hot Shutdown**

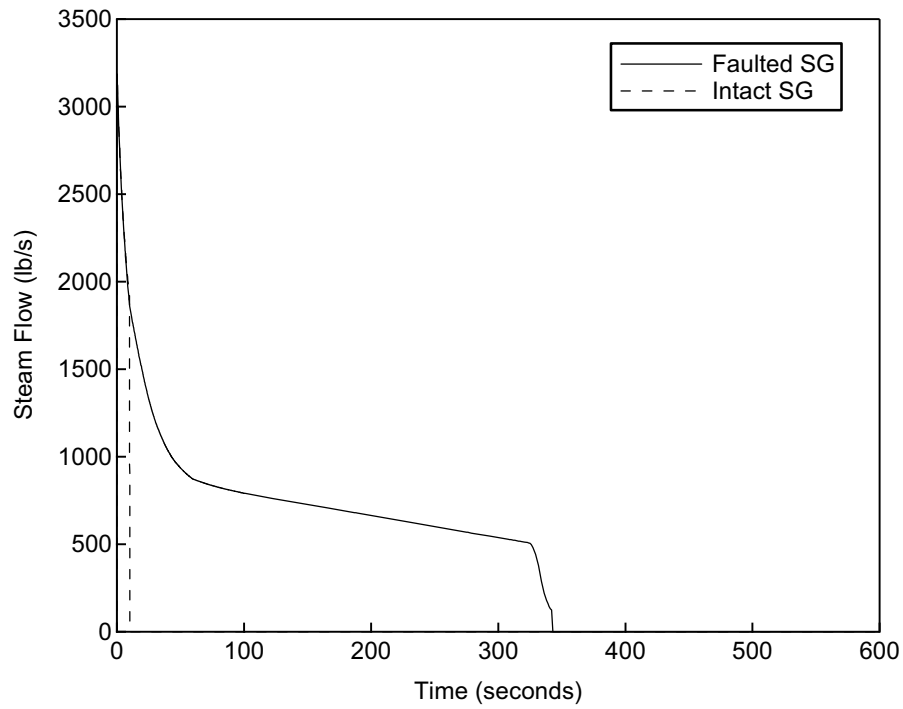


**Figure 6.4-9 Steam Flow Rate versus Time
Steam System Piping Failure – Double-Ended Break from Hot Shutdown**

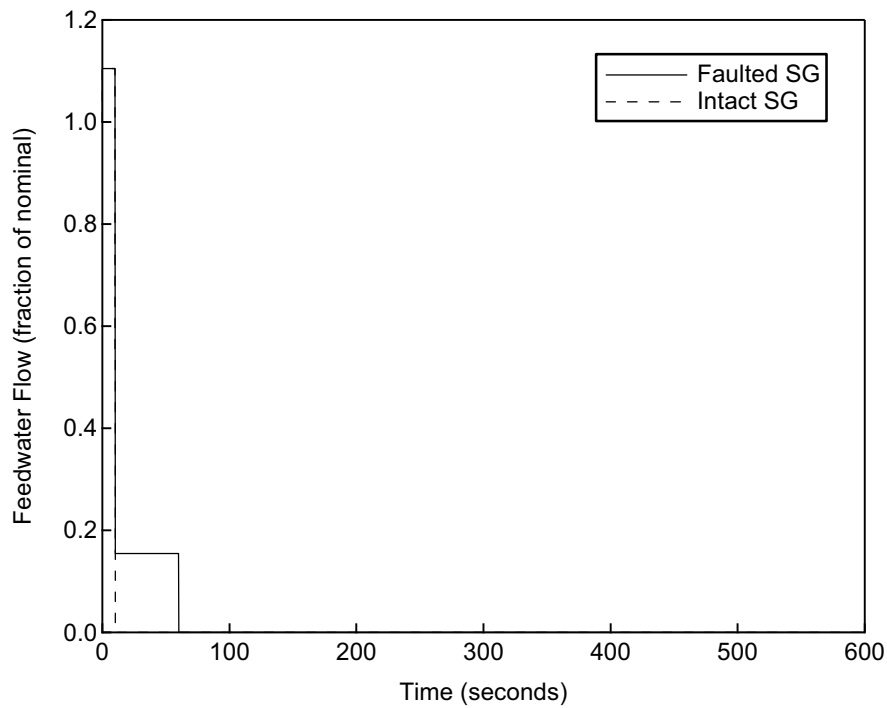


**Figure 6.4-10 Feedwater Flow Rate versus Time
Steam System Piping Failure – Double-Ended Break from Hot Shutdown**

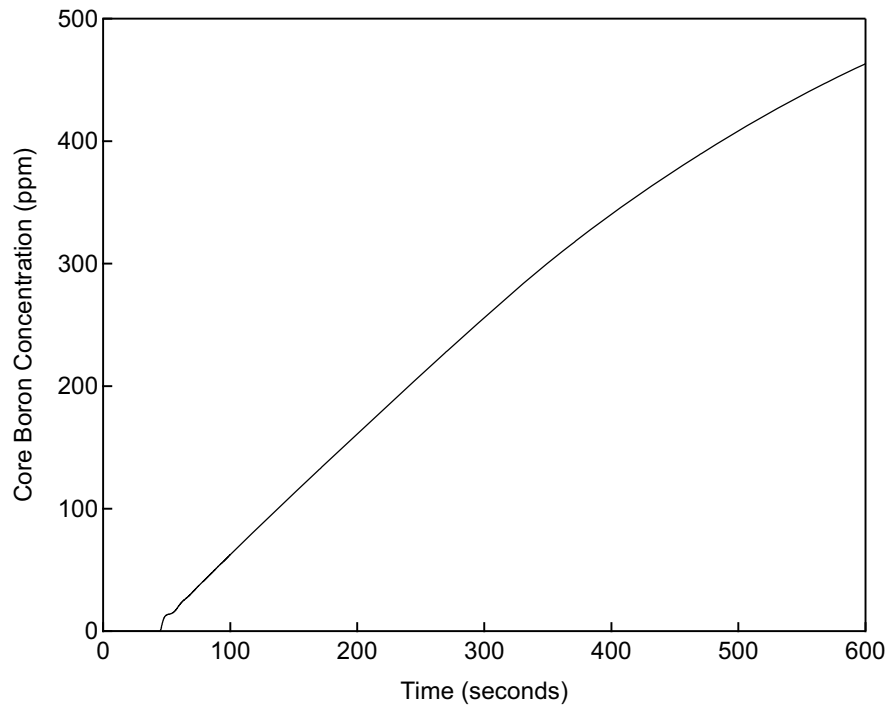


**Figure 6.4-11 Core Boron Concentration versus Time
Steam System Piping Failure – Double-Ended Break from Hot Shutdown**

6.5 Feedwater System Pipe Break

Event Description

SRP 15.2.8 defines a major feedwater line rupture as a feedwater line break large enough to prevent the addition of sufficient feedwater to the steam generators to maintain shell side fluid inventory in the steam generators. The large, double-ended rupture of one feedwater line is classified as a Postulated Accident that results in a limiting heatup and pressurization of the reactor coolant system and the non-affected portion of the secondary system.

Events Analyzed

This analysis evaluates the effects of the most limiting feedwater line break - a double-ended rupture of one feedwater line between the feedwater line check valve and the steam generator. This results in the rapid blowdown of one steam generator through the break. The emergency feedwater system (EFWS) train that would normally supply the broken loop will spill out of the feedwater line and not contribute to removing heat from the primary system. In addition, a single failure of one of the other four EFWS trains is assumed, resulting in degraded heat removal from one of the remaining intact steam generators. The methodology for this accident is described in detail in Section 5.5.

For conservatism, the feedwater system break is assumed to occur when the plant is in a condition where all of the steam generators are at the steam generator water level low trip setpoint. This conservative precondition minimizes the total steam generator inventory available to remove heat from the RCS and makes the reactor protection system response independent of the steam generator pressure and level dynamics of the feedwater line break prior to the reactor trip. As a convenience to the analyst, this is modeled by assuming a loss of normal feedwater at time = 0 with the feedwater pipe break occurring at the time of the steam generator water level low trip. The MARVEL-M code is used to analyze the overall response of the primary and secondary systems. The MARVEL-M code calculates the break flow using the Moody correlation assuming saturated liquid (quality = 0) flow. This assumption maximizes the rate at which the affected steam generator inventory is depleted and primary-to-secondary heat transfer is decreased, resulting in a conservative RCS heatup. The MARVEL-M code also models reactor thermal kinetics (decay heat), reactor coolant system response including temperatures, pressure, pressurizer level, and flow (natural circulation), as well as the non-uniform primary-to-secondary heat transfer caused by the break and EFWS single failure and heat removal from the steam generator safety relief valves in the intact steam generators.

Analysis Results

Table 6.5-1 provides the sequence of events for the analyzed case. The transient responses for key parameters following a main feedwater line break are presented in Figures 6.5-1 through 6.5-11.

The break is assumed to occur immediately following the reactor trip on low steam generator level resulting from the loss of feedwater flow assumed as a precondition. On the sequence of events and figures, this is at time = 47 seconds. A loss of offsite power is assumed to occur at that time concurrent with the turbine trip. The steam generator mass is depleted very rapidly as shown by the break flow and affected steam generator mass in Figures 6.5-7 and 6.5-8.

Primary-to-secondary heat transfer area is reduced when the level is below the top of the tubes in the affected steam generator, resulting in a heatup of the faulted loop as shown in Figure 6.5-3. EFWS is also started on a steam generator water level low signal. EFW flow does not enter the faulted steam generator. EFW is automatically isolated to the affected steam generator by isolation logic developed from main steam line pressure low signals. As a single failure, one of the remaining intact steam generators is assumed to not receive EFW flow. The differences between the response of this steam generator and the others receiving EFW flow can be seen in the RCS loop average temperature and steam generator mass figures. As the transient progresses, the three intact steam generators heat up and pressurize to the steam generator safety valve pressure. The intact steam generator without EFW flow gradually boils off its inventory through the safety valves, and its heat transfer also begins to decrease when level reaches the top of the U-tubes. The two remaining intact steam generators with EFW flow boil off the EFW flow through the safety valves, providing in RCS cooling. The transient “turns around” at the point where decay heat balances the steam generator heat removal capability. This occurs at time = 1585 seconds, at which time the pressurizer water volume peaks and begins to decrease. The pressurizer level peaks before the pressurizer fills. In addition, boiling in the hot leg does not occur in the intact loops receiving EFW flow; subcooling margin is maintained.

It should be noted that fuel rod failure resulting from DNB is of primary concern when the reactor is operating at power, not during a heatup following a reactor trip. As a result of the way the transient is initiated, DNBR is not a parameter calculated during this transient. Subcooling is evaluated to preclude steam binding in the steam generator U-tubes for the steam generators receiving EFW flow during natural circulation flow conditions and to preclude the need to model reflux boiling heat transfer during the transient.

Table 6.5-1 Sequence of Events for the Feedwater System Pipe Failure

Event	Time (sec)
Loss of Feedwater Flow Occurs	0.0
Pressurizer Safety Valves Open	39
SG Water Level Low Analysis Limit Reached	45
Reactor Trip Occurs (Rod Motion Begins)	47
Feedwater Break Initiated	47
Reactor Coolant Pumps Tripped	47
Peak RCS Pressure Occurs	50
SG Safety Valves Open	52
EFWS Isolated to Broken Loop	83
EFWS Pumps Start	187
Peak Pressurizer Water Volume Occurs	1585

Conclusions

The analysis of this event demonstrates that the transient does not result in overpressurization of the RCS, i.e., the peak RCS pressure remains below 120% of RCS design pressure. The peak pressure in the main steam system remains below 120% of the main steam system design pressure. The internal MHI accident-specific acceptance criterion that the pressurizer does not fill has also been met, providing added assurance that the pressurizer safety valves

do not exceed their design basis, precluding the occurrence of another accident (Loss of Coolant). In conclusion, the acceptance criteria for this event described in Section 4.3 have been met.

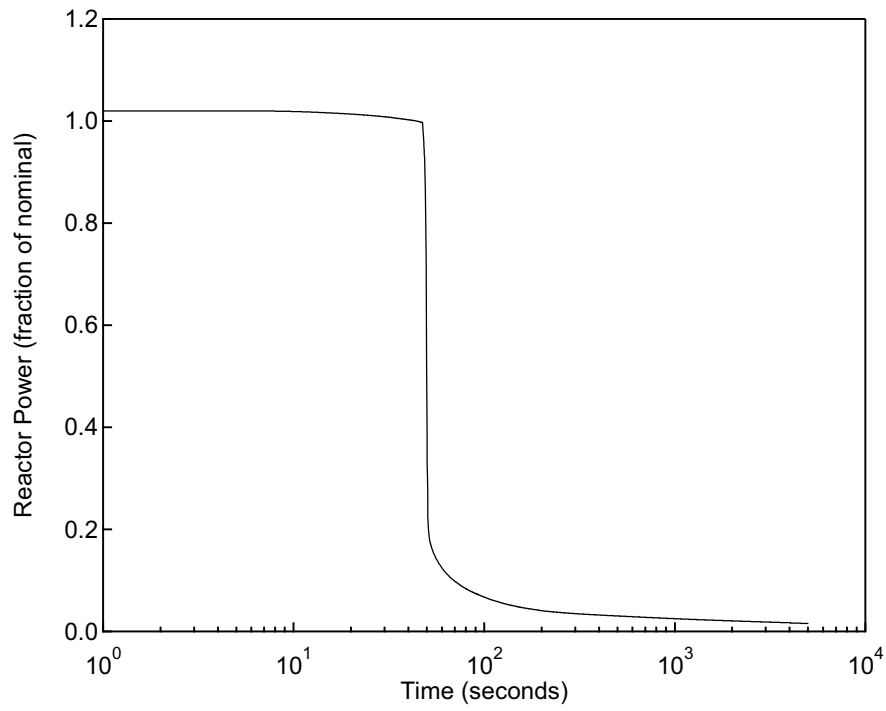


**Figure 6.5-1 Reactor Power versus Time
Feedwater System Pipe Break**

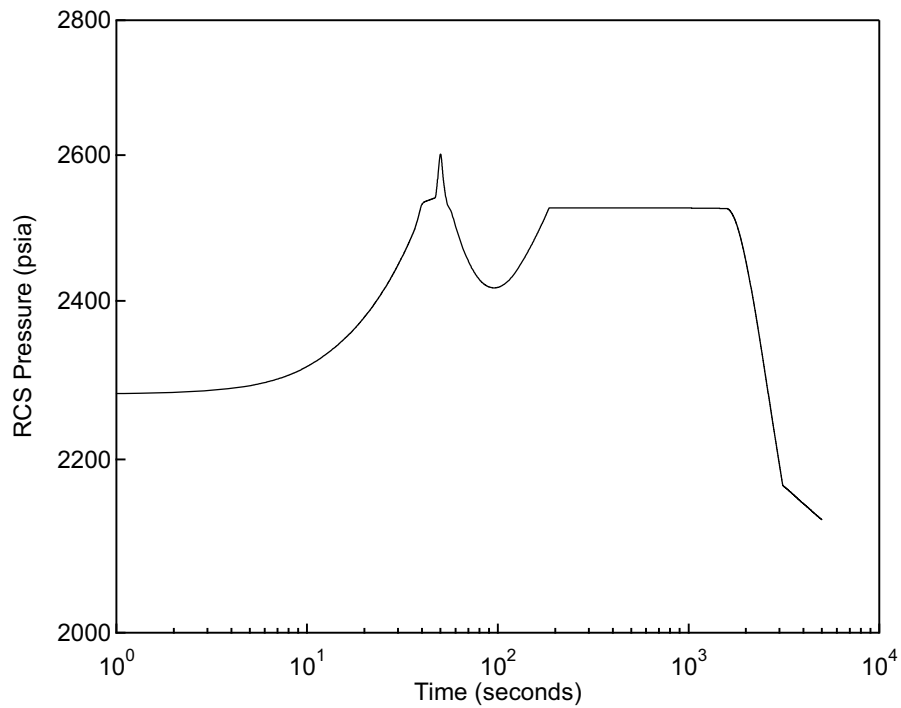


**Figure 6.5-2 RCS Pressure versus Time
Feedwater System Pipe Break**

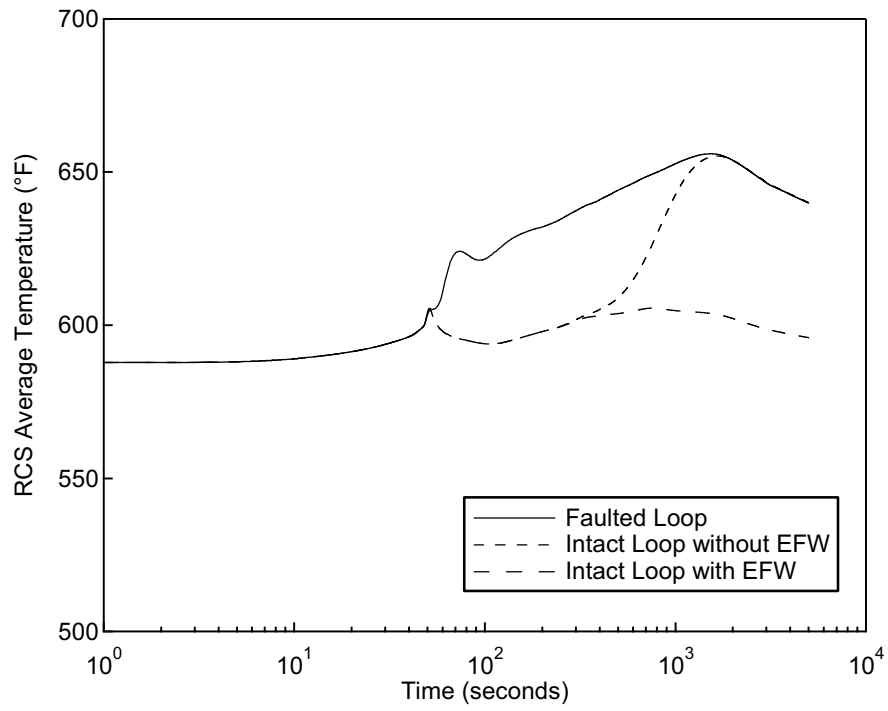


Figure 6.5-3 RCS Average Temperature versus Time Feedwater System Pipe Break

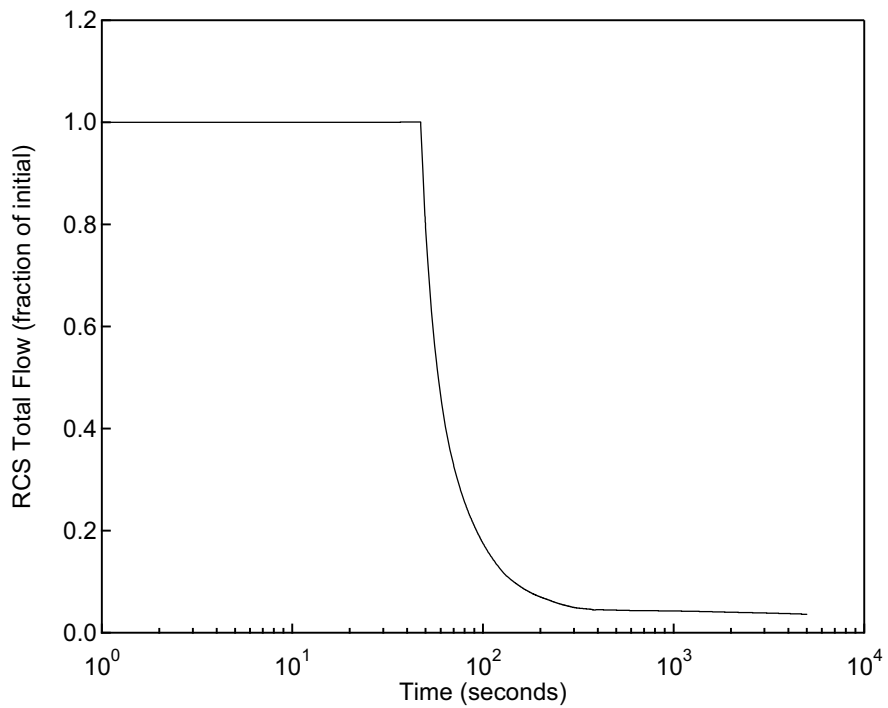


Figure 6.5-4 RCS Total Flow versus Time Feedwater System Pipe Break

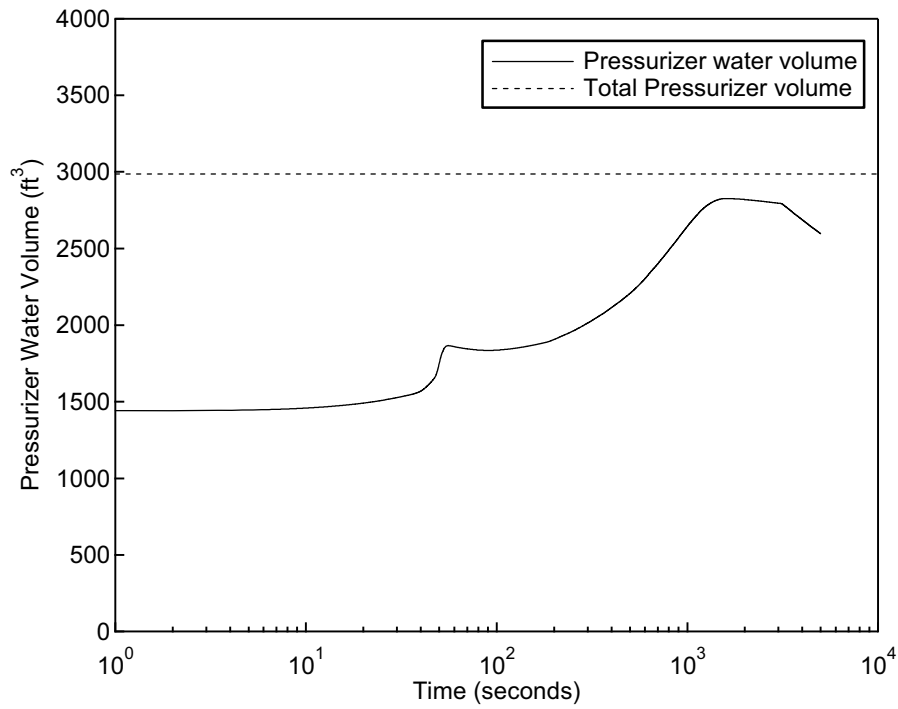


Figure 6.5-5 Pressurizer Water Volume versus Time Feedwater System Pipe Break

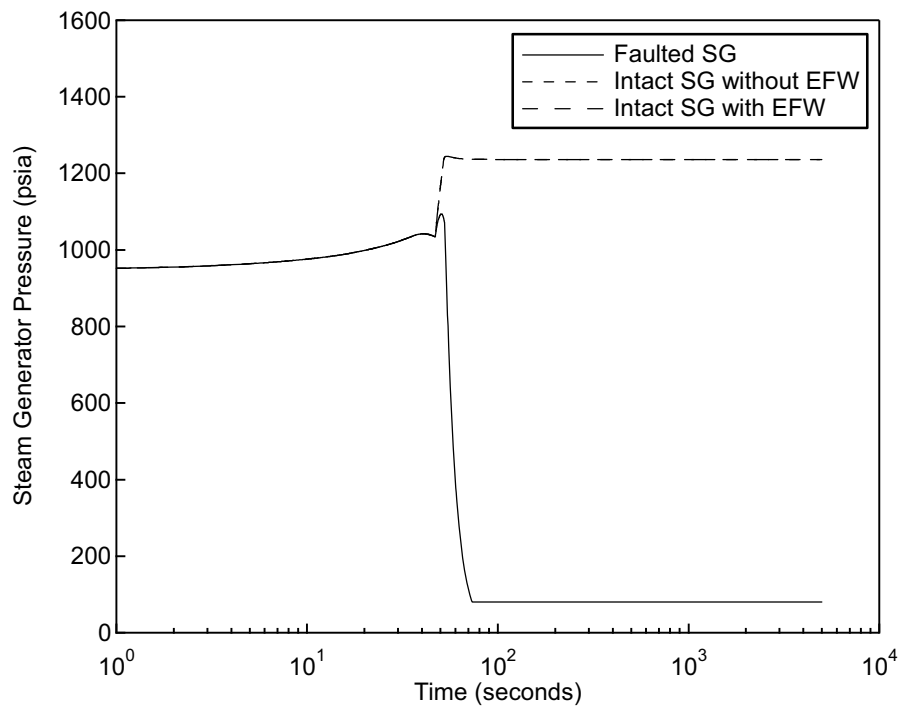


Figure 6.5-6 Steam Generator Pressure versus Time Feedwater System Pipe Break

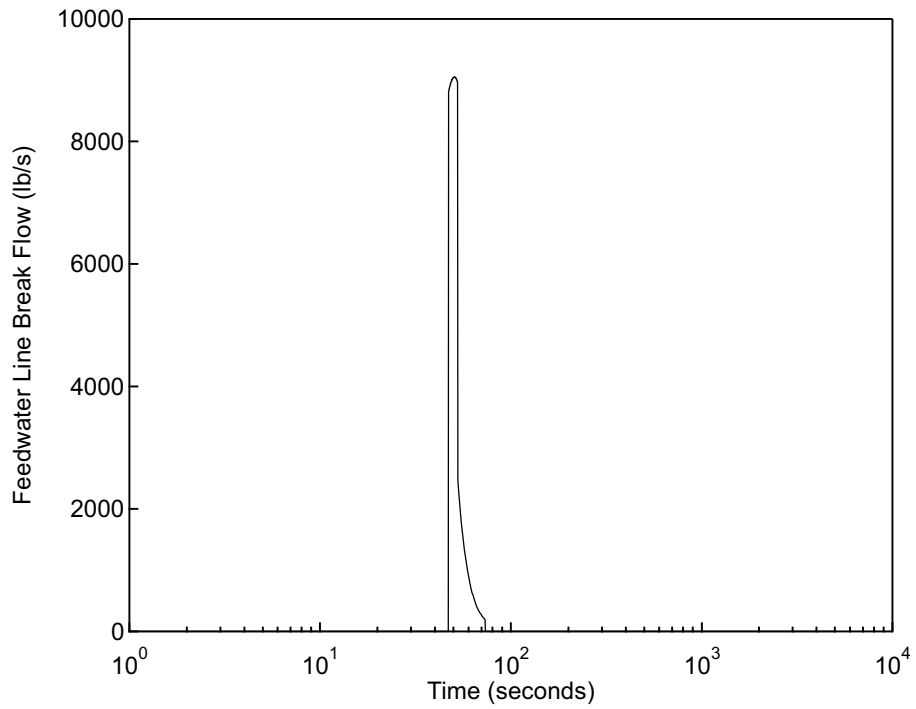


Figure 6.5-7 Feedwater Line Break Flow Rate versus Time Feedwater System Pipe Break

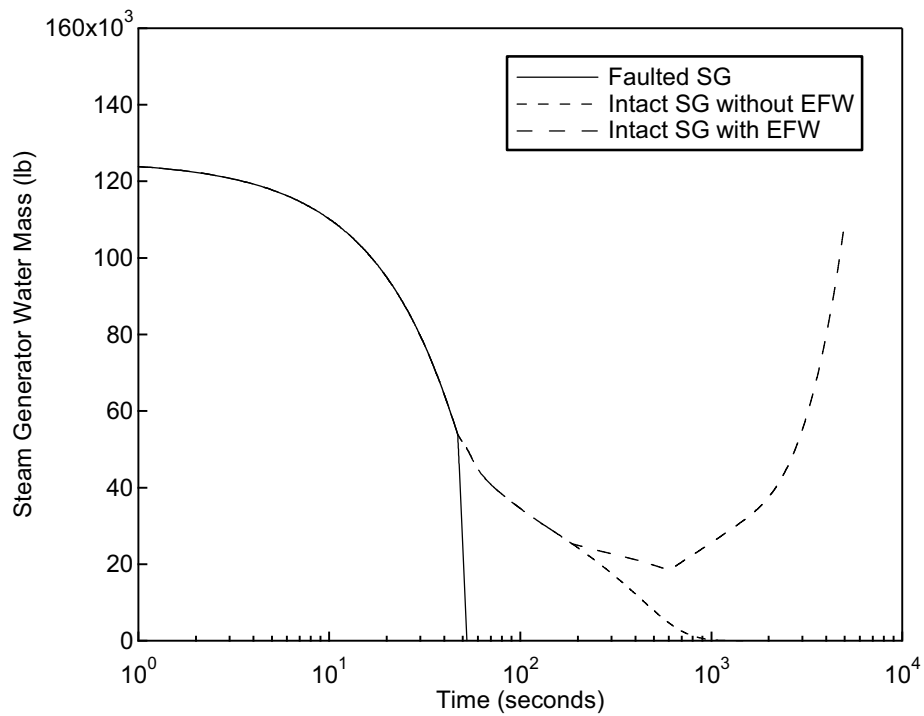


Figure 6.5-8 Steam Generator Water Mass versus Time Feedwater System Pipe Break

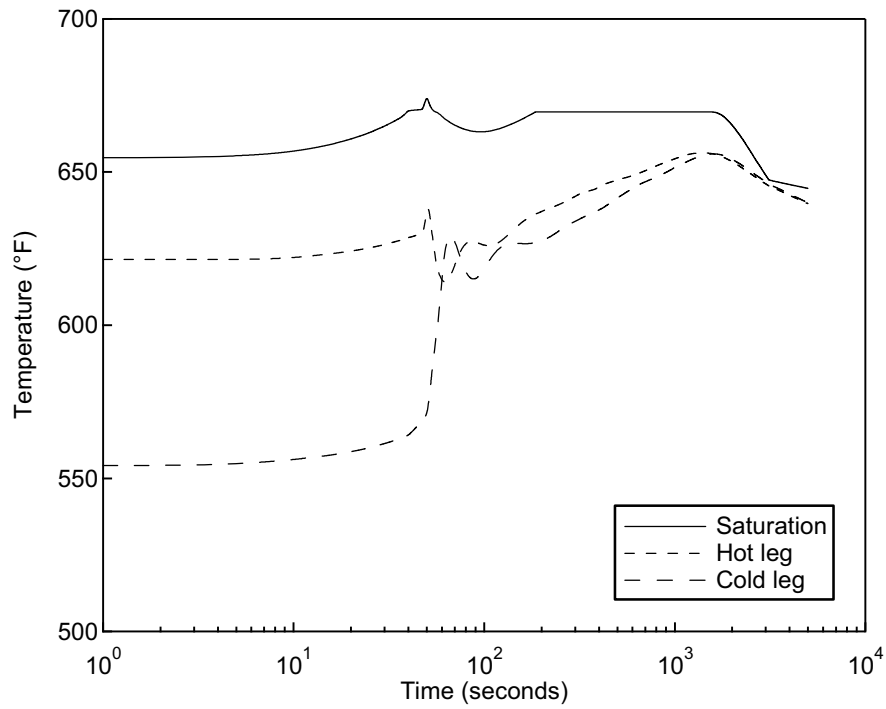


Figure 6.5-9 Temperature versus Time for the Faulted Loop Feedwater System Pipe Break

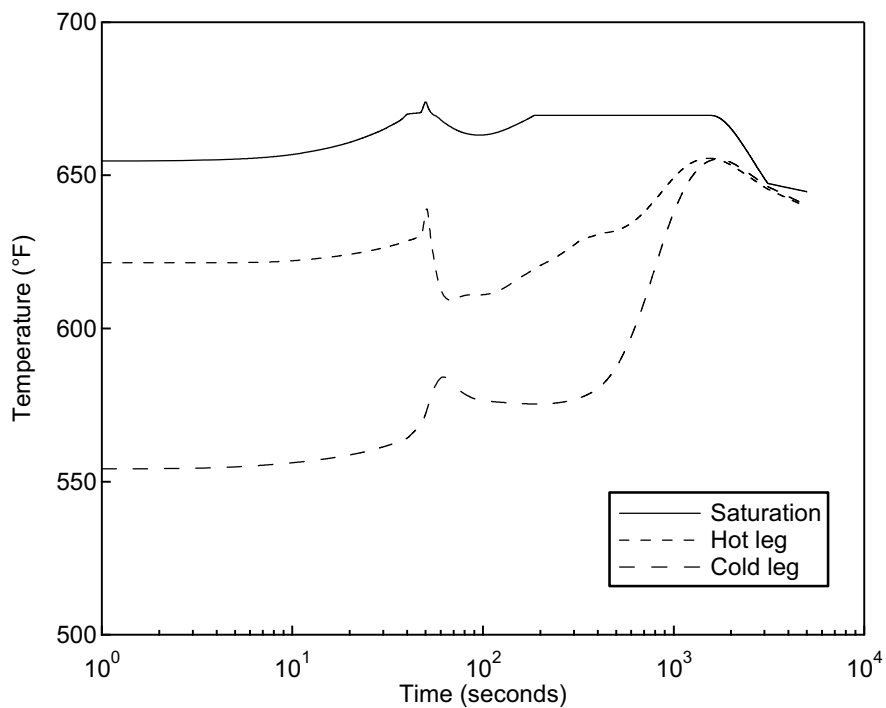


Figure 6.5-10 Temperature versus Time for the Intact Loop without EFW Feedwater System Pipe Break

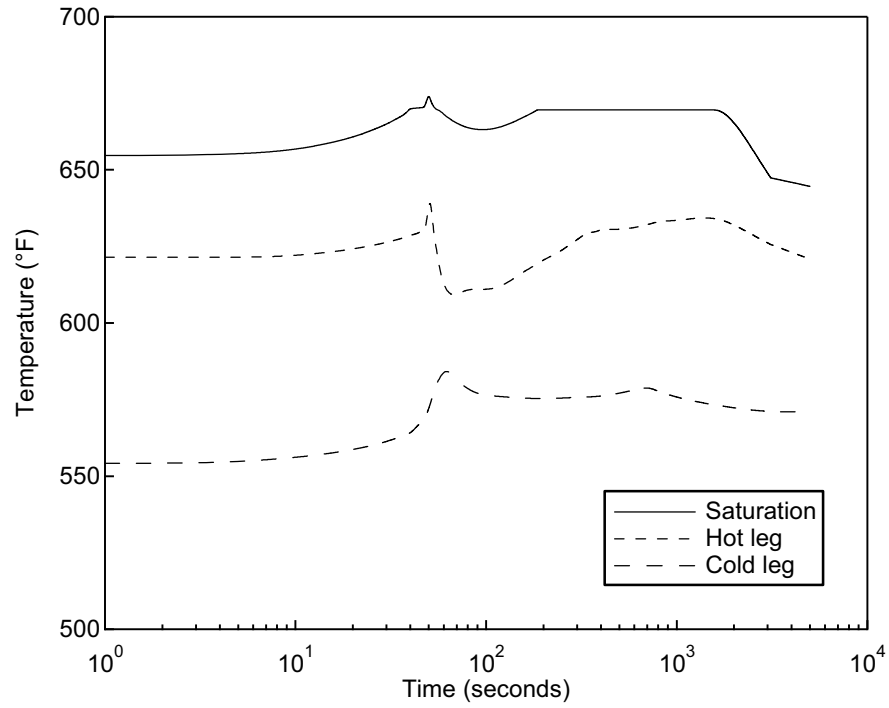


Figure 6.5-11 Temperature versus Time for the Intact Loop with EFW Feedwater System Pipe Break

6.6 Steam Generator Tube Rupture

Event Description

The SGTR event is initiated by a complete severance of a single steam generator U-tube. Leakage of coolant from the primary to secondary side leads to a decrease in the reactor coolant inventory and pressure. The break flow exceeds the makeup capacity of the charging pump causing the pressurizer pressure and level to decrease, leading to a pressurizer pressure low trip.

Events Analyzed

This analysis evaluates the effects of the most limiting SGTR event, which is a double-ended break of a single SG U-tube on the cold leg side just above the tube sheet. The event is terminated when primary-to-secondary leakage stops, which occurs when the RCS pressure is reduced to below the secondary pressure of the ruptured steam generator. Operator action is necessary to recognize the event as a SGTR, terminate ECCS (safety injection), open the pressurizer depressurization valve, isolate the ruptured steam generator, and establish RCS cooling using the main steam relief valves on the intact steam generators to terminate this event. The overall response of the primary and secondary systems is evaluated using the MARVEL-M code.

This event was chosen as one of the six sample analyses because it uses MARVEL-M to model primary-to-secondary coolant flow.

The SGTR is analyzed using different assumptions for the steam generator overflow and the radiological consequence cases. The sample transient analysis presented in this section is for the radiological consequence case.

Analysis Results

Table 6.6-1 presents the sequence of events for the SGTR radiological consequence analysis. Plots of key parameters are presented in Figures 6.6-1 through 6.6-9.

The SGTR is assumed to occur at time = 0. The primary side will exhibit coolant activity during power operation from N-16 and, if present, from fission gap activity as permitted by the Technical Specifications. Following the SGTR, a combination of decreasing pressurizer pressure, decreasing pressurizer level, increasing level in one steam generator, and increased steam line N-16 radioactivity in the same steam generator will alert the operator that a SGTR is in progress as described in Section 5.6. A manual reactor trip is assumed at time = 900 seconds. The pressurizer pressure low reactor trip and over temperature ΔT high trips will protect the DNB limits in the event the manual trip has not occurred.

The primary-to-secondary flow is established by MARVEL-M as described in Section 5.6. When the pressurizer pressure reaches the ECCS setpoint, safety injection will start and deliver flow to the RCS at pressures below the pump shutoff pressure. At time = 1500 seconds, the operators establish secondary cooling with opening the steam generator relief valves in the intact steam generators. As described in Section 5.6, the relief valve on the ruptured steam generator is assumed to fail open and is automatically isolated by the in-line block valve on a pressure signal. At time = 2642 seconds, the operator further reduces primary-to-secondary

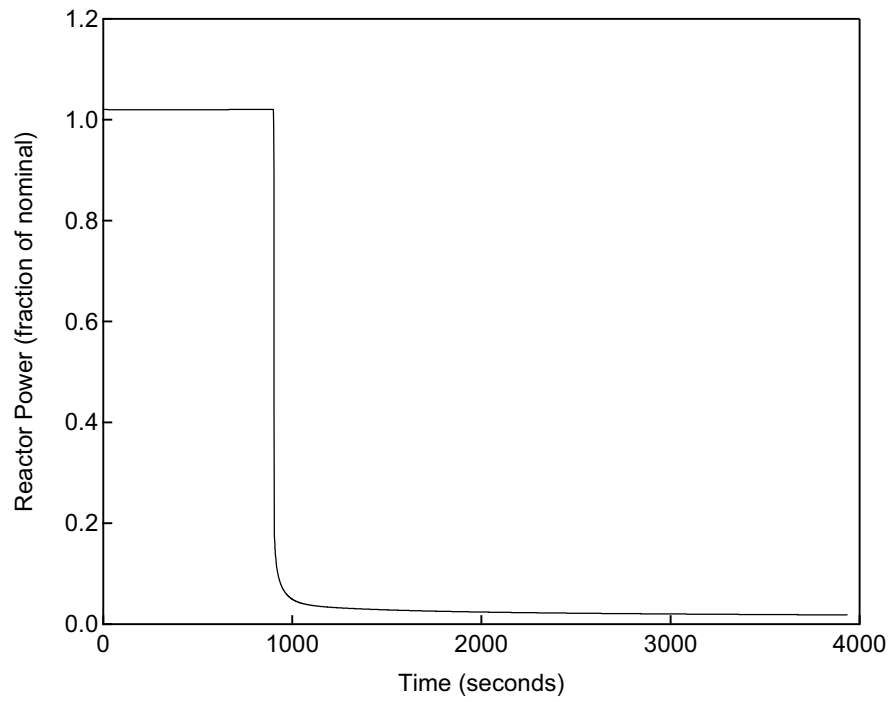
differential pressure by opening the pressurizer depressurization valve based on subcooling margin criteria. The pressurizer depressurization valve is closed when the primary and secondary pressure are equal, which occurs at time = 2972 seconds. At time = 2982 seconds the operator is assumed to have terminated safety injection based on RCS pressure termination criteria. At time = 3934 seconds, the primary pressure is reduced below the ruptured steam generator pressure, and the event is terminated.

Table 6.6-1 Sequence of Events for the SGTR (Radiological Consequence Analysis)

Event	Time (sec)
SG Tube Rupture Occurs	0
Manual Reactor Trip (Rod Motion Begins)	900
Ruptured SG Isolated (EFWS, MSIV)	1200
SG Cooling Established (Intact SGs)	1500
Pressurizer Pressure Low-Low ECCS Analysis Limit Reached	1554
EFWS Pumps Start	1694
Open Pressurizer Depressurization Valve	2642
Close Pressurizer Depressurization Valve	2972
Terminate Safety Injection	2982
Primary Leakage Terminated	3934

Conclusions

This sample analysis is for the radiological release analysis and does not address the acceptance criteria described in Section 4.7. A separate transient for fuel failure analysis and steam generator overfill are not included in this topical report.



**Figure 6.6-1 Reactor Power versus Time
SGTR Radiological Consequence Analysis**

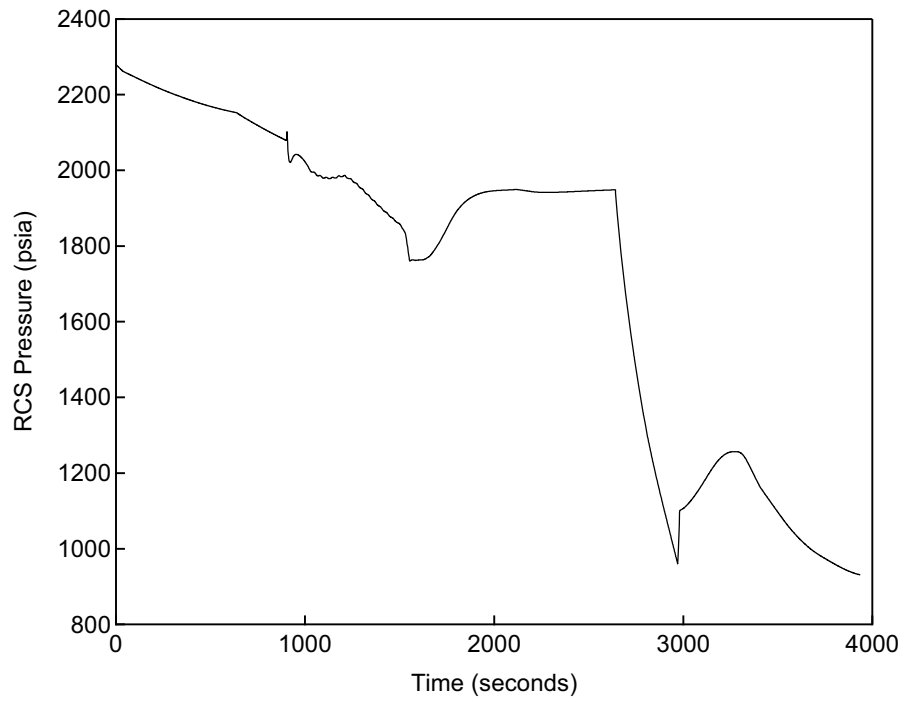


**Figure 6.6-2 RCS Pressure versus Time
SGTR Radiological Consequence Analysis**

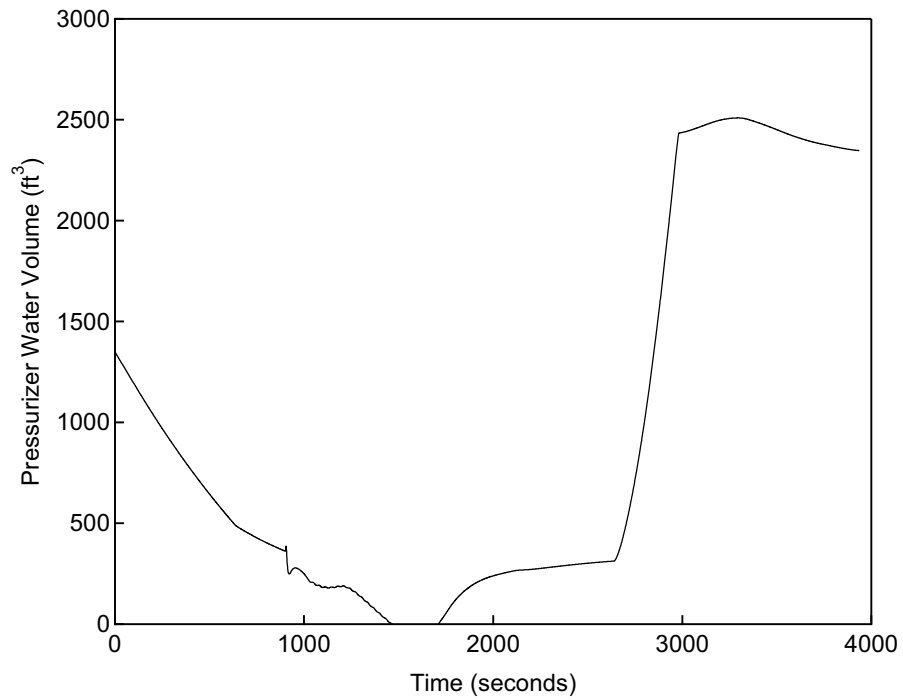


**Figure 6.6-3 Pressurizer Water Volume versus Time
SGTR Radiological Consequence Analysis**

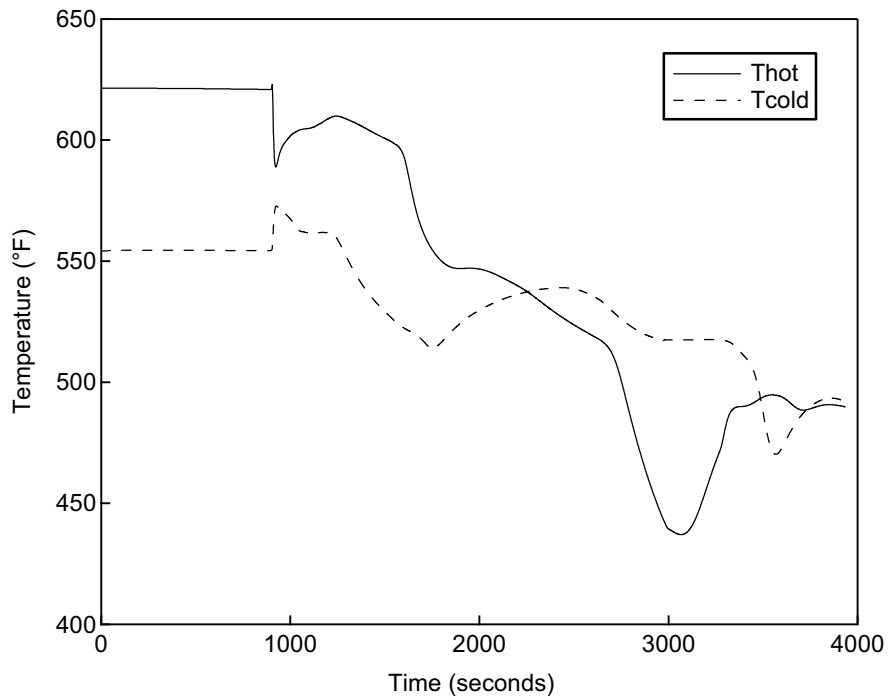


**Figure 6.6-4 Ruptured Loop RCS Temperature versus Time
SGTR Radiological Consequence Analysis**

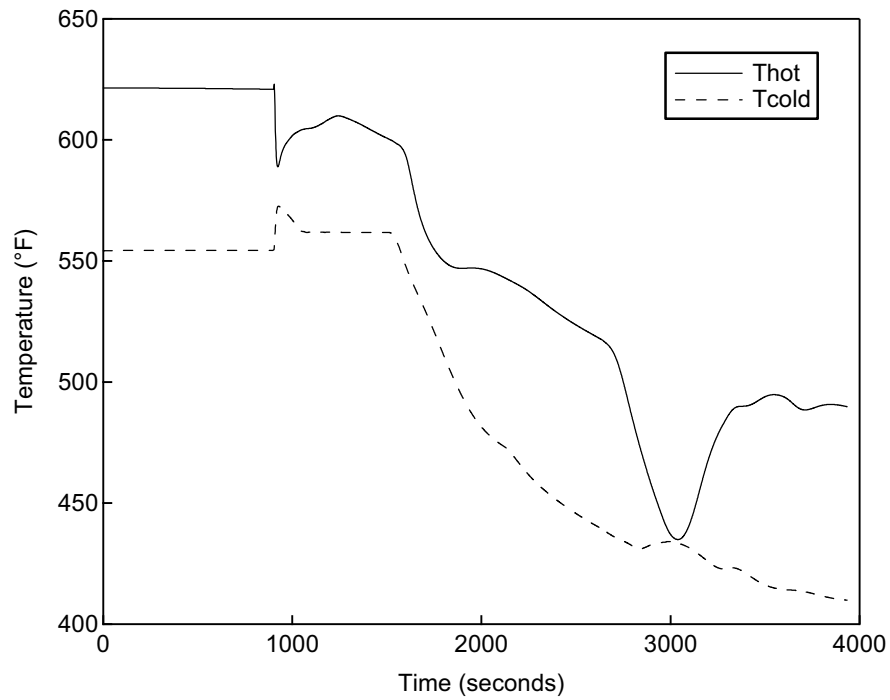


**Figure 6.6-5 Intact Loop RCS Temperature versus Time
SGTR Radiological Consequence Analysis**

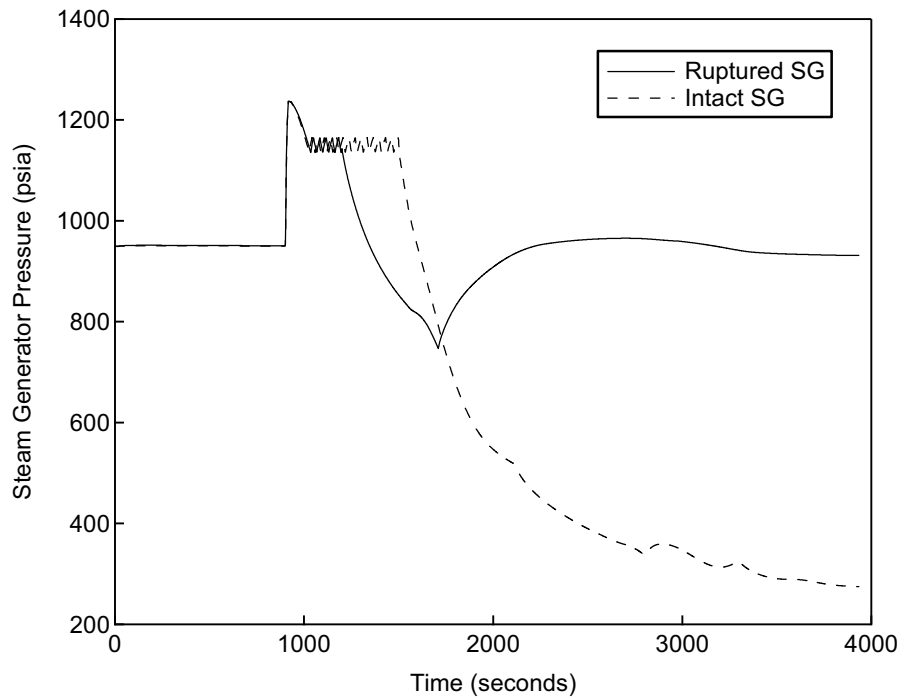


**Figure 6.6-6 Steam Generator Pressure versus Time
SGTR Radiological Consequence Analysis**

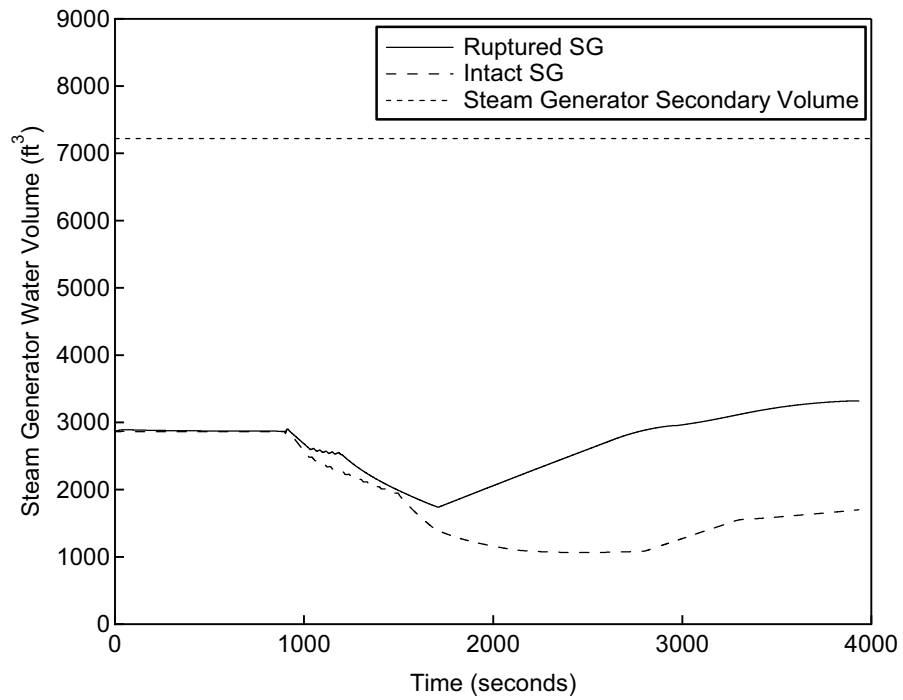


**Figure 6.6-7 Steam Generator Water Volume versus Time
SGTR Radiological Consequence Analysis**

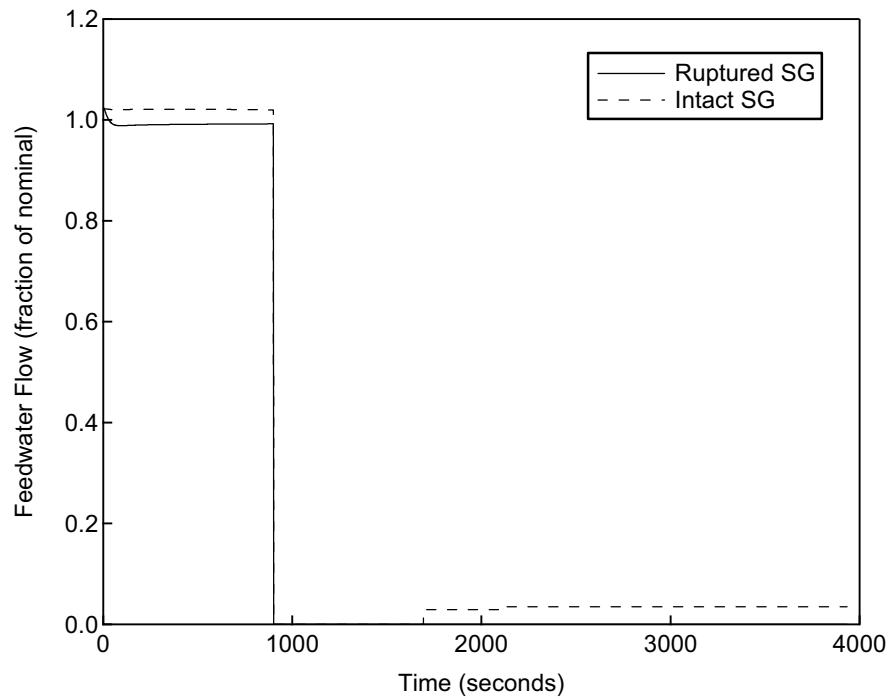


**Figure 6.6-8 Feedwater Flow Rate versus Time
SGTR Radiological Consequence Analysis**

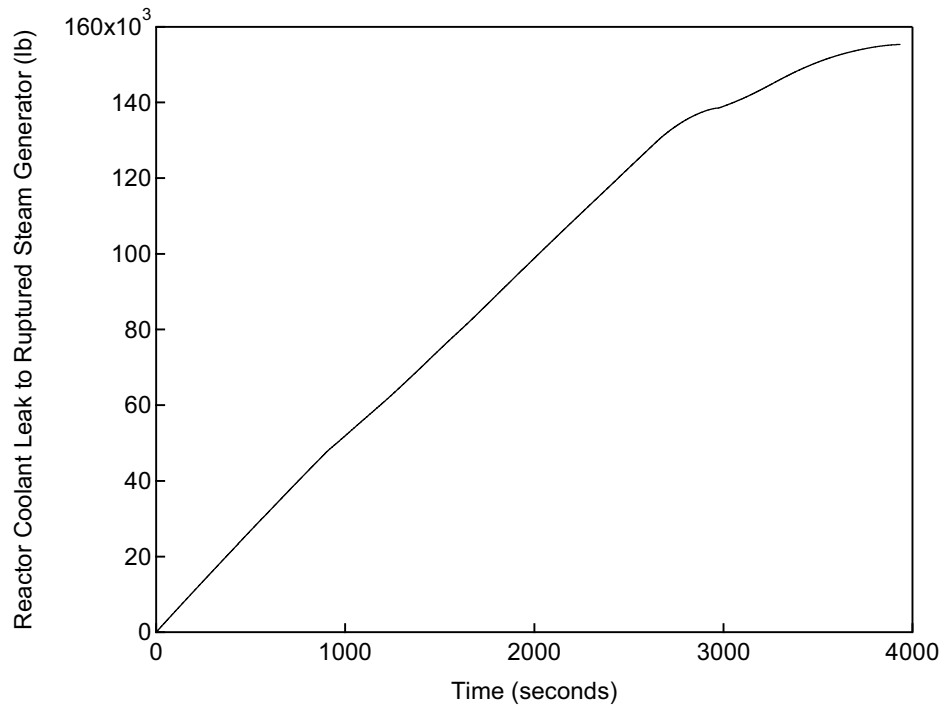


**Figure 6.6-9 Reactor Coolant Leakage versus Time
SGTR Radiological Consequence Analysis**

7.0 CONCLUSIONS

The US-APWR is an advanced PWR design that is functionally similar to existing plants and fuel designs from the perspective of non-LOCA accident analysis. The advanced features of the US-APWR have not created accidents of a different type that are not covered by Chapter 15 of the existing NRC Standard Review Plan, and event classifications and acceptance criteria to be used in the Design Certification License Application have been defined based on existing regulations and regulatory guidance. MHI uses codes and methodologies for non-LOCA analyses of the US-APWR that are similar to NRC-approved codes and methodologies used to evaluate existing plants and fuel. Changes to the codes previously approved by the NRC have been described, justified, and validated by this report.

The codes and methodologies examined were:

- MARVEL-M Plant system transient analysis code
- TWINKLE-M Multi-dimensional neutron kinetics code
- VIPRE-01M Subchannel thermal hydraulics analysis and fuel transient code

The following are confirmed by the analyses in this topical report.

- that the US-APWR responses to various initiating events or conditions are similar to the responses of existing designs and within the range of applicability of MARVEL-M, TWINKLE-M, and VIPRE-01M, and
- that the physical characteristics and phenomena governing the US-APWR responses are similar to those phenomena governing the responses of existing plants.

On the basis of the information in this topical report, it was concluded that the existing codes and methodologies are appropriate for US-APWR analyses. Also, it is concluded that the information provided in this topical report supports its purpose to provide key technical information related to the computer codes, key methods and models and their applicability, event-specific acceptance criteria, and sample results to the NRC during the pre-application phase to facilitate an efficient and timely review of the Design Certification Application.

8.0 REFERENCES

1. "MARVEL-M – A Digital Computer Code for Transient Analysis of a Multi-Loop PWR System", GEN0-LP-480 Rev. 12, Mitsubishi Heavy Industries, October 2010.
2. "TWINKLE-M Input Manual", GEN0-LP-517 Rev. 3, Mitsubishi Heavy Industries, June 2011.
3. D. H. Risher and R. F. Barry, "TWINKLE – A Multi-Dimensional Neutron Kinetics Computer Code", WCAP-7979-P-A (Proprietary), Westinghouse Electric Corporation, January 1975.
4. C. W. Stewart and J. M. Cuta, et al., "VIPRE-01: A Thermal-Hydraulic Code for Reactor Cores, Volume 5 (Revision 4): Guidelines", NP-2511-CCM-A, Electric Power Research Institute (EPRI), February 2001.
5. S. Watanabe, et al, "US-APWR Reactor Vessel Lower Plenum 1/7 Scale Model Flow Test Report", MUAP-07022-P, Mitsubishi Heavy Industries, June 2008.
6. Y. Makino, et al., "Thermal Design Methodology", MUAP-07009-P Rev. 0 (Proprietary) and MUAP-07009-NP Rev. 0 (Non-Proprietary), Mitsubishi Heavy Industries, May 2007.
7. "Quality Assurance Program (QAP) for Design Certification of the US-APWR", PQD-HD-18046-Rev.1, Mitsubishi Heavy Industries, Ltd., 2006.
8. T. Hakata, "Long-Term Transient Analysis Program for Pressurized Reactors (BLKOUT Code)", WCAP-7501, Westinghouse Electric Corporation, July 1970.
9. T. W. T. Burnett, "LOFTRAN Code Description," WCAP-7907-P-A (Proprietary), Westinghouse Electric Corporation, April 1984 and associated NRC approval letter dated July 29, 1983, Cecil O. Thomas (NRC) to E.P. Rahe (Westinghouse), "Acceptance for Referencing of Licensing Topical Reports: WCAP-7907 (P)/(NP) LOFTRAN Code Description; WCAP-7909 (P)/(NP), As Superseded by WCAP-8843 (P)/WCAP-8844 (NP), MARVEL – A Digital Computer Code for Transient Analysis of a Multiloop PWR System".
10. H. G. Hargrove, "FACTRAN – A FORTRAN-IV Code for Thermal Transients in a UO₂ Fuel Rod", WCAP-7908-A, Westinghouse Electric Corporation, December 1989.
11. G. M. Boyd, et.al, "Transient Flow Performance in a Multiloop Nuclear Reactor System", Nucl.Sci.Eng.9 442-454, 1961.
12. "Qualification of Nuclear Design Methodology using PARAGON/ANC", MUAP-07019-P Rev. 0 (Proprietary) and MUAP-07019-NP Rev.0 (Non-Proprietary), December 2007.
13. Y. A. Chao, "SPNOVA – A multidimensional Static and Transient Computer Program for PWR Core Analysis", WCAP-12983-A, Westinghouse Electric Corporation, June 1991.
14. A. J. Friedland, S. Ray, "Revised Thermal Design Procedure", WCAP-11397-P-A, Westinghouse Electric Corporation, April 1989.

-
15. N. Murakami, et al, "Mitsubishi Fuel Design Criteria and Methodology", MUAP-07008-P Rev.2 (Proprietary) and MUAP-07008-NP Rev.2 (Non-Proprietary), Mitsubishi Heavy Industries, July 2010.
 16. Edited by S. L. Davidson, "Reference Core Report VANTAGE 5 Fuel Assembly", WCAP-10444-P-A, Westinghouse Electric Corporation, 1985.
 17. L. S. Tong, "Boiling Crisis and Critical Heat Flux", TID-25887, Atomic Energy Commission, 1972.

Appendix A

Evaluation of MARVEL-M DNBR Calculation Method

This appendix evaluates the method of MARVEL-M DNBR calculation. MARVEL-M interpolates DNBR from DNBR data tables. These tables define the relationship between DNBR, the core inlet temperature, the core pressure and the core heat flux made by VIPRE-01M steady-state calculations. MARVEL-M DNBR result is compared with the DNBR results obtained by VIPRE-01M steady-state calculation for an uncontrolled RCCA bank withdrawal at full power.

Case 1: High reactivity insertion rate at 75 pcm/sec

Case 2: Low reactivity insertion rate at 2.5 pcm/sec

Figure A-1 and A-2 show the MARVEL-M DNBR transient response for Case 1 and Case 2 respectively. MARVEL-M DNBR coincides with the VIPRE-01M DNBR. Therefore, the MARVEL-M is able to calculate DNBR adequately.

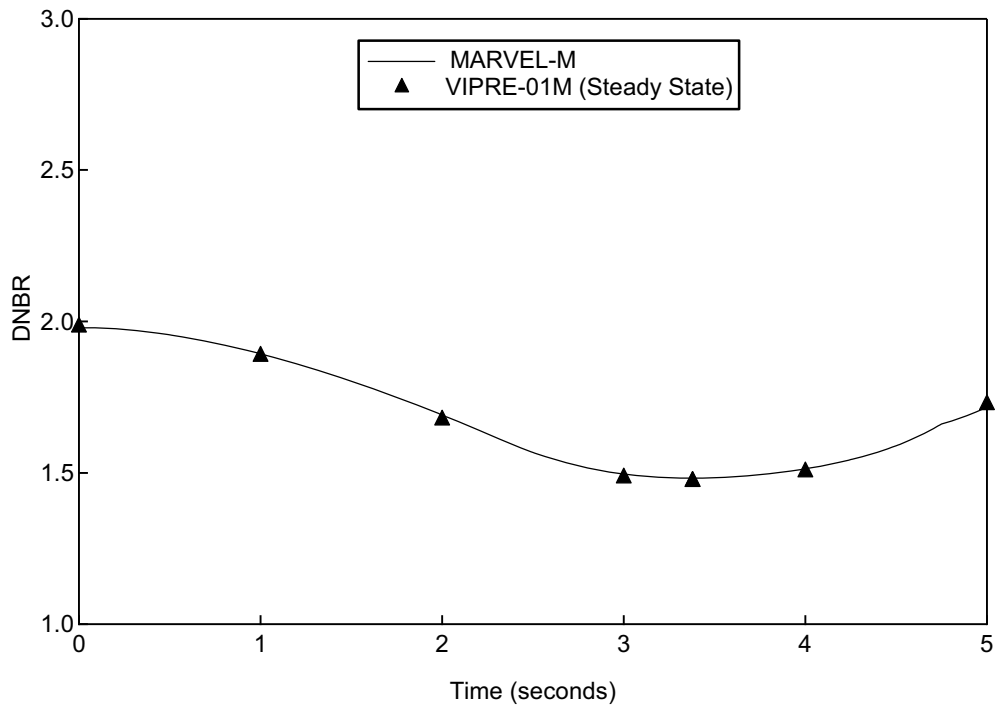


Figure A-1 DNBR Transient, Uncontrolled RCCA Bank Withdrawal at Case 1- Full Power for a High Reactivity Insertion Rate

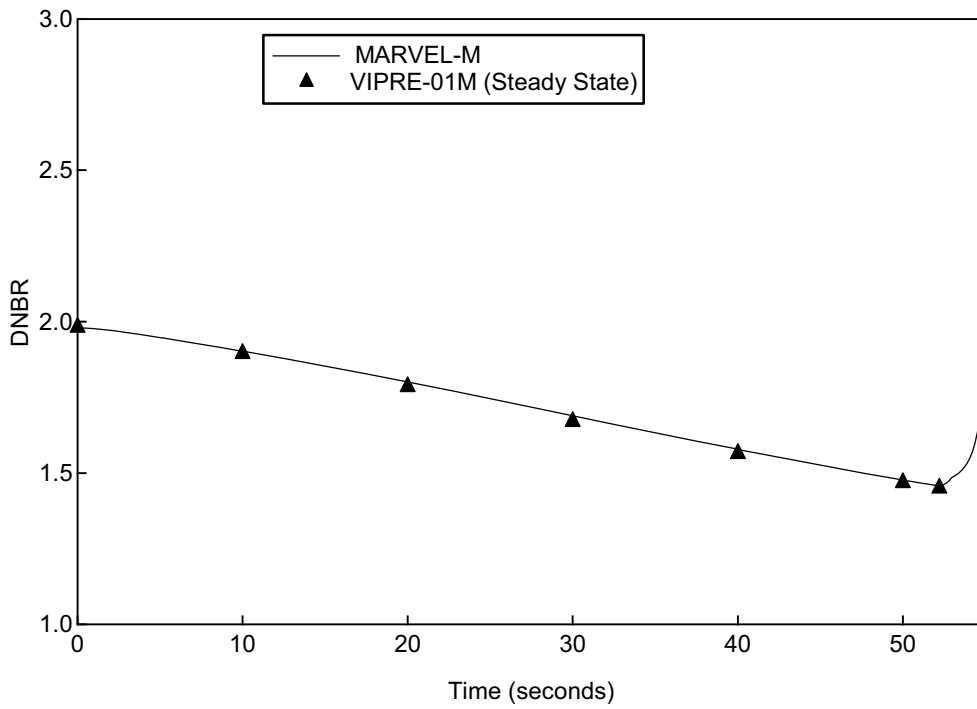


Figure A-2 DNBR Transient, Uncontrolled RCCA Bank Withdrawal at Case 2 - Full Power for a Low Reactivity Insertion Rate

Appendix B

Sensitivity Study of the RCCA Ejection in the 3-D Methodology

Sensitivity Study of the RCCA Ejection in the 3-D Methodology is performed with two key parameters, an ejected reactivity and a hot channel factor, in order to present conservativeness of the MHI RCCA ejection 3-D methodology as described in Section 5.3. The following cases are performed in US-APWR 24 month equilibrium core at the end-of-cycle (EOC).

- Case 1: The ejected reactivity and the hot channel factor are the best estimate which does not include uncertainties.
- Case 2: The ejected reactivity is adjusted to the design limit from the case 1. The design limit includes safety margins and uncertainties.
- Case 3: Conditions of core kinetics are the same as case 2. In the VIPRE-01M calculation, the hot channel factor is adjusted to the design limit.

Note: Other parameters such as delayed neutron fraction, Doppler temperature coefficient and moderator temperature coefficient are the same in three cases.

Table B-1 shows the results of a total maximum fuel enthalpy and a prompt maximum fuel enthalpy rise (adiabatic fuel enthalpy rise) in three cases with these calculation conditions. In the 3-D methodology, a large Doppler feedback effect which consists with a large power peaking factor during transient is expected.

The case 2 and the case 3 have conservative assumptions in the viewpoint of the Doppler feedback effect. In case of the ejected reactivity becomes large, the hot channel factor generally becomes large and the Doppler feedback is expected to be large. However, the case 2 and the case 3 use the same hot channel factor as the case 1 and ignore an increase in effect of the Doppler feedback in the core kinetics. In addition, case 3 has more conservative assumption which is adjusted the maximum hot channel factor to the design limit in the hot spot thermal calculation. This method also ignores an increase in effect of the Doppler feedback.

The case 3 which is licensing case has large conservativeness based on the 3-D methodology and covers uncertainties of parameters and many core variations in the core design.

Table B-1 Calculation Condition and Results of Sensitivity Studies about an Ejected Reactivity and a Hot Channel Factor in the RCCA Ejection

	Case 1	Case 2	Case 3
Reactivity insertion in the TWINKLE-M	600 pcm (Best estimate)	800 pcm ^{*1} (Design limit)	Same as Case 2
Maximum hot channel factor in the TWINKLE-M	27.4 (Best estimate)	Same as Case 1	Same as Case 1
Maximum hot channel factor in the VIPRE-01M	Same as TWINKLE-M ^{*2}	Same as Case 1	35 ^{*3} (Design limit)
Total maximum fuel enthalpy (cal/g)	45.9	68.4	77.8
Prompt maximum fuel enthalpy rise (cal/g) at T_e ^{*4}	18.0	43.5	51.6

*4: Corresponding to one pulse width after the peak of the prompt pulse as shown in Figure B-1

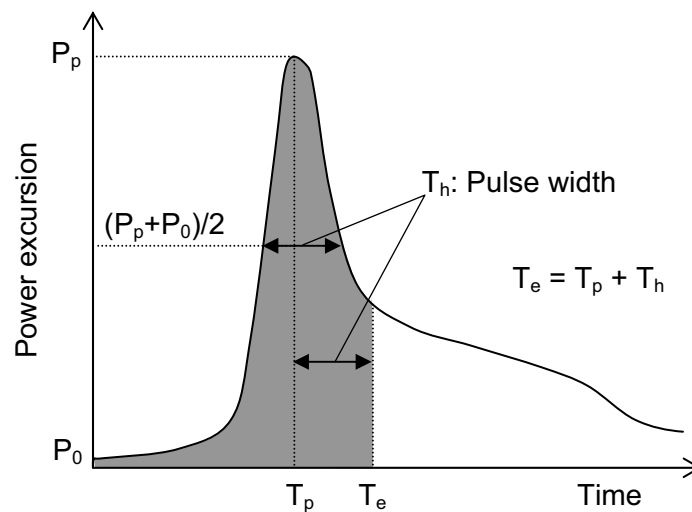


Figure B-1 Definition of the Prompt Maximum Fuel Enthalpy Time

Appendix C

Doppler Weighting Factor of the RCCA Ejection in the 1-D Methodology

A Doppler Weighting Factor (DWF) in the 1-D methodology is used to correct an underestimated effective fuel temperature rise by ignoring an increase in a radial peaking factor. The DWF that is adopted for MHI-designed PWRs is defined as a function of the radial peaking factor (Fxy) as shown in Figure C-1. Conservatism of this DWF is confirmed by the comparison with a 3-D kinetics and a 1-D kinetics results.

Table C-1 shows calculation conditions in US-APWR 24 month equilibrium core at the BOC and EOC. All the key parameters are adjusted to the same condition both in the 3-D and the 1-D analyses. A reactor trip is not simulated to make clear the difference of transient between the 3-D and the 1-D with DWF.

Comparison with the 3-D and the 1-D results of nuclear power transient are shown in Figure C-3 (BOC) and Figure C-4 (EOC). It concludes that the DWF used to the 1-D methodology has a large safety margin during transient.

Table C-1 Calculation Condition of the RCCA Ejection in the Hot Full Power

	BOC (1D / 3D)	EOC (1D / 3D)
Reactivity insertion* ¹ (pcm)	112	138
Effective delayed neutron fraction (%)	0.49	0.44
Prompt neutron lifetime (micro sec.)	8.0	8.0
Doppler temperature coefficient (pcm/°F)	-1.43	-1.65
Average axial power distribution	Figure C-2	Figure C-2
DWF* ²	()	()

*1: External reactivity to prevent the power distribution changes by rod motion

*2: Used in the 1-D methodology only

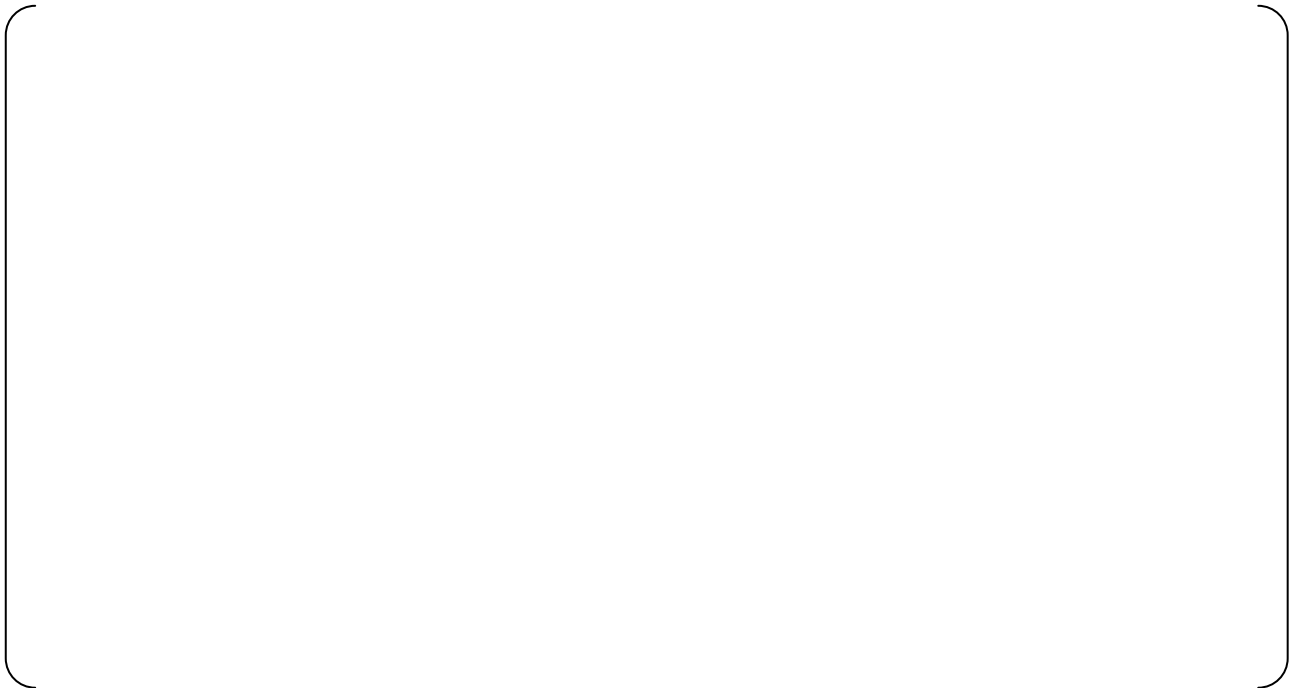


Figure C-1 Radial Doppler Weighting Factor for 1-D Kinetics Analysis

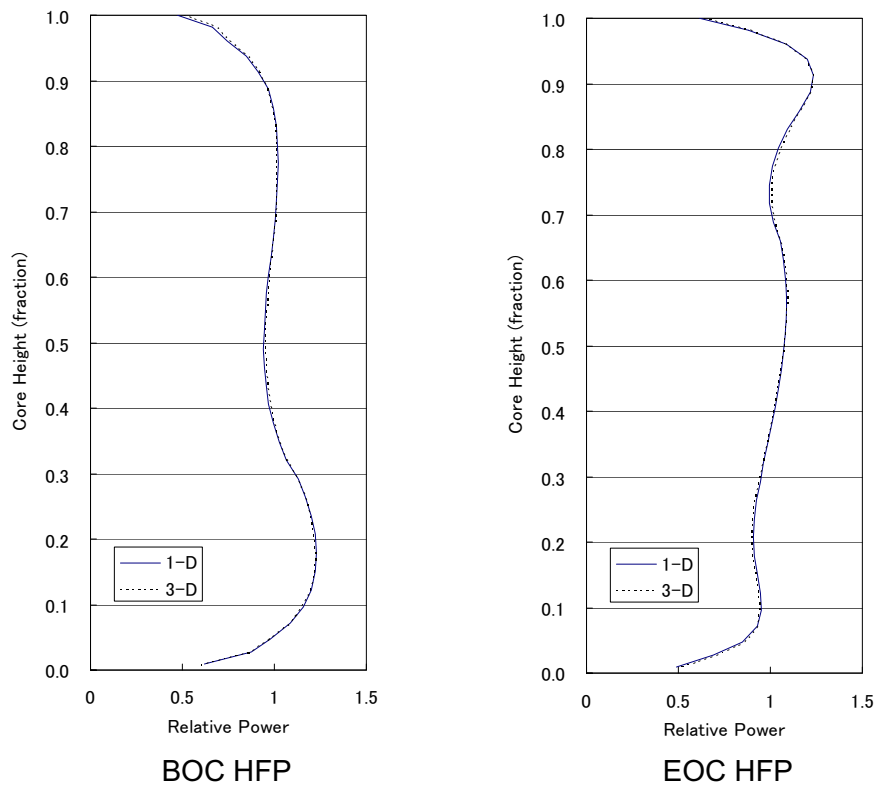


Figure C-2 Average Axial Power Distribution Comparison with 3-D and 1-D (BOC, EOC)

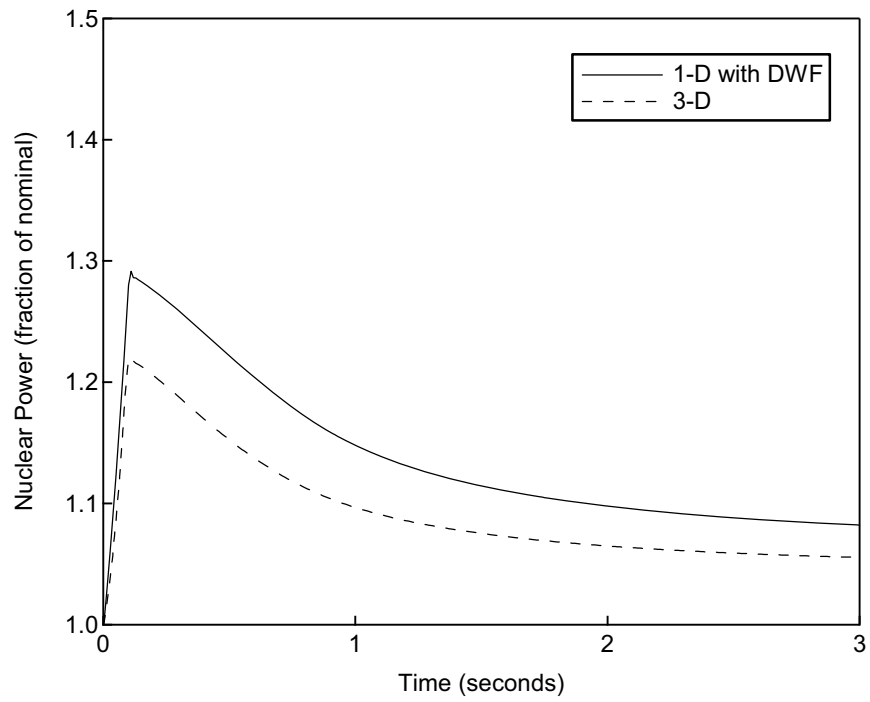


Figure C-3 Nuclear Power versus Time (BOC)
Comparison between 3-D and 1-D with Doppler Weighting Factor

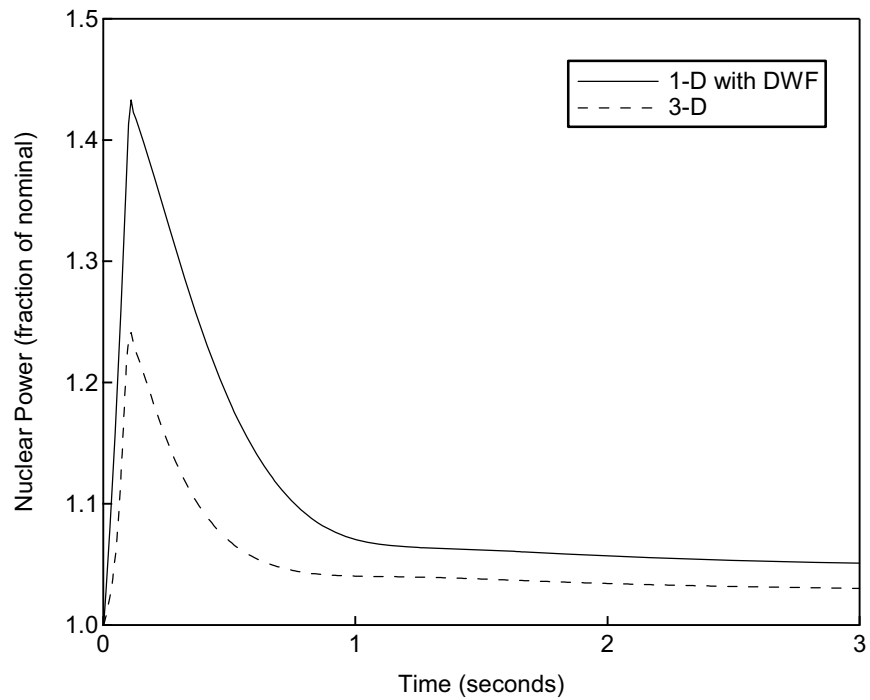


Figure C-4 Nuclear Power versus Time (EOC)
Comparison between 3-D and 1-D with Doppler Weighting Factor

Appendix D

Validation of VIPRE-01M Modeling for Steam System Piping Failure

One-eighth symmetric core model is used in the DNB evaluation for the steam system piping failure. In the model, a hot assembly is assumed to be located in the core center. The core power distribution considering a stuck rod and core inlet temperature distribution are averaged in each of 5 groups, as shown in Figure 5.4-3.

It is confirmed that typical VIPRE-01M analysis model, which has detailed subchannels surrounding the hot channel while the lumped channels represent the remains of the core, can provide sufficiently accurate DNBR [Reference 6]. However the additional study is needed for the applicability of such relatively coarse channel definition and averaged power distribution to the core condition with very steep and asymmetric radial power distribution that may be found in steam system pipe failure event.

The model is validated by comparing with a detailed full core model shown in Figure D-1. Table D-1 shows the calculation model and assumptions. Using a 5-grouped model for a radial power distribution, a detailed power distribution in rod-by-rod is simulated as shown in Figure D-2. Axial distributions of the DNBR and other local fluid parameters at the hot channel in both cases are compared in Figure D-3.

The results show that DNBR evaluated by the both models are in good agreement. The coarse channel definition for the peripherals and the roughly grouped radial power distribution does not affect the prediction of DNBR and other local fluid parameters in the hot channel significantly, in spite of the remarkable radial power distribution. It concludes the one-eighth symmetric core model possesses sufficient calculation accuracy to evaluate the minimum DNBR in the steam system piping failure.

**Table D-1 DNBR Calculation Model and Assumptions
for the Steam System Piping Failure**

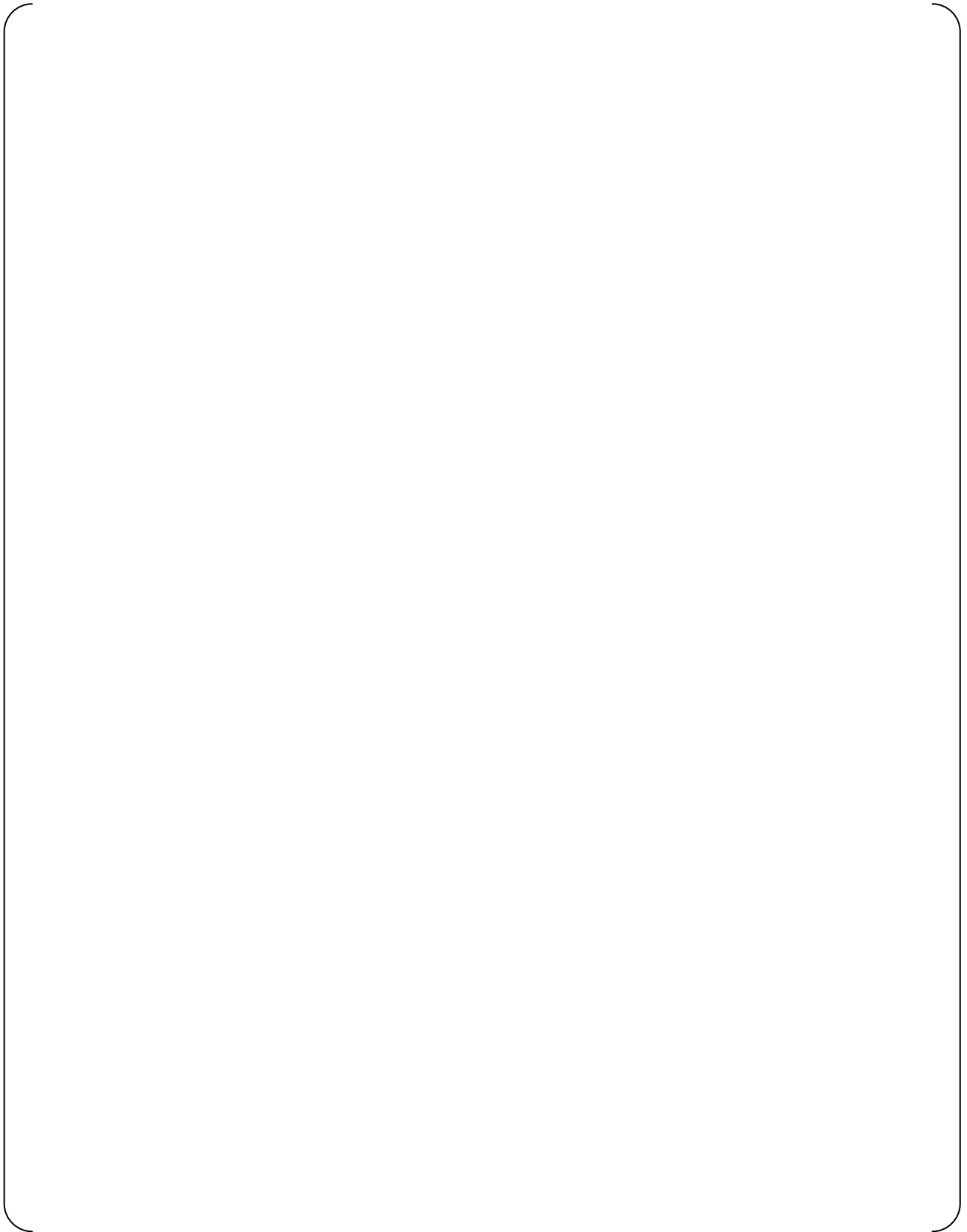


Figure D-1 VIPRE-01M Full Core Analysis Modeling (17x17-257FA Core, 4-Loop Plant)

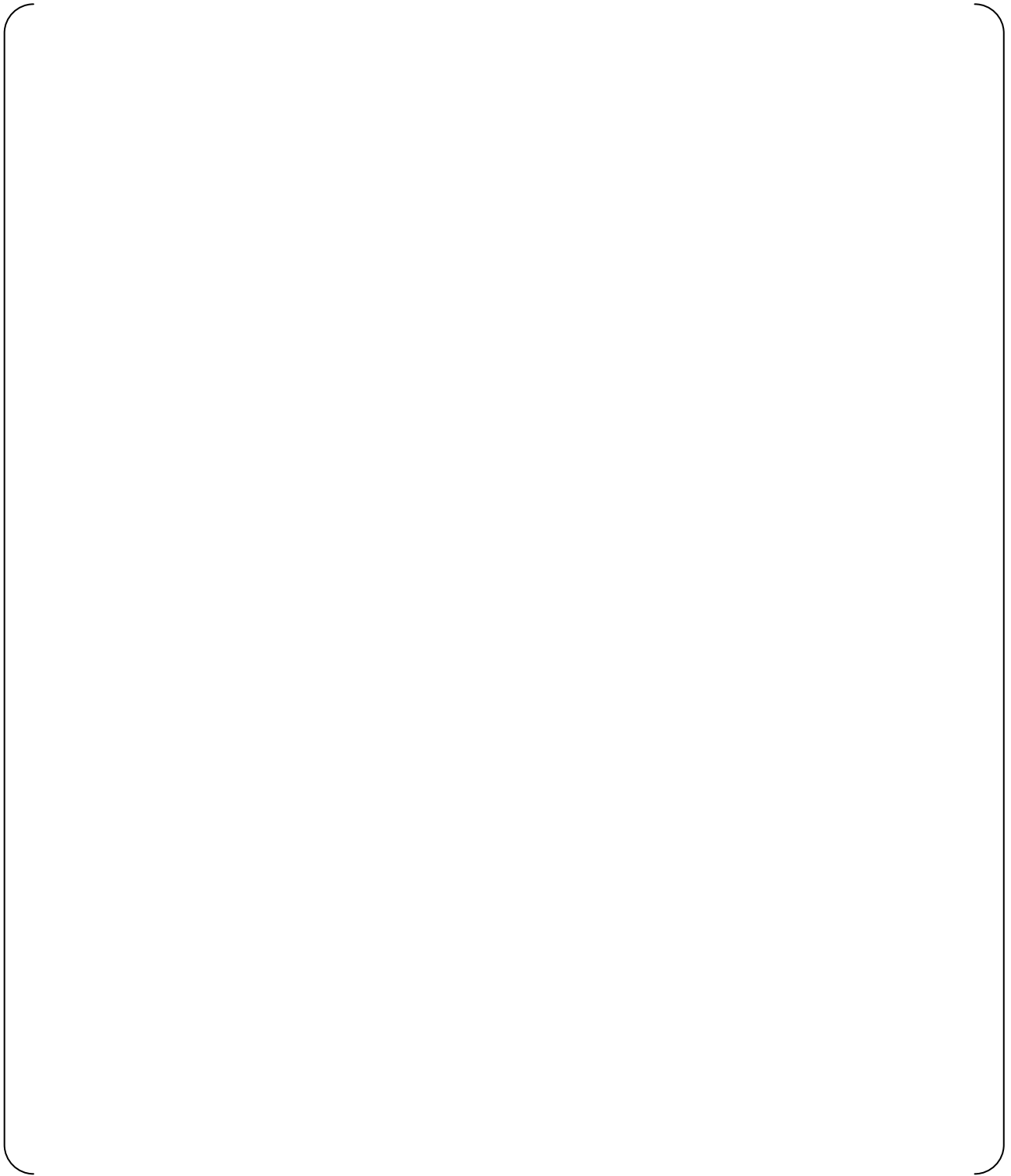


Figure D-2 5-grouped Model for Radial Power Distribution

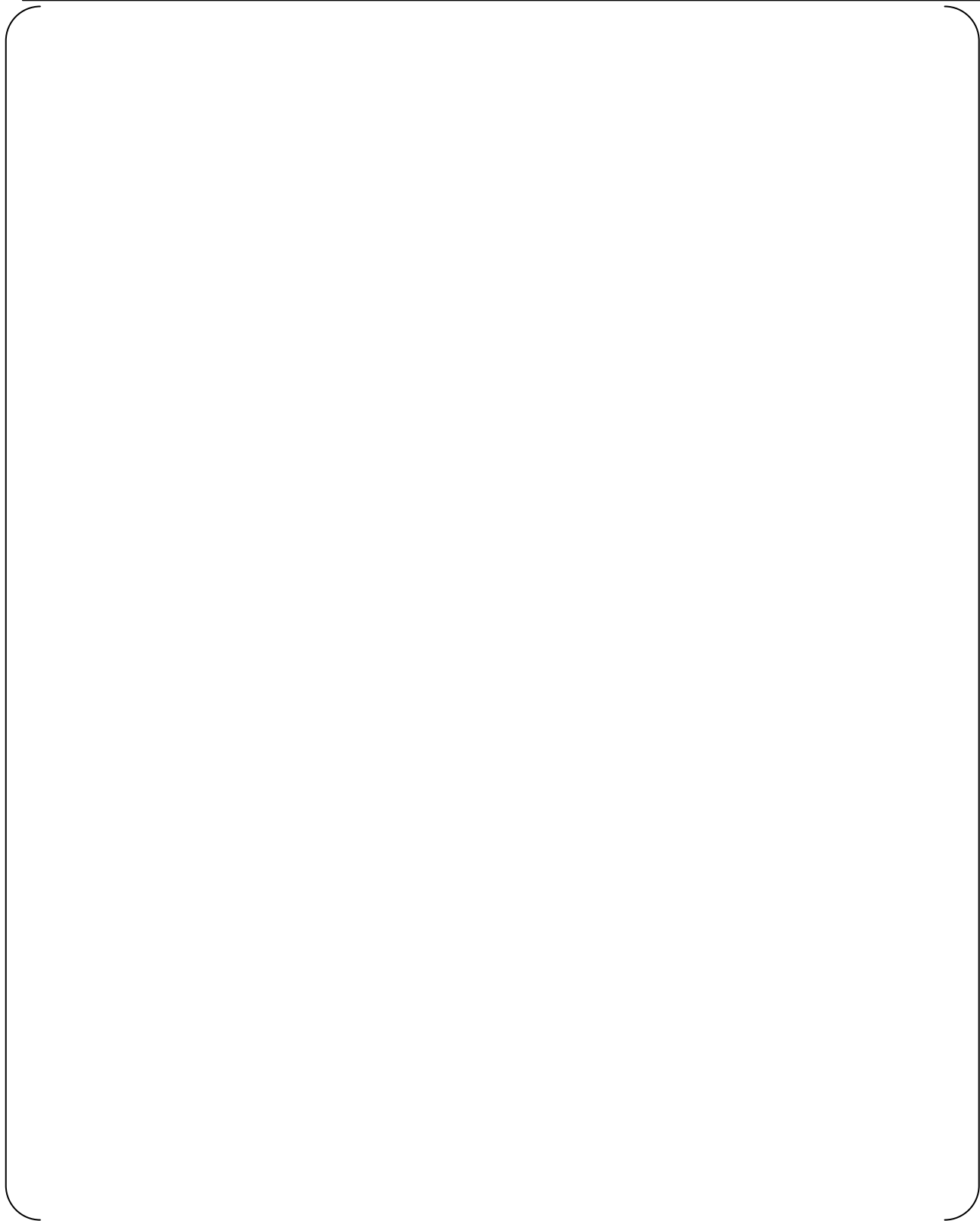


Figure D-3 Comparison of DNBR and Local Fluid Parameters at Hot Channel between the 1/8 Core Model and the Full Core Model

Appendix E

Sensitivity Study of the Inlet Mixing Coefficient for Steam System Piping Failure

The Steam System Piping Failure at hot zero power condition is a transient that is characterized by non-uniform cooling in combination with the assumption that the most reactive control rod be fully withdrawn. The colder inlet temperature at the stuck rod position results in the increase of radial power peaking factor and the decrease of minimum DNBR.

The effect of changes in the vessel inlet mixing factor is shown in Figure E-1. As seen from Figure E-1, assuming no reactor vessel inlet mixing results in a very small reduction in the minimum DNBR and maintains significant margin to the limit.



Figure E-1 DNBR versus Reactor Inlet Mixing for the Steam System Piping Failure

Appendix F

Detailed Break Flow Model for Steam Generator Tube Rupture

This appendix provides a comparison of the conservative break flow model used in the MARVEL-M SGTR analysis with a realistic and more detailed break flow model.

The break flow models applied to licensing analysis and backup analysis

- A simple but conservative break flow model is applied to licensing analysis.
- To indicate the conservatism of this break flow model, its flow is compared to that of the “realistic steam generator tube leak flow model” (realistic model).
- The description of the each model and result of comparison are outlined below.

Description of the conservative break flow model

- The initial break flow rate is calculated conservatively by the Zaloudek correlation applicable to single-phase flow. The conservatism is maintained by adding margin to the value calculated by the Zaloudek correlation.
- The break flow rate in the transient is calculated based on differential pressure of the primary system and secondary system. It is assumed that break flow rate in the transient is proportional to the square root of the differential pressure as following equation.

$$G = G_0 \sqrt{\frac{\Delta P_t}{\Delta P_{nom}}}$$

where

G : Break flow rate

G_0 : initial value of the break flow rate

ΔP_{nom} : Differential pressure between primary and secondary system at initial state

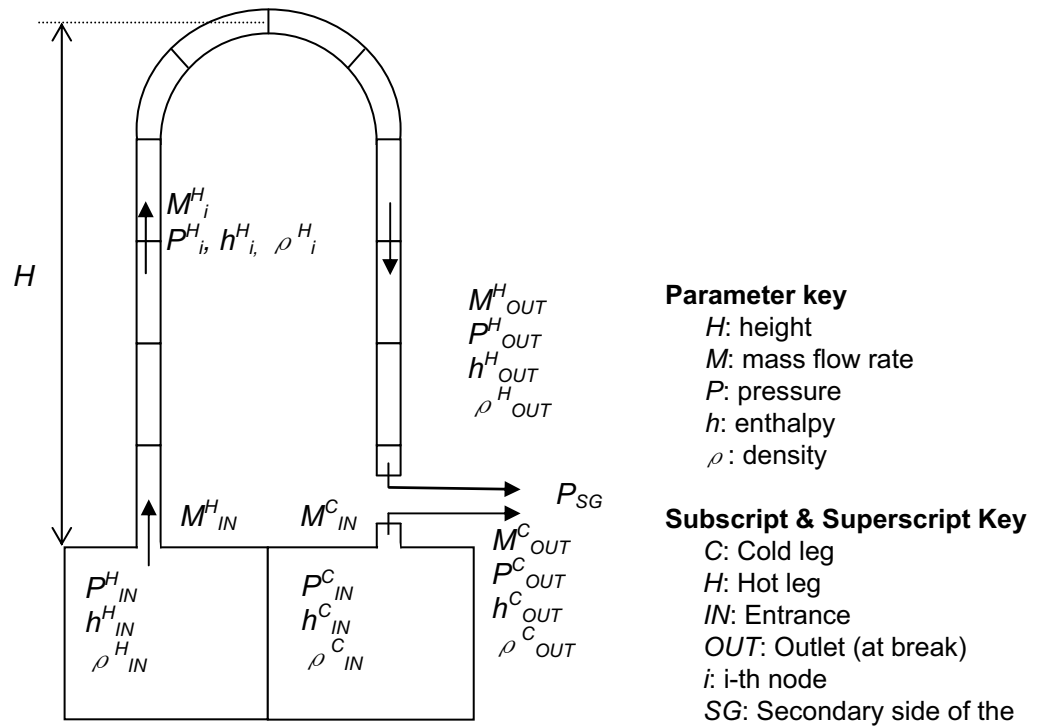
ΔP_t : Differential pressure between primary and secondary system at time = t

Description of the realistic break flow model

- The double ended ruptured SG tube is modeled independently. Also friction loss and resistance due to form losses are considered.
- The conceptual diagram of the realistic model is shown in Figure F-1. For each node, a mass, energy, and momentum balance is performed based on each node's mass flow rate, pressure, enthalpy, and coolant density.

Results of the safety analysis based on each break flow model

- It is assumed that a single tube is ruptured just above the tube sheet of the SG outlet plenum (cold side), because coolant density is the highest at this position in the tube. The type of the rupture is assumed to be a double-ended rupture. For comparison, calculations have also been performed for a rupture just above the tube sheet of the SG inlet plenum (hot side) and a rupture at top of the U-bend. These results are shown in Figure F-2.
- The integrated break flow of the conservative model is larger than that of the realistic model which is evaluated conservatively with discharge coefficient of 1.0 independent of the position of the rupture. Thus, the break flow model applied to licensing analysis is conservative because it bounds the flow predicted by a realistic model using upper-bound assumptions.



- This is sample of rupture just above tube sheet of cold leg.
- The broken tube is modeled independently.

Figure F-1 Realistic Model of the Broken SG Tube



**Figure F-2 Comparison of the Calculation Result for Each Break Flow Model
(Including comparison of the break position)**

Appendix G

Calculation of High Power Range Neutron Flux Reactor Trip for Rod Ejection Event

This appendix provides evaluation methodology for the rod ejection event considering a relationship of an ex-core detector failure and ejected rod location using TWINKLE-M (3D).

G-1: Calculation of Measured Reactor Power

The uncertainty of the high power range neutron flux reactor trip (9%) may not bound the uncertainty of the rod ejection analysis for all possible cases, especially considering the location of the ex-core detectors with respect to the ejected rod. If the ejected rod is located far from the operable ex-core detectors (i.e. near a failed ex-core detector¹), the power increase seen by the operable ex-core detectors may be lower than the average reactor power. MHI evaluated the measured power seen from the ex-core detector for the rod ejection event.

In order to calculate measured reactor power, it is necessary to know the three-dimensional power distribution. The measured power for the rod ejection analysis is calculated according to the following process.

- The initial power level is HFP.
- The burnup is beginning of cycle (BOC) and end of cycle (EOC) of the equilibrium cycle core.
- Ejection from the Rod Insertion Limit (only Bank-D is inserted) is assumed for each burnup. Due to the symmetry of the core, three rod ejection location cases (L9, P14, and R9 rod ejection) represent all of the Bank-D rods. The position of the ex-core detectors relative to control rod Bank-D are shown in Figure G-1.
- A design limit reactivity insertion is assumed for each case (BOC: 110 pcm and EOC: 120 pcm).
- The Doppler feedback is modeled by multiplying the fast absorption cross section for the given change in the calculated fuel effective temperature by a conservative multiplier{ }
- The moderator reactivity feedback is modeled by multiplying the moderator slowing down cross section by a conservative multiplier{ }

$$MP_i(t) = \int P(r,t) \cdot w_i(r) dr / \int P(r,0) \cdot w_i(r) dr$$

Where,
 $MP_i(t)$ is the measured power for detector i at time t
 $P(r,t)$ is the assembly power at location r at time t
 $w_i(r)$ is the detector weighting factor at location r for detector i
 i denotes detector ($i = 1$ to 4)

Note that the denominator ($t=0$) is used to normalize the initial measured power to 1.0. The detector weighting factors are separately calculated based on the geometrical configuration of the core and ex-core detectors using the neutron transport calculation code, DORT.

The ex-core detector ratio is calculated in Step 3. The ex-core detection ratio is defined as the ratio between measured power at the ex-core detector and reactor average power, which can be expressed as

$$E_i(t) = MP_i(t) / RAP(t)$$

Where,
 $E_i(t)$ is the ex-core detection ratio for detector i at time t
 $RAP(t)$ is the reactor average power at time t

The initial ex-core detection ratio is 1.0 from the definition. However, if the power increase in the assemblies located near the ex-core detector is lower than the reactor average power increase, the ex-core detection ratio becomes less than 1.0 (i.e. the ex-core detector sees less than the actual average reactor power).



G-2: High Power Range Neutron Flux Reactor Trip Analytical Limit

The high power range neutron flux reactor trip analytical limit (118%) contains the uncertainty [

)] (The methodology is described in MUAP-09022-P (R2), US-APWR Instrument Setpoint Methodology Technical Report.)





This gives:

$$(\hspace{10em})$$

Therefore, it is appropriate to assume that the high power range neutron flux reactor trip occurs when 2 out of 4 of the measured reactor power channels reach the setpoint (109%) plus $(\hspace{1em})$, that is:

$$(\hspace{10em})$$

Assuming a single failure in one detector¹, the high power range neutron flux reactor trip occurs when the third-highest measured detector power reaches this value.

G-3: Result

Figure G-2 shows the results of the measured (in the third-highest detector) and actual reactor average power for the limiting BOC case. The measured reactor average power reaches $(\hspace{1em})$ within 0.1 seconds.

Note:

- 1) US-APWR DCD Chapter 16 TS LCO 3.3.1 E requires all four channels of power range neutron detectors to be operable. An inoperable channel is required to be placed in trip such that only 1 of the 3 operable detectors would be required to reach the reactor trip setpoint in order for a reactor trip to occur. Therefore, the assumption of an out-of-service detector has no impact on the safety analysis. (This LCO does allow one channel to be bypassed for up to 72 hours for planned bypass and 12 hours for surveillance, testing, and setpoint adjustment; however, these durations are very short compared with the overall operation time.)



Figure G-1 Location of Ex-Core Detectors and Control Rod Bank-D



**Figure G-2 Actual and Measured Reactor Power
Rod Ejection (BOC)**

Appendix H

Summary of MHI's Responses to NRC's Requests for Additional Information

There were many Requests for Additional Information (RAIs) generated during the US-NRC review of MUAP-07010. All of the RAIs on MUAP-07010 are listed in the Table H-1 and Table H-2 below. The actual RAI responses are provided separately as an Attachment.

Table H-1 First Set of MUAP-07010 Historical RAI Responses

RAI Number	Topic	Reference	Related RAI No.
2.1-1	Describe the differences between MARVEL-M 4-loop code and MARVEL 2-loop code.	Ref. 1	
2.1-2	Describe the DNBR model in MARVEL-M.	Ref. 1	2.1-2-1, 2.1-2-2
2.1-3	Provide the comparisons between MARVEL/MARVEL-M.	Ref. 1	
2.1-4	Explain how to deal with homogeneous two-phase flow.	Ref. 1	
2.1-5	Provide the comparisons between mixing models and scaled tests.	Ref. 1	
2.1-6	Provide the methodology for the natural circulation flow modeling.	Ref. 1	
2.1-7	Provide the details of the reactor coolant pump model.	Ref. 1	
2.1-8	Describe the modeling of the overall heat transfer coefficient for the SGs.	Ref. 1	2.1-8-1, 1.5-5, Gen-6
2.1-9	Provide the details of over-temperature ΔT and over-power ΔT trip protection methodologies and specifications.	Ref. 1	
2.1-10	Provide the details of cold leg injection by the safety injection system.	Ref. 1	2.1-10-1
2.1-11	Explain the reason of the changes on the MARVEL-M algorithm for core mixing.	Ref. 1	
2.1-12	Explain how to establish the mixing factors (FMXI).	Ref. 1	
2.1-13	Provide documentation of the 1/7-scale mixing tests.	Ref. 1	2.1-13-1, 1.4-7
2.1-14	Explain how to establish the mixing factors (FMXO).	Ref. 1	
2.1-15	Provide scaled experimental data to determine FMXO.	Ref. 1	
2.1-17	Provide the comparisons between MARVEL-M and scaled experimental data regarding natural circulation flow.	Ref. 1	
2.1-18	Explain the transition to natural circulation depend upon the pump coast down model.	Ref. 1	

Table H-1 First Set of MUAP-07010 Historical RAI Responses

RAI Number	Topic	Reference	Related RAI No.
2.1-20	Explain how to control the usage of "Realistic models" of MARVEL-M.	Ref. 1	
2.2-1	Provide the differences between TWINKLE and TWINKLE-M.	Ref. 1	REA-13
3.1-2	Provide documentation of MARVEL-M/LOFTRAN code comparisons.	Ref. 1	3.1-2-1
3.1-3	Provide the DNBR vs. t for the partial loss of forced reactor coolant flow analyses for both MARVEL-M and LOFTRAN.	Ref. 1	
3.1-4	Provide the DNBR vs. t for the complete loss of forced reactor coolant flow analyses for both MARVEL-M and LOFTRAN.	Ref. 1	
3.1-5	Provide the DNBR vs. t for the partial reactor coolant pump shaft seizure analyses for both MARVEL-M and LOFTRAN.	Ref. 1	
3.2-1	Clarify the introduction of discontinuity factors to TWINKLE-M.	Ref. 1	
3.2-3	Explain the algorithm by which the diffusion coefficient in the reflector is modified.	Ref. 1	3.2-3-1, 3.2-3-2
3.2-4	Explain the differences in modeling Hot Zero Power (HZP) between TWINKLE-M and ANC.	Ref. 1	3.2-4-1
3.2-5	Explain the differences in modeling Hot Full Power (HFP) between TWINKLE-M and ANC.	Ref. 1	3.2-4-1
3.2-6	Provide a comparison of the Doppler coefficient between TWINKLE-M and ANC.	Ref. 1	3.2-6-1
3.2-8	Explain the neutron lifetime given in Table 3.2.2-1(Calculation Condition and Results of the RCCA Ejection).	Ref. 1	3.2-8-1
3.2-9	Explain the delayed neutron fraction calculated for use in TWINKLE-M.	Ref. 1	3.2-9-1
5.2-1	Provide the sensitivity calculations for the complete loss of reactor coolant flow AOO.	Ref. 1	
5.2-2	Provide details of the DNB correlation for the complete loss of reactor coolant flow AOO.	Ref. 1	
5.3-1	Explain the details of the three- and one-dimensional of the REA.	Ref. 1	5.3-1-1, 5.3-1-2, 5.3-1-3
5.3-2	Explain the advantage of using VIPRE-M.	Ref. 1	5.3-2-1, 5.3-2-2, 5.3-2-3
5.3-3	Explain the definition of the hot channel design limit for a transient.	Ref. 1	5.3-3-1
5.3-4	Explain the reason why VIPRE-M doesn't do a single channel calculation.	Ref. 1	
5.3-5	Clarification of TWINKLE-M and VIPRE-01M methodology.	Ref. 1	

Table H-1 First Set of MUAP-07010 Historical RAI Responses

RAI Number	Topic	Reference	Related RAI No.
5.3-6	Verify the symmetric 1/8 core modeled by VIPRE-M.	Ref. 1	5.3-6-1
5.3-7	Explain how the TWINKLE-M one-dimensional model is obtained and how results for the axial power distribution compare with those obtained from a three-dimensional model.	Ref. 1	5.3-7-1, 5.3-7-2
5.3-8	Explain "conservative multiplier" applied for the Doppler feedback.	Ref. 1	
5.3-9	Explain the reason of not using a three-dimensional TWINKLE-M model for the REA analysis at the HFP.	Ref. 1	
5.3-10	Clarify the reactivity insertion curve for the modeling of reactor trip in TWINKLE-M.	Ref. 1	5.3-10-1
5.4-1	Provide the sensitivity calculations for the steam system piping failure.	Ref. 1	
5.4-2	Provide the model of flow mixing in the reactor vessel.	Ref. 1	
5.5-1	Explain the details of the natural circulation model in MARVEL-M for the feedwater system pipe break.	Ref. 1	MSLB-10
5.6-1	Explain the effects of the reactor coolant in the reactor vessel upper head dead volume for the steam generator tube rupture.	Ref. 1	
6.2-1	Clarify the uncertainties of the complete loss of reactor coolant flow AOO.	Ref. 1	
6.3-1	Clarify the ANC code for the rod ejection accident methodology.	Ref. 1	
6.4-1	Explain the effects of the location of the break for the steam system piping failure.	Ref. 1	
6.5-1	Clarify the effects of pressurizer water volume in the feedwater line break analysis.	Ref. 1	
6.6-1	Provide the basis that manual reactor trip is assumed at = 900 seconds	Ref. 1	
App.A-1	Clarification of DNBR model in MARVEL-M.	Ref. 1	
App.E-1	Provide additional comparisons for other AOOs and PAs to substantiate the claim that DNBR is insensitive to the mixing assumptions.	Ref. 1	2.1-13-1
App.F-1	Provide the Zaloudek correlation that MHI has used to perform the steam generator tube rupture break flow calculations.	Ref. 1	App.F-1-1, SGTR-5, SGTR-6
2.1-16	Provide the comparisons between MARVEL-M and pump vendor test data.	Ref. 2	2.1-16-1, 2.1-16-2
3.2-2	Provide additional information which helps validate the code as used at MHI.	Ref. 2	

Table H-1 First Set of MUAP-07010 Historical RAI Responses

RAI Number	Topic	Reference	Related RAI No.
3.2-7	Provide the information to understand why the coarse mesh 2x2 results are in agreement with the 4x4 results.	Ref. 2	3.2-7-1, 3.2-7-2, 3.2-7-3, REA-4
3.2-10	Provide discussion of the effect of axial mesh size on the axial power distribution.	Ref. 2	
5.5-2	Clarify the sensitivity of the feedwater system pipe break calculation.	Ref. 2	
2.1-21	Detail the differences between MARVEL-M and the approved version of MARVEL.	Ref. 3	1.4-6
2.1-22	Describe the limitations of MARVEL-M.	Ref. 3	
2.1-23	Provide the acceptability of utilizing MARVEL-M to analyze many events beyond NRC approved four events.	Ref. 3	
2.2-2	Elaborate further on the development history of TWINKLE-M.	Ref. 3	
2.1-2-1	Confirm the understanding of the DNBR lookup table methodology.	Ref. 4	2.1-2
2.1-2-2	Verify that the DNBR lookup tables cover the full operating space (pressures, temperatures, flow rates) that the methodology is used for.	Ref. 4	2.1-2
2.1-8-1	Provide the bases for the steam generator thermal resistances at nominal conditions.	Ref. 4	2.1-8, 1.5-5
2.1-10-1	Justify why cold leg injection is more conservative.	Ref. 4	2.1-10
2.1-13-1	Clarify the statement "It should also be noted that uniformity in vessel inlet mixing can best be approximated by perfect mixing for very low flows such as during natural circulation conditions. Perfect mixing is assumed for the Steam Generator Tube Rupture event due to natural circulation conditions that exist during most of the event."	Ref. 4	2.1-13, App.E-1
2.1-16-1	Describe or demonstrate that the MARVEL-M's pump model is adequate for the full range of Chapter 15 events.	Ref. 4	2.1-16
2.1-16-2	Explain why the measured and predicted (using MARVEL-M) pump coast down curves are so similar.	Ref. 4	2.1-16
3.1-2-1	Did the Uncontrolled RCCA Bank Withdrawal at Power event have the largest differences between LOFTRAN and MARVEL-M?	Ref. 4	3.1-2
3.2-3-1	Confirm that the approach used in TWINKLE-M modifies the two group diffusion coefficients for both the radial reflector region and two axial reflector regions.	Ref. 4	3.2-3

Table H-1 First Set of MUAP-07010 Historical RAI Responses

RAI Number	Topic	Reference	Related RAI No.
3.2-3-2	Detail the process by which the diffusion coefficient in the reflector is modified before it is input into TWINKLE-M.	Ref. 4	3.2-3
3.2-4-1	Provide further clarification of the responses to RAI 3.2-4 and 3.2-5.	Ref. 4	3.2-4, 3.2-5
3.2-6-1	Comment on the positive Doppler temperature coefficients presented in Table 3.2-6.1(Doppler Temperature Coefficient Comparison with ANC and TWINKLE-M).	Ref. 4	3.2-6
3.2-7-1	Explain the effects of using a finer size in TWINKLE-M.	Ref. 4	3.2-7
3.2-7-2	Describe the time step size used in the TWINKLE-M simulation of the rod ejection accident.	Ref. 4	3.2-7
3.2-7-3	Explain the reason why no adjustment is made of the diffusion coefficient in the reflector region in Figure 3.2-7.6(Average Axial Power Distribution Comparison between ANC and Axial Mesh Sensitivity Cases).	Ref. 4	3.2-7
3.2-8-1	Were the adjustments made to neutron lifetime and delayed neutron fraction adjusted to minimize the difference when changing mesh size?	Ref. 4	3.2-8
3.2-9-1	Explain how the adjustments made in the responses to RAIs 3.2-7 through 3.2-9 relate to the way in which analysis is generally done with TWINKLE-M.	Ref. 4	3.2-9
5.3-1-1	Do operating procedures allow for fully or partially inserted misaligned or inoperable control rods and if so, was this taken into account in the analysis of the design limit?	Ref. 4	5.3-1
5.3-1-2	Does TWINKLE-M use the identical configuration (geometry and mesh) as ANC for the three-dimensional model?	Ref. 4	5.3-1
5.3-1-3	Explain the impact on the analysis of the approximation.	Ref. 4	5.3-1
5.3-2-1	Explain what information is used by VIPRE-M to analyze the hot channel.	Ref. 4	5.3-2
5.3-2-2	Describe the assumed place of the ejected rod in VIPRE-M model.	Ref. 4	5.3-2
5.3-2-3	Clarify the third sentence of the second paragraph in response to RAI 5.3-2.	Ref. 4	5.3-2

Table H-1 First Set of MUAP-07010 Historical RAI Responses

RAI Number	Topic	Reference	Related RAI No.
5.3-3-1	Confirm this understanding of the hot channel design limit, mathematically describe the hot channel factor, uncertainty and safety margin, and explain how the uncertainty and safety margin are applied to the design limit.	Ref. 4	5.3-3
5.3-6-1	Follow-up to RAI5.3-6.	Ref. 4	5.3-6
5.3-7-1	Provide diffusion coefficients and delayed neutron data.	Ref. 4	5.3-7
5.3-7-2	Provide additional information for RAI 5.3-7.	Ref. 4	5.3-7
5.3-10-1	Explain the statement that the trip reactivity is the design limit.	Ref. 4	5.3-10
App.F-1-1	Provide additional validation for the "modified Zaloudek" correlation.	Ref. 4	App.F-1
3.1-6	Present validation data of MARVEL-M for the steam generator tube rupture event.	Ref. 4	
3.1-7	Give the history of the version of LOFTRAN used in MARVEL-M validation.	Ref. 4	
3.1-8	Does MARVEL-M share any significant algorithms, numerical methods or correlations with the version of LOFTRAN used for the comparison?	Ref. 4	
App.E-2	Show the scale on the vertical axis of Figure E-1 (DNBR versus Reactor Inlet Mixing for the Steam System Piping Failure).	Ref. 4	MSLB-10

Table H-2 Second Set of MUAP-07010 Historical RAI Responses

RAI Number	Topic	Reference	Related RAI No.
RAI 1		Ref. 5	1.6-1
RAI 2		Ref. 5	
RAI 3		Ref. 5	
RAI 4		Ref. 5	
Gen-1		Ref. 6	
Gen-2		Ref. 6	
Gen-3		Ref. 6	Gen-3-1
Gen-4		Ref. 6	
Gen-5		Ref. 6	Gen-5-1
Gen-6		Ref. 6	2.1-8, Gen-6-1
Gen-7		Ref. 6	Gen-5-1
1.1-1		Ref. 6	1.1-1-1
1.1-2		Ref. 6	
1.1-3		Ref. 6	1.1-4
1.1-4		Ref. 6	1.1-3
1.1-5		Ref. 6	
1.1-6		Ref. 6	
1.2-1		Ref. 6	1.2-4, 1.2-5
1.2-2		Ref. 6	
1.2-3		Ref. 6	
1.2-4		Ref. 6	1.2-1, 1.2-5
1.2-5		Ref. 6	1.2-1, 1.2-4

Table H-2 Second Set of MUAP-07010 Historical RAI Responses

RAI Number	Topic	Reference	Related RAI No.
1.2-6		Ref. 6	
1.2-7		Ref. 6	
1.2-8		Ref. 6	
1.3-1		Ref. 6	
1.3-2		Ref. 6	
1.3-3		Ref. 6	
1.3-4		Ref. 6	1.3-4-1, 1.3-4-1-1
1.3-5		Ref. 6	
1.3-6		Ref. 6	1.3-6-1, 1.3-6-1-1
1.3-7		Ref. 6	1.3-9
1.3-8		Ref. 6	
1.3-9		Ref. 6	1.3-7, 1.3-9-1
1.3-10		Ref. 6	
1.3-11		Ref. 6	
1.3-12		Ref. 6	1.3-12-1
1.3-13		Ref. 6	
1.3-14		Ref. 6	1.3-14-1, 1.3-15
1.3-15		Ref. 6	1.3-14
1.3-16		Ref. 6	1.3-16-1
1.3-17		Ref. 6	
1.3-18		Ref. 6	
1.4-1		Ref. 6	
1.4-2		Ref. 6	
1.4-3		Ref. 6	
1.4-4		Ref. 6	
1.5-1		Ref. 6	
1.5-2		Ref. 6	
1.5-3		Ref. 6	
1.5-4		Ref. 6	

Table H-2 Second Set of MUAP-07010 Historical RAI Responses

RAI Number	Topic	Reference	Related RAI No.
1.5-5		Ref. 6	2.1-8, 2.1-8-1, 1.5-5-1, 1.5-5-1-1
1.5-6		Ref. 6	
1.5-7		Ref. 6	1.5-7-1
1.5-8		Ref. 6	1.5-8-1, 1.5-8-1-1
1.5-9		Ref. 6	
1.5-10		Ref. 6	1.5-10-1
1.5-11		Ref. 6	
1.5-12		Ref. 6	1.5-12-1
1.5-13		Ref. 6	1.5-13-1
1.6-1		Ref. 6	1.6-1-1, 1.6-1-1-1, RAI 1
1.6-2		Ref. 6	1.6-2-1
1.6-3		Ref. 6	
1.6-4		Ref. 6	1.6-4-1
1.6-5		Ref. 6	1.6-5-1
1.6-6		Ref. 6	1.6-6-1
1.6-7			1.6-9
1.6-8		Ref. 6	
1.6-9		Ref. 6	1.6-7, 1.6-10

Table H-2 Second Set of MUAP-07010 Historical RAI Responses

RAI Number	Topic	Reference	Related RAI No.
1.6-10		Ref. 6	1.6-9
1.7-1		Ref. 6	1.7-1-1, 1.7-1-1-1, RAI 2
1.7-2		Ref. 6	
1.7-3		Ref. 6	
1.7-4		Ref. 6	
1.7-5		Ref. 6	
1.7-6		Ref. 6	
1.7-7		Ref. 6	
1.7-8		Ref. 6	
1.7-9		Ref. 6	
1.8-1		Ref. 6	1.8-1-1, 1.8-3, RAI 7
1.8-2		Ref. 6	RAI 3
1.8-3		Ref. 6	1.8-1
1.8-4		Ref. 6	
1.8-5		Ref. 6	1.8-1-1, 1.8-7
1.8-6		Ref. 6	1.8-6-1, 1.8-6-1-1
1.8-7		Ref. 6	1.8-5

Table H-2 Second Set of MUAP-07010 Historical RAI Responses

RAI Number	Topic	Reference	Related RAI No.
1.8-8		Ref. 6	
1.10-1		Ref. 6	
2.1-1		Ref. 6	
2.1-2		Ref. 6	2.1-2-1, 2.1-2-2
2.3-1		Ref. 6	
2.3-2		Ref. 6	
2.3-3		Ref. 6	
3.1-1		Ref. 6	
4.1-1		Ref. 6	
Gen-3-1		Ref. 7	Gen-3
Gen-5-1		Ref. 7	Gen-5, Gen-7

Table H-2 Second Set of MUAP-07010 Historical RAI Responses

RAI Number	Topic	Reference	Related RAI No.
1.1-1-1		Ref. 7	1.1-1
1.3-4-1		Ref. 7	1.3-4, 1.3-4-1-1
1.3-6-1		Ref. 7	1.3-6, 1.3-6-1-1
1.3-9-1		Ref. 7	1.3-9
1.3-12-1		Ref. 7	1.3-12, CLOF-5
1.3-16-1		Ref. 7	1.3-16
1.5-5-1		Ref. 7	1.5-5, 1.5-5-1-1
1.5-7-1		Ref. 7	1.5-7, 1.5-8-1, 1.5-8-1-1

Table H-2 Second Set of MUAP-07010 Historical RAI Responses

RAI Number	Topic	Reference	Related RAI No.
1.5-8-1		Ref. 7	1.5-7-1, 1.5-8, 1.5-8-1-1
1.5-10-1		Ref. 7	1.5-10
1.5-12-1		Ref. 7	1.5-12
1.5-13-1		Ref. 7	1.5-13
1.6-1-1		Ref. 7	1.6-1, 1.6-1-1-1, 1.6-6-1
1.6-2-1		Ref. 7	1.6-2, 1.6-4-1
1.6-4-1		Ref. 7	1.6-2-1, 1.6-4
1.6-5-1		Ref. 7	1.6-5

Table H-2 Second Set of MUAP-07010 Historical RAI Responses

RAI Number	Topic	Reference	Related RAI No.
1.6-6-1		Ref. 7	1.6-1-1, 1.6-6
1.7-1-1		Ref. 7	1.7-1, 1.7-1-1-1
1.8-1-1		Ref. 7	1.8-1, 1.8-5
1.8-2-1		Ref. 7	
1.8-6-1		Ref. 7	1.8-6, 1.8-6-1-1
1.2-9		Ref. 7	1.2-9-1
1.3-19		Ref. 7	
1.3-20		Ref. 7	
1.4-5		Ref. 7	MSLB-7
1.4-6		Ref. 7	2.1-21
1.4-7		Ref. 7	2.1-13
1.4-8		Ref. 7	

Table H-2 Second Set of MUAP-07010 Historical RAI Responses

RAI Number	Topic	Reference	Related RAI No.
4.1-2		Ref. 7	
4.1-3		Ref. 7	
4.1-4		Ref. 7	
Gen-1		Ref. 7	
Gen-2		Ref. 7	
Gen-3		Ref. 7	Gen-3-1
Gen-4		Ref. 7	
Gen-5		Ref. 7	Gen-5-1
Gen-6		Ref. 7	2.1-8, Gen-6-1
Gen-7		Ref. 7	Gen-5-1
Gen-8		Ref. 7	
MSLB-1		Ref. 7	MSLB-1-1
MSLB-2		Ref. 7	
MSLB-3		Ref. 7	MSLB-4, MSLB-5

Table H-2 Second Set of MUAP-07010 Historical RAI Responses

RAI Number	Topic	Reference	Related RAI No.
MSLB-4		Ref. 7	MSLB-3
MSLB-5		Ref. 7	MSLB-3
MSLB-6		Ref. 7	RAI 5
MSLB-7		Ref. 7	1.4-5, MSLB-7-1, RAI 5
MSLB-8		Ref. 7	
MSLB-9		Ref. 7	
MSLB-10		Ref. 7	5.5-1, App.E-2, RAI 5
MSLB-11		Ref. 7	
MSLB-12		Ref. 7	MSLB-12-1
MSLB-13		Ref. 7	
MSLB-14		Ref. 7	MSLB-14-1, MSLB-15

Table H-2 Second Set of MUAP-07010 Historical RAI Responses

RAI Number	Topic	Reference	Related RAI No.
MSLB-15		Ref. 7	MSLB-14
MSLB-16		Ref. 7	MSLB-16-1, RAI 6
MSLB-17		Ref. 7	
LOL-1		Ref. 7	
SGTR-1		Ref. 7	
SGTR-2		Ref. 7	SGTR-5, SGTR-6
SGTR-3		Ref. 7	
SGTR-4		Ref. 7	
FWLB-1		Ref. 7	
FWLB-2		Ref. 7	
FWLB-3		Ref. 7	
CLOF-1		Ref. 7	

Table H-2 Second Set of MUAP-07010 Historical RAI Responses

RAI Number	Topic	Reference	Related RAI No.
CLOF-2		Ref. 7	
CLOF-3		Ref. 7	
CLOF-4		Ref. 7	
CLOF-5		Ref. 7	1.3-12-1
1.3-4-1-1		Ref. 8	1.3-4, 1.3-4-1
1.3-6-1-1		Ref. 8	1.3-6, 1.3-6-1
1.5-5-1-1		Ref. 8	1.5-5, 1.5.5-1
1.5-8-1-1		Ref. 8	1.5-7-1, 1.5-8, 1.5-8-1

Table H-2 Second Set of MUAP-07010 Historical RAI Responses

RAI Number	Topic	Reference	Related RAI No.
1.6-1-1-1		Ref. 8	1.6-1, 1.6-1-1
1.7-1-1-1		Ref. 8	1.7-1, 1.7-1-1
1.8-2-1-1		Ref. 8	
1.8-6-1-1		Ref. 8	1.8-6, 1.8-6-1, RAI 7
1.2-9-1		Ref. 8	
1.3-14-1		Ref. 8	1.3-14
Gen-6-1		Ref. 8	Gen-6

Table H-2 Second Set of MUAP-07010 Historical RAI Responses

RAI Number	Topic	Reference	Related RAI No.
MSLB-1-1		Ref. 8	MSLB-1
MSLB-7-1		Ref. 8	MSLB-7, MSLB-16-1, RAI 5
MSLB-12-1		Ref. 8	MSLB-12, RAI 5
MSLB-14-1		Ref. 8	MSLB-14
MSLB-16-1		Ref. 8	MSLB-16, MSLB-7-1, MSLB-18, RAI 6
SGTR-5		Ref. 8	App.F-1, SGTR-2, SGTR-6
SGTR-6		Ref. 8	App.F-1, SGTR-2, SGTR-5
FWLB-4		Ref. 8	

Table H-2 Second Set of MUAP-07010 Historical RAI Responses

RAI Number	Topic	Reference	Related RAI No.
FWLB-5		Ref. 8	
MSLB-18		Ref. 8	MSLB-16-1
MSLB-19		Ref. 8	
MSLB-20		Ref. 8	
Non-LOCA Confirmatory Analysis		Ref. 9, Ref. 11	
RAI 1		Ref. 10	1.6-1
RAI 2		Ref. 10	1.7-1
RAI 3		Ref. 10, Ref. 12	1.8-2
RAI 4		Ref. 10	

Table H-2 Second Set of MUAP-07010 Historical RAI Responses

RAI Number	Topic	Reference	Related RAI No.
RAI 5		Ref. 10	MSLB-6, MSLB-7, MSLB-7-1, MSLB-10, MSLB-12-1
RAI 6		Ref. 10	MSLB-16, MSLB-16-1
RAI 7		Ref. 10	1.8-1, 1.8-6-1-1
REA-1		Ref. 13	REA-9
REA-2		Ref. 13	REA-10
REA-3		Ref. 13	
REA-4		Ref. 13	3.2-7, REA-6, REA-7, REA-11

Table H-2 Second Set of MUAP-07010 Historical RAI Responses

RAI Number	Topic	Reference	Related RAI No.
REA-5		Ref. 13	REA-11
REA-6		Ref. 13	REA-4
REA-7		Ref. 13	REA-4
REA-8		Ref. 14	REA-12
REA-9		Ref. 15	REA-1
REA-10		Ref. 15	REA-2
REA-11		Ref. 15, Ref. 18	REA-4, REA-5

Table H-2 Second Set of MUAP-07010 Historical RAI Responses

RAI Number	Topic	Reference	Related RAI No.
REA-12		Ref. 15, Ref. 17	REA-8
REA-13		Ref. 16	2.2-1

References for Tables H-1 and H-2

1. Letter, Yoshiki Ogata (MHI) to Jeffrey A. Ciocco (USNRC), "MHI's Response to NRC's Request for Additional Information on US-APWR Topical Report MUAP-07010-P, Non-LOCA Methodology", UAP-HF-08141, August 22, 2008.
2. Letter, Yoshiki Ogata (MHI) to Jeffrey A. Ciocco (USNRC), "MHI's 2nd Response to NRC's Request for Additional Information on US-APWR Topical Report MUAP-07010-P, Non-LOCA Methodology", UAP-HF-08170, September 11, 2008.
3. Letter, Yoshiki Ogata (MHI) to Jeffrey A. Ciocco (USNRC), "MHI's 3rd Response to NRC's Requests for Additional Information on US-APWR Topical Report: Non-LOCA Methodology, MUAP-07010-P", UAP-HF-08245, November 12, 2008.
4. Letter, Yoshiki Ogata (MHI) to Jeffrey A. Ciocco (USNRC), "MHI's 4th Response to NRC's Requests for Additional Information on US-APWR Topical Report: Non-LOCA Methodology, MUAP-07010-P", UAP-HF-09040, February 12, 2009.
5. Letter, Yoshiki Ogata (MHI) to Jeffrey A. Ciocco (USNRC), "MHI's Non-LOCA Response to NRC's Requests for Additional Information on Topical Reports MUAP-07010, MUAP-07011, and MUAP-07013", UAP-HF-09099, March 24, 2009.
6. Letter, Yoshiki Ogata (MHI) to Jeffrey A. Ciocco (USNRC), "MHI's 5th Response to NRC's Requests for Additional Information on US-APWR Topical Report: Non-LOCA Methodology, MUAP-07010-P", UAP-HF-09358, July 10, 2009.
7. Letter, Yoshiki Ogata (MHI) to Jeffrey A. Ciocco (USNRC), "MHI's 6th, 7th and 8th Responses to NRC's Requests for Additional Information on US-APWR Topical Report: Non-LOCA Methodology, MUAP-07010-P (R0)", UAP-HF-10001, January 7, 2010.
8. Letter, Yoshiki Ogata (MHI) to Jeffrey A. Ciocco (USNRC), "MHI's 9th and 10th Responses to NRC's Requests for Additional Information on US-APWR Topical Report: Non-LOCA Methodology, MUAP-07010-P (R0)", UAP-HF-10101, May 10, 2010.
9. Letter, Yoshiki Ogata (MHI) to Jeffrey A. Ciocco (USNRC), "MHI's 11th Response to NRC's Request for Additional Information on US-APWR Topical Report: Non-LOCA Methodology, MUAP-07010-P (R0) (6th Topical Report RAI)", UAP-HF-10195, July 8, 2010.
10. Letter, Yoshiki Ogata (MHI) to Jeffrey A. Ciocco (USNRC), "MHI's 12th Response to NRC's Requests for Additional Information on US-APWR Topical Report: Non-LOCA Methodology, MUAP-07010-P (R0)", UAP-HF-10226, August 4, 2010.
11. Letter, Yoshiki Ogata (MHI) to Jeffrey A. Ciocco (USNRC), "MHI's Revised 11th Response to NRC's Request for Additional Information on US-APWR Topical Report: Non-LOCA Methodology, MUAP-07010-P (R0) (6th Topical Report RAI)", UAP-HF-10227, August 4, 2010.

12. Letter, Yoshiki Ogata (MHI) to Jeffrey A. Ciocco (USNRC), "MHI's Revised 12th Response to NRC's Request for Additional Information on US-APWR Topical Report: Non-LOCA Methodology, MUAP-07010-P (R0)", UAP-HF-10268, October 5, 2010.
13. Letter, Yoshiki Ogata (MHI) to Jeffrey A. Ciocco (USNRC), "MHI's 13th Response to NRC's Requests for Additional Information on US-APWR Topical Report: Non-LOCA Methodology, MUAP-07010-P (R1)", UAP-HF-11005, January 14, 2011.
14. Letter, Yoshiki Ogata (MHI) to Jeffrey A. Ciocco (USNRC), "MHI's 14th Response to NRC's Request for Additional Information on US-APWR Topical Report: Non-LOCA Methodology, MUAP-07010-P (R1)", UAP-HF-11118, April 22, 2011.
15. Letter, Yoshiki Ogata (MHI) to Jeffrey A. Ciocco (USNRC), "MHI's 15th Response to NRC's Request for Additional Information on US-APWR Topical Report: Non-LOCA Methodology, MUAP-07010-P (R1)", UAP-HF-11129, April 28, 2011.
16. Letter, Yoshiki Ogata (MHI) to Jeffrey A. Ciocco (USNRC), "MHI's 16th Response to NRC's Request for Additional Information on US-APWR Topical Report: Non-LOCA Methodology, MUAP-07010-P (R1)", UAP-HF-11200, June 30, 2011.
17. Letter, Yoshiki Ogata (MHI) to Jeffrey A. Ciocco (USNRC), "MHI's Revised 15th Response to NRC's Request for Additional Information on US-APWR Topical Report: Non-LOCA Methodology, MUAP-07010-P (R1)", UAP-HF-11264, August 12, 2011.
18. Letter, Yoshiki Ogata (MHI) to Jeffrey A. Ciocco (USNRC), "2nd Revision to MHI's 15th Response to NRC's Requests for Additional Information on US-APWR Topical Report: Non-LOCA Methodology, MUAP-07010-P (R1)", UAP-HF-12120, May 11, 2012.

Reference 1

UAP-HF-08141
Docket No. 52-021

MHI's Response to NRC's Request for Additional Information on
US-APWR Topical Report MUAP-07010-P, Non-LOCA Methodology

August 2008

RAI 2.1-1

The evolution of MARVEL-M 4-loop code from the MARVEL 2-loop code was discussed. Please provide details of the significant modeling changes between the two codes.

Response

Section 2.1.3 of MUAP-07010 describes the main differences between the 2-loop MARVEL and 4-loop MARVEL-M codes. The code improvements incorporated into MARVEL-M with the greatest potential impact on the safety analysis methodology are the expansion from 2-loop to 4-loop simulation and the addition of a built-in reactor coolant pump (RCP) model. MUAP-07010 Section 2.1.3.1 provides a detailed discussion of the 4-loop MARVEL-M reactor coolant system model, including schematics of the overall plant and reactor vessel flow models. Section 2.1.3.2 provides a detailed discussion of the mixing equations utilized in MARVEL-M. Section 2.1.3.3 describes the new reactor coolant pump model. The loop noding, transport, and mixing models, as well as the steam generator and core heat transfer models remain essentially the same as in the original MARVEL code.

The following changes from the original version of MARVEL are briefly described in Section 2.1.3.5.

- Pressurizer surge line model
- Hot-spot fuel thermal kinetics model
- Core void simulation
- Feedline break blowdown simulation
- Conversion of RCS volume balance by pressure search

These last five changes are characterized as model refinements in MUAP-07010 rather than significant code changes and have a minimal impact on the safety analysis methodology.

RAI 2.1-2

Please provide a description of the simplified DNBR model in MARVEL-M.

Response

MARVEL-M calculates the value of DNBR during a transient using a simplified DNBR lookup table methodology.

The MARVEL-M lookup table is an array or database of DNBR, core inlet temperature, pressure, and core heat flux data that is created by VIPRE-01M steady state calculations. VIPRE-01M calculates the core inlet temperature corresponding to a given set of parameters such as pressure, core heat flux and DNBR under the steady-state assumptions of constant core flow rate and constant core power distribution.



This simplified DNBR model is used for the evaluation of events which have constant core flow rate and are bounded by the applicable power distribution. For other events whose parameters exceed the limitations of the lookup table, VIPRE-01M is used to directly calculate DNBR based on a DNB correlation.

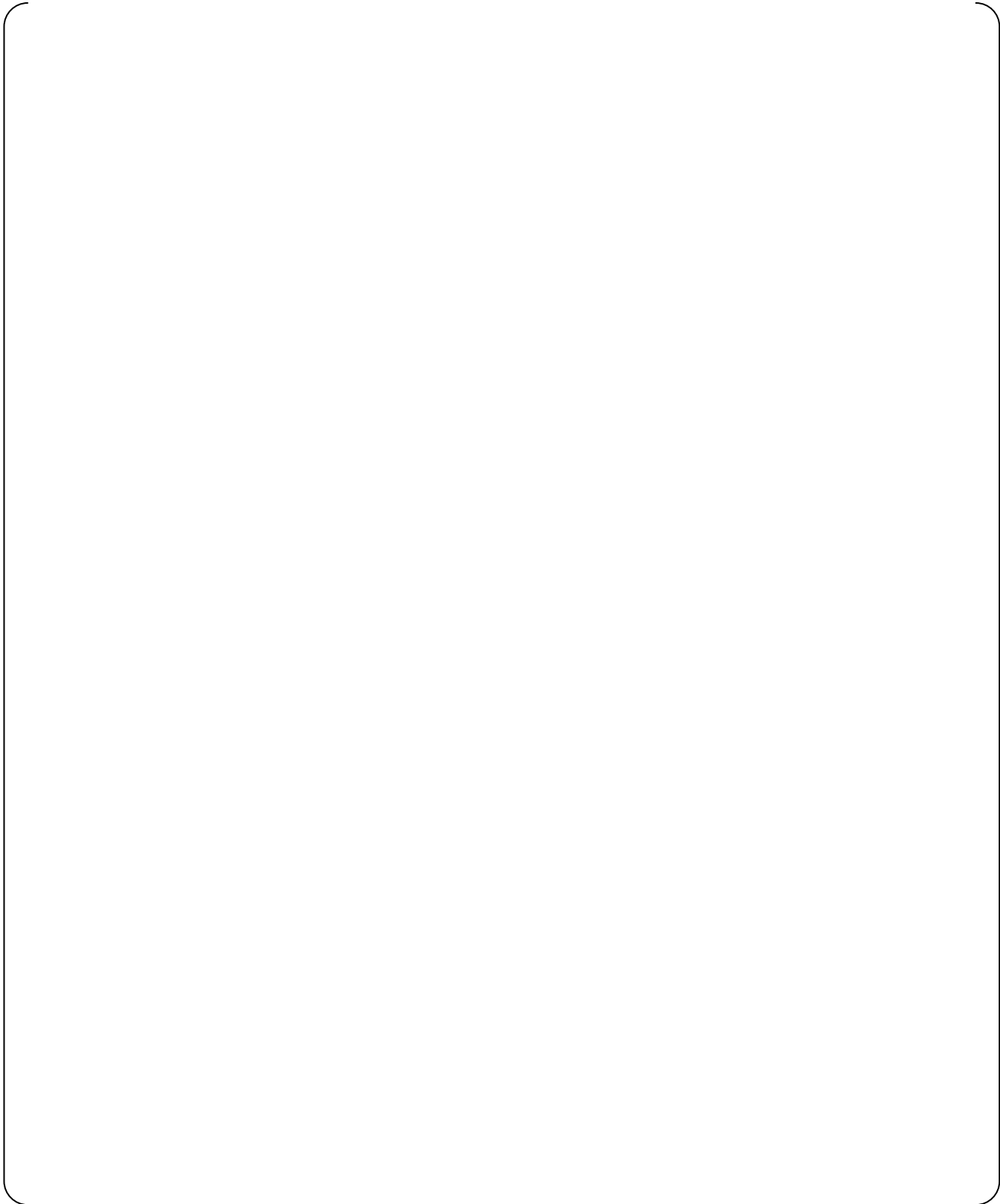


Figure 2.1-2.1 Schematic Description of the Simplified DNBR Model in MARVEL-M

RAI 2.1-3

Have any MARVEL/MARVEL-M code comparisons been performed? Please provide a MARVEL/MARVEL-M code comparison for a typical 2-loop calculation.

Response

Comparisons between the MARVEL and MARVEL-M codes have been performed for non-LOCA events as a verification of the extension from a 2-loop simulation to a 4-loop simulation. The results of these comparisons are introduced in the following figures. Figures 2.1-3.1 through 2.1-3.6 show the comparison of "Loss of Load" as a uniform event and Figures 2.1-3.7 through 2.1-3.17 show the comparison of "Feedwater System Pipe Break" as a non-uniform event. The 4-loop MARVEL-M case is set up to assume the break in a single loop with all of the remaining loops receiving the same emergency feedwater flow. This allows a direct comparison with 2-loop MARVEL, which models these loops as a single loop. Both the 2-loop MARVEL and 4-loop MARVEL-M runs utilize the hyperbolic coast down reactor coolant pump model, again allowing for direct comparison of the code output.

The results demonstrate nearly exact agreement between the 2-loop and 4-loop codes for both primary and secondary parameters of interest.

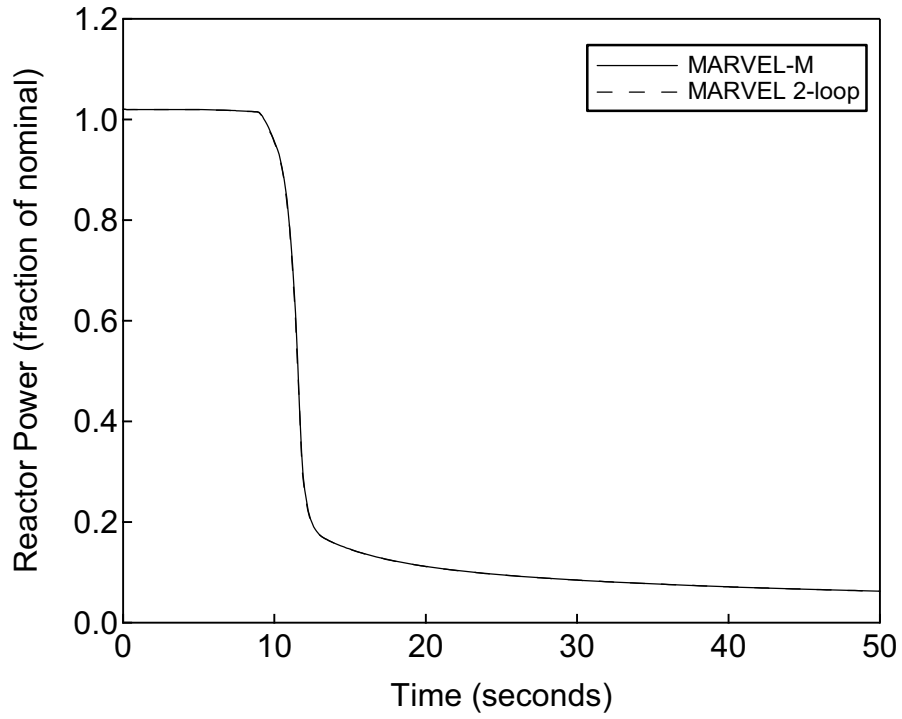


**Figure 2.1-3.1 Reactor Power versus Time
Loss of Load**

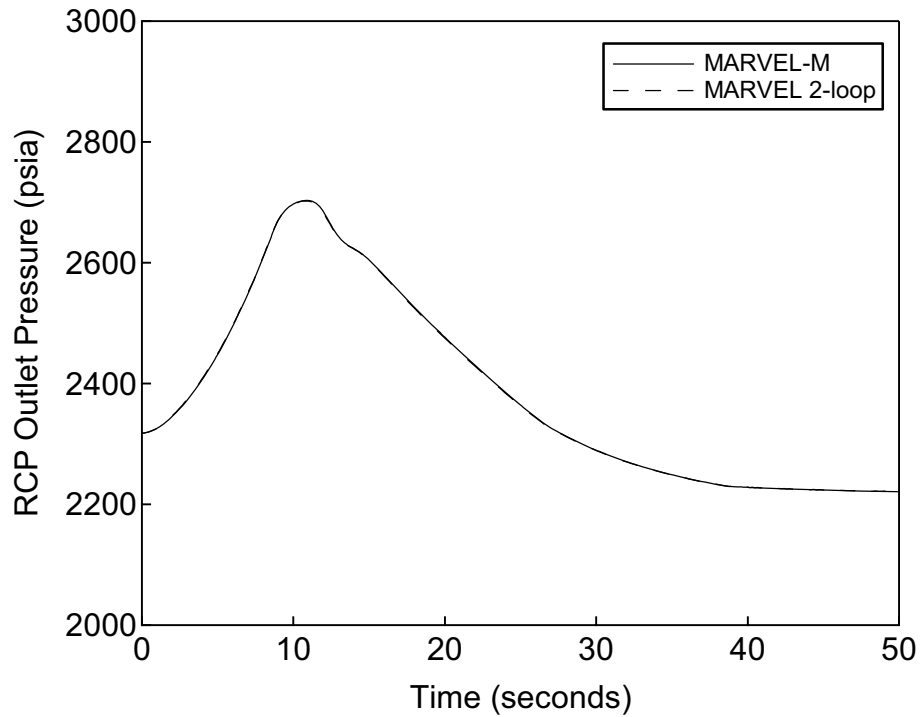


**Figure 2.1-3.2 RCP Outlet Pressure versus Time
Loss of Load**

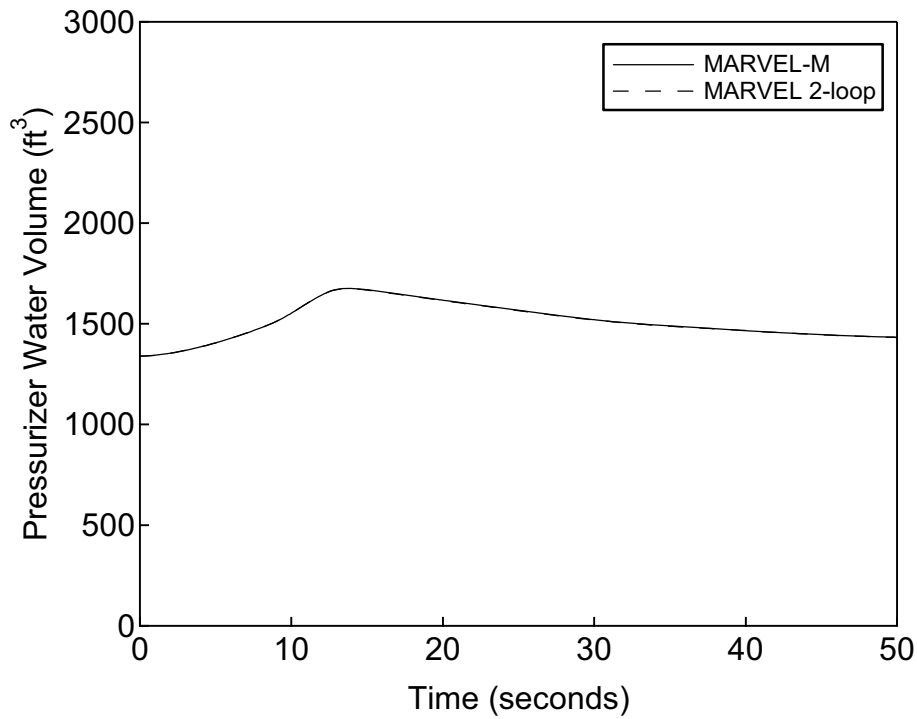


Figure 2.1-3.3 Pressurizer Water Volume versus Time Loss of Load

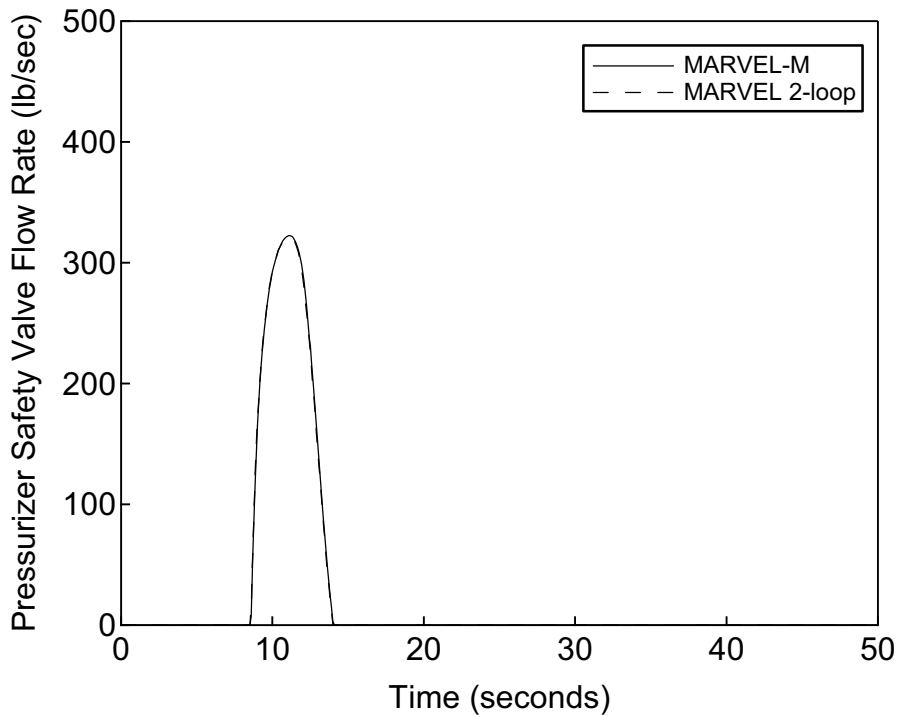


Figure 2.1-3.4 Pressurizer Safety Valve Flow Rate versus Time Loss of Load

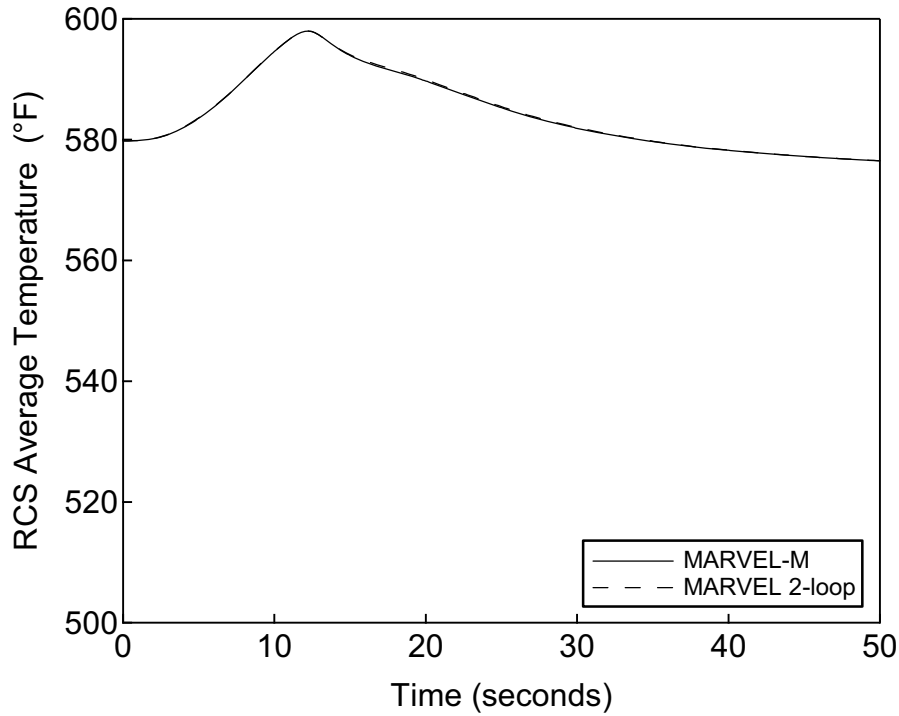


Figure 2.1-3.5 RCS Average Temperature versus Time
Loss of Load

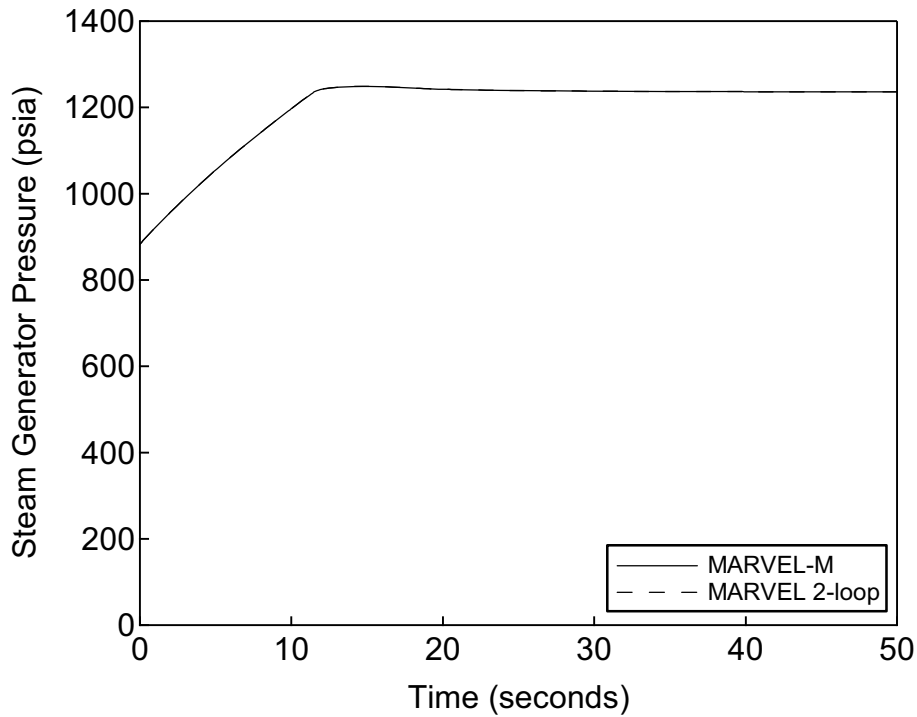
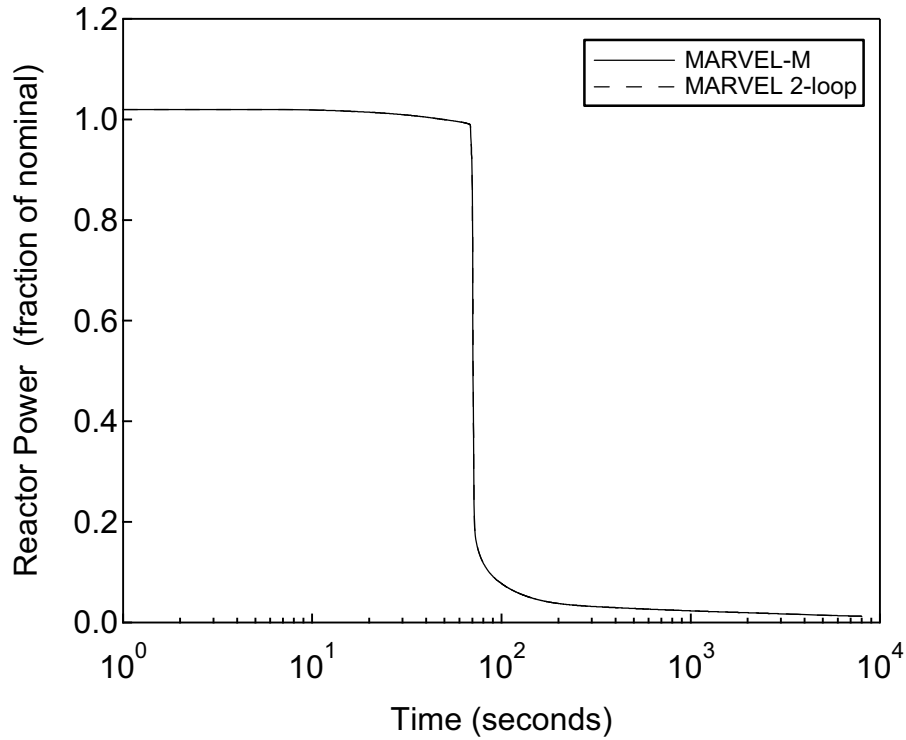
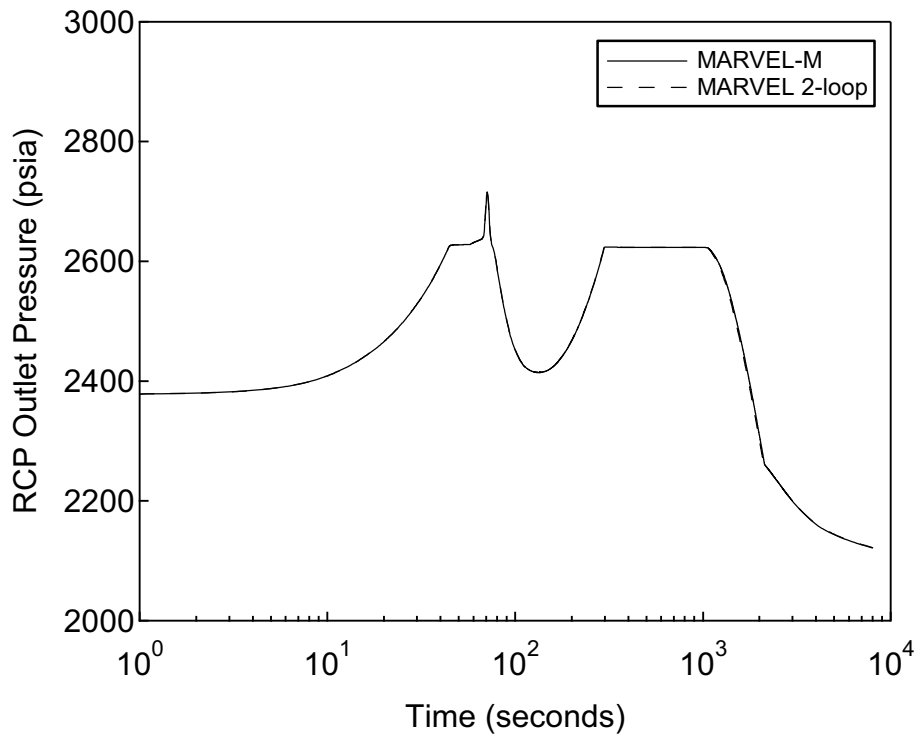


Figure 2.1-3.6 Steam Generator Pressure versus Time
Loss of Load



**Figure 2.1-3.7 Reactor Power versus Time
Feedwater System Pipe Break**



**Figure 2.1-3.8 RCP Outlet Pressure versus Time
Feedwater System Pipe Break**

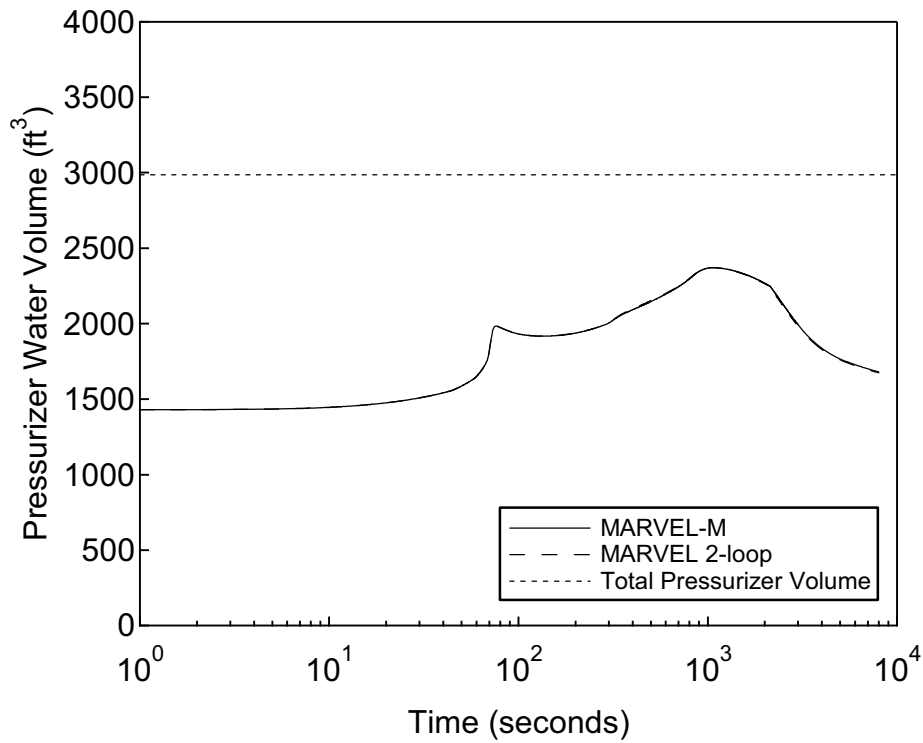


**Figure 2.1-3.9 Pressurizer Water Volume versus Time
Feedwater System Pipe Break**

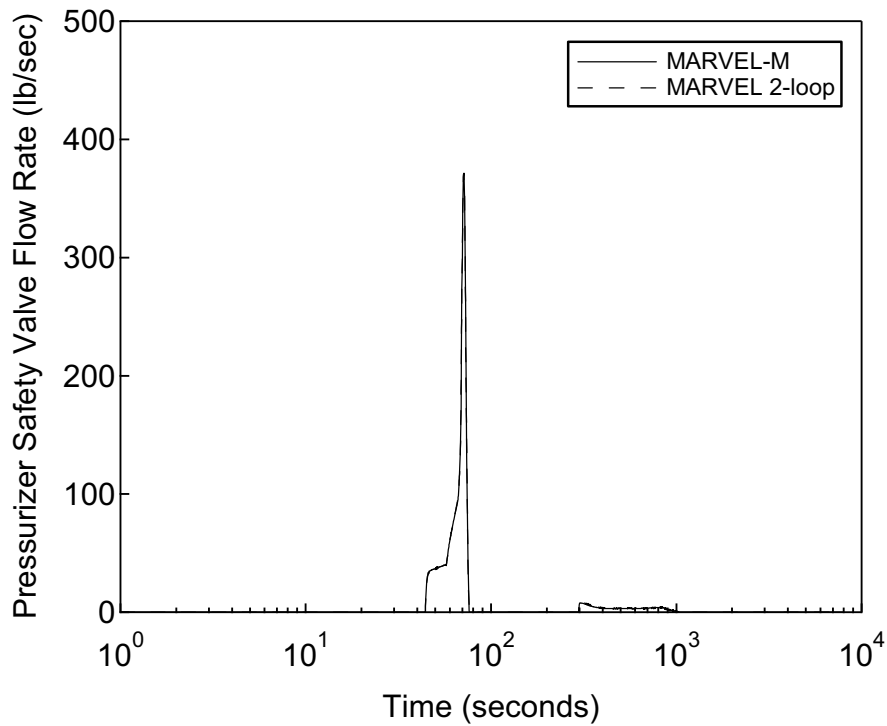


**Figure 2.1-3.10 Pressurizer Safety Valve Flow Rate versus Time
Feedwater System Pipe Break**

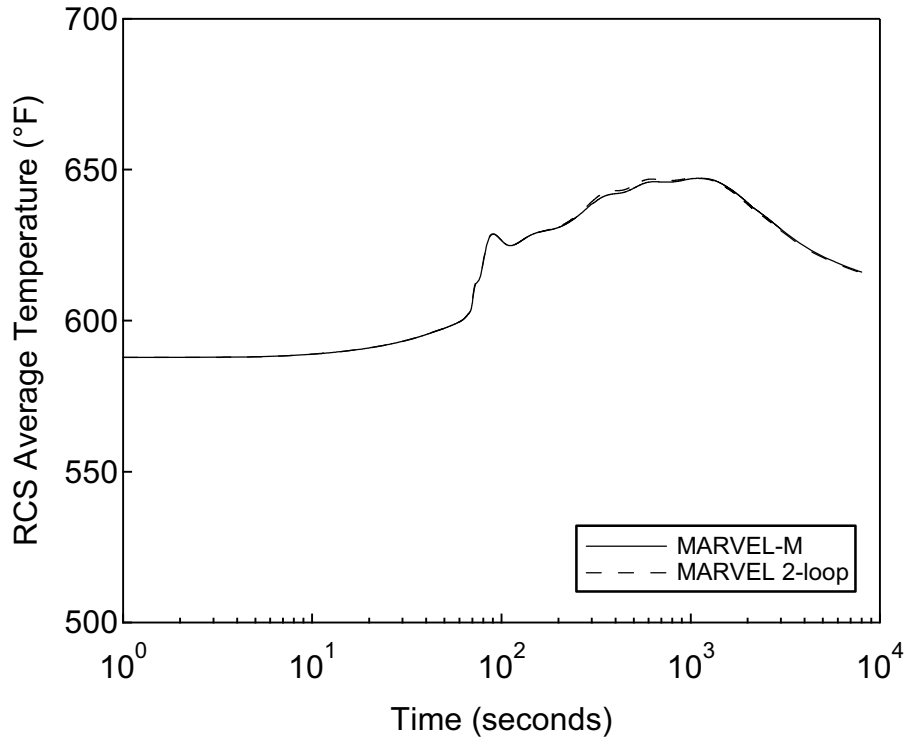


**Figure 2.1-3.11 RCS Average Temperature versus Time
Feedwater System Pipe Break**

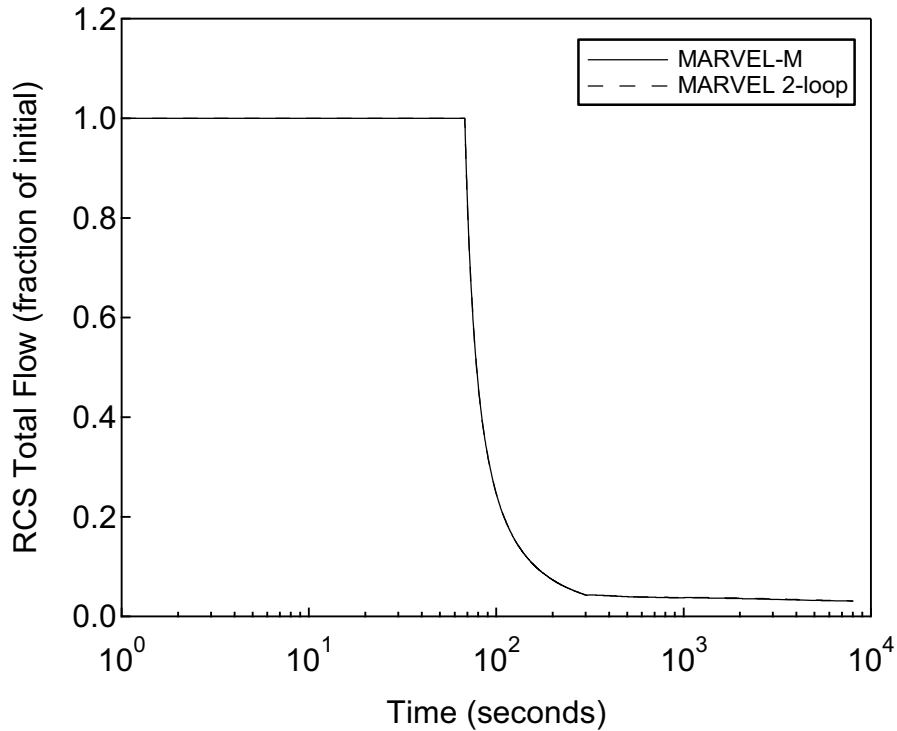


**Figure 2.1-3.12 RCS Total Flow versus Time
Feedwater System Pipe Break**

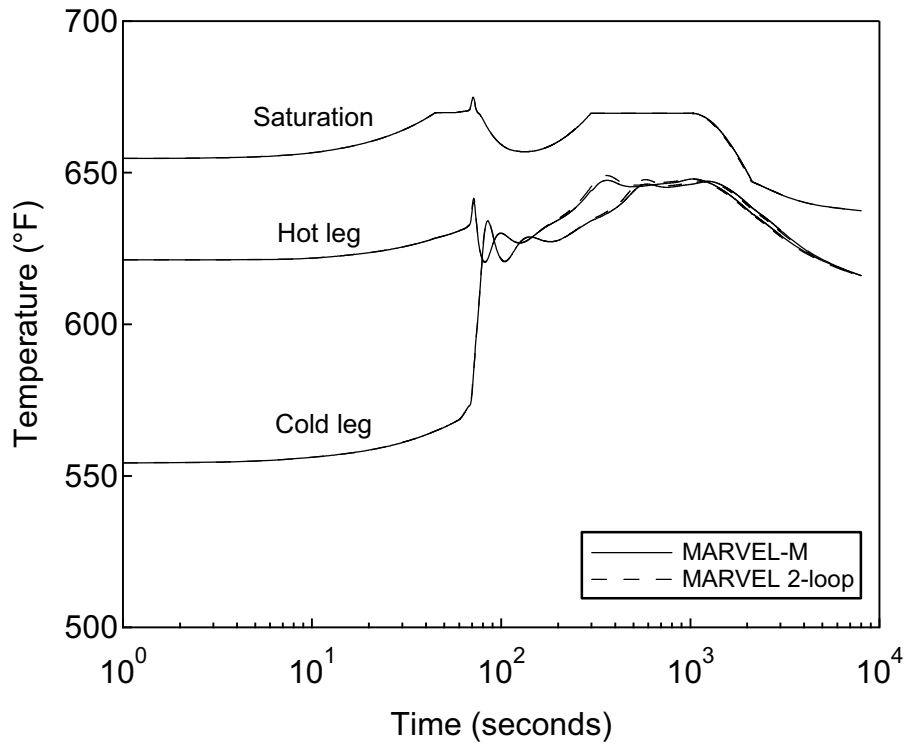


**Figure 2.1-3.13 Temperature of Faulted Loop versus Time
Feedwater System Pipe Break**

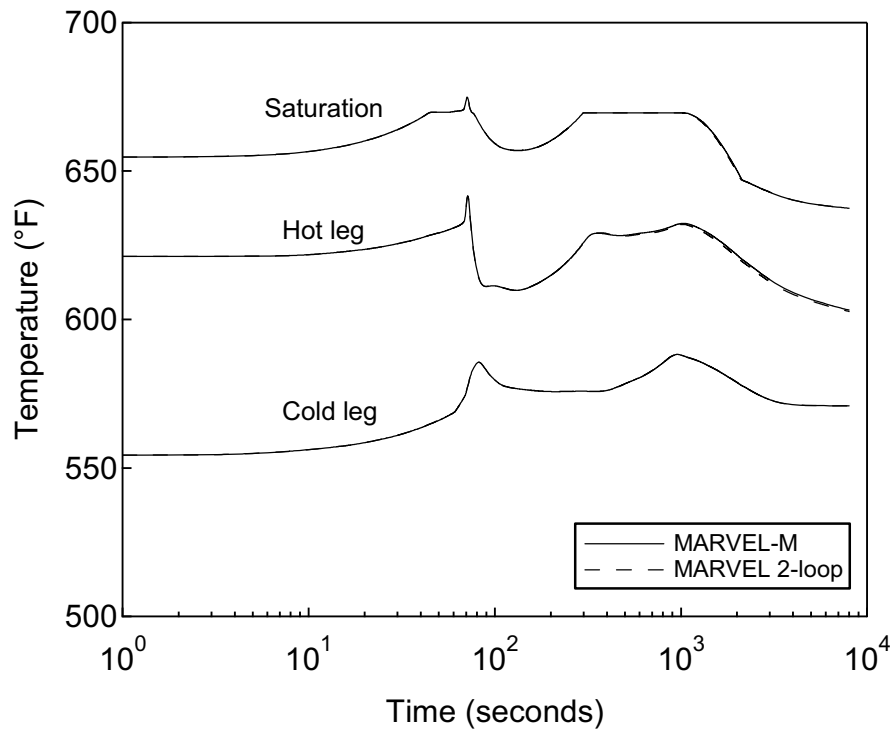


**Figure 2.1-3.14 Temperature of Intact Loop versus Time
Feedwater System Pipe Break**

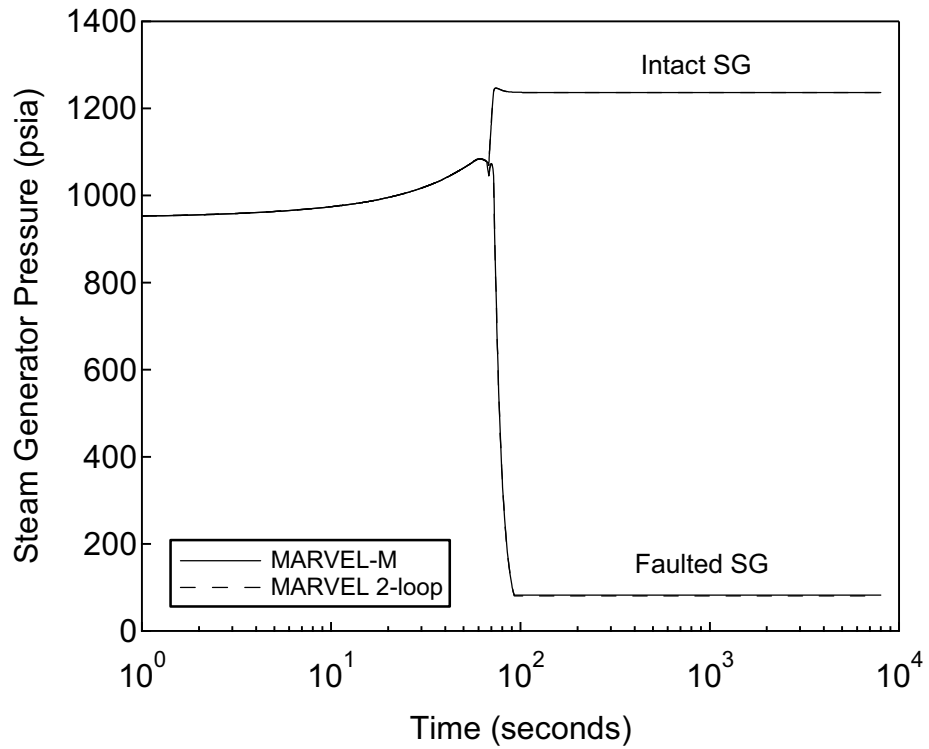


**Figure 2.1-3.15 Steam Generator Pressure versus Time
Feedwater System Pipe Break**

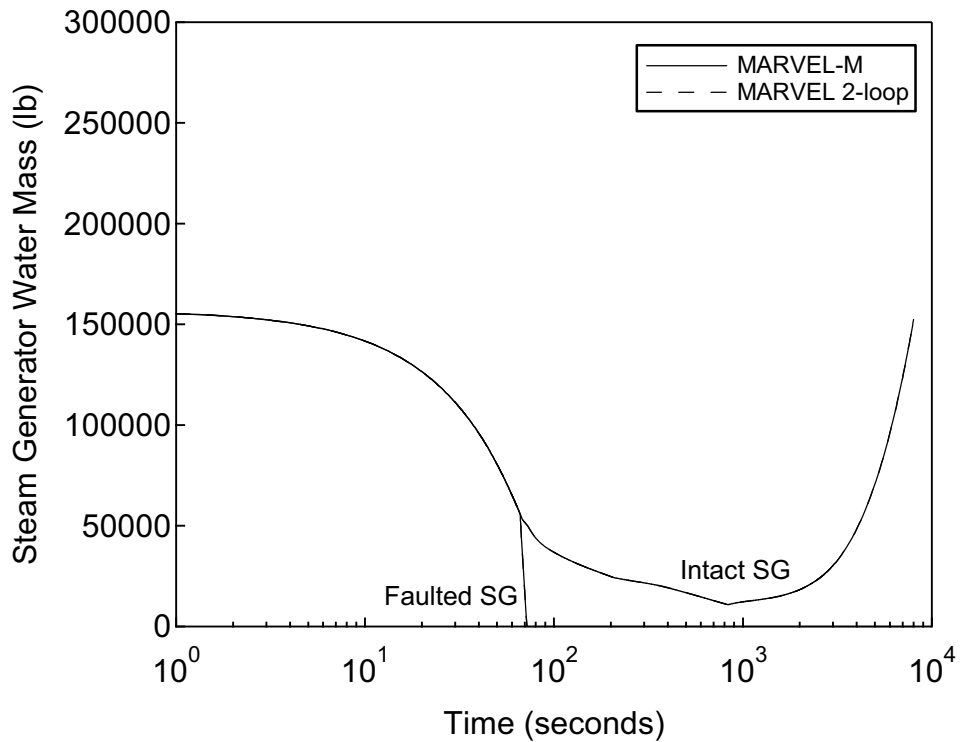


**Figure 2.1-3.16 Steam Generator Water Mass versus Time
Feedwater System Pipe Break**

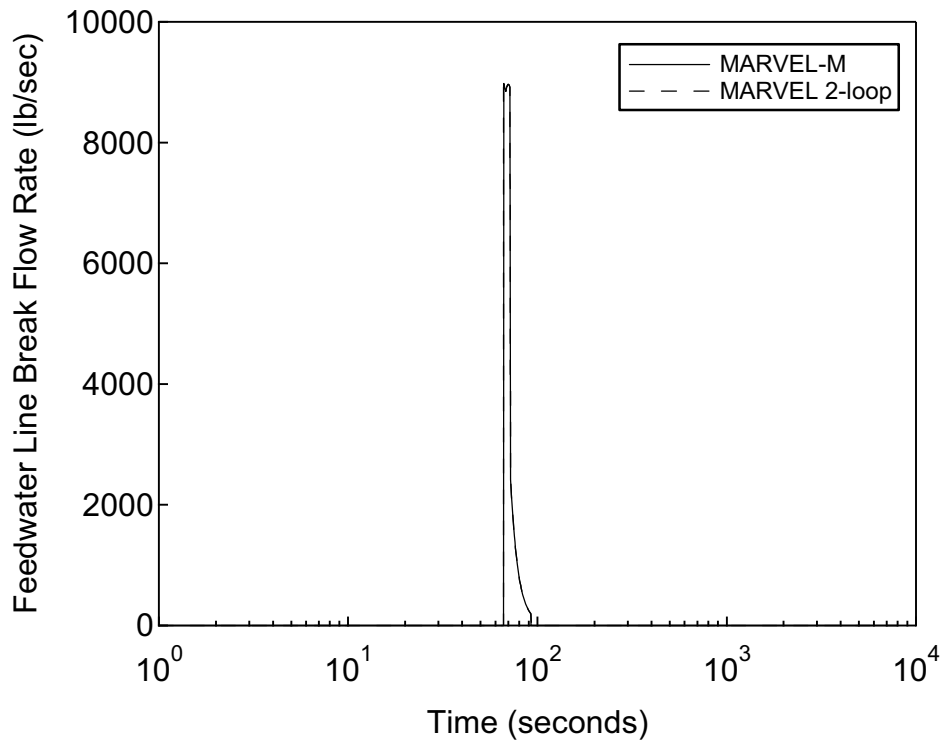


**Figure 2.1-3.17 Feedwater Line Break Flow Rate versus Time
Feedwater System Pipe Break**

RAI 2.1-4

If two-phase homogeneous flow is not applicable, what model does the code use for two-phase flow for $\alpha > \alpha_{\text{homogeneous}}$? How does the user deal with conditions in which homogeneous two-phase flow is not applicable?

Response

For the majority of non-LOCA events analyzed in the US-APWR Chapter 15 analysis, no voids exist in the RCS except in the pressurizer and reactor vessel head. Thus, boiling beyond homogeneous two-phase flow does not occur for non-LOCA analyses which use the MARVEL-M code. MARVEL-M prints a message to inform the user of the occurrence of boiling. The user must determine if the predicted volumetric void fraction has a significant impact on the validity of the computed results.

Localized voids exist for the radiological analysis case of the steam generator tube rupture (SGTR) event. If the pressurizer becomes empty, short-term boiling (~20 seconds) occurs in the hot leg volume where the pressurizer surge line is connected. This phenomenon does not occur in the loops that are not connected to the pressurizer and is not a direct effect of changes in temperature or pressure associated with the reactor coolant system. Since the subcooling in the hot leg is not enough to condense all of the voids from the pressurizer, small portions of the voids remain in the hot leg. The quality at the node connecting the surge line to the hot leg is approximately 0.5% with a corresponding void fraction of about 10%. The voids flow from the hot leg to the steam generator where they are condensed to liquid. A void fraction of 10% corresponds to a dispersed bubbly flow regime, which can be treated as homogeneous two-phase flow for the short-duration of its occurrence during this event. Therefore, it is acceptable to apply MARVEL-M to the SGTR analysis.

In summary, a message in the MARVEL-M output alerts the user to the occurrence of RCS boiling, and a case-by-case review is performed to verify whether the existing result is valid or if an alternative course of action is needed.

RAI 2.1-5

Have any of the mixing models been compared to scaled tests? If so, please provide the comparisons.

Response

The MARVEL-M code inputs derived from the scaled test results are described in the response to RAI 2.1-13.

RAI 2.1-6

Please provide the methodology for the natural circulation flow modeling.

Response

Section 2.1.3.3 of MUAP-07010 describes the MARVEL-M reactor coolant pump (RCP) and flow transient models. MARVEL-M includes an RCP model so that flow transients can be explicitly computed by the pump model in conjunction with the existing reactor coolant system hydraulic models. See the response to RAI 2.1-18 for additional details regarding the use of MUAP-07010 Equation (36) to determine the loop flow for both pump coastdown and natural circulation conditions.

RAI 2.1-7

Please provide the details of the reactor coolant pump model.

Response

MUAP-07010 Section 2.1.3.3 and the response to RAI 2.1-18 provide details regarding the reactor coolant pump and flow transient models utilized in MARVEL-M. Additional details regarding these models are also available in GEN0-LP-480 (the MARVEL-M code manual) Section 1.7. Revision 3 of GEN0-LP-480 was submitted to the NRC by MHI letter UAP-HF-08138 on August 1, 2008.

The original MARVEL code was designed to accept input loop flow tables as a function of time prepared by off-line computation. MARVEL-M now includes a reactor coolant pump (RCP) model so that flow transients can be internally calculated by the pump model in conjunction with the existing reactor coolant system (RCS) hydraulic models. The fundamental flow transient equations in MARVEL-M are based on a momentum balance around each reactor coolant loop and across the reactor vessel, combined with flow continuity and the RCP momentum balance and operational characteristics. Transient operating conditions for the RCP model are determined from homologous head and hydraulic torque curves and pump motor speed-torque characteristics input to MARVEL-M. The overall RCP model methodology described below is similar to the models employed in existing NRC approved codes such as LOFTRAN and PHOENIX.

MUAP-07010 Equation (36) provides the set of simultaneous equations used to describe the overall RCS hydraulic model utilized in MARVEL-M to calculate changes in loop flow. The term H_{pump} in this equation represents the RCP head. Thus, the method of calculating a value of H_{pump} for use in Equation (36) constitutes the RCP model utilized in MARVEL-M.

The user can provide input values for variables defining pump characteristics, homologous head-speed-flow curve and torque-speed-flow curve input, reference pump parameters, and options for pump control. (See GEN0-LP-480 Part II Section 2.5 for a detailed listing of specific MARVEL-M input parameters.)

The pump speed is determined from a torque balance on each RCP. The pump motor torque must equal the sum of the various torques developed in the RCP, as mathematically described below (MUAP-07010 Equation 28).

$$T_M = T_{KE} + T_H + T_W + T_R$$

where

T_M = pump motor torque calculated from the speed-torque curve input to MARVEL-M

T_{KE} = pump kinetic torque = $\frac{1}{g} I_p \cdot \frac{d\omega}{dt}$, where g is the gravitational constant, I_p is the moment of inertia, and ω is the angular speed of rotation

T_H = pump hydraulic torque calculated from the torque-speed-flow homologous curve input to MARVEL-M

T_W = pump windage and friction torque = $K_W \cdot \omega^n$, where K_W and n are constants input to MARVEL-M

T_R = retardation torque due to eddy current in the RCP motor stator

This equation can be rearranged to provide the following equation of motion that is solved to give the transient pump speed:

$$\frac{d\omega}{dt} = (T_M - T_H - K_W \cdot \omega^n - T_R) \cdot \frac{g}{I_p}$$

Once the pump speed has been determined, the pump head is interpolated from the homologous head-speed-flow curves and de-normalized based on reference parameters that are separately input to MARVEL-M. Then the pump head is used to re-calculate the loop flow, which ultimately feeds back into the calculation of a new pump speed at the next time step. Note that T_R is actually treated as part of T_M .

RAI 2.1-8

Describe the modeling of the four major thermal resistances in the calculation of the overall heat transfer coefficient for the steam generators.

Response

The steam generator heat transfer coefficient model is described in detail in Section 1.5.1 of GEN0-LP-480 (the MARVEL-M code manual). Revision 3 of this document was submitted to the NRC by MHI letter UAP-HF-08138 on August 1, 2008.

The overall heat transfer coefficient, U , in the steam generators consists of four major thermal resistance components: the primary convection film resistance, the tube metal resistance, the fouling resistance, and the secondary side boiling heat transfer resistance.

$$U = \frac{1}{R_{tot}} = \frac{1}{(R_{pf} + R_{tube} + R_{foul} + R_{bo})}$$

where

$$R_{pf} = R_{pf}^0 \frac{(1 + 10^{-2}T_0 - 10^{-5}T_0^2)}{(1 + 10^{-2}T - 10^{-5}T^2)} \left(\frac{Q}{Q_0}\right)^{-0.8},$$

$$R_{tube} = R_{tube}^0 \frac{8.0 + 0.0051 \cdot T_{tube}^0}{8.0 + 0.0051 \cdot T_{tube}},$$

$$R_{bo} = R_{bo}^0 \left(\frac{\Delta T}{q''}\right) / \left(\frac{\Delta T}{q''}\right)^0, \text{ and}$$

$$R_{foul} = \text{constant during a transient.}$$

From these equations, it is observed that the absolute value of the overall steam generator heat transfer coefficient at nominal conditions is determined within the MARVEL-M code using the nominal full thermal power, nominal average coolant temperature, nominal steam temperature, and nominal ΔT .

Thus, only the ratios of the major thermal resistances as a fraction of the overall primary-to-secondary heat transfer resistance at nominal full power conditions are directly input to MARVEL-M. The MARVEL-M input parameter variables are provided below with the equations that mathematically describes the ratios in terms of the power, coolant temperature, etc.

$$RRPF = \frac{R_{pf}}{R_{tot}^0} = \left(\frac{R_{pf}^0}{R_{tot}^0}\right) \cdot \left(\frac{1 + 10^{-2}T_0 - 10^{-5}T_0^2}{1 + 10^{-2}T - 10^{-5}T^2}\right) \left(\frac{Q}{Q_0}\right)^{-0.8}$$

$$RRTM = \frac{R_{tube}}{R_{tot}^0} = \left(\frac{R_{tube}^0}{R_{tot}^0}\right) \frac{8.0 + 0.0051 \cdot T_t^0}{8.0 + 0.0051 \cdot T_t}$$

$$RRBO = \frac{R_{bo}}{R_{tot}^0} = \left(\frac{R_{bo}^0}{R_{tot}^0} \right) \left(\frac{q_{sg} / A_{sg}}{q_{sg}^0 / A_{sg}^0} \right)^{-0.75} \cdot \exp\left(\frac{P_s^0 - P_s}{900} \right)$$

The fouling resistance ratio, $\frac{R_{foul}}{R_{tot}^0} = \frac{R_{foul}^0}{R_{tot}^0}$, is not a MARVEL-M input parameter, but is

internally back-calculated within MARVEL-M as $1 - RRPf - RRTM - RRBO$. Note also that the absolute values of these steam generator heat transfer coefficients at nominal conditions are calculated internally by MARVEL-M based on the user-input values of the ratios described above at nominal conditions.

RAI 2.1-9

Please provide the details of over-temperature ΔT and over-power ΔT trip protection methodologies and specifications, including uncertainties.

Response

MARVEL-M simulates both the overtemperature ΔT and overpower ΔT reactor trips. Although most MARVEL-M simulated reactor trip signals compare process variables with fixed setpoints to actuate the reactor protection system (RPS), the overtemperature ΔT and overpower ΔT reactor trip models use more complex setpoint algorithms. Section 2.3.2 of GEN0-LP-480 (the MARVEL-M code manual) provides a detailed description of the core operating limit protection (ΔT) trip models used in MARVEL-M. Revision 3 of GEN0-LP-480 was submitted to the NRC by MHI letter UAP-HF-08138 on August 1, 2008. A summary of the MARVEL-M code manual description is provided below.

Overtemperature ΔT

The overtemperature ΔT trip provides protection to prevent departure from nucleate boiling (DNB) and hot-leg boiling. In MARVEL-M the DNB and hot leg boiling limits are represented by conditions of the temperature difference across the vessel as a function of T_{avg} and pressure. When the reactor coolant loop ΔT exceeds the calculated $\Delta T_{setpoint}$, the reactor is tripped.

The following equation defines the trip setpoint for the DNB limit line:

$$\Delta T_{setpoint} = \Delta T^{nom} \left[K_1 + K_2 (P - P^{nom}) - K_3 \frac{1 + \tau_3 s}{1 + \tau_4 s} (T_{avg} - T_0) - f(\Delta q) \right]$$

where τ_3 and τ_4 are preset adjustable time constants to compensate for the preset manually adjustable bias; K_1 , K_2 , and K_3 are preset manually adjustable constants; T_0 is the nominal value of T_{avg} ; and $f(\Delta q)$ is a penalty function of the flux difference between upper and lower nuclear instrumentation.

A similar overtemperature ΔT trip setpoint without the $f(\Delta q)$ flux difference penalty term can also be defined for hot leg boiling limits using different numerical values of the adjustable constants and time constants. To allow for variations in plant RPS designs, the $\Delta T_{setpoint}$ for DNB and hot leg boiling limits can either be input as separate limits or expressed as the single equation shown above that bounds both limits. If the separate limits are modeled, the trip will occur when either setpoint limit is exceeded.

The overtemperature ΔT trip setpoint in MARVEL-M is selected such that under accidental conditions the trip would occur well within the DNB and hot leg boiling limits, even if all the adverse instrumentation setpoint errors are accumulated in the unfavorable direction. Time delays in signal measurement and processing are also included, which are approximated by a first order delay.

$$T_{avg} = \left[\frac{1}{(1 + \tau_1 s)} \right] \cdot T_{avg-measured} \quad \text{and} \quad \Delta T = \left[\frac{1}{(1 + \tau_2 s)} \right] \cdot \left[\frac{(1 + \tau_6 s)}{(1 + \tau_7 s)} \right] \Delta T_{measured}$$

where τ_1 and τ_2 are the delay time constant in the T_{avg} and ΔT measurement, respectively, and τ_6 and τ_7 are the lead/lag time constants in the ΔT measurement.

Setpoints for the DNB limit and the exit boiling limit are continuously and individually calculated by the RPS using a specific algorithm. Details of the US-APWR overtemperature ΔT setpoint algorithms are provided in DCD Section 7.2.1.4.3.1. DCD Figure 7.2-2 sheet 5 shows the US-APWR logic for this trip function. Although certain notation used in the DCD Chapter 7 description is slightly different, the functionality is the same as that modeled in MARVEL-M.

Overpower ΔT

The overpower ΔT trip provides protection against excessive core thermal power. In MARVEL-M the overpower ΔT trip setpoint is given by

$$\Delta T_{setpoint} = \Delta T^{nom} \left[K_4 - K_5 (T_{avg} - T_o) - K_6 \frac{\tau_5}{1 + \tau_5 s} T_{avg} - f(\Delta q) \right]$$

where τ_5 is a preset adjustable time constant bias applied in the rate/lag operator for increasing average temperature; K_4 , K_5 , and K_6 are preset manually adjustable constants; and $f(\Delta q)$ is a function of flux difference between upper and lower nuclear instrumentation. The time delays in signal measurement and processing are the same as previously described for the overtemperature ΔT trip. Note that while the US-APWR reactor protection system has separate lead/lag units for both overtemperature and overpower ΔT input signals for T_{avg} and ΔT , the MARVEL-M code contains only a single array for lead/lag parameters. Therefore, it is the user's responsibility to assure that the lead/lag parameters associated with the appropriate trip signal are input to MARVEL-M for a given analysis.

The setpoint for this trip is continuously calculated by the RPS using a specific algorithm. Details of the US-APWR overpower ΔT setpoint algorithm are provided in DCD Section 7.2.1.4.3.2. DCD Figure 7.2-2 sheet 5 shows the US-APWR logic for this trip function. Although certain notation used in the DCD Chapter 7 description is slightly different, the functionality is the same as that modeled in MARVEL-M.

RAI 2.1-10

Please provide the details of cold leg injection by the safety injection system and its role in non-LOCA events.

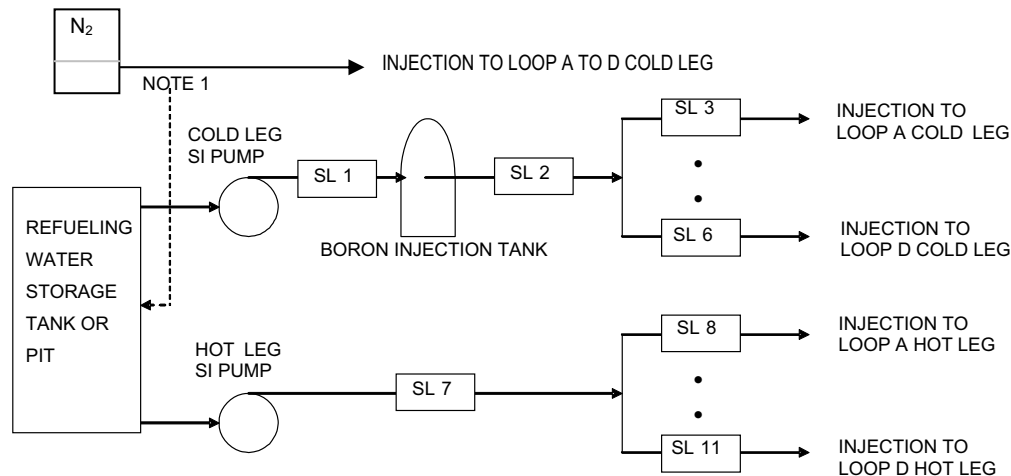
Response

The SIS modeling within MARVEL-M is briefly described on page 2-10 of MUAP-07010 with a more detailed description provided in Section 1.9.1 of GEN0-LP-480 (the MARVEL-M code manual). Revision 3 of GEN0-LP-480 was submitted to the NRC by MHI letter UAP-HF-08138 on August 1, 2008.

The US-APWR has four independent and dedicated safety injection (SI) pump trains which supply boric acid water from the refueling water storage pit (RWSP) directly to the reactor vessel downcomer in the normal system lineup.

As shown in the schematic drawing below from the MARVEL-M code manual, MARVEL-M has the capability to model several different safety injection system configurations. The upper flow path shown on the figure below models one SI pump, a common discharge header, and flow split to the four cold legs. This flow path model includes a Boron Injection Tank consistent with earlier plant designs. For newer plant designs such as the US-APWR that do not have a boron injection tank, this volume can be set to zero. Because for non-LOCA accidents the reactor coolant (RCS) pressure is the same at the cold leg inlets, one or more trains of SI pumps can be modeled with a single pump, as shown in the figure.

ACCUMULATOR (ONE/EACH LOOP)



Note 1: Blow down water from steam generators at secondary line break inside CV may enter the refueling water storage pit, if the storage pit is inside CV.

The lower flow path shown on the figure models a second single SI pump, a common discharge header, and flow split to the four hot legs. The user can select the injection point as the hot legs, the deluge line, or the reactor vessel downcomer.

A separate SI pump pressure-flow characteristic can be specified for each of the systems, and either of the systems can be turned on or off using user inputs. Initial boron concentrations and fluid enthalpies can be specified for the fluid in each of the SI piping volumes.

The SIS is credited in the safety analysis of only the following non-LOCA DCD events:

- inadvertent opening of main steam relief or safety valve,
- secondary steam system piping failure NSSS response,
- secondary steam system piping failure containment mass and energy release, and
- steam generator tube rupture.

The accumulator pressure is not reached for any of these non-LOCA events, so the accumulator model is not used.

For the first three steam flow increase events, the SI both provides RCS makeup to offset the RCS coolant shrinkage due to the cooldown and delivers borated water to the core for negative reactivity. In these events, it is important to accurately model the progression of boron to the core for the purpose of calculating core reactivity. For the steam generator tube rupture, SI is modeled for the purpose of calculating RCS inventory and pressure only. The boron reactivity coefficient is assumed to be zero for this event.

The cold leg injection (upper flow path) is used for all four of the above events for the US-APWR. Modeling considerations and boron transport models associated with the cold leg injection flow path for these events are described below.

For the steam release cooldown events, the time required for borated water to reach the core after SI initiation is determined by taking into consideration: (1) the period from the time the ECCS actuation signal is generated to the time the safety injection pumps reach full speed, and (2) the transport time for the injected water to pass through the SI piping and the reactor coolant piping. These delays and purge volumes are directly modeled in the MARVEL-M code. In the MARVEL-M model the high head ECCS injection cold leg injection point is conservatively assumed to be the cold leg node nearest the reactor vessel, although the actual injection point is the reactor vessel downcomer. The ECCS injection line is simulated in MARVEL-M considering the leading edge of the injection line water slug, which calculates the time delay associated with purging the low concentration borated water from the injection piping by the high concentration borated water from the RWSP. For the purpose of accurately tracking the progression of concentrated borated water through the SI piping, each of the piping volumes in the blocks labeled SL2 through SL6 are subdivided into 20 sub-volumes using slug flow models. The MARVEL-M model also includes the conservative assumption that no mixing occurs in the injection line nodes. Thus, the MARVEL-M SIS model is conservative from the point of view of the boron concentration of the core.

For the inadvertent opening of main steam relief or safety valve, several assumptions about the SIS are made. The boron concentration in the RWSP is assumed to be less than or equal to the minimum allowable Technical Specification value. The total pump flow is defined consistent with the assumptions in the DCD for operating pumps to inject the borated water from the RWSP. The time required for the borated water to reach the core is determined as discussed previously.

Similar assumptions about the SIS are made for the secondary steam system piping failures. Again, the boron concentration in the RWSP is assumed to be less than or equal to the

minimum allowable Technical Specification value, the total pump flow is defined consistent with the assumptions in the DCD for operating pumps, and the time required for the borated water to reach the core is determined as discussed previously. Time delays for the start of the SI pumps are varied to account for whether the pumps are being powered by offsite power or standby emergency power.

For the steam generator tube rupture, the SI boration capability is not credited. Unlike the steam release cooldown events, SI flow is a penalty for the time to equalize the primary and secondary pressures. Maximum flow with all pumps delivering equally to all cold legs is assumed through user input of the system pressure-flow characteristic and uniform injection line split fractions. Because boron concentration is not of concern to the transient response, the boron reactivity coefficient is set to zero. The point of injection (cold leg vs. reactor vessel downcomer) does not affect the transient response for the steam generator tube rupture.

In summary, the cold leg injection flow path in the MARVEL-M code is used for all non-LOCA events, with event-specific inputs to conservatively model each event. The models for boron transport for the SI system volumes have special slug flow provisions that correctly follow the leading edge of borated water as it progresses to the core, resulting in the accurate prediction of core reactivity. These models and associated code inputs are further described in the MARVEL-M code manual. Assumptions made for each of the events crediting SI are described in their respective DCD analysis.

RAI 2.1-11

It is stated that the MARVEL-M algorithm for core mixing is changed from the original MARVEL model. Are the changes due to the expansion of the capability to four loops, or are there fundamental changes in the mixing phenomenology?

Response

The changes to the MARVEL-M algorithm for mixing in the reactor vessel are due to the expansion of the modeling capability from two to four loops. The basic assumptions are the same as the 2-loop version, as described in Section 2.1.3.2 of MUAP-07010, as repeated below.

1. Cross flow may only exist between each downcomer flow section and the adjacent downcomer sections.
2. Cross flow occurs so that coolant flow rates at the downcomer exit are uniform.
3. The cross flows are proportional to the differences of downcomer inlet flows.

From the above assumptions,

$$\left(\right)$$

where

- $N_{loop} = 4$ for the US-APWR.
- W_i represents the portion of flow out of the downcomer node that flows directly into the corresponding reactor vessel lower plenum node for loop i .
- WCR_i represents the cross flow out of the downcomer nodes as defined in MUAP-07010 Figure 2.1-5 and determined by solving the above equations.

$$\left(\right)$$

RAI 2.1-12

Mixing is assumed to occur in the reactor vessel lower plenum as specified in the code input. How are the mixing factors (FMXI) established by the user? What guidance is provided to the user?

Response

The mixing factor in the lower plenum (FMXI) is established using hydraulic test data and the equations described in the response to RAI 2.1-13. Standard 4-loop mixing factors were determined by MHI for the US-APWR and incorporated into a base MARVEL-M input file. Values for specific events are provided to the users in event-specific analysis procedures.

RAI 2.1-13

Some 1/7-scale mixing tests were carried out in the 1970's. It is suggested that mixing assumptions can be inferred from the published results. What justification can be provided to support these claims for evaluating FMXI? Please provide documentation of the 1/7-scale tests.

Response

MHI has utilized hydraulic test data from the 1/7-scale mixing tests for the [] reactor vessel model in order to determine the appropriate values of MARVEL-M input parameters FMXI and FMXO. Although the reactor internal design is different between the [] and the US-APWR (incore instrumentation moved to top of vessel, 14 foot core, etc.), the mixing factor itself has very little effect on the calculated DNBR as described in Appendix E of MUAP-07010 which shows a sensitivity analysis of DNBR as a function of the mixing factor for the steam line break event. An additional discussion of the Appendix E results is provided in the response to RAI App.E-1.

The MARVEL-M modeling of the reactor vessel mixing is described on pages 2-15 through 2-17 of MUAP-07010. A summary of the relevant variables and equations related to the calculation of the MARVEL-M input parameters FMXI and FMXO is provided below (excerpted from MUAP-07010).

The factor, f_m , is defined as the fraction of flow entering the reactor vessel from one loop that returns to the same loop upon exiting the core.

The factor f_{mi} is defined as the fraction of loop coolant flow which flows up the azimuthal sector (per loop) of the core nearest the inlet nozzle from which it emerges. The factor f_{mi} is related to the MARVEL-M input parameter FMXI, as shown below.

$$FMXI = (1 - f_{mi}) \frac{Nloop}{(Nloop - 1)} \quad (1)$$

where $Nloop = 4$ for the US-APWR

Similarly, the factor f_{mo} is defined as the fraction of the vessel outlet flow that comes from the azimuthal part (per loop) nearest the outlet nozzle. The factor f_{mo} is related to the MARVEL-M input parameter FMXO, as shown below.

$$FMXO = (1 - f_{mo}) \frac{Nloop}{(Nloop - 1)} \quad (2)$$

Additionally, f_m and f_{mo} are related to f_{mi} as follows:

$$f_m = f_{mi} \cdot f_{mo} + \frac{(1 - f_{mi}) \cdot (1 - f_{mo})}{(Nloop - 1)} \quad (3)$$

MHI utilizes the following values of f_m and f_{mi} in order to calculate MARVEL-M input parameters FMXI and FMXO from the equations (1), (2), and (3) above. The design value of f_{mi} is utilized for all DCD Chapter 15 non-LOCA events for the US-APWR, except for the steam line break,

which uses the conservative value of f_{mi} .

The values for f_m and f_{mi} are taken from WCAP-7635 (Reference 1). These values are based on the report of the 1/7 scale mixing tests for the () reactor vessel. The test result report is referred to in WCAP-7635, but is not publically available. Although the DNBR analyses are insensitive to the mixing factors, as described previously, MHI recently carried out a 1/7 scale mixing test for the US-APWR reactor vessel in order to confirm the applicability of the () test results. The experimental results indicated that the mixing factors used in the safety analyses that were based on the () test are still applicable for the US-APWR as described in MUAP-07022-P, "US-APWR Reactor Vessel Lower Plenum 1/7 Scale Model Flow Test Report" which was submitted on June 30, 2008 (ML081850466).

Reference (Attached to RAI response letter as Enclosure 4)

- 1) WCAP-7635, "MARVEL – A Digital Computer Code for Transient Analysis of a Multiloop PWR System, dated March 1971.

RAI 2.1-14

The methodology for reactor vessel upper plenum mixing is exactly the same as for mixing in the lower plenum. The mixing factor is FMXO. How are the mixing factors (FMXO) established by the user? What guidance is provided to the user?

Response

The mixing equations for FMXI (Eq. 13) and FMXO (Eq. 18) described in MUAP-07010 Section 2.1.3.2 use the same mathematical expression to describe the portion of the main flow that is mixed rather than directly transferred to the next flow node without undergoing mixing. However, the meaning of the mixing factors in the lower plenum and upper plenum is different.

FMXI represents the fraction of downcomer flow in the corresponding lower plenum node that comes from the other loops. Alternatively, $1 - \text{FMXO}$ represents the fraction of flow leaving the reactor vessel upper plenum lower part that exits the reactor vessel by the nearest hot leg. Refer to Figure 2.1-5 in MUAP-07010.

The mixing factor in the upper plenum (FMXO) is established using hydraulic test data and the equations described in the response to RAI 2.1-13.

Standard 4-loop mixing factors were determined by MHI for the US-APWR and incorporated into a base MARVEL-M input file. Values for specific events are provided to the users in event-specific analysis procedures.

RAI 2.1-15

Are there any scaled experimental data to use for guidance in determining FMXO? If so, please provide the data or guidance.

Response

The response to RAI 2.1-13 describes how to calculate the mixing factors FMXI and FMXO based on the best available mixing test data.

RAI 2.1-17

Transition to natural circulation flow is modeled in MARVEL-M and the elevation head equations are typical. Has this model been tested against scaled experimental data? If so, please provide comparisons.

Response

The MARVEL-M transient flow model has not been compared to scaled experimental data. However, the MARVEL-M model has been compared with LOFTRAN (in a manner similar to the code comparisons provided in MUAP-07010 Section 3) in order to verify the natural circulation model.

Figure 2.1-17.1 shows the loop mass flow rate comparison between MARVEL-M and LOFTRAN for the "Loss of Non-Emergency AC Power to the Station Auxiliaries" event. The natural circulation flow of both the loop without emergency feedwater (EFW) and the loops with EFW after the reactor coolant pump (RCP) coastdown have very good agreement.

The US-APWR safety analysis assumes a conservative lower limit on the friction and windage torque utilized in the MARVEL-M RCP model. (See the response to RAI 2.1-7 for details on the RCP model.) The MARVEL-M results presented in Figure 2.1-17.1 do not include this conservative limitation in order to better compare the results with the LOFTRAN code. Figure 2.1-17.2 presents the results of the case where the safety analysis assumed friction and windage torque lower limit is used in MARVEL-M compared with the same LOFTRAN results previously shown in Figure 2.1-17.1. The figure demonstrates that the safety analysis MARVEL-M predicted results show a larger decrease in flow rate and a lower stable natural circulation flow level than predicted with LOFTRAN. In the DCD Chapter 15 analyses of the US-APWR, this conservative assumption is used in events that feature natural circulation flow conditions.

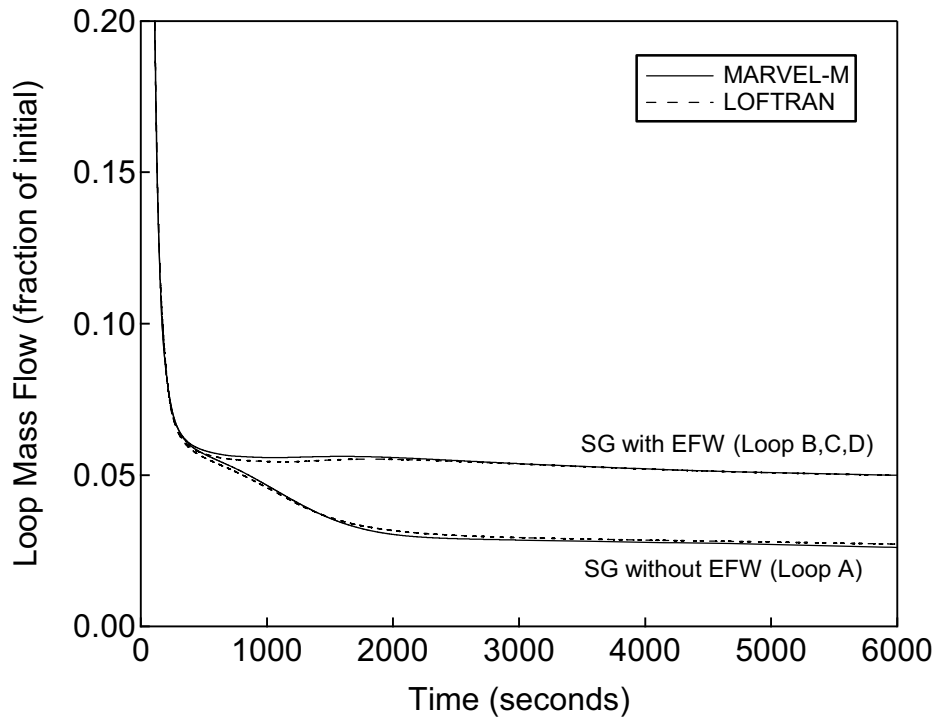


Figure 2.1-17.1 Loss of Non-Emergency AC Power to the Station Auxiliaries Comparison between LOFTRAN and MARVEL-M (1)

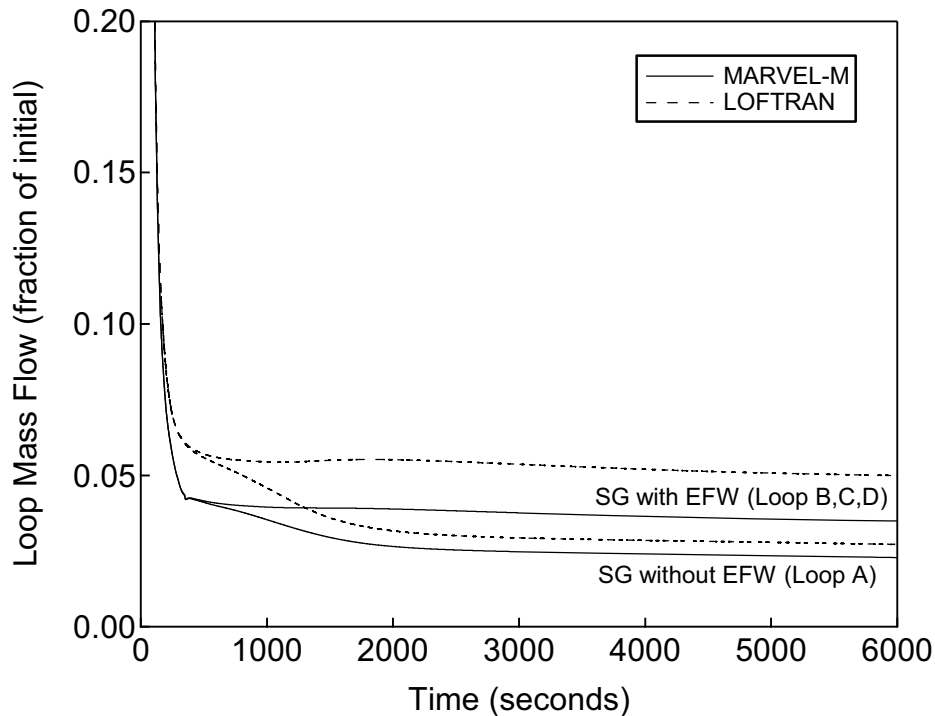


Figure 2.1-17.2 Loss of Non-Emergency AC Power to the Station Auxiliaries Comparison between LOFTRAN and MARVEL-M (2)

RAI 2.1-18

How does the transition to natural circulation depend upon the pump coast down model? Have sensitivity calculations been performed over a range of conditions to demonstrate confidence in the end state? If so, please provide the results.

Response

MARVEL-M now includes a reactor coolant pump (RCP) model so that flow transients can be explicitly computed by the pump model in conjunction with the existing reactor coolant system hydraulic models. Thus, there is no separate transition to natural circulation model because flow transient equations are solved at each time step depending on the status of the pump. Section 2.1.3.3 of MUAP-07010 provides a detailed description of the various equations utilized for modeling flow transients in MARVEL-M.

When the RCP in a reactor coolant loop is running, the head of the pump $[H_{PUMP}]_i$ is calculated from the flow coastdown equations [Equations (29) through (33) in MUAP-07010]. If some pumps are not running, the flow for the loop associated with the idle pump is reversed, and the pump head is replaced with a reverse flow pressure loss. When all the RCPs are not operating, all the pump heads, $[H_{PUMP}]_i$ are replaced with pressure losses and the reactor coolant flow transitions to natural circulation. The natural circulation flow in the multiple loops depends primarily on the power generation in the reactor core and the heat removal in the loops at the steam generators. The flow transition from the forced circulation to the natural circulation is calculated using Equation (36) in MUAP-07010. As a result, there is no need for an approximated model of the transition to natural circulation flow.

RAI 2.1-20

"Realistic models" have been added to MARVEL-M "to simulate real plant transient behavior." Although they are code options, they are not used for licensing evaluations of reactor plants. What controls are in place to ensure that this is the case?

Response

The realistic models available as code options in MARVEL-M are described in Section 2.1.4 of MUAP-07010 and Section 3.0 of GEN0-LP-480 (the MARVEL-M code manual). Details of the input data for MARVEL-M are provided in Part II of the MARVEL-M code manual. Revision 3 of this document was submitted to the NRC by MHI letter UAP-HF-08138 on August 1, 2008.

A standard base MARVEL-M input file has been created by MHI for the US-APWR design. This standard input file is modified for each accident according to the event-specific analysis procedures. Finally, the results of the event-specific calculation are documented in a calculation memo and verified by a qualified reviewer. These quality assurance controls assure that the realistic models are not improperly utilized for licensing evaluations.

RAI 2.2-1

There are several differences between TWINKLE and TWINKLE-M that are mentioned but not discussed in any detail. The introduction of more spatial points and discontinuity factors suggests that the numerical algorithm for solving the diffusion equations may have also been changed although it is not stated. Please list all changes and provide additional description of the differences between the codes.

Response

The solution methods and constitutive models of the TWINKLE-M code have not changed from the original TWINKLE code. MHI has modified several functions which are mainly concerned with the treatment of input data. A brief description of each change is provided below. GEN0-LP-517 Revision 0 (the TWINKLE-M Input Manual), submitted to the NRC by MHI letter UAP-HF-08138 on August 1, 2008, provides additional information regarding TWINKLE-M input.

(1) Spatial Mesh Expansion

In response to a change in the fuel failure thresholds for reactivity initiated events for Japanese LWRs in 1993, the maximum number of spatial mesh points in the TWINKLE-M code was expanded from 2000 meshes to a variable number in order to support a full core three-dimensional representation. The related variables in TWINKLE-M of fuel burnup, macroscopic and microscopic cross section, xenon distribution, fuel temperature, fast and thermal neutron flux, neutron velocities, and delayed neutron fractions were also expanded to accommodate the full core three-dimensional calculations. The capability to solve three-dimensional problems and solution algorithms were not changed.

(2) Introduction of a Discontinuity Factor

A discontinuity factor was added as a new input process in the program. The purpose of the discontinuity factor is to improve the representation of the local power distribution in the three-dimensional calculations. The addition of the discontinuity factor does not change the diffusion equations in TWINKLE. Instead, the discontinuity factor implementation is shown in Figure 2.2-1.1 and described as follows:

- The macroscopic cross section data is divided by the discontinuity factor before solving the diffusion equations (additional process).
- The neutron flux is solved using the unchanged TWINKLE diffusion equation subroutine.
- The neutron flux is divided by the discontinuity factor to determine the mesh averaged neutron flux (additional process).

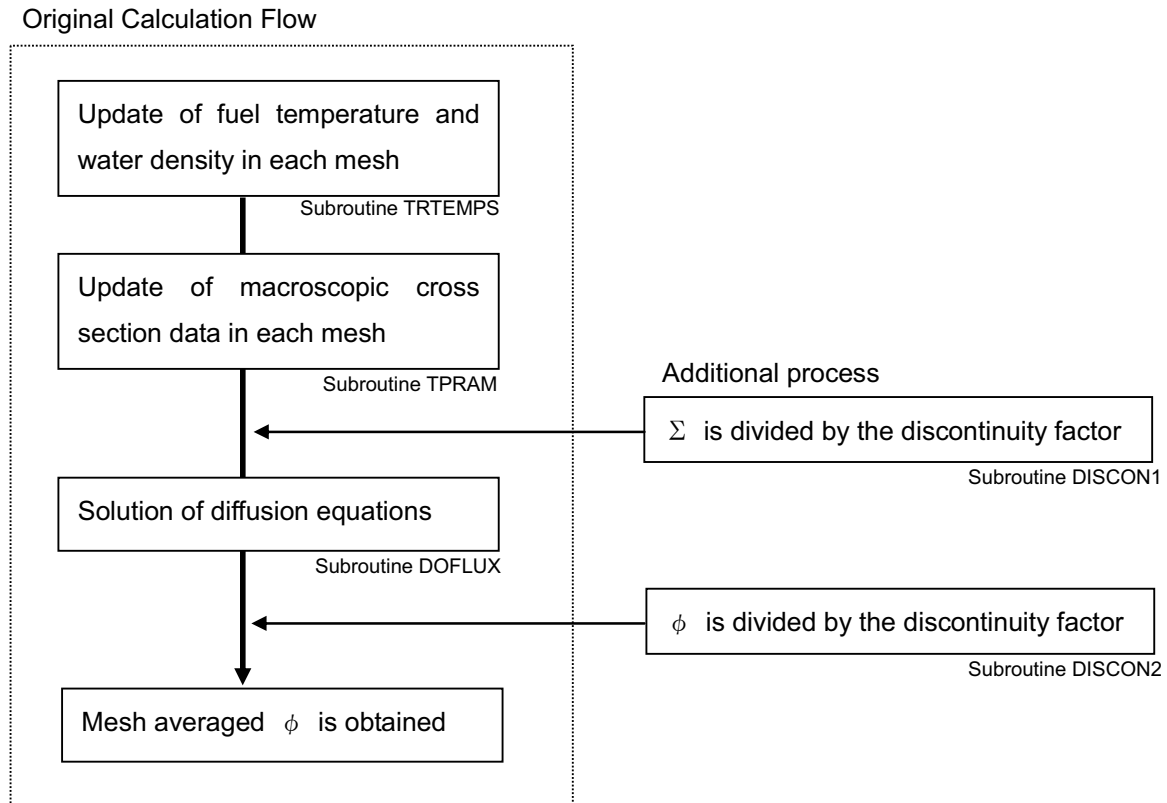


Figure 2.2-1.1 Flowchart of the Discontinuity Factor Process

(3) Input Format

The input format was changed from a numerical identifier form to a Namelist form supported by standard Fortran 77 or 90 compilers. This allows users to identify the input list more clearly.

(4) Additional Options

The following features were added by MHI as input options:

- The nuclear and thermal properties of MOX fuel and BP were included.
- The number of fuel pellet divisions in the radial direction is expanded from 4 meshes to 10 meshes.
- Fuel properties depending on the fuel BU were added such as a thermal conductivity and a radial power depression in the pellet.
- Xenon distribution data calculated by ANC can be passed to TWINKLE-M through an input file. This change provides for a savings in calculation time.
- A separate equation was added to represent the dashpot portion of the trip curve. Prior to this change, the dashpot region was a continuation of the linear portion of the trip curve. The resulting trip curve is now an “S” shaped curve that is more representative of the RCCA displacement curve.
- New outputs were created to aid in the interpretation of code results by allowing for additional data plots and providing the ability to perform sequential calculations with VIPRE-01M. Specific examples of these changes include:
 - Time history of core average power, peaking factor, axial offset, etc.
 - Mesh-wise power distribution map for each time
 - Mesh-wise adiabatic fuel enthalpy rise during a power excursion

RAI 3.1-2

Please provide documentation of MARVEL-M/LOFTRAN code comparisons that may not be in agreement (if available), along with any explanations for the deviations.

Response

The overall agreement between MARVEL-M and LOFTRAN is generally quite good. This response describes a case where a difference between the two codes has been noticed, but can be explained based on known differences in the code models.

MUAP-07010 Section 3.1.1 provides a comparison between MARVEL-M and LOFTRAN for the Uncontrolled RCCA Bank Withdrawal at Power event assuming the pressure control system is turned off. While performing a similar comparison for the same case except with pressurizer pressure control, slight differences were observed in the pressurizer pressure response. After further review, the differences in RCS response for the LOFTRAN and MARVEL-M analyses were shown to be attributed to the following differences between the spray models in LOFTRAN and MARVEL-M:

MARVEL-M

- Saturated steam is assumed in the pressurizer
- If cold water is sprayed, the saturated steam quickly condenses

LOFTRAN

- Superheated steam is assumed in the pressurizer
- If cold water is sprayed, the spray first removes the super heat maintaining pressurizer pressure (the steam phase does not condense but shrinks)
- After sufficient water has been sprayed the pressurizer reaches a saturated condition and condensation of the saturated steam begins

Figures 3.1-2.1 through 3.1-2.4 show the comparison between MARVEL-M and LOFTRAN for the case where the pressure control system is available assuming the pressurizer spray is actuated by the actual pressurizer pressure signal. The LOFTRAN predicted RCS pressure is slightly higher than the MARVEL-M code prediction due to the previously described spray model differences. Because the differences occur below the safety valve pressure, differences in the safety valve models have been ruled out as the cause for the differences. In addition, as stated above, the transient comparison without pressurizer pressure control is virtually identical. The other transient parameters have good agreement between the two codes.

In the RCS pressure analysis, the pressure control system is conservatively turned off to avoid mitigating the pressure increase. Therefore, it can be concluded that MARVEL-M conservatively calculates peak pressures for events that challenge the reactor coolant pressure boundary acceptance criterion. For certain other events such as DNB events, it is conservative to assume the operation of the pressurizer pressure control system. In such cases, MARVEL-M with pressurizer spray operating is expected to calculate pressures slightly lower than LOFTRAN, resulting in a slightly conservative DNBR calculation. However, this effect is very small for the minimum DNBR compared with the other conservative assumptions and treatment of uncertainties for initial conditions for these DNB events. In addition, the minimum DNBR for the limiting Complete Loss of Flow event conservatively assumes constant RCS pressure in the VIPRE-M calculation.

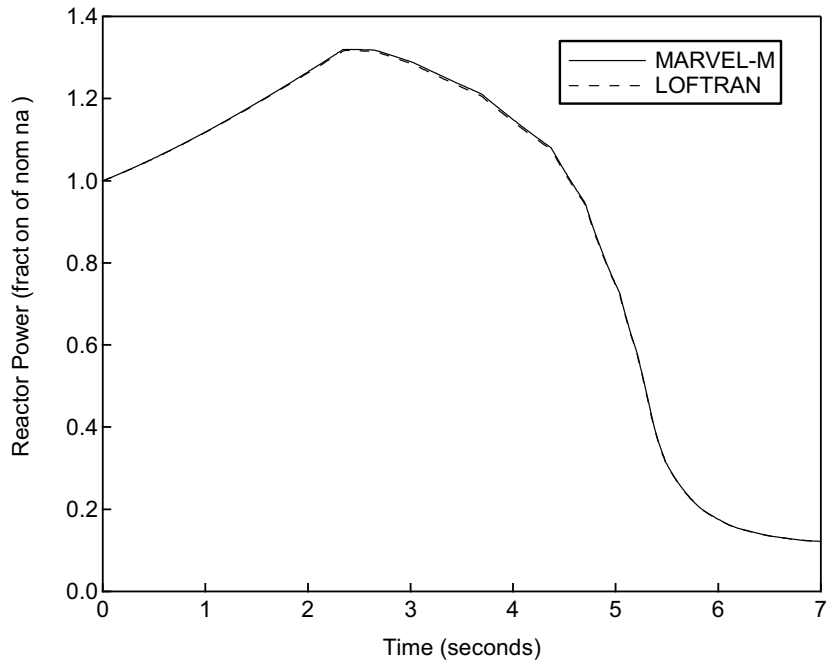


**Figure 3.1-2.1 Reactor Power versus Time
Uncontrolled RCCA Bank Withdrawal at Power
Comparison between MARVEL-M and LOFTRAN**

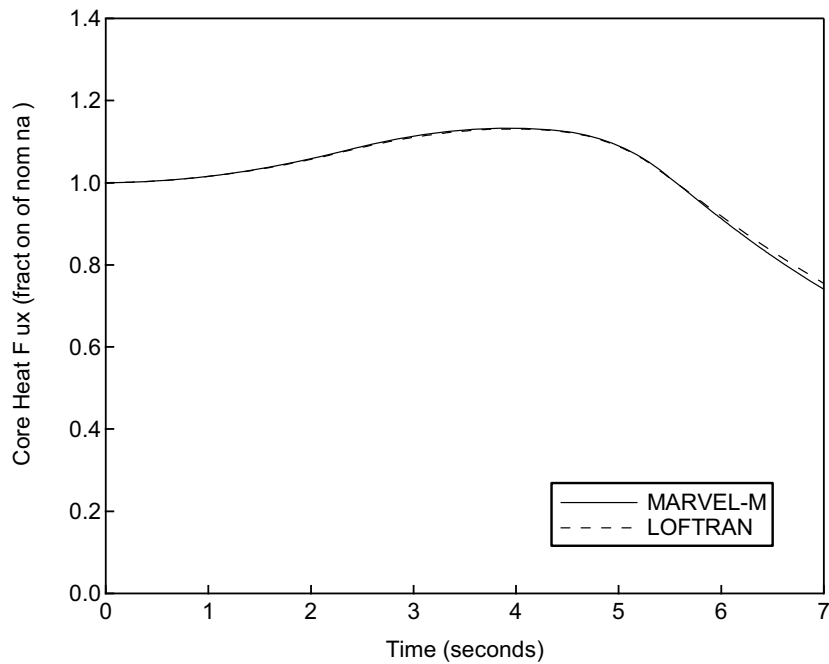


**Figure 3.1-2.2 Core Heat Flux versus Time
Uncontrolled RCCA Bank Withdrawal at Power
Comparison between MARVEL-M and LOFTRAN**

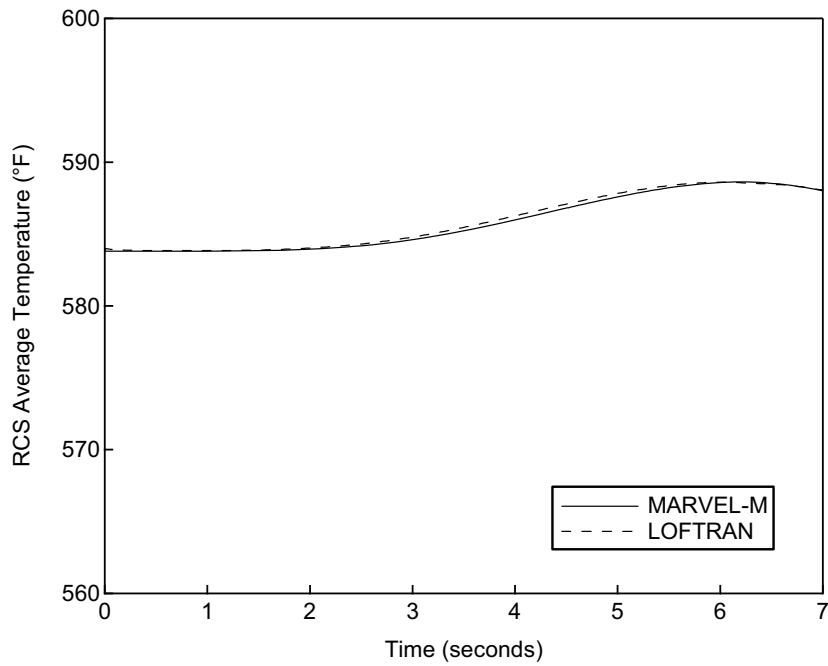


Figure 3.1-2.3 RCS Average Temperature versus Time
Uncontrolled RCCA Bank Withdrawal at Power
Comparison between MARVEL-M and LOFTRAN

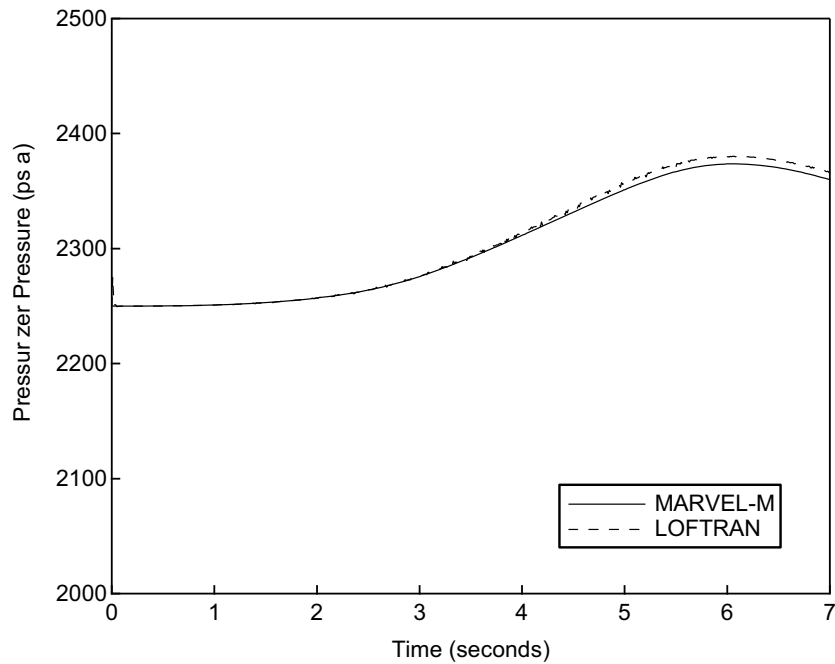


Figure 3.1-2.4 Pressurizer Pressure versus Time
Uncontrolled RCCA Bank Withdrawal at Power
Comparison between MARVEL-M and LOFTRAN

RAI 3.1-3

Please provide the DNBR vs. t for the partial loss of forced reactor coolant flow analyses for both MARVEL-M and LOFTRAN.

Response

As a clarification, DNBR is calculated by the VIPRE-01M code for this event using power and flow calculated by either MARVEL-M or LOFTRAN. The figure below provides a comparison of the DNBR for the partial loss of forced reactor coolant flow event. The two codes provide identical DNBR results for this event.

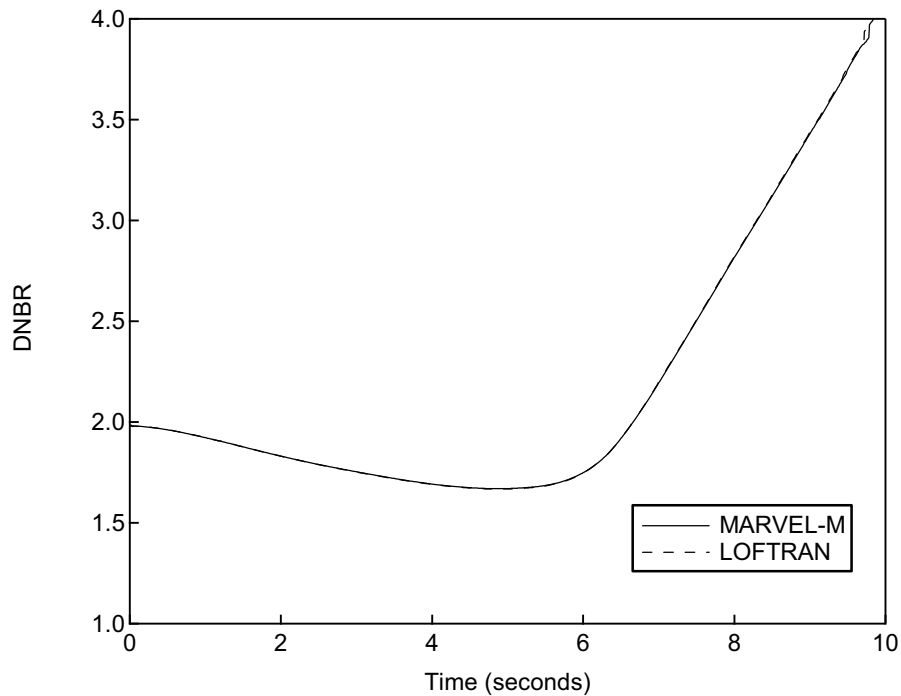


Figure 3.1-3.1 DNBR versus Time
Partial Loss of Forced Reactor Coolant Flow
Comparison between MARVEL-M and LOFTRAN

RAI 3.1-4

Please provide the DNBR vs. t for the complete loss of forced reactor coolant flow analyses for both MARVEL-M and LOFTRAN.

Response

As a clarification, DNBR is calculated by the VIPRE-01M code for this event using power and flow calculated by either MARVEL-M or LOFTRAN. The figure below provides a comparison of the DNBR for the complete loss of forced reactor coolant flow event. The two codes provide identical results for this event.

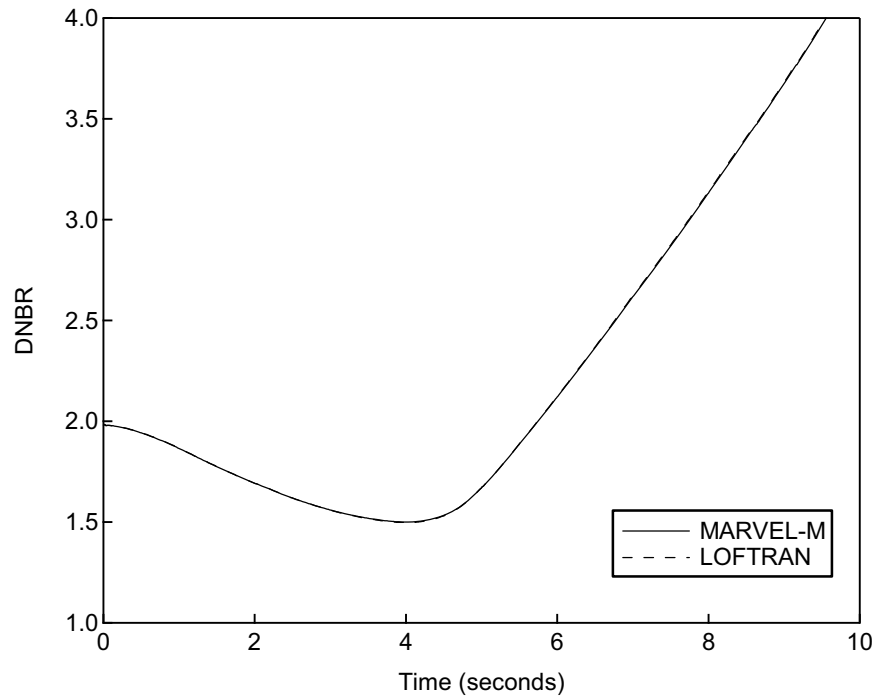


Figure 3.1-4.1 DNBR versus Time
Complete Loss of Forced Reactor Coolant Flow
Comparison between MARVEL-M and LOFTRAN

RAI 3.1-5

Please provide the DNBR vs. t for the partial reactor coolant pump shaft seizure analyses for both MARVEL-M and LOFTRAN.

Response

As a clarification, DNBR is calculated by the VIPRE-01M code for this event using power and flow calculated by either MARVEL-M or LOFTRAN. The figure below provides a comparison of the DNBR results for reactor coolant pump shaft seizure event.

Note that the figure only shows the DNBR transient until the DNBR reaches its safety analysis limit. The two codes show identical results for this transient.

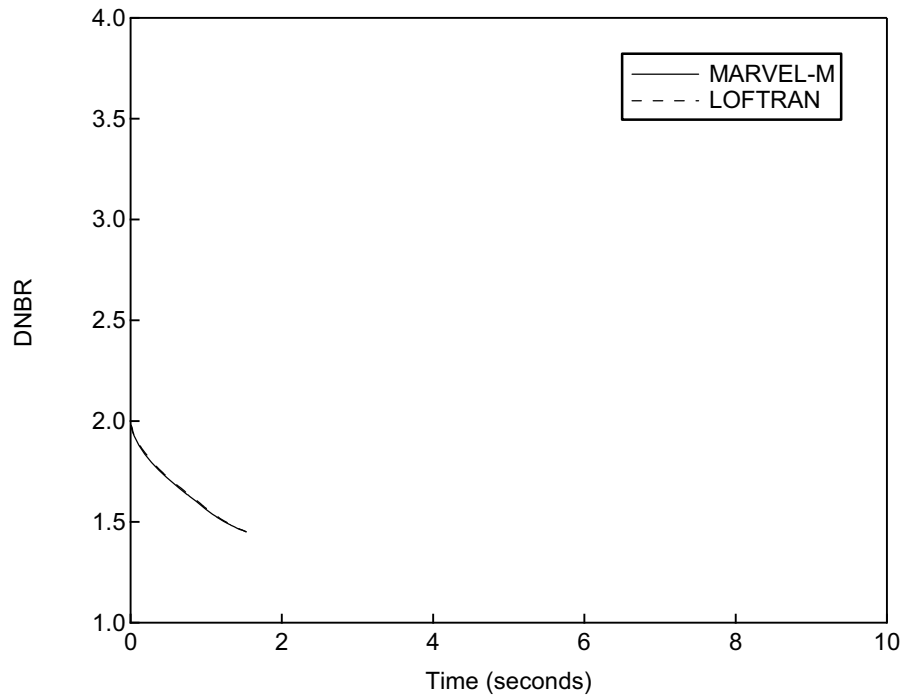


Figure 3.1-5.1 DNBR versus Time
Reactor Coolant Pump Shaft Seizure
Comparison between MARVEL-M and LOFTRAN

RAI 3.2-1

The text says that constitutive models have not changed in TWINKLE-M but the introduction of discontinuity factors can be considered as such. Please respond to this comment.

Response

The response to RAI 2.2-1 provides a detailed discussion of each significant model change between TWINKLE and TWINKLE-M, including the introduction of the new discontinuity factor input process in TWINKLE-M. As depicted in Figure 2.2-1.1 in RAI 2.2-1, MHI considers the addition of the discontinuity factor a pre-processing and post-processing activity outside the solution algorithm of the TWINKLE-M code. Therefore, the solution methods and constitutive models of the TWINKLE-M code have not changed.

RAI 3.2-3

The treatment of the core-reflector boundary condition is important especially when the ejected rod is near the core periphery. Please explain the algorithm by which the diffusion coefficient in the reflector is modified.

Response

The neutron flux distribution changes sharply in the core-reflector boundary which can be simulated accurately using a fine mesh finite difference method or a nodal method such as used in ANC. As an alternative to using such methods, the coarse mesh results can be adjusted to agree with static design code power distribution results in the core. This is done by adjusting the diffusion coefficient of the reflector region once with region-specific multipliers prior to running TWINKLE-M to assure that the TWINKLE-M power distribution agrees with the ANC results both before and after the rod ejection.

The process of modifying the diffusion coefficient is done externally to the code as part of defining the initial condition. Thus there is no change in the computational algorithm in the TWINKLE-M code.

RAI 3.2-4

The comparisons between TWINKLE-M and ANC at HZP show the largest differences in the assemblies with control rods inserted. What are the differences in modeling between the two codes that are claimed to be causing the larger errors?

Response

This difference can be attributed to differences in the numerical solution between TWINKLE-M and ANC. TWINKLE-M uses the finite difference method and ANC uses a nodal expansion method. As explained in the response to RAI 3.2-3, the nodal expansion method used in ANC more accurately calculates steep flux gradients such as near inserted control rods at HZP conditions. Therefore, the differences between TWINKLE-M and ANC in the assemblies with control rods inserted at HZP are larger than those of surrounding fuel assemblies. The differences between TWINKLE-M and ANC tend to decrease as the TWINKLE-M mesh size decreases. It is concluded that the differences between TWINKLE-M and ANC at HZP in assemblies with control rods are attributed to the different numerical solution methods.

RAI 3.2-5

The largest differences between TWINKLE-M and ANC for the HFP case cannot be due to the effect of modeling control rods as all rods are withdrawn. Please comment on the cause of the differences for the HFP case.

Response

This difference can be attributed to differences in the numerical solution between TWINKLE-M and ANC. TWINKLE-M uses the finite difference method and ANC uses a nodal expansion method. As explained in the responses to RAI 3.2-3 and RAI 3.2-4, the nodal expansion method used in ANC more accurately calculates steep flux gradients such as between fresh fuel assemblies and adjacent fuel assemblies in the peripheral region of the core. Therefore, the differences between TWINKLE-M and ANC for adjacent assemblies with large differences in burnup are larger than other combinations of adjacent fuel assemblies. The differences between TWINKLE-M and ANC tend to decrease as the TWINKLE-M mesh size decreases. Therefore, similar to the responses to RAI 3.2-3 and RAI 3.2-4, the reason for the difference between the TWINKLE-M and ANC results is the difference in numerical solution methods.

RAI 3.2-6

Table 3.2.1-1 provides a comparison between TWINKLE-M and ANC for key parameters. A key parameter for the REA that can be calculated with the two codes is the Doppler reactivity coefficient. Please provide a comparison of the Doppler coefficient for at least one core configuration.

Response

The Doppler reactivity coefficient is a key parameter in the control rod ejection event. The response to RAI 5.3-8 describes how the Doppler effect is adjusted in the safety analysis evaluations. A comparison of the Doppler temperature coefficient calculated using both TWINKLE-M and ANC is provided for an end of cycle (EOC) core at hot zero power just prior to the control rod ejection. The comparison between TWINKLE-M and ANC shows good agreement, as the calculated Doppler temperature coefficient is identical for both codes.

Table 3.2-6.1 Doppler Temperature Coefficient Comparison with ANC and TWINKLE-M

Code	Doppler Temperature Coefficient
ANC	1.9 pcm/°F
TWINKLE-M	1.9 pcm/°F

RAI 3.2-8

It is not clear why the neutron lifetime is given in Table 3.2.2-1. If it is meant to be a given reactor condition then how does it enter into the calculation? Whether it is a reactor condition or the result of an edit from the calculation, how is it obtained?

Response

Table 3.2.2-1 provides the core conditions (initial power, average coolant temperature, RCS pressure, ejected worth, delayed neutron fraction, and neutron lifetime) that must be satisfied in order to create a set of TWINKLE-M base cases that represent identical core conditions so that the effects of only changes in the mesh size can be evaluated in Section 3.2.2 of MUAP-07010. Neutron lifetime is an output parameter calculated based on volume averaged power weighted neutron velocity. This is a useful core parameter in characterizing the core response to power excursion events. Per the nuclear design group, the output value of this parameter for both the 2 x 2 mesh case and the 4 x 4 mesh case should be 8.0 microseconds. Adjustments were made to the base model to obtain this value as indicated for both cases in Table 3.2.2-1. Thus, once appropriately adjusted, this parameter does not affect the results of the sensitivity study of the mesh size for the RCCA ejection event.

RAI 3.2-9

How is the delayed neutron fraction calculated for use in TWINKLE-M? If a single number is used for all fuel assemblies, please explain how results would compare if using a number generated for each assembly.

Response

Table 3.2.2-1 provides the core conditions (initial power, average coolant temperature, RCS pressure, ejected worth, delayed neutron fraction, and neutron lifetime) that must be satisfied in order to create a set of TWINKLE-M base cases that represent identical core conditions so that the effects of only changes in the mesh size can be evaluated in Section 3.2.2 of MUAP-07010. The fraction of the six delayed neutron groups is calculated in TWINKLE-M separately for each mesh based on the local burnup. The delayed neutron fraction shown in Table 3.2.2-1 is provided as a core average value calculated by power weighting. This is a useful core parameter in characterizing the core response to power excursion events. TWINKLE-M uses the value for each mesh rather than the core average value in its calculations. Per the nuclear design group, the output value of this parameter for both the 2 x 2 mesh case and the 4 x 4 mesh case should be 0.44%. Adjustments were made to the base model to obtain this value as indicated for both cases in Table 3.2.2-1. Thus, once appropriately adjusted this parameter does not affect the results of the sensitivity study of the mesh size for the RCCA ejection event.

RAI 5.2-1

Are the calculated results for the complete loss of reactor coolant flow AOO sensitive to the reactor coolant pump coast down assumptions? Have any sensitivity calculations been performed?

Response

As described on page 5-5 of MUAP-07010, a conservative reactor coolant pump (RCP) flywheel moment of inertia is assumed for the analysis of the complete loss of forced reactor coolant flow. A sensitivity calculation was performed using the design moment of inertia of the RCP flywheel rather than the conservative value assumed in the topical report analysis. The results of the sensitivity calculation are shown in Figure 5.2-1.1 to Figure 5.2-1.6. The reactor power and hot channel heat flux are identical as can be seen in Figure 5.2-1.1 and Figure 5.2-1.2. The conservative RCP coast down assumption results in conservative values of the reactor coolant system (RCS) total flow, RCS average temperature, RCS pressure, and minimum DNBR, as can be seen in Figure 5.2-1.3, Figure 5.2-1.4, Figure 5.2-1.5, and Figure 5.2-1.6, respectively. It should be noted that the DNBR calculations for both cases assume the same fixed core inlet temperature for the duration of the transient.

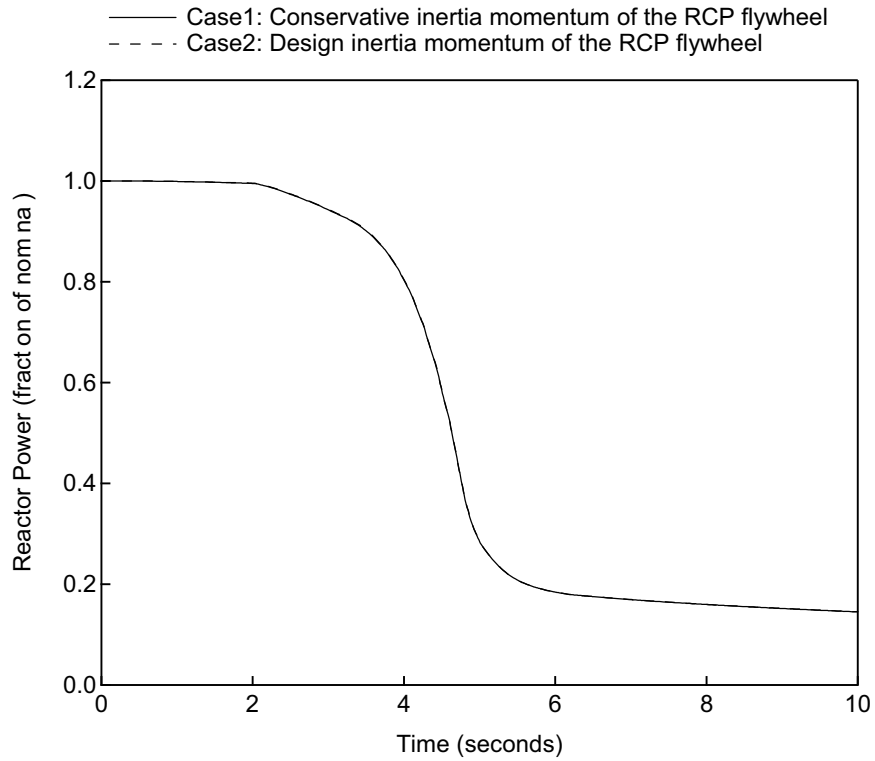


Figure 5.2-1.1 Reactor Power versus Time
Complete Loss of Forced Reactor Coolant Flow

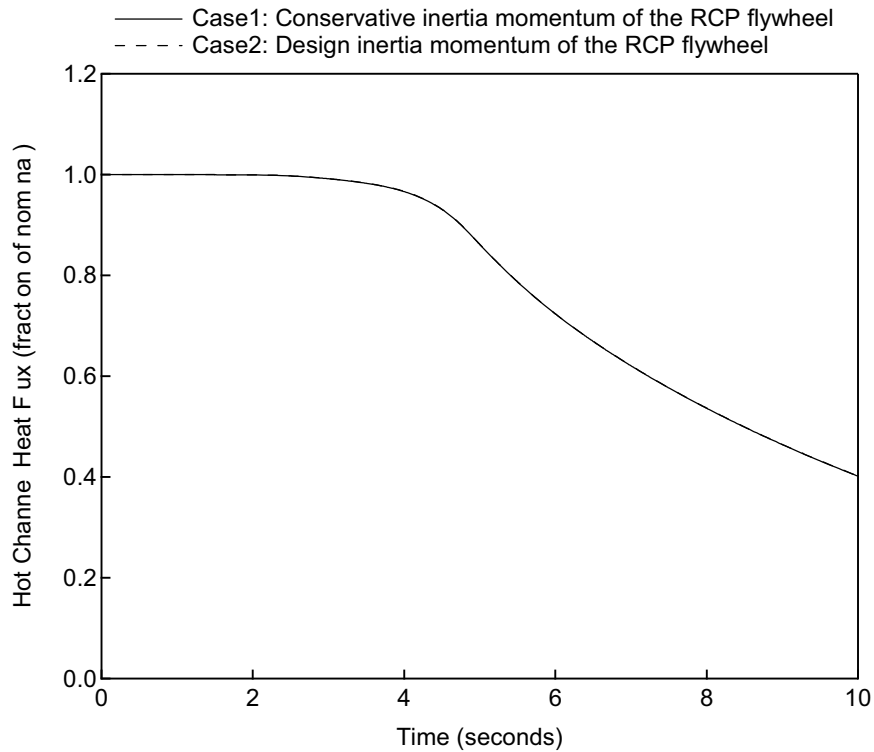
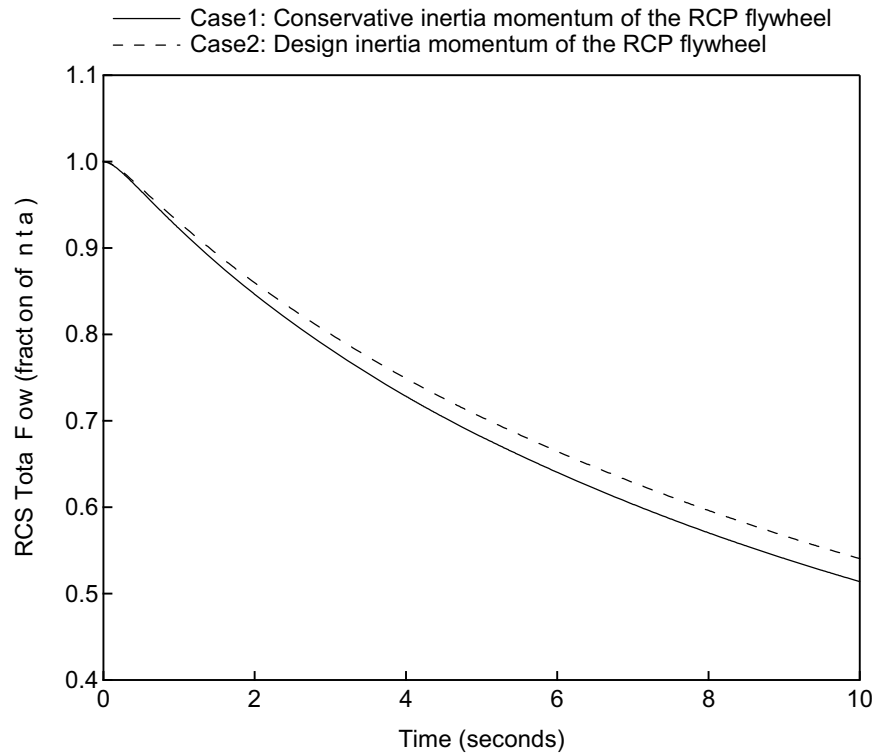
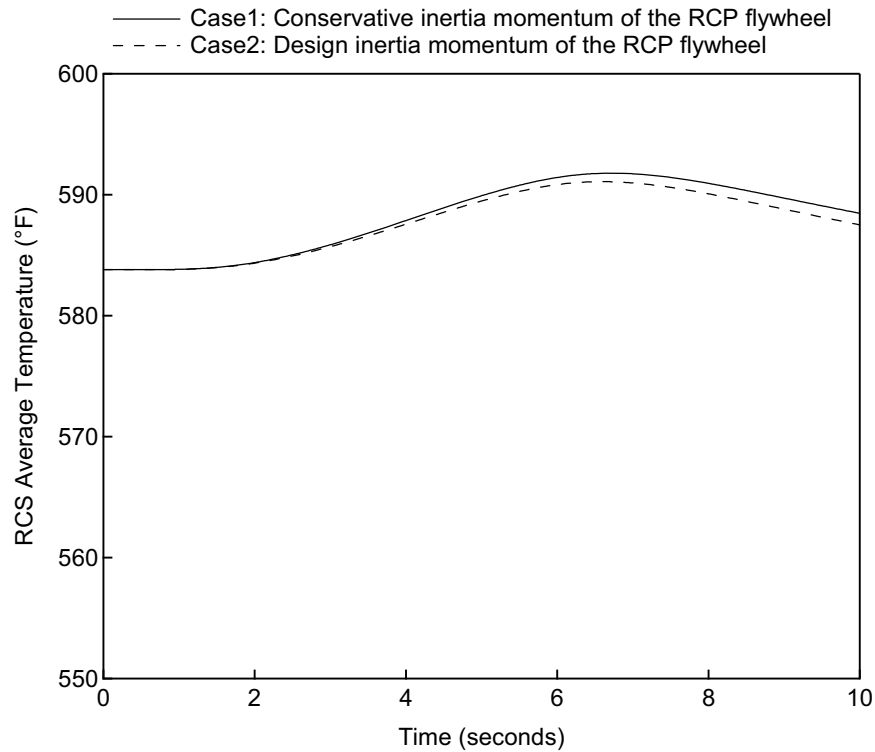


Figure 5.2-1.2 Hot Channel Heat Flux versus Time
Complete Loss of Forced Reactor Coolant Flow



**Figure 5.2-1.3 RCS Total Flow versus Time
Complete Loss of Forced Reactor Coolant Flow**



**Figure 5.2-1.4 RCS Average Temperature versus Time
Complete Loss of Forced Reactor Coolant Flow**

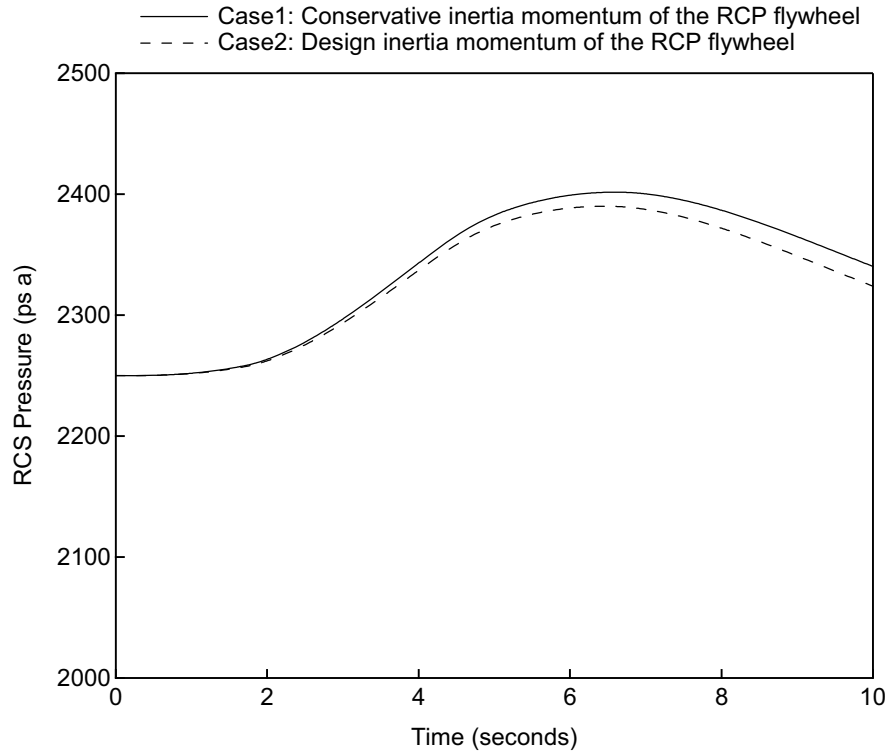


**Figure 5.2-1.5 RCS Pressure versus Time
Complete Loss of Forced Reactor Coolant Flow**

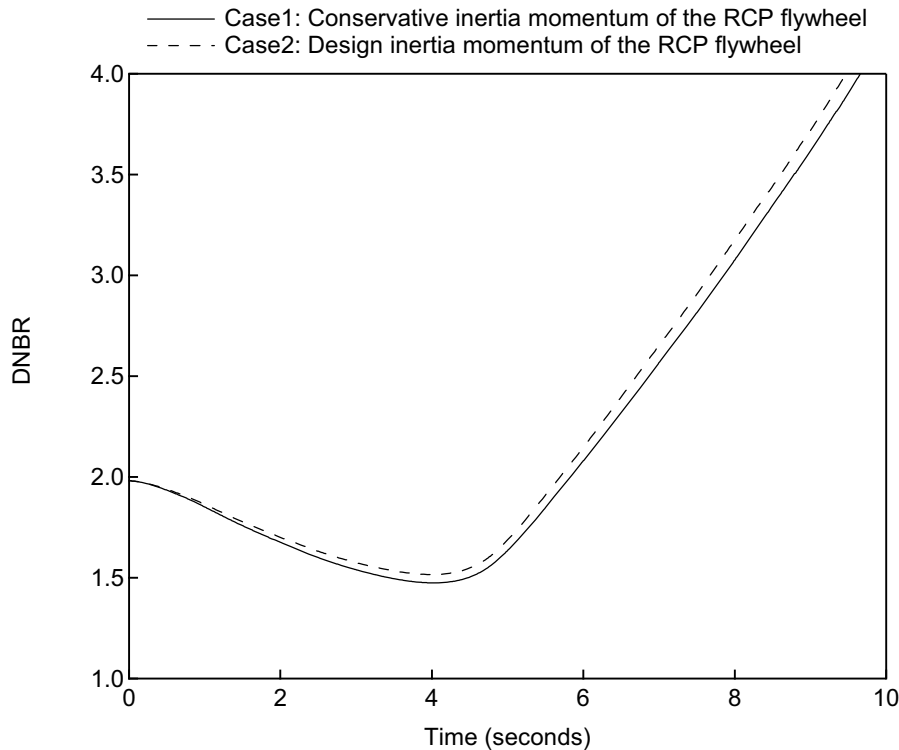


**Figure 5.2-1.6 DNBR versus Time
Complete Loss of Forced Reactor Coolant Flow**

RAI 5.2-2

For the complete loss of reactor coolant flow AOO, it is stated, "a suitable rod bundle DNB correlation...are used." Provide details of the DNB correlation.

Response

The US-APWR applies the WRB-2 correlation. The DNB correlation is intentionally not specified in this Topical Report on "non-LOCA methodology". The DNB correlations applicable to the Mitsubishi fuel design, which include WRB-2, are discussed in Topical Report MUAP-07009 "Thermal Design Methodology".

RAI 5.3-1

In the three- and one-dimensional analysis of the REA, a design limit for the ejected rod worth is used by adjusting the eigenvalue. How is the design limit determined? How is the eigenvalue changed in the calculation to simulate the ejection?

Response

As described on page 5-11 of MUAP-07010, a conservatively large reactivity, chosen at the design limit, is inserted within 0.1 seconds. The design limit for the ejected rod worth is determined as the maximum rod worth for different rod locations and core configurations using the static nuclear design code ANC.

In the case of the three-dimensional methodology which is used for the HZP case, the RCCA which has biggest ejected rod worth (most reactive RCCA) is selected. The inserted reactivity is directly simulated by the change in the absorption cross section caused by the ejection of the most reactive RCCA. The difference between the inserted reactivity and the design limit is accounted for by linearly changing the k_{eff} of the neutron kinetics equation over the course of 0.1 seconds.

In the one-dimensional methodology which is used for the HFP case, the design limit reactivity is externally added to the core only by linearly changing the k_{eff} of the neutron kinetics equation over the course of 0.1 seconds. The methodology in the HFP case differs slightly from the HZP case.

RAI 5.3-2

In the HZP analysis only the hot channel factor and core average power are passed on to VIPRE-M from TWINKLE-M. How is any detailed description of assembly powers and axial power distributions passed on to VIPRE-M? What is the advantage of using VIPRE-M when all the information needed to ascertain whether or not the acceptance criteria are met is contained in the TWINKLE-M results?

Response

The three-dimensional distribution of fuel enthalpy is calculated in TWINKLE-M using a mesh-wise average model, whereas the maximum fuel enthalpy rise is calculated in VIPRE-01M. The maximum enthalpy rise is calculated using a detailed sub-channel model in VIPRE-01M, which is, in turn, used to compensate for the difference between the mesh-wise and pin-wise enthalpy rise. The detailed procedure for how the three-dimensional distribution of enthalpy rise is adjusted to pin-wise enthalpy is provided in Section 5.3 of MUAP-07010.

To calculate the hot spot enthalpy rise in VIPRE-01M for PCMI failure, histories of core average power and hot channel peaking factor (F_Q) calculated in TWINKLE-M are passed to VIPRE-01M. The F_Q history is scaled using a multiplier so that the maximum value is the design limit, which is applied to the hot assembly of the 1/8 core model. The assumption of the power distribution around the hot assembly is the same as the thermal design power distribution and has no effect on the results; therefore, either a 1/8 core model or a single channel calculation can be used for this analysis. However, MHI has selected to use the 1/8 core model for the rod ejection analysis in order to assure consistency of the base input of VIPRE-01M with the core thermal hydraulic design.

In summary, to ascertain whether or not the PCMI acceptance criteria are met, the three-dimensional distribution of enthalpy calculated by TWINKLE-M is applied, considering a peak / average ratio in the mesh using the VIPRE-01M hot spot results. Histories of core average power and hot channel factor are necessary information to calculate the maximum enthalpy rise in VIPRE-01M.

RAI 5.3-3

Since hot channel design limits usually refer to a steady state condition, please explain the definition of the hot channel design limit for a transient.

Response

The hot channel design limit for a transient is determined using the static nuclear design code ANC and takes into account the calculation uncertainty and safety margin. Because the uncertainty and margin are not considered for the transient calculation by the TWINKLE-M code, the calculated maximum value of the hot channel factor history is lower than the design limit from ANC. This assumption is conservative for the core kinetics calculation because the lower hot channel factor decreases the local Doppler effect. On the other hand, for the fuel analysis using VIPRE-01M, the hot channel factor history is scaled by a multiplier so that the maximum value of the time-dependent hot channel factor history is equal to the design limit, which assures a conservative result for the hot spot thermal calculation.

RAI 5.3-4

Since only one hot channel factor (the maximum) is extracted from the TWINKLE-M calculation, how is it applied in VIPRE-M where an entire 1/8 core is represented? Why doesn't VIPRE-M do a single channel calculation?

Response

TWINKLE-M creates an interface file for use with VIPRE-01M that contains a time-dependent history of hot channel factor (not a single maximum value). In order to assure a conservative hot spot calculation, the hot channel factor versus time curve is adjusted upward so that the maximum value of the hot channel factor is equal to the design limit as calculated by ANC (see RAI 5.3-3 response and graphical representation provided in MUAP-07010 Figure 5.3-1). The assumptions of the power distribution in the hot assembly and the other assemblies are the same as the HZP case, as discussed in the response of RAI 5.3.-2. Note that the adjusted hot channel factor time history is only used for the three-dimensional calculation; the 1-D calculation assumes a constant hot channel factor.

The limiting parameters for the rod ejection event are fuel enthalpy, fuel temperature, and cladding temperature, which reach their respective maximum value before the transient coolant condition reaches and affects the core. Therefore, as the reviewer mentioned, a single channel calculation can be applicable for this analysis with an appropriate assumption of the hot spot power transient to be consistent with the peaking factor calculated by TWINKLE-M. However, MHI has selected to use the 1/8 core model for the rod ejection analysis in order to assure consistency of the base input of VIPRE-01M with the core thermal hydraulic design.

RAI 5.3-5

It is recognized that increasing the hot channel factor will make the calculation of fuel temperature and departure-from-nucleate-boiling ratio (DNBR) more conservative in the hot channel. However, assuming that the total power comes from the TWINKLE-M calculation, other channels will have lower powers in the VIPRE-M calculation relative to what was calculated in TWINKLE-M and this will make the calculation of temperature and DNBR in those channels lower. Since one acceptance criterion is a function of clad oxide thickness, the limiting channel may not be the hottest one. Is this taken into account by using the original TWINKLE-M distribution of fuel enthalpy rise rather than the distribution from VIPRE-M?

Response

As the reviewer mentioned, the original TWINKLE-M distribution of mesh-wise fuel enthalpy rise is used to ascertain whether or not the acceptance criteria are met. The hot spot enthalpy rise calculated in VIPRE-01M is used to compensate for the difference between mesh-wise and hot spot enthalpy rise. The detailed PCMI fuel failure evaluation methodology is provided in MUAP-07010 Section 5.3 (2) and Figure 5.3-1.

RAI 5.3-6

The VIPRE-M model uses a 1/8-core representation. This assumes symmetry that is not present in the neutronics calculation. However, this will be acceptable if there is no cross-flow out of that sector or if the time frame is too short for this to be important. Please comment.

Response

Section 4 of MHI topical report MUAP-07009 "Thermal Design Methodology" describes the VIPRE-01M core modeling scheme that coolant mixing between assemblies is conservatively ignored and the effect of mixing is limited to a very local area within the hot assembly. The power distribution in the hot assembly is assumed to be constant for the rod ejection analysis, which is conservative for the mixing effect. Additionally, the power of the hot assembly is assumed to be higher than the power of the surrounding assemblies, which would cause larger flow redistribution from the hot assembly to the surrounding assemblies and result in a more limiting coolant condition in the hot assembly. Therefore, the symmetric 1/8 core model is applicable for the rod ejection hot spot analysis.

RAI 5.3-7

Please explain how the TWINKLE-M one-dimensional model is obtained and how results for the axial power distribution compare with those obtained from a three-dimensional model.

Response

The evaluated state of the reactor core is analyzed with the static nuclear analysis code, ANC. The one-dimensional macroscopic cross sections for TWINKLE-M are created from the three-dimensional results of the ANC calculation. When the macroscopic cross section is collapsed from three dimensions to one dimension, the neutron flux and the volume of the node are used to weight each axial position in order to preserve the reaction rate in the radial direction. The weighting of the macroscopic cross section is shown in the following equation:

$$\bar{\Sigma}_k = \frac{\sum_{i,j} \Sigma_{i,j,k} \cdot \phi_{i,j,k} \cdot V_{i,j,k}}{\sum_{i,j} \phi_{i,j,k} \cdot V_{i,j,k}}$$

Where, $\bar{\Sigma}_k$ = Average macroscopic cross section of axial position k used with TWINKLE-M

$\Sigma_{i,j,k}$ = Macroscopic cross section of position i, j, and k used with ANC

$\phi_{i,j,k}$ = Neutron flux of position i, j, and k calculated with ANC

$V_{i,j,k}$ = Volume of node at position i, j, and k

The comparison of axial power distribution for the TWINKLE-M one-dimensional analysis and the three-dimensional analysis is shown in Figure 5.3-7.1. The analysis condition is beginning of the cycle, all control rods out, and hot full power (HFP). The analytical result of the TWINKLE-M one-dimensional analysis and the three-dimensional analysis agree very well as shown in Figure 5.3-7.1.

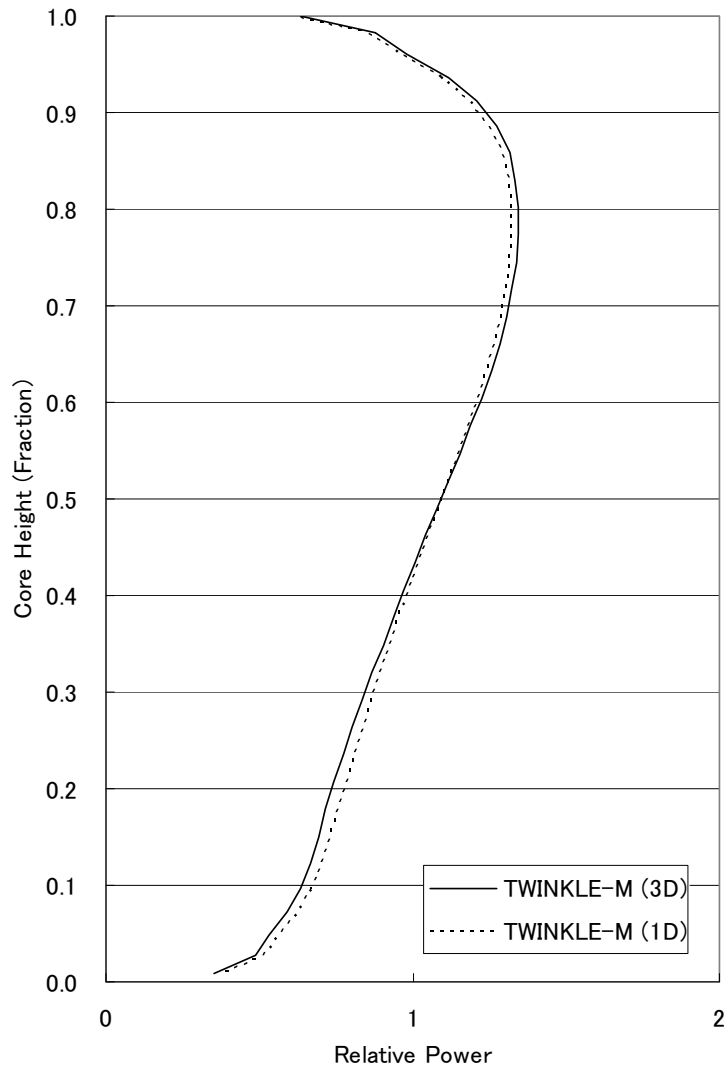


Figure 5.3-7.1 Comparison of Axial Power Distributions for BOC, HFP, ARO

RAI 5.3-8

What "conservative multiplier" is applied for the Doppler feedback?

Response

The Doppler feedback is applied as shown in the following equation. The parameter b is a constant used to adjust the fast absorption cross section for a given change in the calculated effective fuel temperature. In the safety analysis, the constant b is multiplied by 0.8 to apply 20% margin to the design value of the Doppler temperature coefficient.

$$\Sigma_{a1} = \Sigma_{a1}^{\text{ref}} + b \cdot (T_{\text{eff}}^{1/2} - T_{\text{ref}}^{1/2})$$

where

Σ_{a1} = macroscopic absorption cross section for fast group

Σ_{a1}^{ref} = reference macroscopic absorption cross section for fast group

T_{eff} = effective fuel temperature

T_{ref} = reference fuel temperature

RAI 5.3-9

If a three-dimensional model is available in TWINKLE-M for doing the REA analysis at HZP, why isn't this same model used for the HFP case instead of shifting to a one-dimensional model?

Response

The main purpose of using the 3-D methodology is to properly capture the effect of Doppler feedback in the event where the power distribution is highly skewed, such as the RCCA ejection event. The power distribution is less skewed for the hot full power (HFP) case than it is for the hot zero power (HZP) case. As a result, there is not a large advantage in using the 3-D methodology for the HFP case. Thus, although it is technically possible to use the 3-D methodology for the HFP case, MHI opted to use the 1-D model in order to simplify the analysis.

RAI 5.3-10

For the modeling of reactor trip in TWINKLE-M it is stated that the reactivity insertion curve is "simulated." Does this mean that the reactivity insertion is not explicitly modeled by changing cross sections in fuel assemblies? If it is not explicitly modeled, how is the simulation done?

Response

The negative reactivity effect of the control rod is explicitly simulated by increasing the absorption cross section in the calculation mesh associated with inserting the control rod.

RAI 5.4-1

For the steam system piping failure, asymmetric power generation in the core occurs due to a non-uniform cool down. Is this accident sensitive to the user-input mixing factors for the lower and upper plena? Have any sensitivity calculations been performed? If so, please provide the results.

Response

The steam system piping failure event at hot zero power is a transient characterized by non-uniform cooling in combination with the assumption that the most reactive control rod is fully withdrawn. This event is sensitive to the mixing factors. Appendix E of MUAP-07010 evaluates the sensitivity of the calculated minimum DNBR to changes in the vessel mixing factors, FMXI and FMXO. Inlet mixing establishes the core reactivity for this event. The outlet mixing factor is a dependent parameter of f_m^* and f_{mi}^{**} as explained in RAI 2.1-13. The results of the analysis in Appendix E demonstrate that although less inlet mixing does result in small decreases in the calculated minimum DNBR, the DNBR remains significantly above the DNBR limit even assuming no inlet mixing.

* Fraction of flow entering the reactor vessel from one loop that returns to the same loop upon exiting the core.

** Fraction of loop coolant flow which flows up the azimuthal sector (per loop) of the core nearest the inlet nozzle from which it emerges.

RAI 5.4-2

It is stated "flow mixing in the reactor vessel is modeled in the code. The mixing factors for the reactor vessel inlet and outlet plena are defined conservatively by the input referring to the mixing test results by the 1/7 scale reactor vessel model." Please provide the model and substantiate why it is conservative.

Response

The response to RAI 2.1-13 provides details regarding the determination of the design value of f_{mi} used for all non-LOCA events except for the steam line break (SLB) and the conservative value of f_{mi} used for the SLB event. The conservative value of f_{mi} corresponds to the peripheral assemblies closest to the cold loop in the 1/7 scale test results. For the SLB event this maximum value is conservatively applied to the entire 1/4 core sector in MARVEL-M. The outlet mixing factor is a dependent parameter of f_m^* and f_{mi}^{**} as explained in the response to RAI 2.1-13.

* Fraction of flow entering the reactor vessel from one loop that returns to the same loop upon exiting the core.

** Fraction of loop coolant flow which flows up the azimuthal sector (per loop) of the core nearest the inlet nozzle from which it emerges.

RAI 5.5-1

For the feed water system pipe break, the natural circulation model in MARVEL-M is invoked. Are the calculated results sensitive to the timing of the transition to natural circulation flow? Also, are the reactor vessel inlet and outlet plenum mixing factors the same during natural circulation as for the case of forced flow, and what values for the mixing factors are used?

Response

The responses to RAI 2.1-17 and RAI 2.1-18 discuss the treatment of natural circulation flow in MARVEL-M. There is no transition model for natural circulation flow; it is explicitly calculated, therefore, the results are not sensitive to the timing of the transition.

The same inlet and outlet mixing factors (FMXI and FMXO) are used for all flow conditions, the values of which are defined in the response to RAI 2.1-13. It is expected that during natural circulation conditions, the mixing at the lower plenum and the upper plenum will be close to perfect mixing. It is therefore conservative to use the mixing factors from the forced flow condition for the natural circulation condition. A sensitivity study of the feedwater system pipe break results to the assumed mixing factors will be provided in the response to RAI 5.5-2, which will be separately provided to the NRC as agreed upon during the June 26, 2008 conference call.

RAI 5.6-1

For the steam generator tube rupture, "the reactor coolant in the reactor vessel upper head dead volume may flash and form a steam phase at the top..." Does this condition have any effect on upper plenum mixing, and are there any feedbacks to the lower plenum and reactor inlet mixing conditions?

Response

Although it is possible for the upper head dead volume to flash and form a steam phase at the top of the vessel head this is not predicted to occur in the steam generator tube rupture analysis. The following information describes the MARVEL-M model that would be used to describe such as situation.

US-APWR has the design that the primary coolant in the reactor vessel upper head flows into the RV upper plenum lower part through a control rod cluster guide tube, and then it mixes with the flow from the reactor core. MARVEL-M simulates this flow path. If boiling occurs at the reactor vessel upper head, upper plenum mixing occurs as follows:

1. The volume expansion due to boiling displaces the primary coolant from the reactor vessel upper head (20-2) into the RV upper plenum lower part (21-1, 21-2, 21-3, 21-4). See Figure 2.1-5 in MUAP-07010.
2. The mass of the displaced primary coolant is distributed equally to each node of the RV upper plenum lower part.
3. The displaced primary coolant results in an increase of the primary coolant mass in the RV upper plenum lower part. The exit flow from the RV upper plenum lower part (W_{Pi}) also increases due to the flow contributions from the coolant from the core, core bypass coolant flow, and the additional coolant from the reactor vessel upper head.
4. W_{Pi} is distributed between the flow into the node of the RV upper plenum upper part (W_{Pi0}) and the flow to each loop hot leg (W_{Pii}). The distribution is based on the following equations:
(
5. The primary coolant is mixed perfectly in the RV upper plenum upper part (22-1) and flows to each loop hot leg (W_{UPi}).

Therefore, boiling at the reactor vessel upper head has no impact on the lower plenum and reactor inlet mixing conditions.

RAI 6.2-1

For the complete loss of reactor coolant flow AOO, please specify how uncertainties in the input parameters, trip set points, and calculated variables are included in the calculations.

Response

The revised thermal design procedure (RTDP) is used to statistically account for uncertainties in the input parameters such as reactor power, reactor coolant system (RCS) pressure, RCS flow rate, and RCS average temperature. Conservative assumptions for the trip simulation (trip setpoint, signal processing delays, trip reactivity curve, rod drop time) are used in the analysis. The conservative values for parameters such as the inertia of the flywheel, the pressure drop of the primary system, the moderator density coefficient, and the Doppler power coefficient are also used in the analysis. Additional details of the event-specific assumptions are provided in the DCD Chapter 15 analyses rather than in the Non-LOCA Methodology Topical Report.

RAI 6.3-1

In the discussion of the HFP rod ejection accident sample case, it is stated that ANC is used to obtain local peaking factors. No mention of the ANC code is found in the section on the rod ejection accident methodology. Please clarify.

Response

MUAP-07010 Chapter 5 "Event-Specific Methodology" focuses on MHI's general US-APWR non-LOCA analysis methodology which utilizes the following three principal computer codes.

- MARVEL-M plant transient analysis code
- TWINKLE-M multi-dimensional neutron kinetics code
- VIPRE-01M subchannel thermal hydraulics analysis and fuel transient code

The NRC approved nuclear design code ANC is used as a core simulator for the US-APWR design. ANC is a three-dimensional two group diffusion core calculation code based on nodal expansion method. ANC is used for the static evaluation of the peaking factor for the rod ejection accident and the radial power distribution for the steam piping failure event. ANC is one of several nuclear design tools that is related to the core design described in DCD Chapter 4 and related topical reports. These codes are not the central focus of the non-LOCA methodology and are therefore not included in topical report MUAP-07010.

RAI 6.4-1

Is the steam system piping failure event sensitive to the location of the break? Is a break between the steam generator and turbine the most limiting break location for all accident conditions?

Response

The US-APWR design includes both a main steam isolation valve and a check valve in each steam line immediately outside the containment upstream of the main steam header and lines to the turbine. (See MUAP-07010 Figure 5.4-1 for a graphical depiction.) Depending on the combination of break location and single failure assumed, the steam flow may be non-uniform (from only one steam generator) or uniform (all steam generators contribute to the break flow), and may either be automatically isolated or result in an uncontrolled blowdown from one steam generator.

Including single failures, the most limiting break location is inside the main steam line check valve allowing the uncontrolled blowdown of a single steam generator through the flow restrictor integral to the steam generator nozzle. A large double-ended break in the steam header outside the containment vessel will result in all steam generators blowing down until steam line isolation, which will terminate the event. Although the short-term release is greater, the immediate termination makes this case less limiting. As a convenience to the analyst in creating a bounding scenario, ignoring the check valve in the affected steam line results in both a large common blowdown prior to isolation and an uncontrolled single steam generator blowdown after isolation. This is the case analyzed in Section 6.4 of the topical report.

RAI 6.5-1

The analysis assumes that “all of the steam generators are at the steam generator water level low trip set point.” Is the pressurizer water volume sensitive to perturbations in this assumption?

Response

The feedwater line break is assumed to occur concurrent with the low steam generator water level reactor trip signal resulting from the loss of feedwater flow assumed as a precondition. This means that all steam generator water levels are at the low steam generator water level setpoint when the break occurs. This conservative precondition minimizes the total steam generator inventory available to remove heat from the reactor coolant system and makes the reactor trip system response independent of the steam generator pressure and level dynamics of the feedwater line break prior to the reactor trip. This assumption is also conservative regarding the evaluation of the maximum pressurizer water volume.

RAI 6.6-1

For the steam generator tube rupture event, manual reactor trip is assumed at time = 900 seconds because operator action is required to recognize the event. Would the transient results be different if the timing of the manual reactor trip were varied, i.e., 1200 seconds and 1500 seconds, instead of 900 seconds? What was the basis for choosing 900 seconds?

Response

A steam generator tube rupture (SGTR) event initiates the PCMS-based N-16 alarm, which prompts the operator to manually trip the reactor using conventional emergency operating procedures. The N-16 alarm is expected to occur within the first 2 minutes of an SGTR regardless of the coolant activity. In addition, the N-16 alarm is a reliable alarm to immediately identify the event as a SGTR. The analysis assumes that the operators can detect the event within 900 seconds which represents significant time margin for a simple action in the main control room. The assumed 900 second operator action time period will be verified to be conservative during later stages of the plant licensing following development of and training on the procedures.

RAI App.A-1

Appendix A compares the calculated DNBR from MARVEL-M and VIPRE-01M (steady state) for two cases. The code results are identical in both cases. However, the MARVEL-M DNBR analysis uses look-up tables that were generated by calculations with VIPRE-01M. Although it is expected that the VIPRE-01 M model is the same as approved by NRC, this comparison does not validate the DNBR model in MARVEL-M for other transient and accident conditions. Please comment.

Response

As described in the response to RAI 2.1-2, the lookup table consists of DNBR, core inlet temperature, pressure, and core heat flux. The table is created by a VIPRE-01M steady state calculation under the condition of constant primary coolant flow rate and constant power distribution. Therefore, this table can be adopted for transient analysis in each AOO and PA for the condition where the primary coolant flow rate is constant and bounded by the applicable power distribution. MUAP-07010 Appendix A provides a representative comparison between the interpolation of the MARVEL-M DNBR lookup table and the original VIPRE-01M DNBR data for the Uncontrolled Control Rod Assembly Withdrawal at Power event. It is pointed out that the VIPRE-01M data points plotted in Figures A-1 and A-2 are not identical to the data entered into the MARVEL-M tables. This comparison simply demonstrates that the MARVEL-M interpolation methodology adequately calculates DNBR.

RAI App.E-1

Appendix E presents a set of sensitivity analyses based upon reactor inlet plenum mixing for the case of steam system piping failure. Although the case presented indicates that the assumption of no inlet mixing only causes a small reduction in the minimum DNBR, it cannot be extrapolated to other cases on this basis alone. Provide additional comparisons for other AOOs and PAs to substantiate the claim that DNBR is insensitive to the mixing assumptions.

Response

In assessing the importance and sensitivity of events to reactor vessel inlet mixing assumptions, it is important to understand that there is no sensitivity to reactor vessel inlet mixing for uniform events and for rapid transients initiated by the core or for rapid non-uniform transients that are terminated before the effects are felt by the core due to loop transit times. Based on this observation, events such as the RCCA ejection can be analyzed without a NSSS or reactor vessel model, and the partial and locked rotor & sheared shaft events are terminated before the effects of mixing reach the core. It should also be noted that uniformity in vessel inlet mixing is increased with decreasing reactor coolant pump flow and in the limit reactor vessel inlet mixing can best be approximated by perfect mixing for very low flows such as during natural circulation conditions. Perfect mixing is assumed for the Steam Generator Tube Rupture event due to natural circulation conditions that exist during most of the event.

As a result, the extent of reactor plenum inlet mixing has the largest effect on events characterized by non-uniform loop behavior, in particular, events resulting in the heatup or cooldown of a single reactor coolant loop. Among the events that result in a non-uniform loop heatup, the feedwater pipe break event is the most extreme. This event is assumed to be preceded by a uniform loss of feedwater as a precondition that reduces all steam generators to the low-low level trip setpoint, followed by the sudden loss of all inventory from one steam generator due to the break. This event is more extreme and more non-uniform than the loss of feedwater flow event where the non-uniform heatup is caused only by EFW failures assumed in the analysis. The response to RAI 5.5-2 will provide the sensitivity of the feedwater line break event to assumed mixing factors.

The steam system piping failure represents a limiting extreme for analyzing the effects of a single loop cooldown on the NSSS response. Again, by comparison, this non-uniform loop cooldown event is much more severe than the inadvertent opening of a steam generator relief or safety valve. This is the reason why the analysis provided in Appendix E for sensitivity of the event results to reactor vessel inlet mixing was presented for the largest steam system piping failure that results in an uncontrolled blowdown of a single steam generator.

As has already been discussed in the response to RAI 2.1-13, MHI assumes design mixing for all events in which the reactor coolant pumps are assumed to continue to operate, and in the extreme case of the main steam system piping failure, less mixing than expected by test results is assumed for this event. Notwithstanding the extreme non-uniform cooldown characterized by the large steam line break, Appendix E presents a sensitivity study for the steam system piping failure event and concludes that the DNBR would remain above the AOO 95/95 limit for this postulated accident with no mixing and in fact, is relatively insensitive to the mixing assumptions. Therefore, the conclusion that DNBR is relatively insensitive to the mixing assumptions for the most extreme non-uniform cooldown can be extrapolated to other cases.

RAI App.F-1

Please provide the Zaloudek correlation that MHI has used to perform the steam generator tube rupture break flow calculations.

Response

The Zaloudek correlation was originally developed for the critical flow of hot water through a short tube (Reference 1). The Zaloudek correlation is:

$$G = C \sqrt{\frac{2g}{v_f} \cdot (P_{up} - P_{sat})} \quad \text{for } (400 < P_{up} < 1800 \text{ psia})$$

where: G = mass flow rate per unit area for choked flow conditions

P_{up} = upstream pressure

P_{sat} = downstream (SG saturation) pressure

g = gravitational force constant

v_f = specific volume of saturated water

C = constant (0.95)

The Zaloudek correlation was then modified by MHI for use in defining the maximum initial steam generator tube rupture (SGTR) primary-to-secondary flow rate as follows. The constant "C" which was 0.95 in the original correlation was assumed to be 1.0. This assumption is conservative since the larger value of "C" will increase the mass flow rate. The density of saturated water was substituted for the specific volume of saturated water according to the relationship that $\rho_f = 1/v_f$. For the SGTR, the saturation pressure corresponds to the saturation pressure of the secondary side. In the original correlation, the upstream pressure, P_{up} , corresponds very simply to the pressure of the RCS. However, in the SGTR analysis, the upstream pressure varies depending on the RCS pressure and location of the break along the steam generator tube. It must first be reduced by the pressure drop in the length of U-tube between the RCS and the break location. The pressure drop in a single U-tube under nominal RCS flow conditions can easily be determined. However, the pressure drop in the U-tube during the SGTR event will be much larger due to increased rate of flow due to the break, and is proportional to the square of the mass flow. The total pressure drop in the U-tube during the SGTR event can be expressed in terms of the nominal RCS flow and nominal pressure drop between the RCS and the break location by the expression:

$$\Delta P_{SGTR} = \Delta P_{nom} \cdot \left(\frac{G}{G_{nom}} \right)^2$$

where: ΔP_{nom} = pressure drop in the U-tube under nominal conditions

G = mass flow rate in the U-tube under the SGTR conditions

G_{nom} = mass flow rate in the U-tube under nominal conditions

From this expression it is clear that the pressure drop during an SGTR at high-pressure conditions is larger than the nominal pressure drop since the mass flow rate during the SGTR conditions is higher than the mass flow rate under nominal conditions. After the pressure drop in the U-tube has been determined, the upstream pressure can be defined as:

$$P_{up} = P - \Delta P_{SGTR} = P - \Delta P_{nom} \cdot \left(\frac{G}{G_{nom}} \right)^2$$

where: P = pressure in steam generator tube under nominal conditions (may be in hot or cold leg)

Substituting this expression into the original Zaloudek correlation, along with the assumptions described previously, yields the resultant correlation:

$$G^2 = 2g_c \cdot \rho_f \cdot \left\{ P - \Delta P_{nom} \cdot \left(\frac{G}{G_{nom}} \right)^2 - P_{sat} \right\}$$

where: G = SGTR break mass flow rate [lb/(ft²s)]

G_{nom} = mass flow rate under nominal rated conditions [lb/(ft²s)]

P = pressure in steam generator tube under nominal rated conditions (hot or cold leg) [lbf/ft²]

ΔP_{nom} = pressure drop in U-tube to point of SGTR break under nominal rated conditions [lbf/ft²]

P_{sat} = saturation pressure (secondary side) [lbf/ft²]

g_c = gravitational force constant [(lb*ft/s²)/lbf]

ρ_f = density of saturated water [lb/ft³]

In this correlation the mass flow rate during the SGTR event, G , appears on both sides of the equation. Rearranging the terms, the "Modified Zaloudek" correlation used by MHI for calculating a conservatively high initial SGTR primary-to-secondary mass flow per unit area is the following:

$$G = \sqrt{\frac{2g_c \cdot \rho_f \cdot (P - P_{sat}) \cdot G_{nom}^2}{2g_c \cdot \rho_f \cdot \Delta P_{nom} + G_{nom}^2}}$$

Reference

- 1) Zaloudek, R. R., 1963, "The critical flow of hot water through short tubes", HW-77594, Richland, WA: Hanford Lab.

Reference 2

UAP-HF-08170
Docket No. 52-021

MHI's 2nd Response to NRC's Request for Additional Information on
US-APWR Topical Report MUAP-07010-P, Non-LOCA Methodology

September 2008

RAI 2.1-16

A reactor coolant pump model has been added to MARVEL during the evolution to MARVEL-M. Has this model been tested against pump vendor test data? If so, please provide the comparisons.

Response

The reactor coolant pump (RCP) characteristics incorporated into MARVEL-M are based on the RCP unit test data that MHI has performed. MHI has also compared the calculated coast down curve with the test data for a 4-loop Japanese plant in order to confirm the validity of the MARVEL-M RCP model. Figures 2.1-16.1 and 2.1-16.2 compare the measured coast down 4-loop plant data to the MARVEL-M calculation results. Figure 2.1-16.1 shows a test of a two pump coast down (Partial Loss of Forced Reactor Coolant Flow) and Figure 2.1-16.2 shows a test of a four pump coast down (Complete Loss of Forced Reactor Coolant Flow). Both the calculations and the measurements were performed at hot zero power initial conditions. As can be seen from the figures, the calculated values from MARVEL-M show excellent agreement with the measured values. Therefore, the reactor coolant pump model in MARVEL-M is valid for both uniform and non-uniform RCS flow conditions.



**Figure 2.1-16.1 RCS Flow Comparison between a Typical 4-Loop Plant and MARVEL-M
(Partial Loss of Forced Reactor Coolant Flow)**



**Figure 2.1-16.2 RCS Flow Comparison between a Typical 4-Loop Plant and MARVEL-M
(Complete Loss of Forced Reactor Coolant Flow)**

RAI 3.2-2

The TWINKLE code as approved for use by Westinghouse needs to be shown to provide acceptable results when used by MHI. This becomes more important when the code has also been modified. The comparisons in Section 3.2.1 show reasonable agreement with ANC for reactor conditions of interest in rod ejection accident analysis. However, no information is given to show how well TWINKLE-M models steady state power and reactivity measurements at an operating PWR, as well as how it models neutron kinetics. Please provide additional information which helps validate the code as used at MHI.

Response

MHI was introduced to the TWINKLE code by Westinghouse and has been using TWINKLE-M in domestic licensing analyses for many years, as described in MUAP-07010 Section 2.2. The additional comparisons provided in this RAI response supplement the extensive verification and validation activities already performed by MHI for the TWINKLE-M code.

Figures 3.2-2.1 and 3.2-2.2 compare the radial power distributions of two typical 3-loop operating plants to the TWINKLE-M calculations. These comparisons show good agreement and demonstrate the accuracy of the three-dimensional (3D) steady state calculation using TWINKLE-M.

As a verification of the transient capability of TWINKLE-M, the OECD rod ejection 3D transient benchmark problem was performed. This benchmark problem is designed to confirm the ability of various kinetics code solution methods to give common core fuel burnup, cross sections, rod cluster control assembly (RCCA) macroscopic cross sections, fuel properties, and several core physics parameters important to transient calculations. Figures 3.2-2.3 through 3.2-2.5 compare the results calculated using TWINKLE-M to the OECD reference problem solution for the case where one rod is ejected from the bottom of the core at hot zero power initial conditions. These comparisons show good agreement between TWINKLE-M and the reference solution, which demonstrates the validity of the neutron kinetics models used in the TWINKLE-M code.

References:

1. NEACRP-L-335(Revision 1), H. Finnemann and A. G. Galati, "NEACRP 3-D LWR Core Transient Benchmark," Final Specifications, October 1991 (January 1992).
2. NEA/NSC/DOC(93)25, H. Finnemann, H. Bauer, A. Galati, and R. Martinelli, "Results of LWR Core Transient Benchmarks," October 1993.
3. Proc. Joint Int. Conf. Mathematical Methods and Supercomputing for Nuclear Applications, Saratoga Springs, N.Y., American Nuclear Society, 1, 302-313 (1997), M. P. Knight and P. Bryce, "Derivation of a refined PANTHER solution to the NEACRP PWR rod-ejection transients."

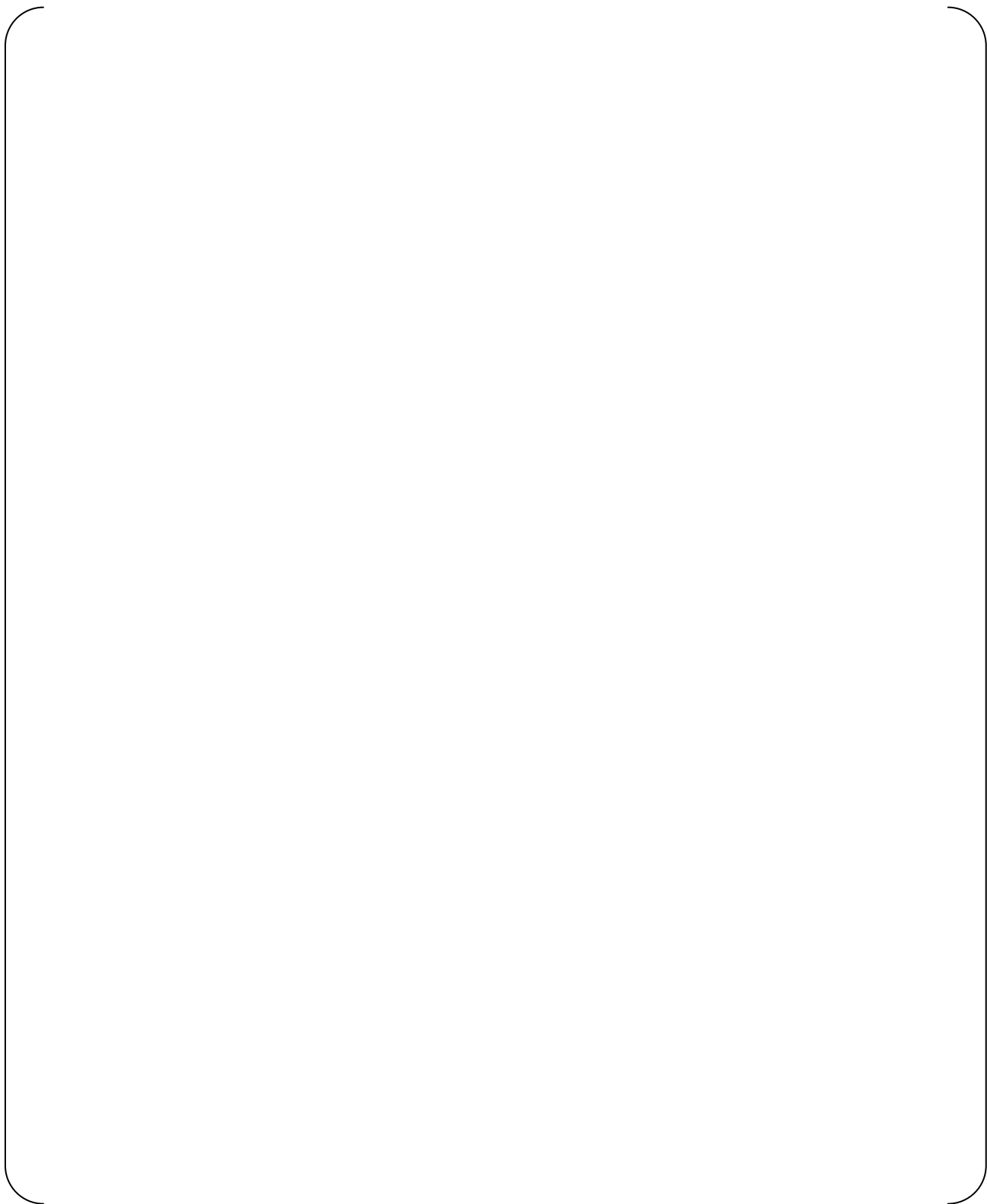


**Figure 3.2-2.1 Radial Power Distribution Comparison between a
Typical 3-loop Operating Plant (Unit-A) and TWINKLE-M**

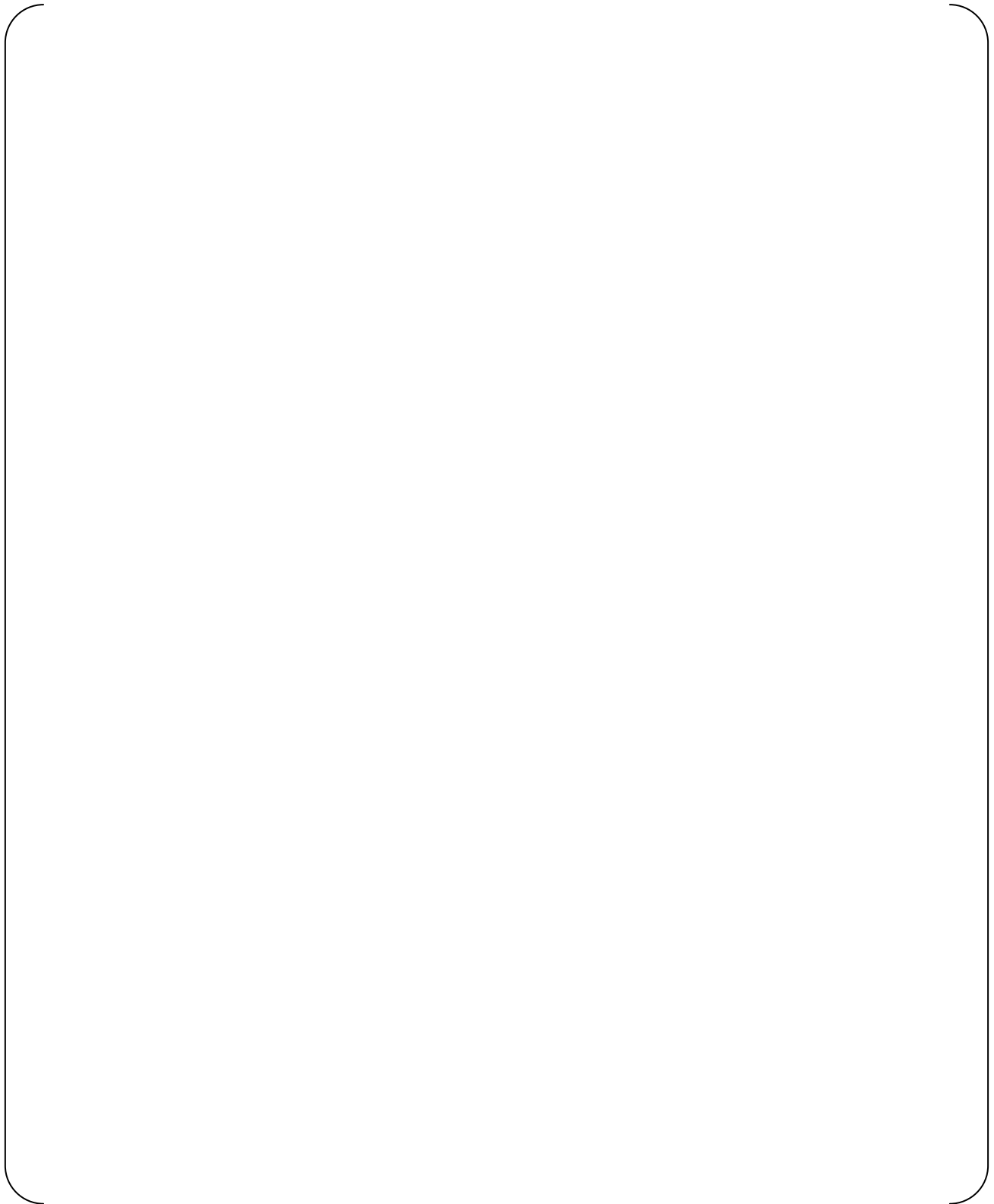


**Figure 3.2-2.2 Radial Power Distribution Comparison between a
Typical 3-loop Operating Plant (Unit-B) and TWINKLE-M**

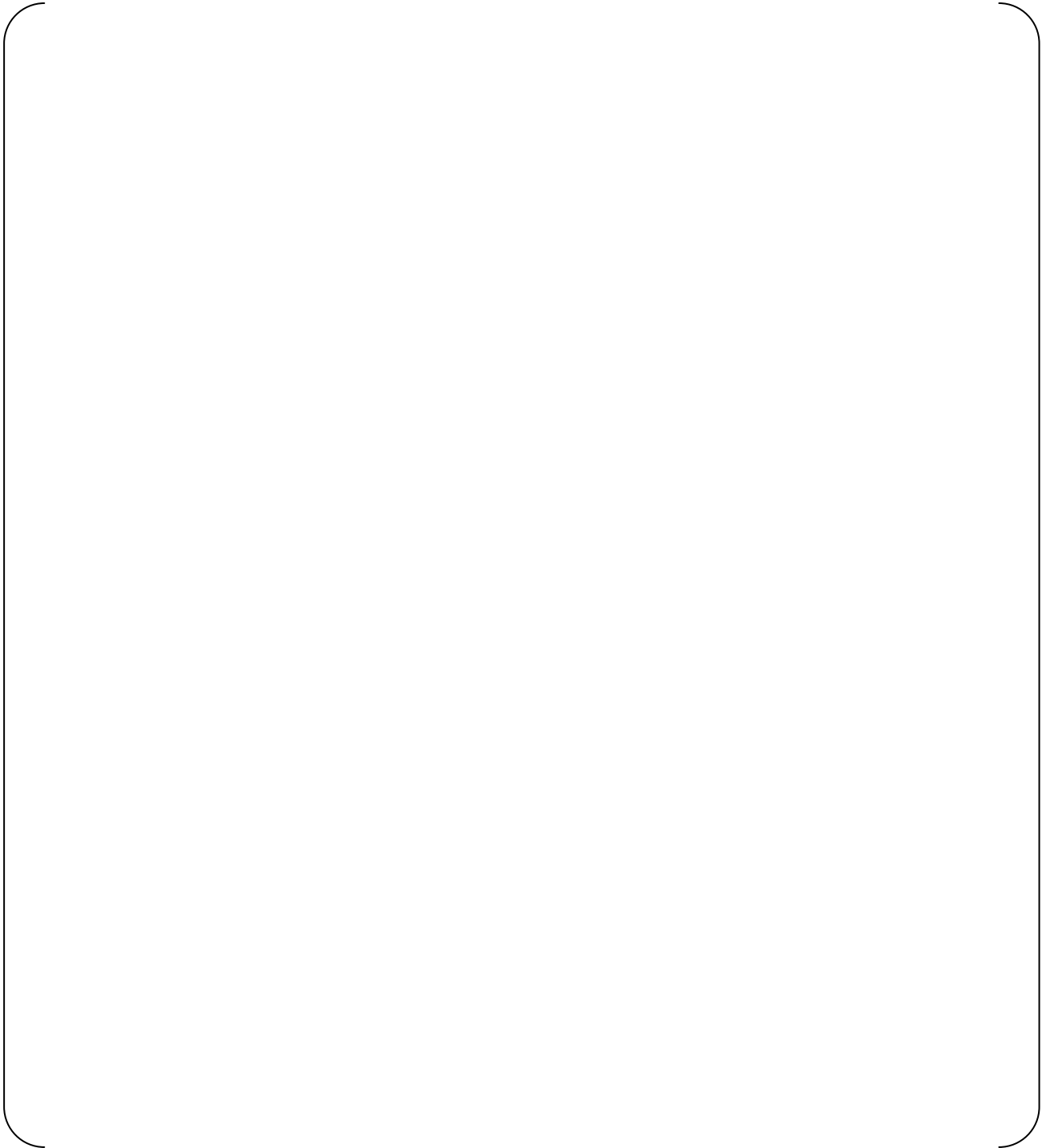


**Figure 3.2-2.3 Average Power Fraction
One Rod Ejection at HZP
Comparison between TWINKLE-M and OECD Reference Solution**

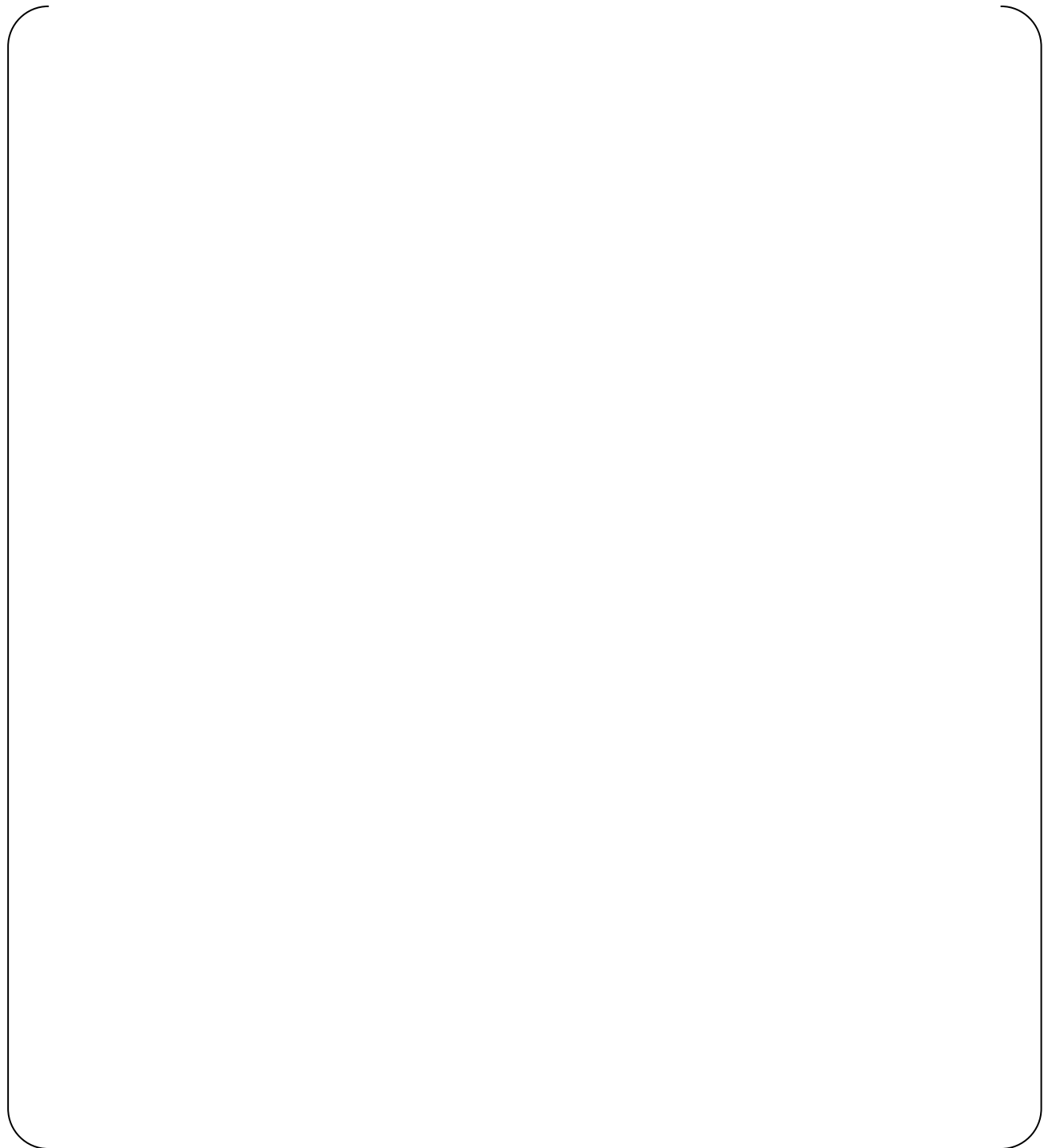


**Figure 3.2-2.4 Doppler Effective Fuel Temperature at Hot Spot
One Rod Ejection at HZP
Comparison between TWINKLE-M and OECD Reference Solution**

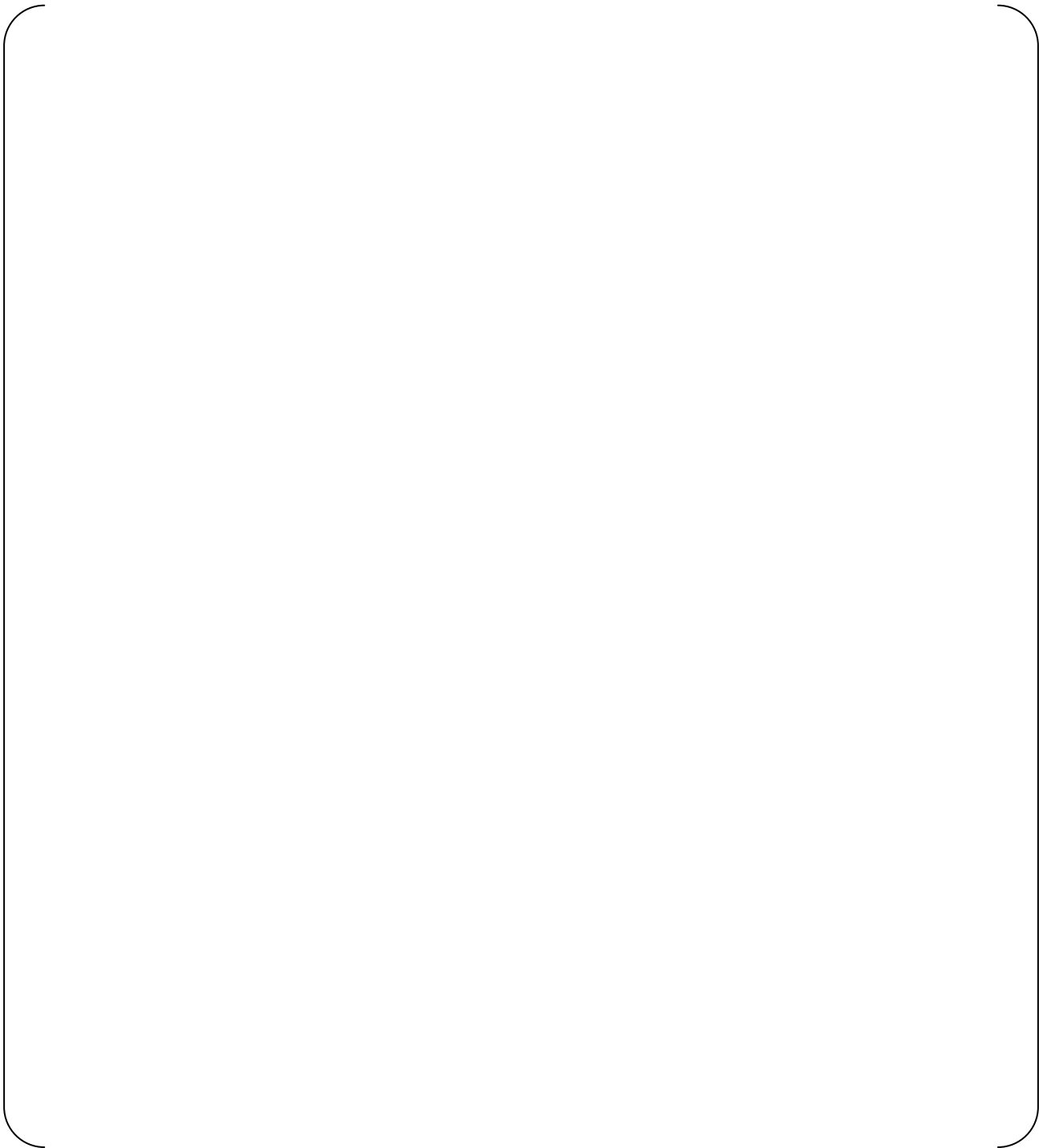


**Figure 3.2-2.5 Radial Power Distribution at Maximum Power
One Rod Ejection at HZP
Comparison between TWINKLE-M and OECD Reference Solution**

RAI 3.2-7

Finite difference codes were originally meant to have mesh sizes on the order of a transport mfp. The mesh spacing used in the comparisons to ANC is 11 cm in all directions. In order to understand why the coarse mesh 2x2 results are in agreement with the 4x4 results please address the following: Is the ejected rod worth calculated for each case (Table 3.2.2-1) or is the worth for one case fixed somehow to be in agreement (within 5 pcm) of the other case? What is the maximum fuel enthalpy (or temperature) for the two cases? It is assumed that the maximum hot channel factor is for an entire assembly. Please provide a comparison of additional hot channel factors (at a minimum for the assemblies surrounding the ejected rod). What would be the result if the axial mesh were also changed?

Response

1. Ejected Rod Worth

The ejected control rod worth (in MUAP-07010-P Table 3.2.2-1) is calculated for both the 2x2 mesh case and the 4x4 mesh case without any adjustment. These values are almost identical because the same cross-section data is used and the power distribution for each case is adjusted to agree with the power distribution of the static design code (ANC). Note that for the safety analysis in Chapter 15 of the Design Control Document, the ejected control rod worth is adjusted to the design limit determined by the ANC calculation because this parameter is critical for the rod ejection analysis and therefore should be conservative. The comparison of the nuclear power transient for the two mesh sizes shown in Figure 3.2.2-1 of MUAP-07010-P would be closer to each other if such an adjustment were performed for those cases.

2. Fuel Temperature

The Doppler effective fuel temperature at the hot spot for the 2x2 and 4x4 mesh calculations generally agree with each other, as shown in Figure 3.2-7.1, although the 2x2 mesh solution conservatively results in a slightly higher maximum effective fuel temperature.

3. Hot Channel Factors

The maximum hot channel factor is calculated for a single mesh. Figures 3.2-7.2 through 3.2-7.5 show the time-varying assembly-wise radial power distribution at the axial height of F_Q for the RCCA ejection transient for the 2x2 and 4x4 mesh calculations. This sequence of figures indicates that the power transient in assemblies around the ejected rod is in good agreement between the 2x2 and 4x4 mesh transient calculations.

4. Axial Mesh Sensitivity

A sensitivity study analysis was performed using { } in the axial direction in the active core region compared to the { } that were utilized in the cases shown in Section 3.2.2 of MUAP-07010-P. For these comparisons, the mesh division in the radial direction is 2x2 mesh per assembly, unless otherwise noted. The results of the axial mesh division sensitivity study are shown in Table 3.2-7.1 and Figure 3.2-7.6 through Figure 3.2-7.8. Figure 3.2-7.6 compares the average axial power distribution for the { } calculation, the { } calculation, and the ANC calculation for three different core conditions. The comparisons indicate that the axial power distributions of the { } calculations are generally closer to the ANC calculations than the { } calculations, but that the differences are not significant. Note that the axial power distributions shown in Figure 3.2-7.6 are calculated by TWINKLE-M without any adjustment of the diffusion coefficients in the reflector region.

The comparisons shown in Figure 3.2-7.7 and Figure 3.2-7.8 indicate that the difference

between the [] calculations has little impact on the nuclear power transient. Note that the diffusion coefficients in the reflector for both cases are adjusted for the transient calculation so that the [] axial power distribution matches the ANC power distribution, as was shown in Figure 3.2.1-5 of MUAP-07010-P. The difference in the nuclear power gradient between the [] cases is caused by the difference in the ejected rod worth, which is shown in Table 3.2-7.1.

In summary, the [] division in the axial direction is sufficient for the non-LOCA safety analyses of the US-APWR.

Table 3.2-7.1 Calculation Conditions and Results of the RCCA Ejection

	[]	[]
Initial power (fraction of nominal)	10 ⁹	Same as left
Average coolant temperature (°F)	557	
RCS pressure (psia)	2250	
Ejected worth (pcm)	600	594
Delayed neutron fraction (%)	0.44	Same as left
Neutron lifetime (microseconds)	8.0	Same as left
Maximum core power (fraction of nominal)	3.12	2.97
Maximum hot channel factor	27.5	27.2

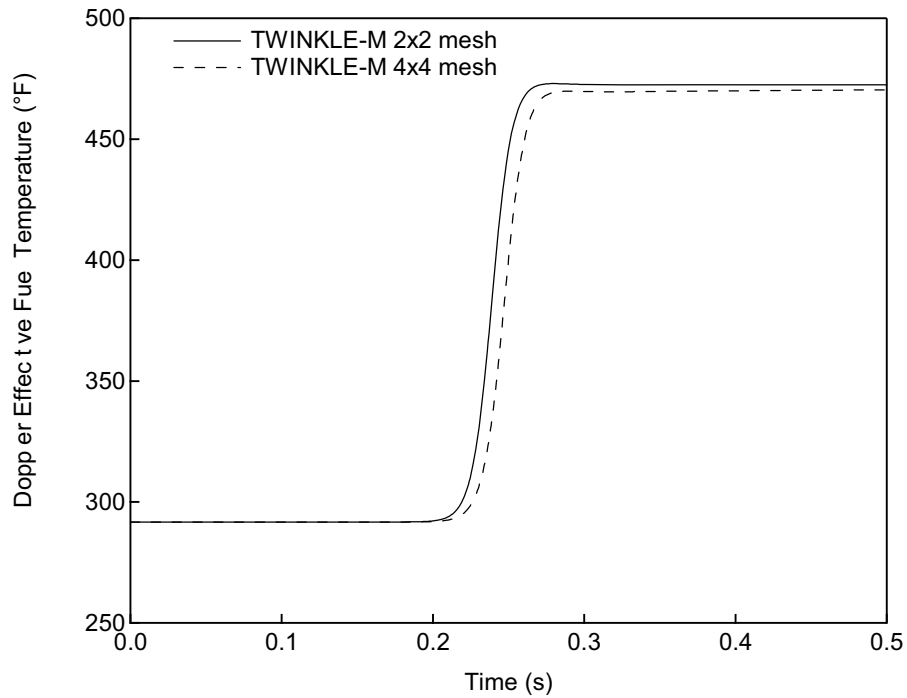


**Figure 3.2-7.1 Doppler Effective Fuel Temperature at Hot Spot
RCCA Ejection at EOC HZP
Comparison between 2x2 and 4x4 Mesh in TWINKLE-M**



**Figure 3.2-7.2 Assembly-wise Radial Power Distribution at Axial Height of F_Q ,
RCCA Ejection at 0.0 second, EOC HZP in TWINKLE-M**



**Figure 3.2-7.3 Assembly-wise Radial Power Distribution at Axial Height of F_Q ,
RCCA Ejection at 0.1 second, EOC HZP in TWINKLE-M**



**Figure 3.2-7.4 Assembly-wise Radial Power Distribution at Axial Height of F_Q ,
RCCA Ejection at 0.2 second, EOC HZP in TWINKLE-M**



**Figure 3.2-7.5 Assembly-wise Radial Power Distribution at Axial Height of F_Q ,
RCCA Ejection at 0.3 second, EOC HZP in TWINKLE-M**

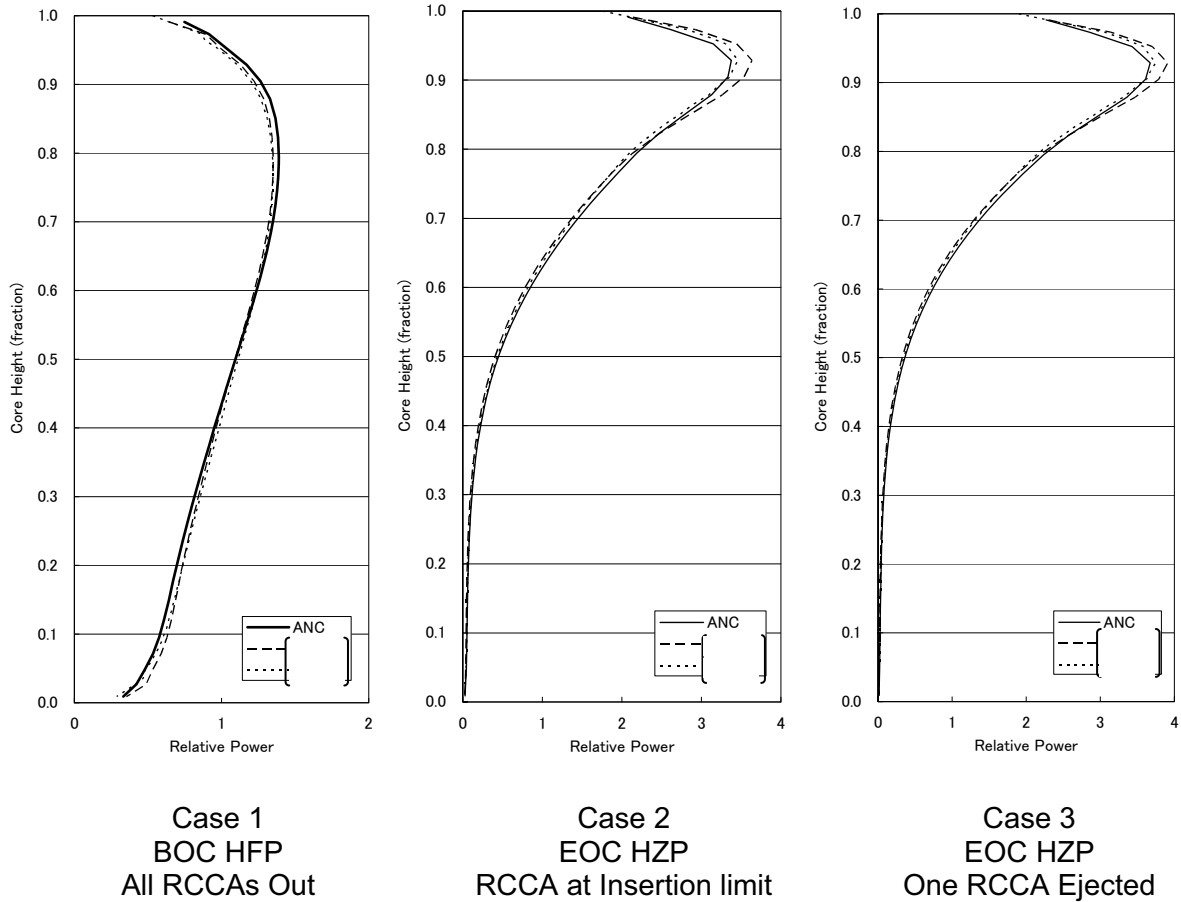


**Figure 3.2-7.6 Average Axial Power Distribution
Comparison between ANC and Axial Mesh Sensitivity Cases
(No adjustment of the diffusion coefficient of the reflector region)**

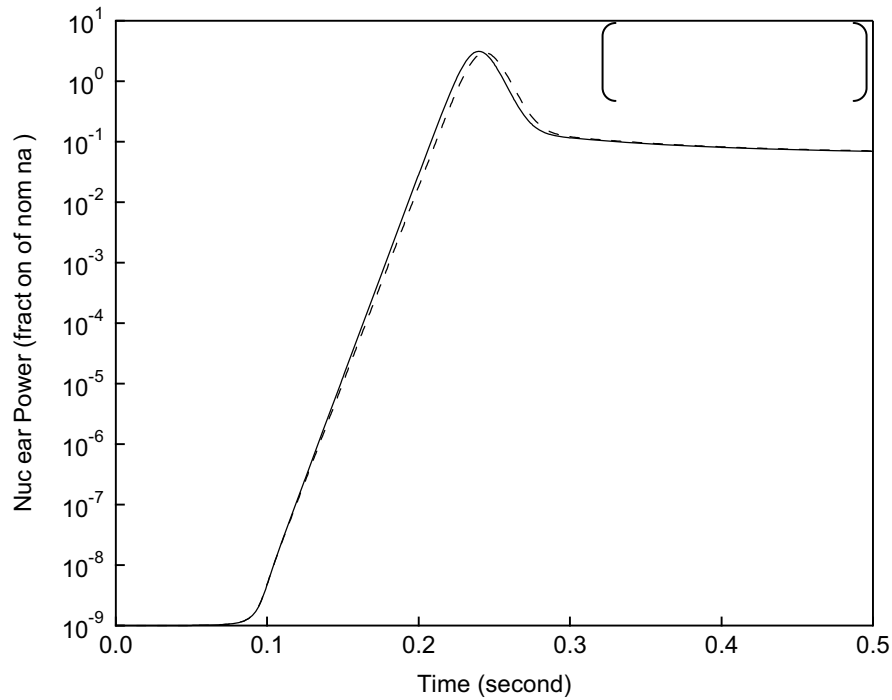


**Figure 3.2-7.7 Nuclear Power, RCCA Ejection at EOC HZP
Comparison between ANC and Axial Mesh Sensitivity Cases**

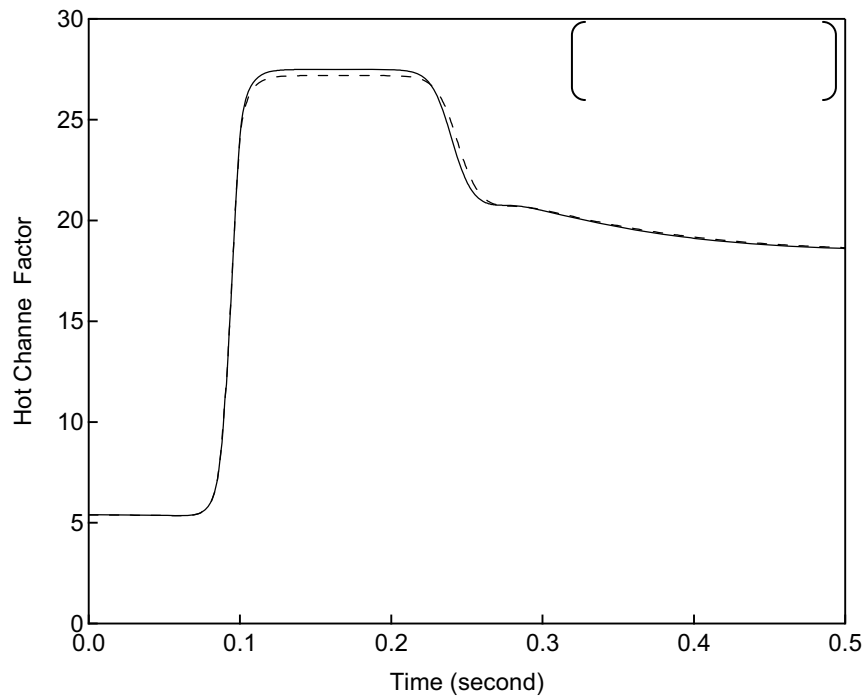


**Figure 3.2-7.8 Hot Channel Factor, RCCA Ejection at EOC HZP
Comparison between ANC and Axial Mesh Sensitivity Cases**

RAI 3.2-10

Please provide discussion of the effect of axial mesh size on the axial power distribution.

Response

See the response to RAI 3.2-7.

RAI 5.5-2

Are the calculated results for the feedwater system pipe break sensitive to the assumed mixing factors, and have any sensitivity calculations been performed? If so, please provide the comparisons.

Response

The extent of reactor plenum inlet mixing has an effect on events characterized by non-uniform loop behavior, in particular, events resulting in the heatup or cooldown of a single reactor coolant loop. Among the events that result in a non-uniform loop heatup, the feedwater system pipe break event is the most extreme. A sensitivity study was performed to confirm the effect of the assumed mixing factors for this event. Two different cases were analyzed: the first case assumes a vessel inlet mixing factor that is 10% less than the base case (Case 1) and the second case assumes a vessel inlet mixing factor that is 10% more than the base case (Case 2). The results of the sensitivity study of the vessel inlet mixing factor for the feedwater system pipe break are shown in Figure 5.5-2.1 through Figure 5.5-2.12. The two cases with modified mixing factors are compared to the base case for various parameters. For these parameters, the effect of the change in the inlet mixing factor is negligibly small. These results demonstrate that the effects of changes to the vessel inlet mixing factor are small for the feedwater system pipe break event.

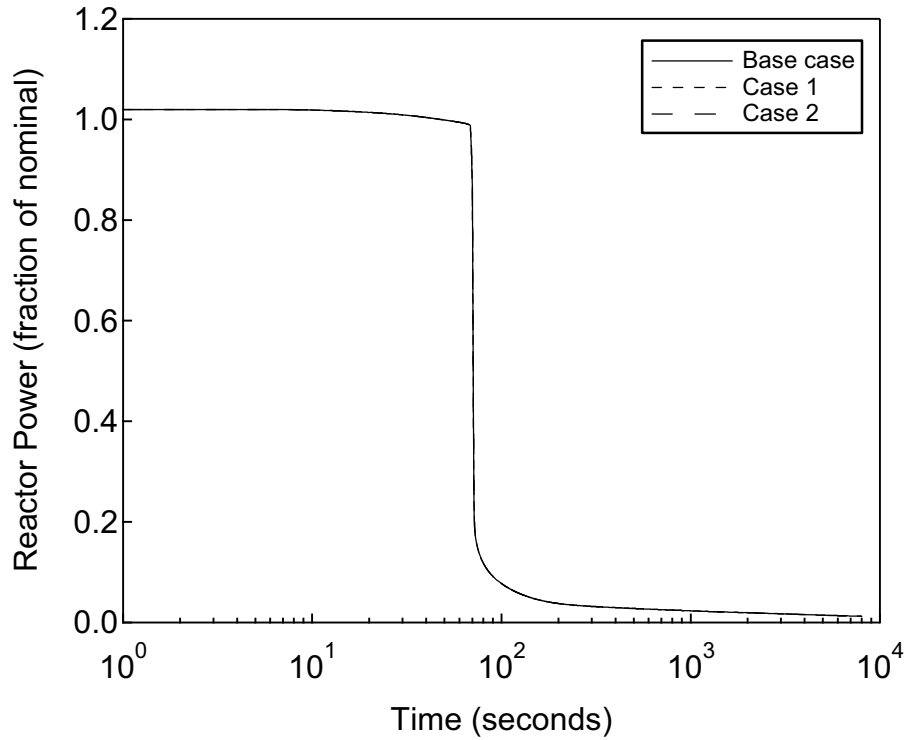


**Figure 5.5-2.1 Reactor Power versus Time
Feedwater System Pipe Break**

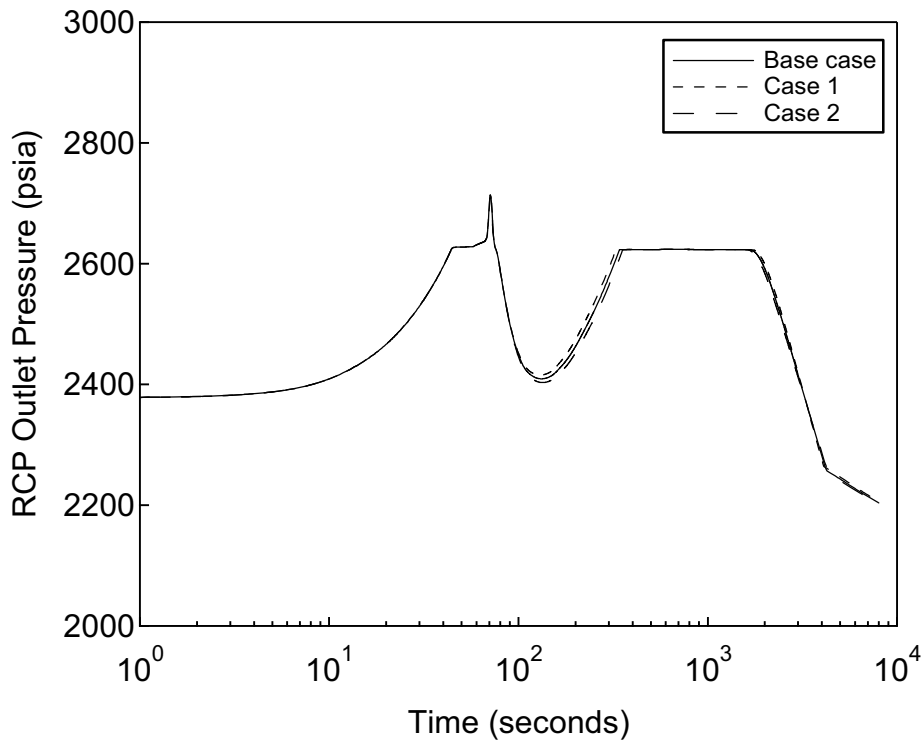


**Figure 5.5-2.2 RCP Outlet Pressure versus Time
Feedwater System Pipe Break**

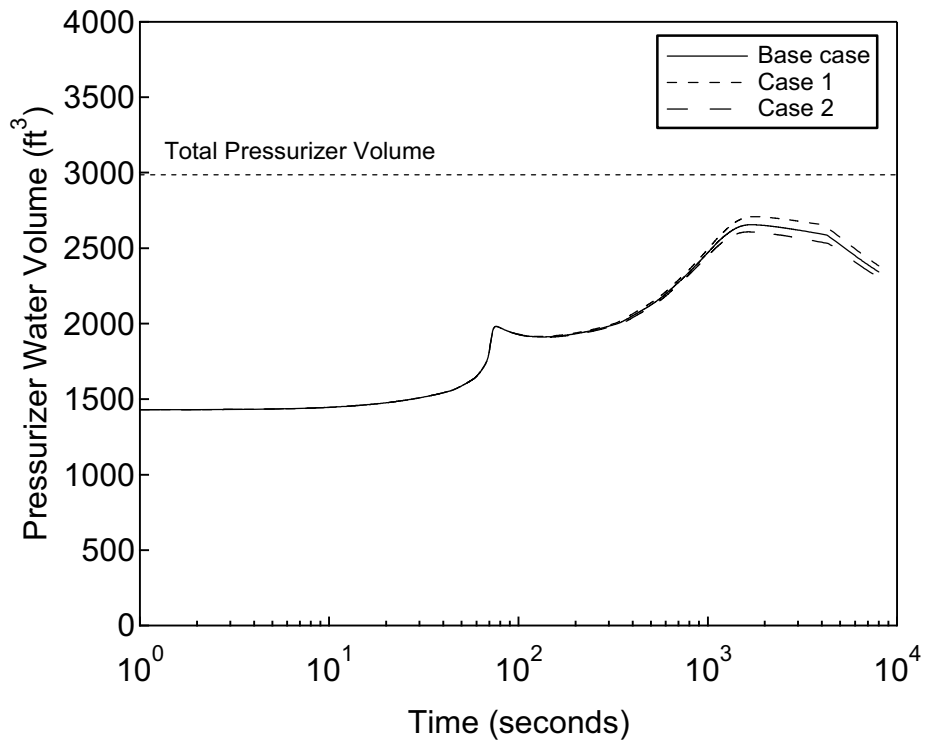


**Figure 5.5-2.3 Pressurizer Water Volume versus Time
Feedwater System Pipe Break**

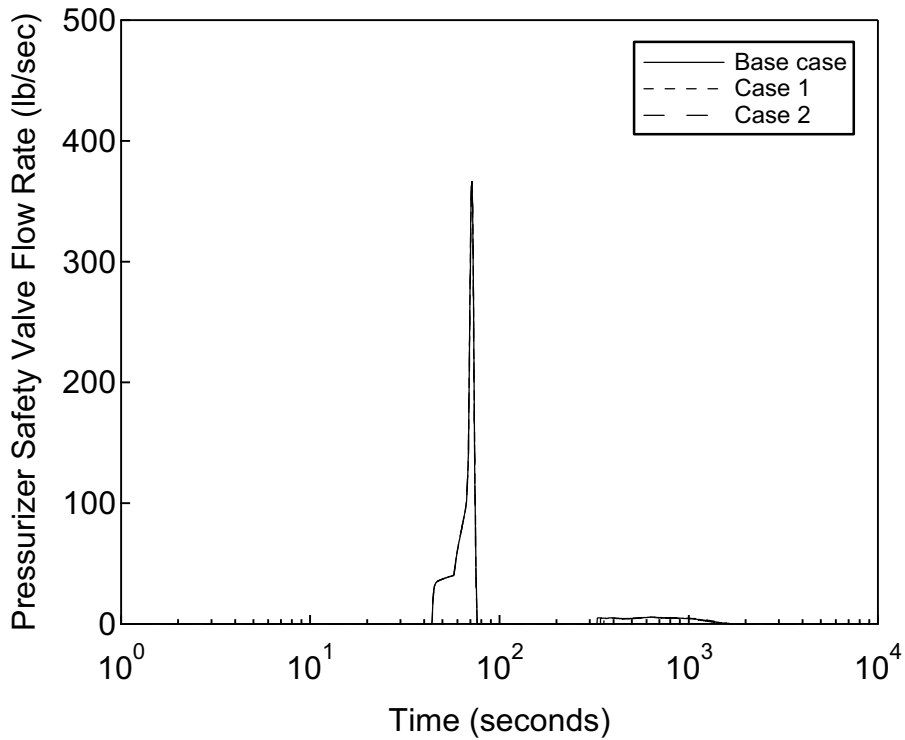


**Figure 5.5-2.4 Pressurizer Safety Valve Flow Rate versus Time
Feedwater System Pipe Break**

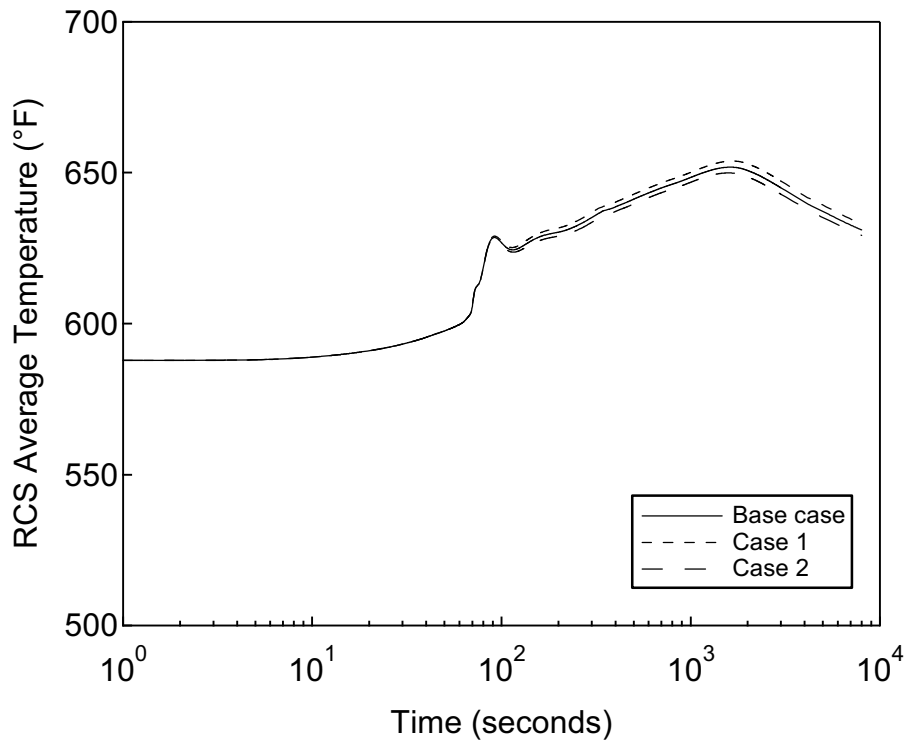


Figure 5.5-2.5 RCS Average Temperature versus Time
Feedwater System Pipe Break

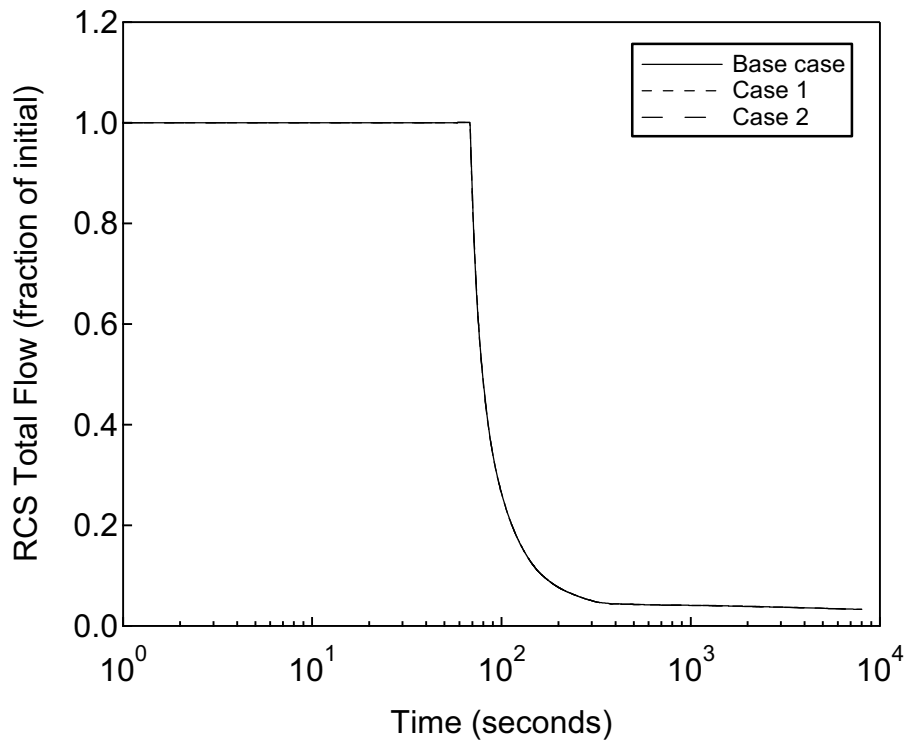


Figure 5.5-2.6 RCS Total Flow versus Time
Feedwater System Pipe Break

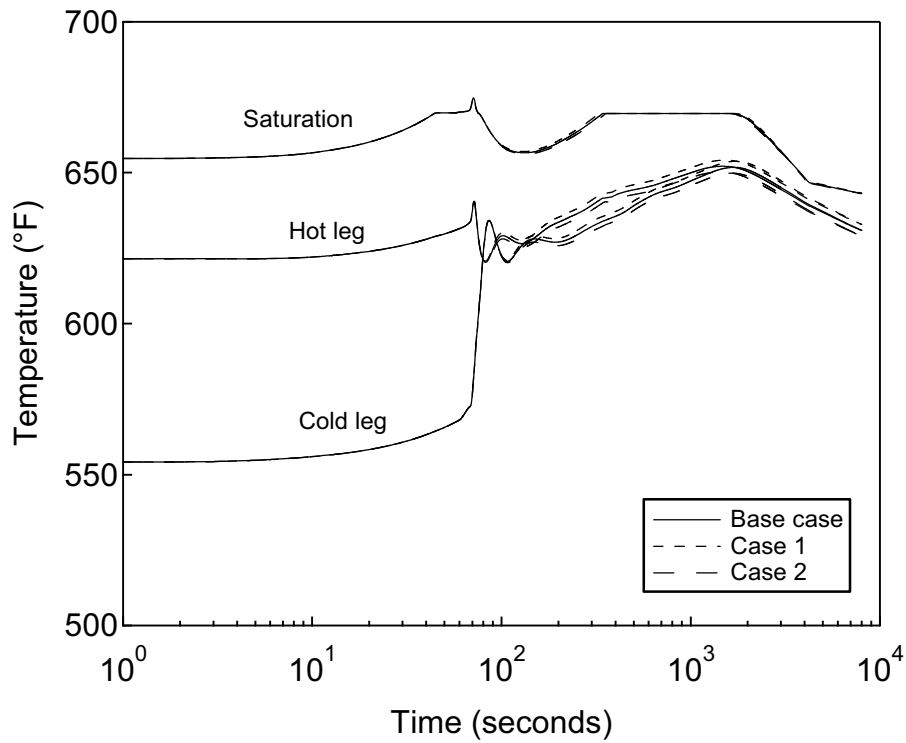


Figure 5.5-2.7 Temperature of Faulted Loop versus Time Feedwater System Pipe Break

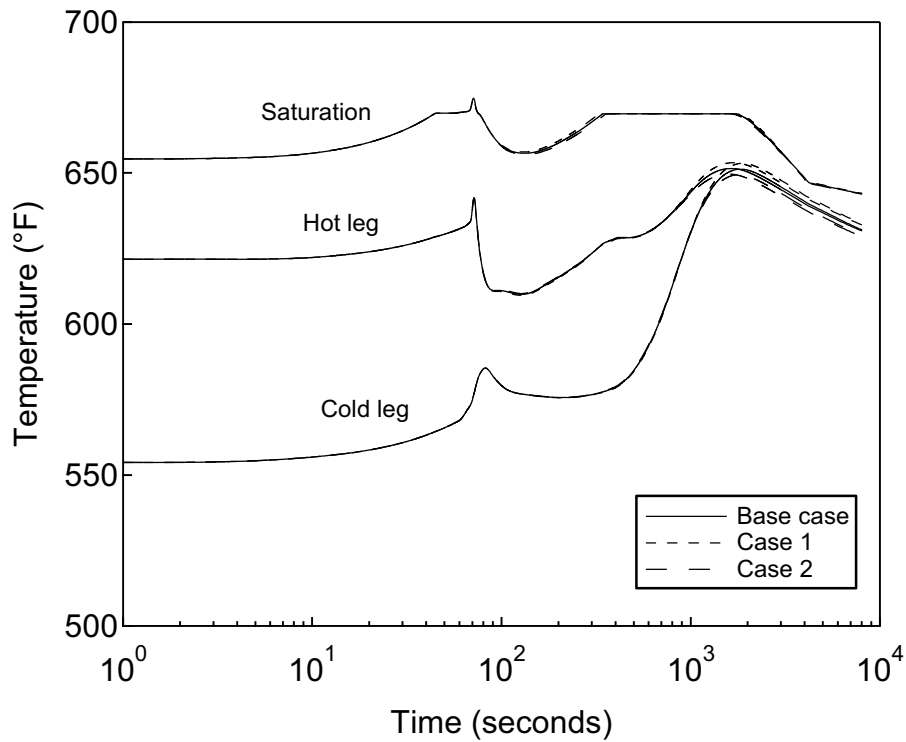


Figure 5.5-2.8 Temperature of Intact Loop without EFW versus Time Feedwater System Pipe Break

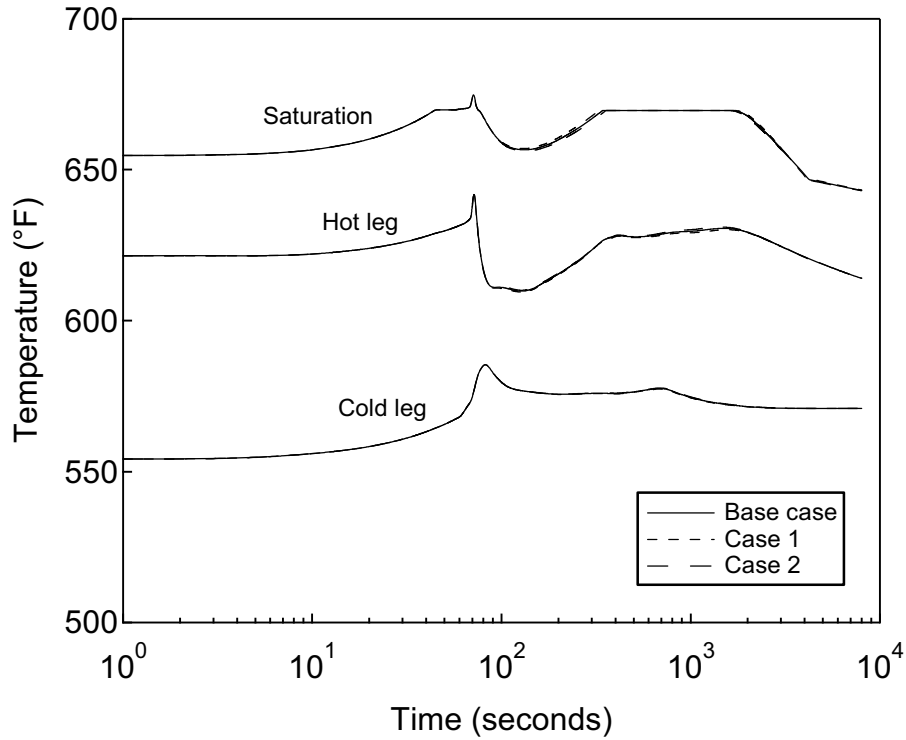


Figure 5.5-2.9 Temperature of Intact Loop with EFW versus Time Feedwater System Pipe Break

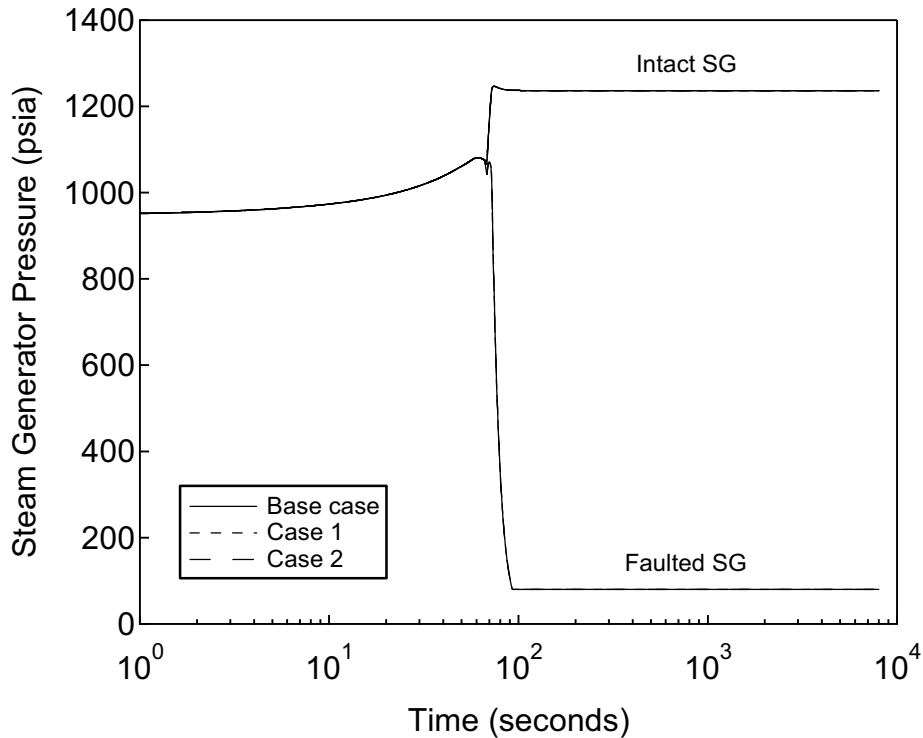


Figure 5.5-2.10 Steam Generator Pressure versus Time Feedwater System Pipe Break

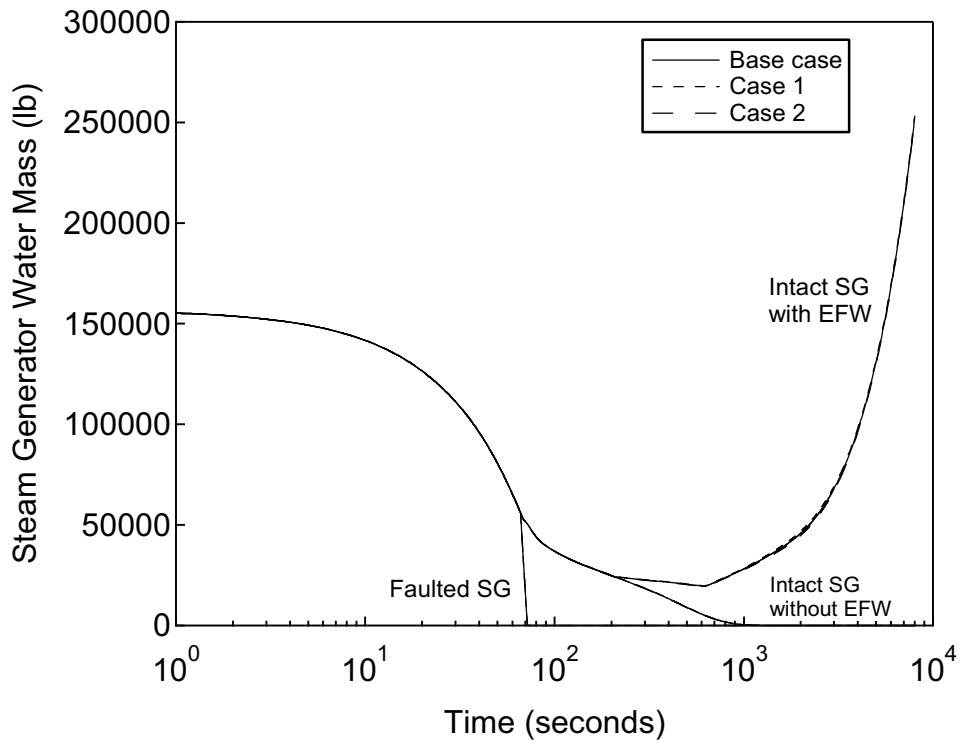


Figure 5.5-2.11 Steam Generator Water Mass versus Time
Feedwater System Pipe Break

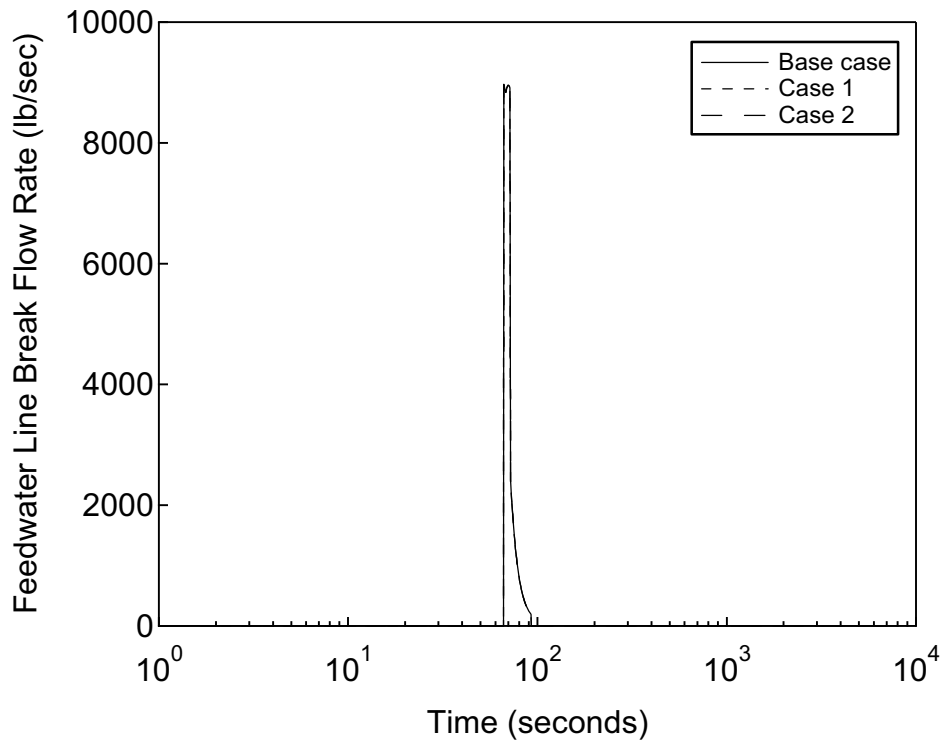


Figure 5.5-2.12 Feedwater Line Break Flow Rate versus Time
Feedwater System Pipe Break

Reference 3

UAP-HF-08245
Docket No. 52-021

MHI's 3rd Response to NRC's Requests for Additional Information on
US-APWR Topical Report: Non-LOCA Methodology, MUAP-07010-P

November 2008

RAI 2.1-21

As shown in the figure on page 2-3 of MUAP-07010-P, MHI did not begin development of MARVEL-M starting with the approved version of MARVEL, but rather an earlier version. Detail the differences between MARVEL-M and the approved version of MARVEL.

Response

History of MARVEL-M

The historical development of the MARVEL-M code is shown in Figure 2.1-21.1 below. It is an updated version of the figure from page 2-3 of the Non-LOCA Methodology Topical Report (MUAP-07010-P) which provides additional information and corrects the LOFTRAN WCAP number and date.



Figure 2.1-21.1 Historical Development of the MARVEL-M Code



In addition to these features, MHI made some improvements and refinements to the MARVEL code independently of Westinghouse. These modifications were described in the Non-LOCA

Methodology Topical Report, MUAP-07010-P, submitted to the NRC in July of 2007. The resultant code was designated MARVEL-M and is described in the MARVEL-M manual (GEN0-LP-480). The latest revision of the MARVEL-M manual, Revision 5, is being submitted to the NRC for approval concurrent with this RAI response as Enclosure 4 to MHI letter UAP-HF-08245.

The purpose of the response to this RAI is to compare the previously approved version of MARVEL to MARVEL-M. The comparison between the approved version and MARVEL-M is divided into two separate discussions: (1) features that are available in the approved version that were not in the original MHI version of MARVEL in 1972 and (2) new features that were added to the code by MHI during the creation of MARVEL-M. All of the features from case (1) and (2) are shown in Table 2.1-21.1. Each of the differences in Table 2.1-21.1 will also be described here in detail.

Given the description of the differences between the approved version of MARVEL and MARVEL-M, the parts of MARVEL-M that need to be reviewed for NRC approval and the parts that can be considered as having been previously reviewed and approved by the NRC can be determined.

Proprietary vs. Non-Proprietary Versions of Approved MARVEL

Comparison between Approved Version and MARVEL (1972)

There are eight features described below in the NRC approved version of MARVEL that were not included in the original version of MARVEL in 1972.

For the first six features, MHI independently added equivalent models of these features to the MHI version of MARVEL, currently designated MARVEL-M. These features are mainly used for the steamline break mass and energy release in the US-APWR DCD Chapter 6 analyses.

The last two features that were in the approved version of MARVEL but not the original MHI version of MARVEL have not been incorporated into the MHI version of MARVEL because these features are not needed for the non-LOCA safety analyses in Japanese domestic plants or the US-APWR design.

Comparison between MARVEL (1972) and MARVEL-M (MUAP-07010-P)

The previous discussion focused on features available in the approved version of MARVEL that were not included in the original version of MARVEL in 1972. As mentioned before, there are also features that have been added to MARVEL-M that do not exist in the approved version of MARVEL. These features are described in the Non-LOCA Topical Report, MUAP-07010, in the MHI RAI responses on that topical report, and in the latest revision of the MARVEL-M manual (Revision 5). The new MARVEL-M features are listed here, along with the corresponding references to sections in the topical report, responses to RAIs, or the MARVEL-M manual. MHI expects these models (listed below) to be the focus of the NRC review of the MARVEL-M code for use in analyzing the US-APWR. Major modifications are described in numbers 9 through 12 and other refinements are described in numbers 13 through 18.

- 9) *4-Loop Reactor Coolant System Model*: The approved version of MARVEL uses a 2-loop reactor coolant system (RCS) model. MHI has modified MARVEL-M to have a 4-loop RCS model. The details of the 4-loop RCS model are found in Section 2.1.3.1 of the Non-LOCA Methodology Topical Report, Section 1.3 of the MARVEL-M manual, and the response to RAI 2.1-1.
- 10) *Flow Mixing in the Reactor Vessel for a 4-Loop Model*: The approved version of MARVEL uses a 2-loop mixing model. MHI has modified MARVEL-M to have a 4-loop mixing model. The details of the 4-loop mixing model are found in Section 2.1.3.2 of the Non-LOCA Methodology Topical Report, Section 1.4 of the MARVEL-M manual, and the response to RAIs 2.1-5, 2.1-11, 2.1-12, 2.1-13, 2.1-14, and 2.1-15.
- 11) *Explicit Reactor Coolant Pump Model*: The approved version of MARVEL uses a simplified empirical flow coastdown model and a transition from this flow model to natural circulation. MHI has modified MARVEL-M to use an explicit reactor coolant pump (RCP) model. The details of the explicit RCP model are found in Section 2.1.3.3 of the Non-LOCA Methodology Topical Report, Section 1.7 of the MARVEL-M manual, and the responses to RAIs 2.1-6, 2.1-7, 2.1-16, 2.1-17, and 2.1-18.
- 12) *Secondary Steam System for a 4-Loop Model*: The approved version of MARVEL uses a 2-loop secondary steam system model. MHI has modified MARVEL-M to have a 4-loop steam system model. The details of the 4-loop steam system model are described in Section 2.1.3.4 of the Non-LOCA Methodology Topical Report and Section 1.8 of the MARVEL-M manual.
- 13) *Pressurizer Surge Line Model*: MHI has modified MARVEL-M to include a pressurizer surge line model. The details of the pressurizer surge line model are found in Section 2.1.3.5 of the Non-LOCA Methodology Topical Report. The surge line node is shown in Table 2.1-1 and Figure 2.1-3.
- 14) *Hot-spot Fuel Thermal Kinetics Model*: MHI has modified MARVEL-M to include a hot-spot fuel thermal kinetics model. The details of the hot-spot fuel thermal kinetics model are found in Section 2.1.3.5 of the Non-LOCA Methodology Topical Report and Section 1.2.3 of the MARVEL-M manual.
- 15) *Core Void Simulation*: MHI has modified MARVEL-M to include a core void simulation model. The details of the core void simulation model are found in Section 2.1.3.5 of the Non-LOCA Methodology Topical Report and Section 4.0 of the MARVEL-M manual.
- 16) *Feedline Break Blowdown Simulation*: MHI has modified MARVEL-M to include a feedline break blowdown simulation model. The details of the feedline break blowdown simulation model are found in Section 2.1.3.5 of the Non-LOCA Methodology Topical Report and further discussed in Section 5.5. It is also discussed in Section 1.5.5 of the MARVEL-M manual and the feedline break simulation parameters are described in Section 2.8 of Part II.
- 17) *Conversion of RCS Volume Balance by Pressure Search*: MHI has modified MARVEL-M to include conversion of RCS volume balance by pressure search. The details of this model are found in Section 2.1.3.5 of the Non-LOCA Methodology Topical Report. It is also discussed in Section 4.0 of the MARVEL-M manual and the input parameters are given in Section 2.13.2 of Part II.
- 18) *Realistic Models*: MHI has modified MARVEL-M to include the optional ability to model realistic events. The details of the realistic models are found in Section 2.1.4 of the Non-LOCA Methodology Topical Report, Section 3.0 of the MARVEL-M manual, and the response to RAI 2.1-20.

Verification of the Improvements to the MARVEL-M Code

The features numbered 9 through 14 and 17 were verified by comparisons with the NRC approved 4-loop LOFTRAN code from the viewpoint of total RCS behavior, including 4-loop simulation and the built-in RCP model. MARVEL-M and LOFTRAN were compared for the "Uncontrolled RCCA Bank Withdrawal at Power", "Partial Loss of Forced Reactor Coolant Flow", "Complete Loss of Forced Reactor Coolant Flow", and "Reactor Coolant Pump Shaft Seizure" events as described in Section 3.1 of the Non-LOCA Methodology Topical Report, as well as the "Loss of Non-Emergency AC Power to the Station Auxiliaries" event as described in the MHI response to RAI 2.1-17. Confirmation of feature 16 is included in this response by the steamline break comparison with the LOFTRAN code described in the following paragraph. Feature number 15 is only used for transferring data from VIPRE-01M to MARVEL-M in the reactivity initiated events. Feature number 18 is not used in the US-APWR safety analysis although a sample transient analysis of a steam generator tube rupture is shown in Appendix F of the Non-LOCA Methodology Topical Report.

In this response, MHI performed a comparison between MARVEL-M and LOFTRAN to confirm the features numbered 1 through 5 and 16 (the feedline break blowdown uses the Moody correlation, the same as the steamline break flow). Figures 2.1-21.2 through 2.1-21.13 compare relevant parameters associated with the steamline break mass and energy release that is described in US-APWR DCD Chapter 6*. In Figure 2.1-21.12, MARVEL-M overestimates the feedwater flow because MARVEL-M conservatively assumes no pressure drop in the feedwater line during feedwater flashing. Other than the difference in feedwater flow, the results of the two codes agree very well for each parameter of interest in the figures. Therefore MHI concludes that the features numbered 1 through 5 and 16 have been correctly incorporated into the MARVEL-M code.

(

Conclusion

- MHI's development of MARVEL-M began from an earlier version rather than the NRC approved version of MARVEL.
 - There are some differences between the approved version and the original MHI version; the approved version has additional features.
 - MHI incorporated equivalent models of these features into MARVEL-M and verified them through comparisons with the 4-loop LOFTRAN code approved by the NRC.
 - Therefore, MARVEL-M includes these features of the NRC approved MARVEL version.
 - MHI then made additional modifications and improvements to MARVEL-M that are not in the approved version of MARVEL.
 - MHI expects the additional modifications described in the Non-LOCA Methodology Topical Report to be the focus of the NRC review of the MARVEL-M code for use in analyzing the US-APWR.
-)

References

- 1) "Non-LOCA Methodology Topical Report", MUAP-07010-P, dated July 2007.
- 2) "MHI's Response to NRC's Request for Additional Information on US-APWR Topical Report MUAP-07010-P, Non-LOCA Methodology," MHI Letter UAP-HF-08141, dated August 22, 2008.
- 3) "MHI's 2nd Response to NRC's Request for Additional Information on US-APWR Topical Report MUAP-07010-P, Non-LOCA Methodology," MHI Letter UAP-HF-08170, dated September 12, 2008.

Table 2.1-21.1 Comparison between Approved Version of MARVEL and MARVEL-M

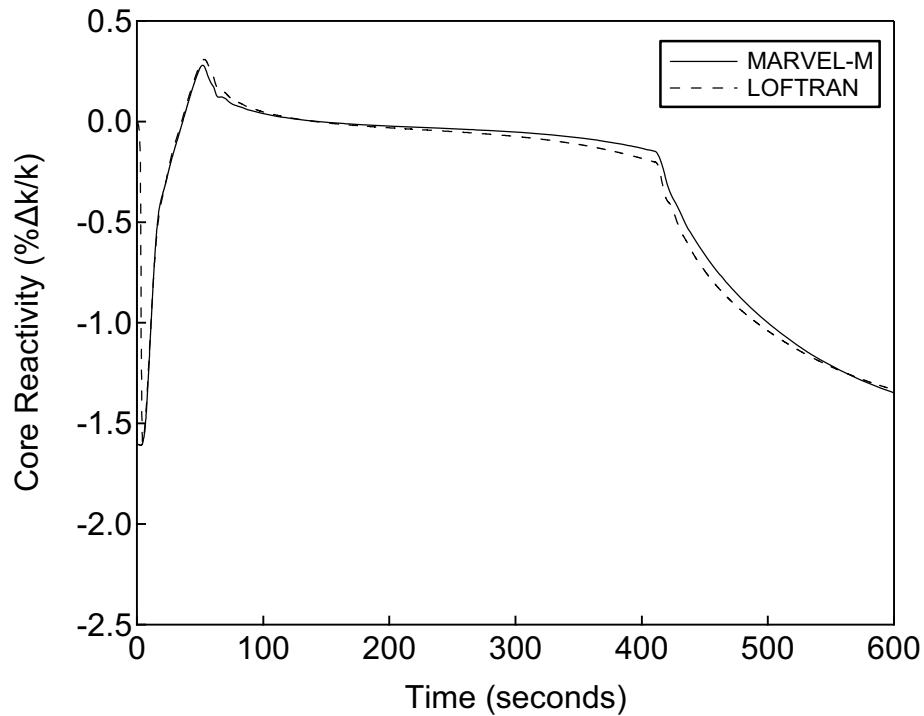


**Figure 2.1-21.2 Core Reactivity versus Time
Mass and Energy Release for Steam System Piping Ruptures
Comparison between MARVEL-M and LOFTRAN**

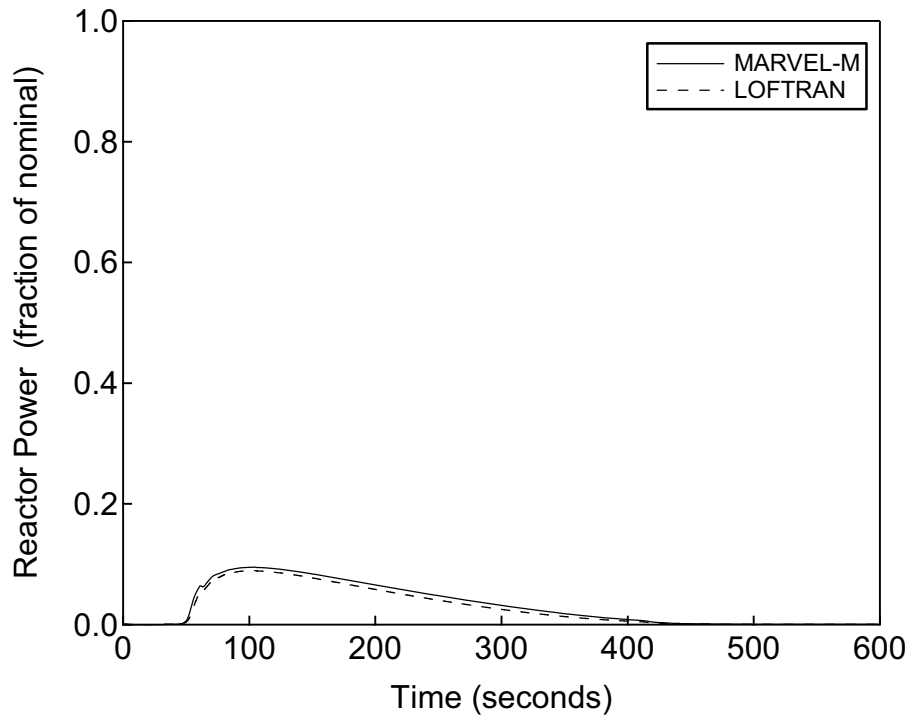


**Figure 2.1-21.3 Reactor Power versus Time
Mass and Energy Release for Steam System Piping Ruptures
Comparison between MARVEL-M and LOFTRAN**

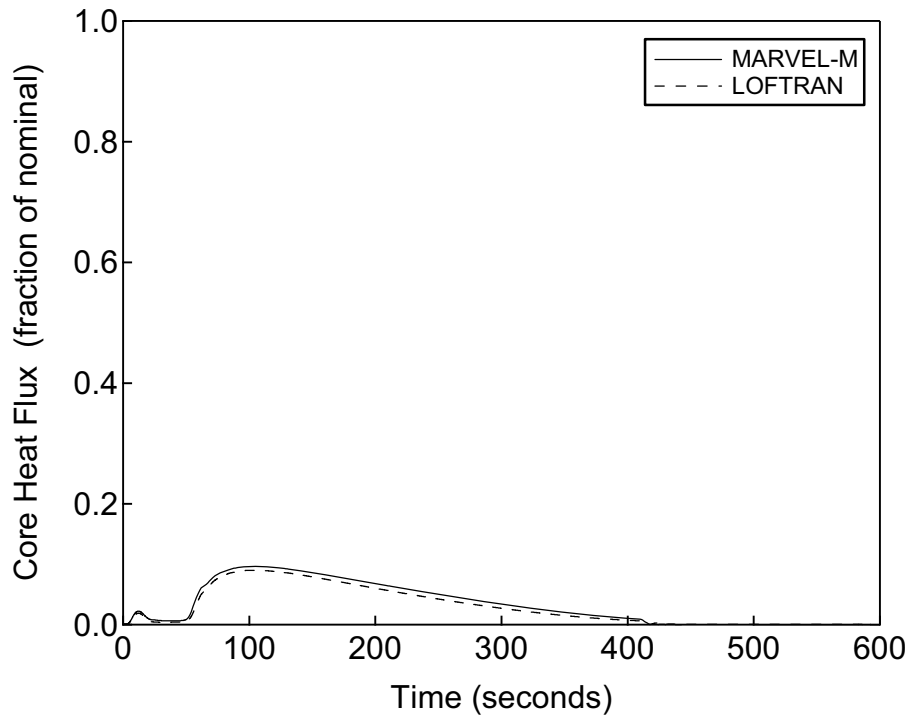


Figure 2.1-21.4 Core Heat Flux versus Time
Mass and Energy Release for Steam System Piping Ruptures
Comparison between MARVEL-M and LOFTRAN

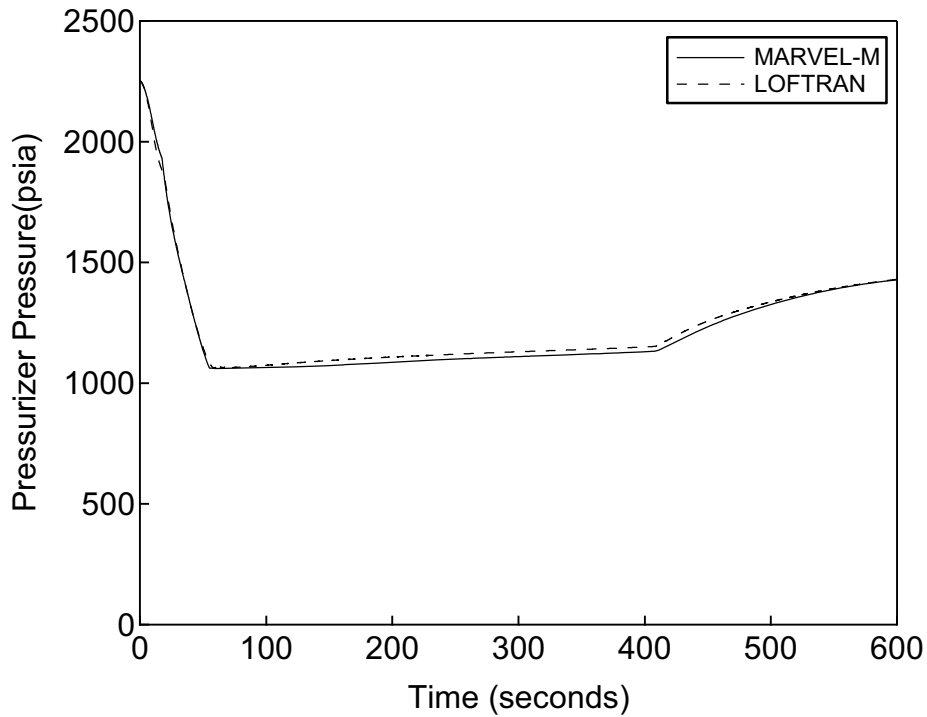
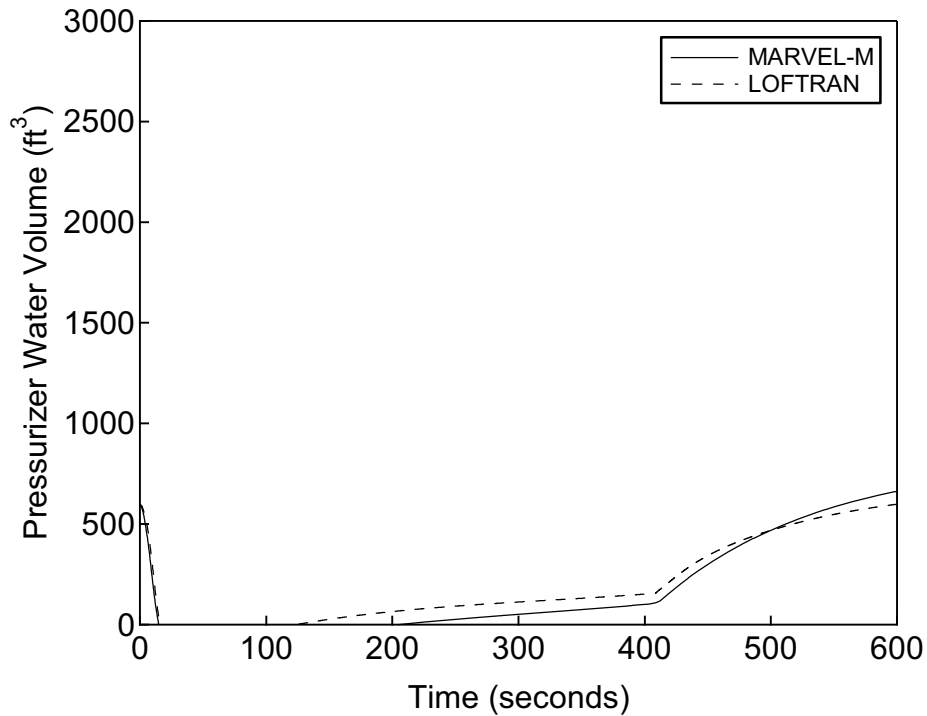
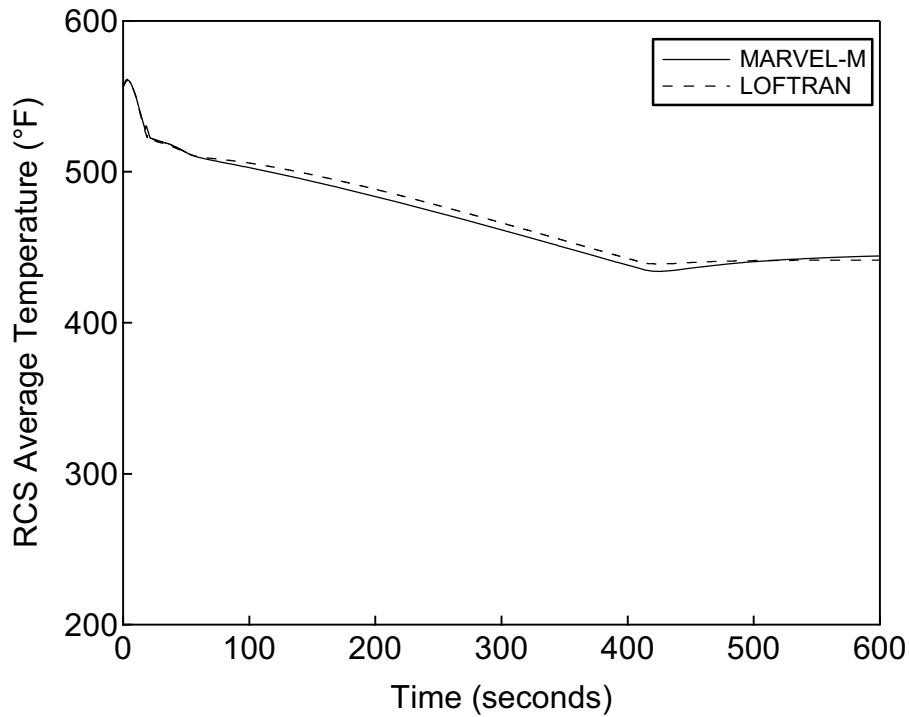


Figure 2.1-21.5 Pressurizer Pressure versus Time
Mass and Energy Release for Steam System Piping Ruptures
Comparison between MARVEL-M and LOFTRAN



**Figure 2.1-21.6 Pressurizer Water Volume versus Time
Mass and Energy Release for Steam System Piping Ruptures
Comparison between MARVEL-M and LOFTRAN**



**Figure 2.1-21.7 RCS Average Temperature versus Time
Mass and Energy Release for Steam System Piping Ruptures
Comparison between MARVEL-M and LOFTRAN**

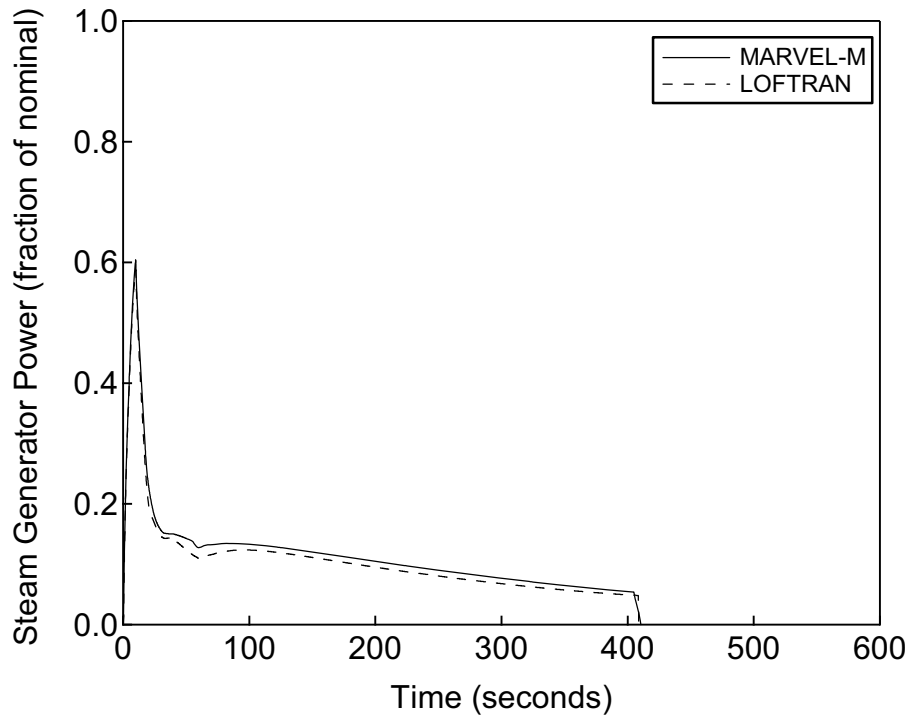


**Figure 2.1-21.8 Steam Generator Power versus Time
Mass and Energy Release for Steam System Piping Ruptures
Comparison between MARVEL-M and LOFTRAN**

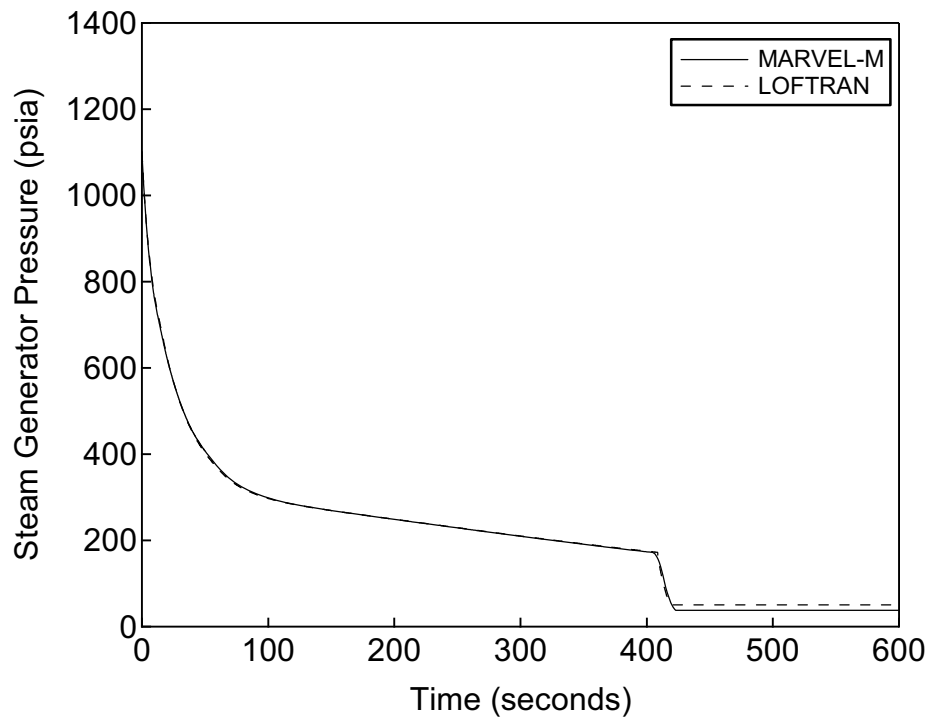


**Figure 2.1-21.9 Steam Generator Pressure of Faulted SG versus Time
Mass and Energy Release for Steam System Piping Ruptures
Comparison between MARVEL-M and LOFTRAN**

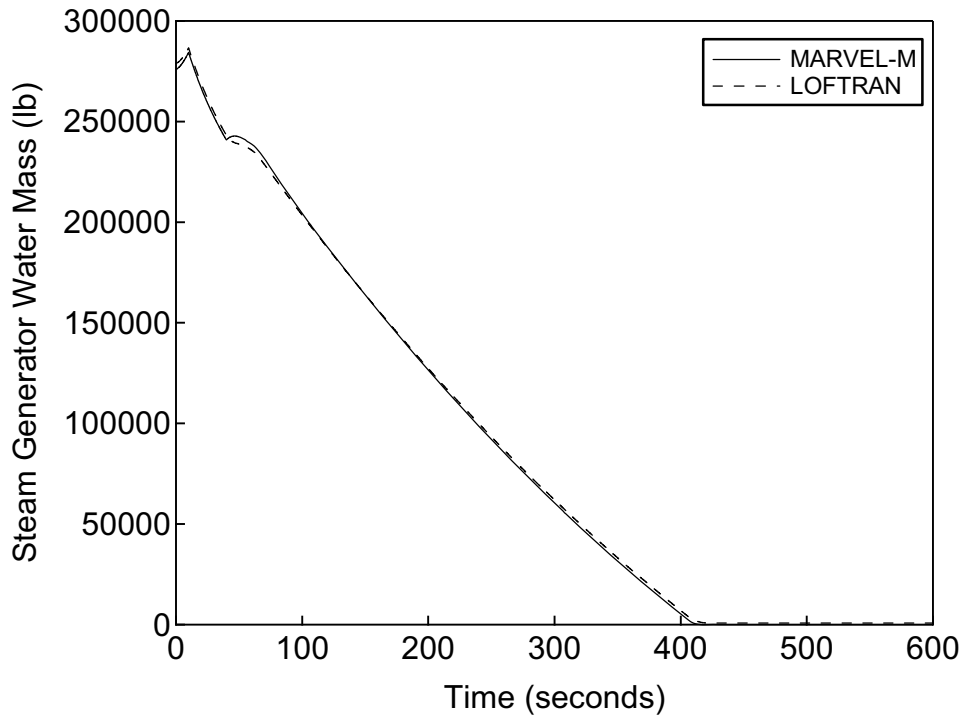


**Figure 2.1-21.10 Steam Generator Water Mass of Faulted SG versus Time
Mass and Energy Release for Steam System Piping Ruptures
Comparison between MARVEL-M and LOFTRAN**

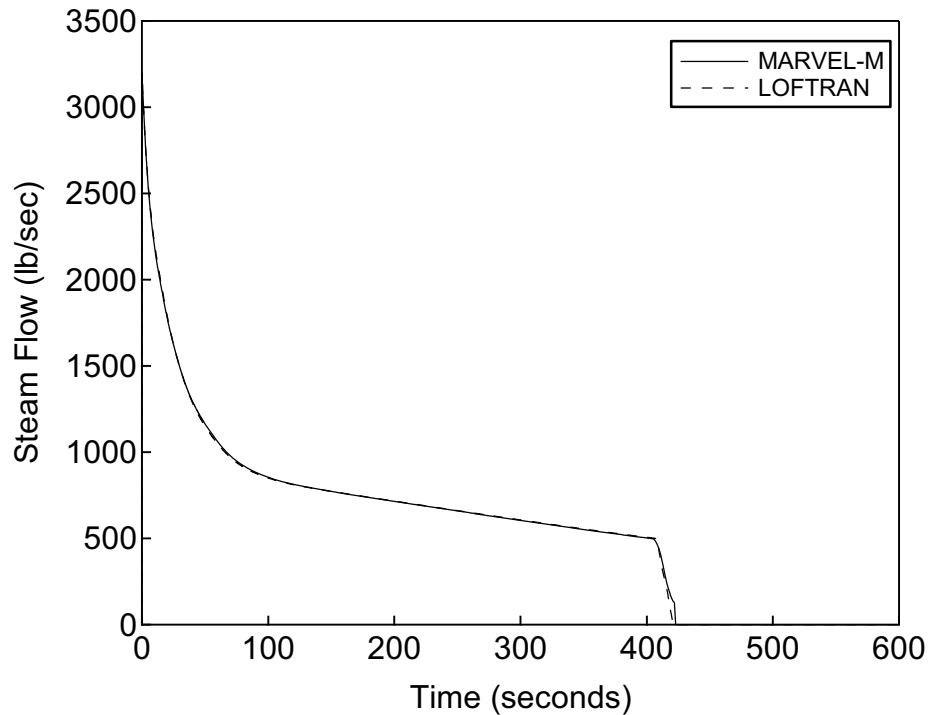


**Figure 2.1-21.11 Steam Flow Rate of Faulted SG versus Time
Mass and Energy Release for Steam System Piping Ruptures
Comparison between MARVEL-M and LOFTRAN**

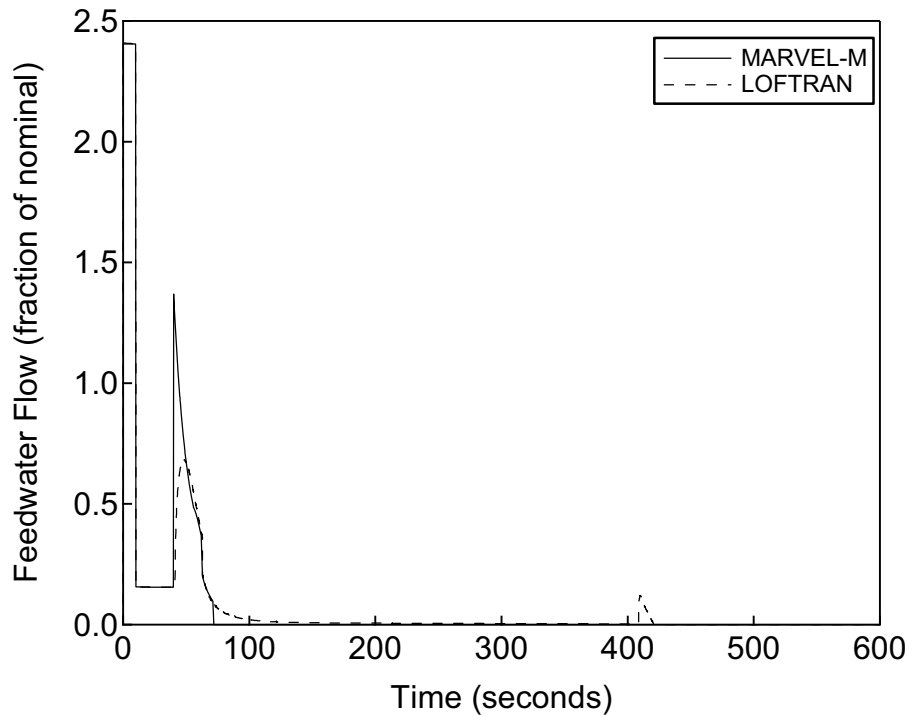


**Figure 2.1-21.12 Feedwater Flow Rate of Faulted SG versus Time
Mass and Energy Release for Steam System Piping Ruptures
Comparison between MARVEL-M and LOFTRAN**

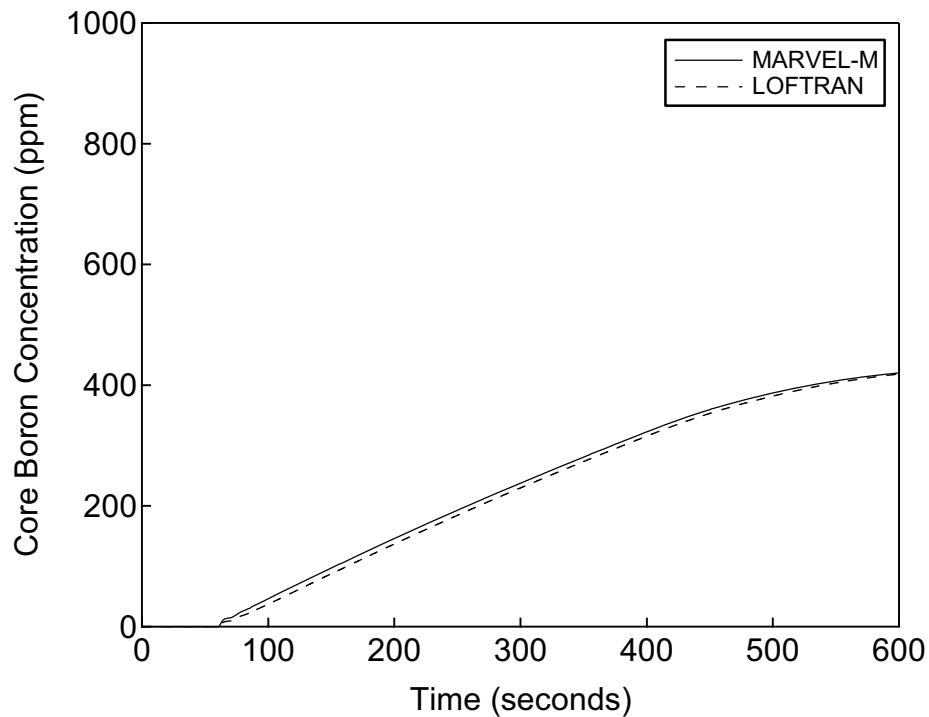


**Figure 2.1-21.13 Core Boron Concentration versus Time
Mass and Energy Release for Steam System Piping Ruptures
Comparison between MARVEL-M and LOFTRAN**

RAI 2.1-22

In accounting for the differences between MARVEL-M and the NRC approved version of MARVEL, are there any limitations beyond those already described in MUAP-07010 which are applicable to the use of MARVEL-M for the US-APWR design?

Response

There are no limitations in MARVEL-M compared to the NRC approved version of MARVEL (WCAP-8843-P/WCAP-8844-NP). The program is designed to be run within the following ranges of operating variables described in Section 2.1.5.1 of Non-LOCA Methodology Topical Report:

- Reactor Coolant System Temperature and Pressure
 - Temperature : 50°F to approximately 1100°F
 - Pressure : 50 psia to critical pressure (about 3200 psia)
- Pressurizer Water Level
 - From empty to full including water discharge. (After the pressurizer is emptied, the program may analyze the system behavior until the coolant in the reactor vessel inactive volume (dead volume) is boiled off.)
- Steam Generator
 - Steam Pressure : 14 psia to 1500 psia
 - Water Inventory : Empty to moderately high level
- Reactor Coolant Loop Flow
 - Forward, reverse and natural circulation flows are computed. Two phase flows are also permitted as a homogeneous equilibrium mixture of vapor and liquid.
- Reactor Core Kinetics
 - Reactor power : Neutron source level to overpower level
 - Reactivity : Sub-critical to super-prompt critical

The program is intended to cover a very wide range of operating parameters. However, when the plant operating variables deviate excessively from the normal operating conditions, care must be used in interpreting the results in context with the accuracy and limitations of the code models over the regions where the variables are extreme.

RAI 2.1-23

In the NRC evaluation of Westinghouse topical reports WCAP-7909-P and WCAP-8843-P, MARVEL was approved for use to analyze the following four events: steamline rupture, feedwater line rupture, startup of an inactive reactor coolant loop, and excessive heat removal due to a feedwater system malfunction. However, MHI is utilizing MARVEL-M to analyze many events in DCD Chapter 15 beyond these four. Explain why MHI believes this is acceptable.

Response

The disturbances caused by postulated uniform events are milder than those of non-uniform events. Moreover, almost all of the MARVEL models used for the postulated non-uniform events are common to uniform events except for certain specific models related to the initiating events, such as rod withdrawal and primary depressurization.

In order to show that the MARVEL code could be used to analyze other events, MHI made comparisons of MARVEL-M to the NRC approved 4-loop LOFTRAN. The MARVEL-M and 4-loop LOFTRAN comparisons for a variety of uniform and non-uniform events are described in detail in the Non-LOCA Methodology Topical Report, MUAP-07010. Sections 3.1.1 through 3.1.4 compare MARVEL-M to 4-loop LOFTRAN for an uncontrolled RCCA bank withdrawal at power (a uniform event), a partial loss of forced reactor coolant flow (a non-uniform event), a complete loss of forced reactor coolant flow (a uniform event), and a reactor coolant pump (RCP) shaft seizure (a non-uniform event), respectively. Overall, the MARVEL-M results agree very well with the results of the NRC approved 4-loop LOFTRAN code. MHI also supplemented the comparisons for these four events as part of the response to RAIs 3.1-2 through 3.1-5 on the Non-LOCA Methodology Topical Report. The response to RAI 2.1-17 provides a comparison of MARVEL-M and LOFTRAN for a loss of non-emergency AC power to station auxiliaries (a uniform event before auxiliary feedwater initiation and a non-uniform event after auxiliary feedwater initiation). Not only does this provide a comparison for an additional event, it also provides a verification of the ability of the explicit RCP model in MARVEL-M to transition to natural circulation flow.

MHI has also made comparisons of MARVEL-M results to measured data. The response to RAI 2.1-16 shows comparisons of MARVEL-M results to measured data from a 4-loop plant for a partial loss of forced reactor coolant flow and a complete loss of forced reactor coolant flow. These results show that MARVEL-M matches data for both uniform and non-uniform events as well as verifying the explicit RCP model.

In addition to the comparisons of MARVEL-M with LOFTRAN, MHI has also compared MARVEL-M (4-loop) to the original 2-loop MARVEL code from Westinghouse. The response

to RAI 2.1-3 shows the results of the comparisons for a loss of load (a uniform event) and a feedwater system pipe break (a non-uniform event). This comparison was performed as part of the verification of the transition to an explicit 4-loop code.

Despite the fact that the NRC evaluation of MARVEL was focused on four specific (non-uniform) events, MARVEL-M has been shown to provide excellent agreement with the NRC approved version of LOFTRAN, measured plant data, and the original MARVEL for a variety of events. For this reason, MHI believes that it is acceptable to use MARVEL-M for the DCD Chapter 15 accident analyses.

RAI 2.2-2

Elaborate further on the development history of TWINKLE-M. Are there any differences between the TWINKLE version used to develop TWINKLE-M and the NRC approved version described in WCAP-7979-P-A? Include, if possible, a figure describing the development of TWINKLE-M analogous to the figure describing the development of MARVEL-M found on page 2-3 of MUAP-07010-P.

Response

MHI then made modifications to this version of TWINKLE to create TWINKLE-M. The modifications made by MHI have been described in detail in Section 2.2 of the Non-LOCA Methodology Topical Report (MUAP-07010), in the response to RAIs 2.2-1, 3.2-1, and 3.2-2 on the Non-LOCA Methodology Topical Report, and in Section 1 of the TWINKLE-M input manual which was submitted to the NRC on August 1, 2008 by MHI letter UAP-HF-08138. A figure detailing the development of TWINKLE-M is shown below.

Figure 2.2-2.1 Historical Development of the TWINKLE Code

The following description of the differences between the approved version of TWINKLE and TWINKLE-M is taken directly from the response to RAI 2.2-1, which was submitted to the NRC on August 22, 2008 by MHI letter UAP-HP-08141:

The solution methods and constitutive models of the TWINKLE-M code have not changed from the original TWINKLE code. MHI has modified several functions which are mainly concerned with the treatment of input data. A brief description of each change is provided below. GEN0-LP-517 Revision 0 (the TWINKLE-M Input Manual), submitted to the NRC by MHI letter UAP-HF-08138 on August 1, 2008, provides additional information regarding TWINKLE-M input.

(1) Spatial Mesh Expansion

In response to a change in the fuel failure thresholds for reactivity initiated events for Japanese LWRs in 1993, the maximum number of spatial mesh points in the TWINKLE-M code was expanded from 2000 meshes to a variable number in order to support a full core three-dimensional representation. The related variables in TWINKLE-M of fuel burnup, macroscopic and microscopic cross section, xenon distribution, fuel temperature, fast and thermal neutron flux, neutron velocities, and delayed neutron fractions were also expanded to accommodate the full core three-dimensional calculations. The capability to solve three-dimensional problems and solution algorithms were not changed.

(2) Introduction of a Discontinuity Factor

A discontinuity factor was added as a new input process in the program. The purpose of the discontinuity factor is to improve the representation of the local power distribution in the three-dimensional calculations. The addition of the discontinuity factor does not change the diffusion equations in TWINKLE. Instead, the discontinuity factor implementation is shown in Figure 2.2-2.2 and described as follows:

- The macroscopic cross section data is divided by the discontinuity factor before solving the diffusion equations (additional process).
- The neutron flux is solved using the unchanged TWINKLE diffusion equation subroutine.
- The neutron flux is divided by the discontinuity factor to determine the mesh averaged neutron flux (additional process).

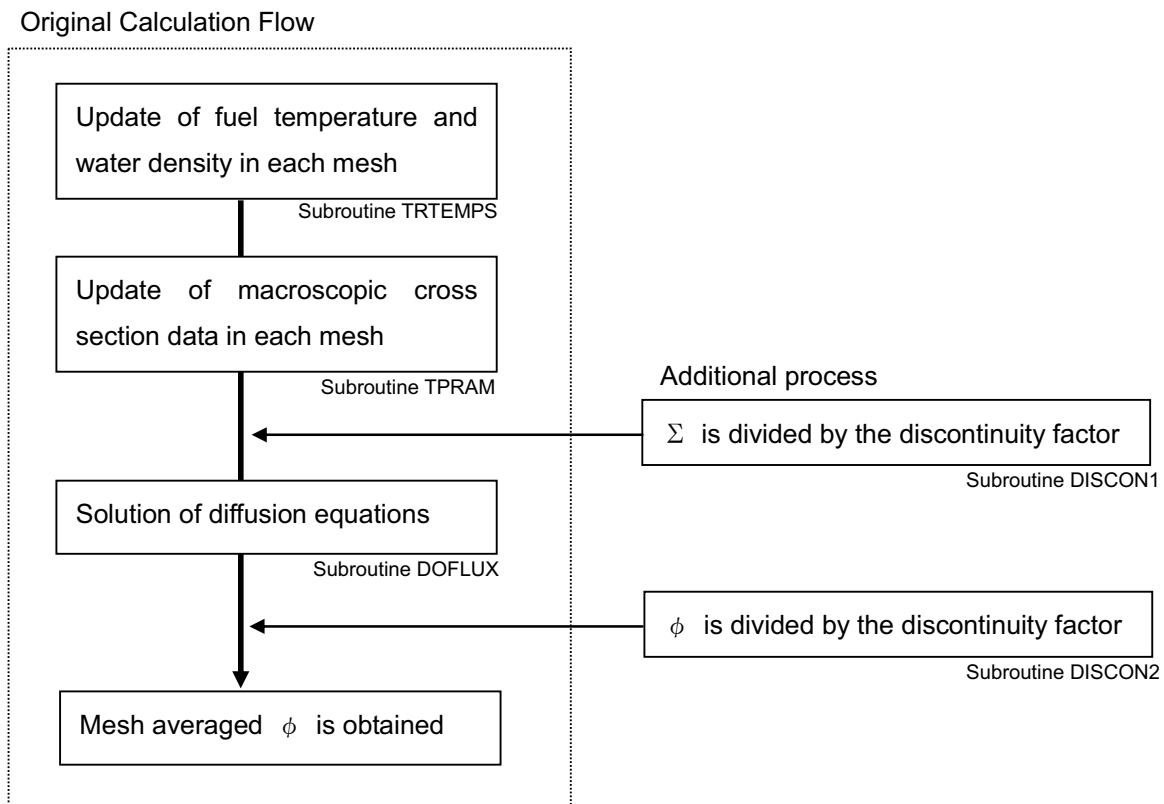


Figure 2.2-2.2 Flowchart of the Discontinuity Factor Process

(3) Input Format

The input format was changed from a numerical identifier form to a Namelist form supported by standard Fortran 77 or 90 compilers. This allows users to identify the input list more clearly.

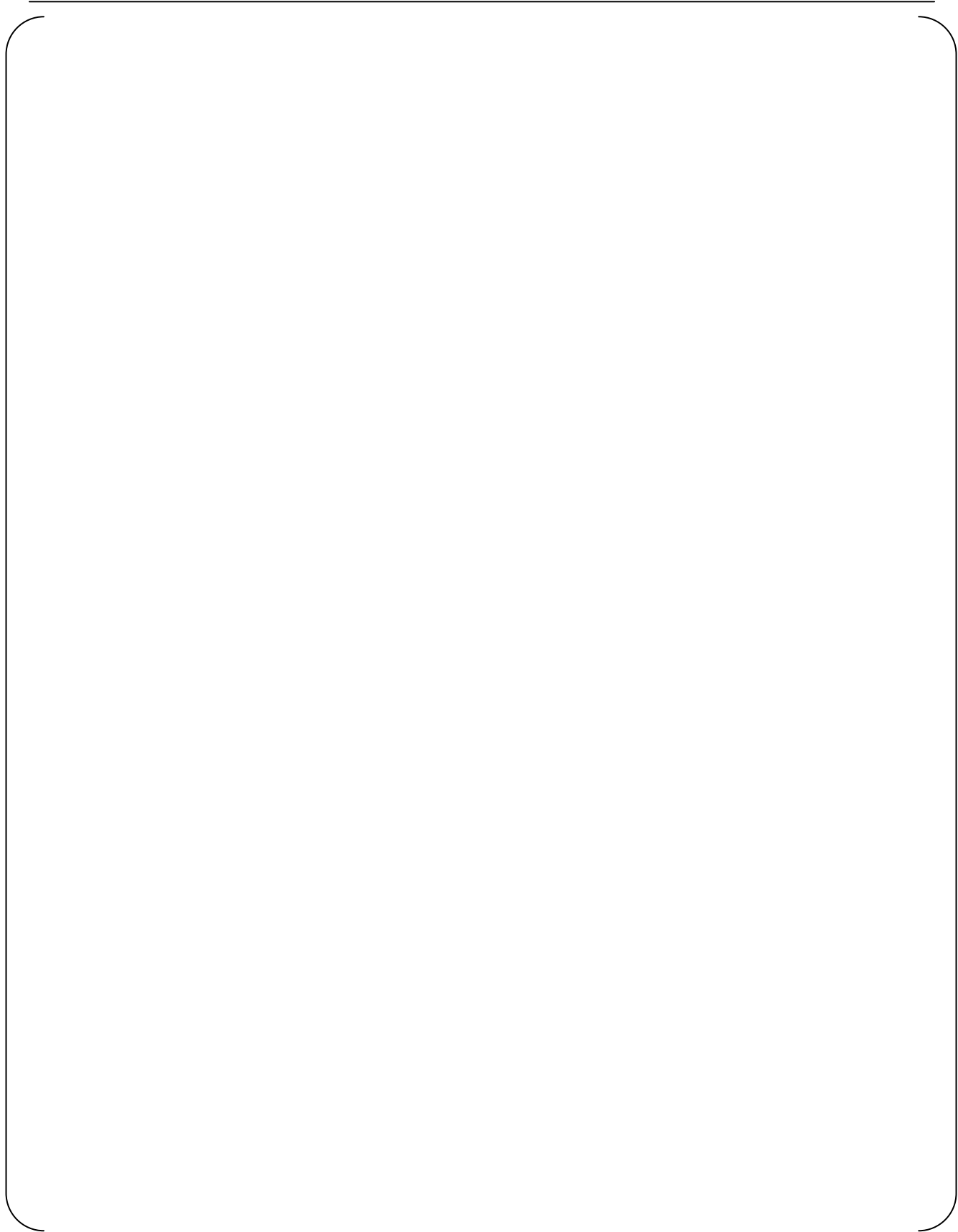
(4) Additional Options

The following features were added by MHI as input options:

- The nuclear and thermal properties of MOX fuel and BP were included.
- The number of fuel pellet divisions in the radial direction is expanded from 4 meshes to 10 meshes.
- Fuel properties depending on the fuel BU were added such as a thermal conductivity and a radial power depression in the pellet.
- Xenon distribution data calculated by ANC can be passed to TWINKLE-M through an input file. This change provides for a savings in calculation time.
- A separate equation was added to represent the dashpot portion of the trip curve. Prior to this change, the dashpot region was a continuation of the linear portion of the trip curve. The resulting trip curve is now an "S" shaped curve that is more representative of the RCCA displacement curve.
- New outputs were created to aid in the interpretation of code results by allowing for additional data plots and providing the ability to perform sequential calculations with VIPRE-01M. Specific examples of these changes include:
 - Time history of core average power, peaking factor, axial offset, etc.
 - Mesh-wise power distribution map for each time
 - Mesh-wise adiabatic fuel enthalpy rise during a power excursion

Appendix A

Proprietary vs. Non-Proprietary Versions of Approved MARVEL



Reference 4

UAP-HF-09040
Docket No. 52-021

MHI's 4th Response to NRC's Requests for Additional Information on
US-APWR Topical Report: Non-LOCA Methodology, MUAP-07010-P

February 2009

RAI 2.1-2-1

Please confirm the following understanding of the DNBR lookup table methodology: The MARVEL-M lookup table is a database of DNBR, core inlet temperatures, system pressures, and core heat flux data generated from VIPRE-01M steady state calculations. Using system analyses to determine the core inlet temperature and system pressure during a transient, an interpolative scheme is used to determine the normalized heat flux and thus the DNBR at each time step through the analysis. This simplified DNBR lookup table methodology is only used for non-LOCA events that have constant core flow rate and “are bounded by the applicable power distribution.” In the event that the parameters of the calculation exceed the limitations of the lookup table, the analyst is flagged to use VIPRE-01M to directly calculate DNBR based on a DNB correlation in VIPRE-01M.

Response

The reviewer's understanding of the DNBR lookup table methodology is basically correct. There is no MARVEL-M output message that alerts the user that they have exceeded the limitations of the lookup table. The user must know the limitations of the methodology and apply it appropriately. The MARVEL-M input variable PMAXDNB allows the user to input an upper limit on the RCS pressure associated with the DNBR lookup tables. If the RCS pressure exceeds the user input upper limit, the pressure is assumed to be equal to the upper limit value when determining DNBR.





Figure 2.1-2-1.1 **DNBR versus Time**
One or More Dropped RCCAs within a Group or Bank

RAI 2.1-2-2

How is the number of DNBRs evaluated in the generating the DNBR lookup tables (N) chosen? What degree of interpolation is used when using the table?

Verify that the DNBR lookup tables cover the full operating space (pressures, temperatures, flow rates) that the methodology is used for. Explain what is meant by "applicable power distribution" with regard to the use of the simplified DNBR tables.

Response

The MARVEL-M simplified DNBR lookup table array is defined by the MARVEL-M variables MDNB for a thimble cell and MDNBS for a typical cell. The array is defined for { } of DNBR (MARVEL-M variable WMIRC) corresponding to the DNBR limit, the DNBR at nominal conditions and { } additional DNBR points between these { }

Additional details of these input variables are described in Section 2.4 \$DNBRD of Part II of the MARVEL-M Manual (GEN0-LP-480). Revision 5 of the MARVEL-M Manual was submitted to the NRC by MHI letter UAP-HF-08245 on November 11, 2008.

The DNBR is interpolated using a third order Lagrange interpolation formula at the normalized heat flux calculated by MARVEL-M.

The power distribution assumed in the lookup table is the same as that used in the thermal hydraulic design, which is described in Section 4.4 of the US-APWR DCD, and covers normal operating conditions. For events where the power distribution exceeds the design power distribution, VIPRE-01M is used to calculate DNBR rather than the MARVEL-M DNBR lookup table, except for the RCCA drop as was described in the response to RAI 2.1-2-1.

The DNBR lookup tables cover the operating range of pressure and temperature that are protected by the over temperature ΔT , over power ΔT , low pressurizer pressure and high pressurizer pressure reactor trips. The DNBR lookup tables are not applied for decreasing core flow rate conditions.

RAI 2.1-8-1

The discussion provided in response to RAI 2.1-8 by MHI contained an error and was inadequate for the reviewer to evaluate the modeling of the four major thermal resistances in the calculation of the overall heat transfer coefficient for the steam generators. Provide clarification on the calculation of the initial values of the four thermal resistances, R_{pf}^0 , R_{tube}^0 , R_{bo}^0 , and R_{foul}^0 , and define all parameters and variables. Provide clarification on their calculation during the transient, and their combination to yield the overall heat transfer coefficient during the transient. Provide a (hypothetical) numerical example to clarify for the reviewer the overall procedure as modeled in the code from initial conditions through a transient. Discuss the overall heat balance and the fouling resistance. Provide the bases for the steam generator thermal resistances at nominal conditions? Provide comparisons to data if possible.

Response

The previous response to RAI 2.1-8 did contain errors in the formulas for the thermal resistances. The last several formulas in the response for the MARVEL-M input variables $RRPF$, $RRTM$, $RRBO$ and $RRFOUL$ should be written as follows:

$$RRPF = \frac{R_{pf}^0}{R_{tot}^0}$$

$$RRTM = \frac{R_{tube}^0}{R_{tot}^0}$$

$$RRBO = \frac{R_{bo}^0}{R_{tot}^0}$$

$$RRFOUL = 1 - RRPF - RRTM - RRBO$$

Note: $RRFOUL$ is not an actual MARVEL-M input variable, but is calculated internally using the above equation.

The superscript zeroes denote nominal conditions in these equations.

These equations, as written above, show the relationship between the mathematical models and the input variables. Descriptions of the equations and input are also found in Section 1.5.1 of the MARVEL-M Manual (GEN0-LP-480). As noted by the NRC, the values of $RRPF$, $RRTM$, $RRBO$ and $RRFOUL$ are input as constants into MARVEL-M. The MARVEL-M input parameters of $RRPF$, $RRTM$, $RRBO$ and $RRFOUL$, are evaluated at nominal conditions.

R_{tot}^0 is internally scaled at nominal conditions as follows:

At nominal conditions, the SG overall heat transfer coefficient $(UA)_{SG}$ can be calculated internally from the nominal SG power (q_{SG}), the nominal SG temperature (T_s) and the nominal primary side temperature (T_{avg}^0) as shown in the equation below.

$$q_{SG} = (UA)_{SG} (T_{avg}^0 - T_s)$$

U_0 can be calculated from the overall heat transfer coefficient and the total resistance at nominal conditions is calculated with the equation below.

$$R_{tot}^0 = 1/U_0$$

Next, the overall heat transfer coefficient in the steam generators as a fraction of the nominal value can be obtained by combining the above equations as shown below:

$$\frac{U}{U^0} = \frac{R_{tot}^0}{(R_{pf} + R_{tube} + R_{foul} + R_{bo})}$$

$$\frac{U}{U^0} = \frac{1}{\left(\frac{R_{pf}}{R_{tot}^0} + \frac{R_{tube}}{R_{tot}^0} + \frac{R_{foul}}{R_{tot}^0} + \frac{R_{bo}}{R_{tot}^0}\right)}$$

where

$$\frac{R_{pf}}{R_{tot}^0} = \left(\frac{R_{pf}^0}{R_{tot}^0}\right) \cdot \left(\frac{1 + 10^{-2}T_0 - 10^{-5}T_0^2}{1 + 10^{-2}T - 10^{-5}T^2}\right) \left(\frac{Q}{Q_0}\right)^{-0.8}$$

$$\frac{R_{tube}}{R_{tot}^0} = \left(\frac{R_{tube}^0}{R_{tot}^0}\right) \frac{8.0 + 0.0051 \cdot T_t^0}{8.0 + 0.0051 \cdot T_t}$$

$$\frac{R_{foul}}{R_{tot}^0} = \frac{R_{foul}^0}{R_{tot}^0}$$

$$\frac{R_{bo}}{R_{tot}^0} = \left(\frac{R_{bo}^0}{R_{tot}^0}\right) \left(\frac{q_{sg} / A_{sg}}{q_{sg}^0 / A_{sg}^0}\right)^{-0.75} \cdot \exp\left(\frac{P_s^0 - P_s}{900}\right)$$

As described, nominal $(UA)_{SG}$ is internally calculated and its transient value is modified based on transient conditions. Likewise, the thermal resistances are also modified based on transient conditions.

Table 2.1-8-1.1 gives an example of the required parameters in the equations above and the calculation results for the resistances in the Complete Loss of Forced Coolant Flow analysis discussed in Section 6.2 of MUAP-07010. Figure 2.1-8-1.1 shows the transient of these resistances calculated by MARVEL-M. These results indicate that the primary convection film resistance (R_{pf}) increases associated with the decrease in reactor coolant flow and the secondary side boiling heat transfer resistance (R_{bo}) increases associated with the decrease in feedwater flow caused by a reactor trip, while the tube metal resistance (R_{tube}) and the fouling resistance (R_{foul}) stay constant.

**Table 2.1-8-1.1 Calculation of Thermal Resistances during a Transient
 - Complete Loss of Forced Reactor Coolant Flow**

Parameter	0.0 seconds	5.0 seconds	10.0 seconds
T (°F)			
T_t (°F)			
Q (fraction)			
q_{sg} (fraction)			
A_{sg} (fraction)			
P_s (psia)			
R_{pf} / R_{tot}^0			
R_{tube} / R_{tot}^0			
R_{foul} / R_{tot}^0			
R_{bo} / R_{tot}^0			
R_{tot} / R_{tot}^0			



**Figure 2.1-8-1.1 Thermal Resistances versus Time
 - Complete Loss of Forced Reactor Coolant Flow**

RAI 2.1-10-1

There may be physical effects in the coolant flow not captured by modeling safety injection into the cold leg instead of the Direct Vessel Injection featured in the US-APWR. Justify why cold leg injection is more conservative.

Response

The MARVEL-M pressure model is not dependent on the location of injection. Therefore, the only effect of this modeling difference is in the time for the safety injection to reach the core. The previous response to RAI 2.1-10 describes that modeling safety injection into the cold leg instead of the direct vessel injection, as is physically done in the plant, adds additional purge volume which conservatively delays the effect of the boron reaching the core. Therefore, modeling the safety injection by cold leg injection rather than direct vessel injection is more conservative.

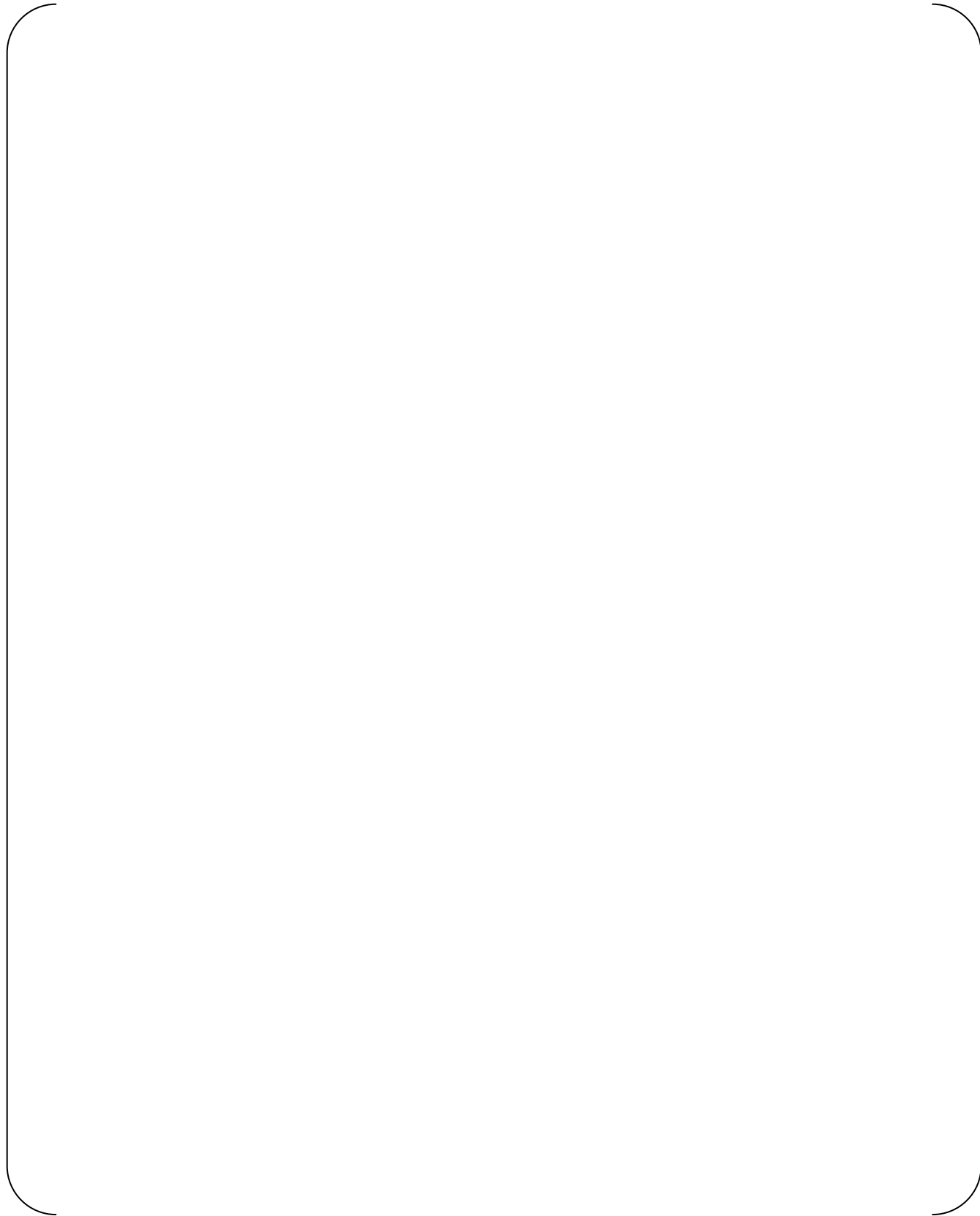
RAI 2.1-13-1

In the MHI response to RAI Appx.E-1 (in UAP-HF-08141, Docket No. 52-021, August 22, 2008), it is stated, "It should also be noted that uniformity in vessel inlet mixing can best be approximated by perfect mixing for very low flows such as during natural circulation conditions. Perfect mixing is assumed for the Steam Generator Tube Rupture event due to natural circulation conditions that exist during most of the event." This statement appears to contradict the MHI response to RAI 2.1-13. MHI is requested to clarify and comment on the discussion above.

Response

The original RAI response stated that, "The design value of f_{mi} is utilized for all DCD Chapter 15 non-LOCA events for the US-APWR, except for the steam line break, which uses the conservative value of f_{mi} ." This statement was incorrect because there are other Chapter 15 events that do not use the design or conservative values. The purpose of this response is to clarify the MARVEL-M mixing values that are used for the DCD Chapter 15 non-LOCA events that require this input. Table 2.1-13-1.1 shows the mixing factor in each of the non-LOCA events that are analyzed using the MARVEL-M code. In addition, the basis for the values used in the mixing model for each event is also shown in the notes below the table.

Table 2.1-13-1.1 Mixing Factors in Non-LOCA Events Analyzed Using MARVEL-M





RAI 2.1-16-1

Describe or demonstrate that the MARVEL-M's pump model is adequate for the full range of Chapter 15 events.

Response

For the Chapter 15 events where the reactor coolant pumps (RCPs) are running, constant reactor coolant system (RCS) flow is used, so there is no need for the RCP model. For other events, the RCP parameters are verified from the RCP scale data used to generate the homologous curves used in the Chapter 15 analysis. Three of the Chapter 15 events, partial loss of flow, complete loss of flow, and locked rotor (shaft seizure) have already been verified by comparisons to LOFTRAN, shown in Sections 3.1.2 through 3.1.4 of topical report MUAP-07010. Additionally, the partial loss of flow and complete loss of flow were verified by comparison to actual test data as shown in the response to RAI 2.1-16 provided in UAP-HF-08170-P.

RAI 2.1-16-2

Explain why the measured and predicted (using MARVEL-M) pump coast down curves are so similar. Have these measured data of pump coast down used to validate MARVEL-M been compared to the LOFTRAN code?

Response

For the comparison of MARVEL-M to actual plant test data, best estimate values are used in MARVEL-M rather than the more conservative values used in the DCD Chapter 15 safety analyses. In particular, the best estimate values for pump inertia and loop pressure drops lead to the excellent agreement between MARVEL-M and plant data shown in Figures 2.1-16.1 and 2.1-16.2. In the response to RAI 2.1-16, the measured plant data was compared to MARVEL-M, not LOFTRAN. However, MARVEL-M and LOFTRAN were compared for these same events, partial and complete loss of flow, in Sections 3.1.2 and 3.1.3 of the Non-LOCA Methodology Topical Report MUAP-07010. The comparisons show that MARVEL-M agrees very well with actual plant data and with LOFTRAN results for the pump coast down.

RAI 3.1-2-1

Did the Uncontrolled RCCA Bank Withdrawal at Power event have the largest differences between LOFTRAN and MARVEL-M?

Response

MHI has performed numerous comparisons between MARVEL-M and LOFTRAN. Only cases which resulted in significant differences between the results were investigated further to determine the reason for the differences. Two primary differences between the code models have been identified and previously described.

- (1) Topical report MUAP-07010 identifies differences in the core heat flux model that results in differences for peak pressure for the loss of flow event.
- (2) The UAP-HF-08141-P response to RAI 3.1-2 discusses differences in the pressurizer spray models that result in differences in results for the uncontrolled RCCA bank withdrawal at power event.

Overall, MARVEL-M compares extremely well with LOFTRAN and is suitable for Chapter 15 analyses.

RAI 3.2-3-1

Please confirm that the approach used in TWINKLE-M modifies the two group diffusion coefficients for both the radial reflector region and two axial reflector regions.

Response

The first (fast) group diffusion coefficient is modified for both the axial and radial reflector regions. The second (thermal) group diffusion coefficient is not modified because the desired effect on the TWINKLE-M power distributions is achieved by modifying the first group diffusion coefficient for these reflector regions.

RAI 3.2-3-2

Detail the process by which the diffusion coefficient in the reflector is modified before it is input into TWINKLE-M.

Response

[]

RAI 3.2-4-1

MHI asserts that the differences between the two codes in the assemblies with control rods inserted for the HZP case is due to the different modeling of the spatial dependence and the fact that there is a strong spatial gradient near the control rods. This is a reasonable explanation; however, it is not consistent with their response to 3.2-5. The explanation of the differences at the location of a control rod for the HFP case is claimed to be because the burnup is different in the controlled and surrounding assemblies. However, since the reactor is expected to be operated with control rods withdrawn, the burnup differential between controlled assemblies and surrounding assemblies should be no different than between any other set of adjacent assemblies. Please provide further clarification of the responses to RAI 3.2-4 and 3.2-5.

Response

The topical report provided comparisons of the radial power distribution between TWINKLE-M and ANC for several cases. The BOC, HFP, all RCCAs out case was shown in Figure 3.2.1-2 and the EOC, HZP, RCCAs at the insertion limit case was shown in Figure 3.2.1-3. There were several RAIs about the differences in these comparisons. RAI 3.2-4 discussed the HZP case (Figure 3.2.1-3) and RAI 3.2-5 discussed the HFP case (Figure 3.2.1-2). In the response to RAI 3.2-4, it was stated that the largest differences between TWINKLE-M and ANC for the HZP case were in assemblies with the control rods inserted. This could be verified by Figure 3.2.1-1 in the topical report that showed the locations of the RCCAs. In the response to RAI 3.2-5, it was stated that the largest differences between TWINKLE-M and ANC for the HZP case were in assemblies near the periphery of the core where adjacent fuel assemblies had large differences in burnup. However, no burnup information was included in that response.

The example that was provided by MHI in the responses to RAIs 3.2-4 and 3.2-5 included adjacent assemblies with significant differences in burnup, as shown in Figure 3.2-4-1.1. The figure also indicates the assemblies with the largest differences in power between ANC and TWINKLE-M for the HFP case (based on Figure 3.2.1-2 of the topical report). The figure confirms the explanation in the response to RAI 3.2-5 that the largest differences in power for the HFP case occur in assemblies with fresh fuel that are adjacent to high-burnup assemblies near the periphery of the core. As a result, the differences between TWINKLE-M and ANC can be attributed to the large differences in burnup.

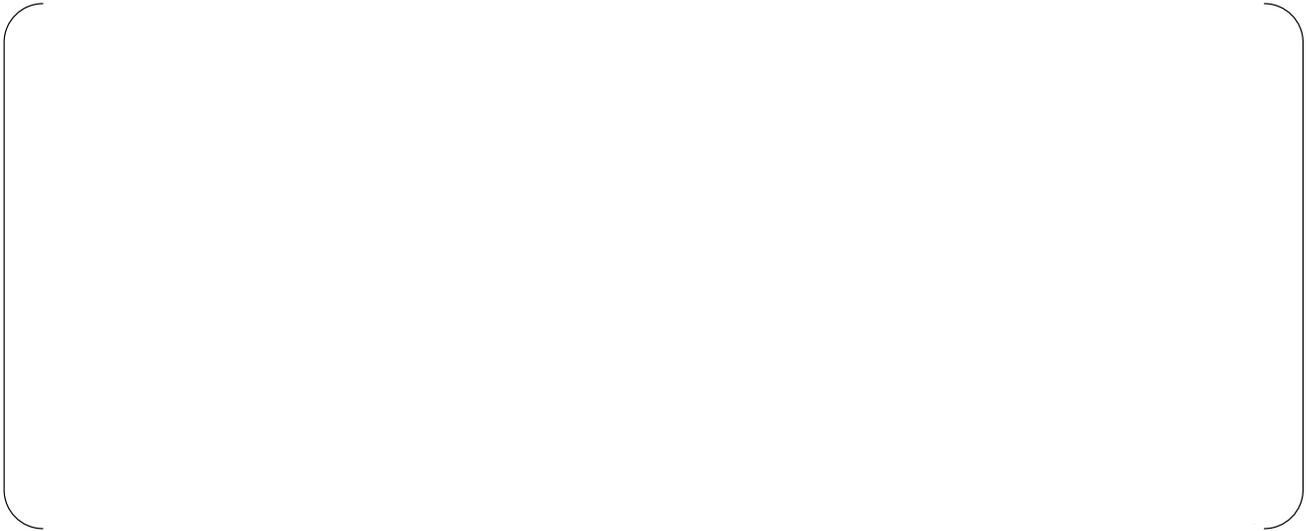


Figure 3.2-4-1.1 Burnup Distribution at BOC (0.15 GWD/MTU)

RAI 3.2-6-1

Comment on the positive Doppler temperature coefficients presented in Table 3.2-6.1.

Response

The positive values in Table 3.2-6.1 are typographical mistakes. The Doppler temperature coefficient values for both TWINKLE-M and ANC should be $-1.9 \text{ pcm}/^{\circ}\text{F}$.

RAI 3.2-7-1

MHI states that the ejected rod worth is the same with both mesh sizes in part because the steady state power distributions are the same. It is true that the power distributions should be similar as they are both tuned to the same ANC-generated power distributions. The result shown for the Doppler fuel temperature is similar for the two meshes with the 2x2 mesh giving a higher value. MHI also supplies radial power distributions at different times during a rod ejection accident to show that the effect of mesh size is small. Several comparisons of the effect of axial mesh are also shown to be insensitive to mesh size. The conclusions implicitly assume that the 4x4 mesh yields a converged solution. What changes would occur if a smaller mesh (6x6 or 8x8 radially or >76 mesh points axially) were used?

Response

As discussed in previous RAI responses, the nodal expansion method used in ANC can more accurately calculate steep flux gradients than the finite difference method used in TWINKLE-M. In general, using a finer mesh size in a finite difference code will allow for a more accurate calculation in regions of steep flux gradients. Therefore, it is expected that using a finer mesh size in TWINKLE-M would result in power distributions that more closely match those generated by ANC. However, the reactivity insertion and peaking factor from TWINKLE-M are already adjusted to match the safety limit value which is determined based on the ANC calculations. The hot spot temperature response is highly dependent on the reactivity insertion and peaking factor and is not affected by the small differences in power distribution between TWINKLE-M and ANC. Therefore, it is not necessary to use a finer mesh size, since the final result will not be affected.

RAI 3.2-7-2

What is the time step size used in the TWINKLE-M simulation of the rod ejection accident?
How is this time step size determined?

Response

Section 4.6 of the TWINKLE-M Input Manual, GEN0-LP-517(R0), provides a standard set of time steps, reproduced in the table below. This standard set of time step values were used in the TWINKLE-M analysis of the rod ejection accident. In addition to this standard set of time steps, a sensitivity analysis is performed to judge that the time steps used in the analysis are appropriate. If necessary, the time steps are adjusted appropriately. The TWINKLE-M Input Manual was submitted to the NRC by letter UAP-HF-08138 on August 1, 2008.



RAI 3.2-7-3

In Figure 3.2-7.6, why is no adjustment made of the diffusion coefficient in the reflector region?

Response

Figure 3.2-7.6 showed the average axial power distribution comparison between ANC and the results from TWINKLE-M. No adjustment is made to the diffusion coefficient in order to better see the difference between the case. If the diffusion coefficient in TWINKLE-M was adjusted, then the cases would agree very well and would be difficult to distinguish from each other in the figure.

RAI 3.2-8-1

Were the adjustments made to neutron lifetime and delayed neutron fraction adjusted to minimize the difference when changing mesh size? Were these only made for the comparison of mesh sizes or is this part of the procedure for calculating transients?

Response

The neutron lifetime and delayed neutron fraction are key parameters that affect the transient calculation. These parameters are adjusted in order to match the safety limit. The parameters were adjusted separately for the two mesh sizes, but in each case the adjustment is only made in order to match the safety limit. This adjustment is part of the procedure for calculating transients; it occurs uniquely for every analysis.

RAI 3.2-9-1

Explain how the adjustments made in the responses to RAIs 3.2-7 through 3.2-9 relate to the way in which analysis is generally done with TWINKLE-M.

Response

As described in the preceding response to RAI 3.2-8-1, adjustments to key parameters are made as part of each analysis. The parameters are adjusted to match the values from the safety analysis limit.

RAI 5.3-1-1

Do operating procedures allow for fully or partially inserted misaligned or inoperable control rods and if so, was this taken into account in the analysis of the design limit?

Response

All transients are assumed to begin with the most severe power distributions that are consistent with operation within the Technical Specifications (TS). In Chapter 16 of the DCD, Limiting Condition for Operation (LCO) 3.1.4 states that all shutdown and control rods shall be operable and that individual indicated rod positions shall be within 12 steps of their group step counter demand position. The impact of this LCO on the safety analysis is described in the Bases section of TS 3.1.4. The operability of the shutdown and control rods is an initial assumption in all safety analyses that assume rod insertion upon reactor trip. The maximum rod misalignment is another initial assumption in the safety analysis that directly affects core power distributions and assumptions of available shutdown margin.

RAI 5.3-1-2

The TWINKLE-M model is adjusted to give the same design limit worth as from the ANC calculation. Is the identical configuration represented in the TWINKLE-M three-dimensional model?

Response

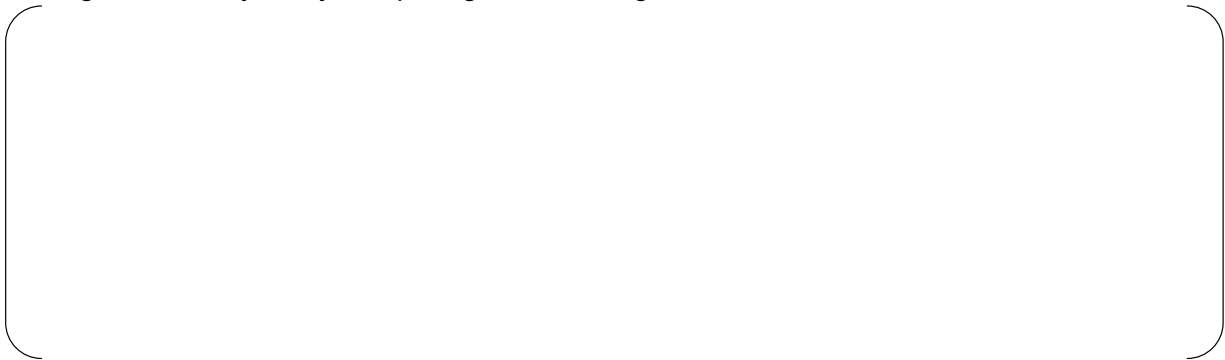
TWINKLE-M uses the identical configuration (geometry and mesh) as ANC for the three-dimensional model.

RAI 5.3-1-3

The adjustment is done by "changing the eigenvalue" in both the three- and one dimensional models. In the former, this would mean that a multiplier is applied to the fission rate throughout the reactor rather than to a local property of the controlled fuel assembly (e.g., absorption cross section). What is the impact on the analysis of this approximation?

Response

For the RCCA ejection analysis, there are two methods to add reactivity to the core. One method is to change the eigenvalue, which modifies the fission rate in all regions of the core. The second method is to decrease the local absorption cross section in the assembly where the RCCA is being ejected. While these two methods seem very different, the end results for the RCCA ejection analysis are similar. To show evidence that the results are similar, MHI is providing a sensitivity study comparing the following two cases:



The sequence of events for the sensitivity study is shown in Table 5.3-1-3.1 below. The results of the sensitivity study for the nuclear power and the fuel enthalpy as a function of time are shown in Figures 5.3-1-3.1 and 5.3-1-3.2, respectively. As the figures show, the two methods give very similar results. The hot spot peak fuel enthalpy is 77.8 cal/g for the topical report analysis, 51.1 cal/g for Case 1, and 50.9 cal/g for Case 2. The general shape of the two results is also similar to the topical report results, although the absolute values are different due to the difference in total reactivity insertion (600 pcm for the sensitivities vs. 800 pcm for the topical report). In addition, Figure 5.3-1-3.3 shows the radial enthalpy distributions for both cases^{*1}. These results show that the two methods give similar results and it is therefore acceptable to use the method of "changing the eigenvalue" in the R/E analysis.

*1 Note that Figure 5.3-1-3.3 is generated from TWINKLE-M. As described in Section 5.3 (2) of MUAP-07010 "Non-LOCA Methodology", a local fuel enthalpy rise is calculated in TWINKLE-M code by integration of the local power and power density in each mesh. The values in Figure 5.3-1-3.3 are adjusted to match the fuel enthalpy of the hottest assembly to the result of VIPRE-01M. The fuel enthalpy in each assembly is the maximum fuel enthalpy of the axial nodes.

Table 5.3-1-3.1 Sequence of Events for the RCCA Ejection (EOC HZP)

Event	Topical Report Time (sec)	Case1 Time (sec)	Case2 Time (sec)
Rod Ejection Occurs	0.0	0.0	0.0
Neutron Flux High (low setting) Analysis Limit Reached	0.15	0.20	0.22
Peak Nuclear Power Occurs	0.16	0.22	0.24
Reactor Trip Initiated (Rod Motion Begins)	1.05	1.10	1.12
Maximum Fuel Temperature Occurs	-	-	-
Maximum Fuel Enthalpy Occurs	1.60	1.66	1.68

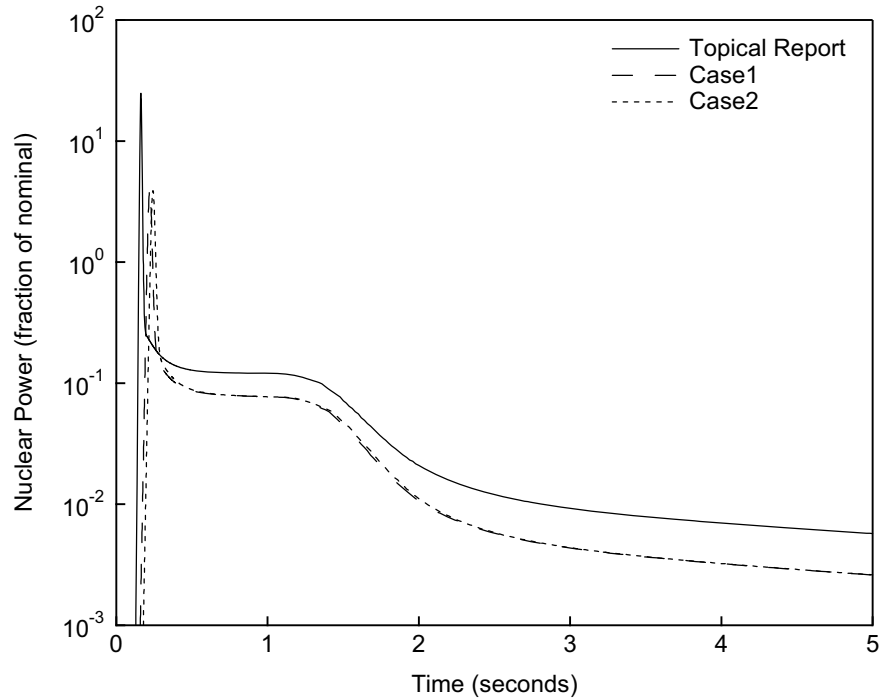


Figure 5.3-1-3.1 Nuclear Power versus Time – RCCA Ejection (EOC HZP)

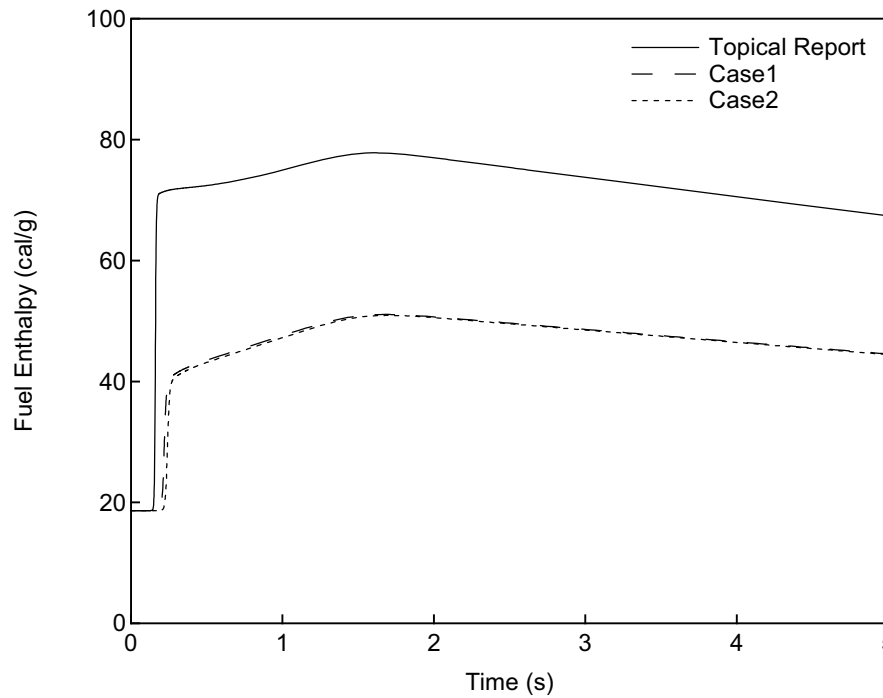
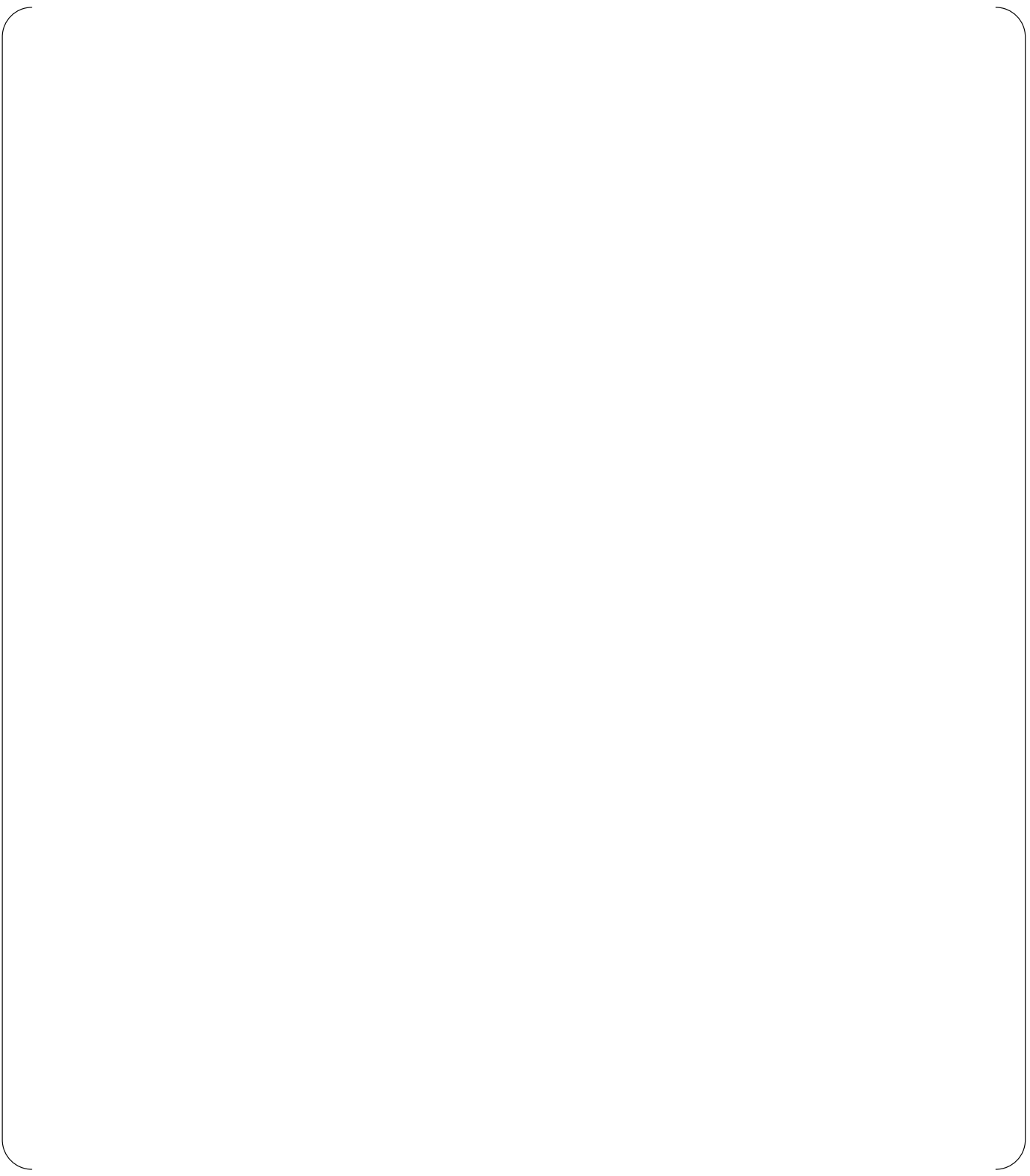


Figure 5.3-1-3.2 Fuel Enthalpy versus Time – RCCA Ejection (EOC HZP)



**Figure 5.3-1-3.3 Radial Enthalpy Distribution at the Time of Maximum Enthalpy
RCCA Ejection (EOC HZP)**

RAI 5.3-2-1

According to Figure 5.2-1, the VIPRE-M calculation needs rod power factors for 23 rods; TWINKLE-M presumably provides the "hot channel factor" for the hottest quarter (based on a 2x2 mesh) of a fuel assembly, i.e., not even for one fuel rod. Please explain what information is used by VIPRE-M to analyze the hot channel.

Response

[Empty response box]

RAI 5.3-2-2

The response to this RAI indicates that whatever the model is, it is not necessary to do a detailed 1/8 core calculation; all information is obtained by focusing on the hot channel. Does this allow you to make the assumption that the VIPRE-M model can place the ejected rod at the center of the core rather than at its realistic position?

Response

The reviewer's understanding of the VIPRE-01M model is correct. As discussed in the response for RAI 5.3-4 in UAP-HF-08141, the limiting parameters for the rod ejection event are fuel enthalpy, fuel temperature, and cladding temperature, which reach their respective maximum values before the transient coolant condition significantly changes and is able to affect the core. This allows for calculating the behavior of the hottest rod in the center of the VIPRE-01M 1/8 core model by applying appropriate boundary conditions.

RAI 5.3-2-3

The third sentence of the second paragraph in response to RAI 5.3-2 is grammatically incorrect; clarify.

Response

MHI would like to clarify this sentence by rewriting it as follows: The power distribution around the hot assembly is assumed to be the thermal design power distribution. This assumption has no effect on the results and, therefore, either a 1/8 core model or a single channel calculation can be used for this analysis.

The intent of the sentence is to explain that as long as the channels around the hot assembly are modeled, it does not matter what portion of the core is modeled.

The response to RAI 5.3-2, including this correction, is shown in entirety below:

The three-dimensional distribution of fuel enthalpy is calculated in TWINKLE-M using a mesh-wise average model, whereas the maximum fuel enthalpy rise is calculated in VIPRE-01M. The maximum enthalpy rise is calculated using a detailed sub-channel model in VIPRE-01M, which is, in turn, used to compensate for the difference between the mesh-wise and pin-wise enthalpy rise. The detailed procedure for how the three-dimensional distribution of enthalpy rise is adjusted to pin-wise enthalpy is provided in Section 5.3 of MUAP-07010.

To calculate the hot spot enthalpy rise in VIPRE-01M for PCMI failure, histories of core average power and hot channel peaking factor (F_Q) calculated in TWINKLE-M are passed to VIPRE-01M. The F_Q history is scaled using a multiplier so that the maximum value is the design limit, which is applied to the hot assembly of the 1/8 core model. The power distribution around the hot assembly is assumed to be the thermal design power distribution. This assumption has no effect on the results and, therefore, either a 1/8 core model or a single channel calculation can be used for this analysis. However, MHI has selected to use the 1/8 core model for the rod ejection analysis in order to assure consistency of the base input of VIPRE-01M with the core thermal hydraulic design.

In summary, to ascertain whether or not the PCMI acceptance criteria are met, the three-dimensional distribution of enthalpy calculated by TWINKLE-M is applied, considering a peak / average ratio in the mesh using the VIPRE-01M hot spot results. Histories of core average power and hot channel factor are necessary information to calculate the maximum enthalpy rise in VIPRE-01M.

RAI 5.3-3-1

The response suggests that the design limit is actually just the ANC generated peak/average fuel assembly power (with some unknown adjustment for uncertainty and "safety margin") for the case with the ejected rod out and no other change in rod configuration. It is used to add a conservative factor to the analysis only because it turns out to be larger than the same ratio calculated by TWINKLE-M. Please confirm this understanding of the hot channel design limit, mathematically describe the hot channel factor, uncertainty and safety margin, and explain how the uncertainty and safety margin are applied to the design limit.

Response

The reviewer's understanding is basically correct. The design limit is determined based on the value calculated using the core design code ANC, considering calculation uncertainty and safety margin. The TWINKLE-M value does not include calculation uncertainty or safety margin and is therefore less than the ANC value. By using the lower (TWINKLE-M) value of the hot channel factor, the result is a higher peak power excursion. This larger peak power from TWINKLE-M is used as input to the VIPRE-01M analysis. (

)

The mathematical description of the hot channel factor is as follows: The "hot channel" is the coolant channel in which the maximum heat flux occurs and the "hot channel factor" is the maximum heat flux in the core (the heat flux in the "hot channel") divided by the average heat flux in the core.

(

RAI 5.3-6-1

In MUAP-07009-P and in the response to RAI 5.3-6, it is noted that mixing between assemblies is "conservatively ignored." Yet later in the response to RAI 5.3-6, it is stated that "the power of the hot assembly is assumed to be higher than the power of the surrounding assemblies, which would cause *larger flow redistribution from the hot assembly to the surrounding assemblies* and result in a more limiting coolant condition in the hot assembly." As written, these two statements are contradictory. Clarify.

Response

In the response to RAI 5.3-6, the word "mixing" is meant to refer to the turbulent mixing of energy and momentum, which is associated with equal mass exchange between adjacent channels due to turbulence. This is more clearly explained in MUAP-07009-P but was unclear as was written in the original response to RAI 5.3-6. The response should have used the term "turbulent mixing" rather than "mixing" for clarity.

RAI 5.3-7-1

The response explains how cross sections are averaged radially, but does not address other parameters such as diffusion coefficients and delayed neutron data. Please provide the missing information.

Response

The nuclear parameters such as the diffusion coefficients and delayed neutron data are also averaged using a neutron flux and volume weighting method. The equation for the averaging of the diffusion coefficients and the delayed neutron data is the same as was shown for the macroscopic cross section, which was given in the UAP-HF-08141-P response to RAI 5.3-7.

RAI 5.3-7-2

In response to RAI 5.3-7 of UAP-HF-08141-P MHI provided a comparison between the TWINKLE-M 3-D and 1-D core average axial power in Figure 5.3-7.1. Is the difference given in Figure 5.3-7.1 a representative or maximum expected difference? If representative, please explain if a larger difference would have a significant impact on the number of rods in DNBR.

Response

The comparison provided in Figure 5.3-7.1 is a representative example of the axial power distribution for the 1-D and 3-D TWINKLE-M analyses for the beginning of cycle. The difference in axial power distribution has only a very slight impact on the number of rods in DNBR, even if the differences were larger than those shown in the representative example. Additionally, the rod ejection analysis using 1-D methodology assumes a large amount of conservatism in the inserted reactivity, the hot channel factor and the Doppler weighting factor. These other conservative assumptions are more than large enough to bound the impact of the relatively small differences in axial power distribution.

RAI 5.3-10-1

According to the response, the control rods are modeled explicitly. However, the report says that the trip reactivity is the design limit, i.e., not what is calculated by TWINKLE-M. Please explain further.

Response

The rod absorption cross section is adjusted so that the total worth of the tripped rods is equal to the design limit.

RAI App.F-1-1

Although the final form of the “modified Zaloudek” correlation is attractive due to its simple dependence on $(P - P_{sat})$, comparison to experimental data is necessary to show that the correlation is accurate under the conditions for which it was developed. Please provide additional validation for the “modified Zaloudek” correlation.

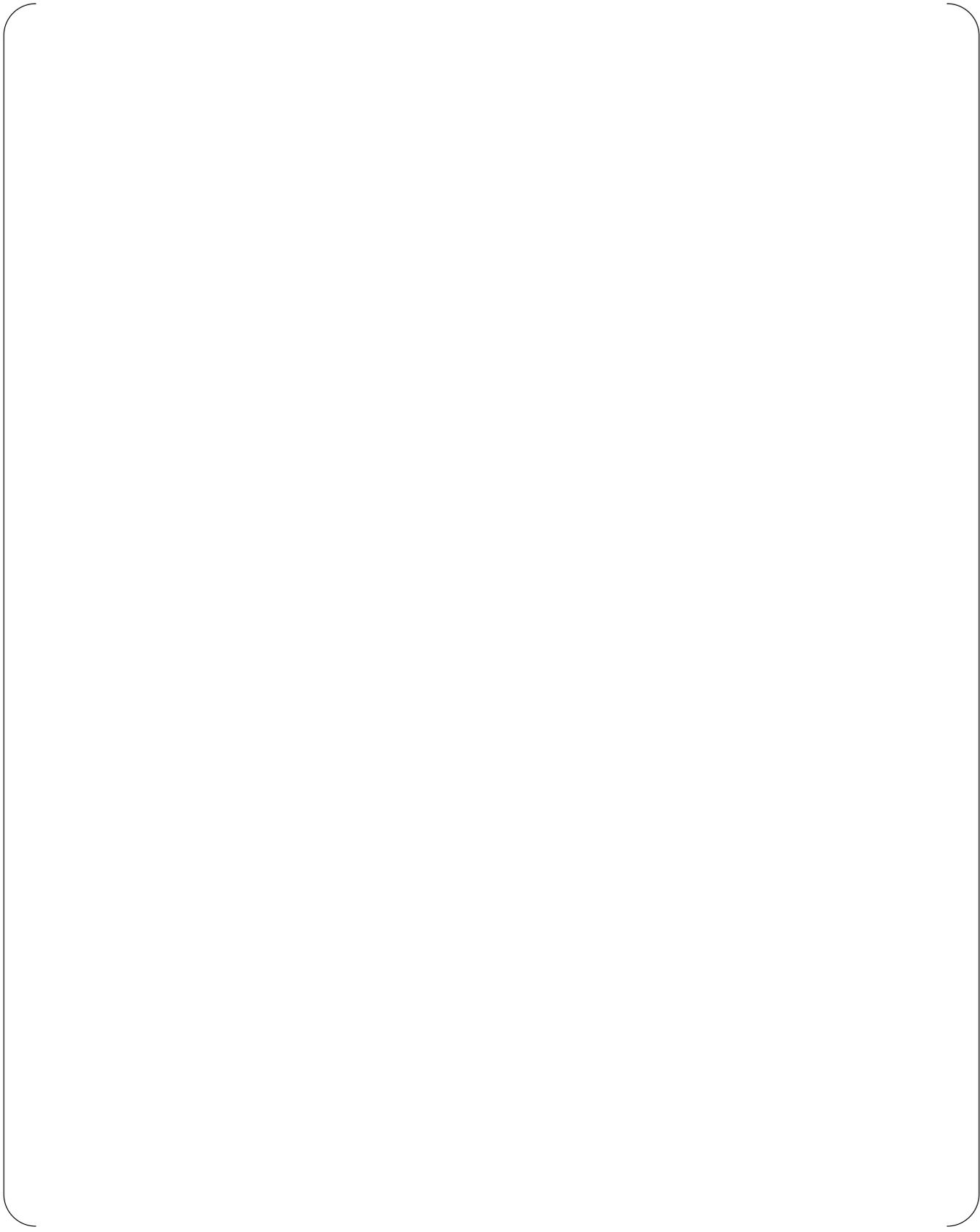
Response

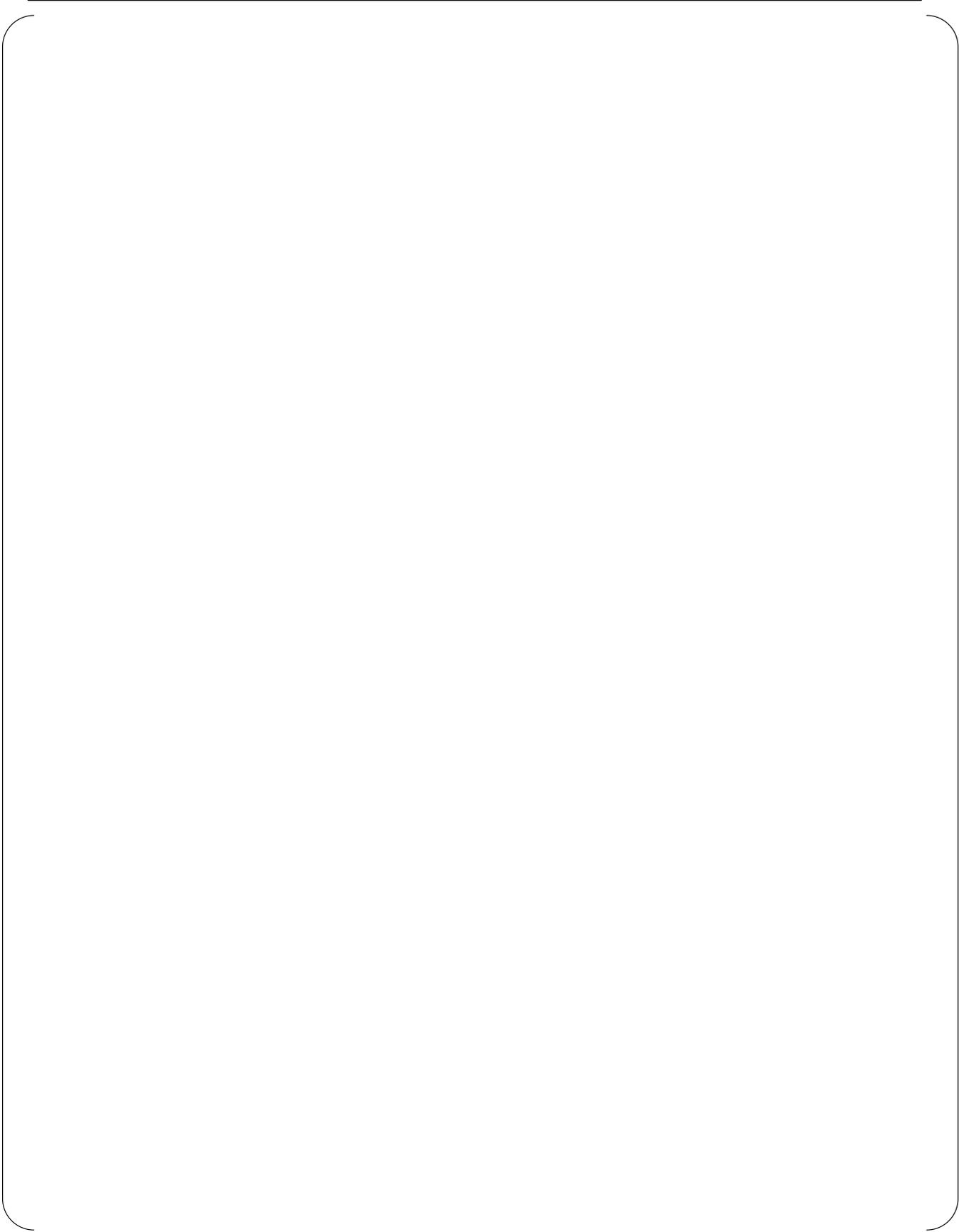
The modified Zaloudek correlation is part of the conservative break flow model used in MARVEL-M for the steam generator tube rupture (SGTR) analysis. The SGTR analysis in MARVEL-M was validated by a comparison to an actual SGTR event at the [] The MARVEL-M validation used a realistic break flow model with a discharge coefficient (C_D) of [] and is described in detail in the response to RAI 3.1-6. In Appendix F of the “Non-LOCA Methodology Topical Report” (MUAP-07010), the calculation results for the US-APWR with a conservative break flow model (in which the initial break flow rate is calculated by the modified Zaloudek correlation) are compared to those of the realistic break flow model (using $C_D=1.0$). Figure F-2 in the topical report shows that the conservative break flow model is conservative with respect to the realistic break flow model. Since the realistic break flow model was shown to give accurate results when compared to data from an actual SGTR event, as described in the response to RAI 3.1-6, the conservative break flow model will likewise give conservative results for an actual SGTR event. Therefore, the use of the modified Zaloudek correlation is both reasonable and conservative for the SGTR event.

RAI 3.1-6

Present validation data of MARVEL-M for the steam generator tube rupture event.

Response





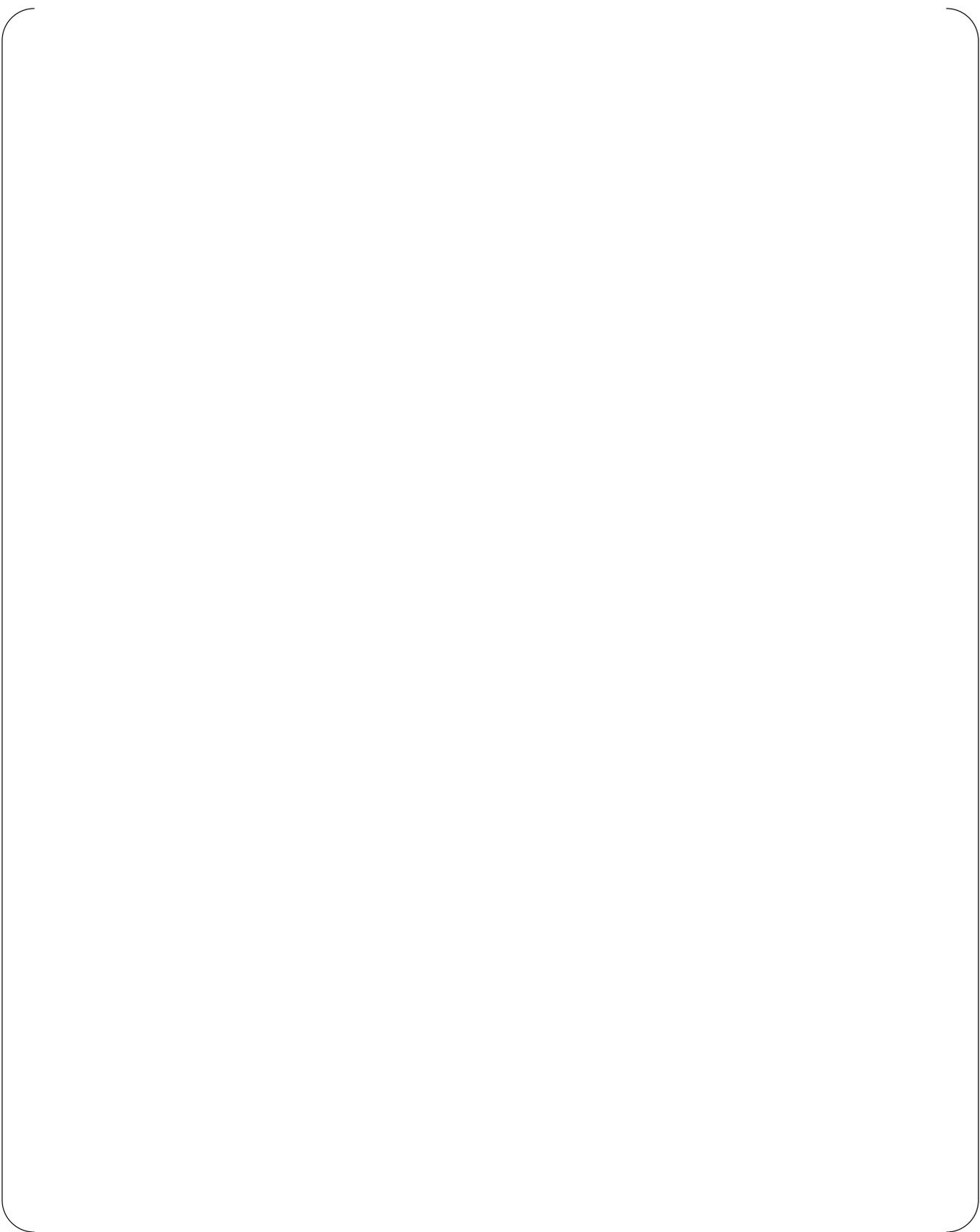






Figure 3.1-6.1 RCS Pressure versus Time



Figure 3.1-6.2 Ruptured Steam Generator Pressure versus Time



Figure 3.1-6.3 Intact Steam Generator Pressure versus Time



Figure 3.1-6.4 Ruptured Steam Generator Water Level versus Time



Figure 3.1-6.5 Intact Steam Generator Water Level versus Time



**Figure 3.1-6.6 Intact Steam Generator Water Level versus Time
Sensitivity Analysis to Steam Generator Model**



Figure 3.1-6.7 Pressurizer Water Level versus Time



Figure 3.1-6.8 Ruptured Loop Hot Leg Temperature versus Time



Figure 3.1-6.9 Intact Loop Hot Leg Temperature versus Time



Figure 3.1-6.10 Safety Injection Flow Rate to Deluge Line versus Time



Figure 3.1-6.11 Safety Injection Flow Rate to Cold Leg versus Time

RAI 3.1-7

Give the history of the version of LOFTRAN used in MARVEL-M validation. Is the version of LOFTRAN employed by MHI for validation the same as that which was approved by the NRC? Detail any changes MHI has made to LOFTRAN. This is necessary because MHI is using LOFTRAN to validate the results from MARVEL-M, and it must be clear that the version of LOFTRAN employed has received licensing approval in the United States.

Response

[Empty response box]

RAI 3.1-8

MHI uses LOFTRAN as one of the means to demonstrate that the MARVEL-M code behaves as expected. For the comparison to be meaningful, the algorithms, numerical methods and, if used, correlations should be sufficiently different. Does MARVEL-M share any significant algorithms, numerical methods or correlations with the version of LOFTRAN used for the comparison? If yes, please describe the similarities. If no, provide examples where there are fundamental differences.

Response

MARVEL and LOFTRAN are completely different codes with respect to the FORTRAN programming. The two codes were developed independently by different individuals, and the internal subroutine structure and variable names are different. MARVEL was used for selected FSAR Chapter 15 analyses for events with non-uniform behavior (prior to the availability of 4-loop LOFTRAN in the late 1970s) such as:

- Inadvertent opening of a steam generator relief or safety valve
- Startup of an inactive loop at an incorrect temperature
- Steam system piping failure

The NRC approved the use of MARVEL for those FSAR Chapter 15 analyses. MARVEL and 4-loop LOFTRAN were both approved in 1984 by the NRC. The NRC continues to approve the use of 4-loop LOFTRAN in FSAR Chapter 15 analyses of recent US PWRs. However, MARVEL has not been used in recent US PWR plant FSAR Chapter 15 analyses since the 4-loop LOFTRAN code was approved by the NRC.

As described in detail in the response to RAI 2.1-21 in MHI letter UAP-HF-08245, MHI made some improvements and refinements to certain original MARVEL models. As part of the validation of MARVEL-M, comparisons of MARVEL-M and 4-loop LOFTRAN have been made and presented to NRC in the Non-LOCA Topical Report (MUAP-07010) and the associated RAI responses. The MARVEL-M and 4-loop LOFTRAN calculation results agree very well and in some cases are almost identical. Therefore, MARVEL-M has the same capabilities as 4-loop LOFTRAN, which continues to be approved by the NRC. MHI believes that the comparison of MARVEL-M to an NRC approved code, 4-loop LOFTRAN, is a reasonable method of code of code certification and validation.

RAI App E-2

Show the scale on the vertical axis of Figure E-1.

Response

The revised version of Figure E-1 that includes the axes scales is shown in Figure E-2.1 below.



Figure E-2.1 DNBR versus Reactor Inlet Mixing for the Steam System Piping Failure

Reference 5

UAP-HF-09099
Docket No. 52-021

MHI's Non-LOCA Response to NRC's Requests for Additional Information
on Topical Reports MUAP-07010, MUAP-07011, and MUAP-07013

March 2009

RAI 1

Description and software (either provide or identify commercial source) to generate plotted output from MARVEL-M results. Provide method and directions for retrieving plot data from MARVEL-M binary output file.

Response

A simple FORTRAN program is used to convert the binary output file from MARVEL-M into a delimited text file that can be read using a spreadsheet application, such as Microsoft Excel. The delimited output is grouped according to the MARVEL-M output variables. The description of the output variables is included in Section 3.2 of the latest revision of the MARVEL-M Manual (Rev. 6), which is being submitted along with this response. The FORTRAN program to convert the binary output file to a delimited text file is attached as an executable file, including its source code. Once the delimited data has been imported into a spreadsheet application, such as Microsoft Excel, the spreadsheet application can be used to generate various plots as specified by the user. For completeness, this response also includes the version of the MARVEL-M executable file consistent with Rev. 6 of the MARVEL-M Manual (and compatible with the FORTRAN converter program).

The FORTRAN program requires the user to request, by number (from Section 3.2 of the MARVEL-M Manual), the MARVEL-M output variables to convert. The user specifies these requests using a very simple text input file; a sample file has been included as an attachment. The result will be a delimited file that contains a column for each of the user requested MARVEL-M output variables. The first column of data is always time. Each row of data is for a single MARVEL-M output time interval.

RAI 2

Electronic copies of the input files for MARVEL-M analysis corresponding to:

- a. Uncontrolled RCCA bank withdrawal at power.
- b. Partial loss of forced reactor coolant flow.
- c. Complete loss of forced reactor coolant flow.
- d. Reactor coolant pump shaft seizure.
- e. Main steam line break (hot zero power with offsite power available).

Response

Electronic copies of all of the requested MARVEL-M input files are included with this submittal.

It is the understanding of MHI that the purpose of providing the input files is to independently confirm the results and/or assist in performing confirmatory analyses. The five input files that were requested and are being provided (as attached files) are:

- Uncontrolled RCCA bank withdrawal at power (US-APWR DCD Section 15.4.2)
- Partial loss of forced reactor coolant flow (US-APWR DCD Section 15.3.1.1)
- Complete loss of forced reactor coolant flow (US-APWR DCD Section 15.3.1.2)
- Reactor coolant pump shaft seizure (US-APWR DCD Section 15.3.3)
- Main steam line break (hot zero power with offsite power available case) (US-APWR DCD Section 15.1.5)

These five input files are the same as those used for the analyses of the corresponding sections of Chapter 15 of the DCD indicated above in the parentheses.

RAI 3

Please provide access to M-RELAP5 source code and PC executable. This will be used exclusively by the NRC and its contractor (ISL) in support of the M-RELAP5 code review.

Response

The response to this RAI question is included in the LOCA portion of the response, which will be submitted in a separate letter.

RAI 4

For the following two bullets, please provide the requested information if it is available in English (or some combination of English/Japanese). If the referenced material is solely written in Japanese, do not send this material but rather provide a listing of these items so that we can later decide which items may need to be translated into English.

- Documentation for M-RELAP5 SBLOCA US-APWR plant model – preferably a model development notebook. This will be used to aid in understanding the basis for the plant model that was developed (NRC and ISL will return to MNES Arlington on April 22, 2009 to review this material).
- Documentation (calculation notebooks) for the specific limiting SBLOCA, LBLOCA and Non-LOCA cases. Currently plans are to evaluate all limiting cases presented in the DCD for the SBLOCA, the limiting LBLOCA case in the DCD (including all parametric selections used for that case), the MSLB non-LOCA cooldown limiting case in the DCD (including hot zero power initialization and reactivity feedback effects), the loss-of-load non-LOCA limiting heatup case in the DCD and a SGTR transient. This information is requested to facilitate setting up the confirmatory RELAP5/MOD3.3 models.

Response

This RAI question refers to both LOCA (the entire first bullet and the first half of the second bullet) and non-LOCA (the second half of the second bullet) items. The LOCA portion of the response will be submitted in a separate letter. The non-LOCA portion of the response is below:

It is the understanding of MHI that the purpose of requesting the calculations memos (notebooks) is to assist with preparing the confirmatory analyses. MHI calculation memos are written in Japanese with the input parameters and values written in English. The calculation memos also describe initial conditions and event-specific input assumptions in Japanese. However, most of this information is provided in the applicable section for each event in Chapter 15 of the DCD. An English version of a summary of the initial conditions and event-specific input assumptions is included in the attachment to this response for the following three non-LOCA events:

- Main steam line break (hot zero power with offsite power available case)
- Loss of load (peak pressure case)
- Steam generator tube rupture (offsite dose evaluation case)

In addition to this information, electronic copies of the input files for these three events are also included as attachments to this response.

Reference 6

UAP-HF-09358
Docket No. 52-021

MHI's 5th Response to NRC's Requests for Additional Information on
US-APWR Topical Report:
Non-LOCA Methodology, MUAP-07010-P

July 2009

All RAI responses in this letter are redacted due to proprietary content

Reference 7

UAP-HF-10001
Docket No. 52-021

MHI's 6th, 7th, and 8th Responses to NRC's Requests for Additional
Information on US-APWR Topical Report:
Non-LOCA Methodology, MUAP-07010-P (R0)

January 2010

All RAI responses in this letter are redacted due to proprietary content

Reference 8

UAP-HF-10101
Docket No. 52-021

MHI's 9th and 10th Responses to NRC's Requests for Additional
Information on US-APWR Topical Report:
Non-LOCA Methodology, MUAP-07010-P (R0)

May 2010

All RAI responses in this letter are redacted due to proprietary content

Reference 9

UAP-HF-10195
Docket No. 52-021

MHI's 11th Response to NRC's Request for Additional Information on
US-APWR Topical Report:
Non-LOCA Methodology, MUAP-07010-P (R0)
(6th Topical Report RAI)

July 2010

All RAI responses in this letter are redacted due to proprietary content

Reference 10

UAP-HF-10226
Docket No. 52-021

MHI's 12th Response to NRC's Requests for Additional Information on
US-APWR Topical Report:
Non-LOCA Methodology, MUAP-07010-P (R0)

August 2010

All RAI responses in this letter are redacted due to proprietary content

Reference 11

UAP-HF-10227
Docket No. 52-021

MHI's Revised 11th Response to NRC's Request for Additional Information
on
US-APWR Topical Report:
Non-LOCA Methodology, MUAP-07010-P (R0)
(6th Topical Report RAI)

August 2010

All RAI responses in this letter are redacted due to proprietary content

Reference 12

UAP-HF-10268
Docket No. 52-021

MHI's Revised 12th Response to NRC's Request for Additional Information
on
US-APWR Topical Report:
Non-LOCA Methodology, MUAP-07010-P (R0)

October 2010

All RAI responses in this letter are redacted due to proprietary content

Reference 13

UAP-HF-11005
Docket No. 52-021

MHI's 13th Response to NRC's Requests for Additional Information on
US-APWR Topical Report:
Non-LOCA Methodology, MUAP-07010-P (R1)

January 2011

All RAI responses in this letter are redacted due to proprietary content

Reference 14

UAP-HF-11118
Docket No. 52-021

MHI's 14th Response to NRC's Request for Additional Information on
US-APWR Topical Report:
Non-LOCA Methodology, MUAP-07010-P (R1)

April 2011

All RAI responses in this letter are redacted due to proprietary content

Reference 15

UAP-HF-11129
Docket No. 52-021

MHI's 15th Response to NRC's Request for Additional Information on
US-APWR Topical Report:
Non-LOCA Methodology, MUAP-07010-P (R1)

April 2011

All RAI responses in this letter are redacted due to proprietary content

Reference 16

UAP-HF-11200
Docket No. 52-021

MHI's 16th Response to NRC's Request for Additional Information on
US-APWR Topical Report:
Non-LOCA Methodology, MUAP-07010-P (R1)

June 2011

All RAI responses in this letter are redacted due to proprietary content

Reference 17

UAP-HF-11264
Docket No. 52-021

MHI's Revised 15th Response to NRC's Request for Additional Information
on US-APWR Topical Report:
Non-LOCA Methodology, MUAP-07010-P (R1)

August 2011

All RAI responses in this letter are redacted due to proprietary content

Reference 18

UAP-HF-12120
Docket No. 52-021

2nd Revision to MHI's 15th Response to NRC's Requests for Additional
Information on US-APWR Topical Report: Non-LOCA Methodology,
MUAP-07010-P (R1)

May 2012

All RAI responses in this letter are redacted due to proprietary content